

## Numerical Simulation of Steady States Associated with Thermomechanical Processes - Application to Welding and Rolling

Yabo JIA<sup>\*</sup>, Rémi Lacroix<sup>\*\*</sup>, Jean-Christophe Roux<sup>\*\*\*</sup>, Eric Feulvarch<sup>\*\*\*\*</sup>, Jean-Michel Bergheau<sup>\*\*\*\*\*</sup>

<sup>\*</sup>University Lyon, ENISE, CNRS, UMR 5513, Laboratoire de Tribologie et Dynamique des Systèmes, 58 rue Jean Parot, 42023 Saint-Etienne Cedex 02, France, <sup>\*\*</sup>ESI Group 70 Rue Robert, 69006 Lyon, France, <sup>\*\*\*</sup>University Lyon, ENISE, CNRS, UMR 5513, Laboratoire de Tribologie et Dynamique des Systèmes, 58 rue Jean Parot, 42023 Saint-Etienne Cedex 02, France, <sup>\*\*\*\*</sup>University Lyon, ENISE, CNRS, UMR 5513, Laboratoire de Tribologie et Dynamique des Systèmes, 58 rue Jean Parot, 42023 Saint-Etienne Cedex 02, France, <sup>\*\*\*\*\*</sup>University Lyon, ENISE, CNRS, UMR 5513, Laboratoire de Tribologie et Dynamique des Systèmes, 58 rue Jean Parot, 42023 Saint-Etienne Cedex 02, France

### ABSTRACT

The numerical simulation of thermo-mechanical processes is based on the modeling of the couplings between several physical phenomena such as heat transfer, metallurgy and mechanics. The classical time-stepping methods enable accurate predictions of the physical variables but are generally time consuming because these processes often involve moving loadings leading to fast evolutions and high gradients of the physical variables, and consequently to the choice of very small time steps. For simulations of thermomechanical forming processes like welding, the thermal, mechanical and metallurgical fields associated with moving loadings can reach steady states. Several authors have therefore proposed eulerian or mixed lagrangian-eulerian computation methods to determine directly or incrementally the steady states ([1][2][3]). In this paper, an eulerian approach with nodal integration is presented. Using nodal integration, the transfers are still necessary but may be performed in a more rigorous way, and this method permits to use standard linear tetrahedral elements in plasticity. In order to demonstrate the performance of eulerian approach with nodal integration, we propose first to compare this method with an incremental approach of calculation of the steady states associated to the welding process. Then, a simulation of the steady state with an application to rolling is presented and discussed in relation to existing arbitrary lagrangian-eulerian approaches ([4] [5]).

REFERENCES [1] J. Huetink, P.T. Vreede, J. Van der Lugt, Progress in mixed eulerian-lagrangian finite element simulation of forming processes, Int. J. for Numer. Meth. Engng 1990, Vol. 30, 1441-1457. [2] J.-M. Bergheau, D. Pont and J.-B. Leblond, « Three-dimensional simulation of a LASER surface treatment through steady state computation in the heat source comoving frame », Mechanical Effects of Welding, IUTAM Symposium Lulea (Sweden), 1991, edited by L. Karlsson, L.-E. Lindgren, M. Jonsson, 1992, Springer-Verlag, Berlin Heidelberg, pp. 85-92. [3] J.Y. Shanghvi and P. Michaleris, « Thermo-elasto-plastic finite element analysis of quasi-state processes in Eulerian reference frames », Int. J. Numer. Meth. Engng 2002 Volume 53, pages 1533-1556 [4] J.M BERGHEAU, J.B LEBLOND, 'A nouvel finite element method based on a nodal integration technique for nonlinear problems of solid mechanics', complas 2017, 5 -7 September 2017, Barcelona, Spain. [5] Y. Crutzen, R.Boman, L. Papeleux, J.P Ponthot, 'Arbitrary Lagrangian Eulerian simulations cold roll formaing processes including inline welding' complas 2017, 5 -7 September 2017, Barcelona, Spain.

## **The Cosserat Point Element (CPE) for Modeling Static and Dynamic Response of Structures at Finite Deformations**

Mahmood Jabareen\*

\*Technion - Israel Institute of Technology

### **ABSTRACT**

The theory of a Cosserat point has been used to develop a 3D brick Cosserat point element (CPE) for the static and dynamic numerical solutions of elastic structures that undergo finite deformations. The Cosserat approach postulates an average form of the deformation measure and connects the kinetic quantities to derivatives of a strain energy function. Once this strain energy has been specified, the procedure for obtaining the kinetic quantities needs no integration over the element region and it ensures that the response of the CPE is hyperelastic. Also, the constitutive equations of the CPE were designed to analytically satisfy a nonlinear form of the patch test. Specifically, the strain energy function is additively decomposed into two parts: one controlling the homogeneous deformations and the other controlling the inhomogeneous deformations. Developing a functional form for the strain energy of the inhomogeneous deformations has proven to be challenging. Recently, a functional form of the inhomogeneous strain energy function was developed, which causes the CPE to be a truly user friendly element that can be used with confidence for problems with finite deformation. It was observed that the three-dimensional brick CPE is a robust, an accurate element that can be used to accurately predict the response of thin plates and shells with only one element through the thickness. Also, the CPE does not exhibit unphysical locking or hourglassing for thin structures or nearly incompressible material response.

## Urban Flow Simulations Using LES Lattice Boltzmann Method

Jerome Jacob\*, Pierre Sagaut\*\*

\*Aix Marseille Univ, CNRS, Centrale Marseille, M2P2, Marseille, France, \*\*Aix Marseille Univ, CNRS, Centrale Marseille, M2P2, Marseille, France

### ABSTRACT

Urban flow simulation on full scale configurations are widely used in the literature to assess pedestrian wind comfort, pollutant dispersion and thermal comfort inside cities. Urban flows are very complex three dimensional turbulent flows with several physical processes such as building wake interaction or channeling mechanisms. Most of these simulations have been performed using Reynolds Average Navier-Stokes (RANS) approach due to reasonable computational cost whereas Large Eddy Simulation (LES) are mainly used for simplified areas such as isolated buildings or street canyon. In this work we propose the use of lattice Boltzmann method[1] (LBM) based on the resolution of Boltzmann equation which describes the evolution of particle distribution function instead of Navier Stokes equations. This method is a very efficient method for massively parallel simulation due to local and linear algorithm. Furthermore the use of immersed boundary conditions and embedded uniform meshes with a ratio of 2 for the grid step between two successive refinement levels permit to mesh complex areas such as city more easily that make LBM a very interesting method for urban flow simulation. In this work the Boltzmann equation is discretized on a D3Q19 lattice and a single relaxation time regularized collision operator[2] is used to ensure the stability of the model. Some properties of this regularized collision operator have been used to perform implicit and explicit wall modeled LES simulations inside the Shinjuku area, a 1 km<sup>2</sup> part of Tokyo city center. These simulations are compared with several RANS simulation available in the literature and validated by comparisons with wind tunnel and in-situ measurements provided by the Architectural Institute of Japan. [1] X. He, L.-S. Luo, Theory of the lattice Boltzmann method: From the Boltzmann equation to the lattice Boltzmann equation, Physical Review E 56 (6) (1997) 6811-6817 [2] O. Malaspinas, Increasing stability and accuracy of the lattice Boltzmann scheme: recursivity and regularization. ArXiv, pages 1-31, 2015

## Modeling the Biomechanics of a Four Chamber Cardiac Model with Myocardial Infarction

Arian Jafari<sup>\*</sup>, Edward Pszczolkowski<sup>\*\*</sup>, Adarsh Krishnamurthy<sup>\*\*\*</sup>

<sup>\*</sup>Iowa State University, <sup>\*\*</sup>Iowa State University, <sup>\*\*\*</sup>Iowa State University

### ABSTRACT

Abstract: Cubic-Hermite finite element meshes are widely used for simulating cardiac biomechanics due to their superior convergence characteristics and their ability to capture smooth geometries compactly compared to linear tetrahedral meshes. However, such meshes have previously been used only with simple ventricular geometries with non-physiological boundary conditions due to challenges associated with creating cubic-Hermite meshes of the complex heart geometry. The complex geometry of the heart, especially near atrial regions and valves necessitates the appearance of extraordinary nodes (nodes with 3 or  $\geq 5$  adjacent elements in 2D) in the mesh. Extraordinary nodes allow the mesh to capture the geometric characteristics of the heart accurately and apply physiologically accurate boundary conditions. However, consistently interpolating the finite element fields in the presence of extraordinary nodes requires additional mathematical formulation. In this work, we created a four-chamber cardiac model utilizing cubic-Hermite elements and simulated a full cardiac cycle by coupling the 3D finite element model with a lumped circulation model. The  $G_1$  continuity of the finite-element fields in the neighborhood of extraordinary nodes were maintained using an ensemble coordinate system with a linear global-to-local transformation. The myocardial fiber orientations were interpolated within the mesh using the Log-Euclidean method to overcome the singularity associated with interpolation of orthogonal matrices. Physiologically accurate boundary conditions were applied to the nodes along the valve plane. We then simulated a complete cardiac cycle of a healthy heart and of a heart with myocardial infarction. We compared the pumping function of the heart for both cases by calculating the work done by the ventricle (area enclosed inside the left ventricular Pressure-Volume (P-V) loop) and the base-apex shortening. We observed a 12% reduction in work done by the heart after myocardial infarction and a corresponding reduction in the base-apex shortening. The displacement of the infarcted region and the corresponding region in a healthy heart was also compared to understand the influence of myocardial infarction on the local displacements of the myocardium. The myocardial wall displacements obtained from the four-chamber cardiac model are comparable to actual patient data without requiring complicated non-physiological boundary conditions usually required in truncated ventricular heart models. References: 1) Adarsh Krishnamurthy, Matthew J. Gonzales, Gregory Sturgeon, W. Paul Segars, Andrew D. McCulloch, Biomechanics simulations using cubic Hermite meshes with extraordinary nodes for isogeometric cardiac modeling, In Computer Aided Geometric Design, Volume 43, 2016, Pages 27-38, ISSN 0167-8396.

## An Isogeometric Collocation Method for Karhunen-Loeve Discretization of Random Fields

Ramin Jahanbin\*, Sharif Rahman\*\*

\*The University of Iowa, \*\*The University of Iowa

### ABSTRACT

Many uncertainty quantification problems in engineering and applied sciences require modeling spatial variability of random input parameters. For instance, the tensile and fracture toughness properties of engineering materials, the size and shape characteristics of mechanical components, and the wind and snow loads in structural systems all exhibit randomness that varies not only from sample to sample, but also from point to point in their respective domains. Therefore, random field treatment of spatial varying randomness is a vital ingredient in computational analysis. Loosely speaking, a random field represents a random quantity at each point of the domain and, therefore, engenders an infinite number of random variables. In practice, though, the number of random variables must be finite and manageable but also large enough to ensure an optimal or accurate approximation of the original random field. This process is often referred to as random field discretization. This paper presents an isogeometric collocation method for solving a Fredholm integral eigenvalue problem, leading to random field discretization by the Karhunen-Loeve expansion. The method involves a projection onto finite-dimensional a subspace of a Hilbert space, basis splines (B-splines) and non-uniform rational B-splines (NURBS) spanning the subspace, and standard methods of eigensolutions. Like the existing isogeometric Galerkin method [1], the NURBS-based collocation method also preserves exact geometrical representation of the physical or computational domain and exploits regularity of basis functions delivering globally smooth eigensolutions. However, in the collocation method, the construction of the system matrices for a d-dimensional eigenvalue problem requires at most d-dimensional domain integrations, as compared with 2d-dimensional integrations in the Galerkin method. Therefore, the introduction of the isogeometric collocation method for random field discretization offers a huge computational advantage over the existing Galerkin methods. Numerical examples illustrate the accuracy, efficiency, and convergence properties of the proposed isogeometric method for obtaining eigensolutions. [1] Rahman, S. "A Galerkin Isogeometric Method for Karhunen-Loeve Approximation of Random Fields," submitted to Computer Methods in Applied Mechanics and Engineering, 2017.

## Using Deep Neural Networks for Data-Driven Inverse Modeling of Turbulent Wake Dynamics

Rajeev Jaiman<sup>\*</sup>, Tharindu Miyanawala<sup>\*\*</sup>

<sup>\*</sup>National University of Singapore, <sup>\*\*</sup>National University of Singapore

### ABSTRACT

An efficient deep learning technique for the model reduction of the Navier-Stokes equations for unsteady flow problems is proposed. The proposed technique relies on the Convolutional Neural Network (CNN) and the stochastic gradient descent method. Of particular interest is to predict the unsteady fluid forces for different bluff body shapes for 3D high-Reynolds number flows. The discrete convolution process with a non-linear rectification is employed to approximate the mapping between the bluff-body shape and the fluid forces. The deep neural network is fed by the Euclidean distance function as the input and the target data generated by the full-order Navier-Stokes computations for primitive bluff body shapes. The convolutional networks are iteratively trained using the stochastic gradient descent method with the momentum term [1] to predict the fluid force coefficients of different geometries and the results are compared with the full-order computations. We attempt to provide a physical analogy of the stochastic gradient method with the momentum term with the simplified form of the incompressible Navier-Stokes momentum equation. We also construct a direct relationship between the CNN-based deep learning and the Mori-Zwanzig formalism [2] for the model reduction of dynamical system. A systematic convergence and sensitivity study is performed to identify the effective dimensions of the deep-learned CNN process such as the convolution kernel size, the number of kernels and the convolution layers. We perform the CNN predictions initially for low Re (laminar wake) and then for high Re (turbulent wake) flows. Within the error threshold, the prediction based on our deep convolutional network has a speed-up nearly four-orders of magnitude for the low Re and five-orders of magnitude for the high Re compared to the full-order results. The CNN only consumes a very small fraction of computational resources as well. The proposed CNN-based approximation procedure enables to perform the parametric design of bluff bodies on personal computers and devices. Overall, this method has a profound effect on design space exploration and the feedback control of separated flows. References: [1] D. E. Rumelhart, G. E. Hinton, and R. J. Williams, "Learning representations by back-propagating errors", *Cognitive modeling*, vol. 5, no. 3, pp. 1-4, 1988. [2] Tharindu P. Miyanawala and Rajeev K. Jaiman, "An Efficient Deep Learning Technique for the Navier-Stokes Equations: Application to Unsteady Wake Flow Dynamics," arXiv preprint arXiv:1710.09099, 2017.

## Construction of Basis Functions for Algebraic Dual Space

Varun Jain<sup>\*</sup>, Yi Zhang<sup>\*\*</sup>, Artur Palha<sup>\*\*\*</sup>, Marc Gerritsma<sup>\*\*\*\*</sup>

<sup>\*</sup>Delft University of Technology, <sup>\*\*</sup>Delft University of Technology, <sup>\*\*\*</sup>Eindhoven University of Technology, <sup>\*\*\*\*</sup>Delft University of Technology

### ABSTRACT

In this work we develop a discretization method that explicitly uses functions from the algebraic dual space. Duality pairing between functions from the primal space and the dual space can be done in terms of the degrees of freedom only and do not (directly) depend on the basis functions, [2]. First, we prove the duality of these basis functions using the two examples from [1]. We prove the equivalence at discrete level between i) a pair of Dirichlet-Neumann problem in  $H(\text{div}, K)$ , and ii) a pair of Dirichlet-Neumann problem in  $H(\text{curl}, K)$ . We corroborate these proofs with numerical tests. Second, we demonstrate the application of these basis functions for two model constraint problems: i) scalar Laplacian, and ii) vector Laplacian. In both the applications we observe that the discretization of the constraint eq. is purely topological and is independent of grid shape and grid size. The corresponding matrix block consists of 1, -1 and 0 only, and is extremely sparse. Consequently, the condition number for the system is very low. The method is inf-sup stable. The error shows exponential convergence for both the applications. [1] C. Carstensen, L. Demkowicz, J. Gopalakrishnan, Breaking spaces and forms for the DPG method and applications including Maxwell equations, *Computers and Mathematics with Applications* 72 (2016) 494–522. [2] V. Jain, Y. Zhang, A. Palha and M. Gerritsma, Construction and application of algebraic dual polynomial representations for finite element methods, arXiv1712.09472, 2017.

## **Taking into Account Thermal Constraints in Topology Optimization of Structures Built by Additive Manufacturing**

Lukas Jakabcin\*, Grégoire Allaire\*\*

\*Ecole Polytechnique, France, \*\*Ecole Polytechnique, France

### **ABSTRACT**

In this talk, we introduce a model and several constraints for shape and topology optimization of structures, built by additive manufacturing techniques. The goal of these constraints is to take into account the thermal residual stresses or the thermal deformations, generated by processes like Selective Laser Melting, right from the beginning of the structural design optimization. In other words, the structure is optimized concurrently for its final use and for its behavior during the layer by layer production process. It is well known that metallic additive manufacturing generates very high temperatures and heat fluxes, which in turn yield thermal deformations that may prevent the coating of a new powder layer, or thermal residual stresses that may hinder the mechanical properties of the final design. Our proposed constraints are targeted to avoid these undesired effects. Shape derivatives are computed by an adjoint method and are incorporated into a level set numerical optimization algorithm. Several 2-d and 3-d numerical examples demonstrate the interest and effectiveness of our approach. References: G. Allaire, L. Jakabcin, Taking into account thermal residual stresses in topology optimization of structures built by additive manufacturing, submitted. HAL preprint: hal-01666081 (2017).

## **Space-Time Discretization for the Enhanced Velocity Mixed Finite Element Method: Applications to Modeling Fractures in Large Scale Reservoir Simulators**

Mohamad Jammoul<sup>\*</sup>, Benjamin Ganis<sup>\*\*</sup>, Gurpreet Singh<sup>\*\*\*</sup>, Ivan Yotov<sup>\*\*\*\*</sup>, Mary Wheeler<sup>\*\*\*\*\*</sup>, Sanghyun Lee<sup>\*\*\*\*\*</sup>

<sup>\*</sup>University of Texas at Austin, <sup>\*\*</sup>University of Texas at Austin, <sup>\*\*\*</sup>University of Texas at Austin, <sup>\*\*\*\*</sup>University of Pittsburgh, <sup>\*\*\*\*\*</sup>University of Texas at Austin, <sup>\*\*\*\*\*</sup>Florida State University

### **ABSTRACT**

Hydraulic fracturing is a widely used technology to stimulate tight and unconventional reservoirs and increase their ultimate recovery. Fractures are propagated in the rock matrix to create a fracture network and enhance the flow of hydrocarbons from the reservoir into the wellbore. The numerical simulation of hydraulic fracturing involves multiple multiphysics phenomena including: (1) fractures propagation, (2) fluid flow in the fractures and the reservoir, and (3) the accompanying mechanical deformations. Various computational models have been developed to simulate these coupled processes, yet many hydraulic fracture models focus on the near wellbore effects and fail to represent the holistic reservoir behavior. In this work, we develop a numerical framework to integrate non-planar fractures in large scale reservoir simulator (IPARS). The fracture permeability and geometry are obtained using the phase field fracture propagation method (IPACS). Fractures are then represented in the reservoir as small subdomains with high permeability coupled to the surrounding permeable formation. This configuration allows the simulation of the fluid flow in the reservoir and the fractures, yet restricts the time step. This means that fractured reservoir on the scale of kilometers would need to have its time steps governed by flow through fractures with apertures on the scale of millimeters. A space-time discretization is thus adopted, where the spatial domain is decomposed into overlapping or non-overlapping subdomains and a space-time variational formulation is employed. The flow in the reservoir is discretized using an Enhanced Velocity Mixed Finite Element Method. EVFEM adds additional velocity degrees of freedom on non-matching spatial and temporal interfaces to ensure the continuity of the flux. Numerical results are presented to show the impact of the induced fractures on the overall reservoir productivity.

## Numerical and Experimental Investigation on Fracture Characteristics of Multilayer Graphene

Bongkyun Jang<sup>\*</sup>, Byungwoon Kim<sup>\*\*</sup>, Jae-Hyun Kim<sup>\*\*\*</sup>, Hak-Joo Lee<sup>\*\*\*\*</sup>

<sup>\*</sup>Korea Institute of Machinery and Materials, <sup>\*\*</sup>Korea Institute of Machinery and Materials, <sup>\*\*\*</sup>Korea Institute of Machinery and Materials, <sup>\*\*\*\*</sup>Korea Institute of Machinery and Materials

### ABSTRACT

Graphene is 2-dimensional carbon layer with sp<sup>2</sup>-bondings like carbon nanotube and fullerene, and shows outstanding electrical, thermal, optical, and mechanical properties. Its excellent physical properties have been utilized for the various applications such as transparent conductor and, high-performance energy harvester and storage. Among them, extraordinary mechanical properties of graphene attract the attention to many fundamental researchers [1]. For fracture behavior of single crystalline and polycrystalline graphene, several experimental and analytical researches are performed, until now [2]. However, fracture mechanisms of multilayer graphene have not been fully studied, yet. In this study, we investigated fracture characteristics of multilayer graphene with experimental and numerical methods. For the fracture experiments, multilayer graphene specimens are fabricated by mechanical exfoliation from natural graphite and transferred onto tensile jigs, which can realize precise alignment and accurate application of loads to the specimens. In addition, narrow notches are fabricated with focused ion beam on the edges of the graphene specimens. Using these specimens, in situ fracture tests are performed under the scanning electron microscope. Load-displacement curves measured in the fracture experiments, and fracture load is obtained for each fracture specimen. Under the consideration of the shapes of the fracture specimens, we construct finite element models. By comparing the experimental results and the load-displacement curves calculated by finite element analyses, Young's modulus of multilayer graphene is estimated. In addition, the stress distribution near the crack tip of the specimen can be calculated by the analysis. At the failure load, singular stress fields near the crack tip imply the intensified stress at the crack propagation, and the fracture toughness can be derived from them. Based on the experiments and finite element analysis, the fracture toughness of multilayer graphene is enhanced compared to the monolayer. From in situ observation of the fracture surface, interlayer slippages occur near the crack tip and fracture surface at the fracture. To elucidate the fracture mechanisms of multilayer graphene, molecular dynamics simulation is performed on the multilayer graphene specimens with single edge crack. The numerical simulation helps to explain how the fracture of multilayer graphene occurs when a uniaxial load applied. The experimental and numerical research on fracture of multilayer graphene can contribute to developing graphene-based electronic devices, and enhance the reliability of them. References [1] Lee, C., Wei, X., Kysar, J. W. & Hone, J. Science 321, 385-388 (2008). [2] Jang, B., et al. Nanoscale 9, 17325 (2017)

## Topology Optimization for Three-dimensional Ultrasonic Acoustic Lens Design

Gang-Won Jang\*, Quang Dat Tran\*\*

\*Sejong University, Republic of Korea, \*\*Sejong University, Republic of Korea

### ABSTRACT

For topology optimization of acoustic problems, the use of the finite element method (FEM) is limited to low or mid frequency applications because of considerable computational efforts especially in three-dimensional problems. To resolve this, a new method for efficiently solving topology optimization of high-frequency ultrasonic acoustic problems is proposed by combining the edge-based smoothed finite element method (ES-FEM) [1] and the wave based method (WBM) [2]. The ES-FEM is formulated by incorporating the gradient smoothing techniques of mesh free methods into the FEM. The ES-FEM is very suitable for acoustic problems due to the proper softening effect provided by the edge-based gradient smoothing operation. Because a close-to-exact stiffness of the system can be obtained in the ES-FEM, the dispersion error can be effectively suppressed in high frequency problems. Meanwhile, the WBM can give very accurate solutions with small number of degrees of freedom when applied to problems with simple geometries because it employs exact solutions of the governing equation as field variables. Through the hybrid use of the ES-FEM and WBM, great efficiency in the reduction of computational effort for high-frequency acoustic problems can be expected while retaining high analysis accuracy. The primary objective of this study is to develop shape and topology optimization of high-frequency acoustic problems based on the combined use of the ES-FEM and WBM. In the present paper, the entire domain is separated into design and non-design domains; the ES-FEM is applied to the design domain while the WBM is applied to the non-design domain. The interface tracking phase field approach in [3] is employed to implicitly parameterize the boundaries of acoustic lenses, which move according to design sensitivities during optimization. The effectiveness of the proposed hybrid method of the ES-FEM and WBM is verified by solving three-dimensional acoustic topology optimization problems with high frequency range (0.5-1MHz). Keywords: Acoustic topology optimization, Phase field method, Edge-based smoothed finite element method, Wave based method, Ultrasonic acoustic waves  
References [1] Liu GR, Nguyen TT (2010) Smoothed Finite Element Methods, CRC Press, ISBN 978-1-4398-2027-8. [2] Desmet W (1998) A Wave Based Prediction Technique for Coupled Vibro-acoustic Analysis (Ph.D. thesis), KULeuven. [3] Takezawa A, Nishiwaki S, Kitamura M (2010) Shape and topology optimization based on the phase field method and sensitivity analysis. Journal of Computational Physics 229(7):2697-2718.

## Linear Smoothed eXtended Finite Element Method for Hyperelastic Materials

Chintan Jansari<sup>\*</sup>, Sundararajan Natarajan<sup>\*\*</sup>, Krishna Kannan<sup>\*\*\*</sup>

<sup>\*</sup>Indian Institute of Technology Madras, <sup>\*\*</sup>Indian Institute of Technology Madras, <sup>\*\*\*</sup>Indian Institute of Technology Madras

### ABSTRACT

In this talk, we propose the Linear Smoothed eXtended Finite Element Method for large deformation problems of hyperelasticity, with material interfaces in plane strain approximation. The eXtended Finite Element Method (XFEM) allows for the interior discontinuities to be represented independent of the underlying discretization. This is done by augmenting the conventional approximation space with suitable ansatz that carries the information of the local behaviour. However, this leads to difficulties in the numerical integration of the weak form and poor convergence properties due to the blending elements. The difficulty with the numerical integration is alleviated by employing the strain smoothing technique. And the stable XFEM is used to suppress the blending issues. Some numerical examples are solved and verified with the conventional FEM based on conforming mesh.

## Immersive Simulation at Extreme Scale

Kenneth Jansen<sup>\*</sup>, John Evans<sup>\*\*</sup>, Alireza Doostan<sup>\*\*\*</sup>, Kurt Maute<sup>\*\*\*\*</sup>, Felix Newberry<sup>\*\*\*\*\*</sup>, Corey Nelson<sup>\*\*\*\*\*</sup>

<sup>\*</sup>University of Colorado Boulder, <sup>\*\*</sup>University of Colorado Boulder, <sup>\*\*\*</sup>University of Colorado Boulder, <sup>\*\*\*\*</sup>University of Colorado Boulder, <sup>\*\*\*\*\*</sup>University of Colorado Boulder, <sup>\*\*\*\*\*</sup>University of Colorado Boulder, <sup>\*\*\*\*\*</sup>University of Colorado Boulder

### ABSTRACT

Parallel computing now delivers simulations in a time scale that could change the paradigm of how scientists, engineers, and other practitioners address discovery and design questions. Tools have been developed to precisely define a specific, complex simulation which can then be executed in seconds on computers. However, for discovery and design questions where the next variant of the problem requires change to the problem definition, the time to redefine the problem takes much longer. This delay interrupts intuition and learning about how the change in problem definition relates to a change in solution. To realize this innovative paradigm shift, referred to here as immersive simulation, requires the development of new approaches to problem definition editing that allow practitioners to interact with the simulations (visual model iteration) in a manner where they can dynamically experience (via in situ visualization that employs massive data reduction) the influence of parameter variations. In this talk we will describe our research efforts to advance state of the art tools into more generic components that, when integrated, will make the following capabilities available to any partial differential equation (PDE) solver: i) live, reconfigurable visualization of ongoing simulations, ii) live, reconfigurable problem definition to allow the dynamic solution insight to guide the choice of key problem parameters, iii) real-time parameter sensitivity feedback, iv) error estimation and adaptivity, and v) integration and demonstration of reliable, immersive simulation. This research will not only drive several of its science components in innovative and new directions, but, once integrated, will provide the field of simulation (and the science community that has developed an increasing dependence on it) with the ability to intuitively explore the behavior of the system. Furthermore, this research will allow interactively redefining the geometry, boundary conditions, and other parameters, to experience the science, and thereby greatly accelerate discovery and innovation.

## Time-resolved Adaptive Direct FEM Simulation Prediction of Flow Separation

Johan Jansson\*

\*KTH Royal Institute of Technology

### ABSTRACT

We present an adaptive finite element method for time-resolved simulation of aerodynamics without any turbulence model parameters, which is applied to a benchmark problem from the HiLiftPW-3 workshop to compute the flow past a JAXA Standard Model (JSM) aircraft model at realistic Reynolds number. The mesh is automatically constructed by the method as part of an adaptive algorithm based on a posteriori error estimation using adjoint techniques. No explicit turbulence model is used, and the effect of unresolved turbulent boundary layers is modeled by a simple parametrization of the wall shear stress in terms of a skin friction. In the case of very high Reynolds numbers we approximate the small skin friction by zero skin friction, corresponding to a free slip boundary condition, which results in a computational model without any model parameter to be tuned, and without the need for costly boundary layer resolution. We introduce a numerical tripping noise term to act as a seed for growth of perturbations, the results support that this triggers the correct physical separation at stall, and has no significant effect pre-stall. We show that the methodology quantitatively and qualitatively captures the main features of the JSM experiment - aerodynamic forces and the stall mechanism - with a much coarser mesh resolution and lower computational cost than the state of the art methods in the field, with convergence under mesh refinement by the adaptive method. Thus, the simulation methodology appears to be a possible answer to the challenge of reliably predicting turbulent-separated flows, for a complete air vehicle. We also present recent comparison against leading high-order frameworks in connection to the 5th International Workshop on High Order CFD Methods, showing that adaptivity and large timesteps enables high computational efficiency. The methodology is further extended to fluid-structure interaction with an embedded discontinuity in the phase interface by doubling the solution field, and we show a snapshot of the development. [1] J. Hoffman, J. Jansson, N. Jansson, R. V. de Abreu, and C. Johnson. Computability and Adaptivity in CFD. Encyclopedia of Computational Mechanics (Ed. E. Stein, R. de Borst and T.J.R. Hughes), John Wiley and Sons, (2017). [2] J. Jansson, E. Krishnasamy, M. Leoni, N. Jansson, and J. Hoffman. Time-resolved adaptive direct fem simulation of high-lift aircraft configurations. Springer Brief: Numerical simulation of the aerodynamics of high-lift configurations, 2017.

## **A Mixed Variational Framework for Structure-preserving Space-time Discretization for Non-linear Electro-elastodynamics**

Alexander Janz<sup>\*</sup>, Peter Betsch<sup>\*\*</sup>, Marlon Franke<sup>\*\*\*</sup>, Rogelio Ortigosa<sup>\*\*\*\*</sup>

<sup>\*</sup>Institute of Mechanics, Karlsruhe Institute of Technology (KIT), Germany, <sup>\*\*</sup>Institute of Mechanics, Karlsruhe Institute of Technology (KIT), Germany, <sup>\*\*\*</sup>Institute of Mechanics, Karlsruhe Institute of Technology (KIT), Germany, <sup>\*\*\*\*</sup>Zienkiewicz Centre for Computational Engineering, Swansea University, Wales

### **ABSTRACT**

The present talk deals with a new approach to the design of energy and momentum (EM) consistent integration schemes in the field of non-linear electro-elastodynamics, see Ortigosa, Franke, Janz, Gil and Betsch (submitted in *Comput. Methods Appl. Mech. Engrg.*, 2017). The importance of electro-active polymers (EAPs) in different applications such as actors and sensors, soft robotics or artificial muscles requires advanced simulation techniques to prognosticate the behavior of such smart materials. Typically, these materials are described as electro-static but nevertheless the consistent time-integration of the electro-mechanical model plays an important role concerning the numerical stability and accuracy. In this talk we present a new approach to the design of energy-momentum consistent algorithms motivated by the structure of polyconvex stored energy functions and tailor-made for the consistent space-time discretization of EAPs. The presented time-integrator is based on the internal energy of the system, which is in accordance with the concept of polyconvexity for nonlinear electro-mechanics, see Gil and Ortigosa (*Comput. Methods Appl. Mech. Engrg.*, 302: 293-328, 2016). Based on a Hu-Washizu-type mixed variational framework with a novel cascade form of kinematic constraints a new algorithmic stress formula is proposed, see Betsch, Janz and Hesch (accepted in *Comput. Methods Appl. Mech. Engrg.*, 2017), which is a typical feature of energy-momentum methods. Furthermore, a tensor-cross product operator for second order tensors is used, which greatly simplifies the algebraic formulation. In addition, the time-discrete weak form of the Gauss's law and Faraday's law along with the concept of partitioned discrete derivatives leads to an implicit one-step time integrator which consistently approximates the linear momentum, the angular momentum as well as the total energy. The resulting structure-preserving integrator shows superior numerical stability and robustness compared to alternative formulations. Moreover, the mixed variational framework makes possible a wide variety of alternative finite element formulations. Along with an appropriate combination of the interpolation spaces high performance finite elements can be generated. Several numerical examples dealing with large strains and electric fields are shown. These examples demonstrate the advantageous properties of the newly developed structure-preserving discretization scheme.

## **A Reliability Based Design Optimization Method for MASH TL-3 Concrete Barriers under Vehicle Crashes**

Erica Jarosch<sup>\*</sup>, Qian Wang<sup>\*\*</sup>, Hongbing Fang<sup>\*\*\*</sup>, Hangfeng Yin<sup>\*\*\*\*</sup>

<sup>\*</sup>Manhattan College, <sup>\*\*</sup>Manhattan College, <sup>\*\*\*</sup>The University of North Carolina at Charlotte, <sup>\*\*\*\*</sup>Hunan University

### **ABSTRACT**

Concrete barriers are commonly adopted on state highways to redirect impacting vehicles and reduce occupant injury risks. Due to the rigidity of a concrete barrier compared to other types of traffic barriers, its performance primarily depends on its cross-sectional shape. Besides physical crash tests, numerical simulations based on high-fidelity finite element (FE) analyses can be conducted to assess the performance of traffic barriers. This research work focused on the development of a reliability based design optimization (RBDO) method for concrete barriers subjected to vehicle impacts. The concrete barriers met the test level-3 (TL-3) requirements specified in the Manual for Assessing Safety Hardware (MASH). The proposed design optimization method started with nonlinear FE simulations at certain sample points so that crash responses could be used to evaluate barrier performance. A successive metamodeling technique developed using augmented radial basis functions (RBFs) was applied to create approximate functions of implicit crash responses. Once the RBF metamodels were created to approximate crash simulation results, the design constraints that included reliability calculations were evaluated using any sampling method such as Monte Carlo simulations (MCS). Finally, a genetic algorithm (GA) was adopted to optimize the objective function subjected to all the design constraints. The RBDO method integrated FE simulations, metamodels, MCS, and GA, and provided a useful tool for the design of roadside barriers. A concrete barrier example was solved and numerical results were presented to demonstrate the effectiveness of the design optimization method.

## **Error Estimation in Discontinuous Galerkin Method with Polygonal Finite Elements**

Jan Jaskowiec\*

\*Cracow University of Technology, Institute for Computational Civil Engineering, Poland

### **ABSTRACT**

In the paper three methods for error estimation in the two-dimensional (2D) discontinuous Galerkin method (DGM) are presented. The applied DGM version uses arbitrary polygonal finite elements [1,2]. The Chebyshev basis functions are used for approximation. They are constructed recursively which makes the method very efficient and flexible. It is then quite easy to calculate higher order derivatives of the basis functions on the polygonal finite elements. In the first error estimation method, the residual error from the strong form can be obtained directly from the approximate solution. The residual error is discontinuous, so the Zienkiewicz-Zhu smoothing procedure is employed for the continuous error distribution. In the DGM the recursive basis functions are utilized. In this case, it is very easy to obtain a low order solution of the considered problem in a situation when the higher order solution is already calculated. It is because the stiffness matrix has hierarchical construction, and so the lower order stiffness matrix is just a part of the primary stiffness matrix. In the second method, the error is estimated by comparison of two approximate solutions. The two solutions are of different orders and the lower-order solution is calculated with marginal cost. In the third method, a special boundary value problem (PVB) is constructed to estimate the error. The error PVB is obtained and solved with low computational costs due to some special properties of the DGM utilized in this method. The quality of the error estimation is very high in the last method. The paper is illustrated with two-dimensional benchmark examples where the standard scalar Poisson's boundary value problems are considered. In the examples the correctness and flexibility of the proposed error estimation methods are shown. The two-dimensional examples of linear elasticity are also presented, in which the errors are estimated in situations when stress concentrations occur in the final solution. [1] E. B. Chin, J. B. Lasserre, and N. Sukumar (2015) Numerical integration of homogeneous functions on convex and nonconvex polygons and polyhedra. *Computational Mechanics*, 56(6):967–981 [2] J. Jaskowiec, P. Plucinski and A. Stankiewicz (2016) Discontinuous Galerkin method with arbitrary polygonal finite elements *Finite Elements in Analysis and Design* 120:1–17

## Higher Order Multipoint Meshless FDM for Two-scale Analysis of Heterogeneous Materials

Irena Jaworska\*

\*Cracow University of Technology

### ABSTRACT

The paper focuses on application of the Multipoint solution approach – the higher order extension of the Meshless Finite Difference Method (MFDM) to the numerical homogenization of the heterogeneous material with periodic structure. The Finite Element Method (FEM) has been the most commonly applied method of computer modeling for the multiscale problem. However, this fact does not mean that one should not search for the alternative, perhaps more efficient approaches, especially based on the meshless technique which uses only a set of nodes for discretization of the continuum and therefore leads to greater flexibility. Recently developed Multipoint meshless method is discussed here for this purpose. The higher order Multipoint approach is followed the original Collatz [1] concept and the essential idea of the MFDM [2] – the moving weighted least squares approximation, using the arbitrarily irregular cloud of nodes as well as various formulations of b.v. problem. The higher order approximation, applied in the Multipoint method, is based on the additional degrees of freedom at all stencil nodes, taking into account e.g. the right hand side of considered differential equation. It improves obtained solution without necessity of providing additional unknowns to both – the mesh and the MFD operator, and also may be used e.g. for high quality a posteriori error estimation of the results. The higher order Multipoint meshless method, like the MFDM solution approach [3], may be used at both – the macro and the micro levels in the two-scale analysis of heterogeneous materials based on the single RVE. The analysis of the convergence results of the effective material parameters for the set of meshes with increasing number of nodes as well as comparison with FEM was conducted. The error analysis done at the micro level confirm the high quality of the Multipoint solution, which may be used as the improved reference solution instead of the true analytical one for the a posteriori error estimation. Further research is planned.

1. L. Collatz, *Numerische Behandlung von Differential-gleichungen*, Springer-Verlag, Berlin, 1955.
2. J. Orkisz, *Finite Difference Method (Part III)*, in *Handbook of Computational Solid Mechanics*, ed. M. Kleiber, Springer-Verlag, Berlin, 336–431, 1998.
3. I. Jaworska, *On some aspects of the meshless FDM application for the heterogeneous materials*, *International Journal for Multiscale Computational Engineering*, 15(4):359–378, 2017.

# MACROSCOPIC INELASTIC BEHAVIORS SIMULATED BY A STOCHASTIC MULTI-SCALE NUMERICAL MODEL FOR HETEROGENEOUS MATERIALS

PIERRE JEHEL

Laboratory MSSMat-UMR 8579 (CentraleSupélec/CNRS)  
Université Paris-Saclay, CentraleSupélec, 3 rue Joliot-Curie, 91190 Gif-sur-Yvette, France  
E-mail: pierre.jehel[at]centralesupelec.fr

**Key words:** Random heterogenous material; Inelastic cyclic behavior; Uncertainty quantification; Global sensitivity analysis; Variance decomposition.

**Abstract.** *The uncertainty and the sensitivity of the response of a nonlinear stochastic multi-scale numerical model for randomly heterogenous material is investigated. 9 input parameters and 10 descriptors of the time-dependent output response are considered. The material model has been presented elsewhere and is introduced as a 'black box function' in the present paper, parameterized so that the model is deterministic and that variability in the outputs only comes from the variability introduced in the inputs. The objective is twofolds: (i) surveying the variety of macroscopic behaviors the material model considered is capable of representing, and (ii) assessing the relative importance of the model inputs in the model outputs to, for instance, define efficient parameters identification protocols. A preliminary analysis of the linear dependency between the output descriptors is presented and a reduced set of 6 descriptors is eventually selected. Then, the influence of the model input parameters on each of these model response descriptors is investigated using a global sensitivity analysis technique based on the functional decomposition of their respective total variance.*

## 1 INTRODUCTION

The mechanical behavior of a wide range of natural or manufactured materials is characterized by macroscopic engineering parameters that depend on phenomena at heterogeneous smaller scales (concrete, nano-engineered materials [12]). On the one hand, experimental devices and techniques allow characterizing the spatial distribution of material properties at micro-scales as for instance the combination of atomic force microscope imaging and quantitative nanomechanical property mapping techniques employed in [14] for a study of Young's modulus distribution in the so-called interfacial transition zone in concrete material. On the other hand, computational material models allow carrying out numerical experiments that have the potential of investigating the material behavior in a range of configurations that can be difficult to reach with sole experimental investigation. There is therefore a need for developing such numerical material models that can simulate engineering properties at macro-scale from relevant

information coming from lower scales. This has been a topic of continuing research in the field of computational mechanics for decades.

The development of the inelastic stochastic multi-scale numerical model investigated in the present work (see [5] and [6]) was initially motivated by the need for a concrete model that is capable of representing the contribution of material damping to the overall structural damping in the seismic analysis of civil engineering assets. In earthquake engineering, structural damping is indeed commonly introduced in numerical simulations using ad hoc damping models such as the pervasive so-called Rayleigh damping model. Unfortunately, as nonlinear structural analysis is performed, resorting to such ad hoc approach potentially results in large uncertainties when assessing structural seismic performance.

This concrete model [5, 6] is based on a meso-scale where the heterogeneous structure is represented by random vector fields. Local behavior at meso-scale is nonlinear and can be seen as the homogenized response of other mechanisms at lower scales when explicit construction of smaller scales is not possible. The model is constructed with a set of parameters that describes the structure of the random vector fields (correlation coefficients, correlation lengths and functions); a set of parameters that characterizes the mean, variance and distribution of physical parameters at meso-scale (initial stiffness, yield stress and stiffness degradation ratio); and a set of parameters for spatial discretization of the material domain (finite element method) and of the random fields (spectral representation method [11]). A representative volume element (RVE) can be retrieved with the ability to represent salient features of the concrete uniaxial cyclic compressive response that are not explicitly represented at meso-scale, like for instance the hysteresis loops experimentally observed in unloading-reloading cycles.

The objective of this paper is twofolds: (i) surveying the variety of macroscopic behaviors this numerical inelastic stochastic multi-scale material model is capable of representing, and (ii) assessing the relative importance of the model inputs in the model outputs to, for instance, define efficient parameters identification protocols. Next section is focussed on introducing the model input parameters. Then, a probabilistic framework is set in section 3 for uncertainty and global sensitivity analysis. In section 4, the results of an application are presented and, finally, a list of conclusions closes the paper.

## 2 THE MATERIAL MODEL AND ITS INPUT PARAMETERS

The material model used in this paper has been developed to represent the restoring force  $f(t)$  of a 1D nonlinear material in a given cyclic quasi-static loading displacement time history  $u(t)$  where  $t$  is the pseudo-time (Fig. 1). This material model is referred to as  $\mathcal{M}$ , it takes  $t$  along with a set of parameters  $\mathbf{x}$  as inputs, and yields the restoring force history  $f(t)$  as output.

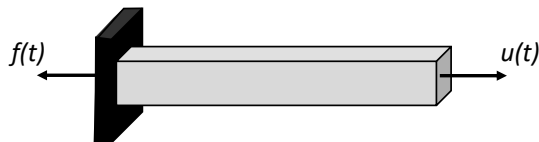


Figure 1: The experiment: bar with quasi-static displacement  $u(t)$  imposed at one end, with other end fixed where reaction  $f(t)$  develops; it is assumed that the experiment is such that the strain field is homogeneous in the bar.

The material model  $\mathcal{M}$  that is used in this work has been presented in [5, 6]. Therefore, we only introduce here its main characteristics along with the list of input parameters that will be used for uncertainty and sensitivity analyses hereafter. Also, for the sake of illustrating, we

consider that the modeled material is concrete; but any other random heterogeneous material described by 3 scales as introduced in Tab. 1 and Fig. 2 could fit this setting.

Scale	Observations	Modeling assumptions
Micro	Physical and chemical mechanisms occur	Internal variables are considered in the framework of continuum thermodynamics [1, 8] to convey information from this scale to the meso-scale (see Fig. 3).
Meso	Aggregates and the cement paste are observable and build an heterogeneous material structure	The heterogeneity at this scale is represented using random fields rather than an explicit representation of the structure.
Macro	Homogeneous quantities are retrieved for engineering purposes	Classical homogenization technique in the framework of the Finite Element Method is used [9, 10].

Table 1: The 3 scales introduced in the model  $\mathcal{M}$ . Concrete material is considered here as an illustrating example.

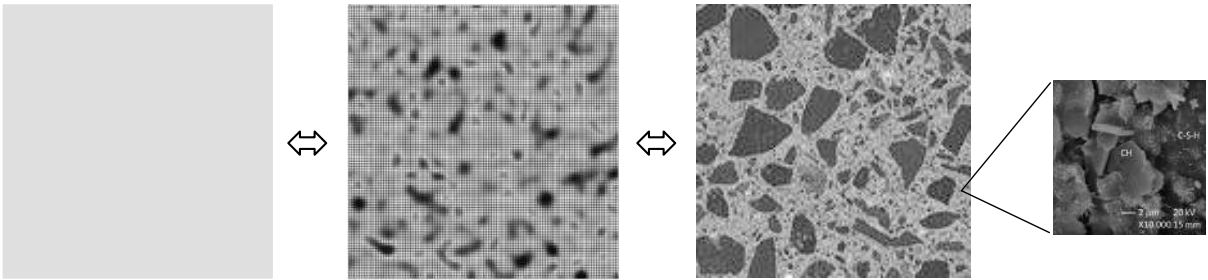


Figure 2: From left to right: [a] equivalent homogeneous concrete (macro-scale), [b] representation of the heterogeneous concrete at meso-scale ( $5 \text{ cm} \times 5 \text{ cm}$ -square), [c] actual heterogeneous concrete ( $5 \text{ cm} \times 5 \text{ cm}$ -square), and [d] zoom on the underlying microstructure in the cement paste ( $20 \mu\text{m} \times 20 \mu\text{m}$ -square observed through Scanning Electron Microscope, courtesy A.P.M. Trigo [13]).

The model uses stochastic fields to represent spatial variations – that is random heterogeneity – in the material properties at meso-scale. The actual meso-scale shown in Fig. 2[c] is replaced by random vector fields as shown in Fig. 2[b]. In the particular case of a 1D material behavior, which this work is limited to, three parameters are represented as spatially variable as illustrated in Fig. 3: the initial stiffness  $C(\mathbf{p}, \omega)$  (or Young’s modulus at meso-scale), the yield stress  $\sigma_y(\mathbf{p}, \omega)$ , and the stiffness degradation ratio  $r(\mathbf{p}, \omega) \in [0, 1]$ , where  $\mathbf{p}$  is a position in the material and  $\omega$  recalls the randomness in the quantity. The three quantities are correlated and the same correlation coefficient  $\rho$  is considered for any pair of parameters. The parameters  $\mathbf{x}$  of model  $\mathcal{M}$  are listed in Tab. 2.

The model  $\mathcal{M}$  can be stochastic: same input parameters  $\mathbf{x}$  and imposed displacement history  $u(t)$  can yield different outputs. Nevertheless, it has been shown in [5, 6] that the model can also be deterministic: same input parameters  $\mathbf{x}$  and loading history  $u(t)$  would yield same output. In other words, it is possible to parameter the model in such a way that a material Representative Volume Element (RVE) is simulated. This can be achieved using particular set of spatial parameters ( $N = 16$ ,  $M = 32$ ,  $M_f = 96$ ,  $L_0/\ell = 0.1$ ,  $\epsilon_R = 0.01$  using the same notations as in [5]). This parameterization is used in this paper so that uncertainty observed in the output parameters  $\mathbf{y}$  would only come from uncertain input parameters  $\mathbf{x}$ .

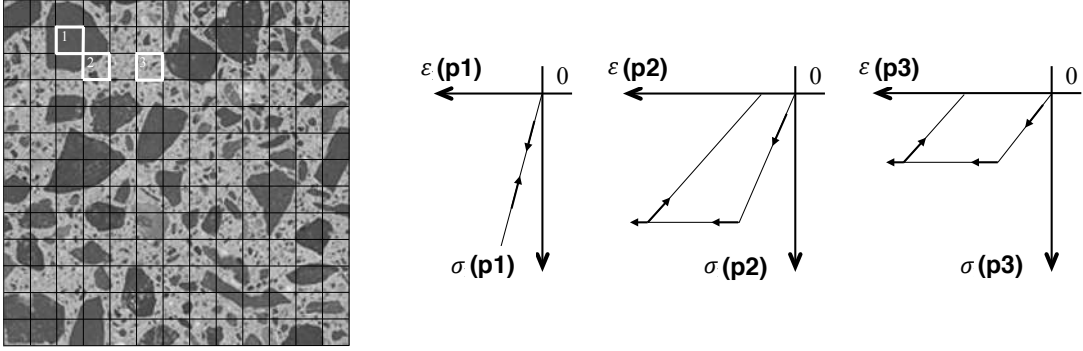


Figure 3: Behavior law at meso-scale depends on the position  $\mathbf{p}$  in the heterogeneous material. Initial stiffness, yield stress, and stiffness degradation ratio at any point  $\mathbf{p}$  are modeled as random variables.

$\mathbf{x}$	Description
$x_1 = law_C$	Initial stiffness $C$ distribution (log-normal or uniform)
$x_2 = a_C$	Mean of $law_C$
$x_3 = b_C$	Variance of $law_C$
$x_4 = law_{\sigma_y}$	Yield stress $\sigma_y$ distribution (log-normal or uniform)
$x_5 = a_{\sigma_y}$	Mean of $law_{\sigma_y}$
$x_6 = b_{\sigma_y}$	Variance of $law_{\sigma_y}$
$x_7 = a_r$	Mean of the stiffness degradation ratio uniform distribution $law_r$
$x_8 = b_r$	Variance of $law_r$
$x_9 = \rho$	Correlation coefficient between $(C$ and $\sigma_y)$ , $(C$ and $r)$ , or $(\sigma_y$ and $r)$

Table 2: List of the  $N^x = 9$  model input parameters  $x_j, j = 1 \dots N^x$  considered in this work.

### 3 UNCERTAINTY AND SENSITIVITY ANALYSES OF THE MODEL OUTPUT

Let introduce the probability space  $(\Theta, \mathcal{S}, P)$  with sample space  $\Theta$ , collection of events  $\mathcal{S}$ , and probability measure  $P$ . To introduce a certain degree of belief in the set  $\mathbf{x}$  of the model input parameters, we consider them as random variables  $\mathbf{X} : \theta \in \Theta \mapsto \mathbf{X}(\theta)$ . Consequently, the model output  $f(t)$  also is a random variable  $F(t) : \theta \mapsto F(t, \theta)$  for all  $t \in [0, T]$  and we have the deterministic model  $\mathcal{M}$  that is the mapping

$$\mathcal{M} : (\theta, t) \mapsto F(t) = \mathcal{M}(\mathbf{X}, t) \quad (1)$$

#### 3.1 Uncertainty analysis

The uncertainty in the model output can be analyzed computing quantities such as the mean, variance, and cumulated density function for all  $t \in [0, T]$ :

$$E[F(t)] = \int_{\Theta} \mathcal{M}(\mathbf{X}(\theta), t) dP(\theta) \quad (2)$$

$$V[F(t)] = \int_{\Theta} (E[F(t)] - \mathcal{M}(\mathbf{X}(\theta), t))^2 dP(\theta) \quad (3)$$

$$\Pr[F(t) \leq f(t)] = \int_{\Theta} \delta_{f(t)}[\mathcal{M}(\mathbf{X}(\theta), t)] dP(\theta) \quad \text{with} \quad \delta_{f(t)}[\cdot] = \begin{cases} 1 & \text{if } \cdot \leq f(t) \\ 0 & \text{if } \cdot > f(t) \end{cases} \quad (4)$$

This requires computing integrals over the sample space  $\Theta$ . To this purpose, Monte Carlo simulations are performed from a Latin hypercube sample (LHS) of size  $N^s$ . LHS is adopted here for its efficiency compared to random sampling [3, 7] with the  $N^x$  input random variables in  $\mathbf{X}$  assumed as mutually independent.

### 3.2 Sensitivity analysis

For the analysis of the sensitivity of the model output to the inputs, the approach adopted in this work is based on a functional decomposition of the variance (see e.g. [4]),  $\forall t \in [0, T]$ , as:

$$V[F(t)] = \sum_{j=1}^{N^x} D_j[F(t)] + \sum_{1 \leq j < k \leq N^x} D_{jk}[F(t)] + \dots + D_{12\dots N^x}[F(t)] \quad (5)$$

where  $D_j[F(t)] = V[E[F(t)|X_j]]$ ,  $D_{jk}[F(t)] = V[E[F(t)|X_j, X_k]] - D_j[F(t)] - D_k[F(t)]$  and so on. Then, the following first-order and total indices are computed from  $(N^x + 2) \times N^s$  computations of the model response as:

$$s_j = \frac{D_j[F(t)]}{V[F(t)]} \quad (6)$$

$$s_{jT} = s_j + \frac{\sum_{k=1, k \neq j}^{N^x} D_{jk} + \sum_{1 \leq k \neq j < l \neq j}^{N^x} D_{jkl} + \dots + D_{12\dots N^x}}{V[F(t)]} \quad (7)$$

where  $s_j$ , respectively  $s_{jT}$ , is the portion of  $V[F(t)]$  due to input  $x_j$  alone, respectively to  $x_j$  and all the interactions of  $x_j$  with the other input variables.

## 4 APPLICATION

### 4.1 Uncertainty in the model input parameters

The distributions selected for the uncertain input parameters are introduced in Tab. 3.

$\mathbf{X}(\theta)$	Distribution: <i>law(mean, variance)</i>	
$X_1 = LAW_C$	$\mathcal{B}_{0.5}$ : either $\mathcal{U}(a_C, b_C)$ or $\mathcal{L}(a_C, b_C)$	with probability 0.5 each
$X_2 = A_C$ [MPa]	$\mathcal{U}(\tilde{a}_C = 30e3, 0.04 \tilde{a}_C^2)$	such that $C \geq 0$
$X_3 = B_C$ [MPa <sup>2</sup> ]	$\mathcal{U}(\tilde{b}_C = 15e3, 0.04 \tilde{b}_C^2)$	such that $C \geq 0$
$X_4 = LAW_{\sigma_y}$	$\mathcal{B}_{0.5}$ : either $\mathcal{U}(a_{\sigma_y}, b_{\sigma_y})$ or $\mathcal{L}(a_{\sigma_y}, b_{\sigma_y})$	with probability 0.5 each
$X_5 = A_{\sigma_y}$ [MPa]	$\mathcal{U}(\tilde{a}_{\sigma_y} = 35, 0.04 \tilde{a}_{\sigma_y}^2)$	such that $\sigma_y \geq 0$
$X_6 = B_{\sigma_y}$ [MPa <sup>2</sup> ]	$\mathcal{U}(\tilde{b}_{\sigma_y} = 20, 0.04 \tilde{b}_{\sigma_y}^2)$	such that $\sigma_y \geq 0$
$X_7 = A_r$	$\mathcal{U}(\tilde{a}_r = 0.5, 0.04 \tilde{a}_r^2)$	such that $r \in [0, 1]$
$X_8 = B_r$	$\mathcal{U}(\tilde{b}_r = 0.02, 0.04 \tilde{b}_r^2)$	such that $r \in [0, 1]$
$X_9 = Rho$	$\mathcal{U}(0.5, 1/12)$	(support is $[0, 1]$ )

Table 3: Random variables and there distributions characterized by their mean and variance.  $\mathcal{B}$ ,  $\mathcal{U}$ , and  $\mathcal{L}$  are Bernoulli, uniform, and log-normal distributions. How to find the support of a uniform distribution from its mean and variance is shown in the Annex. Quantities with superimposed tilde  $\tilde{\cdot}$  are some nominal mean values; a coefficient of variation of 20% is considered to calculate the variance associated to these nominal mean values.

## 4.2 Model response descriptors

We start by simulating the material response in one symmetric loading cycle with macroscopic strain amplitude  $E = 3.5e^{-3}$ .  $N^s = 500$  simulations are run and model responses are plot in Fig. 4. From the observation of this figure we choose a series of  $N^y$  model response descriptors as introduced in Fig. 5, gathered in vector  $y$ . Then, we seek possible linear dependencies – other types of dependencies could of course be sought too – and build Fig. 6. From Fig. 6, it is observed that model response after point D is strongly correlated to model response between points O and D. Accordingly, only the following  $N^y = 6$  model response descriptors will be considered thereafter:  $y_1 = C_O$ ,  $y_2 = C_B$ ,  $y_3 = \Sigma_A$ ,  $y_4 = \Sigma_B$ ,  $y_5 = \Sigma_D$ , and  $y_6 = E_C$ .

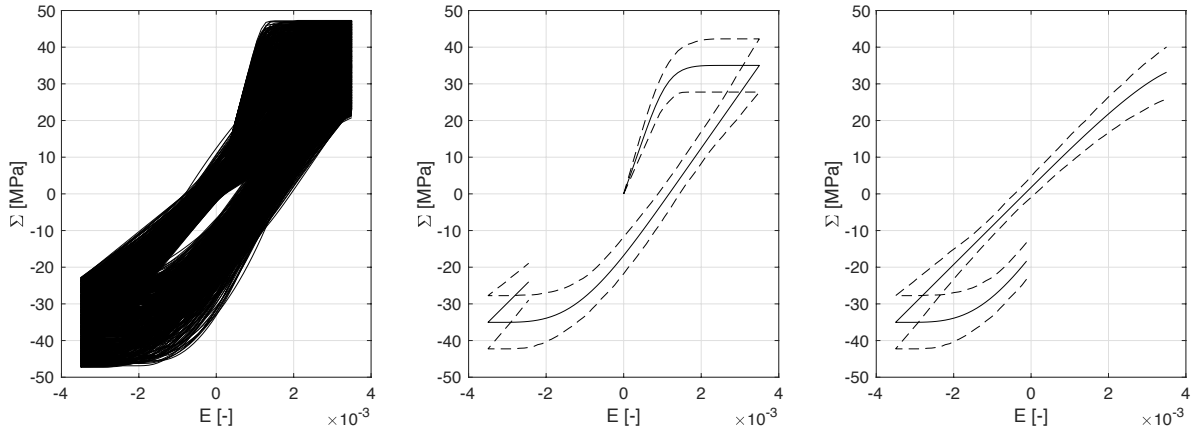


Figure 4: [left]  $N^s = 500$  model response curves. [middle] and [left] Sample mean along with the 10% and 90% percentiles (dashed line); response curves are split into two parts for better readability.

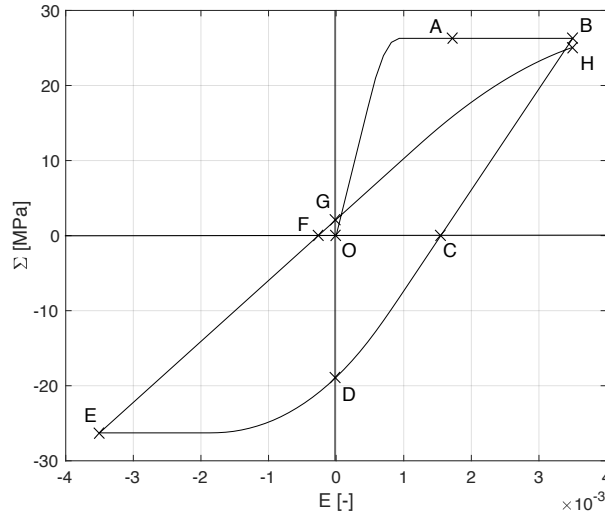


Figure 5: Model response descriptors: initial tangent modulus  $C_O$  and unloading tangent modulus at point B  $C_B$ ; stresses  $\Sigma_A$  ( $E = 1.75e^{-3}$ ),  $\Sigma_B$ ,  $\Sigma_D$ ,  $\Sigma_E$ ,  $\Sigma_G$ , and  $\Sigma_H$ ; strains  $E_C$  and  $E_F$ .

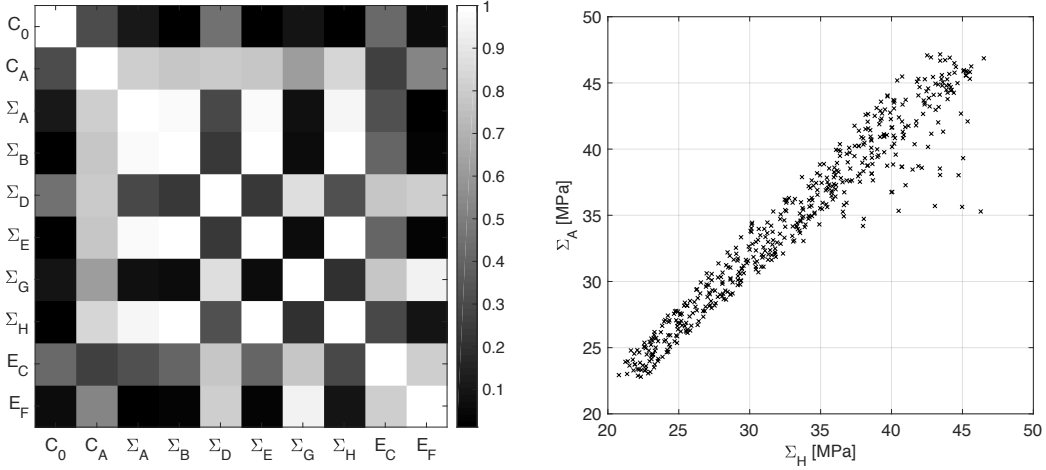


Figure 6: [left] Absolute value of the sample Pearson correlation coefficients between model response descriptors  $y_k$ ,  $k = 1 \dots N^y$ ; [right] scatterplot of  $\Sigma_A$  versus  $\Sigma_H$  showing strong linear correlation.

### 4.3 Uncertainty and sensitivity estimators

To estimate global sensitivity of the model outputs  $\mathbf{y}$  to the inputs  $\mathbf{x}$ , the method detailed in [2] (Sect. 6.13) has been implemented. Accordingly:

1. A first LHS  $[x_{ij}]$ ,  $i \in [0, N^s]$  and  $j \in [0, N^x]$ , is generated and the model response  $\mathbf{y}_i(t) = \mathcal{M}(\mathbf{x}_i, t)$  is computed for each set of input parameters  $\mathbf{x}_i = [x_{i1} \dots x_{iN^x}]$ . From these quantities, estimators of the mean and variance in Eqs. (2) and (3) are computed  $\forall k \in [1 \dots N^y]$  as:

$$\hat{E}[Y_k] = \frac{1}{N^s} \sum_{i=1}^{N^s} y_{k,i}(t) \quad ; \quad \hat{V}[Y_k] = (\hat{\sigma}[Y_k])^2 = \frac{1}{N^s} \sum_{i=1}^{N^s} (\hat{E}[Y_k] - y_{k,i}(t))^2 \quad (8)$$

2. Another sample  $[\bar{x}_{I,j}] = [p(\mathbf{x}_1) \dots p(\mathbf{x}_{N^s})]$ ,  $I \in [0, N^s]$ , is built, where  $p(\mathbf{x}_j)$  is a random permutation without replacement of the  $N^s$  elements of the  $j$ -th column of  $[x_{ij}]$ . The model response  $\bar{\mathbf{y}}_I(t) = \mathcal{M}(\bar{\mathbf{x}}_I, t)$  is computed for each  $\bar{\mathbf{x}}_I = [\bar{x}_{I1} \dots \bar{x}_{IN^x}]$ . Then,  $N^x$  samples of  $N^s$  model responses are obtained by reordering the computed  $\bar{\mathbf{y}}_I(t)$ 's as follows:  $\bar{\mathbf{y}}_i^{(j)}(t) = \mathcal{M}([\bar{x}_{I1} \dots \bar{x}_{Ij} = x_{ij} \dots \bar{x}_{IN^x}], t)$ ,  $j \in [0, N^x]$ .
3. A last LHS  $[\check{x}_{ij}]$ ,  $i \in [0, N^s]$  and  $j \in [0, N^x]$ , is generated and  $N^x$  samples of  $N^s$  model responses are computed as  $\bar{\mathbf{y}}_i^{(j)} = \mathcal{M}(\bar{\mathbf{x}}_i^{(j)}, t)$ ,  $\bar{\mathbf{x}}_i^{(j)} = [\bar{x}_{i1}^{(j)} \dots \bar{x}_{iN^x}^{(j)}]$ , with  $\bar{x}_{iJ}^{(j)} = x_{iJ}$  for  $J \in [0, N^x]$  except for  $J = j$  where  $\bar{x}_{iJ}^{(j)} = \check{x}_{ij}$ .

Estimators for the sensitivity indices are then computed,  $\forall k \in [1 \dots N^y]$ , as:

$$\hat{s}_{k,j} = \frac{1}{\hat{V}[Y_k]} \left( \frac{1}{N^s} \sum_{i=1}^{N^s} y_{k,i}(t) \times \bar{y}_{k,i}^{(j)}(t) - \hat{E}[Y_k]^2 \right) \quad (9)$$

$$\hat{s}_{k,jT} = \frac{1}{N^s \times \hat{V}[Y_k]} \sum_{i=1}^{N^s} y_{k,i} \left( y_{k,i} - \bar{y}_{k,i}^{(j)} \right) \quad (10)$$

Altogether, the model has to be run  $(2 + N^x) \times N^s$  times. In the present work,  $N^x = 9$ ,  $N^s = 300, 400$ , or  $1,000$ , and computing one model response takes less than 2 seconds. The calculated estimations are shown in Tab. 4.

	$N^s$	$y_1 = C_0$	$y_2 = C_B$	$y_3 = \Sigma_A$	$y_4 = \Sigma_B$	$y_5 = \Sigma_D$	$y_6 = E_C$
$\hat{E}[Y_k]$	300	29,998 MPa	15,034 MPa	34.470 MPa	35.034 MPa	-16.801 MPa	1.156e-3
	600	29,997 MPa	15,040 MPa	34.441 MPa	35.035 MPa	-16.776 MPa	1.155e-3
	1,000	29,997 MPa	15,008 MPa	34.344 MPa	35.030 MPa	-16.700 MPa	1.152e-3
$\hat{\sigma}[Y_k]$	300	6,001 MPa	2,822 MPa	6.565 MPa	7.007 MPa	5.509 MPa	3.06e-4
	600	6,000 MPa	2,848 MPa	6.507 MPa	7.000 MPa	5.561 MPa	3.09e-4
	1,000	6,000 MPa	2,835 MPa	6.413 MPa	7.006 MPa	5.494 MPa	3.04e-4
$\hat{s}_1 (x_1 = law_C)$	300	0.012	0.058	0.112	0.056	-0.012	0.058
	600	-0.074	-0.021	-0.003	-0.029	-0.050	-0.068
	1,000	0.003	-0.006	0.119	-0.011	0.046	0.075
$\hat{s}_2 (x_2 = a_C)$	300	<b>1.000</b>	0.070	-0.018	-0.104	0.256	0.269
	600	<b>1.000</b>	0.127	0.068	0.016	0.268	0.225
	1,000	<b>1.000</b>	0.159	0.137	-0.018	0.294	0.204
$\hat{s}_3 (x_3 = b_C)$	300	0.077	0.087	-0.004	-0.081	0.083	0.062
	600	-0.015	0.013	0.022	-0.021	-0.003	-0.039
	1,000	0.008	0.029	0.157	0.017	-0.028	-0.034
$\hat{s}_4 (x_4 = law_{\sigma_y})$	300	-0.024	0.167	0.135	0.048	0.112	0.144
	600	-0.056	0.028	-0.004	-0.038	0.063	0.025
	1,000	-0.011	0.056	0.149	0.017	0.076	0.072
$\hat{s}_5 (x_5 = a_{\sigma_y})$	300	-0.042	<b>0.626</b>	<b>1.032</b>	<b>1.002</b>	0.023	0.218
	600	-0.034	<b>0.573</b>	<b>0.994</b>	<b>1.000</b>	0.014	0.131
	1,000	-0.014	<b>0.614</b>	<b>1.103</b>	<b>1.003</b>	0.046	0.187
$\hat{s}_6 (x_6 = b_{\sigma_y})$	300	-0.078	0.030	0.035	-0.014	-0.034	0.022
	600	0.003	0.042	0.054	-0.016	-0.017	-0.114
	1,000	0.004	0.017	0.106	-0.018	0.016	0.012
$\hat{s}_7 (x_7 = a_r)$	300	-0.070	0.331	0.097	0.049	<b>0.679</b>	<b>0.709</b>
	600	0.011	0.300	0.040	0.030	<b>0.644</b>	<b>0.595</b>
	1,000	0.029	0.335	0.130	0.002	<b>0.697</b>	<b>0.618</b>
$\hat{s}_8 (x_8 = b_r)$	300	-0.066	-0.004	0.074	0.016	-0.034	0.073
	600	0.026	0.000	-0.012	-0.049	-0.003	-0.075
	1,000	0.011	0.088	0.173	0.042	0.076	0.058
$\hat{s}_9 (x_9 = \rho)$	300	-0.021	0.066	0.102	0.019	-0.053	-0.041
	600	-0.007	0.006	0.063	0.015	-0.007	0.008
	1,000	-0.074	0.010	0.115	-0.001	0.011	0.034
$\hat{s}_{1T} (x_1 = law_C)$	300	0.000	0.000	-0.001	0.000	0.002	-0.002
	600	0.000	-0.002	0.002	0.002	-0.003	0.004
	1,000	0.000	0.000	0.000	-0.000	0.001	-0.001
$\hat{s}_{2T} (x_2 = a_C)$	300	<b>1.020</b>	0.038	0.017	-0.002	0.212	0.179
	600	<b>0.914</b>	0.230	0.046	0.002	0.374	0.297
	1,000	<b>0.945</b>	0.067	-0.083	-0.001	0.246	0.202
$\hat{s}_{3T} (x_3 = b_C)$	300	0.000	0.001	0.000	0.000	0.004	-0.002
	600	0.000	0.000	0.001	0.001	-0.001	0.000
	1,000	0.000	-0.001	0.000	0.000	-0.003	-0.001
$\hat{s}_{4T} (x_4 = law_{\sigma_y})$	300	0.000	0.000	-0.005	-0.002	0.019	-0.001
	600	0.000	0.002	-0.004	-0.001	0.008	-0.004
	1,000	0.000	0.000	-0.003	-0.002	0.001	-0.001
$\hat{s}_{5T} (x_5 = a_{\sigma_y})$	300	0.000	<b>0.581</b>	<b>0.894</b>	<b>0.939</b>	0.111	0.180
	600	0.000	<b>0.547</b>	<b>0.920</b>	<b>1.005</b>	0.049	0.223
	1,000	0.000	<b>0.565</b>	<b>0.893</b>	<b>1.023</b>	0.078	0.171
$\hat{s}_{6T} (x_6 = b_{\sigma_y})$	300	0.000	-0.002	0.007	-0.004	0.006	0.001
	600	0.000	-0.003	0.004	0.001	-0.003	-0.004
	1,000	0.000	-0.001	0.000	-0.000	-0.002	-0.001
$\hat{s}_{7T} (x_7 = a_r)$	300	0.000	0.174	-0.003	-0.003	<b>0.572</b>	<b>0.554</b>
	600	0.000	0.316	0.000	0.000	<b>0.619</b>	<b>0.566</b>
	1,000	0.000	0.343	-0.004	-0.003	<b>0.721</b>	<b>0.607</b>
$\hat{s}_{8T} (x_8 = b_r)$	300	0.000	-0.008	-0.001	0.000	0.002	-0.008
	600	0.000	-0.006	0.002	0.002	0.001	-0.007
	1,000	0.000	-0.004	-0.001	-0.000	-0.004	-0.003
$\hat{s}_{9T} (x_9 = \rho)$	300	0.000	0.000	0.000	0.000	-0.001	0.002
	600	0.000	0.007	0.003	0.005	0.012	0.007
	1,000	0.000	0.009	-0.004	-0.004	-0.005	0.021

Table 4: Estimates  $\hat{E}[Y_k]$  and  $\hat{\sigma}[Y_k]$  for expected value and standard deviation of the model response descriptors  $y_k$  with  $k = 1 \dots N^y$ ; estimates  $\hat{s}_j$  for the contribution of each input  $x_j$  with  $j = 1 \dots N^x$ ; estimates  $\hat{s}_{jT}$  for the contribution of each input  $x_j$  and all its interactions with the other inputs  $x_p$  with  $p = 1 \dots N^x$  and  $p \neq j$ .

## 5 CONCLUSIONS

In the particular case of the experiment shown in Fig. 1, and from the above presented work, the following conclusions can be drawn about the inelastic stochastic multi-scale numerical model for random heterogeneous materials developed in [5] and [6]:

- Fig. 4: The model simulates macroscopic behaviors of analogous shapes for all the sets of input parameters considered.
- Tab. 4: Clear trends regarding the relative importance of the model input parameters on the outputs can be observed with a relatively small number of simulations.
- Tab. 4: 3 out of 9 input parameters are key to control the simulated macroscopic response, namely the means of the random fields at meso-scale:  $a_C$ ,  $a_{\sigma_y}$ , and  $a_r$ .
- Tab. 4: Combined actions of two or more input parameters on the model outputs are very limited ( $\hat{s}_{k,j} \approx \hat{s}_{k,jT}$ ,  $\forall (j, k) \in [1, N^x] \times [1, N^y]$ ).
- Tab. 4: Initial stiffness  $C_O$  at macro-scale solely depends on the mean  $a_C$  of the initial stiffness marginal distribution at meso-scale (see Fig. 4). This is in accordance with the way the model is built: by definition  $C_O = \langle C(\mathbf{p}, \omega) \rangle$  with  $\langle C(\mathbf{p}, \omega) \rangle$  the spatial mean of the initial stiffness field over the material RVE, and, consequently to ergodicity properties of the random vector field at meso-scale  $a_C = \langle C(\mathbf{p}, \omega) \rangle$ ; accordingly:  $C_O = a_C$ .

## ACKNOWLEDGEMENT

Part of this work has been developed while visiting the Department of Civil Engineering and Engineering Mechanics at Columbia University in the City of New York.

## REFERENCES

- [1] Germain P., Nguyen Q.S., Suquet P. Continuum thermodynamics. ASME Journal of Applied Mechanics (1983) 50:1010–1020.
- [2] Helton J.C., Johnson J.D., Sallaberry C.J., Storlie C.B. Survey of sampling-based methods for uncertainty and sensitivity analysis. Reliability Engineering & System Safety (2006) 91:1175–1209.
- [3] Helton J.C., Davis F.J. Latin hypercube sampling and the propagation of uncertainty in analyses of complex systems. Reliability Engineering & System Safety (2003) 81:23–69.
- [4] Iooss B., Lemaître P. *A review on global sensitivity analysis methods*. In: Meloni C. and Dellino G. (Eds.) Uncertainty management in Simulation-Optimization of Complex Systems: Algorithms and Applications, Springer, 2015.
- [5] Jehel P. A Stochastic Multi-scale Approach for Numerical Modeling of Complex Materials – Application to Uniaxial Cyclic Response of Concrete. In: Ibrahimbegovic A. (ed.), Computational Methods for Solids and Fluids. Springer, pp. 123–160 (2016).
- [6] Jehel P., Cottureau R. On damping created by heterogeneous yielding in the numerical analysis of nonlinear reinforced concrete frame elements. Computers and Structures (2015) 154:192–203.

- [7] Mc Kay M.D., Conover W.J., Beckman, R.J. A comparison of three methods for selecting values of input variables in the analysis of output from a computer code. *Technometrics* (1979) 21:239–245.
- [8] Maugin G. The thermodynamics of nonlinear irreversible behaviors: An introduction. World Scientific, Singapore (1999).
- [9] Miehe C., Koch A. Computational micro-to-macro transitions of discretized microstructures undergoing small strains. *Archive of Applied Mechanics* (2002) 72:300–317.
- [10] Nemat-Nasser S., Hori M. *Micromechanics: Overall properties of heterogenous materials*. Elsevier Science Publishers B.V., Amsterdam, The Netherlands (1993).
- [11] Popescu R., Deodatis G., Prevost J.H. Simulation of homogeneous nonGaussian stochastic vector fields. *Probabilistic Engineering Mechanics* (1998) 13(1):1–13.
- [12] Savvas D., Stefanou G., Papadopoulos V., Papadrakakis M. Effect of waviness and orientation of carbon nanotubes on random apparent material properties and RVE size of CNT reinforced composites. *Composite Structures* (2016) 152:870–882.
- [13] Trigo A.P.M., Liborio J.B.L. Doping technique in the interfacial transition zone between paste and lateritic aggregate for the production of structural concretes. *Materials Research* (2014) 17(1):16–22.
- [14] Zhu X., Gao Y., Dai Z., Corr D.J., Shah S.P. Effect of interfacial transition zone on the Young’s modulus of carbon nanofiber reinforced cement concrete. *Cement and Concrete Research* (2018) 107:49–63.

### ANNEX - Support of a uniform distribution with know mean and variance

Let  $\mathcal{U}(a, b)$  be a uniform distribution over the range  $[x; y]$  ( $x < y$ ) with mean  $a$  and variance  $b^2 > 0$ . In this annex, we show how to calculate  $x$  and  $y$  from  $a$  and  $b$ . By definition, the following nonlinear system has to be solved:

$$\begin{cases} x + y = 2a \\ (y - x)^2 = 12b^2 \end{cases} \quad (11)$$

Introducing  $C^2 = 4a^2$  and  $D^2 = 12b^2$ , Eqs. (11) implies that:

$$\begin{cases} (x + y)^2 = C^2 \\ (x - y)^2 = D^2 \end{cases} \quad \Rightarrow \quad \begin{cases} x + y = \pm C \\ x - y = \pm D \end{cases} \quad (12)$$

Consequently, we have the following four possible couples of solutions:

$$\begin{aligned} (x_1, y_1) &= ((C + D)/2, (C - D)/2) \\ (x_2, y_2) &= ((C - D)/2, (C + D)/2) \\ (x_3, y_3) &= ((-C + D)/2, (-C - D)/2) \\ (x_4, y_4) &= ((-C - D)/2, (-C + D)/2) \end{aligned} \quad (13)$$

From Eqs. (13), the following table can be built:

$i$	$(x_i + y_i)/2$	$x_i - y_i$	$(C, D) = (2a, \sqrt{12}b)$	$(C, D) = (2a, -\sqrt{12}b)$	$(C, D) = (-2a, \sqrt{12}b)$	$(C, D) = (-2a, -\sqrt{12}b)$
1	$C/2$	$D$	<i>No</i>	<i>Yes</i>	<i>No</i>	<i>No</i>
2	$C/2$	$-D$	<i>Yes</i>	<i>No</i>	<i>No</i>	<i>No</i>
3	$-C/2$	$D$	<i>No</i>	<i>No</i>	<i>No</i>	<i>Yes</i>
4	$-C/2$	$-D$	<i>No</i>	<i>No</i>	<i>Yes</i>	<i>No</i>

A *Yes* means that both conditions  $(x_i + y_i)/2 = a$  and  $x_i < y_i$  are true for the corresponding values of  $C$  and  $D$ , while a *No* is indicated otherwise. Because there is always one and only one *Yes* for each value of  $i$ , this table shows the intuitive fact that  $x$  and  $y$  are uniquely determined from  $a$  and  $b$ . Besides, if for instance we consider that  $(x, y) = (x_2, y_2)$  in Eqs. (13) with  $C = 2a$  and  $D = \sqrt{12}b$  (corresponding to a *Yes*), we have:

$$x = a - \sqrt{3}b \quad \text{and} \quad y = a + \sqrt{3}b \quad (14)$$

As a direct application of Eqs. (14), it is for instance straightforward to guarantee that  $[x, y] \subset [0, 1]$  if, for any  $a \in [0, 1]$ ,  $b$  is calculated as

$$\begin{cases} a - \sqrt{3}b \geq 0 \\ a + \sqrt{3}b \leq 1 \end{cases} \Rightarrow b \leq \min\left(a/\sqrt{3}; (1-a)/\sqrt{3}\right) \quad (15)$$

## Acoustic Black Holes: from Generalization to Realization

Wonju Jeon\*

\*KAIST

### ABSTRACT

This study starts with a simple question: can we efficiently reduce the vibration of plates or beams using a lightweight structure that occupies a small space? As an efficient technique to dampen vibration, we adopted the concept of an Acoustic Black Hole (ABH) with a simple modification of the geometry. The original shape of an ABH has a straight wedge-type profile with power-law thickness, with the reduction of vibration in beams or plates increasing as the length of the ABH increases. However, in real-world applications, there exists an upper bound of the length of an ABH due to space limitations. Therefore, in this study, the authors propose a curvilinear shaped ABH using the simple mathematical geometry of an Archimedean spiral, which allows a uniform gap distance between adjacent baselines of the spiral. In numerical simulations, the damping performance increases as the spiral length of the Archimedean spiral increases regardless of the curvature of the spiral in the mid- and high-frequency ranges. Adding the damping material to the ABH could strongly enhance the damping performance while not significantly increasing the weight. In addition, the authors experimentally investigate the effect of curvatures of the curved ABH on the vibration damping performance. The curved ABHs studied in this work are divided into two cases: (1) the curved ABH with the baseline of constant curvatures which has a circular arc shape, (2) the curved ABH with the baseline of varying curvatures. After manufacturing the spiral ABH with high precision, the authors perform experiments to investigate the effect of curvatures on the damping performance of the circular arc shaped ABHs. An Archimedean spiral ABH, a particular form of the curved ABH of slowly varying curvatures is also investigated experimentally in order to create the possibility of using the spiral ABH as a new and efficient method of damping vibration in real-world problems.

## Identification of Elastic Moduli and Length Scale Parameter for Strain Gradient Theory from Full-field Measurements

Iksu Jeong<sup>\*</sup>, Euiyoung Kim<sup>\*\*</sup>, Maenghyo Cho<sup>\*\*\*</sup>

<sup>\*</sup>Department of Mechanical and Aerospace Engineering, Seoul National University, Seoul, Republic of Korea, <sup>\*\*</sup>4th Industrial Revolution R & D Center, Korea Institute of Machinery & Materials, Daejeon, Republic of Korea, <sup>\*\*\*</sup>Department of Mechanical and Aerospace Engineering, Seoul National University, Seoul, Republic of Korea

### ABSTRACT

Classical continuum solid mechanics have been widely used in various fields for decades, but cannot demonstrate some phenomena such as size effects and deformation of micro- and nano-scale structures. To overcome these limitations, many researchers have developed the strain gradient theory in which the classical theory is enriched by adding first derivatives of macroscopic strains, i.e. second derivatives of displacements, to the constitutive equations. Additional parameters called length scale parameters need to be introduced for the higher order terms and it is necessary to experimentally measure the exact value of the parameters for the practical application of the strain gradient theory. Recent advances in optical devices and image processing have led to the development of methodologies such as digital image correlation which can measure full-field displacements of structures. Full-field measurements make it possible to identify more accurate and realistic material parameters compared to the traditional method especially when the stresses and strains are not uniform. Furthermore, identification methods based on full-field measurement can extract the parameters from a relatively small number of experiments even though the material has heterogeneous or nonlinear constitutive properties. In this research, constitutive parameters for gradient elasticity including length scale parameter are identified from full-field displacements by minimizing the gap between measured and numerical quantities. For the numerical analysis, finite element method with staggered gradient elasticity based on Ru-Aifantis theorem is used since it only need C0-continuous interpolation functions. Finite element analysis of the strain gradient theory basically requires C1-continuity due to the higher order terms, but staggered gradient elasticity divides the solution process into two step so that C0 elements suffice. The accuracy and robustness of the proposed method are verified in a couple of numerical examples. Keywords: Identification, Full-field measurement, Gradient elasticity, Length scale parameter References [1] H. Askes, I. Morata, E.C. Aifantis, Finite element analysis with staggered gradient elasticity, Computers and Structures, 2008, Vol. 86, pp. 1266-1279 [2] S. Avril et al., Overview of identification methods of mechanical parameters based on full-field measurements, 2008, Exp. Mech., Vol. 48, pp. 381-402 Acknowledgement This work was supported by the National Research Foundation of Korea(NRF) grant funded by the Korea government(MSIP) (No. 2012R1A3A2048841

## Calculation of Surface Energy Barriers of Droplet Adhesion to Textured Solid Surface in Cassie-Baxter Wetting Mode by Using Numerical Modeling

Minsoo Jeong<sup>\*</sup>, Seunghwa Ryu<sup>\*\*</sup>, Keonwook Kang<sup>\*\*\*</sup>

<sup>\*</sup>Department of Mechanical Engineering, Yonsei University, Republic of Korea, <sup>\*\*</sup>Department of Mechanical Engineering, KAIST, Republic of Korea, <sup>\*\*\*</sup>Department of Mechanical Engineering, Yonsei University, Republic of Korea

### ABSTRACT

The phenomenon that particles stick to the solid surface is called particle surface adhesion. The wettability of a particle on the surface can be tuned by changing the topology of the surface. In this work, we developed a line tension model to understand the surface adhesion phenomenon of a deformable body to solid surface. Our model is validated by comparing with analytical solutions of D. Kim et al.(2016)[1] and Young et al.(1805)[2] which calculate the surface energy and contact angle of water droplet adhered to the solid surface in Cassie-Baxter wetting mode. The model produces consistent result that the wettability of the patterned solid surface is lower than that of flat surface. Besides, the unrealistic non-smooth droplet shape is avoided in our numerical modeling. In addition, the surface energy barriers that are generated when the contact angle changes in the Cassie-Baxter wetting mode are calculated. [1] Kim et al., "Wetting theory for small droplets on textured solid surfaces", Scientific Reports, 6:, 37813 (2016) [2] Young et al., "An Essay on the Cohesion of Fluids", Phil. Trans. R. Soc. Lond., 95:, 65–87 (1805)

## High Fidelity Modeling and Simulation of Earthquake Soil Structure Interaction Effects for Infrastructure Objects

Boris Jeremic\*, Yuan Feng\*\*, Han Yang\*\*\*, Hexiang Wang\*\*\*\*, Francis McKenna\*\*\*\*\*, David McCallen\*\*\*\*\*

\*UCD, LBNL, \*\*UCD, \*\*\*UCD, \*\*\*\*UCD, \*\*\*\*\*LBNL, \*\*\*\*\*LBNL

### ABSTRACT

Interaction of dynamics of three components: (1) an earthquake, (2) soil/rock and (3) the structure, control the response of structures during earthquakes. It is postulated that this interaction, called Earthquake Soil Structure Interaction (ESSI) can sometimes be beneficial and sometimes detrimental to dynamic response of infrastructure objects. Accurate modeling of ESSI effects is possible when modeling uncertainties, that are introduced in results when modeling simplifications are made, are controlled and that their influence on results is known. A hierarchy of models, from simpler toward more sophisticated, is used to estimate influence of modeling uncertainties. Higher modeling sophistication models require high performance computing (HPC) approach to simulations. Presented here is our approach to modeling ESSI effects for dynamic behavior of buildings and other safety related structures (bridges, dams, etc.). Approach is based on a notion of availability of a hierarchy of modeling and simulation tools, from low to high fidelity, that allow for deterministic and probabilistic models to be used in the analysis. Effects of modeling simplifications on ESSI modeling and simulation results are tested through the use of multiple levels of sophistication for models, from simple 1D elastic stick models, to sophisticated 3D inelastic solid, contact, shell, beam models. In addition, accurate following of seismic energy, as it propagates through the soil structure system, is used to improve safety and economy of infrastructure objects. HPC approach to modeling and simulation of ESSI effects is presented on both fine and coarse grained levels. Fine grain level HPC is based on application of Small Linear Algebra (SLA) to tensor computations on the constitutive and finite element level. Coarse grained level HPC is based on massively parallel computations using Ring Buffer (RB) dynamic load balancing that is applicable to local clusters, to Cloud Computing (Amazon Web Services (AWS) for example) as well as to large national supercomputers (EDISON and CORI at LBNL for example). A number of examples will illustrate aspects of modeling and simulation of ESSI behavior using HPC approach. All simulations are performed using the Real ESSI Simulator system (<http://real-essi.info/>).

## Free Damage Propagation with Memory

Prashant Jha<sup>\*</sup>, Robert Lipton<sup>\*\*</sup>

<sup>\*</sup>Department of Mathematics Louisiana State University, <sup>\*\*</sup>Center for Computation and Technology and  
Mathematics Louisiana State University

### ABSTRACT

We introduce a simple model for free damage propagation based on non-local potentials. The model is developed using a state based peridynamic formulation. The resulting evolution is shown to be well posed. At each instant of the evolution we identify the damage set. On this set the local strain has exceeded critical values either for tensile or hydrostatic strain and damage has occurred. For this model the damage set is nondecreasing with time and associated with damage variables defined at each point in the body. We show that energy balance holds for this evolution. For differentiable displacements away from the damage set we show that the nonlocal model converges to the linear elastic model. We provide several numerical examples modeling fatigue and fracture.

## Dynamics of Thin Liquid Films on Vertical Cylindrical Fibers

Hangjie Ji<sup>\*</sup>, Claudia Falcon<sup>\*\*</sup>, Abolfazl Sadeghpour<sup>\*\*\*</sup>, Zezhi Zeng<sup>\*\*\*\*</sup>, Andrea Bertozzi<sup>\*\*\*\*\*</sup>,  
Sungtaek Ju<sup>\*\*\*\*\*</sup>

<sup>\*</sup>University of California, Los Angeles, <sup>\*\*</sup>University of California, Los Angeles, <sup>\*\*\*</sup>University of California, Los Angeles, <sup>\*\*\*\*</sup>University of California, Los Angeles, <sup>\*\*\*\*\*</sup>University of California, Los Angeles

### ABSTRACT

Viscous thin liquid films flowing down vertical fibers can exhibit interesting dynamics via the formation of droplets driven by a Rayleigh mechanism with the presence of gravity. Motivated by experimental results on the effects of nozzle geometry on the dynamics of these viscous droplets by Sadeghpour et al. (2017), we further study a thin film model for the gravity-driven flow in the Rayleigh-Plateau Regime. The governing equation is a fourth-order nonlinear parabolic PDE for the film thickness that takes into consideration hydrodynamic boundary conditions, surface tension, intermolecular forces, and gravity. Time-dependent computations of the spatial evolution of the film reveal a strong influence of inlet boundary conditions that characterize different nozzle geometry. Numerical solutions of traveling wave solutions also yield information on the profile and propagation velocity of fluid beads, which are compared to experiments.

## Buffering Capacity of Non-spherical Granular Materials Based on DEM Simulations with Super-quadric Elements

Shunying Ji<sup>\*</sup>, Ying Yan<sup>\*\*</sup>, Siqiang Wang<sup>\*\*\*</sup>

<sup>\*</sup>State Key Laboratory of Structural Analysis for Industrial Equipment, Dalian University of Technology, Dalian 116023, China, <sup>\*\*</sup>School of civil and Safety Engineering, Dalian Jiaotong University, Dalian, 116028, China, <sup>\*\*\*</sup>State Key Laboratory of Structural Analysis for Industrial Equipment, Dalian University of Technology, Dalian 116023, China

### ABSTRACT

Granular systems commonly encountered in industry or nature are comprised of non-spherical grains. Compared to spherical particles, high discretization and interlocking among particles can dissipate effectively the system energy and improve the buffer capacity. The superquadric element based on continuous function representation can construct the geometric shape of irregular particles accurately, and then its contact detection between particles can be calculated easily. In this paper we study the buffer capacity of non-spherical particles under impact load by the discrete element method (DEM). To examine the validity of the algorithms and this model, we compare with the analytical results for a single cylinder impacting a flat wall and the previous experimental result for spherical granular material under impact load, and this method is verified by the good agreement between the simulated results and the previous experiments. Furthermore, the influences of granular thickness and particle shapes on the buffer capacity are discussed. The results show that a critical thickness  $H_c$  is obtained for different particle shapes. The buffer capacity is improved for increasing the granular thickness when  $H < H_c$ , but is independent of the granular thickness and particle shapes when  $H > H_c$ . Moreover, decreasing the particle blockiness and increasing or decreasing the aspect ratio of cylinder-like particles and box-like particles have more effective buffer capacity for the non-spherical particle systems.

## **An Accurate Weakly Compressible SPH Method for Simulating Interfacial Multiphase Fluid Flow Involving Complex Geometries and Motions**

Zhe Ji<sup>\*</sup>, Michael Gestrich<sup>\*\*</sup>, Milos Stanic<sup>\*\*\*</sup>, Thomas Indinger<sup>\*\*\*\*</sup>

<sup>\*</sup>FluiDyna GmbH, <sup>\*\*</sup>FluiDyna GmbH, <sup>\*\*\*</sup>FluiDyna GmbH, <sup>\*\*\*\*</sup>FluiDyna GmbH

### **ABSTRACT**

Numerical simulations of interfacial multiphase fluid flow have a wide range of applications across engineering fields. Simulations of oil distribution in transmission systems regularly involve complex geometries and high-speed motions. Robust and accurate handling of multiple material phases and the interaction with complex moving geometries is a challenging problem for any numerical method. As a particle-based method, Smoothed Particle Hydrodynamics (SPH) conserves mass and momentum. The sharp interface condition is inherently satisfied and characterized by particles carrying distinct material properties, which is the main advantage over the grid-based methods. Nonetheless, regarding to multiphase simulations, traditional SPH suffers from several numerical difficulties and extra treatments are required in order to maintain stability and sharpness of the interface. In this work, an accurate weakly compressible SPH method is developed to simulate interfacial multiphase flow involving complex geometries and rigid-body motions. In order to decrease numerical oscillation of the pressure field, the pair-wised particle interaction is calculated by solving a one-dimensional Riemann problem. An extended HLLC Riemann solver [1] is tailored to handle interactions between different materials with general equations of state and large density ratio. For continuous region within one phase, a modified Riemann solver [2] is employed to decrease the intrinsic numerical dissipation. In addition, a generalized wall boundary condition, based on solving a one-side Riemann problem, is extended to multiphase situation to handle interactions regarding to complex moving geometries with the existence of triple points. Moreover, to go beyond 1st order of accuracy and overcome some well-known difficulties of the traditional SPH method, a second-order gradient estimator as well as the MUSCL-Hancock scheme are utilized. Lastly, to avoid the disorder of particle positions and creation of void regions, the transport velocity formulation is embedded as well. The proposed SPH method is implemented in a high performance multi-GPU code developed by FluiDyna GmbH. Extensive numerical tests including academic and industrial benchmarks are carried out in the end to validate the accuracy of proposed numerical method. The results exhibit significant improvement over traditional SPH. More physically plausible results are observed by producing better-resolved fluid structures and a more accurate pressure field. [1] C. Zhang, X. Hu, N. Adams, *Journal of Computational Physics* 335 (2017) 605–620. [2] X. Hu, N. Adams, G. Iaccarino, *Journal of Computational Physics* 228 (2009) 6572–6589.

## An Adaptive IGA Collocation Method with a Recovery-based Error Estimator

Yue Jia<sup>\*</sup>, Cosmin Anitescu<sup>\*\*</sup>, Yongjie Zhang<sup>\*\*\*</sup>, Timon Rabczuk<sup>\*\*\*\*</sup>

<sup>\*</sup>Northwestern Polytechnical University, Xi'an, China, <sup>\*\*</sup>Institute of Structure Mechanics, Bauhaus University Weimar, Germany, <sup>\*\*\*</sup>Carnegie Mellon University, Pittsburgh, USA, <sup>\*\*\*\*</sup>Institute of Structure Mechanics, Bauhaus University Weimar, Germany

### ABSTRACT

Abstract The current work presents an enhanced isogeometric analysis (IGA) [1] collocation method, where the collocation points are different from the usual Greville-abcissae. It is well known that the location of the collocation points plays an important role in the accuracy and stability of IGA collocation methods. This is particularly true for non-uniform meshes and domains generated from multi-patch geometries. We propose a collocation method based on Gaussian points [2], which has improved accuracy as compared to using C1 splines and a recovery-based error estimator can be derived by sampling the solution at particular points in the domain. Adaptivity is implemented using a hierarchical spline basis [3], which satisfies the C1 continuity requirement. The proposed approach is demonstrated for arbitrary polynomial degrees and has been tested by several benchmark problems, including multipatch domains and geometries with re-entrant corners. Key words: IGA collocation method; Gaussian-collocation points; PHT-Spline; linear elasticity; error estimation References [1] Hughes T J R, Cottrell J A, Bazilevs Y. Isogeometric analysis: CAD, finite elements, NURBS, exact geometry and mesh refinement [J]. Computer Methods in Applied Mechanics and Engineering, 2005, 194(39-41): 4135-4195 [2] De Boor C, Swartz B. Collocation at Gaussian Points [J]. SIAM Journal on Numerical Analysis, 1973, 10(4): 582-606 [3] Deng J S, Chen F, Li X, et al. Polynomial splines over hierarchical T-meshes[J]. Journal Graphical Models, 2008, 70(4): 76-86

## Quasi-nonlocal Coupling of State-based Peridynamics Model with Classical Continuum Mechanics Model

Feng Jiang\*, Yongxing Shen\*\*

\*University of Michigan-Shanghai Jiao Tong University Joint Institute, Shanghai Jiao Tong University, \*\*University of Michigan-Shanghai Jiao Tong University Joint Institute, Shanghai Jiao Tong University

### ABSTRACT

The peridynamics and continuum models of elasticity have their pros and cons. The peridynamics model can be naturally applied to a region where a crack propagates or damage emerges, while the continuum mechanics model is most cost efficient and easier to enforce boundary conditions. Coupling of these models provides a way to fully take advantage of their merits. However, the energy based coupling schemes usually suffer from the spurious “ghost force” effect. To relieve this issue, in this work, a quasi-nonlocal coupling technique has been developed to couple the state-based peridynamics model with continuum mechanics model. The essential idea of the coupling is that the transition region interacts with the peridynamics region in a nonlocal way while it interacts with the continuum region in a local way. In the transition region, the stiffness tensor and the influence function are modified so that both the force patch test and the energy patch test are passed at the nodal points. Since there are more equations than parameters, the parameters are determined with  $l^1$ -minimization. Numerical examples demonstrating the accuracy and efficiency of the coupling model are presented. [1] S.A. Silling et al., Peridynamic states and constitutive modeling, *J. Elasticity*, 88:151-184, 2007. [2] C. Ortner, L. Zhang, Energy based atomistic-to-continuum coupling without ghost forces, *Comput. Methods Appl. Mech. Engrg.*, 279:29-45, 2014. [3] X. H. Li and J. Lu, Quasi-nonlocal coupling of nonlocal diffusions. *SIAM J. Numer. Anal.*, 55 (5):2394-2415, 2017.

## Offline-Enhanced Reduced Basis Method through Adaptive Construction of the Surrogate Training Set

Jiahua Jiang<sup>\*</sup>, Yanlai Chen<sup>\*\*</sup>, Akil Narayan<sup>\*\*\*</sup>

<sup>\*</sup>University of Massachusetts Dartmouth, <sup>\*\*</sup>University of Massachusetts Dartmouth, <sup>\*\*\*</sup>University of Utah

### ABSTRACT

The Reduced Basis Method (RBM) is a popular certified model reduction approach for solving parametrized partial differential equations. It has been combined with many multiscale methods such as domain decomposition. One critical stage of the offline portion of the algorithm is a greedy algorithm, requiring maximization of an error estimate over parameter space. In practice this maximization is usually performed by replacing the parameter domain continuum with a discrete ‘‘training’’ set. When the dimension of parameter space is large, it is necessary to significantly increase the size of this training set in order to effectively search parameter space. Large training sets diminish the attractiveness of RBM algorithms since this proportionally increases the cost of the offline phase. However, the large size of parameter inputs leads to high computational costs in offline stage. In this work we propose novel strategies for offline RBM algorithms that mitigate the computational difficulty of maximizing error estimates over a training set. The main idea is to identify a subset of the training set, a ‘‘Surrogate Training Set’’ (STS), on which to perform greedy algorithms. The STSs we construct are much smaller in size than the full training set, yet our examples suggest that they are accurate enough to induce the solution manifold of interest at the current offline RBM iteration. We propose two algorithms to construct the STS: Our first algorithm, the Successive Maximization Method (SMM) method, is inspired by inverse transform sampling for non-standard univariate probability distributions. The second constructs an STS by identifying pivots in the Cholesky Decomposition of an approximate error correlation matrix. We demonstrate the algorithm through numerical experiments, showing that it is capable of accelerating offline RBM procedures without degrading accuracy, assuming that the solution manifold has rapidly decaying Kolmogorov width.

## **A Multi-Material Structural Topology Optimization Based on Parametric Level Set Approach Using Cardinal Basis Functions**

Long Jiang\*, Shikui Chen\*\*

\*Department of Mechanical Engineering, State University of New York at Stony Brook, \*\*Department of Mechanical Engineering, State University of New York at Stony Brook

### **ABSTRACT**

As a further development of the conventional level set methods, the parametric level set method is an improvement over its predecessor in the topology optimization area. By parameterizing the level set function, the topology optimization not only can preserve clear design result boundaries but also can avoid some undesired deficiencies in the conventional level set approach, such as the reinitialization scheme. Integrated with mathematical programming, the parametric level set approach can achieve higher numerical robustness and better handling of multiple constraints. To get an accurate material property interpolation from the level set model to the physical model, the level set function is preferred to be maintained as a signed distance function (SDF). In this research, this feature is realized by introducing a distance regularization energy functional. With this energy functional minimized, the level set function around the design boundary will be maintained as a signed distance function. At the same time, the level set function can be kept flat at the locations away from the design boundaries. Overall, this type of level set function is referred as the distance-regularized level set function. By being flat at areas away from the design boundaries, the level set function can penetrate the zero level easier, improving the design robustness by creating new holes. When extended to the multi-material structure designing, different level set functions are utilized to represent different material phases, and the overlapping areas are reconciled via the Merriman-Bence-Osher (MBO) operator. However, the distance-regularized-shape level set function may cause numerical issues while applying this operator. A sub-optimization scheme is introduced to reshape the level set function before and after the MBO operation to ensure its success. Conventionally, the parametric level set approach uses radial basis function (RBF) in the parameterization. However, due to the overlapping of the neighboring RBFs, the range of the corresponding weights, to be used as the optimization design variable, cannot be explicitly determined. In this research, a newly-constructed cardinal basis function (CBF) is utilized to parameterize the level set function. This CBF is equal to one at the selected node and is equal to zero elsewhere. By using this CBF in the parameterization, the design variable range can be explicitly determined, as the range of the level set function itself.

## Effects of grain size and shape on the plasticity of FCC polycrystals : A Dislocation Dynamics Study

Maoyuan Jiang<sup>\*</sup>, Benoit Devincre<sup>\*\*</sup>, Ghiath Monnet<sup>\*\*\*</sup>

<sup>\*</sup>EDF R&D, Department MMC, France, <sup>\*\*</sup>Laboratoire d'Etude des Microstructures, CNRS-ONERA, France, <sup>\*\*\*</sup>EDF R&D, Department MMC, France

### ABSTRACT

From the seminal work of Hall and Petch (HP), the effect of grain size on the mechanical properties of polycrystal is well known. Nevertheless, the elementary properties responsible for the HP effect are still matter of debate. Besides, theoretical and experimental investigations are today essentially focused on polycrystals made of equiaxial grains. However, industrial materials are usually formed with grains having non-equiaxed shapes (perlite, matensite, bainite etc.). In this work, Dislocation Dynamics (DD) simulation is used to identify the elementary mechanisms controlling the HP effect at the dislocations scale. In addition, the influence of grain shape is explored by considering simple periodic polycrystalline aggregates made of grains with cube, plate or needle shapes. First, simulations have been made with a very simple periodic model of aggregates. Grain boundaries (GBs) are considered impenetrable to the dislocation gliding inside the grains. Results show that the HP effect is globally obeyed and the interaction with GBs is strongly affected by the number of active slip systems. Secondly, we designed simulations to test the influence of grain shape on the HP effect. We show that the HP effect is strongly affected by the grain shapes. A simple model based on the calculation of the dislocation mean free path is proposed to account for the influence of the grains morphology. In the context of strain gradient plasticity, the HP effect is explained by the presence of a back-stress inside the grains that emerges from strain incompatibility between grains in a deformed polycrystal. In other words, geometrically necessary dislocations (GNDs) must accumulate at GBs to accommodate the different distortion field imposed to the grains during plasticity. By virtue of the Nye's tensor, the above property can be directly tested and quantified in DD simulations. For the simplest simulation geometry, the computed back-stress as function of the distance to the GB interface can be compared with theoretical models. Essentially, a crystal plasticity field model is found to correctly calculate the back-stress amplitude close to the GB interface while the DD simulation results exhibit a decay trend for the stress components. A twist subgrain calculation accounting for the finite size of the GND microstructure gives much better agreement with the DD simulation results.

## **A Coupled Finite Volume Methods and Extended Finite Element Methods for the Dynamic Crack Propagation Modelling with the Pressurized Crack Surfaces**

Shouyan Jiang\*, Chengbin Du\*\*

\*Department of Engineering Mechanics, Hohai University, Nanjing 210098, China, \*\*Department of Engineering Mechanics, Hohai University, Nanjing 210098, China

### **ABSTRACT**

In this paper, we model the fluid flow within the crack as one-dimensional flow and assume that the flow is laminar, the fluid is incompressible, and accounts for the time-dependent rate of crack opening. Here, we discretise the flow equation by finite volume methods. The extended finite element methods are used for solving solid medium with crack under dynamic loads. Having constructed the approximation of dynamic extended finite element methods, the derivation of governing equation for dynamic extended finite element methods are presented. The implicit time algorithm is elaborated for the time discretization of dominant equation. In addition, the interaction integral method is given for evaluating stress intensity factors. Then, the coupling model for modelling hydraulic fracture can be established by the extended finite element methods and the finite volume methods. We compare our present numerical results with our experimental results for verifying the proposed model. Finally, we investigate the water pressure distribution along crack surface and the effect of water pressure distribution on the fracture property.

## **3D Multi-scale Modeling of Microstructure Dependent Inter-granular Fracture in UO<sub>2</sub> Using a Phase-field Approach**

Wen Jiang<sup>\*</sup>, Larry Aagesen<sup>\*\*</sup>

<sup>\*</sup>Idaho National Laboratory, <sup>\*\*</sup>Idaho National Laboratory

### **ABSTRACT**

The brittle fracture behavior of UO<sub>2</sub> fuels is strongly influenced by the porosity and grain size distributions in the underlying microstructure. In service, there is significant evolution of these microstructural features, which can alter the fracture properties and subsequently the thermo-physical-mechanical behavior of the nuclear fuels. To incorporate these microstructural effects on the fracture behavior, a three-dimensional multi-scale modeling framework is developed in the present work. Within this framework, the grain-boundary fracture properties obtained from molecular dynamics simulations are utilized in a phase-field fracture model to investigate the inter-granular brittle crack propagation in this material. The fission gas bubble formation model is coupled with fracture to study their interaction and influence on the fracture properties. Subsequently, the parameters of an engineering scale fracture model are obtained by fitting the stress-strain evolution obtained from the phase-field simulations. This framework provides a hierarchical coupling of properties evaluated at the atomistic scale to perform more realistic engineering level predictions of fracture in nuclear fuel pellets.

## **Evaluation of the Benefit of Strengthening Shield Tunnels by Epoxy-bonded Filament Wound Profiles by Means of a Parametric Study Based on Multiscale Analysis**

Zijie Jiang<sup>\*</sup>, Xian Liu<sup>\*\*</sup>, Lele Zhang<sup>\*\*\*</sup>, Yong Yuan<sup>\*\*\*\*</sup>, Herbert A. Mang<sup>\*\*\*\*\*</sup>

<sup>\*</sup>Department of Geotechnical Engineering, Tongji University, China, <sup>\*\*</sup>Department of Geotechnical Engineering, Tongji University, China, <sup>\*\*\*</sup>Department of Geotechnical Engineering, Tongji University, China, <sup>\*\*\*\*</sup>Department of Geotechnical Engineering, Tongji University, China, <sup>\*\*\*\*\*</sup>Institute for Mechanics of Materials and Structures, Vienna University of Technology, Austria

### **ABSTRACT**

Large deformations of shield tunnels may be the consequence of a long period of operation or of nearby pit construction. Epoxy-bonded filament wound profiles (FWP) have been employed more recently to strengthen the deformed segmental tunnel linings. Full-scale tests were performed to prove the effectiveness of this method. The present paper contains a report on a macroscopic numerical model, which has been validated by comparing numerical results with experimental results. Multiscale analysis is an important ingredient of the modeling process, aimed at improving computational efficiency and fidelity. In this model, the reinforced concrete segments and the strengthening material, i.e. FWP, are simulated by means of beam elements. The joints which connect adjacent reinforced concrete segments are modeled by a group of nonlinear spring elements. Previous research has shown that the behavior of the joints may have significant influence on the mechanical behavior of the overall structure. Based on the developed numerical model, a comprehensive parametric study of the influence of several design parameters, such as, for example, Young's modulus of the FWP and the mechanical properties of the bond between the FWP and a segment of the tunnel, on the increase of both the load-carrying capacity and the overall stiffness of the structure was performed. Based on the results from this study, an optimal combination of design parameters for strengthening of shield tunnels by FWP is proposed. Moreover, the influence of the geometric dimensions of the strengthened structure and of the soil environment on the overall benefit of this strengthening was obtained. The soil environment is intergraded into the model by means of a specific scheme of loading. It is shown that this influence is smaller than the one of the geometric dimensions of the lining, which is itself relatively small.

## **A Link between Multiplicative Hyper-Elasto-Plasticity and Additive Hypo-Elasto-Plasticity Models: the Kinetic Logarithmic Stress Rate**

Yang Jiao\*, Jacob Fish\*\*

\*Columbia University, \*\*Columbia University

### **ABSTRACT**

Plasticity is one of the most common energy dissipation mechanisms featuring large strain in solids. Geometric nonlinearity is therefore often involved in constitutive models adopted for numerical simulation of plastic behavior of solids. Such constitutive models are usually developed through extension of the corresponding infinitesimal-deformation models into the large strain regime. Distinct large-strain plasticity models, however, can be obtained as large-strain generalizations of the same classical infinitesimal-deformation model. Understanding of the relation between these different models for the same purpose is thus of crucial importance for ensuring reliability of the computational approaches to studying plasticity. In the present study, two well-recognized categories of large-strain elastoplasticity models, i.e. the multiplicative hyper-elasto-plasticity and additive hypo-elasto-plasticity models, are analyzed with relation between them revealed. At first, the well-known additive hypo-elasto-plasticity models, which are based on additive decomposition of the rate of deformation into elastic and plastic parts, are critically examined. Through an unloading stress ratchetting obstacle test, it is shown that even a relatively recent, self-consistency-oriented variant of such models, which features the logarithmic stress rate, exhibits physical inconsistency (nonphysical energy dissipation) in an unloading process. A remedy is accordingly proposed through a simple modification to the logarithmic stress rate employed by the model. It is demonstrated that the resulting objective stress rate, termed the kinetic logarithmic rate due to its dependency on stress, renders the corresponding additive models capable of representing energy dissipation-free elastic response whenever plastic flow is absent. The multiplicative hyper-elasto-plasticity models, which are usually considered to be distinct from the additive ones in that they assume multiplicative decomposition of the deformation gradient into elastic and plastic parts, are then analyzed. It is proved that for isotropic materials the multiplicative models coincide with the additive ones if a newly discovered objective stress rate is employed by the later. This objective stress rate, termed the modified kinetic logarithmic rate, reduces to the kinetic logarithmic rate in the absence of strain-induced anisotropy. Such equivalence between the two categories of elastoplasticity models is illustrated through numerical model problems which consider homogeneous deformation along with J2 plasticity with associative plastic flow rule. It is also demonstrated in these problems that other well-known additive models, such as those based on the Jaumann and logarithmic rates, may considerably deviate from the multiplicative models.

## Multi-Phase-Field Simulation of Eutectic Solidification of Binary Alloys Using a Thermodynamically Consistent Model

Peter Jimack<sup>\*</sup>, Peter Bollada<sup>\*\*</sup>, Andrew Mullis<sup>\*\*\*</sup>

<sup>\*</sup>University of Leeds, <sup>\*\*</sup>University of Leeds, <sup>\*\*\*</sup>University of Leeds

### ABSTRACT

This presentation will introduce the derivation of a consistent temperature equation for phase-field models of non-isothermal alloy solidification, and demonstrate its application in two dimensions for the eutectic solidification of a binary alloy based upon an appropriate multi-phase-field model. This non-isothermal model is derived using a formulation based upon the dissipative bracket of Beris and Edwards [1]. Originally designed for modelling complex fluids, the dissipative bracket has ready application in phase field modelling. In outline, we design the bracket to return the phase and alloy concentration field equations, and then use the mechanism of the bracket to automatically return the entropy field, which in turn, using generalised standard thermodynamic identities, gives the thermal field [2]. Our numerical scheme for solving the resulting system is based upon the use of spatial adaptivity and implicit time-stepping via a nonlinear multigrid scheme (the Full Approximation Scheme, FAS). The core components of this implementation will be described, including parallelization based upon a domain decomposition approach. We will illustrate both the quantitative and the qualitative importance of the non-isothermal model by contrasting numerical results against isothermal runs for a range of multiphase solidification problems, including eutectic solidification of a binary alloy, where multiple solid phases grow simultaneously in a cooperative manner. [1] A.N. Beris, B.J. Edwards, *Thermodynamics of Flowing Systems: With Internal Microstructure*, Oxford Engineering Science Series, OUP, USA, 1994. [2] P.C. Bollada, P.K. Jimack, A.M. Mullis, Bracket formalism applied to phase field models of alloy solidification, *Computational Materials Science* 126:426–437, 2017.

## Estimation of Bridge Frequency from Traversing Vehicle by Short-time Stochastic Subspace Identification

Nan Jin<sup>\*</sup>, Themelina S. Paraskeva<sup>\*\*</sup>, Elias G. Dimitrakopoulos<sup>\*\*\*</sup>, Lambros S. Katafygiotis<sup>\*\*\*\*</sup>

<sup>\*</sup>Hong Kong University of Science and Technology, Department of Civil and Environmental Engineering, Clear Water Bay, Kowloon, Hong Kong, <sup>\*\*</sup>Hong Kong University of Science and Technology, Department of Civil and Environmental Engineering, Clear Water Bay, Kowloon, Hong Kong, <sup>\*\*\*</sup>Hong Kong University of Science and Technology, Department of Civil and Environmental Engineering, Clear Water Bay, Kowloon, Hong Kong, <sup>\*\*\*\*</sup>Hong Kong University of Science and Technology, Department of Civil and Environmental Engineering, Clear Water Bay, Kowloon, Hong Kong

### ABSTRACT

The eigenfrequencies of the bridge are important for various engineering applications, such as the health monitoring and the damage detection of the bridge. Over the past decade, there is a growing interest in an “indirect” approach to extract the bridge dynamic properties from vibration of the traversing vehicles. Compared with the traditional technique of installing sensors at multiple locations on the bridge, this approach is more economical, time-saving, portable and most importantly, applicable to every bridge. The traversing vehicle plays the role of a “vibration shaker” exciting the bridge, and at the same time is also a “receiver” collecting information from the bridge. Thus, it is feasible to extract modal parameters of the bridge by processing the vibration response of the vehicle. In general, the frequencies of the bridge and the traversing vehicle are not strictly constant, if the interaction between the two sub-systems and the mass of the vehicle is non-ignorable. However, their time variations are by far longer than their dynamics. For such a time-variant system, the Short-time Stochastic Subspace Identification (ST-SSI) method is proposed to extract the bridge frequencies from the vibration response and the dynamic characteristics of the traversing vehicle. Specifically, the present study assesses the accuracy and the effectiveness of the ST-SSI method that is used to identify the frequencies of a straight reinforced concrete bridge, from the vibration response of a traversing vehicle. As a proof of concept, herein the response of the vehicle is estimated from the vehicle-bridge interaction dynamic analysis. The dynamic characteristics of the vehicle are assumed known. For the needs of the ST-SSI method, the equations of motion for the vehicle and the bridge are discretized in state space, and then transformed to a series vectors by separating the known vehicle-related parameters from the unknown parameters. Finally, the observability matrix containing the bridge dynamic properties is derived by linear algebra techniques, including the Hankel matrix, LQ decomposition, orthogonal projection and singular value decomposition. The bridge frequencies identified with the proposed ST-SSI method are validated against the theoretically correct values, and conclusions regarding the feasibility of the method are drawn.

## **Bending Analysis of Multilayered Composite Beams in Terms of a New Mixed Global-local Higher-order Theory**

Qilin Jin<sup>\*</sup>, Weian Yao<sup>\*\*</sup>, Xiaofei Hu<sup>\*\*\*</sup>

<sup>\*</sup>Dalian University of Technology, Dalian, China, <sup>\*\*</sup>Dalian University of Technology, Dalian, China, <sup>\*\*\*</sup>Dalian University of Technology, Dalian, China

### **ABSTRACT**

Accurately predicting of the transverse shear stresses for multilayered composite structure based on the equivalent single-layer theory is still challenging. In the existing method, the complex post-processing procedure based on three dimensional (3D) equilibrium equation was used. Thus, an improved equivalent single-layer theory which describe transverse shear stresses of multilayered composites accurately is expected. In this study, an accurate and computationally attractive mixed-form global-local higher-order theory (MGLHT) is developed for the bending analysis of multilayered composite beams. The theory is derived using the kinematic assumptions of global-local higher-order theory (GLHT) and employs the Reissner mixed variational theorem (RMVT). Moreover, the MGLHT retains a fixed number of displacement variables regardless of the number of layers. The benefit of the proposed MGLHT over the GLHT is that no post-processing approach is needed to accurately calculate the transverse shear stresses. The equilibrium equations and analytical solution of the present model can be obtained based on the Reissner mixed variational equation. The effects of transverse shear stress on the displacements and in-plane stress have been investigated in detail. Numerical results show that the transverse shear stresses can be accurately determined from the proposed model. In addition, the transverse shear stresses derived from the RMVT have a slight effect on displacements and in-plane stress for symmetric beams. For antisymmetric beams, such effect on transverse displacement and in-plane stress is slight, but it is significant on in-plane displacement.

## **A Comparative Study of Modeling Shear Band Propagation via Embedded Weak Discontinuity with Global, Local and No-tracking Strategies in Three Dimensions**

Tao Jin<sup>\*</sup>, Hashem Mourad<sup>\*\*</sup>, Curt Bronkhorst<sup>\*\*\*</sup>

<sup>\*</sup>Los Alamos National Laboratory, <sup>\*\*</sup>Los Alamos National Laboratory, <sup>\*\*\*</sup>Los Alamos National Laboratory

### **ABSTRACT**

A tracking strategy has been proposed by Oliver et al. [1] to ensure the continuous propagation of discontinuity surfaces in three dimensions (3D). The basic idea of this strategy is to solve a heat-conduction type boundary value problem for a family of isosurfaces of a scalar level set function as the potential discontinuity surface in the same discretized domain of the mechanical problem. In literature, this strategy has been implemented locally (the local tracking) [2] and globally (the global tracking) [3] to model Mode I fracture via the embedded strong discontinuity. In this research, for the first time we manage to integrate the tracking strategy with the embedded weak discontinuity approach to model shear band propagation that mimics Mode II fracture in the context of explicit finite element formulation. The algorithmic and implementation details regarding the global and local tracking strategies are provided. By comparing the numerical results obtained from simulations using the global, local and no-tracking strategies with the experimental results of the split-Hopkinson pressure bar test, we demonstrate the necessity of ensuring the continuity of the shear band surface to treat shear band propagation. Moreover, we discuss the suitability and the computational cost related to the global and local tracking strategies through several numerical examples. [1]. Oliver, J., Huespe, A.E., Samaniego, E., Chaves, E.W.V., 2002. On strategies for tracking strong discontinuities in computational failure mechanics. Proceedings of the Fifth World Congress on Computational Mechanics (WCCM V), July 7-12, 2002, Vienna, Austria Mang HA, Rammerstorfer FG, Eberhardsteiner J (eds). [2]. Armero, F., Kim, J., 2012. Three-dimensional finite elements with embedded strong discontinuities to model material failure in the infinitesimal range. *Int. J. Numer. Methods Eng.* 91, 1291–1330. [3]. Linder, C., Zhang, X., 2013. A marching cubes based failure surface propagation concept for three-dimensional finite elements with non-planar embedded strong discontinuities of higher-order kinematics. *Int. J. Numer. Methods Eng.* 96, 339–372.

## Simulation of the Cutting Process in Softening and Hardening Soils

Zhefei Jin<sup>\*</sup>, James Hambleton<sup>\*\*</sup>

<sup>\*</sup>Northwestern University, <sup>\*\*</sup>Northwestern University

### ABSTRACT

Ploughing and cutting processes in soils are difficult and inefficient to simulate using conventional approaches, such as the finite element method and discrete element method, due to the occurrence of extremely large, potentially discontinuous plastic deformation. Recently, a numerical technique for modeling this process in sands was proposed by Kashizadeh and Hambleton [1] and Hambleton et al.[2]. This approach is based on incremental plastic analysis, which has high efficiency and stability to capture the essential physics and features of the problem. The present study refines this technique in two key respects. Firstly, a shear band with finite thickness is incorporated in the new model, thus introducing a key length scale and parameter that influences the predicted deformed shape. Secondly, and more importantly, a more sophisticated material law is implemented. The effects of hardening and softening, as well as the dilatancy and compaction within the shear band, are introduced. With the modified model, it is observed in the case of hardening (compaction) that the occurrence of multiple successive shear bands appearing at variable locations gives the impression of continuous shearing. This is markedly different from the previously predicted response in the case of softening (dilatancy). In that case, the shear bands appear at distinct locations, and the transition from one location to the next is reflected in distinct peaks in the force-displacement history [1,2]. In the more general case, where an initial hardening phase is followed by softening, only one peak force is obtained in the modified model. The computational results are compared with some preliminary experimental data obtained in the Soil-Structure and Soil-Machine Interaction Laboratory at Northwestern University, which utilizes a six-axis robot for actuation and data acquisition. [1] Kashizadeh, E., Hambleton, J.P., and Stanier, S.A. (2014). A numerical approach for modelling the ploughing process in sands. Proc. 14th International Conference of the International Association for Computer Methods and Advances in Geomechanics, Kyoto, Japan, Sept. 22-25, pp. 159-164. [2] Hambleton, J.P., Stanier, S.A., White, D.J., and Sloan SW. (2014). Modelling ploughing and cutting processes in soils. Australian Geomechanics, 49(4), 147-156.

## Eigenspace-Based Characterization of Structural Uncertainty in Large-Eddy Simulation Closures

Lluís Jofre<sup>\*</sup>, Stefan Domino<sup>\*\*</sup>, Gianluca Iaccarino<sup>\*\*\*</sup>

<sup>\*</sup>Stanford University, <sup>\*\*</sup>Sandia National Laboratories, <sup>\*\*\*</sup>Stanford University

### ABSTRACT

Large-eddy simulation (LES) has gained significant importance as a high-fidelity technique for the numerical resolution of complex turbulent flow. In comparison to direct numerical simulation (DNS), LES approaches reduce the computational cost of solving turbulent flow by removing small-scale information from the conservation equations via low-pass filtering. However, the effects of the small scales on the resolved flow field are not negligible, and therefore their contribution in the form of subgrid-scale (SGS) stresses needs to be modeled. As a consequence, the assumptions introduced in the closure formulations result in potential sources of structural uncertainty that can affect the quantities of interest (QoI). Therefore, the aim of this work is to characterize their model-form uncertainty and its impact on the QoIs by means of recently developed eigenspace-based strategies [1,2,3] that decompose the SGS stress tensor in terms of magnitude (trace), shape (eigenvalues) and orientation (eigenvectors) to facilitate the analysis. In the presentation, the strategy will be described in detail and investigations based on filtered DNS and LES of turbulent free shear flow will be discussed. [1] L. Jofre, S. P. Domino, and G. Iaccarino. A framework for characterizing structural uncertainty in large-eddy simulation closures. *Flow Turbulence and Combustion*, 1-23, 2017. [2] G. Iaccarino, A. A. Mishra, and S. Ghili. Eigenspace perturbations for uncertainty estimation of single-point turbulence closures. *Physical Review Fluids* 2, 024605. [3] M. Emory, J. Larsson, and G. Iaccarino. Modeling of structural uncertainties in Reynolds-averaged Navier-Stokes closures. *Physics of Fluids* 25, 110822, 2013.

## Multimesh: Finite Element Methods on Arbitrarily Many Intersecting Meshes

August Johansson\*, Mats Larson\*\*, Anders Logg\*\*\*, Benjamin Kehlet\*\*\*\*

\*Simula Research Laboratory, \*\*Umea University, \*\*\*Chalmers University of Technology, \*\*\*\*Simula Research Laboratory

### ABSTRACT

We will present a framework for expressing finite element methods on arbitrarily many intersecting meshes: multimesh finite element methods [1]. The framework enables the use of separate meshes to discretize parts of a computational domain, such as the components of an engine, the domains of a multiphysics problem, or solid bodies interacting under the influence of forces from surrounding fluids or other physical fields. Multimesh finite element methods are particularly well suited to problems in which the computational domain undergoes large deformations as a result of the relative motion of the separate components of a multi-body system. This is a challenging situation if one would use a single mesh. The key feature of the framework is that arbitrarily many (but finite) meshes are allowed to intersect. To make this possible, accurate quadrature rules for performing the necessary volume and boundary integrals are crucial. We will in this talk present a novel procedure to systematically construct quadrature rules with appropriate positive and negative weights using a basic result from combinatorics. Furthermore, suitable stabilization are needed to ensure an optimal method also for elements of high order. Here we follow [2]. The condition at the interface (continuity) is enforced weakly by the Nitsche method. In the presentation, we formulate the multimesh finite element method for the Poisson equation and show that it is optimal and stable. We also present numerical examples to demonstrate the optimal order convergence also for high order elements, optimal conditioning of the linear system, the numerical robustness of the formulation and implementation, as well as the applicability of the methodology. [1] Johansson, A., Larson, M.\ G., Logg, A and Kehlet, B. \textit{MultiMesh: Finite Elements on Arbitrarily Many Intersecting Meshes}. In preparation, 2017. [2] Johansson, A., Larson, M.\ G., and Logg, A. \textit{High order cut finite element methods for the Stokes problem}. Advanced Modeling and Simulation in Engineering Sciences, Vol.\ \textbf{2}, 2015.

## On the Modelling of Technical Rubber Regarding Multiphysical Environmental Conditions

Michael Johlitz\*, Alexander Lion\*\*

\*Institute of Mechanics, Bundeswehr University Munich, Germany, \*\*Institute of Mechanics, Bundeswehr University Munich, Germany

### ABSTRACT

In more or less all thinkable applications, polymer parts are thermomechanically loaded and exposed to different environmental media. In the most general case, the loadings are time-dependent and nonstationary and the composition of the media can change. An example is a hydraulic tube of a dredge which consists of fibre reinforced elastomers. The outer side of the tube is surrounded by water, dry or by humid air with a time-dependent temperature and its inner side is in contact with hydraulic oil whose temperature and pressure are time-dependent too. The outer side is also commonly also exposed to electromagnetic radiation like UV. The combination of all these influences leads to diffusion, dissolution, physicochemical reactions and changing material properties of the polymer. In order to simulate such phenomena with numerical methods, it is necessary to combine the theory of continuum mechanics with thermodynamics, chemistry and material transport. Due to the complex nature of these problems, it is impracticable to formulate one single model that can take all possible phenomena into account. As a good starting point, the thermomechanical balance equations are formulated for an open system which consists of only two materials: a deformable solid and a liquid. The liquid can diffuse into and out of the solid and can react with it. The diffusion is accompanied by reversible or irreversible swelling and changing material properties of the solid. Based on the structure of the balance relations and motivated by experience, a constitutive model for a suitable thermodynamic potential is developed and evaluated. For simplification, the dry solid is assumed to be nonlinearly elastic and the liquid to be non-viscous. The talk closes with the discussion of the final set of equations and some numerical simulations.

## Predicting Baseplate Preheating Effects on Residual Stress and Microstructure in LENS Parts

Kyle Johnson<sup>\*</sup>, Theron Rodgers<sup>\*\*</sup>, Shaun Whetten<sup>\*\*\*</sup>, Joseph Bishop<sup>\*\*\*\*</sup>, Phillip Reu<sup>\*\*\*\*\*</sup>, Kurtis Ford<sup>\*\*\*\*\*</sup>, Michael Stender<sup>\*\*\*\*\*</sup>, Lauren Beghini<sup>\*\*\*\*\*</sup>

<sup>\*</sup>Sandia National Laboratories, <sup>\*\*</sup>Sandia National Laboratories, <sup>\*\*\*</sup>Sandia National Laboratories, <sup>\*\*\*\*</sup>Sandia National Laboratories, <sup>\*\*\*\*\*</sup>Sandia National Laboratories, <sup>\*\*\*\*\*</sup>Sandia National Laboratories, <sup>\*\*\*\*\*</sup>Sandia National Laboratories, <sup>\*\*\*\*\*</sup>Sandia National Laboratories

### ABSTRACT

Additive Manufacturing (AM) has many potential benefits as a manufacturing technique such as complex shape production, rapid prototyping capability, and cost reduction. However, barriers to widespread adoption still exist in the form of detrimental effects like high residual stresses and non-uniform grain microstructures. Both of these effects are highly dependent on the extreme thermal gradients and high cooling rates found in the AM process. Prediction of the resulting residual stress profile and microstructure opens up many options for process optimization in order to tailor microstructure and stress profiles. This work presents methods of predicting the thermal, residual stress, and resultant microstructure for 304L stainless steel cylinders using the Laser Engineered Net Shape (LENS) AM process. The spatial and temporal evolutions of thermal history are first modeled using the Sierra finite element code. The thermal history is then used as input into a solid mechanics simulation in which material is deposited and builds residual stress upon cooling due to thermal strain. The material constitutive behavior is modeled using the Bammann-Chiesa-Johnson temperature and history-dependent viscoplastic internal state variable model. In addition to room temperature, four additional baseplate preheat temperatures up to 450°C were then modeled to investigate the effect on residual stress. Corresponding builds were produced and relaxation-based residual-stress measurement techniques were used to compare results to those predicted by the simulations. Finally, the thermal model is used in a Potts Kinetic Monte Carlo simulation using the SPPARKS code suite. Grain formation and solid-state evolution is predicted by using a cubic lattice of sites with grain “spins” that switch to neighboring spins based on a temperature-dependent grain mobility. Rapid grain growth occurs in the high thermal gradients near the melt pool and decreases with distance. The microstructure predictions for each preheat temperature are presented, along with experimental results. Sandia National Laboratories is a multitechnology laboratory managed and operated by National Technology and Engineering Solutions of Sandia LLC, a wholly owned subsidiary of Honeywell International Inc. for the U.S. Department of Energy’s National Nuclear Security Administration under contract DE-NA0003525.

## Peridynamics Modelling of Weibull-Type Behaviour in Ceramic Nuclear Fuel Pellets

Lloyd Jones\*, Glyn Rossiter\*\*, Mark Wenman\*\*\*

\*Imperial College London, \*\*National Nuclear Laboratory (UK), \*\*\*Imperial College London

### ABSTRACT

During operation, nuclear fuel experiences large temperature changes, with a steep thermal gradient from the hot centre to the cooler surface. Some information may be gleaned from in situ measurements at test reactors, and some from studying fuel once it is removed from service. Both of these options are expensive and limited. Computer models potentially allow for much greater insight into the processes that damage fuel, and those that allow it to function properly. Since uranium dioxide (UO<sub>2</sub>) fuel is ceramic, its fracture behaviour should be well described by Weibull theory, also known as weakest link theory. Weibull theory posits that ceramic fracture is caused by cracks nucleating on microscopic flaws. Since these flaws are of a distribution of sizes, the fracture strength of ceramics follow a similar distribution. Peridynamics is well suited to modelling this problem due to its strengths in handling discontinuities. Randomisation of bond strengths is common in peridynamics(1). In this work, a link is made between the random properties of ceramics and the random strengths of the peridynamics bonds. The problems with simple randomisation methods are discussed, and a method for recreating Weibull characteristics in peridynamics simulations is presented. REFERENCES 1. Oterkus S, Madenci E. Peridynamic modeling of fuel pellet cracking. Eng Fract Mech. 2017 May 1;176:23–37. ?

## Modeling Material Variability with Uncertainty Quantification and Machine Learning Techniques

Reese Jones<sup>\*</sup>, Francesco Rizzi<sup>\*\*</sup>, Jeremy Templeton<sup>\*\*\*</sup>, Jake Ostien<sup>\*\*\*\*</sup>, Coleman Alleman<sup>\*\*\*\*\*</sup>, Moe Khalil<sup>\*\*\*\*\*</sup>, Ari Frankel<sup>\*\*\*\*\*</sup>

<sup>\*</sup>Sandia, <sup>\*\*</sup>Sandia, <sup>\*\*\*</sup>Sandia, <sup>\*\*\*\*</sup>Sandia, <sup>\*\*\*\*\*</sup>Sandia, <sup>\*\*\*\*\*</sup>Sandia, <sup>\*\*\*\*\*</sup>Sandia

### ABSTRACT

Material variability originating from heterogeneous microstructural features, such as grain and pore morphologies, can have significant effects on component behavior and creates uncertainty around performance. Current engineering material models typically do not incorporate microstructural variability explicitly, rather functional forms are chosen based on intuition and parameters are selected to reflect mean behavior. Conversely, mesoscale models that capture the microstructural physics, and inherent variability, are impractical to utilize at the engineering scale. An enhanced design methodology must be developed for materials with significant variability, such as current additively manufactured metals. To address these challenges we have developed a method based on the Embedded Uncertainty formulation of Sargsyan, Najm, and Ghanem (2015) to calibrate distributions of material parameters from high-throughput experimental data. With this method, material variability is directly associated with commonly-used material parameters using a chosen nominal model. One of the benefits of this approach is that expert knowledge can be extended to interpret the effect of (hidden) microstructure on variable mechanical response. In a complementary effort, we are also developing machine learning techniques to handle the large volume of data from high-throughput methods. The focus of this aspect of the work is on adapting common machine learning models, such as neural networks, to obey the same exact properties and symmetries as traditional constitutive models while representing features in the data in a flexible, bias-less manner. Sandia National Laboratories is a multi-mission laboratory managed and operated by National Technology and Engineering Solutions of Sandia, LLC., a wholly owned subsidiary of Honeywell International, Inc., for the U.S. Department of Energy's National Nuclear Security Administration under contract DE-NA-0003525

## A Particle Based Modelling Approach for Predicting Charge Dynamics in Tumbling Ball Mills

Pär Jonsén<sup>\*</sup>, Simon Larsson<sup>\*\*</sup>, Bertil Pålsson<sup>\*\*\*</sup>, Samuel Hammarberg<sup>\*\*\*\*</sup>, Göran Lindkvist<sup>\*\*\*\*\*</sup>

<sup>\*</sup>Division of Mechanics of Solid Materials, Luleå University of Technology, Sweden, <sup>\*\*</sup>Division of Mechanics of Solid Materials, Luleå University of Technology, Sweden, <sup>\*\*\*</sup>Minerals and Metallurgical Engineering, Luleå University of Technology, Sweden, <sup>\*\*\*\*</sup>Division of Mechanics of Solid Materials, Luleå University of Technology, Sweden, <sup>\*\*\*\*\*</sup>Division of Mechanics of Solid Materials, Luleå University of Technology, Sweden

### ABSTRACT

Wet grinding of minerals in tumbling mills is a highly important process in the mining industry. During grinding in tumbling mills, lifters submerge into the charge and create motions in the ball charge, the lifters is exposed for impacts and shear loads that will wear down the lifters. Increased loading can accelerate the wear and the lining has to be replaced. Replacing the lining is an expensive and time consuming operation that is preferred to be done within planned maintenance stops. Prediction of the charge motion and wear rate for different grinding operations and linings are therefore desirable to predict the lining life. Modelling of wet grinding in tumbling mills that include pulp fluid and its interaction with both the grinding balls and the mill structure is an interesting challenge and some different approaches have been suggested, see [1-2]. For an effective and successful prediction, the numerical model has to be able to handle the pulp fluid and its simultaneous interactions with both the ball charge and the mill structure, in a computationally efficient approach. In this work, the pulp fluids are modelled with a Lagrange based method called incompressible computational fluid dynamics, (ICFD), which gives the opportunity to model free surface flow. This method gives robustness and stability to the fluid model and is efficient as it gives possibility to use larger time steps than the conventional CFD. The ICFD solver can be coupled to other solvers as in this case the finite element method, (FEM) solver for the mill structure and the discrete element method (DEM) solver for the ball charge. The combined ICFD-DEM-FEM model can predict both charge motion and responses from the mill structure, as well as the pulp liquid flow and pressure. The numerical grinding case presented here is validated against experimentally measured driving torque signatures from an instrumented small-scale batch ball mill, see [3]. This approach opens up the possible to predict the volume of the high-energy zone and optimise lifter design and operating conditions. The ICFD solver show improve efficiency and robustness for studying tumbling mill systems and can predict the charge dynamics in such systems. [1] Jonsén, P. et al., Minerals Engineering. Accepted publication [2] Jonsén, P., Stener, J.F., Pålsson, B.I. and Häggblad, H.-Å., Min. Eng., Vol. 73, 77–84, 2015. [3] Jonsén, P. Stener, J. F. Pålsson, B. I. and Häggblad, H.-Å., Minerals and Metallurgical Processing, vol. 30, No. 4, 220-225, 2013.

## Mixed Nonlinear Localization: Two-Scale Approximation of the Robin Parameter

Hinojosa Jorge\*, Saavedra Karin\*\*

\*Universidad de Talca, Chile., \*\*Universidad de Talca, Chile.

### ABSTRACT

Performing nonlinear analysis of large structures at fine scale is one of the industrial challenges of our times. The post-buckling analysis of aeronautical structures is a typical example. During the structural tests for certification achieved on complete fuselages of aircraft, local buckling of the skin between stiffeners occurs. For increasing loads, these nonlinear areas can expand and provoke redistributions of stresses in the structures. For workloads usually met in service, these phenomena are reversible, the material remaining in the elastic domain. However, they can provoke stress concentrations at the bases of stiffeners and may be at the origin of local damages leading to global failure. The idea of the nonlinear localization strategy [1, 2, 3] is the treatment of the localized nonlinearities at the subdomain level, avoiding dealing with a high number of different local buckling modes, improving the robustness of the method. The other point on this strategy is to use a mixed domain decomposition scheme in order to favour neither the displacement continuity, which is a too stiff condition, nor the interface equilibrium, but a combination of both (a Robin-like condition). This mixed scheme shares similar features with continuation methods to control the algorithm convergence. In previous works [1] was shown that the decomposition choice could lead to different equilibrium paths depending on the followed "numerical" path. When a subdomain that buckles is decomposed into two subdomains its behaviour could be modified leading to a different solution. In [1] it also has been shown the convergence equilibrium of a stiffened panel when skin buckling occurs, showing a 5-lobes buckling for the non-subdivided subdomain and 4-lobes for the subdivided subdomain. Also, the equilibrium path are consequently different and the global buckling deformed shape are different as well as the global compressive behaviour, reducing the final load in 30%. In this work, we focus on the choice of dedicated Robin operator for common industrial features. A two-scale approximation [2] is implemented. [1] Hinojosa J, Allix O, Guidault P-A, Cresta P. "Domain decomposition methods with nonlinear localization for the buckling and post-buckling analyses of large structures". *Advances in Engineering Software*. 2014;70:13-24 [2] Gendre L, Allix O, Gosselet P. "A two-scale approximation of the Schur complement and its use for non-intrusive coupling". *International Journal for Numerical Methods in Engineering*. 2011;87(9):889-905.

## **Coarse-grained Twinning Characteristics for Crystal Plasticity Gleaned from Atomistic Simulations**

Shailendra Joshi\*

\*University of Houston

### **ABSTRACT**

We employ molecular dynamics (MD) simulations to investigate the evolution of extension twinning in magnesium single crystals under a range of multi-axial loading. The objective is to understand the evolution of variant twin volume fraction and number of twins, which enable describing the evolution of the twinning at the coarser, crystal plasticity length-scales. We investigate the role of stress state in the activation and interaction between different twin variants through signatures of nucleation, growth, coalescence and detwinning. Significant dislocation plasticity occurs on basal and prismatic  $\langle a \rangle$  slip systems during and after twinning. Prior to coalescence phase, twinning volume fraction exhibits an exponentially decaying distribution. We propose phenomenological formulae for the evolution of volume fraction and number of twins, which should serve as a starting point for constructing improved coarse-grained crystal plasticity models for twinning.

## **Gradient Crystal Plasticity Modeling of Twin Boundary Migration Effects on Deformation Stability in Nanotwinned Metals**

Shailendra Joshi\*

\*University of Houston

### **ABSTRACT**

Our ongoing work is to understand the role of twin boundaries (TBs) in the deformation and failure characteristics of nanotwinned (NT) materials. To that end, we implemented a gradient crystal plasticity model within a finite element framework, which accounts for slip and slip rate gradients that are intrinsically coupled to TB migration. Using this framework, we extract intricate coupling between TB migration and twin size, load orientation and the energy barrier of dislocation-TB interactions. The resulting kinetic relation is then adopted in probing the size-dependent stress-strain responses and microstructural instabilities in polycrystalline NT materials without explicitly modeling twins.

## A 3D Partitioned Coupled Variational Formulation for Multifield and Multiphase Modeling

Vaibhav Joshi<sup>\*</sup>, Rajeev K. Jaiman<sup>\*\*</sup>, Pardha S. Gurugubelli<sup>\*\*\*</sup>

<sup>\*</sup>National University of Singapore, <sup>\*\*</sup>National University of Singapore, <sup>\*\*\*</sup>National University of Singapore

### ABSTRACT

A 3D coupled variational framework has been proposed to solve a nonlinear dynamical multifield problem of multiphase turbulent fluid flow interacting with a flexible multibody dynamic system. The proposed coupled solver is motivated by the modeling of offshore vessel-riser system which is exposed to harsh environmental conditions, viz, free-surface ocean waves and high velocity ocean currents. The dynamical response of such offshore system can be quite challenging due to strong two-way interaction of the vortex-induced vibration of riser and the wave-induced motion of vessel. We address three key numerical challenges in the proposed variational coupled formulation: (i) stable and robust coupling of incompressible turbulent flow with a system of nonlinear elastic bodies described in a co-rotated frame, (ii) a conservative and positivity preserving two-phase coupling based on the phase-field approach, and (iii) the stable integration of phase-field solver with fluid-flexible multibody solver involving moving boundaries. In the proposed formulation, the modeling of the air-water interface is accomplished by the positivity preserving variational method [1] applied to the conservative Allen-Cahn phase-field equation [2] and the turbulence is modeled by Delayed Detached Eddy Simulation [3]. The structural domain consisting of multibodies is solved using a nonlinear co-rotational method, whereas the fluid domain is solved by the Petrov-Galerkin variational method. The flow, turbulence and two-phase equations are written in an arbitrary Lagrangian-Eulerian (ALE) framework which takes into effect the moving boundaries of the structure. This multifield formulation consisting of fluid, structure, turbulence, two-phase and ALE, is solved in a partitioned iterative implicit manner. The partitioned scheme utilizes the nonlinear iterative force correction at the fluid-structure interface for stability at low structure-to-fluid mass ratios typically found in the offshore systems. We verify accuracy and robustness of our formulation on simple and reproducible academic examples and applicability to large-scale scenario of offshore vessel-riser system interacting with ocean waves and current flow. References: [1] Joshi, V. and Jaiman, R.K., A positivity preserving variational method for multi-dimensional convection-diffusion-reaction equation. *Journal of Computational Physics*, 339, Pg. 247-284 (2017). [2] Joshi, V. and Jaiman, R.K., A positivity preserving and conservative variational scheme for phase-field modeling of two-phase flows. *Journal of Computational Physics*, Accepted for publication (2018). [3] Joshi, V. and Jaiman, R.K., A variationally bounded scheme for delayed detached eddy simulation: Application to vortex-induced vibration of offshore riser. *Computers and Fluids*, 157, Pg. 84-111 (2017).

## Goal-oriented Adaptivity for Micromorphic Problems Based on Duality Techniques

Xiaozhe Ju<sup>\*</sup>, Rolf Mahnken<sup>\*\*</sup>

<sup>\*</sup>University of Paderborn, <sup>\*\*</sup>University of Paderborn

### ABSTRACT

It is well-known that the classical Cauchy-Boltzmann continuum, in spite of its simplicity, has its limitations, e.g. on the simulation of strain localization phenomena or size effects. For a remedy, one may resort to the so-called generalized continuum theories, see e.g. [1] and references therein. Amongst others, we consider a class of higher order continua, namely the micromorphic continua, where the kinematics is enriched by means of a microstructure undergoing an affine micro deformation. The increasing number of the degrees of freedom in such a theory clearly motivates an application of adaptive methods. In this contribution, we present a general framework of goal-oriented adaptivity for such kind of problems. To this end, we derive a goal-oriented error estimator, leading to an effective adaptive method for controlling the discretization errors of the finite element method. For illustration, we address both elasticity and plasticity problems. For linear elastic micromorphic problems, we show the consistency of the resulted dual problem, ensuring an optimal convergence order, see [2]. For plasticity (time-dependent) problems, as shown in [3], we construct a specific dual problem tracking backwards in time to account for the accumulation of errors over time. Additionally, numerical examples are shown. References: [1] T. Dillard, S. Forest, P. Ienny: Micromorphic continuum modelling of the deformation and fracture behaviour of nickel foams, *European Journal of Mechanics A/Solids* 25, 526-549 (2006). [2] X. Ju, R. Mahnken: Goal-oriented adaptivity for linear elastic micromorphic continua based on primal and adjoint consistency analysis, *Int. J. Numer. Meth. Engng.* 112, 1017-1039 (2017). [3] M. Schmich, B. Vexler: Adaptivity with dynamic meshes for space-time finite element discretizations of parabolic equations, *SIAM J. Sci. Comput.* 30(1), 369-393 (2008).

## Towards Efficient Isogeometric Matrix Assembly: Partial Tensor Decomposition and Numerical Quadrature Rules for Trimmed Domains

Bert Juettler<sup>\*</sup>, Angelos Mantzaflaris<sup>\*\*</sup>, Felix Scholz<sup>\*\*\*</sup>

<sup>\*</sup>Johannes Kepler University, Linz, <sup>\*\*</sup>Johannes Kepler University, Linz, <sup>\*\*\*</sup>RICAM, Austrian Academy of Sciences

### ABSTRACT

The efficient assembly of matrix elements for isogeometric simulations poses many challenging problems. On the one hand, the high polynomial degrees and the large overlap of the basis functions motivates the use of new approaches to achieve computational efficiency. Among the various approaches to address this issue, we mention the use of special numerical integration techniques for spline functions [1]. On the other hand, the use of trimming operations increases the geometric complexity of the domains. Consequently, there is a need to develop suitable techniques for numerical integration. More information is provided in the survey article [2]. The talk reports on two recent developments to address these two issues. First, we describe the method of partial tensor decomposition, which allows to increase the efficiency of numerical quadrature by systematically exploiting the tensor-product structure of isogeometric discretizations, thereby reducing the dimension of the occurring integrals. Compared to the full decomposition approach, which has been established in [3], it is easier to implement, since it relies entirely on standard techniques from numerical linear algebra. It also provides a further reduction of the computational costs when used in connection with h-refinement. Second, we show how to derive special quadrature rules for trimmed domains by considering the implicit representation of the trimming curves and surfaces. This representation can be obtained via (exact or approximate) implicitization. Based on the implicit form, we use linearization to simplify the trimmed elements. Our quadrature rules combine integration over the simplified trimmed element with an integration of an auxiliary function over the linearized cutting curve or surface. The latter integration gives a correction term that restores the required order of convergence. This approach allows us to perform numerical quadrature on trimmed domains without having to compute intersections explicitly. Both methods have been implemented in the G+Smo C++ library [4].

References [1] R.R. Hiemstra, F. Calabro, D. Schillinger, T.J.R. Hughes: Optimal and reduced quadrature rules for tensor product and hierarchically refined splines in isogeometric analysis, *Comp. Meth. Appl. Mech. Engrg.* 316 (2017), 966-1004. [2] B. Marussig, T.J.R. Hughes: A Review of Trimming in Isogeometric Analysis: Challenges, Data Exchange and Simulation Aspects, *Archives of Computational Methods in Engineering*, in press (2017), doi 10.1007/s11831-017-9220-9. [3] A. Mantzaflaris, B. Juettler, B.N. Khoromskij, U. Langer: Low-rank tensor methods in Galerkin-based isogeometric analysis, *Comp. Meth. Appl. Mech. Engrg.* 316 (2017), 1062-1085. [4] *Geometry + Simulation Modules*, gs.jku.at/gismo.

## Architected Piezoelectrics for Dynamic Control of Mechanical Wave Propagation

Abigail Juhl<sup>\*</sup>, Carson Willey<sup>\*\*</sup>, Vincent Chen<sup>\*\*\*</sup>, Phillip Buskohl<sup>\*\*\*\*</sup>

<sup>\*</sup>Air Force Research Laboratory, <sup>\*\*</sup>Air Force Research Laboratory, <sup>\*\*\*</sup>Air Force Research Laboratory, <sup>\*\*\*\*</sup>Air Force Research Laboratory

### ABSTRACT

Periodically repeating resonant substructures are the building blocks of many acoustic metamaterials and phononic crystals. The usefulness of a component made from such an array of unit cells is that the vibratory, or wave propagation behavior can be engineered to create frequency bands in which mechanical motion is forbidden, or highly attenuated, termed bandgaps. One major drawback of producing bandgaps through structural design is that the bandgap is fixed once the structure is decided upon leaving no opportunity for bandgap reconfiguration. In order to create a tunable bandgap structure some portion of the locally resonant unit cells must be variable and controllable by outside, preferably remote, stimulus. An approach for tuning a structure experiencing forces or practical origin and magnitude is the use of piezoelectric elements acting as electrically tunable stiffness and damper elements. Due to the difficulty in fabricating complex architectures in piezoelectric materials and integrating electrodes, research in this area has been mostly theoretical, or limited to 1D plates or patches of piezoelectrics. This talk will focus on steps made towards simulating structures augmented by the addition of shunted piezoelectric patches for the suppression of particular structural mode shapes.

## Fast Spectral Solvers without Linear Reference Medium

Till Junge\*

\*École polytechnique fédérale de Lausanne

### ABSTRACT

In the field of computational homogenization of periodic representative volume elements (RVE), over the last two decades, fast Fourier transform (FFT)-based spectral solvers have emerged as a promising alternative to the finite element method (FE). Most of these spectral methods are based on the work of Moulinec and Suquet [1] and split an RVE's mechanical response into the response of a linear reference medium and a periodic fluctuation due to heterogeneities. The main advantage of this formulation over FE is that it can be both significantly faster and have a much smaller memory-footprint. The two main problems are 1) the choice of the linear reference medium, which is typically based on heuristics, is not trivial and has a strong impact on the method's convergence (A bad choice can render the method non-convergent), and 2) a high-frequency numerical artifact (Gibbs ringing) around areas of sharp phase contrast due to non-uniformly converging Fourier series coefficients. Numerous studies have suggested mitigations to both of these problems (e.g. [2]), but they have remained substantial disadvantages compared to the more expensive, but also more robust FE. Recent work by Zeman et al. [3] proposes a new formulation for spectral solvers which dispenses with the linear reference problem and converges unconditionally. We present  $\mu$ Spectre, an open implementation of this novel method and use it to show that the new approach is frequently more computationally efficient than its linear reference medium-based predecessors, converges in the presence of arbitrary phase contrast - including porosity - and eliminates or drastically reduces Gibbs ringing. [1] H. Moulinec and P. Suquet. A numerical method for computing the overall response of nonlinear composites with complex microstructure. *Computer Methods in Applied Mechanics and Engineering*, 157(1):69–94, 1998 [2] M. Kabel, T. Böhlke, and M. Schneider. Efficient fixed point and Newton-Krylov solvers for FFT-based homogenization of elasticity at large deformations. *Computational Mechanics*, 54:1497–1514, 2014 [3] J. Zeman, T. W. J. de Geus, J. Vondřejc, R. H. J. Peerlings, and M. G. D. Geers. A finite element perspective on non-linear FFT-based micromechanical simulations. *International Journal for Numerical Methods in Engineering*, 2016

## IGA-BEM for Lifting Flows

PANAGIOTIS KAKLIS\*, SOTIRIOS CHOULIARAS\*\*, CONSTANTINOS POLITIS\*\*\*,  
ALEXANDROS-ALVERTOS GINNIS\*\*\*\*, KONSTANTINOS KOSTAS\*\*\*\*\*

\*UNIVERSITY OF STRATHCLYDE, GLASGOW (UK), \*\*UNIVERSITY OF STRATHCLYDE, GLASGOW (UK),  
\*\*\*TECHNOLOGICAL EDUCATIONAL INSTITUTE OF ATHENS (GR), \*\*\*\*NATIONAL TECHNICAL UNIVERSITY  
OF ATHENS (GR), \*\*\*\*\*NAZARBAYEV UNIVERSITY, ASTANA (KZ)

### ABSTRACT

Combining Iso-Geometric analysis (IGA) with Boundary Element Methods (BEM) for inviscid lifting flows imposes a number of difficulties. Firstly, an IGABEM collocation scheme has to take into account the tangent-plane discontinuity occurring along the trailing edge (TE). More important, the scheme has to handle the non-linear Kutta condition, securing continuity of the normal velocity and pressure through the a-priori unknown wake, a force-free boundary surface emanating from TE. In this presentation we shall review the status of our work towards developing a pair of IGABEM collocation schemes for computing steady lifting flows around 2D and 3D bodies, e.g., hydrofoils, marine propellers; [1,2]. In the latter case, the ansatz functions are inherited from T-spline representations which are free from singularities occurring, e.g., at the tip of a propeller blade, when NURBS are used. [1] Kostas, K.V., Ginnis, A.-A. I., Politis, C.G., Kaklis, P.D, "Shape-optimization of 2D hydrofoils using an Isogeometric BEM solver", Computer-Aided Design, vol. 82, pp. 79-87, (2017). [2] Chouliaras, S.P., Kaklis, P.D., Ginnis, A.-A.I., Kostas, K.V., Politis, C.G., "An IGA-BEM method for the open-water marine propeller flow problem", International Conference on Isogeometric Analysis, Pavia (IT), 11-13 September 2017.

## Topology Optimization for Shape-Memory Alloys

ZILIANG KANG\*, Kai James\*\*

\*University of Illinois at Urbana-Champaign, Department of Aerospace Engineering, \*\*University of Illinois at Urbana-Champaign, Department of Aerospace Engineering

### ABSTRACT

Shape-memory alloys are a unique class of active materials, as some of them exhibit a bidirectional shape-memory effect. This effect enables shape memory alloys to deform and recover under a prescribed temperature cycle, which makes shape memory alloys an ideal material for use in self-actuated morphing applications. However, the most widely used titanium-based shape memory alloys have large electrical resistance when using joule heating from electrical current as a source of actuation. By contrast copper-based shape-memory alloys are efficient electrical conductors but they have poor deformation caused by the shape memory effect. Therefore, we present a novel method for the design of shape-memory activated structures based on a multimaterial topology optimization method, which aims to create structures that are manufacturable via 3D printing, and also exhibit desirable shape-memory effects. Assuming isotropy throughout the structure, we consider a two-dimensional stress-free problem in which we optimize the distribution of several distinct candidate materials plus a void phase to get optimal strain caused by the shape-memory effect, under a predetermined temperature cycle caused by joule heating. The thermomechanical response of the structures is modeled using nonlinear, multi-physics finite element analysis. The electrical conductivity and shape-memory transformation temperature of each finite element within the discretized structure are represented via a series of coefficient functions that implicitly define the material distribution. The design task is carried out using gradient-based optimization, with the design sensitivities obtained via adjoint sensitivity analysis. We demonstrate the proposed design framework using a series of two-dimensional thermomechanical benchmark problems. Keywords: shape-memory alloys, topology optimization, multimaterial optimization, multi-physics design

## The Contact Problem of a Two Deformable Orthotropic Elastic Solids

Aysegul KUCUKSUCU\*

\*Unfortunately, Bursa Orhangazi University, which was the university I worked, closed after 15th July 2016 coup attempt in Turkey. So, I could not write the name of the university.

### ABSTRACT

In this study, the contact problem of two deformable orthotropic solids is considered. The problem is solved by using analytical method. The Poisson's ratio of the cylinders are assumed to be constant and the contact is frictional, obeying the Coulomb law of dry friction with constant friction coefficient and the contact is assumed to be the Hertzian. In the formulation of the contact problem, it is assumed that the principal axes of orthotropy are parallel and perpendicular to the contact. Four independent engineering constants are replaced by a stiffness parameter, a stiffness ratio, a shear parameter, and an effective Poisson's ratio, Cauchy-type singular integral equations of the mixed-boundary value contact problem are prevailed using Fourier transform and solved numerically to obtain contact pressure and in-plane stress distribution. The analytical solution of the study presents correlation between contact stress and in-plane stress distributions and orthotropic material parameters, length parameters and the coefficient of friction.

## **Modelling and Simulation of Engineered Cementitious Composites with Shape Memory Alloy Fibres**

Mieczyslaw KUCZMA\*

\*Poznan University of Technology, Institute of Structural Engineering

### **ABSTRACT**

A thermodynamically consistent model for cementitious composites reinforced with shape memory fibres is considered. Cementitious composites, including concrete being the most used structural material, possess some inherent shortcomings. They are very weak in tension in comparison to their compressive strengths and are brittle materials with low ductility which results from development of micro-cracks. The addition of shape memory alloy fibres to cementitious composites will enhance their ductility and damping capacity. Shape memory alloys exhibit very large (up to 8-10%) recoverable strains, as a result of stress and temperature induced transformations between austenite and martensite phases. The SMA are smart materials which demonstrate unusual phenomena: the shape memory effect, and pseudoelasticity (superelasticity) with characteristic flag-shaped hysteresis loops in loading/unloading cycles. For cementitious matrix of the composite a constitutive model for concrete with progressive damage is used, whereas for the monolithic shape memory alloy fibre a constitutive model is applied that accounts for occurrence of three phases (austenite and two variants of martensite). The evolution law for volume fractions of martensite variants is derived from the second law of thermodynamics in Clausius-Duhem inequality form. From the computational point of view, the deformation process of the cementitious composite with shape memory fibres is discretized in space by the FEM and solved incrementally in time as an implicit strain driven problem (sequence of complementarity problems). Results of numerical simulations will illustrate the observed influence of shape memory alloy fiber reinforcement on the response of the cementitious composite.

## **Modelling and Simulation of Dynamic Fracture of Polycrystalline TiAl Alloys under High Velocity Particle Impact**

Mohammad Rizviul Kabir\*

\*German Aerospace Center

### **ABSTRACT**

Multi-phase polycrystalline TiAl alloys show complex fracture behaviour under high velocity particle impact (HVPI). The front-side damage and back-side crack networks are found to be microstructure sensitive, which implies that the local microstructure variations of this alloy may lead to unwanted blade failure during operation. Therefore, it is important to know how these microstructures influence crack initiation and crack propagation. To this aim in the present work a numerical modelling approach has been proposed that takes into account the microstructural statistics via polycrystal modelling and a combined damage and fracture ansatz for impact fracture behaviour. The polycrystal models were generated using Voronoi cells considering grain aspect ratio and texture. The grain boundaries were modelled applying thin cohesive layers between grains. Two types of microstructures have been studied; one with the globular grains and the other with elongated grains. The material data were obtained from detail experimental work [1]. The proposed approach allows a quantitative prediction of crack networks as observed by the experiments for different TiAl microstructures. Under dynamic impact, cracks mainly propagate through grain boundaries which have been captured using cohesive damage model. It was found that for globular grains star-shaped crack network was formed and for the elongated grains the crack extends longitudinally. The length of the crack branches can be studied for varying damage parameters at the grain boundaries. This information is useful for further analysis of fatigue life and durability of the TiAl alloy. [1] S. Gebhard, Partikel-Impact an  $\alpha$ -Titanaluminid-Legierungen. PhD Thesis, University of Stuttgart, Germany, 2011

## Phase Field Modeling of Fission Gas Bubble Growth in Nuclear Fuels

Amy Kaczmarowski<sup>\*</sup>, Dane Morgan<sup>\*\*</sup>, Shiva Rudraraju<sup>\*\*\*</sup>

<sup>\*</sup>Sandia National Laboratories, <sup>\*\*</sup>University of Wisconsin Madison, <sup>\*\*\*</sup>University of Wisconsin Madison

### ABSTRACT

Fission gas bubble growth is critical to the behavior of nuclear fuels in fission nuclear reactors. Bubbles can induce fuel swelling that could lead to fuel-cladding contact, generate increased stresses on the cladding and lead to undesired fuel-cladding chemical interactions. In addition, the bubbles also decrease the thermal conductivity of the fuel and thus effect the performance of the nuclear reactors. In this talk, we present a novel coupled phase field formulation for tracking bubble growth and the resulting deformation of the surrounding matrix material. The model demonstrates the application of moving Neumann conditions corresponding to the gas pressure from the equation of state, and its relative advantage over other relevant interface tracking methods. Numerical examples will demonstrate the evolution of mechanics and stress concentrations in single bubble and multiple bubble growth scenarios.

## NONLINEAR PHENOMENA OF SHORT AND LONG WAVELENGTH RAIL DEFECTS ON VEHICLE-TRACK INTERACTION

CHATPONG CHIENGSON\*, SAKDIRAT KAEWUNRUEN\*, AND AKIRA AIKAWA<sup>†</sup>

\*School of Engineering, The University of Birmingham  
52 Pritchatts Road  
Edgbaston B152TT United Kingdom

Email addresses: c.chiengson@gmail.com (C. Chiengson); s.kaewunruen@bham.ac.uk (S. Kaewunruen)

<sup>†</sup>Railway Dynamics Division, Railway Technical Research Institute  
Hikari-cho, Kokubunji  
Tokyo 185-8540 Japan  
Email address: aikawa.akira.11@rtri.or.jp

**Key words:** Dynamic interaction, Coupling vehicle-track modeling, short wavelength defect, long wavelength defect, coupled rail surface defects.

**Abstract.** Every day, over 100 million of train traffics are being operated globally. The first priority in train operation management is ‘*safety*’. During each operation, the dynamic interactions between vehicle and track usually impose vibrations and acoustic radiations and become a moving source of vibroacoustics along the railway network. Especially when there is imperfection of either wheel or rail, the dynamic amplification of loading conditions and reflected vibration effects on infrastructure and rolling stocks is significantly higher. In practice, imperfection of rail tracks is inevitable and can be classified into short wave length and long wave length defects. The imperfections can statistically induce high-intensity impact loadings up to 25% of *annual* track loading conditions. The short wavelength defects include high-frequency related rail surface defects such as dipped joint rails, rail squats, rolling contact fatigues (RCFs), rail gabs and crossing noses. The long wavelength defects are those associated with low frequency vibrations such as differential track settlement, mud pumping, bridge ends, stiffness transition zone, etc. Most previous studies into vehicle-track interactions were concerned only to a single one of the defect separately. This study is the world first to evaluate the coupling dynamic vehicle-track interactions over coupled short and long wavelength rail defects. The vehicle model has adopted multi degrees of freedom coupling with a discrete supported track model using Herizian contact theory. This paper highlights the nonlinear dynamic impact load factors experienced by railway track components due to wheel/rail contacts. The insight into the nonlinear phenomena will enable predictive track maintenance and risk-based track inspection planning adaptation to enhance public safety and reduce unplanned maintenance costs.

## 1 INTRODUCTION

There are two types of modern railway tracks suitable for various purposes of railway operations. A selection of trackform (ballasted vs ballastedless track) is commonly based on capital cost, lifecycle cost, asset management and operations (e.g. train speeds, axle load, and ride quality). For over 200 years, railway tracks have evolved. Considering the whole life cycle values, modern ballasted railway tracks have become the most efficient and effective infrastructure for the railway industry operating *below* 250 km/h of train speed for over centuries. The ballasted tracks have been tailored and optimised over and over; and they are often used in light rail tracks, metro networks, suburban rail network and intercity rail lines since they are relatively inexpensive and quite superior in terms of maintainability and constructability [1-4]. In contrast, ballastless tracks or concrete slab tracks are often utilised for highspeed rail lines (with train speed over 250 km/h) to reduce maintenance costs due to highspeed related swift degradation of traditional track components (e.g. accelerated densification and dilation of ballast, poor ride comfort due to differential track settlement/stiffness, ground-borne noise and vibration problems, etc.) [1, 5-9]. In practice, railway maintainers and operators are suffering from many of rail surface defects that lead to increased maintenance (either planned or unplanned), operational downtime and delay, more frequent monitoring and track patrol, and possibly the broken rails leading to train derailments [10-12].

Commonly, urban rail operators experience social problems of ground-borne, structure-borne noise and vibration induced by short and long wavelength rail defects. For instance, extra level of noise excited by rail squats (short wavelength type) was observed by residents near Woolloomooloo viaduct in Sydney, Australia [13-14]. Reportedly, the cost of rail replacement due to rail squats and studs has become a major part of the whole track maintenance cost in European countries [15]. Note that the rail squats and studs are typically classified as the growth of any cracks that has grown longitudinally through the subsurface. The subsurface lamination crack later results in a depression of rail surface sometimes called 'dark spot' [16]. There are two initiation types of the rail surface defects. Such rail defects are commonly referred to as 'squats' when they were initiated from rolling contact fatigue (RCF) cracks, and as 'studs' when they were associated with white etching layer due to wheel slips or excessive tractive effort [16].

Moreover, with heavier and faster trains, the dynamic load transferring on to track and its components such rails, sleepers, ballast and formations is higher and amplified by the traffic speeds and rail surface defects. These dynamic impact loading conditions often damage the track support and cause initial differential settlement and plastic deformation. The track issue does not stop here. Such the plastic deformation and initial differential settlement further form and couple with short wavelength defects (if any) to exponentially aggravate the dynamic loading condition [17-19]. Therefore, it is highly important to understand the coupled dynamic effect of rail defects on the rail infrastructure so that rail operators and maintainers can develop suitable cost-effective strategies for operations and maintenance. An example of strategies is to carry out preventative track maintenance (such as re-tamping, re-grinding and ballast cleaning when early sign of damage is inspected). In many regional railways (such as freight services), speed restrictions have been adopted to delay the maintenance regime when the rail defects exist. Note that these strategies are often called 'Base Operating Conditions (BOCs)' in railway industry practices. The BOCs have been developed from internal R&D activities and extensive empirical experience in

the rail industry over the centuries. On this ground, the established railway authorities of course do not lack of expertise and best practices. However, they might lose sight of nonlinear combined effects and might lead to inefficient and ineffective track maintenance if such effects are not being investigated or inspected timely. This current study will fill this gap by establishing a new insight into nonlinear phenomena of combined short and long wavelength rail defects so that the *safety-critical* track inspection regime can be effectively adapted.

Initially, the detailed modelling of rail track dynamic and wheel-rail interaction was studied in 1992 while D-track program for dynamic simulation also have been created by Cai for his PhD's thesis of Queen's University in Canada [20]. Afterward, Iwnick has done a benchmark, which was called Manchester Benchmarks in 1998 [21]. In 2005; Steffens [22] has adopted the parameter of Manchester Benchmarks to compare performance of vary dynamic simulation programs and also developed the user-interface of D-track. On the other hand, D-track had still an issue of lower result than others and then the owner has revised the program after this benchmark. Subsequently, Leong has done the Benchmark II with the revised version of D-Track in 2007 [23].

In this present study, the dynamic simulation concept by Cai [20] has been adopted as seen in Figure 1 since the track model has included Timoshenko beam theory for rail and sleepers, which enable a more accurate behaviours of tracks. Note that rail cross section and sleeper pre-stressing are among the key influences on shear and rotational rigidities of Timoshenko beam behaviors in numerical modelling of railway tracks [24-27]. The irregularity of wheel and rail will cause higher dynamic impact force that the design condition level or serviceability limit state. The exceeding magnitude of the force generated by wheel and rail irregularities will damage track components and impair ride quality [28]. This study thus is the first to present the wheel-rail dynamic forces over both single defects and coupled defects. The dynamic amplification factor will be highlighted to identify the effect of train speeds. The scope of this study will be focused on ballasted railway tracks. The commonly used 106t freight wagons will be modeled and coupled with the discrete supported track model. The track model will be based on a standard rail gauge (1.435m). The outcome of this study will help railway organization in improving the predictive maintenance and inspection regimes.

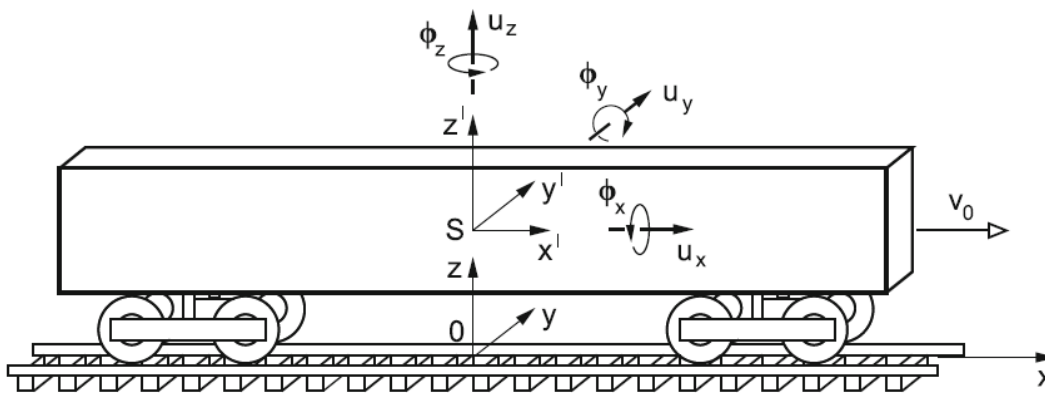


**Figure 1:** Coupling vehicle-track model [22]

## 2 DYNAMIC BEHAVIOURS

To design a ballasted railway track, it is important to assure safety and satisfy all the requirements of various stakeholders. The variety of dynamic loads from vehicle-track interaction and different environments make the rail infrastructure design highly complicated.

### 2.1 Dynamic wheel load

The dynamic loads induced by the vehicle moving on track structure will be considered as quasi-static force (equivalent to a static load times a factor) when the loads contain typically less than 10 Hz and is used to study behaviour of vehicle and design of the track foundation. In many cases, the perfect rail and wheel surfaces will be used to calculate of contact force and a factor (dynamic factor) to apply to the static wheel load and give a result for quasi static wheel load. The low-frequency load from a vehicle will apply to track geometry at a few cycles per second (up to 20 Hz).

In Australia, the most common method for calculation is presented by the Railway of Australia (ROA) manual or called “A Review of Track Design Procedures” or the “Blue Book”. The Dynamic Impact Factor (DIF) from this method ignores vertical track elasticity. The dynamic vertical wheel load (PD) is expressed empirically as a function of the static wheel load ( $P_s$ ) where  $\emptyset$  is the Dynamic impact factor (always  $\geq 1$ ). For example,  $PD = \emptyset P_s$ .

### 2.2 Eisenmann’ Classical Formula

The Eisenmann formula is the most common method used for calculation the dynamic impact factor, used in a general track design. At the same time, the Eisenmann formula is modified by ROA and is used internationally. The Eisenmann formula (Eq. 1) and modified Eisenmann (Eq. 2) are shown respectively.

$$P_D = (1 + \delta\eta t) \cdot P_s \quad (1)$$

$$P_D = (1 + \delta\beta\eta t) \cdot P_s \quad (2)$$

where  $\delta$  = Track condition factor;  $\eta$  = Speed factor, where  $\eta = 1$  for speed ( $v$ ) < 60 km/h and  $\eta = 1 + [(v-60)/140]$  for  $v > 60$  km/h;  $t$  = Upper confidence level (UCL) factor;  $\beta = 1$  for loaded vehicles; and 2 for unloaded vehicles.

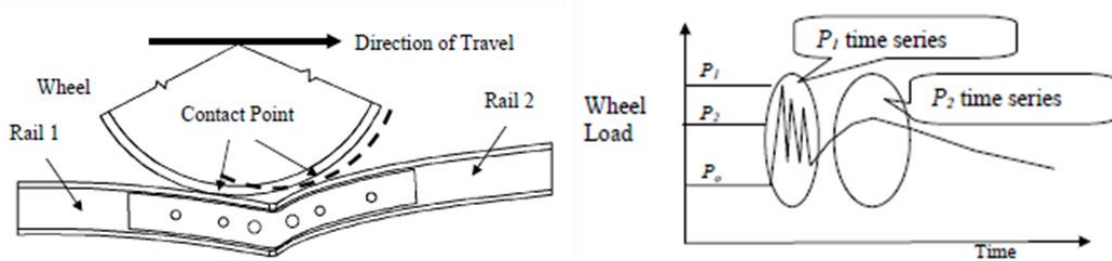


**Figure 2:** Impact force of wheel/rail contact at dipped rail joint [13]

### 2.3 Wheel trajectory over short wavelength rail defect

Dipped rail joint is termed to define the sum of an angle of dipped trajectory between each rail and the horizontal (in milli-radians). The two components of this angle consist of permanent deformation of the rail ends and the deflection of the joint under load. Jenkins et al. [29] described that the wheel travelling across a dipped rail joint creates the force peak as P1 and P2. The shape of the irregularity and characteristics of the vehicle create impact loading which the force at dipped joint increases almost linearly with the speed and angle of the dip. When the trains travelling at high speed approach a rail joint, the wheel lose will lose contact with the railhead of rail and land on the connected rail that generate the high dynamic impact force as illustrated in Figure 2.

The P1 force is a very high frequency ( $\cong 200$  Hz -1000Hz) that is less than 0.5 millisecond in length (0.25 - 0.5 millisecond after crossing the joint). The compression of contact zone between wheel and rail create the inertia of rail and sleepers which does not directly transform to ballast or subgrade settlement. However, it has a significant effect on wheel/rail contact force. The P2 is occurred at a lower frequency range ( $\cong 50$  Hz -200Hz) than P1 occurring much later at typically 6 – 8 milliseconds. The unsprung mass and the rail/sleeper mass are moving down together influencing the compression of the ballast below the sleeper. P2 forces therefore increase the contact stresses and also induce the loads on sleepers and ballast. P2 force will be considered mostly by the track design engineer. Jenkins et al. [29] provided a method of calculation as follows:

$$P_1 = P_0 + (2\alpha v) \cdot \sqrt{\frac{k_H m_e}{1 + \frac{m_e}{m_u}}} \quad (3)$$

$$P_2 = P_0 + (2\alpha v) \cdot \sqrt{\frac{M_u}{M_u + M_t}} \quad (4)$$

$$\times \left[ 1 - \frac{\pi C_t}{4\sqrt{K_t(M_u + M_t)}} \right] \times \sqrt{K_t M_u}$$

where:  $P_1$  and  $P_2$  = dynamic rail force (kN);  $P_0$  = vehicle static single wheel load (kN);  $k_H$  = a chord stiffness to the Hertzian contact stiffness;  $m_e$  = the effective track mass (kg);  $m_u$  = the vehicle unsprung mass (kg);  $2\alpha$  = Total joint angle (rad);  $v$  = speed of vehicle (m/s);  $K_t$  = equivalent track stiffness (MN/m);  $M_t$  = equivalent track mass (kg); and  $C_t$  = Equivalent track damping (kNs/m).

### 2.4 Track settlement

Track settlement can cause the train passing the track with higher dynamic load increasing high-frequency variations to the ballast and subgrade. It will then cause non-elastic or plastic deformations with permanent setting. In normal situation, the track will generally not return to the same position but to the very close point (accumulated deformation). As time passes, all of non-elastic deformations will create a new track position and this phenomenon becomes

differential track settlement. The track alignment and surface level of track also change due to the accumulated non-elastic deformations. The irregularity of track will increase low-frequency oscillation of vehicle. However, the track settlement often takes place at the transition area to a bridge. In addition, the quality of ballast, sub-ballast and the subgrade are also the factor inducing permanent deformation [30-31].

Track settlements typically consist of two phases. The first phase is after tamping that the gap between ballast particles is reduced quickly and so this layer is consolidated. The second phase is slower while the densification and inelastic behaviour of the ballast and subgrade materials are concerned as the two majors parameters influencing the ballast settlement that are the deviatoric stress, vibrations, degradation and subgrade stiffness. The empirical settlement equation for the substructure is shown below. It does only consider the ballast settlement not including subgrade settlement:

$$Z_{iN} = Z_{i0} + f(\log N, \sigma_{be}, I_{dyn}, I_{dec}, I_{Esub}) \quad (5)$$

This equation describes the settlement of ballast below the sleeper  $I$  where:  $Z_{i0}$  = the given void amplitude;  $N$  = Number of load cycles;  $\sigma_{be}$  = the vertical equivalent stress in the ballast layer;  $I_{dyn}$  = the dynamic factor;  $I_{dec}$  = the degradation factor; and  $I_{Esub}$  = the subgrade stiffness factor.

### 3 COUPLING VEHICLE-TRACK MODELLING

The track model (D-Track) is simulated on Winkler foundation principal which only cross-section of track dynamic responses is considered symmetrically. Rail and sleeper were represented on elastic beam of either the Timoshenko type. The sleepers also support the rail as discrete rigid masses. Free-body diagram of track model are shown in the Figure 3(a) where  $P(t)$  is a moving wheel force at constant speed ( $v$ ). Figure 3 (b) represents the force from rail to sleeper through the rail seat ( $i^{th}$ ) and reaction force  $k_s z_i(y, t)$  per unit length.

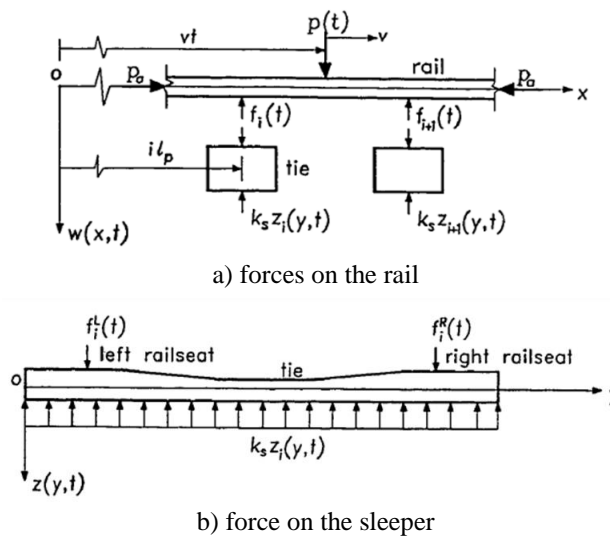


**Figure 3:** Free-body diagram of track model [22]

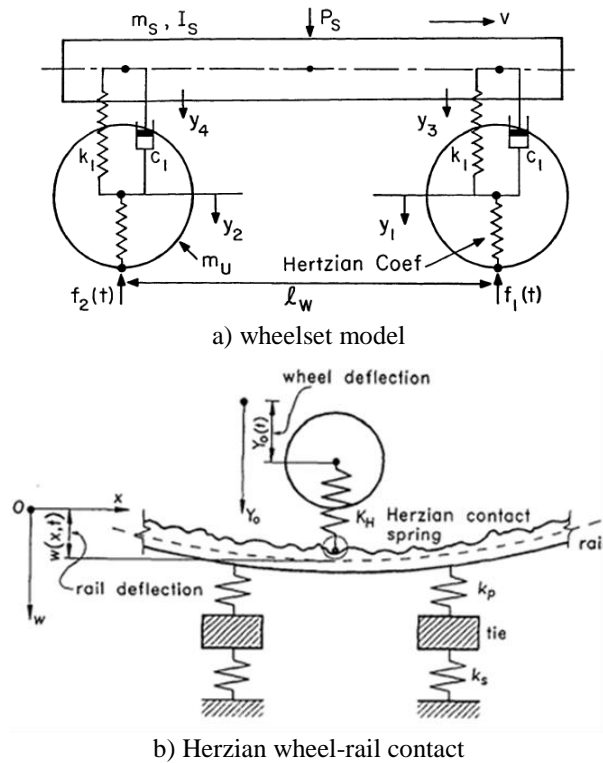


**Figure 4:** Free-body diagram of vehicle-track model [22]

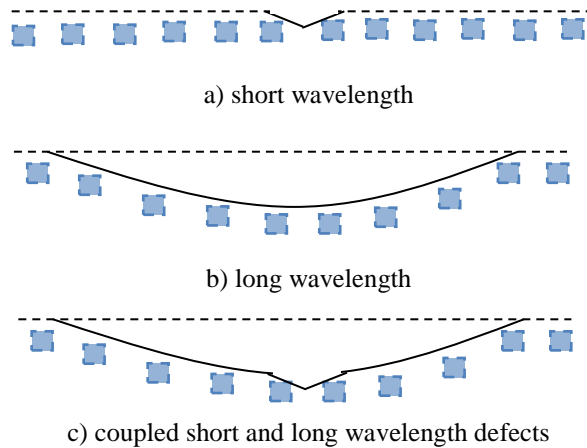


**Figure 5:** Rail irregularity models

The wheelset model in this modelling consists of a four-degree of freedom which include of one bogie with two-axle, rail and track. The wheelset model uses the unsprung masses ( $\mu$ ) and the sideframe mass ( $m_s, I_s$ ) to calculate on one rail through the primary suspension ( $k_1, c_1$ ) as shown in Figure 4(a). The components of vehicles are demonstrated as a spring load by using Hertzian contact model. Moreover, the equations of motion in this model used the principles of Newton's law and beam vibration to apply. Integration between wheelset and track equations can be calculated by the non-linear Hertzian wheel-rail interaction model as illustrated in Figure 4 (b). The D-Track model has been benchmarked by [23, 24] in order to assess the accuracy and

verify the precision of numerical results. D-Track is thus adopted for this study. Rail surface profile irregularities can be estimated as inverse half-sinusoidal curve as shown in Figure 5(a). For track settlement, the study focus on a long span defect (such as large mud pumping tracks) with a wavelength of 10m as shown in Figure 5(b).

#### 4 RESULTS AND DISCUSSIONS

The numerical simulations have been carried out using 106t freight wagon with wheel radius of 0.46m and Hertzian spring constant of  $0.87 \times 10^{11} \text{ N/m}^{3/2}$ . The dynamic wheel/rail contact forces can be seen in Figure 6.

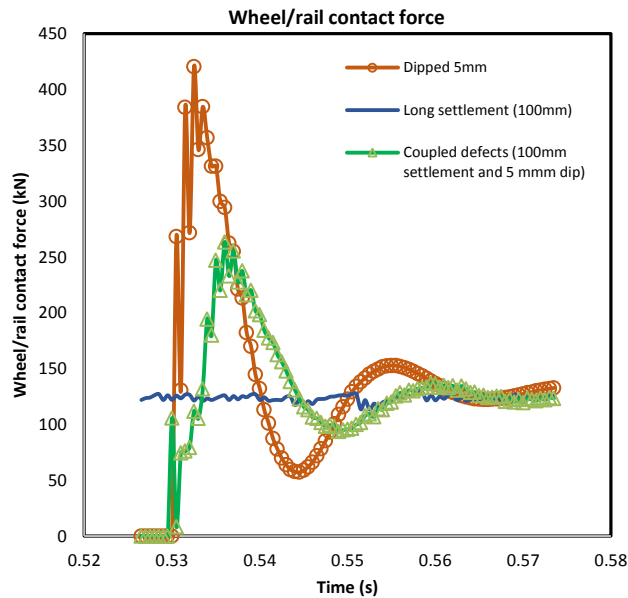


Figure 6: Wheel/rail contact force

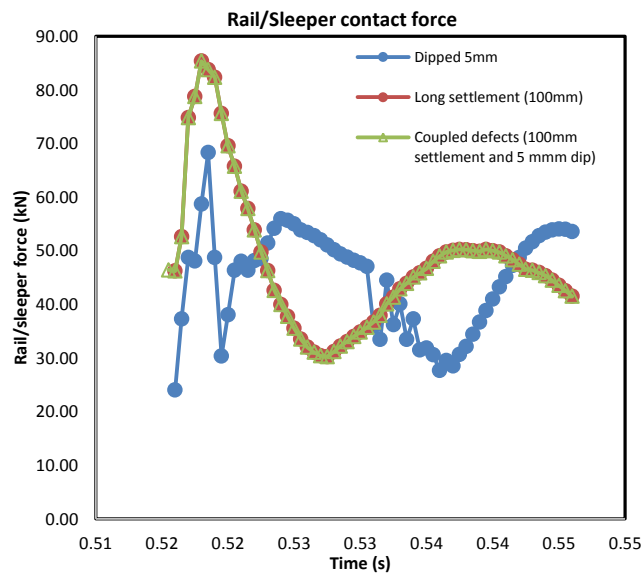


Figure7: Rail/sleeper contact force

Short wavelength defects have significant effects on the wheel/rail contact force in comparison with long wavelength defects. In contrast, surprisingly, it is apparent that long wavelength defect plays higher influence on the dynamic railseat loads (rail/sleeper contact) as shown in Figure 7.

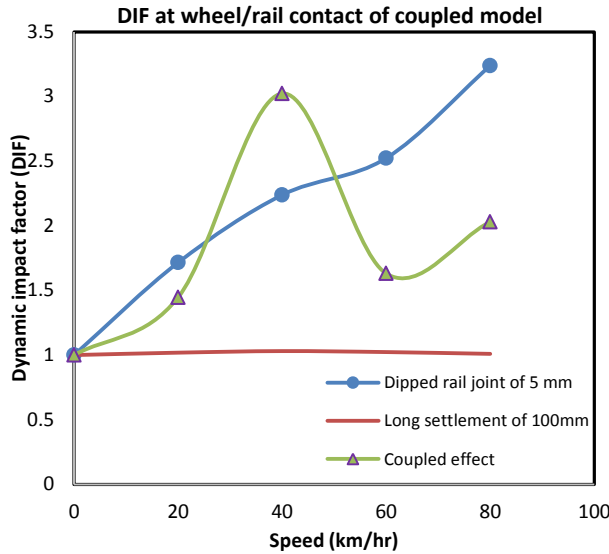


Figure 8: DIF at wheel/rail contact force

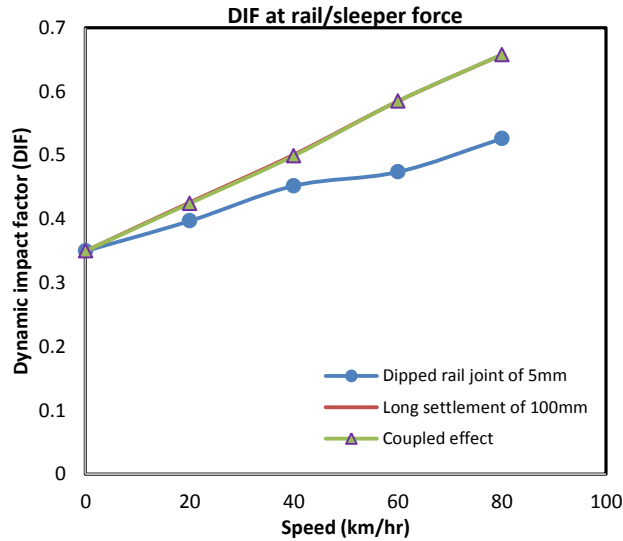


Figure 9: DIF at rail/sleeper contact force

The dynamic impact factor (DIF) can be evaluated from dynamic over static wheel force ratio. Figures 8 and 9 demonstrate the coupling dynamic vehicle-track interaction on contact forces and railseat loading conditions. It is clear that the coupling wheel/rail contact force is nonlinear (Figure 8) whilst rather linear relationships can be observed on the load sharing (Figure 9). It is clear that the individual short rail surface defects influence significantly the high frequency force at wheel/rail contact. However, the coupled short and long wavelength defects does not seem to play a strong influence on wheel/rail contact, but instead influence how the load is distributed on the sleepers.

## 5 CONCLUSION

This paper presents the nonlinear dynamic interactions between vehicle and track, which can cause vibrations and acoustic radiations to railway neighborhood. The nonlinear effects of coupled short and long wavelength rail defects on vehicle-track interaction have been highlighted. It is the first to evaluate the coupling dynamic vehicle-track interactions over coupled short and long wavelength rail defects. The results show that the coupled effect plays a key role on magnifying the rail/sleeper contact forces (railseat loads). The insight implies that sleepers will experience excessive dynamic loads and they can deteriorate and abrade at a relatively faster rate. More results on parametric effects of short and long wavelength as well as the effect of defect severity will appear elsewhere in the near future. This understanding into the nonlinear phenomena will help track engineers to manage and operate infrastructure assets more effectively.

## ACKNOWLEDGEMENT

The second author wishes to thank the Australian Academy of Science and Japan Society for the Promotion of Sciences for his Invitation Research Fellowship (Long term), Grant No. JSPS-L15701 at the Railway Technical Research Institute and The University of Tokyo, Tokyo Japan. The authors wish to gratefully acknowledge the financial support from European Commission for H2020-MSCA-RISE Project No. 691135 “RISEN: Rail Infrastructure Systems Engineering Network,” which enables a global research network that tackles the grand challenges [32] in railway infrastructure resilience and advanced sensing under extreme events ([www.risen2rail.eu](http://www.risen2rail.eu)). This project is also financially sponsored by H2020-S2R Project No. 730849 “S-CODE: Switch and Crossing Optimal Design and Evaluation”.

## REFERENCES

- [1] Esveld, C., *Modern Railway Track*, The Netherlands MRT Press, (2001).
- [2] Remennikov, A.M., Kaewunruen, S., A review on loading conditions for railway track structures due to wheel and rail vertical interactions. *Structural Control and Health Monitoring*, 15(2): 207-234, (2008).
- [3] Thompson, D.J., *Railway Noise and Vibration*. Elsevier, Amsterdam, The Netherlands, (2010).
- [4] Indraratna, B, Salim, W and Rujikiatkamjorn, C, *Advanced Rail Geotechnology - Ballasted Track*, The Netherlands: CRC Press/Balkema, (2011).
- [5] Griffin, D.W.P., Mirza, O., Kwok, K., and Kaewunruen, S., “Composite slabs for railway construction and maintenance: A mechanistic review”, *IES Journal of Civil and Structural Engineering*, 7(4): 243-262, (2014).
- [6] Griffin, D.W.P., Mirza, O., Kwok, K., and Kaewunruen, S., “Finite element modelling of modular precast composites for railway track support structure: A battle to save Sydney Harbour Bridge”, *Australian Journal of Structural Engineering* 16 (2), 150-168, (2014).

- [7] Binti Sa'adin, S. L., Kaewunruen, S., and Jaroszweski, D. "Risks of Climate Change with Respect to the Singapore-Malaysia High Speed Rail System". *Climate* 4, 65, (2016).
- [8] Binti Sa'adin, S. L., Kaewunruen, S., Jaroszweski, D., "Operational readiness for climate change of Malaysia high-speed rail", *Proceedings of the Institution of Civil Engineers – Transport*, 169 (5), 308-320, (2016).
- [9] Binti Sa'adin, S. L., Kaewunruen, S., and Jaroszweski, D. Heavy rainfall and flood vulnerability of Singapore-Malaysia high speed rail system. *Australian Journal of Civil Engineering*, 14(2): 123-131, (2016). doi:10.1080/14488353.2017.1336895
- [10] Kaewunruen, S., Sussman, J. M., and Einstein, H. H. "Strategic framework to achieve carbon-efficient construction and maintenance of railway infrastructure systems." *Frontiers in Environmental Sciences*, 3:6, (2015), doi:10.3389/fenvs.2015.00006
- [11] Setsobhonkul S, Kaewunruen S and Sussman JM, "Lifecycle assessments of railway bridge transitions exposed to extreme climate events". *Frontiers in Built Environments*, 3:35, (2017), doi: 10.3389/fbuil.2017.00035
- [12] Kaewunruen, S., Ishida, M., Marich, S., "Dynamic wheel–rail interaction over rail squat defects", *Acoustics Australia*, 43(1): 97-107, (2015).
- [13] Sun, Y.Q., Cole, C., McClanachan, M., Wilson, A., Kaewunruen, S. and Kerr, M.B., "Rail short-wavelength irregularity identification based on wheel-rail impact response measurements and simulations", *Proceedings of the 9th International Heavy Haul Conference*, June 21-23, Shanghai, China, (2009).
- [14] Kaewunruen, S. and Remennikov, A.M., "Current state of practice in railway track vibration isolation: an Australian overview", *Australian Journal of Civil Engineering* 14 (1), 63-71, (2016).
- [15] Tuler, M.V., Kaewunruen, S., "Life cycle analysis of mitigation methodologies for railway rolling noise and groundbourne vibration", *Journal of Environmental Management* 191, 75-82, (2017).
- [16] Wilson, A., Kerr, M., Marich, S., and Kaewunruen, S. "Wheel/rail conditions and squat development on moderately curved tracks". in: *CORE 2012: Global Perspectives; Conference on railway engineering*, 10-12 September 2012, Brisbane, Australia. Barton, A.C.T.: Engineers Australia, 2012: 223-230, (2012).
- [17] Kaewunruen, S. and Remennikov, A.M., "Dynamic properties of railway track and its components: Recent finding and future research directions." *Insight - Non-Destructive Testing and Condition Monitoring*, 52(1): 20-22, (2010).
- [18] Kaewunruen, S., Ishida, M., "Field monitoring of rail squats using 3D ultrasonic mapping technique," *Journal of the Canadian Institute for Non-Destructive Evaluation*, 35(6): 5-11, (2014) (invited).
- [19] Kaewunruen, S., Remennikov, A.M., "Field trials for dynamic characteristics of railway track and its components using impact excitation technique," *NDT & E International* 40 (7), 510-519, (2007).
- [20] Cai, Z. Modelling of rail track dynamics and wheel/rail interaction. PhD Theses, Queen's University, Canada, (1992).

- [21] Iwnicki, S. Manchester Benchmarks for Rail Vehicle Simulation, *Vehicle System Dynamics*, 30 (3-4): 295-313, (1998).
- [22] Steffens, D. M. Identification and development of a model of railway track dynamic behavior. MEng Thesis, Queensland University of Technology, Australia (2005).
- [23] Leong, J. Development of Limit State Design of Methodology for Railway Track. MEng Thesis, Queensland University of Technology, Australia (2007).
- [24] Kaewunruen, S. and Remennikov, A.M., "Experimental determination of the effect of wet/dry ballast on dynamic sleeper/ballast interaction." *ASTM J of Testing and Evaluation*, 36(4): 412-415, (2008).
- [25] Kaewunruen, S. and Remennikov, A.M., "Sensitivity analysis of free vibration characteristics of an in-situ railway concrete sleeper to variations of rail pad parameters." *Journal of Sound and Vibration*, 298(1-2), 453-461, (2006).
- [26] Kaewunruen, S. and Remennikov, A.M., "Experimental determination of the effect of wet/dry ballast on dynamic sleeper/ballast interaction." *ASTM J of Testing and Evaluation*, 36(4): 412-415, (2008).
- [27] Remennikov, A. and Kaewunruen, S., "Determination of dynamic properties of rail pads using instrumented hammer impact technique," *Acoustics Australia*, 33(2): 63-67. (2005).
- [28] Kaewunruen, S. Lewandowski, T., Chamniprasart, K. "Dynamic responses of interspersed railway tracks to moving train loads", *International Journal of Structural Stability and Dynamics*, 18(1): 1850011, (2018).
- [29] Jenkins, H.H., Stephenson, J.E., Clayton, G.A. The effect of track and vehicle parameters on wheel/rail vertical dynamic force. *Rail engineering Journal*, 2-16, 1974.
- [30] Kaewunruen, S., Minoura, S., Papaalias, M., Remennikov, A.M., [Asymmetrical influences on nonlinear dynamics of railway turnout bearers](#), The 24<sup>th</sup> International Congress on Sound and Vibration, London, U.K., 23-27 July (2017).
- [31] Kaewunruen, S., Ngamkhanong, C., Janeliukstis, R., You, R., Influences of surface abrasions on dynamic behaviours of railway concrete sleepers, The 24<sup>th</sup> International Congress on Sound and Vibration, London, U.K., 23-27 July (2017).
- [32] Kaewunruen, S., Sussman, J. M., and Matsumoto, A. Grand challenges in transportation and transit systems. *Frontiers in Built Environments*, 2:4, (2016) doi:10.3389/fbuil.2016.00004

## Phase Field Material Point Method for Impact Induced Fracture

Emmanouil Kakouris\*, Savvas Triantafyllou\*\*

\*Centre for Structural Engineering and Informatics, The University of Nottingham, \*\*Centre for Structural Engineering and Informatics, The University of Nottingham

### ABSTRACT

Predictive modelling of impact induced fracture is of extreme interest to the engineering community as it pertains to various applications, e.g., projectile impact and rocking of deformable medium. Dynamic failure mechanisms in brittle solids are governed by complex fracture phenomena such as crack initiation, multiple crack branching, or crack arrest. Mesh distortion errors that are inevitable in large displacement FEA hinder the fidelity of dynamic impact simulations where the deformability of the contact surfaces significantly affects the resulting contact forces and corresponding failure surfaces. Material point methods provide high fidelity solutions for large displacement and large deformation problems [1]. Rather than relying on the notion of a deforming mesh, material point methods introduce a particle based approximation for the deformable body that move within a non-deforming mesh. This introduces a considerable advantage as opposed to purely particle based methods as the continuum approximation is preserved thus releasing the requirement for high particle densities. To this point, material point implementations for brittle fracture have proven efficient in tackling quasi-static crack propagation in terms of computational simplicity and robustness. Phase Field Material Point Method (PF-MPM) has been successfully introduced [2] for quasi-static brittle fracture problems. In this, the phase field is resolved at material points and mapped onto grid nodes where the phase field governing equations are solved. PF-MPM has further been extended to account for surface energy densities with strongly anisotropy [3]. In this work, the PF-MPM is originally extended to account for dynamic brittle fracture within an anisotropic regime. Furthermore, a frictional contact framework is adopted to accurately capture the intriguing effects governing impact fracture problems. The phase field governing equations are solved independently for each contact body employing a predictor-corrector algorithm. The merits of the proposed scheme in tackling impact dynamics are investigated through a set of benchmark cases. [1] Sulsky D., Chen Z. and Schreyer H.L. (1994). A particle method for history-dependent materials. *Computer Methods in Applied Mechanics and Engineering*, 118 (1-2), pp. 179-196 [2] Kakouris, E. G., and Triantafyllou, S. P. (2017) Phase-Field Material Point Method for Brittle Fracture, *International Journal for Numerical Methods in Engineering* 112 (12), pp. 1750 -1776. [3] Kakouris, E.G., and Triantafyllou, S. P., (2017). Material point method for crack propagation in anisotropic media: a phase field approach, *Archive of Applied Mechanics*, DOI: <https://doi.org/10.1007/s00419>.

## Particle-based Flow Simulations for Complicated Viscous Fluid

Kazuhiko Kakuda<sup>\*</sup>, Wataru Okaniwa<sup>\*\*</sup>, Ituki Nishino<sup>\*\*\*</sup>, Shinichiro Miura<sup>\*\*\*\*</sup>

<sup>\*</sup>Nihon University, <sup>\*\*</sup>Nihon University, <sup>\*\*\*</sup>Nihon University, <sup>\*\*\*\*</sup>Nihon University

### ABSTRACT

The numerical simulations of three-dimensional (3D) viscous fluid flows including multi-scale/physics and moving boundary/obstacle are indispensable in science and engineering fields from a practical point of view. Numerical difficulties have been experienced in the solution of the Navier-Stokes equations at higher Reynolds numbers. In particular, it is well known that the centered finite difference and standard Galerkin finite element formulations lead to spurious oscillatory solutions for flow problem at high Reynolds number regimes. To overcome such spurious oscillations, various upwind/upstream-based schemes have been significantly presented by many researchers in both frameworks. On the other hand, there are various gridless/meshless-based particle methods, such as SPH (Smoothed Particle Hydrodynamics) method[1], MPS (Moving Particle Semi-implicit) one[2], and PFEM (Particle Finite Element Method)[3] to simulate effectively such complicated flow problems. Recently, the physics-based computer simulations on the GPU (Graphics Processing Units) have increasingly become an important strategy for solving efficiently various problems, such as fluid dynamics, solid dynamics, and so forth. The purpose of this paper is to present the application of the GPU-based SPH/MPS method to 3D complicated fluid flow problems, namely the dam-breaking flow problem and the droplet-falling with surface tension. As the surface tension model, we adopt the inter-particle potential force with a potential coefficient. The problems of the dam-breaking flow and the droplet-falling with surface tension have been widely used to verify the applicability and validity of the numerical methods. The GPU-implementation consists mainly of the search for neighboring particles in the local grid cell using hash function for both methods. The MPS scheme is also applied to solve implicitly the Poisson equation with respect to the pressure fields by using GPU-based SCG (Scaled Conjugate Gradient) method. The workability and validity of the present approaches are compared with experimental data and other numerical ones. References [1] Gingold, R.A. and Monaghan, J.J., Smoothed Particle Hydrodynamics: Theory and Application to Non-spherical Stars, *Mon. Not. R. astr. Soc.*, Vol.181, 1977, pp.375-389, 1977. [2] Koshizuka, S. and Oka, Y., Moving-particle Semi-implicit Method for Fragmentation of Incompressible Fluid, *Nucl. Sci. Eng.*, Vol.123, pp.421-434, 1996. [3] Idelsohn, S.R., Onate, E. and Pin, F.Del, The Particle Finite Element Method: A Powerful Tool to Solve Incompressible Flows with Free-surfaces and Breaking Waves, *Int. J. Numer. Meth. Engng.*, Vol.61, pp.964-989, 2004.

## **Data Analytics for Mining Process-Structure-Property Linkages for Hierarchical Materials**

Surya Kalidindi\*

\*Georgia Tech

### **ABSTRACT**

A majority of the materials employed in advanced technologies exhibit hierarchical internal structures with rich details at multiple length and/or structure scales (spanning from atomic to macroscale). Collectively, these features of the material internal structure are here referred to as the material structure, and constitute the central consideration in the development of new/improved hierarchical materials. Although the core connections between the material's structure, its evolution through various manufacturing processes, and its macroscale properties (or performance characteristics) in service are widely acknowledged to exist, establishing this fundamental knowledge base has proven effort-intensive, slow, and very expensive for most material systems being explored for advanced technology applications. The main impediment arises from lack of a broadly accepted framework for a rigorous quantification of the material's structure, and objective (automated) identification of the salient features that control the properties of interest. This presentation focuses on the development of data science algorithms and computationally efficient protocols capable of mining the essential linkages from large ensembles of materials datasets (both experimental and modeling), and building robust knowledge systems that can be readily accessed, searched, and shared by the broader community. The methods employed in this novel framework are based on digital representation of material's hierarchical internal structure, rigorous quantification of the material structure using n-point spatial correlations, objective (data-driven) dimensionality reduction of the material structure representation using data science approaches (e.g., principal component analyses), and formulation of reliable and robust process-structure-property linkages using various machine learning techniques. This new framework is illustrated through a number of case studies.

## Modeling and Simulation of Magnetorheological Elastomers Filled with Magnetically Hard Particles

Karl Alexander Kalina<sup>\*</sup>, Jörg Brummund<sup>\*\*</sup>, Philipp Metsch<sup>\*\*\*</sup>, Markus Kästner<sup>\*\*\*\*</sup>

<sup>\*</sup>Institute of Solid Mechanics, TU Dresden, Germany, <sup>\*\*</sup>Institute of Solid Mechanics, TU Dresden, Germany,  
<sup>\*\*\*</sup>Institute of Solid Mechanics, TU Dresden, Germany, <sup>\*\*\*\*</sup>Institute of Solid Mechanics, TU Dresden, Germany

### ABSTRACT

Magnetorheological elastomers (MREs) are a class of active composites which can alter their macroscopic properties if an external magnetic field is applied. Typically, these materials consist of a polymer matrix filled with micron-sized magnetically soft particles such as carbonyl iron. Another type of fillers are magnetically hard particles as NdFeB which exhibit significant magnetic hysteresis effects. MREs with this kind of composition have features as field dependent coercivity and remanent magnetization which are typical for conventional magnetically hard materials. Recently published experiments [1, 2] indicate a significant influence of the effective hysteresis loops on the matrix stiffness in such MREs. In this contribution we investigate the microstructural causes of this effect by the use of a computational modeling approach. The analyzed MREs are described by a microscopic model [2], i. e. the heterogeneous microstructure consisting of magnetizable inclusions embedded into a polymer matrix is taken into account explicitly. The constitutive models for the magnetizable particles and the polymer matrix are formulated separately. In order to describe the irreversible magnetic behavior of the NdFeB particles a thermodynamically consistent vector-hysteresis model based on [3] is used. The governing equations of the coupled magneto-mechanical problem are solved by a nonlinear finite element formulation [2]. Therein, the evolution equation of the hysteresis model is solved by means of an implicit integration scheme. In order to connect the macroscopic and the microscopic magnetic and mechanical quantities, a suitable computational homogenization scheme is applied [2]. The presented simulations indicate a rotation of the particles within the soft polymer matrix material. Due to this effect, the effective hysteresis of the MRE are significantly smaller than the hysteresis of pure NdFeB. The presented computational results are qualitatively in good agreement with the experiments discussed in [1]. References [1] J. M. Linke, D. Yu. Borin, S. Odenbach, First-order reversal curve analysis of magnetoactive elastomers, *RSC Adv.*, 6, pp. 100407-100416, (2016). [2] K. A. Kalina, J. Brummund, P. Metsch, M. Kästner, D. Yu. Borin, J. M. Linke, S. Odenbach, Modeling of magnetic hysteresis in soft MREs filled with NdFeB particles, *Smart Mater. Struct.*, 26, pp. 105019-105031, (2017). [3] A. Bergqvist, Magnetic vector hysteresis model with dry friction-like pinning, *Physica B*, 233, pp. 342-347 (1997).

## **Efficient and Reliable Simulation of Failure of Reinforced Concrete Structures under Impact (RTG 2250: Mineral-bonded Composites for Enhanced Structural Impact Safety)**

Michael Kaliske<sup>\*</sup>, Viktor Mechtcherine<sup>\*\*</sup>, Aurel Qina<sup>\*\*\*</sup>, Alexander Fuchs<sup>\*\*\*\*</sup>

<sup>\*</sup>Institute for Structural Analysis, TU Dresden, <sup>\*\*</sup>Institute of Construction Materials, TU Dresden, <sup>\*\*\*</sup>Institute for Structural Analysis, TU Dresden, <sup>\*\*\*\*</sup>Institute for Structural Analysis, TU Dresden

### **ABSTRACT**

Existing concrete or reinforced concrete structures feature, as a rule, a relatively low resistance to various sorts of impact loading, such as shock, collision or explosion. The primary goal of Research Training Group 2250 (RTG 2250) is to bring substantial improvements in the impact-resistance of existing buildings by applying thin layers of strengthening material. By using innovative, mineral-bonded composites, public safety and the reliability of vitally important infra-structure should be significantly enhanced. The scientific basis to be developed will additionally enable to build new, impact-resistant structures economically and ecologically. In order to elaborate a deep understanding of the specific structural behavior under impact loading, theoretical and numerical models extending far beyond current knowledge have to be developed. An important role is played by the simulation of the bond between the fibers and the matrix under very high strain rates as well as the development of relevant constitutive laws. For a realistic description of the macroscopic structural failure of strengthened concrete structures under impact by an extended microplane model and by the discrete implementation of local damage by the eigenstrain approach, a large number of detail developments (material description at impact with microplane model for reinforced concrete and reinforcement layer, effective nonlocal description of extended inelasticity, formulation of eigenstrain for inelasticity) needs to be taken into account. Moreover, challenges in the combination of the methods (e.g. description of the wave propagation for the selected modelling) have to be overcome. The contribution introduces the RTG generally and elaborates on the simulation of structural behavior of this class of structures and loading cases.

## Investigation of the Properties of Dislocation Structures by XRD and HR-EBSD Experiments Coupled with 2D DDD Simulations

Szilvia Kalácska<sup>\*</sup>, Péter Dusán Ispánovity<sup>\*\*</sup>, István Groma<sup>\*\*\*</sup>

<sup>\*</sup>Eötvös Loránd University (ELTE), <sup>\*\*</sup>Eötvös Loránd University (ELTE), <sup>\*\*\*</sup>Eötvös Loránd University (ELTE)

### ABSTRACT

X-ray diffraction (XRD) is a well-established experimental method for determining the dislocation density values in materials science, that helped developing basic models of crystal plasticity. To evaluate the X-ray line profiles measured on bulk samples the so called “strain broadening” setup is applied and the asymptotic properties of the X-ray intensity distributions are investigated with the momentum method [1]. The recently developed technique for investigating the statistical properties of dislocation structures by high resolution electron backscatter diffraction (HR-EBSD) enables us to calculate and examine the internal stress distribution in deformed crystalline materials. The application of the momentum method to HR-EBSD is a novel way to determine the total dislocation density [2]. The comparison of the two methods will be shown in the presentation to corroborate the results measured on copper single crystals. To explore the relevance and potential of the HR-EBSD-based evaluation method a 2D discrete dislocation dynamics simulation is applied [3]. The model establishes the understanding of the unexpected behaviour observed in the calculated HR-EBSD moments. It is also shown that the dislocation arrangement does not affect the tail of the probability distribution of the internal stress. The availability of spatially resolved stress maps opens further perspectives for the evaluation of correlation properties and mesoscale parameters of heterogeneous dislocation structures. [1] I. Groma, X-ray line broadening due to an inhomogeneous dislocation distribution. *Physical Review B* 57, 7535 (1998). [2] Sz. Kalácska, I. Groma, A. Borbély and P.D. Ispánovity, Comparison of the dislocation density obtained by HR-EBSD and X-ray profile analysis. *Applied Physics Letters* 110, 091912 (2017). [3] P.D. Ispánovity, I. Groma, G. Györgyi, F.F. Csikor and D. Weygand, Submicron plasticity: yield stress, dislocation avalanches, and velocity distribution. *Physical Review Letters* 105, 085503 (2010).

## Variational Sea Ice Mechanics in the Regional Arctic System Model

Samy Kamal<sup>\*</sup>, Andrew Roberts<sup>\*\*</sup>, Elizabeth Hunke<sup>\*\*\*</sup>, William Lipscomb<sup>\*\*\*\*</sup>, Wieslaw Maslowski<sup>\*\*\*\*\*</sup>

<sup>\*</sup>Naval Postgraduate School, <sup>\*\*</sup>Naval Postgraduate School, <sup>\*\*\*</sup>Los Alamos National Laboratory, <sup>\*\*\*\*</sup>National Center or Atmospheric Research, <sup>\*\*\*\*\*</sup>Naval Postgraduate School

### ABSTRACT

Since the 1970s, large-scale sea ice models have approximated compressive ice strength and mechanical thickening using empirical functions that modify the areal ice thickness distribution,  $g(h)$ , under horizontal compression and shear. Yet, observational and modeling research since the 1980s has demonstrated that these empirical functions are flawed: compressive strength approximations that parameterize constant frictional loss relative to potential energy gain during ridging may perform no better than simple and unphysical estimates of ice strength.  $g(h)$  is itself a scale-dependent representation of sea ice thickness that should not be applied to models with resolution less than 10 km and it is missing the critical dimension of macro-porosity associated with fracture and fragmentation of individual ridges just a few meters across. Most importantly, empirical redistribution of  $g(h)$  overlooks the principle of stationary action as applied to non-conservative systems. Without considering the variational principles of ice mechanics, it is difficult to derive well-posed physics to represent ridging within the grid cells or elements of Eulerian or Lagrangian sea ice models, respectively, for horizontal resolutions of less than 1km to more than 50km. This work presents the first known application of variational sea ice ridging to a basin-scale coupled model – the Regional Arctic System Model (RASM) – that rectifies the problems highlighted above. Ridging statistics are computed by coarse-graining the degrees of freedom associated with individual ridge formation. Equations governing sea ice momentum and mass conservation have been derived using variational principles upwards from the scale of individual ridges, and therefore do not require empirical functions for sub-grid redistribution of sea ice thickness in our 9km model. Instead, the principle of virtual work determines the prevalence, shape, and porosity of ridges of different sizes that in turn ascertain the compressive strength of the pack within each model grid cell. This is achieved using an expanded state-space for the thickness distribution that includes macro-porosity. Results presented are objectively assessed against previous RASM simulations using both isotropic (EVP) and anisotropic (EAP) rheologies using freeboard skill scores obtained with an ICESat emulator.

## Fast Level Set Topology Optimization by Means of a Sparse Hierarchical Data Structure

Sandilya Kambampati<sup>\*</sup>, Carolina Jauregui<sup>\*\*</sup>, Ken Museth<sup>\*\*\*</sup>, Hyunsun Alica Kim<sup>\*\*\*\*</sup>

<sup>\*</sup>University of California San Diego, <sup>\*\*</sup>University of California San Diego, <sup>\*\*\*</sup>Voxel Tech Inc., <sup>\*\*\*\*</sup>University of California San Diego

### ABSTRACT

The application of level set methods for topology optimization offers several advantages, such as being able to handle complex topological changes and having an implicit definition of the dynamic boundary. However, a common criticism is that they tend to suffer in terms of computational efficiency when compared to the traditional topology optimization based on material distribution. We note that common level set topology optimization methods utilize dense (vs sparse) grid data structures, which significantly limits the memory efficiency and hence the available resolution of the dynamic interface. Another common numerical technique in the level set methods is the Fast Marching Method, which is an inherently a serial algorithm with a time complexity of  $O(N \log N)$  and does not easily parallelize. In this paper we demonstrate how the efficiency of level set methods for topology optimization can be substantially improved by employing the sparse data structure VDB [1], which is a hierarchical data structure that shares some of the performance characteristics of B+ trees traditionally used for high-performance file systems and relation data bases. As such VDB offers fast grid data access (average  $O(1)$ ) and high grid resolutions with low memory footprints. We also employ more modern algorithms like the Fast Sweeping Methods, that has recently been parallelized for sparse grids and offers a superior time complexity of  $(N)$  [2]. Specifically we present benchmark studies of level set topology optimization. This includes discussions of the computational times and memory footprints of topology optimization based on the sparse VDB data structure as well as a reference implementation based on a dense grid. The efficiency and scalability of advection schemes used to update the level set method such as the inverse square distance interpolation, Fast Marching Method, and Fast Sweeping Method, will also be discussed. References: [1] K. Museth, "VDB: High-Resolution Sparse Volumes With Dynamic Topology". ACM Transactions on Graphics, Volume 32, Issue 3, Pages 27:1-27:22, June 2013. [2] K. Museth, "Novel Algorithm for Sparse and Parallel Fast Sweeping: Efficient Computation of Sparse Signed Distance Fields, ACM SIGGRAPH 2017 Talks, Pages 74:1--74:2, July 2017.

## Crack Progress Analysis of Plain Concrete Using Prescribed Displacement Based on Hybrid-type Penalty Method

Atsushi Kambayashi<sup>\*</sup>, Norio Takeuchi<sup>\*\*</sup>, Yoshihiro Fujiwara<sup>\*\*\*</sup>, Tadahiko Shiomi<sup>\*\*\*\*</sup>

<sup>\*</sup>Graduate School of Engineering and Design, Hosei University, <sup>\*\*</sup>Graduate School of Engineering and Design, Hosei University, <sup>\*\*\*</sup>Mind Inc., <sup>\*\*\*\*</sup>Mind Inc.

### ABSTRACT

Crack progress analysis of plain concrete using prescribed displacement based on hybrid-type penalty method Atsushi Kambayashi / Norio Takeuchi Graduate School of Engineering and Design, Hosei University Yoshihiro Fujiwara / Tadahiko Shiomi Mind Inc. We studied a new function of a crack opening utilizing the hybrid-type penalty method (HPM) developed by Takeuchi [1] to analyze the strength characteristics of the structural members of reinforced concrete structures. In fracture analysis, the measurement of crack mouth opening displacement (CMOD) is important because it is directly related to the fracture energy,  $G_f$ . The HPM can accurately assess the CMOD in discrete cracks at intersection boundaries between the subdomains of the HPM, thereby reflecting accurate fracture energy of the discrete cracks. Using the HPM, we simulated experimental tests conducted for a concrete structure and showed good qualitative and quantitative agreements between the simulated and the experimental results. [2]. Although most of analyses were conducted using load control method and satisfactory results were obtained only the region from continua to discontinua, deformation control method used to obtain further analysis such as softening phenomena. In this work, we introduced a new function for a prescribed displacement control with the HPM. This involved introducing an algorithm for the prescribed displacement in the rmin method [3], which is an incremental load method. The rmin method can accurately track tensile cracking and compressive failure in concrete structure. To validate the accuracy of the displacement control analysis with the new function, we conducted several analyses using uniform triangular mesh and Delaunay triangular mesh. And , we also simulated the three-point bending test for notched beams, which is a standard test of the plain concrete. Finally, we discuss the load-displacement relationship between the experimental tests and numerical results. References [1] N. Takeuchi, Elasto-plastic analysis in soil and rock mechanics by using hybrid-type penalty method, Proc. of International Conference dedicated to the 95th Anniversary of Academician Nagush Kh. Arutyunyan, Institute of Mechanics National Academy of Sciences of Armenia, Yerevan-2007, pp.492–496. [2] Y. Fujiwara, N. Takeuchi, T. Shiomi, and A. Kambayashi, Discrete Crack Modeling of RC Structure Using Hybrid-Type Penalty Method, Int. J. Aerospace and Lightweight Structures, 3(2), 2013, pp. 263–275. [3] Y. Yamada, Y., N. Yoshimura and T. Sakurai, Plastic stress–strain matrix and its application for the solution of elasto-plastic problem by a finite element method, Int. J. Mechanical Sciences, 10, 1968, pp. 343–354.

## Partially-Averaged Navier-Stokes Formulation of Two-Layer Turbulence Model

Chetna Kamble\*, Sharath Girimaji\*\*

\*Texas A&M; University, \*\*Texas A&M; University

### ABSTRACT

Seamless transition between the Reynolds-Averaged Navier-Stokes (RANS) and Direct Numerical Simulation (DNS) is achieved by the Partially-Averaged Navier-Stokes (PANS) bridging strategy. In PANS, the physical resolution is controlled by filter widths which quantify the extent of partial averaging via the unresolved to total kinetic energy and dissipation ratios. This scale-resolving simulation method offers resolution of large scale turbulent structures at reasonable computational costs. In the present study, the PANS closure modeling is applied to a two-layer turbulence model which couples the standard k-epsilon model in the outer layer with a one-equation model in the near wall region. In RANS context, this turbulence model exhibits a superior near wall behavior compared to other near wall treatments. The PANS modified two-layer model aims to improve upon the near wall predictions by resolving the unsteady flow features of turbulence. The outer region in the PANS two-layer turbulence model is a PANS modified k-epsilon turbulence model, whereas, the inner layer comprises of a PANS modified one equation model of unresolved kinetic energy. The unresolved eddy viscosity and dissipation in the inner layer are specified in terms of unresolved kinetic energy and length scales. The effectiveness of the proposed PANS modified two-layer turbulence model is studied by a detailed comparison with a PANS k-omega turbulence model for a three-dimensional Channel flow for frictional Reynolds number,  $Re_{\tau} = 180$  and  $Re_{\tau} = 590$ . The proposed model is assessed on the performance in reproducing the mean statistics, the turbulent flow quantities and the resolution of the turbulent flow structures. The PANS modified two-layer model displays improved accuracy in capturing the turbulent flow physics and thereby solidifying the effectiveness of the two-layer PANS scheme in the near wall region.

## Isogeometric Analysis Using FEniCS

David Kamensky\*, Yuri Bazilevs\*\*

\*University of California, San Diego, \*\*University of California, San Diego

### ABSTRACT

This talk introduces recent work on implementing extraction-based isogeometric analysis (IGA) [1] on top of the FEniCS open source finite element (FE) software project [2], while retaining many of the powerful features that make the latter an attractive analysis platform. We hopefully dispel the sentiment that FEniCS and IGA present conflicting visions for automating numerical solution of partial differential equations (PDEs). Several aspects of our implementation differ from the algorithms for Bézier extraction put forward by Borden et al. [3] in 2011, and our alternative approach may be useful for retrofitting other FE codes as well. A collection of object-oriented abstractions separate PDE solution from generation of extraction operators and thereby permit the use of a wide variety of spline types. We cover, as illustrative examples, the discretization of various PDEs that benefit from IGA and the use of T-splines imported from CAD software. We conclude by discussing possible future directions, and welcome input from the FE(niCS) and IGA communities. References: [1] <https://doi.org/10.1016/j.cma.2004.10.008> [2] <https://doi.org/10.1007/978-3-642-23099-8> [3] <https://doi.org/10.1002/nme.2968>

## High-Order Meshes for the 3D Simulation of Electro-Magnetic-Induced Fusion

Kazem Kamran<sup>\*</sup>, Mark S. Shephard<sup>\*\*</sup>, Cameron W. Smith<sup>\*\*\*</sup>, Tzanio Kolev<sup>\*\*\*\*</sup>, Syun'ichi Shiraiwa<sup>\*\*\*\*\*</sup>, Mark L. Stowell<sup>\*\*\*\*\*</sup>

<sup>\*</sup>Rensselaer Polytechnic Institute, <sup>\*\*</sup>Rensselaer Polytechnic Institute, <sup>\*\*\*</sup>Rensselaer Polytechnic Institute, <sup>\*\*\*\*</sup>Lawrence Livermore National Laboratory, <sup>\*\*\*\*\*</sup>Massachusetts Institute of Technology, <sup>\*\*\*\*\*</sup>Lawrence Livermore National Laboratory

### ABSTRACT

Fusion reactors have sophisticated detailed 3D geometries, especially in the SOL/antenna region, which their inclusion is crucial for a reliable simulation of fusion process. In this work, a fully automated parallel mesh infrastructure, PUMI1, that generates adapted curved meshes classified on the CAD model, is integrated in to a state-of-the-art plasma simulation solver<sup>2</sup>. This 3D edge plasma wave solver is implemented in the MFEM3 open source scalable C++ library that supports elements of different type i.e. H1 to L2 and order. To demonstrate the effect of the high-order geometry representation, a realistic detailed 3D CAD model of the antenna placed in the fusion chamber is chosen and the effect of the adapted curve mesh on the quality of the RF wave solution is studied. [1] D.A. Ibanez, E.S. Seol, C.W. Smith and M.S. Shephard, &quot;PUMI: Parallel unstructured mesh infrastructure.&quot; ACM Transactions on Mathematical Software (TOMS) 42.3 (2016): 17. [2] S. Shiraiwa, J.C. Wright, P.T. Bonoli, T. Kolev, and M. Stowell, &quot;RF wave simulation for cold edge plasmas using the MFEM library.&quot; EPJ Web of Conferences. Vol. 157. EDP Sciences, 2017. [3] <http://ceed.exascaleproject.org/mfem/>

## Efficient Numerical Solution of the Hydraulic Fracture Problem for Planar Cracks

Sergey Kanaun\*

\*Tecnológico de Monterrey, México

### ABSTRACT

Efficient Numerical Solution of the Hydraulic Fracture Problem for Planar Cracks S. Kanaun Tecnológico de Monterrey, México An infinite elastic medium with a planar crack is considered. The crack is subjected to pressure of fluid injected inside the crack at a point of its surface. Description of the crack growth is based on the lubrication equation (local balance of the injected fluid and the crack volume), the elasticity equation for crack opening caused by fluid pressure, Poiseuille equation related the fluid flux with crack opening and the pressure gradient, and the criterion of crack propagation of linear fracture mechanics. The crack growth is simulated by a series of discrete steps. Each step consists of three stages: increasing the crack volume by a constant crack size, crack jump to a new size defined by the fracture criterion, and filling the new crack configuration by the fluid presented in the crack [1]. The problem is ill-posed and requires specific methods for numerical solution. The proposed method is based on an appropriate class of approximating functions for fluid pressure distributions on the crack surface and the theory of solution of ill-posed problems. It is shown that for small fluid viscosity, the three-parameter model of pressure distribution on the crack surface can be used [2]. The model allows one to satisfy the condition at the point of fluid injection, the balance equation of the volume of injected fluid and the crack volume, and fracture criterion at the crack edge. The analysis of evolution of the crack boundary is based on an original method of fast numerical solution of the integral equations of the crack problem of elasticity. The method allows constructing the crack boundary at discrete time moments for media with varying elastic properties and fracture toughness [3]. Evolution of the crack boundary in the process of fluid injection, time dependence of pressure distributions and crack openings are presented for examples of hydraulic fracture crack growth in layered heterogeneous media. [1] Kanaun S, Discrete model of hydraulic fracture crack propagation in homogeneous isotropic elastic media, International Journal of Engineering Sciences,10:1-14, 2017. [2] Kanaun S, Hydraulic fracture crack propagation in an elastic medium with varying fracture toughness, International Journal of Engineering Sciences,120:15-30, 2017. [3] Kanaun S, Markov A, Discrete and Three-Parameter Models of Hydraulic Fracture Crack Growth, WSEAS Transactions on Applied and Theoretical Mechanics, 12:147-156, 2017.

## **Constraints Handling in Multi-Objective Evolutionary Algorithm by Two-Stage Non-Dominated Sorting Using Direct/ Neighborhood Mating for Multi-Disciplinary Optimization**

Masahiro Kanazaki<sup>\*</sup>, Minami Miyakawa<sup>\*\*</sup>, Hiroyuki Sato<sup>\*\*\*</sup>

<sup>\*</sup>Tokyo Metropolitan University, <sup>\*\*</sup>Hosei University, <sup>\*\*\*</sup>The University of Electro-Communications

### **ABSTRACT**

A non-dominated sorting and dieted mating (TNSDM) is an operator to handle the constraint in evolutionary algorithms and authors have shown its applicability to real-world multi-disciplinary design problems with difficult-constraints. In original two-stage non-dominated sorting and dieted mating, parents are selected by non-dominated sorting based on constraint violation values and objective functions sequentially. NSGA-II with original TNSDM has achieved better performance than the well-known existent method. Extreme Pareto solutions, which are the end of the Pareto front and are equivalent to the optimum solution of the single objective problem, could not be acquired well only by the TNSDM. To overcome this problem, we developed a new method by introducing local mating in identical ranks in the TNSDM. We propose the expansion of TNSDM by adding neighborhood mating in identical ranks, and this is decided by non-dominated sorting. The proposed constrained handling method is employed in NSGA-II. We investigated the proposed approach by solving a test function and hybrid rocket design problem, a real-world problem. Each problem has six constraints. These problems are solved by the constrained NSGA-II, which is based on the simple penalty method, and the original TNSDM based NSGA-II. According to investigations, the proposed approach and TNSDM based optimizations acquire better Pareto front than the simple penalty based method does. In addition, the proposed method can acquire not only compromised solutions but also extreme Pareto solutions in good agreement with the TNSDM method. Comparing convergence history via hypervolume, the best performance also can be observed by the proposed method.

## Dynamic Behaviour of Different Pulmonary Monocusp Valve Designs

Harkamaljot Kandail\*, Marcelle Uiterwijk\*\*, Jolanda Kluin\*\*\*, Frans van de Vosse\*\*\*\*, Carlijn Bouten\*\*\*\*\*, Anthal Smits\*\*\*\*\*, Sandra Loerakker\*\*\*\*\*

\*Eindhoven University of Technology, Netherlands, \*\*Academic Medical Centre, University of Amsterdam, Netherlands, \*\*\*Academic Medical Centre, University of Amsterdam, Netherlands, \*\*\*\*Eindhoven University of Technology, Netherlands, \*\*\*\*\*Eindhoven University of Technology, Netherlands, \*\*\*\*\*Eindhoven University of Technology, Netherlands

### ABSTRACT

Purpose: Right ventricular outflow tract in children with congenital heart diseases is often reconstructed with a transannular patch and a monocusp valve. However, there are no set standards for the monocusp valve design and as such, these designs vary from clinic to clinic. The aim of this investigation is to propose an optimal pulmonary monocusp valve design with physiologic opening and closing behaviour, good coaptation and minimal aortic regurgitation. Methods: Dynamics of a pulmonary monocusp valve which is currently under pre-clinical evaluation within 1Valve program, hereinafter referred to as PMV-1 valve, were simulated using finite element (FE) methods to optimise the monocusp design. A second hypothetical valve design was then proposed to overcome the limitations of PMV-1 valve and its dynamic behaviour was also simulated using FE methods. The native pulmonary artery was modelled as an anisotropic material using a Holzapfel-Gasser-Ogden model while the monocusp valves and transannular patches were modelled as isotropic Neo-Hookean hyperelastic materials. Valve dynamics were simulated by imposing the pressure difference between the right ventricle and the pulmonary artery on the ventricular side of the respective monocusp valve designs and all simulations were performed for three cardiac cycles. Results: Dynamics of PMV-1 valve from the FE model were compared with dynamics from an ex-vivo heart model and a good agreement between the numerical and experimental results was observed. PMV-1 valve was implanted in the pulmonary artery in the closed position and its free-edge was prone to folding when the monocusp valve opened during systole. During diastole, only an edge-based coaptation between the free-edge of PMV-1 valve and pulmonary artery was observed. Unlike the initial design, the proposed design of the second monocusp valve is meant to be implanted in the open position. FE results for the second monocusp valve predicted that the free-edge of this valve design does not fold during the entire cardiac cycle. Also, better coaptation was seen for this valve design as the coaptation length between the free-edge and pulmonary artery was approximately 2.1 mm. Conclusion and future work: FE results from this investigation suggest that it is desirable to implant the pulmonary monocusp valve in the open instead of the closed position to achieve physiologic valve dynamics. This is an ongoing research project and fluid-structure interaction simulations are currently being performed to quantify aortic regurgitation and the risk of thrombosis associated with each valve design.

## **Spectral Element Solutions for Heat Transfer Augmentation**

Kento Kaneko\*, Paul Fischer\*\*

\*UCIC, \*\*UCIC

### **ABSTRACT**

We consider spectral element based simulations of thermal transport to study heat transfer augmentation in pipe flow with wire coil inserts, which induce turbulence and a rotational mode. We compare our numerical results with available experimental data for three distinct coil geometries and several Reynolds numbers. Several additional simulations were run to determine the change in the Nusselt number when the rotational mode is completely removed. Three cases have geometries with equally-spaced tori whose distance corresponds to the pitch in the coil cases and a fourth case has a meandering coil with no net helicity. We present Nusselt number vs. Reynolds number results for all of these cases and analyze the effectiveness of gradient-diffusion based models for prediction of mean thermal transport in these configurations.

## Modeling of Locked Particle Behavior in Magnetic Separation Using DEM and FEM

Masanori Kaneko<sup>\*</sup>, Yuki Tsunazawa<sup>\*\*</sup>, Takuma Tokoro<sup>\*\*\*</sup>, Giuseppe Granata<sup>\*\*\*\*</sup>, Chiharu Tokoro<sup>\*\*\*\*\*</sup>

<sup>\*</sup>Graduate School of Creative Science and Engineering, Waseda University, <sup>\*\*</sup>National Institute of Advanced Industrial Science and Technology, <sup>\*\*\*</sup>Graduate School of Creative Science and Engineering, Waseda University, <sup>\*\*\*\*</sup>Faculty of Science and Engineering, Waseda University, <sup>\*\*\*\*\*</sup>Faculty of Science and Engineering, Waseda University

### ABSTRACT

Magnetic separation is one of the mineral processing technology. Its technology utilizes magnetic susceptibility of different substances to separate them. In conventional magnetic separation studies, a particle was assumed as a free particle composed of one component. On the other hand, in actual operations, feed particles usually consist of locked particles composed of some components. The efficiency of magnetic separation was affected by locked particles. To achieve high efficiency, it is necessary that locked particles are appropriately controlled in the magnetic separation. However, there has not been little knowledge about the magnetic force acting on locked particles and the behavior of the locked particles in magnetic separators. Therefore, it is important to model the magnetic force acting on locked particles in magnetic field. This study modeled the magnetic force acting on locked particles by the magnetic field analysis. This study assumed that locked particles composed of two components with different magnetic susceptibilities. The finite element method (FEM) was used to calculate the magnetic force acting on a locked particle. According to the FEM analysis on the different composition ratio of locked particles, it was introduced that the model formula of the relationship between the magnetic susceptibility and the composition ratio of locked particles in the magnetic field. The FEM analysis suggested that this model formula depended on distribution of components within particles. Based on the FEM analysis results, magnetic separation incorporating locked particles model was simulated. In this simulation, the behavior of locked particles was calculated by the discrete element method (DEM), and the magnetic field in a magnetic separator was calculated by the FEM. Using this simulation, it was analyzed that the relationship between the applied magnetic field and the efficiency of magnetic separation. Furthermore, the simulation result was compared with the experimental results. In the case of particles consisting of only free particles, the simulation results qualitatively agreed with the experimental result. However, there was some quantitative difference between the simulation and experimental results. In the case of particles containing locked particles, the difference between the simulation and experimental results became smaller. As a result, it was suggested that the behavior of locked particles could be appropriately simulated by the locked particle model.

## Development of a Stable Structure-fluid-electrostatic Analysis System

Shigeki Kaneko<sup>\*</sup>, Tomonori Yamada<sup>\*\*</sup>, Shinobu Yoshimura<sup>\*\*\*</sup>, Giwon Hong<sup>\*\*\*\*</sup>, Naoto Mitsume<sup>\*\*\*\*\*</sup>

<sup>\*</sup>The University of Tokyo, <sup>\*\*</sup>The University of Tokyo, <sup>\*\*\*</sup>The University of Tokyo, <sup>\*\*\*\*</sup>The University of Tokyo, <sup>\*\*\*\*\*</sup>The University of Tokyo

### ABSTRACT

Fluid-structure interaction (FSI) is an important phenomenon in engineering because it often causes unexpected mechanical vibration and sometimes brings the structural destruction. Numerical simulation is effective for the research on the control of FSI because numerical simulation is proper for parametric study and can cut the cost of experiments. In our previous study [1], we proposed FSI analysis with active control, where both fluid and structural analyses were performed in detail, but specific models of actuators and sensors were not considered. It was assumed that the mass and volume of the actuators and sensors could be neglected and arbitrary control force could be given. It is necessary to introduce a specific model in order to put the previous analysis to practical use. For reducing the vibration caused by FSI, piezoelectric actuators and sensors are widely used because it has excellent electromechanical properties. For examples, flutter phenomenon which causes undesired vibration to the aircraft is diminished by using piezoelectric materials. In this study, we implement the model of piezoelectric materials to our previous system. In order to analyze strictly all the physics of piezoelectric materials, the host structure, and the surrounding fluid, we develop a general-purpose structure-fluid-electrostatic analysis system by integrating electrostatic analysis and partitioned iterative FSI analysis of the previous system. To find an optimal balance between accuracy and computational cost, we propose and verify three coupling approaches. In the first approach, structure-fluid-electrostatic analysis is split into electrostatic analysis and FSI analysis. The second approach splits into fluid analysis and structure-electrostatic analysis. The structure-electrostatic is solved by monolithic approach. In the third approach, electrostatic analysis is inserted into FSI iteration. In the present study, we investigate the stability of each system by simulating various control of FSI, and we compare three systems in the viewpoint of stability. References [1] S.Kaneko, G.Hong, N.Mitsume, T.Yamada, S.Yoshimura, Partitioned-coupling FSI analysis with active control, Computational Mechanics, Vol.60, Nos.4, pp.549-558, 2017.

## **A Study on Accuracy Improvement of Decomposed Surrogate Model with Random Samples for High Dimension Problem**

Kyeonghwan Kang\*, Ikjin Lee\*\*

\*KAIST (Korea Advanced Institute of Science and Technology), \*\*KAIST (Korea Advanced Institute of Science and Technology)

### **ABSTRACT**

Surrogate model has been widely used to solve engineering problems with heavy computation, and there have been many studies to generate surrogate model with limited samples due to the computation cost. However, practical surrogate model generating method dealing with high dimensional design space are still challenging. Among the approaches dealing with high dimensional surrogate model, decomposition is one of popular approach for its efficiency and flexibility. There are various approaches of decomposition, but accurate decomposition results require to generate samples not in the decomposed design space. Furthermore, there can exist random samples in practice engineering problem, but these samples are also difficult to be utilized in the decomposed surrogate model. In this study, the potential accuracy improvement method using the samples not in the decomposed design space is proposed. Previously unused samples are considered for approximation using Gaussian process and variable screening, and virtual samples are generated to improve the accuracy of each decomposed surrogate model. Numerical examples and engineering problem are used to check the performance of proposed method, and it is shown that the accuracy of the surrogate model is surely improved with random samples.

## Topology Optimization with Manufacturing-related Constraints Expressed by Domain Integral of Level Set Function

Zhan Kang<sup>\*</sup>, Yaguang Wang<sup>\*\*</sup>, Pai Liu<sup>\*\*\*</sup>

<sup>\*</sup>Dalian University of Technology, China, <sup>\*\*</sup>Dalian University of Technology, China, <sup>\*\*\*</sup>Dalian University of Technology, China

### ABSTRACT

In topology optimization of continuum structures, certain geometrical constraints and interfacial behaviors, as well as uncertain geometrical manufacturing imperfections, are often of great importance to ensure the manufacturability or integrity of the structures. This talk will present some of our new developments on the study of manufacturing-related topology optimization problems in the level set function-based framework. The level set, as an implicit geometrical model, offers a natural description of shape and topology evolution and thus can be suitably used for representation of some geometrical constraints [1]. In our previous work, we proposed a unified integral-form constraint to avoid overlaps, to control the distances among the embedded objects in the topology optimization of multi-component structures [2]. Now we extend the idea of integral-form constraints to expression of other geometrical constraints to ensure the manufacturability of topology optimization results, including the casting constraint, the overhang angle constraint in additive manufacturing, and the shell-infill configuration description. All these constraints have explicit domain-integral forms, facilitating their sensitivity analysis with respect to shape variations. This approach inherits the properties of easier geometric information extraction of the implicit level set model. We also propose a level set-based implicit description model for modeling geometrical uncertainties arising from manufacturing errors. In particular, this model can mimic topological defects often exhibited by micro-size fabrication, which may result in breakage of load transmission paths of the optimized designs. Such a model is then combined with the uncertainty quantification techniques and employed in robust topology optimization considering random manufacturing errors. Keywords: topology optimization, level set, manufacturing constraint, geometrical constraints, geometrical uncertainty References 1. G. Allaire, F. Jouve, G. Michailidis, Thickness control in structural optimization via a level set method, *Struct. Multidiscip. Optim.* 53 (2016) 1349-1382. 2. Z. Kang, Y. Wang, Y. Wang, Structural topology optimization with minimum distance control of multiphase embedded components by level set method, *Comput. Methods Appl. Mech.* 306 (2016) 299-318.

## Exchange-correlation Potentials from Electron Densities Using a Complete Basis

Bikash Kanungo\*, Vikram Gavini\*\*

\*Mechanical Engineering, University of Michigan, Ann Arbor, MI, \*\*Mechanical Engineering, University of Michigan, Ann Arbor, MI

### ABSTRACT

Exchange-correlation (xc) functionals, the cornerstone of the success of density functional theory (DFT), encapsulate the quantum many-electron interactions in terms of a mean-field. Although known to be unique functionals of the ground-state electronic charge density,  $n(r)$ , the exact form of these functionals - expressed either as energy ( $\text{Exc}[n(r)]$ ) or potential ( $\text{Vxc}[n(r)]$ ) - are unknown, necessitating the use of approximate functionals. The existing xc functionals, despite their success in predicting wide range of materials properties, exhibit notable failures - under-predicted bandgaps, incorrect bond-dissociation curves, wrong charge-transfer excitations, to name a few. Typically, these approximations are constructed through semi-empirical parameter fitting in model systems, thereby making systematic improvement and conformity to certain known exact conditions difficult. We attempt to address this through data-driven modeling of xc functionals. This involves, generating a training data set comprising of  $n(r)$  to  $\text{Vxc}(r)$  map, and then, use of machine learning algorithms to learn the functional form of  $\text{Vxc}[n(r)]$  (and  $\text{Exc}[n(r)]$ ), conforming to the exact conditions. In this work, we tackle the first step of generating the training data. To elaborate, it involves generating accurate  $n(r)$  from wavefunction-based calculations (e.g., quantum Monte-Carlo, full Configuration-Interaction), and then inverting the Kohn-Sham (KS) eigenvalue problem to obtain the  $\text{Vxc}(r)$  that yields the same  $n(r)$ . We perform the inversion by posing it as a PDE-constrained optimization problem with  $\text{Vxc}(r)$  as the control variable and the KS eigenvalue problem as the PDE-constraint. We note that all previous attempts at this inverse problem have suffered from non-unique solutions or spurious oscillations in  $\text{Vxc}(r)$ , both of which are attributed to the incompleteness of the Gaussian basis that was employed in the inversion. We resolve them by using spectral finite-elements - a complete basis - to discretize the problem. We employ limited-memory BFGS (a quasi-Newton solver) to solve the nonlinear optimization problem. Additionally, we make use of appropriate weights for the objective function to expedite convergence as well as to avoid ill-conditioning in the low density region. We validate the algorithm, to an accuracy of  $\leq 1$  mHa, for cases where the densities are obtained from known xc functionals (LDA and GGA). Next, we demonstrate the capability of the algorithm for densities obtained from wavefunction-based calculations. Time permitting, we demonstrate preliminary results from simple regression techniques, that can faithfully generate bond-dissociation curves, using a few data points, thereby holding promise for future machine learning algorithms on the training data.

## **Genetic Algorithm for Optimizing an Airfoil Shape of Wind Turbine by Direct-forcing Immersed Boundary Modeling**

Chao-Ching Kao<sup>\*</sup>, Ming-Jyh Chern<sup>\*\*</sup>, Tzyy-Leng Horng<sup>\*\*\*</sup>, Nima Vaziri<sup>\*\*\*\*</sup>

<sup>\*</sup>National Taiwan University of Science and Technology, <sup>\*\*</sup>National Taiwan University of Science and Technology,  
<sup>\*\*\*</sup>Feng-Chia University, <sup>\*\*\*\*</sup>Islamic Azad University Karaj Branch

### **ABSTRACT**

Renewable energy is a popular topic nowadays due to energy shortage. Especially wind energy converted by a wind turbine receives more attentions. In the present study, the blade design of the wind turbine using a couple method with computational fluid dynamics (CFD) and genetic algorithm (GA) is discussed. The blade shape is the most significant effective parameter in the wind energy conversion. Hence, we dedicated to utilizing an optimal method for the cross-sectional shape of blade, i.e., an airfoil, in order to get the better efficiency for producing the higher lift and lower drag to drive the wind turbine. According to the previous study, the Genetic Algorithm (GA) is known to be the robust method in the optimal design area. The Real-coded Genetic algorithm is considered because it can solve the defect of binary code. That is, the chromosomes length is too long to code. While the PARSEC parameterization method is used to represent the shape of airfoil through the eleven parameters as the control variables. Furthermore, a direct-forcing immersed boundary (DFIB) method is employed for simulations of interaction of rotating blades in a flow field at moderate low Reynolds number. Numerical results reveal that the shape of airfoil can be optimized and the proposed DFIB model coupled with GA successfully simulates the moving blade in flow field for obtaining the high lift-drag ratio.

# Investigating Strain Localization in Additively Manufactured Ti-alloys Using Detailed Material Characterization, Crystal Plasticity Finite Element Modeling and High Resolution Digital Image Correlation

Kartik Kapoor\*, Todd Book\*\*, Michael Sangid\*\*\*

\*Purdue University, \*\*Purdue University, \*\*\*Purdue University

## ABSTRACT

Titanium alloys, produced via additive manufacturing techniques, offer tremendous benefits over conventional manufacturing processes such as reduction in production lead time and increased geometrical flexibility. However, there is inherent uncertainty associated with their material properties, often stemming from the variability in the manufacturing process itself along with the presence of residual stresses in the material, which prevents their use as critical components. The current work investigates Ti-6Al-4V, a dual phase Titanium alloy produced via direct metal laser sintering by carrying out crystal plasticity finite element (CPFE) simulations which models both the alpha and beta phases of the material explicitly and high-resolution digital image correlation (HR-DIC) on samples subject to cyclic loading. This is preceded by detailed material characterization using electron backscatter diffraction and back-scattered electron imaging whose results are utilized to create a realistic finite element microstructural mesh with spatial and crystallographic information about both the alpha and beta phases of the material. In addition, results from TEM studies, informing about distribution of the total dislocation density are utilized to inform the CPFE model itself. A method to incorporate the effect of grain-level residual stresses via geometrically necessary dislocations (GNDs) is developed and implemented within the CPFE framework. Using this approach, grain level information about residual stresses, in the form of GND densities obtained spatially over the region of interest, directly from the experimental material characterization, is utilized as an input to the model. Results indicate that the simulation strain maps show good match with those obtained using HR-DIC. In addition, possible sites for damage nucleation are identified, which correspond to regions of high plastic strain accumulation and occur near prior beta boundaries suggesting that prior beta boundaries play a critical role in strain localization. Further, a more robust method to incorporate residual stresses that involves modifying the elastic-plastic decomposition of the deformation gradient is proposed and implemented within the CPFE model. This is then tested with an available dataset of High-Energy Diffraction Microscopy experiments performed on Ti-alloys.

## Fibrous Materials Characterization through a 3-D Fiber Network Model

Alp Karakoc\*, Jouni Paltakari\*\*, Eero Hiltunen\*\*\*

\*Aalto University, \*\*Aalto University, \*\*\*Aalto University

### ABSTRACT

The current work presents a 3-D fiber network model mimicking fibrous materials such as non-woven felt, paper and paperboards [1]. The objective is to investigate the effects of geometric properties and interactions of fibers on the overall stiffness and strength characteristics. In consideration to the objective, a stochastic micro-mechanical approach using random sequential adsorption was implemented to generate fiber geometries, alignments and positions in a confined space. Thereafter, material properties were assigned to each fibers and cohesive properties on the surface of each fiber intersection. Dirichlet boundary conditions were applied on the confined space and the problem was solved in explicit time integration scheme to determine the fiber network characteristics. [1] Karakoç A., Hiltunen E., Paltakari J. Geometrical and spatial effects on fiber network connectivity. *Composite Structures*, 2017; 168: 335-344.

## The Elusive Granular Length Scale: Continuum vs Discrete

Konstantinos Karapiperis\*, Jose Andrade\*\*

\*California Institute of Technology, \*\*California Institute of Technology

### ABSTRACT

Classical Cauchy continuum theories are known to be ill-posed after the onset of shear banding instability in granular materials. More elaborate continuum descriptions have provided a remedy by introducing a length scale, but have not enjoyed general acceptance due to the lack of a sound micromechanical basis. The renewed interest in such theories is largely due to grain-scale observations providing partial justification of the underlying assumptions. In this work, we provide a critical assessment of micropolar plasticity by comparing continuum predictions with grain-scale measurements in virtual triaxial experiments of real sands. Particularly, we employ the recently developed 3D Level-Set Discrete Element Method to shed light into the kinematics (rotational vortices) and kinetics (force chain buckling, couple stress) of shear bands obtained by means of advanced homogenization schemes. Upon identifying the major limitations of current theoretical models, we propose elements of an alternative framework possessing a direct physical interpretation of the granular length scale, towards the final goal of developing an enhanced multiscale theory.

# PARALLEL PARTITIONED FINITE ELEMENT SOLVERS WITH NON-MATCHING TIME-STEPS

SAEID KARIMI  
FullRank Software LLC  
3139 W. Holcombe Blvd. #325  
Houston, TX 77025, USA  
skarimi@fullranksoftware.com; www.fullranksoftware.com

**Key words:** multi-time-step, time-integration methods, structural dynamics, domain decomposition, differential-algebraic equations.

## 1. INTRODUCTION AND MOTIVATION

Computational methods play an increasingly important role in modern engineering and scientific practice. Availability of high-performance computers along with the advanced (and easy-to-use) software, has enabled practitioners to successfully model complex physical, chemical and biological processes. For instance, fluid-structure interaction problems are some of the most challenging to efficiently model [1]. Irrespective of the problem, any large real-world computer modeling of engineering or scientific applications typically relies on partitioning (domain decomposition) of computational domain and parallel computing.

Domain partitioning (or domain decomposition) algorithms have become a popular approach to develop fast parallel solvers for various problems [2; 3]. In these algorithms, the spatial computational domain is split into a number of subdomains. This allows distribution of the computation among a pool of processors (CPUs and GPUs) available [4]. Obviously, such algorithms need some information (either primal or dual quantities) to be transferred across to adjacent subdomains. The domain partitioning can be either overlapping or non-overlapping. In general, the interface variables and compatibility of solution near the interface are defined implicitly.

In addition to work distribution among parallel processors, domain partitioning algorithms have other advantages. One can use different numerical formulations in different subdomains. Therefore, based on the nature of the process occurring at a particular subdomain, a suitable numerical formulation can be implemented to approximate the solution in the desired subdomain. A class of methods that offers such flexibility in terms of time-stepping (i.e., with different time-steps in different subdomains) is labeled *multi-time-step* or *sub-cycling* methods [6; 7]. Under this class of methods, the user can choose non-matching time-steps for time-integration in different subdomains. This feature is particularly of interest when a mix of implicit and explicit time-integration algorithms are used in different

subdomains [8; 9; 10]. In light of domain partitioning algorithms, multi-time-step methods can be of strong or weak types.

Weak multi-time-step algorithms rely on iterative approximation of variables in subdomains and their respective interfaces. These updated quantities are then used to advance the solution in other subdomains in time, which will in turn be used to update interface quantities. This iteration continues until desired convergence criteria are satisfied. This type of algorithm is extremely popular and forms the basis for many partitioned and multi-physics simulations. One of the main reasons why such algorithms are common is that the available (or legacy) solvers can be easily adopted in this approach, hence, accelerating the development phase. Some (but not all) of successful applications of weak algorithms can be found in [10; 11; 12]. Despite the attractive concept, weak partitioned algorithms are prone to numerical instability, especially in time-dependent problems. An alternative approach to multi-time-step simulation is to use strong coupling [13]. Unlike the weak algorithms, strong partitioning algorithms update the subdomain variables and the interface conditions monolithically. This means that iterations from one subdomain to another are not needed. These algorithms have better properties with respect to numerical stability. However, these algorithms are not as popular as the weak type. The reason being that development of software based on strong algorithms needs major modification to the existing computer codes. This hurdle translates into longer and more complicated development process. This drawback, however, has not stopped researchers to investigate strong multi-time-step algorithms. Some results in this area can be found in [14; 15; 16; 17].

This article is devoted to an overview of strong partitioning algorithms with non-matching time-steps. The theory and other aspects of these algorithms will be outlined. For the sake of presentation, we will limit our scope to elastodynamics problems. The rest of this paper is organized as follows: Section 2 is devoted to the theory and numerical formulation, Section 3 presents some numerical examples to demonstrate the discussed algorithms, and the conclusions are drawn in Section 4.

## 2. MATHEMATICAL MODELS AND NUMERICAL ALGORITHMS

**2.1. Governing equations.** Consider an open domain  $\Omega \subset \mathbb{R}^{nd}$  and  $\Gamma_D \cup \Gamma_N = \partial\Omega$ . Boundary subsets  $\Gamma_D$  and  $\Gamma_N$  are mutually exclusive. The time-interval of interest is  $\mathcal{I} = [0, T)$ . The displacement field of the solid body,  $\mathbf{u}$  defined in  $\Omega$ , evolves according to conservation of linear momentum. We take the density of the solid to be  $\rho$  and the specific body force to be  $\mathbf{b}$ . The governing PDE can hence be written as:

$$\rho \frac{\partial^2 \mathbf{u}}{\partial t^2} = \text{div} [\mathbf{T}] + \rho \mathbf{b} \quad \mathbf{x} \in \Omega, t \in \mathcal{I} \quad (2.1a)$$

$$\mathbf{u} = \mathbf{u}_p \quad \mathbf{x} \in \Gamma_D, t \in \mathcal{I} \quad (2.1b)$$

$$\mathbf{T} \hat{\mathbf{n}} = \mathbf{t}_p \quad \mathbf{x} \in \Gamma_N, t \in \mathcal{I} \quad (2.1c)$$

$$\mathbf{u} = \mathbf{u}_0 \quad \mathbf{x} \in \Omega, t = 0 \quad (2.1d)$$

$$\frac{\partial \mathbf{u}}{\partial t} = \mathbf{v}_0 \quad \mathbf{x} \in \Omega, t = 0 \quad (2.1e)$$

where  $\mathbf{u}_p$  and  $\mathbf{t}_p$  are prescribed values for displacement and traction on boundary. The initial displacement and velocity are shown as  $\mathbf{u}_0$  and  $\mathbf{v}_0$ . The stress tensor is denoted by  $\mathbf{T}$  and  $\text{div}[\cdot]$  is the divergence operator. The stress tensor is related to the displacement field

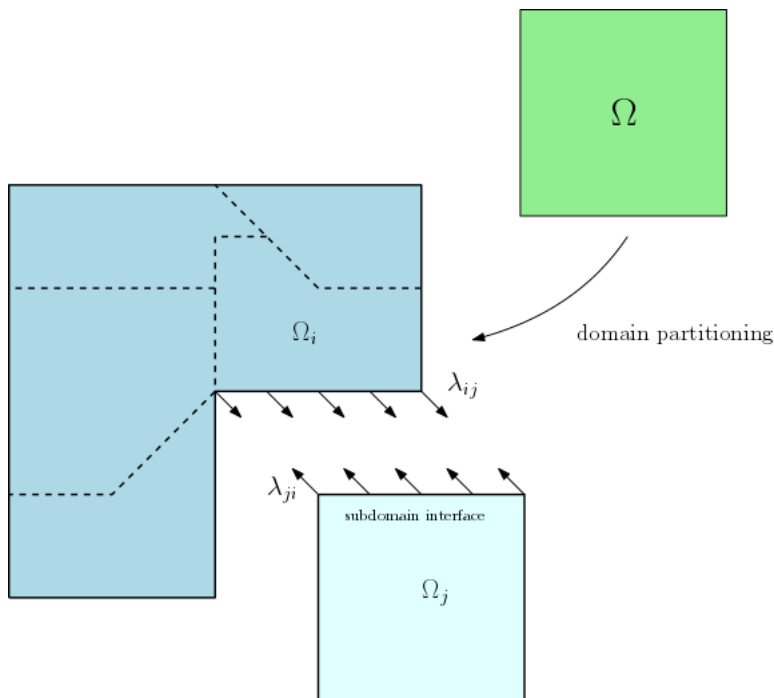


FIGURE 1. Domain partitioning of initial domain  $\Omega$  into an arbitrary number of subdomains is shown (dashed lines show the interfaces between subdomains). Subdomains  $\Omega_i$  and  $\Omega_j$  share an interface (subdomain interface in the figure), where the Lagrange multipliers  $\lambda_{ij} = -\lambda_{ji}$  are used to enforce compatibility of solution.

through a constitutive relation. For a more detailed account of constitutive models for solids and their finite element treatment, the reader can consult [18] and references therein.

In this paper, we are concerned with solving coupled PDEs of the form given in (2.1) on multiple subdomains that share interface with one another. Hence, in addition to the typical initial and boundary conditions given in (2.1), one needs constraints to ensure compatibility of the displacement fields at the interface of subdomains. As shown in figure 1, we will use Lagrange multipliers defined on subdomain interfaces to enforce an algebraic constraint of form

$$\mathbf{u}_i - \mathbf{u}_j = \mathbf{0} \quad (2.2)$$

on the interface of  $\Omega_i$  and  $\Omega_j$  (and all other neighboring subdomains). Subindices  $i$  and  $j$  indicate the respective subdomains. This equation, in addition to the conservation equation in (2.1) for each subdomain, completes the formulation of the problem on a partitioned domain. One can derive a weak form using a desired formalism (e.g., Galerkin) and discretize using the finite element methods.

**2.2. Finite element discretization.** Consider domain  $\Omega$  partitioned into  $\mathcal{S}$  non-overlapping subdomains. The boundary of each subdomain  $\Omega_i$  is comprised of  $\partial\Omega_i \cap \Gamma_D$ ,  $\partial\Omega_i \cap \Gamma_N$  and  $\tilde{\Gamma}_i$ . The part of boundary that is shared with other subdomains' boundaries is denoted by

$\tilde{\Gamma}_i$ . The function spaces needed for a FEM discretization of the problem at hand include

$$\mathcal{U}_i = \left\{ \mathbf{u}_i \in (H^1(\Omega_i))^{nd} \mid \mathbf{u}_i = \mathbf{u}_p \text{ on } \mathbf{x} \in \Gamma_D \cap \partial\Omega_i, \frac{\partial \mathbf{u}_i}{\partial t} \in (L^2(\Omega_i))^{nd}, \frac{\partial^2 \mathbf{u}_i}{\partial t^2} \in (L^2(\Omega_i))^{nd} \right\} \quad (2.3a)$$

$$\mathcal{W}_i = \left\{ \mathbf{w}_i \in (H^1(\Omega_i))^{nd} \mid \mathbf{w}_i = \mathbf{0} \text{ on } \mathbf{x} \in \Gamma_D \cap \partial\Omega_i \right\} \quad (2.3b)$$

for all subdomains  $i = 1, \dots, \mathcal{S}$ . In addition, trace operators are needed that are defined on the subdomain interfaces

$$\mathcal{M} = \left\{ \boldsymbol{\mu} \in \left( H^{-1/2} \left( \bigcup_{i=1}^{\mathcal{S}} \tilde{\Gamma}_i \right) \right)^{nd} \right\}. \quad (2.4)$$

Furthermore, the inner product on any subset  $K$  of  $\Omega$  is defined as

$$(a, b)_K = \int_K a \cdot b \, d\Omega, \quad (2.5)$$

with  $a \in \mathcal{W}_i$  and  $b \in \mathcal{U}_i$ . Given these definitions, a weak form for the partitioned can be written on finite element  $e$  belonging to the triangulation (mesh) on subdomain  $i$  (i.e.,  $\forall \Omega_e \subset \mathcal{T}(\Omega_i)$ ,  $i = 1, \dots, \mathcal{S}$ ) as: find  $\mathbf{u}_i \in \mathcal{U}_i$  and  $\boldsymbol{\lambda} \in \mathcal{M}$ , such that

$$\left( \mathbf{w}, \rho \frac{\partial^2 \mathbf{u}_i}{\partial t^2} \right)_{\Omega_e} = (\mathbf{w}, \mathbf{t}_p)_{\partial\Omega_e \cap \Gamma_N} + (\mathbf{w}, \text{Sign}[\tilde{\Gamma}_i] \boldsymbol{\lambda})_{\partial\Omega_e \cap \tilde{\Gamma}_i} - (\text{grad}[\mathbf{w}^T], \mathbf{T})_{\Omega_e} + (\mathbf{w}, \rho \mathbf{b})_{\Omega_e} \quad \forall \mathbf{w} \in \mathcal{W}_i \quad (2.6a)$$

$$(\boldsymbol{\mu}, \mathbf{u}_i - \mathbf{u}_j)_{\tilde{\Gamma}_i \cap \tilde{\Gamma}_j} = 0 \quad i, j = 1, \dots, \mathcal{S}, \quad i \neq j \text{ and } \tilde{\Gamma}_i \cap \tilde{\Gamma}_j \neq \emptyset \quad \forall \boldsymbol{\mu} \in \mathcal{M} \quad (2.6b)$$

where  $\text{Sign}[\Gamma_i]$  is an arbitrary sign of +1 or -1 assigned to the subdomain interfaces such that

$$\text{Sign}[\tilde{\Gamma}_i \cap \tilde{\Gamma}_j] = -\text{Sign}[\tilde{\Gamma}_j \cap \tilde{\Gamma}_i]. \quad (2.7)$$

It should be noted that proper inf-sup conditions [19] need to be satisfied to ensure stability of this discretization. Finite element discretization results in a differential/algebraic equation [20] in terms of the nodal displacement values and the Lagrange multipliers as given below:

$$\mathbf{M}_i \ddot{\mathbf{u}}_i = \mathbf{f}(\dot{\mathbf{u}}_i, \mathbf{u}_i; t) + \mathbf{C}_i^T \boldsymbol{\Lambda} \quad i = 1, \dots, \mathcal{S} \quad (2.8a)$$

$$\sum_{i=1}^{\mathcal{S}} \mathbf{C}_i \mathbf{u}_i = \mathbf{0} \quad (2.8b)$$

where  $\mathbf{M}_i$  and  $\mathbf{u}_i$  are the mass matrix and nodal displacements, respectively. The vector of nodal Lagrange multipliers is denoted by  $\boldsymbol{\Lambda}$  and  $\mathbf{C}_i$  are the signed Boolean matrices (discretized trace operators). The superposed dots show differentiation with respect to time. Equation (2.8) is a differential/algebraic equation of index 3. This equation can be solved in a multitude of ways.

**2.3. Algebraic interface constraint.** Note that in a time-continuous setup, the algebraic constraint can be replaced by its derivatives given below

$$\sum_{i=1}^{\mathcal{S}} \mathbf{C}_i \mathbf{u}_i = \mathbf{0}, \quad \sum_{i=1}^{\mathcal{S}} \mathbf{C}_i \dot{\mathbf{u}}_i = \mathbf{0}, \quad \sum_{i=1}^{\mathcal{S}} \mathbf{C}_i \ddot{\mathbf{u}}_i = \mathbf{0} \quad (2.9)$$

However, the time discretization of equations (2.8) with either of the constraints given in (2.9) will indeed yield different numerical values (as it is expected). Also, enforcing one type of interface constraint (e.g., displacements or velocities) does not imply compatibility of the other kinematic variables at the subdomain interface [21]. This phenomena is known as *drift-off*, which refers to deviation of the numerical solution from the constraints manifold [20]. Hence, one of the main difficulties in developing numerical algorithms for differential/algebraic equations compared to purely differential equations is recognizing the drift-off in the numerical solution. Drift-off is usually not avoidable. Hence, various numerical methodologies for controlling this effect have been developed [22; 23].

A method for controlling the drift-off was proposed by Baumgarte in [24]. The motivation behind using the Baumgarte stabilization method is to control drift-off from the displacement, velocity and acceleration constraints. The Baumgarte stabilization method for the current problem reads as follows:

$$\sum_{i=1}^S \mathbf{C}_i \ddot{\mathbf{u}}_i + \alpha_1 \sum_{i=1}^S \mathbf{C}_i \dot{\mathbf{u}}_i + \alpha_2 \sum_{i=1}^S \mathbf{C}_i \mathbf{u}_i = \mathbf{0} \quad (2.10)$$

where  $\alpha_1$  and  $\alpha_2$  are user-defined constants that control (supress) the values of drift-off. Note that the Baumgarte stabilization method is an efficient way of controlling the drift-off, as only one algebraic constraint (as a result only one Lagrange multiplier) is used. For comparison, the Gear-Gupta-Leimkuhler (GGL) methodology [21; 25; 26] requires more than one algebraic constraint (and consequently more than one Lagrange multiplier). Hence, the size of the problem is smaller and more suitable for computer simulations, especially in practical problems with a large number of subdomains. However, GGL method often provides better accuracy because the extra interface constraints are directly enforced.

In this article, Newmark time-integration methods will be used. Time discretization using the Newmark method [27] can be written as:

$$\mathbf{v}^{(n+1)} = \mathbf{v}^{(n)} + (1 - \gamma)\Delta t \mathbf{a}^{(n)} + \gamma \Delta t \mathbf{a}^{(n+1)} \quad (2.11a)$$

$$\mathbf{d}^{(n+1)} = \mathbf{d}^{(n)} + \Delta t \mathbf{v}^{(n)} + \Delta t^2 \left(\frac{1}{2} - \beta\right) \mathbf{a}^{(n)} + \Delta t^2 \beta \mathbf{a}^{(n+1)} \quad (2.11b)$$

where  $\Delta t$  is the time-step,  $\beta$  and  $\gamma$  are time-integration parameters. The time-discretized values of displacement, velocity and acceleration are denoted by  $\mathbf{d}$ ,  $\mathbf{v}$  and  $\mathbf{a}$ , respectively. Note that with domain partitioning one can choose subdomain-specific time-steps and integration parameters. Having subdomain-specific parameters give the user the freedom to choose different members of the Newmark time-stepping family of algorithms for different subdomains. An important application of this feature is the implicit-explicit time-integration. The Newmark time-stepping algorithms (and its descendants) are well studied in numerical solution of second-order differential equations. Application of this class of methods to solution of differential algebraic equations (such as in equation (2.8)) is studied to a lesser extent. In the following section, we will explore the differences in the outcome of numerical simulations based on the type of interface constraint utilized.

### 3. NUMERICAL EXAMPLE

Consider a unit square domain agitated by a time-dependent force applied at the point  $(0, 0)$  described as:

$$f(t) = e^{-t} \sin(t) \quad t \in [0, 5). \quad (3.1)$$

The boundaries on  $x = 1$  and  $y = 1$  are non-absorbing (Dirichlet-type) and the rest of the boundary is free. We will model propagation of a scalar wave over the domain by splitting it into three non-overlapping subdomains. In figure 2 the domain decomposition is shown. We will use linear triangular elements for finite element discretization. The speed of propagation in this medium is set to be  $c_0 = 0.1$ . The time-integration parameters in all subdomains will be  $\beta = 1/4$  and  $\gamma = 1/2$  (see (2.11)). The subdomain time-steps are set to  $\Delta t_1 = 0.02$ ,  $\Delta t_2 = 0.002$  and  $\Delta t_3 = 0.002$ . The system time-step is  $\Delta t = 0.02$ .

The interface compatibility criteria of interest will be the v-continuity method and the Baumgarte stabilization methods. In the v-continuity method, we will only enforce continuity of velocities near the interface. Constraints on compatibility of displacements and accelerations will not be enforced. In the Baumgarte stabilization method, as given in equation (2.10), a linear combination of displacement, velocity and acceleration values at the interface is set to zero. In this numerical illustration, we will choose  $\alpha_1 = 2/\Delta t$  and  $\alpha_2 = \sqrt{2}/\Delta t^2$ .

The numerical values at time  $t = 15$  are shown in figure 3. It can be seen that the difference in the two numerical results is about 0.1% of the values. In both cases of v-continuity and Baumgarte stabilization methods, the time-stepping parameters are exactly the same. Hence, the difference shown is only a result of interface compatibility conditions. Notably, the two methods give different values in energy as well. Figure 4 shows this quantity against time. This difference in energy,  $\Delta E$ , at every time-step is defined as

$$\Delta E^n = |E_{\text{v-continuity}}^{(n)} - E_{\text{Baumgarte}}^{(n)}| \quad \forall n \quad (3.2)$$

which is the difference in energy based on the v-continuity and the Baumgarte stabilization method. As a result, one can conclude that the two methods have different numerical energy dissipation properties as well. This numerical example shows that the interface condition alone causes a deviation in the resulting numerical values.

### 4. CONCLUSION

With growing accessibility to computational capacity (such as cloud services, etc.) development of numerical algorithms designed to take full advantage of this architecture is more necessitated than ever before. A popular approach to distribution of work among a cluster of processors is the domain decomposition (domain partitioning) method. In this class of methods, the computational domain is split into several subdomains and the arrays associated with each subdomain can be manipulated by a few of the processors available, independently. The interface variables are used to enforce compatibility of numerical solution, and need to be transferred to other processors.

In this article, we overviewed the non-overlapping domain partitioning approach for a simple structural dynamics model. We looked into the mathematical theory of partitioned finite element discretization which results in differential/algebraic equations. Through a numerical example, two popular interface compatibility methods for partitioned algorithms were compared. Multi-time-step and strongly coupled time-integration algorithm was used

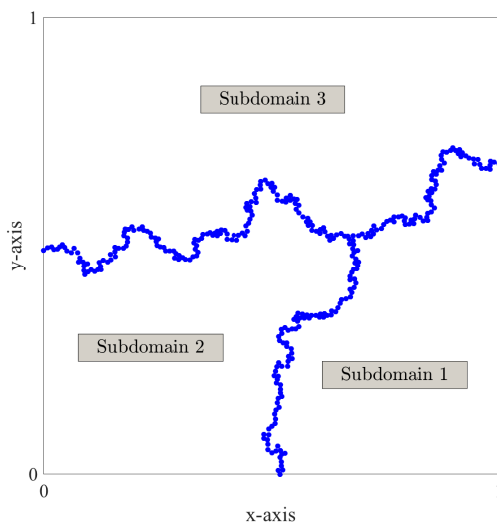


FIGURE 2. Partitioning of the computation domain into three non-overlapping subdomains.

to show how different subdomain interface conditions can affect the final numerical values. It was also shown that interface conditions lead to particular numerical energy dissipation characteristics. Based on the application, the user needs to identify the proper subdomain interface constraints to be used.

## REFERENCES

- [1] Y. Bazilevs, K. Takizawa, and T. E. Tezduyar. *Computational Fluid-Structure Interaction: Methods and Applications*. John Wiley & Sons, 2013.
- [2] V. Dolean, P. Jolivet, and F. Nataf. *An Introduction to Domain Decomposition Methods: Algorithms, Theory, and Parallel Implementation*. SIAM, 2015.
- [3] A. Toselli and O. Widlund. *Domain Decomposition Methods: Algorithms and Theory*. Springer Science & Business Media, 2006.
- [4] M. Papadrakakis, G. Stavroulakis, and A. Karatarakis. A new era in scientific computing: Domain decomposition methods in hybrid CPU–GPU architectures. *Computer Methods in Applied Mechanics and Engineering*, 200:1490–1508, 2011.
- [5] K. B. Nakshatrala, A. Prakash, and K. D. Hjelmstad. On dual Schur domain decomposition method for linear first-order transient problems. *Journal of Computational Physics*, 228:7957–7985, 2009.
- [6] S. Karimi and K. B. Nakshatrala. On multi-time-step monolithic coupling algorithms for elastodynamics. *Journal of Computational Physics*, 273:671–705, 2014.
- [7] S. Karimi and K. B. Nakshatrala. A monolithic multi-time-step computational framework for first-order transient systems with disparate scales. *Computer Methods in Applied Mechanics and Engineering*, 283:419–453, 2015.
- [8] T. J. R. Hughes and W. K. Liu. Implicit-explicit finite elements in transient analysis: Stability theory. *Journal of Applied Mechanics*, 45(2):371–374, 1978.

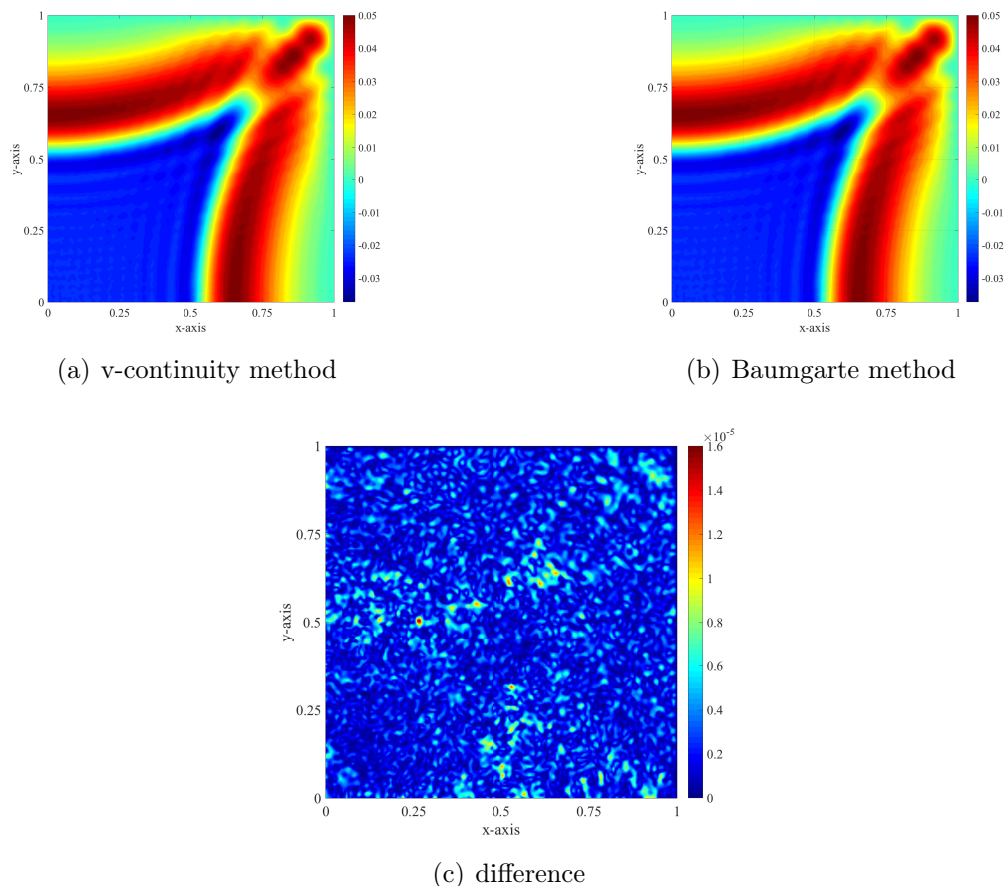


FIGURE 3. In this figure, the value of displacements at time  $t = 15$  using both the v-continuity and Baumgarte stabilization methods is shown. The difference from the two solutions is also shown.

- [9] T. Belytschko and R. Mullen. Stability of explicit-implicit mesh partitions in time integration. *International Journal for Numerical Methods in Engineering*, 12(10):1575–1586, 1978.
- [10] C. Farhat, M. Lesoinne, and N. Maman. Mixed explicit/implicit time integration of coupled aeroelastic problems: Three-field formulation, geometric conservation and distributed solution. *International Journal for Numerical Methods in Fluids*, 21(10):807–835, 1995.
- [11] C. Farhat, M. Lesoinne, P. LeTallec, K. Pierson, and D. Rixen. FETI-DP: a dual-primal unified FETI method—Part I: A faster alternative to the two-level FETI method. *International Journal for Numerical Methods in Engineering*, 50(7):1523–1544, 2001.
- [12] S. Piperno and C. Farhat. Partitioned procedures for the transient solution of coupled aeroelastic problems—Part II: Energy transfer analysis and three-dimensional applications. *Computer Methods in Applied Mechanics and Engineering*, 190(24-25):3147–3170, 2001.
- [13] A. Gravouil and A. Combescure. Multi-time-step explicit-implicit method for non-linear structural dynamics. *International Journal for Numerical Methods in Engineering*,

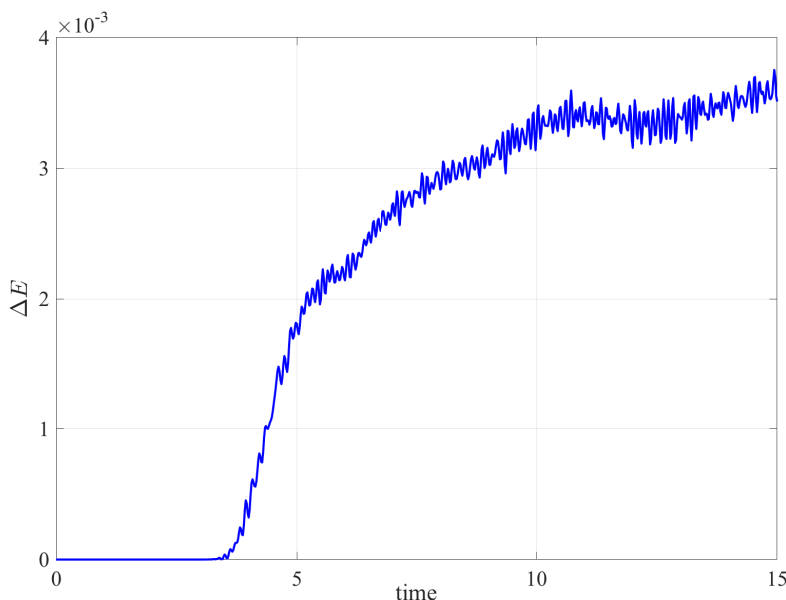


FIGURE 4. The difference in the calculated value of the energy from the v-continuity and the Baumgarte methods is shown.

- 50(1):199–225, 2001.
- [14] M. W. Gee, U. Küttler, and W. A. Wall. Truly monolithic algebraic multigrid for fluid–structure interaction. *International Journal for Numerical Methods in Engineering*, 85(8):987–1016, 2011.
- [15] N. Mahjoubi, A. Gravouil, A. Combescure, and N. Greffet. A monolithic energy conserving method to couple heterogeneous time integrators with incompatible time steps in structural dynamics. *Computer Methods in Applied Mechanics and Engineering*, 200(9–12):1069–1086, 2011.
- [16] O. S. Bursi, Z. Wang, C. Jia, and B. Wu. Monolithic and partitioned time integration methods for real-time heterogeneous simulations. *Computational Mechanics*, 52(1):99–119, 2013.
- [17] M. Beneš. Convergence and stability analysis of heterogeneous time step coupling schemes for parabolic problems. *Applied Numerical Mathematics*, 121:198–222, 2017.
- [18] P. Wriggers. *Nonlinear Finite Element Methods*. Springer, 2008.
- [19] F. Magoulès and F. X. Roux. Lagrangian formulation of domain decomposition methods: A unified theory. *Applied Mathematical Modeling*, 30(7):593–615, 2006.
- [20] G. Wanner and E. Hairer. *Solving Ordinary Differential Equations II: Stiff and Differential–Algebraic Problems*. Springer, 1991.
- [21] O. Brüls, V. Acary, and A. Cardona. Simultaneous enforcement of constraints at position and velocity levels in the nonsmooth generalized- $\alpha$  scheme. *Computer Methods in Applied Mechanics and Engineering*, 281:131–161, 2014.
- [22] W. Blajer. Methods for constraint violation suppression in the numerical simulation of constrained multibody systems—A comparative study. *Computer Methods in Applied Mechanics and Engineering*, 200(13–16):1568–1576, 2011.

- [23] P. Flores, M. Machado, E. Seabra, and M. T. da Silva. A parametric study on the Baumgarte stabilization method for forward dynamics of constrained multibody systems. *Journal of Computational and Nonlinear Dynamics*, 6(1):011019, 2011.
- [24] J. Baumgarte. Stabilization of constraints and integrals of motion in dynamical systems. *Computer Methods in Applied Mechanics and Engineering*, 1(1):1–16, 1972.
- [25] C. W. Gear, B. Leimkuhler, and G. K. Gupta. Automatic integration of Euler–Lagrange equations with constraints. *Journal of Computational and Applied Mathematics*, 12:77–90, 1985.
- [26] C. Lunk and B. Simeon. Solving constrained mechanical systems by the family of Newmark and  $\alpha$ -methods. *ZAMM-Journal of Applied Mathematics and Mechanics*, 86(10):772–784, 2006.
- [27] N. M. Newmark. A method of computation for structural dynamics. *Journal of the Engineering Mechanics*, 85(3):67–94, 1959.

## Squeeze-film Flow in the Presence of a Thin Anisotropic Porous Bed: an Application to Knee Joint

Timir Karmakar\*, Raja Sekhar G. P.\*\*

\*Indian Institute of Technology Kharagpur, India, \*\*Indian Institute of Technology Kharagpur, India

### ABSTRACT

We consider a theoretical model of squeeze-film flow in the presence of a thin porous bed. It is assumed that a flat bearing is approaching towards the porous bed. The gap between the porous bed and the bearing is assumed to be filled with a Newtonian fluid. The liquid porous interface is assumed to be flat. Assuming that the fluid is Newtonian, we use Navier-Stokes equation in the fluid region and Darcy equation in the fluid saturated porous region. Lubrication approximation is used to the hydrodynamic equation of motion in the gap and in the porous region. We use Beavers & Joseph (1967) and Le Bars & Worster (2006) conditions at the liquid-porous interface and present a detailed analysis on the corresponding impact. We assume that the porous bed is anisotropic in nature with permeabilities  $K_2$  and  $K_1$  along the principal axes. Accordingly, the anisotropic angle  $\theta$  is taken as the angle between the horizontal direction and the principal axis with permeability  $K_2$ . We show that the anisotropic permeability ratio and the anisotropic angle make a significant influence on contact time, flux, velocity etc. The analysis is presented when a bearing approaches the porous bed for a given constant velocity or a given constant load is presented. We present some important findings relevant to knee joint based on the anisotropic of the human cartilage. The permeability of the articular cartilage depends on the proteoglycan matrix especially glycosaminoglycan (GAG) chains and the properties are influenced by the arrangement of the collagen fibres in different directions which form a anisotropic network of the human cartilage. In case of constant load, we have estimated the time duration a healthy human knee remains fluid lubricated. While in case of a constant velocity, we have estimated the load a human knee can sustain. 1. Beavers G S, Joseph D D, Boundary conditions at a naturally permeable wall, Journal of fluid mechanics, 30, pp. 197-207, 1967. 2. Le Bars M, Worster M G, Interfacial conditions between a pure fluid and a porous medium: implications for binary alloy solidification, Journal of fluid mechanics, 550, pp. 149-173, 2006. 3. Knox D J, Wilson S K, Duffy B R, McKee S, Porous squeeze-film flow, IMA Journal of applied mathematics, 80, pp. 376-409, 2013

## Physics Informed Deep Learning

George Karniadakis\*

\*Brown University

### ABSTRACT

For more than two centuries, solutions of partial differential equations (PDEs) have been obtained either analytically or numerically based on well-behaved forcing and boundary conditions for well-posed problems. However, in real-life applications the available input data are often incomplete, noisy, and of variable fidelity, rendering existing computational methods ineffective. Moreover, despite the availability of big data in many domains, high-fidelity scientific data are small and expensive to obtain. We are changing this paradigm in a fundamental way by establishing an interface between probabilistic machine learning and PDEs that express known physical laws and constraints. We develop data-driven algorithms for general nonlinear PDEs using Gaussian processes and deep neural networks tailored to the corresponding integro-differential operators. The only observables are scarce and noisy multi-fidelity data for the forcing/solution, which could be scattered anywhere in the domain. We refer to these smart systems that encode the proper physical laws in their description as Physics-Informed Learning Machines (PILM). This work is based on work of Maziar Raissi and Paris Perdikaris.

## On Nonlocal Theories: Mathematical Models and Computational Approaches

Aansi Karttunen\*, J.N. Reddy\*\*

\*Aalto, \*\*Texas A&M; University

### ABSTRACT

Structural continuum theories require a proper treatment of the kinematic, kinetic, and constitutive issues accounting for possible sources of non-local and non-classical continuum mechanics concepts and solving associated boundary value problems. There is a wide range of theories, from higher gradient to truly nonlocal. These include, for example, strain gradient theories [1, 2], couple stress theories, Eringen's stress gradient theories [3], and micropolar theories [4] (the micropolar theory of elasticity includes an independent microrotation), and thermodynamically consistent structural theories. In this lecture, an overview of recent research on strain gradient, stress gradient, couple stress, micropolar, and thermodynamically consistent theories in developing the governing equations beams, plates, and sandwich structures will be presented and their computational aspects will be discussed. In addition, a graph-based finite element framework (GraFEA) suitable for the study of damage in brittle materials will be discussed [5]. Acknowledgements: The author is pleased to acknowledge the collaboration on non-local and non-classical mechanics with Arun Srinivasa (TAMU), and Karan Surana (KU), and Debasish Roy (IISc). References 1. R.D. Mindlin, Influence of couple-stresses on stress concentrations. *Experimental Mechanics*, 3(1), 1-7, 1963. 2. A.R. Srinivasa and J.N. Reddy, *Journal of Mech Phys Solids*, 61(3), 873-885, 2013. 3. A.C. Eringen, *International Journal of Engineering Science*, 10, p. 1, 1972. 4. A.T. Karttunen, J.N. Reddy, and J. Romanoff, *Composite Structures*, 185, 656-664, 2018. 5. Parisa Khodabakhshi, J.N. Reddy, and Arun Srinivasa, *Meccanica*, 51(12), 3129-3147, Dec 2016

## Simulation and Auralization for Noise Using Virtual Reality Technology

Kazuo Kashiya\*

\*Chuo University

### ABSTRACT

The evaluation of noise is very important for planning and designing of various construction works in urban area. There have been presented a number of evaluation methods for noise simulation. Based on the frame of reference used, those methods can be classified into two categories: 1) Methods based on the geometrical acoustic theory and 2) Methods based on acoustic wave theory. Both methods have advantages and disadvantages. For the methods based on the geometrical acoustic theory, the CPU time is very short but the numerical accuracy is low comparing with the methods based on the acoustic wave theory. On the other hand, the method based on the acoustic wave theory gives accurate solutions but the simulation becomes a large scale simulation. In the conventional studies, the computed noise level is described by the visualization using computer graphic such as iso-surface. Although the visualization is a powerful tool to understand the distribution of noise, it is difficult to recognize the noise level intuitively. This paper presents noise evaluation systems based on acoustic wave theory using virtual reality technology. The system exposes to users the computed noise level with both the auditory information using sound source signal and the visual information using CG image. The CIP method using AMR and FEM are employed for the discretization of wave equation. The ambisonics based on the spherical surface function expansion is employed to realize the stereoscopic sound field using computational results and sound source data. We performed the observation to obtain the sound source data for the auralization. The present system is shown to be a useful tool for planning and designing tool for various construction works in urban area, and also for consensus building for designers and the local residents.

## The Effect of Water on the Wrinkling Formation in Graphene, and the Interlayer Shear between Graphene Bilayers

Jatin Kashyap<sup>\*</sup>, Dibakar Datta<sup>\*\*</sup>

<sup>\*</sup>New Jersey Institute of Technology, <sup>\*\*</sup>New Jersey Institute of Technology

### ABSTRACT

Graphene, a two-dimensional material, is the cynosure in nanotechnology with wide ranges of applications. Wrinkling, a ubiquitous phenomenon in graphene, severely weakens its performance. In some cases, however, wrinkling is advantageous such as hydrophobic surface, energy storage. Whether beneficial or not, it is crucial to understand the wrinkle formation mechanism in graphene. Experimental investigations suggest that during the growth process, because of the humid environment in the growth chamber, water diffuses into graphene and substrate and plays a significant role in the wrinkle formation in graphene. There is no systematic computation investigation at all to address this critical issue. We, therefore, performed molecular dynamics simulation to analyze this important phenomenon by considering a simplistic model with graphene on graphene substrate and diffused water inside. First, we consider the absence of water inside and observe the formation of bigger wrinkle due to the coalescence of initial small wrinkles. However, if the initial wrinkles have a very high angle, the final wrinkle formed after coalescence is too high to maintain its stability and collapses to form multifold graphene structure. Next, we consider the humidity effect. The configuration of final wrinkle structure is governed by the competition between bending energy of wrinkled graphene and the van der Waals (vdW) energy between graphene, substrate, and water in-between. At low initial angle (e.g., 6 degrees), condensation of diffused water dominates the final wrinkle structure. At the intermediate initial angle (e.g., 11 degrees), when only one water layer is present, the bending energy dominates. However, with the increase in water density, i.e., more water layer inside, condensation of water droplet governs the final structure. At higher initial angle (e.g., 21 degrees), bending energy dominates and regulates the final wrinkle configuration. With the increase in initial wrinkle angle, the width of the final wrinkle formed after coalescence decreases while the final height shows a reverse trend. We further investigated the effect of water in the interlayer shear of graphene bilayer. We notice when the water is absent in between the layers, the interlayer shear shows a symmetric trend and the maximum shear is around 60 MPa. However, the presence of water droplet significantly reduces the maximum shear. Our systematic computational analysis provides a deeper insight into the role of water in the wrinkling formation in graphene and the interlayer shear between graphene bilayers.

## Material Design of Elastoplastic Media with Decoupling Multi-scale Analysis

Junji Kato<sup>\*</sup>, Shun Ogawa<sup>\*\*</sup>, Hiroya Hoshihara<sup>\*\*\*</sup>, Takashi Kyoya<sup>\*\*\*\*</sup>

<sup>\*</sup>Tohoku University, <sup>\*\*</sup>Tohoku University, <sup>\*\*\*</sup>Tohoku University, <sup>\*\*\*\*</sup>Tohoku University

### ABSTRACT

The present study proposes material design of elastoplastic media in the framework of a decoupling multi-scale analysis. The objective function is to maximize the energy absorption capacity of macrostructure with a prescribed material volume in the microstructure. Isotropic von Mises elastoplastic material model is employed for the constituents of microstructure and the anisotropic Hill plasticity model is used for the macroscopic constitutive law. In the framework of the decoupling multi-scale analysis, material parameters in the Hill's material model are identified by solving the microscopic boundary value problems based on the finite element analysis. This process is called numerical material testing. In the topology optimization of microstructure, conventional SIMP approach is utilized and gradient-based method is employed. In this study, the methodology to obtain the accurate sensitivity with low computational costs is proposed, where the sensitivity of the incremental strain with respect to design variables can be eliminated using the return mapping algorithms. It is verified by a series of numerical examples that the proposed method has a great potential to design elastoplastic media, especially advanced materials such as functional materials.

## Strain Shielding in Femurs with an Implant

Yekutiel Katz\*, Zohar Yosibash\*\*

\*Tel Aviv University, \*\*Tel Aviv University

### ABSTRACT

More than half a million hip replacement surgeries are performed annually in the US, and similarly in Europe. The inserted metallic prosthesis in these surgeries changes the femur's natural loading conditions, leading to bone remodeling and resorption. This phenomenon, commonly known as "stress shielding", leads to reduction of implant's mechanical stability and increases the risk of periprosthetic femoral fracture. Thirteen percent of hip replacement surgeries undergo a revision surgery within ten years [1]. Orthopedic surgeons usually choose a prosthesis based on clinical outcome reports, statistical data and their personal experience. No scientific tool exists that may assist surgeons to determine the biomechanically optimal prosthesis for a specific patient. Finite element analyses may be used as such a tool. The first essential step must be their verification and experimental validation. Intact femurs mechanical response had already been shown to be well predicted by high-order finite element models based on patient-specific QCT scans [2]. The generation of finite element models representing implanted femurs followed by their experimental validation will be presented. The experiments were conducted on fresh frozen cadaver femurs, loaded in different configurations. Measurements were performed using the "gold standard" strain gauges, and also novel methods as digital image correlation. Once the models were validated, they were used to compare the mechanical behavior before and after the implantation. To quantify the implant's performance, comparison of the strain fields was performed. Strains were addressed rather than stresses due to their stimulation of the biological remodeling mechanism [3]. Norms to quantify strain shielding will be suggested. Such norms may assist orthopedic surgeons to choose an optimal implant for the specific patient, from the vast available variety of implants. [1] G. Labek, M. Thaler, W. Janda, M. Agreiter, and B. Stockl, "Revision rates after total joint replacement: Cumulative results from worldwide joint register datasets", *Bone Joint J.*, vol. 93-B, no. 3, pp. 293–297, 2011. [2] N. Trabelsi, Z. Yosibash, C. Wutte, P. Augat, and S. Eberle, "Patient-specific finite element analysis of the human femur-A double-blinded biomechanical validation," *J. Biomech.*, vol. 44, no. 9, pp. 1666–1672, 2011. [3] E. H. Burger and J. Klein-Nulend, "Mechanotransduction in bone - role of the lacuno-canalicular network," *FASEB J.*, vol. 13, no. 9001, pp. S101–S112, 1999.

## **An Overset Mesh Framework Applied to the Hybridizable Discontinuous Galerkin Finite Element Method for Dynamic Meshes**

Justin Kauffman\*, Jonathan Pitt\*\*

\*The Pennsylvania State University, \*\*The Pennsylvania State University

### **ABSTRACT**

Fluid-structure interaction simulations where the solid bodies are undergoing larger deformations require special handling of the mesh motion for Arbitrarily Lagrangian-Eulerian (ALE) formulations. Such formulations are necessary when body-fitted meshes with certain characteristics, such as boundary layer resolution, are required to properly resolve the problem. This work presents an overset mesh method to accommodate such problems in which flexible bodies undergo large deformations, or where rigid translation modes of motion are present as well. To accommodate these motions of the bodies through the computational domain, an overset mesh enabled ALE formulation for fluid flow is discretized with the hybridizable discontinuous Galerkin (HDG) finite element method. The overset mesh framework applied to the HDG method enables the deforming and translating dynamics meshes to maintain mesh quality without re-meshing. Verification and validation are presented along with an example calculation.

## A Hybrid Quasicontinuum Method

Aditya Kavalur\*, Woo Kyun Kim\*\*

\*University of Cincinnati, \*\*University of Cincinnati

### ABSTRACT

Quasicontinuum (QC) is a spatial multiscale method which approximates the potential energy of an atomistic system with reduced computational cost. Like other partitioned-domain approaches, QC divides the simulation domain into atomistic and continuum regions. A full-atomistic description is restricted only to the atomistic region with the continuum region adopting a finite element method-based coarse-graining scheme and a continuum constitutive relation called the Cauchy-Born (CB) rule. While the CB rule can capture the full-nonlinearity of the strain energy density in the continuum region, its computational cost is one order of magnitude higher than the linear elastic (LE) constitutive relation, which is adopted by other partitioned-domain methods. In this study we propose a novel hybrid QC method where CB and LE are combined to increase the efficiency of the original QC method. The extension consists of two main steps. First, the continuum region is further divided into sub-domains such that the CB rule is applied only to those sub-regions adjoining the atomistic region with the energy of the remaining continuum region being approximated using the linear elastic constitutive relation. Second, a corrective force term is added as dead load to the nodes in the LE region in order to retain the higher order accuracy. Two test examples of Lomer dislocations and nanoindentation are employed to validate the proposed method. The simulation results reveal that the hybrid method is numerically more efficient than the original QC method while maintaining virtually the same accuracy.

## Design of Cultivation Environment Scenario of *Oryza sativa* L.

E. Kawabe<sup>\*</sup>, S. Nishiuchi<sup>\*\*</sup>, E. Kita<sup>\*\*\*</sup>

<sup>\*</sup>Nagoya University, <sup>\*\*</sup>Nagoya University, <sup>\*\*\*</sup>Nagoya University

### ABSTRACT

While Japanese agriculture is high productivity, farmers are aging. Once the skillful farmers are retired, their knowledge should be lost. The aim of this study is to design the cultivation environment scenario of *Oryza sativa* L. "Koshihikari". If the optimized scenario is obtained, the newcomers can do like the skillful farmers. The yield and the quality data in the rice cultivation and the environment scenario are collected by Agricultural Research Center of each prefecture and Japan Meteorological Agency, respectively. The prediction models of the yield and the quality of the *Oryza sativa* L. are defined by the multiple regression analysis or neural network analysis of the rice cultivation data (yield and quality) and the environment scenario such as average temperature, maximum temperature, minimum temperature, precipitation, hours of sunlight and diurnal temperature range. The objective function of the optimization problem is defined so as to maximize the yield and the quality of the *Oryza sativa* L. Design variables are composed of the part of the environment scenario variables such as maximum and minimum temperatures. Constraint conditions for the design variables are the upper and the lower bounds of the temperatures. Optimization problem is solved by L-BFGS-B method. The initial temperature fluctuation is the average year temperature in Nagoya. The optimized year temperature is considerably lower and then, very similar to that in Tadami. References [1] L. Taiz, E. Zeiger, Plant Physiology. Fifth Edition, 2010. [2] S. Yoshida, Fundamentals of Rice Crop Science. The International Rice Research Institute, 1981. [3] T. Mitchell, Machine Learning. McGraw-Hill, 1997.

## Subdomain Local FE Solver Design for DDM on Many-core Architectures

Hiroshi Kawai<sup>\*</sup>, Masao Ogino<sup>\*\*</sup>, Ryuji Shioya<sup>\*\*\*</sup>, Tomonori Yamada<sup>\*\*\*\*</sup>, Shinobu Yoshimura<sup>\*\*\*\*\*</sup>

<sup>\*</sup>Toyo University, <sup>\*\*</sup>Nagoya University, <sup>\*\*\*</sup>Toyo University, <sup>\*\*\*\*</sup>The University of Tokyo, <sup>\*\*\*\*\*</sup>The University of Tokyo

### ABSTRACT

Exa-scale supercomputers will appear around 2020–2022. To obtain high intra-node performance, efficient utilization of processor cache memory should be considered. The traditional memory access-intensive approach, which prefers less computing and more storage on main memory, might not be effective for supercomputers in near future. The Domain Decomposition Method (DDM) is one of the effective parallel finite element schemes. We have been developing an FE-based parallel structural analysis code, ADVENTURE Solid, based on DDM, with the Balancing Domain Decomposition (BDD) pre-conditioners. The re-design of the subdomain local FE solver part, which is a performance sensitive kernel in the DDM code, is required. Here in this work, an “on-cache” iterative solver based on the DDM framework is developed. The subdomain local FE solver of the DDM code is implemented using CG solvers with element-by-element matrix storage-free approaches. These iterative solvers are parallelized using OpenMP, so that each subdomain can be solved by multiple cores. By adjusting the subdomain size so that the footprint fits within the last-level cache of a processor, this DDM code can be considered as a kind of an “on-cache” iterative solver”. Performance benchmark results are shown on various kinds of HPC platform having many core scalar processors, such as Skylake Xeon, Knights Landing and Fujitsu PRIMEHPC FX100.

## Effect of Strain Path on Microstructure and Texture Inhomogeneity during Accumulative Angular Drawing Process of Ti-6Al-4V

Jakub Kawalko<sup>\*</sup>, Krzysztof Muszka<sup>\*\*</sup>, Piotr Bala<sup>\*\*\*</sup>, Marcin Kwiecien<sup>\*\*\*\*</sup>, Paulina Lisiecka-Graca<sup>\*\*\*\*\*</sup>, Maciej Szymula<sup>\*\*\*\*\*</sup>

<sup>\*</sup>AGH University of Science and Technology, Academic Centre for Materials and Nanotechnology, <sup>\*\*</sup>AGH University of Science and Technology, Faculty of Metals Engineering and Industrial Computer Science, <sup>\*\*\*</sup>AGH University of Science and Technology, Academic Centre for Materials and Nanotechnology, <sup>\*\*\*\*</sup>AGH University of Science and Technology, Faculty of Metals Engineering and Industrial Computer Science, <sup>\*\*\*\*\*</sup>AGH University of Science and Technology, Faculty of Metals Engineering and Industrial Computer Science, <sup>\*\*\*\*\*</sup>AGH University of Science and Technology, Faculty of Metals Engineering and Industrial Computer Science

### ABSTRACT

Accumulative Angular Drawing (AAD) process is a novel method used to produce wires with controlled inhomogeneity of microstructure and properties. Similarly to Severe Plastic Deformation (SPD) processes, it introduces high accumulation of deformation energy in the cross-section of the drawn wire and enables activation of additional deformation mechanisms compared to conventional drawing processes. In the current work, AAD process will be applied to produce wires made of Ti-6Al-4V alloy. This alloy is characterized by a limited ductility at room temperature due to hexagonal closed packed (HCP) structure. During AAD process strain path changes occur, what besides reduction of the cross-section area, introduces additional bending, shearing, burnishing and torsion to the deformed wires, and thanks to that, activates additional slip planes allowing successful realization of deformation process. In the present work, level of inhomogeneity of microstructure, texture and properties resulting from applied strain path history will be assessed. Conclusions regarding interrelationships between deformation history and resulting microstructural changes will be drawn in the light of possible texture mechanisms that are activated during AAD process. Due to a number of process parameters that affect the microstructural inhomogeneity, acquired data can be used for the numerical modeling. Understanding of the AAD of Ti alloys with the aid from computer simulation will enable optimization of the process towards better control of microstructure and texture inhomogeneity what, in turn, will allow production of titanium wires with controlled gradual changes in their microstructure and properties.

## SEISMIC RESPONSE CONTROL FOR EQUIPMENT WITH CASTERS USING SWITCHING WHEEL LOCK CONDITIONS

YOSUKE KAWANISHI\*, MASAYUKI KOHIYAMA\*

\*Graduate School of Science and Technology, Keio University  
3-14-1 Hiyoshi, Kohoku-ku, Yokohama 223-8522, Japan  
yosuke.kawanishi@keio.jp

**Key words:** Seismic Response Control, Caster Wagon, Furniture, Rocking, Sliding,  
Numerical Analysis

**Abstract.** When an earthquake occurs, the people in and/or contents of buildings may suffer damage due to the sliding or overturning of furniture and equipment or the falling of objects even if the structure of the building experiences no damage. In this study, using numerical analyses, we investigate a model of effective equipment caster wheel control to reduce damage caused by the moving and overturning of equipment during earthquakes and propose a control method to switch the lock and free conditions of the caster wheel. In the numerical analyses, a simulator library of three-dimensional rigid body dynamics is used and two-direction earthquake ground motion is input into a model of a 10-story steel frame building. The horizontal displacement and the falling down of the equipment model are expressed depending on the caster lock condition.

### 1 INTRODUCTION

In an earthquake event, to protect people in a building, we need to consider not only the damage to a building's structure but also the damage caused by furniture in the building. When an earthquake occurs, furniture in a building and/or their contents may hit people or may overturn and hinder evacuations, as reported in the 2011 Great East Japan Earthquake. In particular, the seismic resistance of medical equipment is important because it affects whether medical activities can be performed following an earthquake. Most medical equipment are equipped with casters for convenience, and in the case of the 1995 Hyogo-ken Nanbu Earthquake, it was reported that medical equipment with high centers of gravity overturned when the casters were locked and moved around and collided with other equipment and the walls when the casters were not locked. Nikfar and Konstantinidis <sup>[1]</sup> estimated the seismic responses of hospital equipment supported by casters. They determined the frictional resistance of the casters, evaluated the seismic response of the equipment, and performed shaking table experiments. Kamada et al. <sup>[2]</sup> proposed an earthquake response control of caster-supported wagons using an ER, variable-type brake and demonstrate its effectiveness via simulations and excitation

experiments. In past studies of furniture earthquake response analyses, it has been common to use a spring–mass model; however, this model does not consider the shape of the structure. Saomoto and Yoshimi <sup>[3]</sup> analyzed furniture earthquake responses using a physics engine, the Open Dynamics Engine (ODE) and performed numerical analyses considering the shape of the furniture. Masatsuki and Midorikawa <sup>[4]</sup> quantitatively examined the fluctuations of large displacements considering the collisions of multiple pieces of furniture and walls using a physical simulator, Springhead2. Isobe et al. <sup>[5]</sup> developed an effective numerical code based on the adaptively shifted integration (ASI)–Gauss technique for analyzing the motion of furniture subjected to seismic excitations.

In this study, using an ODE numerical analysis, we investigate effective caster wheel control to reduce damage due to equipment moving and overturning during earthquakes and propose a control method to switch the lock and free conditions of the caster wheels.

## **2 OUTLINE OF THE SIMULATION AND CASTER CONTROL METHOD**

In the numerical analysis, we use ODE, which is a simulator library of three-dimensional rigid body dynamics. The modeled equipment with casters consists of a box and four wheels. The width, depth, height, and mass of the model are 0.45 m, 0.30 m, 0.80 m, and 10 kg, respectively. First, we input the two-direction earthquake ground motion (NS and EW) into a model of a 10-story steel frame building with a first natural period of 0.8 s and obtained the acceleration response time history on the top (9<sup>th</sup>) floor. We assumed that the equipment is placed on the top floor of the building and input the response acceleration waves to the floor slab to obtain the response time history of the equipment model. We compared the responses for the following three caster conditions: (1) setting the casters as locked, (2) setting the casters as free, and (3) switching the casters between locked and free at constant time intervals.

### **2.1 THE EQUIPMENT MODEL**

In this study, we consider the equipment model shown in Figure 1 and define the variables as shown in Table 1. The value obtained in the experiment conducted by Saito et al. <sup>[6]</sup> is used as the friction coefficient.

We name the casters as shown in Figure 1(c). In addition, for the sake of simplicity, the caster swivels do not rotate and are fixed at the position shown in Figure 1.

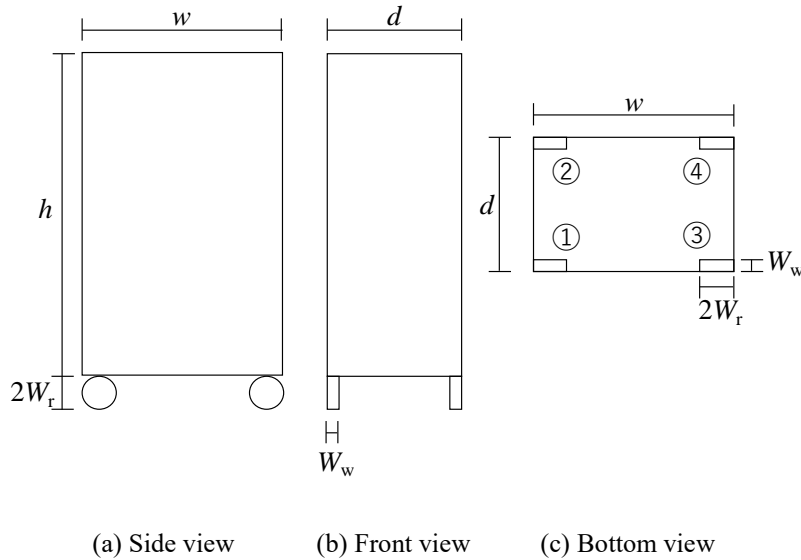


**Figure 1.** The equipment model.

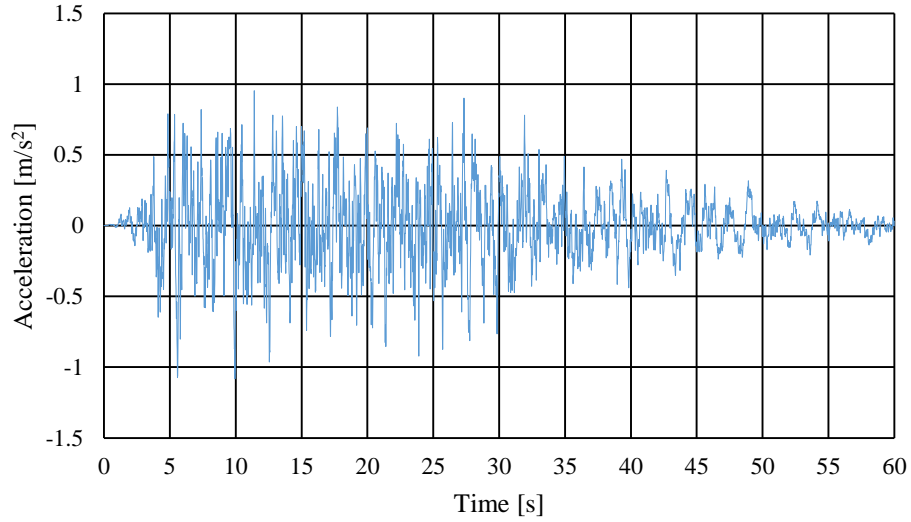
**Table 1.** Parameters of the equipment with casters.

Specification	Variable	Value
Equipment width	$w$	0.40 m
Equipment depth	$d$	0.30 m
Equipment height	$h$	0.80 m
Equipment mass	$M$	10 kg
Caster mass	$M_c$	0.05 kg
Caster wheel radius	$W_r$	0.0375 m
Caster wheel width	$W_w$	0.75 m
Friction coefficient when the casters are locked	$\mu_0$	0.3
Static friction coefficient	$\mu_s$	0.4
Friction coefficient when the casters are released	$\mu_{free}$	0.02

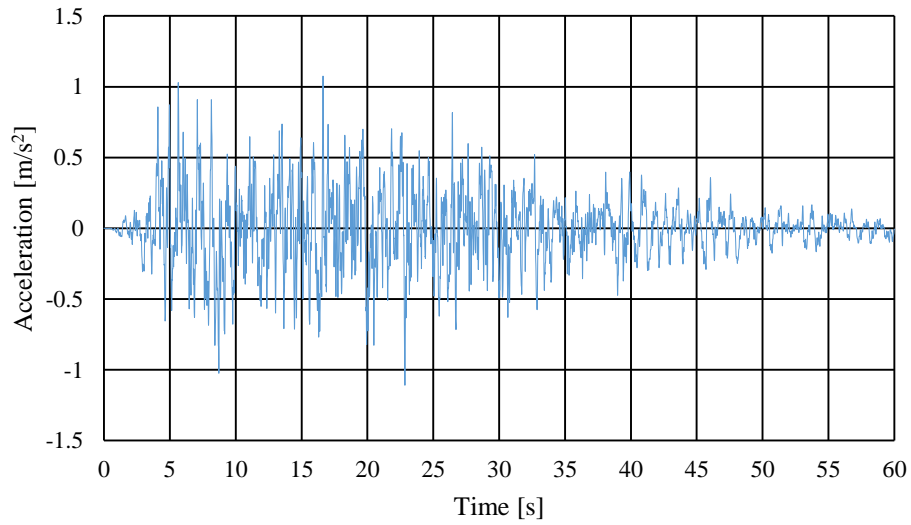
## 2.2 DYNAMIC ANALYSIS OF A BUILDING MODEL

With respect to the input ground motions, we use simulated ground motions of “rare earthquake ground motion” at an outcrop engineering bedrock with random phase components, as prescribed in Notification No. 1461 of the Ministry of Construction, Japan, May 31, 2000. The ground motions correspond to a return period of approximately 50 years. Figure 2 shows the

time history of the input ground acceleration, and Figure 3 shows the target acceleration spectrum and acceleration response spectra of the input waves.



(a) EW direction



(b) NS direction

**Figure 2.** Time history of the ground acceleration input to a 10-story building model.

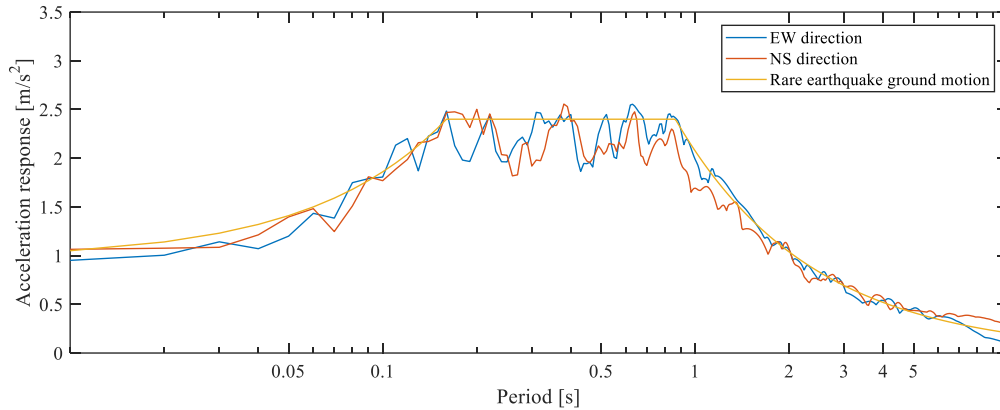


**Figure 3.** Target acceleration response spectrum of the rare earthquake ground motion and those of the input waves (5% damping).

We enter these input acceleration waves into the building model and obtained the acceleration response for each floor. We use the Newmark  $\beta$  method for the time history response analysis. With respect to the behavior of the specimen from a previous study by Purvance et al. [7], we consider the influence of the input wave in the vertical direction to be small. Therefore, in this analysis, we only input the horizontal acceleration waves and obtained the horizontal acceleration response of the building. The results of the time history response analysis for the 9<sup>th</sup> floor are shown in Figure 4, and Figure 5 shows the floor response spectrum on the 9<sup>th</sup> floor.

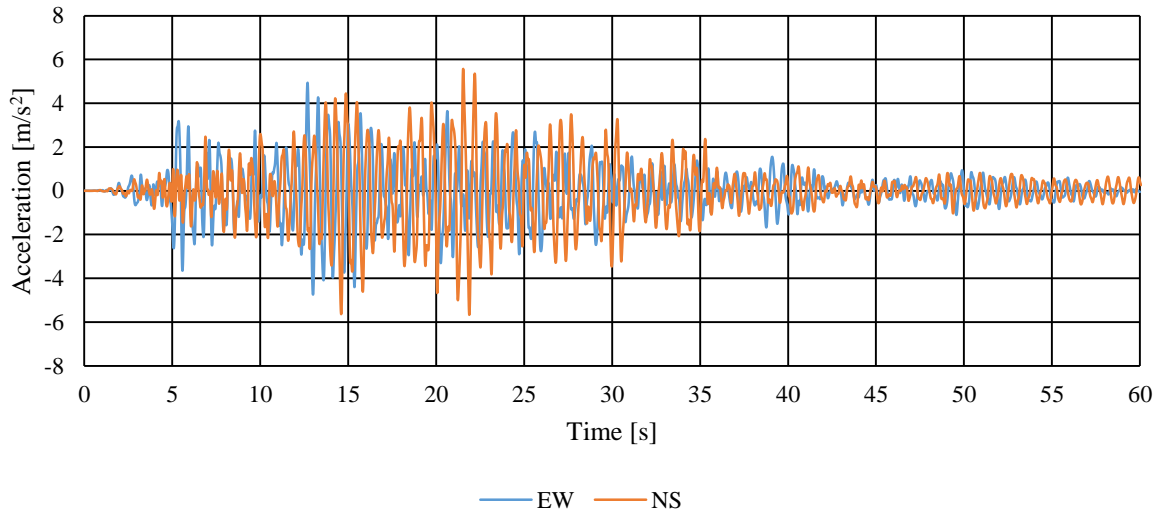


**Figure 4.** The results of the time history acceleration response analysis for the 9<sup>th</sup> floor of the building model.

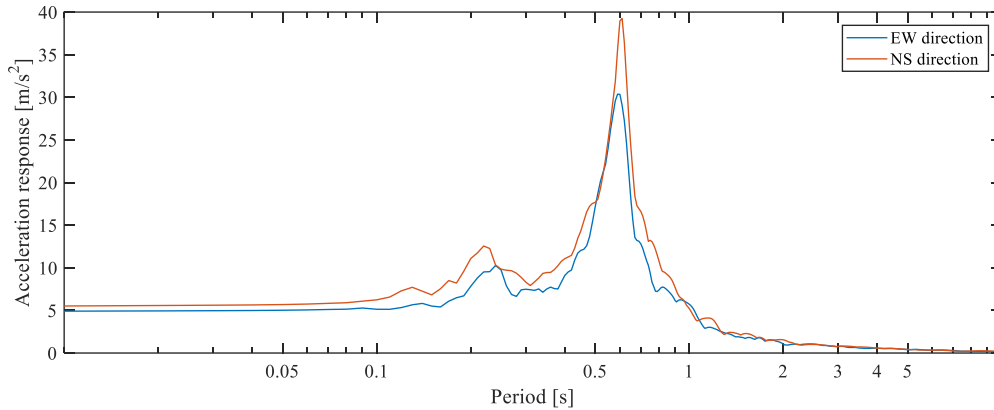


**Figure 5.** The floor response spectrum on the 9<sup>th</sup> floor of the building model (5% damping).

### 3 NUMERICAL ANALYSIS OF THE EQUIPMENT RESPONSE

#### 3.1 ANALYSIS CONDITIONS

In the numerical analysis of equipment response, we set the time step to 0.01 s and the number of analysis steps to 6000. When a floor responds to the earthquake and the equipment model vibrates, the position and posture of the equipment change. Therefore, we consider the following 10 patterns for the possible posture of the equipment as shown in Table 2.

**Table 2.** The posture of the equipment.

Case	Condition
(a)	The case when all casters touch the floor.
(b1)	The case when casters 1 and 2 touch the floor.
(b2)	The case when casters 3 and 4 touch the floor.
(b3)	The case when casters 1 and 3 touch the floor.
(b4)	The case when casters 2 and 4 touch the floor.
(c1)	The case when only caster 1 touches the floor.
(c2)	The case when only caster 2 touches the floor.
(c3)	The case when only caster 3 touches the floor.
(c4)	The case when only caster 4 touches the floor.
(d)	The case when the equipment jumps and none of the casters touch the floor.

For the sake of simplicity, we assume the following.

- Only the inertial force and the frictional force are applied to the equipment.

- The inertial force is applied to the center of gravity of the equipment box model and the four casters of the equipment model.
- The equipment model is a rigid body and the casters do not swing or roll.
- After the equipment model falls down, we assume that the equipment does not move anymore.
- We consider the equipment model to have fallen when part of the upper surface of the equipment model touches the ground.
- We consider both static and dynamic friction forces.
- The angular velocity and angular acceleration are obtained from the rotation angle via the finite difference method.
- We assume that the normal forces of each caster wheel are equal. They are actually different; however, what matters is the resultant of the normal forces. There is no difference in the movement of the equipment model if these forces are assumed to be equal.

First, we consider the case when the caster  $i$  is locked. The frictional force vector  $\mathbf{F}_{\text{frc},i}$  is defined as

$$\mathbf{F}_{\text{frc},i} = \begin{pmatrix} -\mathbf{F} & \left( |\mathbf{F}| < \sum_{i=1}^4 F_{s,i} \wedge \dot{\mathbf{x}}_i = 0 \right) \\ -\mu_0 N_i \times \left( \frac{\dot{\mathbf{x}}_i}{|\dot{\mathbf{x}}_i|} \right) & \left( \left( |\mathbf{F}| \geq \sum_{i=1}^4 F_{s,i} \wedge \dot{\mathbf{x}}_i = 0 \right) \vee \dot{\mathbf{x}}_i \neq 0 \right) \end{pmatrix}, \quad (1)$$

$$F_{s,i} = \mu_s N_i, \quad (2)$$

where  $\mathbf{F}$  is the inertial force vector applied at the center of gravity of an equipment model,  $F_{s,i}$  is the maximum static friction force calculated at the caster  $i$ ,  $\mu_0$  is the static frictional coefficient,  $\mu_s$  is the dynamic friction coefficient,  $N_i$  is the normal force at the wheel of caster  $i$ ,  $\mathbf{x}_i$  is the displacement of caster  $i$ , and  $\dot{\mathbf{x}}_i$  is the velocity of caster  $i$ . The friction force is applied to the position where the casters touch the ground.

Di Egidio and Contento<sup>[8]</sup> defined the normal force  $N_i$  using a formula balancing the horizontal direction, the vertical direction, and rotation such that

$$N_i = m(g + b'_1 \ddot{\theta} - h'_1 \dot{\theta}^2), \quad (3)$$

where  $m$  is the mass of the equipment model and  $g$  is the gravitational acceleration. Suppose  $\phi$  is defined by the angle between the yaw axis of a rigid body and the horizontal vector perpendicular to its rotating axis, then  $\theta$  is calculated such that  $\theta = \frac{\pi}{2} - \phi$ .  $b'_1$  is the distance between the projected point of the center of gravity on  $xy$ -plane and the position where the casters touch the floor, and  $h'_1$  is the height of the center of gravity of the equipment model. In the cases (b1) and (b2),  $b'_1$  and  $h'_1$  are shown in Figure 6 and are described as

$$b'_1 = h_1 \cos \theta - b_1 \sin \theta + W_r \cos \theta, \quad (4)$$

$$h'_1 = h_1 \sin \theta + b_1 \cos \theta + W_r (1 + \sin \theta). \quad (5)$$

where  $b_1$  is the difference between a half of the equipment width  $w$  and the caster wheel radius  $W_r$ , and  $h_1$  is a half height of the equipment height  $h$ .

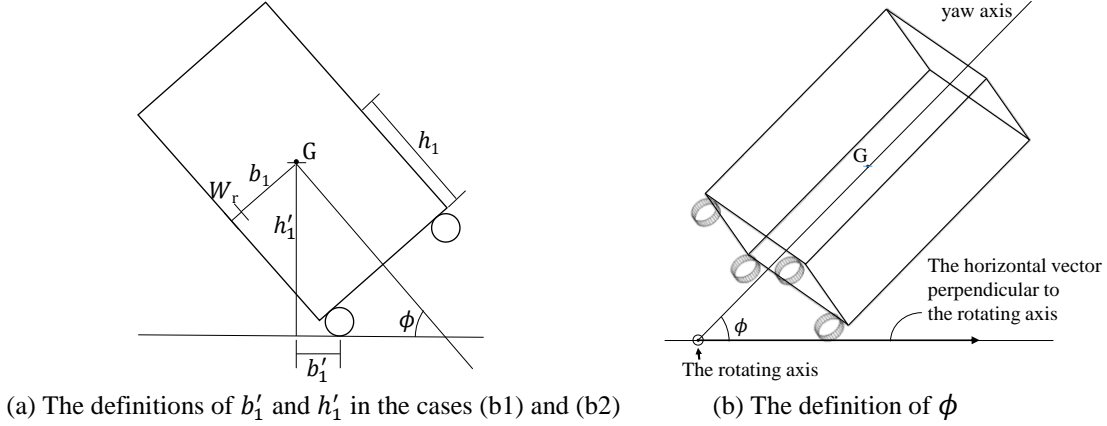


**Figure 6.** The definitions of parameters

Next, we consider the case when the casters are released. In addition to the friction force when the casters are locked, we apply an external force vector  $\mathbf{F}_{\text{free}}$ , which is equivalent to the casters rolling and is expressed as

$$\mathbf{F}_{\text{free}} = (\mu_0 - \mu_{\text{free}})Nr, \quad (6)$$

where  $\mu_{\text{free}}$  is the dynamic friction coefficient when the casters are rolling and  $\mathbf{r}$  is the direction in which the casters are rolling. When  $\theta$  is greater than  $\frac{\pi}{4}$ , the caster wheel rolls inward, and when  $\theta$  is smaller than  $\frac{\pi}{4}$ , the caster wheel rolls outward. As with the friction force, the external force vector  $\mathbf{F}_{\text{free}}$  is applied to the position where casters touch the ground.

### 3.2 FLOW DIAGRAM OF THE NUMERICAL ANALYSIS

A flow diagram of the numerical analysis is shown in Figure 7; the variables are defined in Table 3.

**Table 3.** The variables for the flow diagram in Figure 7.

Parameter	Explanation
$t$	The current step number
$\Delta t$	The time step width (= 0.01 s)
flg <sub>fd</sub>	If 1, the equipment model has fallen down, and if 0, it has not.
flg <sub>lk</sub>	If 1, the caster wheels are locked, and if 0, they are not.

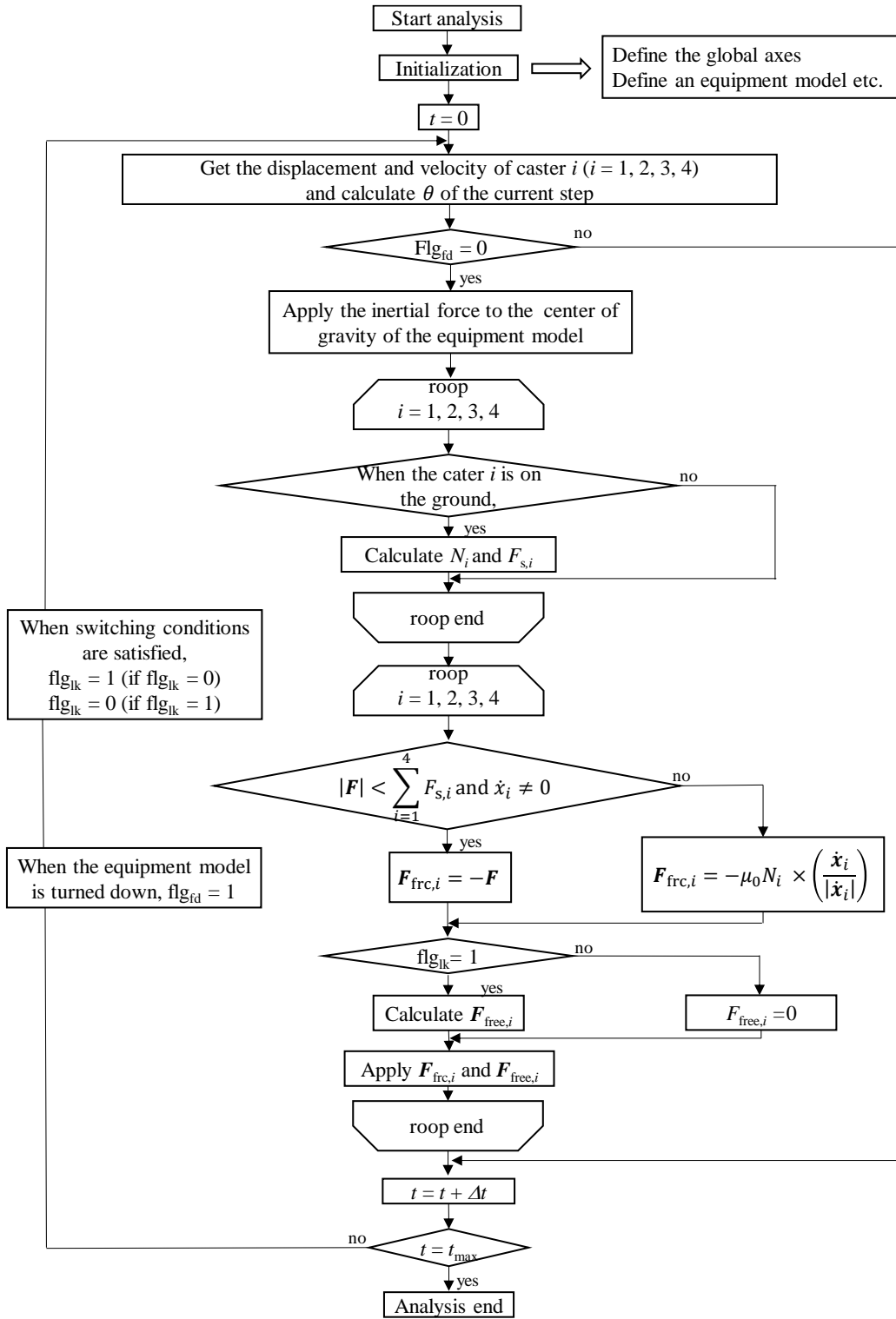


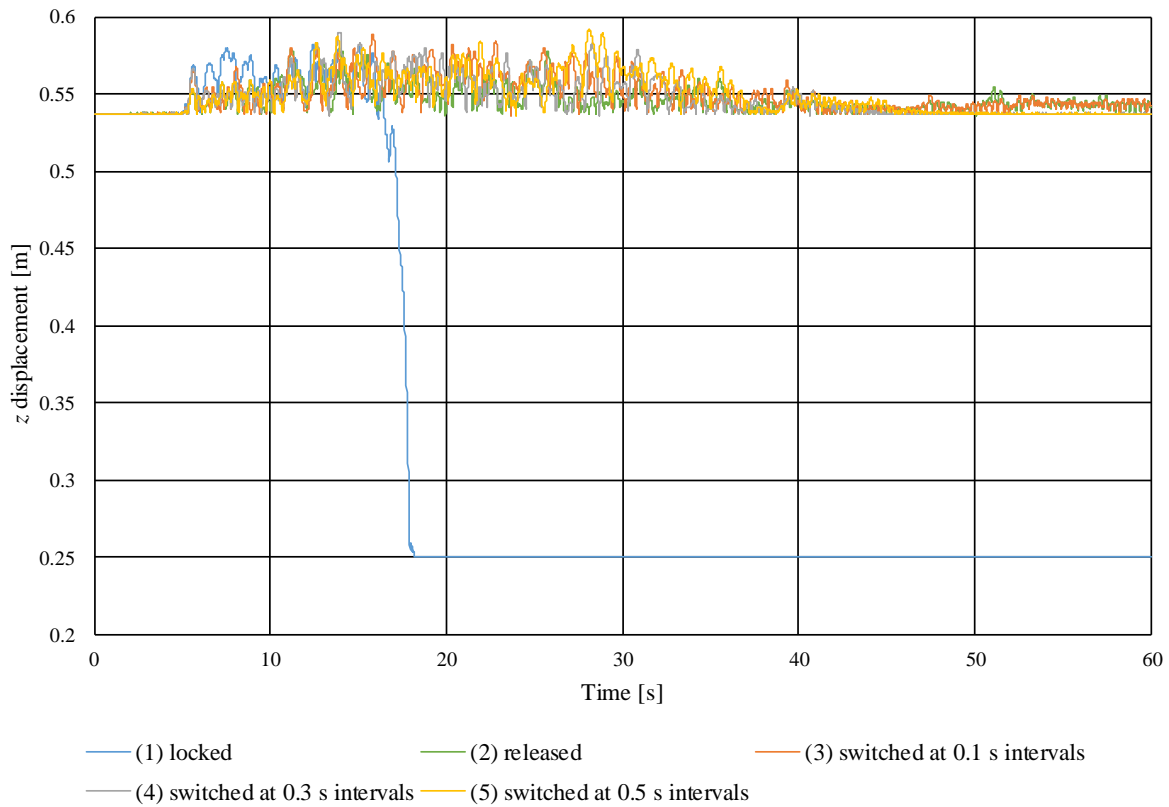
Figure 7. Flow of the numerical analysis.

### 3.3 CONTROL OF THE CASTERS

We consider the following five conditions to control the casters.

- (1) All casters locked.
- (2) All casters released.
- (3) All casters switched between locked and released at 0.1 s intervals.
- (4) All casters switched between locked and released at 0.3 s intervals.
- (5) All casters switched between locked and released at 0.5 s intervals.

The results of the equipment time history response analysis with control patterns (1)–(5) are shown in Figure 8.



(a) z displacement of the center of gravity of the equipment model

**Figure 8.** The results of the equipment time history response analysis for the five control patterns.

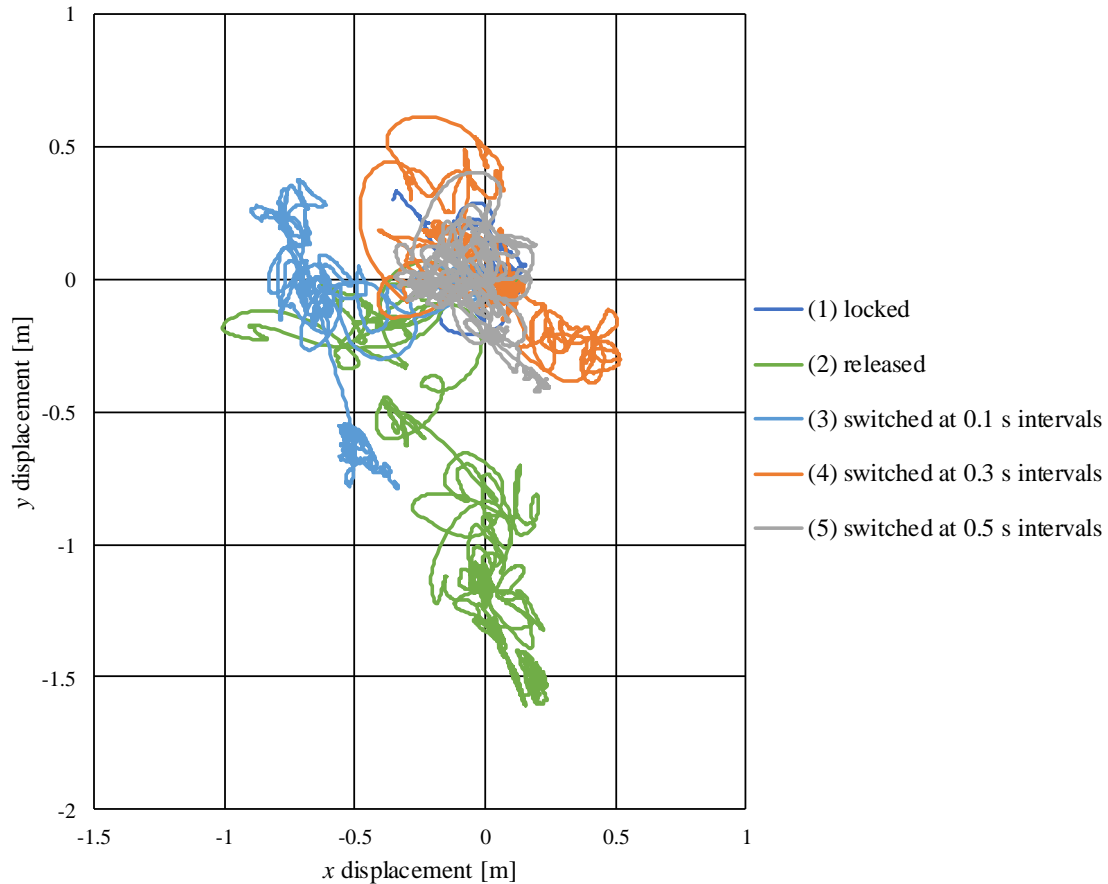


**Figure 8.** The results of the equipment time history response analysis for the five control patterns (continued).

From the  $z$  displacement of the center of gravity of the equipment model in Figure 8(a), the equipment model fell down only for condition (5), and from the  $x$  and  $y$  displacement of the center of gravity of the equipment in Figure 8(b), the equipment model moved to the farthest for condition (5) and moved the least for condition (4). Condition (3) resulted in a pattern where the displacement was small and the equipment did not fall down. We found that the caster switching control affects the behavior of the equipment model during seismic excitation. Therefore, caster switching control could reduce the damage in a building. However, more precise control methods need to be investigated.

#### 4 CONCLUSIONS

We developed a simulation code to analyze the behavior of equipment with casters in a building and analyzed the motion of such equipment subjected to earthquake excitation. As a result of the numerical analysis, we confirmed that the proposed switching control could reduce the displacement and the probability of the equipment overturning. In a future study, we will derive

the overturning condition of furniture with casters from large amounts of damping control data, we will propose an optimal fixed/non-fixed switching control based on that condition, and we will perform shaking table experiments to validate our simulation results.

## ACKNOWLEDGEMENTS

This work was supported by JSPS KAKENHI Grant Number 16H04455. The authors acknowledge Ms. Arisa Sugimoto for her contribution to fundamental formulation of control scheme.

## REFERENCES

- [1] Nikfar, F. and Konstantinidis, D. Shake table investigation on the seismic performance of hospital equipment supported on wheels/casters. *Earthq. Eng. Struct. Dyn.* (2017) 46:243–266.
- [2] Kamada, T., Ogata, Y., Sato, E., and Kakehi, A. Seismic response mitigation of medical wagon with casters by ER brake. *Proceedings of the 10th International Conference on Motion and Vibration Control (2010)* 2C35-1–2C35-9.
- [3] Saomoto, H. and Yoshimi, M. Seismic response simulation of furniture: Rational input including shape effect of building. *Journal of Japan Society of Civil Engineers, Ser. A1* (2013) 69: I\_1642–I\_1649.
- [4] Masatsuki, T. and Midorikawa, S. Simulation of seismic behavior of furniture in high-rise residential building due to long-period ground motion. *Journal of Japan Association for Earthquake Engineering* (2015) 15:6\_1–6\_11.
- [5] Isobe, D., Yamashita, T., Tagawa, H., Kaneko, M., Takahashi, T., and Motoyui, S. Motion analysis of furniture under seismic excitation using the finite element method. *Japan Architectural Review* (2018) 1: 44–45.
- [6] Saito, T., Takahashi, T., Hasegawa, R., Morita, K., Azuhata, T., and Noguchi, K. Shaking table test on indoor seismic safety of highrise buildings (Part II. Movement of furniture under long period earthquake ground motion), *Proceedings of the 14<sup>th</sup> World Conference on Earthquake Engineering* (2008) S10–014.
- [7] Purvance, D.M., Anoshepoor, A., and Brune, J.N. Freestanding block overturning fragilities: Numerical simulation and experimental validation. *Earthq. Eng. Struct. Dyn.* (2008) 37:791–808.
- [8] Di Egidio, A. and Contento, A. Base isolation of slide-rocking non-symmetric rigid blocks under impulsive and seismic excitations. *Engineering Structures* (2009) 31:2723–2734.

## PROBLEM-SOLVING ENVIRONMENT (PSE) IN COMPUTATIONAL ENGINEERING AND SCIENCE

SHIGEO KAWATA\*

\* Graduate School of Eng., Utsunomiya University  
Yohtoh 7-1-2, Utsunomiya 321-8585, Japan  
kwt@cc.utsunomiya-u.ac.jp

**Key Words:** Problem Solving Environment, Computer assisted computations, Scientific simulation, e-Science, PSE, Uncertainty in scientific computing.

**Abstract.** In this paper a review is presented on the PSE (Problem Solving Environment) concept in computational engineering and science. In the PSE concept, human concentrates on target problems and works out solutions, and a part of application of solutions, which can be solved mechanically, is performed by computers or machines or software. PSE provides integrated human friendly innovative computational services and facilities for easy incorporation of novel solution methods to solve a target class of problems. PSE is an innovative concept to enrich our e-Science, e-Life, e-Engineering, e-Production, e-Commerce, e-Home, etc. The PSE-relating studies were started in 1970's to provide a higher-level programming language than Fortran, etc. in scientific computations. The trend at that time was natural to deliver more human-friendly programming environment, and was resulting in PSE, CAE (Computer Assisted Engineering), libraries, etc. At present PSE covers a rather wide area, for example, program generation support PSEs, education support PSEs, CAE software learning support PSEs, Grid/Cloud computing support PSEs, job execution support PSEs, e-Learning support PSEs, etc. This review paper includes the PSE definition, a brief history of PSE, example PSE study activities, uncertainty management PSE and a future research directions in PSE.

### 1 INTRODUCTION

Problem Solving Environment (PSE) concept provides integrated human-friendly innovative computational services and facilities for easy incorporation of novel solution methods to solve a target class of problems. For example, a PSE generates a computer program automatically to solve differential equations<sup>[1-12]</sup>. Now the PSE concept covers rather wide areas in our society. PSE is an innovative concept to enrich science, human life, engineering, production and our society toward a programming-free environment in computing science. In the PSE concept, human concentrates on his/her target problems and works on solutions, and a part of application of solution, which can be solved mechanically, is performed by computers or machines or software. At present many kinds of computer-assisted problem solving environments are found everywhere in our life and in our society.

On the other hand, even today human power still contributes greatly to develop and write new softwares. For example, in scientific researches scientific discoveries are supported by theory, experiments and computer simulations. New researches tend to require new computer programs to simulate phenomena concerned. In another example, in developing new products engineers would also need new computer programs to develop the products cost-effectively. They may have to develop the new programs or learn how to use the programs for the product development. New services may also need new software systems. Therefore, the researchers and engineers may write or develop the new computer programs or learn how to use the programs. They do not like to develop nor learn the computer programs to solve their problems, but they like to devote their efforts to solve their target problems themselves.

In addition, computer simulations became the third important method after theoretical and experimental methods in science and engineering. Computer assisted problem solving is one of key methods to promote innovations in science and engineering, and contributes to enrich our society and our life from scientific and engineering sides.

The PSEs have provided the new directions to support users, engineers and scientists for

developing new services and new softwares, and also for solving their target problems based on computer systems.

The PSE-relating studies were started in 1970's to provide a higher-level programming language than Fortran, COBOL, ALGOL, PL/I and others in scientific computations. The trend at the time was reasonable to deliver more human-friendly programming environment beyond the higher-level languages shown above. Then the PSE research activity was started as well as activities of Computer Assisted Engineering (CAE) and software libraries. After the intensive developments in computer hardware and also in computer algorithms, researchers and engineers had expected an innovation in program writing and developing power. However, the enhancement in the programming power was relatively slow and weak compared with the enormous evolutions in the present hardware and algorithm power enhancements.

At present PSE covers a rather wide area, for example, program generation support PSE, education support PSE, CAE software learning support PSE, grid/cloud computing support PSE, job execution support PSE, learning support PSE, uncertainty management in scientific computing, PSE for PSE generation support (PSE for PSE), etc.

The paper includes a brief history of PSE, example PSE study activities and a future of PSE, including uncertainty management in scientific computing.

## 2 COMPUTER-ASSISTED PROBLEM SOLVING ENVIRONMENT (PSE)

PSE is defined as follows: "A system that provides all the computational facilities necessary to solve a target class of problems. It uses the language of the target class and users need not have specialized knowledge of the underlying hardware or software"<sup>[6]</sup>. PSE provides integrated human-friendly innovative computational services and facilities to enrich science, life, engineering, production, commerce and our society. Based on the PSEs, human concentrates on target problems themselves, and a part of solution is performed mechanically by computers or machines or software.

In computing sciences, we need the computer power, the excellent algorithms and the programming power in order to solve scientific problems leading to scientific discoveries and development of innovative new products and services. So far, the computer power and the computing algorithms have been developed incredibly, and have provided enormous contributions to sciences, productions and services. On the other hand, the programming power has not been developed well. The concept of PSE was proposed to support the programming power in science and engineering, and has been explored for decades.

In 1985, IFIP (International Federation for Information Processing) WG2.5 (Numerical Software)<sup>[16]</sup> organized a working conference on PSE and published the proceedings<sup>[17]</sup>. In 1991, a working conference on Programming Environments for High-Level Scientific Problem Solving was held<sup>[18]</sup>. In addition, a book on PSE was also published<sup>[19]</sup>. In 2007, a working conference on Grid-Based Problem Solving Environments was held<sup>[20]</sup>. A working conference on Uncertainty Quantification in Scientific Computing was held in 2012<sup>[21]</sup>. The PSE activity including scientific computing environments is one of research projects in IFIP WG2.5<sup>[16]</sup>. In these decades, international conferences tend to include the topic of PSE as one of standard topics in scientific computing. It has been recognized that PSE is an important research area in scientific computation and high-performance computing. In parallel, the PSE activities have started in several societies, scientific groups and countries. For example, in Japan, the PSE research group started in 1998 based on the previous individual PSE study activities, and the Japan Society for Computational Engineering and Science (JSCES) started in 1995, including the Study Group on PSE<sup>[22, 23]</sup>.

The PSE studies have been extensively explored over the past few decades. The explorations have been supported by the reinforced computer power and algorithm power. PSE has boosted the programming power, and have enriched problem solving methods in science and engineering to bring us innovations.

One of PSE studies<sup>[1-12]</sup> has been extensively explored in order to support engineers and

scientists to compute or solve their own problems based on for partial differential equations (PDEs), for example. One of the major objectives in PSE researches is to help users compute or solve their problems without heavy tasks, for example, without complete knowledge for computations<sup>[24]</sup> and/or the programs used. In this sense, the PSE provides an infrastructure for software for computational engineering and sciences.

One of typical PSEs for PDEs-based problems is ELLPACK<sup>[8, 24]</sup>. ELLPACK is a high level system for solving elliptic boundary value problems. One can solve routine problems by simply writing them down and naming the methods to be used. The ELLPACK high-level language can reduce the programming effort for a "routine" elliptic problem.

Another typical PSE for PDEs-based problems is DEQSOL<sup>[7, 10, 11]</sup>. DEQSOL was designed to develop an easy-to-use system for problem solving of PDE-based problems by finite difference method and finite element method. DEQSOL creates optimal Fortran codes oriented to the Hitachi vector processors.

Another PSE system of NCAS<sup>[1, 2, 4, 9]</sup> inputs a problem information including PDEs, initial and boundary conditions, and discretization and computation schemes, and outputs a program flow graph, a C-language source code for the problem and also a document for the program and for the problem (see Fig. 1). On a host computer a user inputs his/her problem, and NCAS guides the user to solve the problem. The distributed PSE for PDEs consists of several modules: problem description, discretization, equation manipulation, program design, program generation, documentation support, module liaison and job execution service. Each module is distributed on distributed computers. Each distributed module communicates with the host module, so that outputs from each module are visualized. Independent modules, which are developed by other engineers or users for one of the functions specified above can also be used after adjustments to the distributed PSE interface<sup>[25]</sup>, if necessary. The module liaison module generates an adapter module for the distributed PSE modules. The adapter module generated by the module liaison system inputs output data from preceding modules and/or external modules, and connects the data to the input data for the next module. The PSE contains all the information of the problem, PDEs, discretization scheme, mesh information, equation manipulation results, program design structure, variables and constant definitions and program itself. Therefore, the documentation support module also generates a document for the program generated together with the problem itself in the PSE<sup>[26]</sup>.

A PSE module in NCAS also helps users generate MPI-based parallel simulation programs based on PDEs<sup>[4]</sup>. The NCAS capability explores possibilities to visualize and steer the parallel program design process. At present NCAS supports a domain decomposition in a design of a parallel numerical simulation program, and the domain decomposition is designed or steered by users through a visualization window. After designing the domain decomposition, the parallel program itself is also designed and generated in NCAS, and the designed parallel program is visualized and steered by a Problem Analysis Diagram (PAD). In NCAS, MPI functions<sup>[27]</sup> are employed for message passing, and a single program multiple data (SPMD) model is

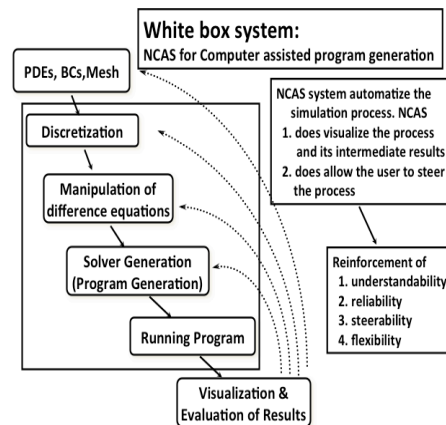


Fig. 1 An example PSE for computer assisted scientific program generation support: NCAS. NCAS inputs partial differential equations (PDEs), initial and boundary conditions, discretization method and algorithm, and outputs a C language program. The PDEs are automatically discretized and the program is generated mechanically. NCAS is a white box system, in which users can see and steer all the processes of program generation. NCAS system contains all the information for program generation, including basic equations, discretization schemes, discretized equations, boundary and initial conditions, mesh structure, program structure, and definitions of variables and constants. Therefore, a document for the corresponding program is also generated together with the program itself.

supported. The visualization and steering capabilities provide users a flexible design possibility of parallel programming.

Some PSEs provide a job execution support service on cloud or grid<sup>[28, 29]</sup>. It is difficult for users to submit jobs to distributed computers and to retrieve calculation data from them in scientific computing. A robust job execution service system was also developed in a closed distributed computer system<sup>[28]</sup>. The job execution service system consists of dynamic system management servers, execution servers and data servers. The dynamic system management server is duplicated in order to keep the system robust, and has an assistant management server. The dynamic system management server has a function of the job execution system management, including software deployment, program compilation, job execution, job status retrieval and computing data retrieval. This system does not require special middleware such as Globus<sup>[30]</sup> or UNICORE<sup>[31]</sup> or so. Users access the WWW page on the dynamic system management server, and the clients submit jobs. After the submitted job finishes, the dynamic system management server collects the information from other distributed computers. The dynamic management server and its assistant server move dynamically to new servers, if the present servers become busy. The dynamic system management server also demands the execution server to transfer the result data to the optimal data server. The dynamic system management server copies the computing data and sends the compressed computing data to another optimal data server in order for a robust data storage system. The clients can deploy their programs, execute jobs and retrieve the result data by accessing only the WWW page in the job execution service system. This job execution management server also has a function of automatic system construction, so that the users can manage the setup of the job execution management system easily on their closed distributed computers.

Another remarkable example of PSE is an education support PSE<sup>[32]</sup>. Network-based learning has been taking an important role in education as helpful education tools. However, it is difficult for teachers to retrieve education data from students or to obtain data from the student activities. Therefore, a problem solving environment (PSE) for the education and learning support: TSUNA-TASTE<sup>[32]</sup> was developed. The TSUNA-TASTE system collects the system-usage statistics, the information for the windows used and the operation situation of the mouse and key board of all students. The data, which the system TSUNA-TASTE collects, are stored in a database on the TSUNA-TASTE system server. Based on the data collected, teachers can have the learning status data for each student, and can guide the students in a better way.

Another research issue in PSE is validation, verification and uncertainty control in scientific simulations. When a software gives incorrect results for users, it may cause some difficulties, errors and accidents, depending on target problems<sup>[21, 33-37]</sup>. The validation and verification mechanism is essentially important in scientific computing. This point was also pointed out by E. Houstis, J. Rice and his colleagues<sup>[38]</sup>. Standardization and benchmark problems in each field may help to perform the validation and verification. In addition, uncertainty management must be addressed intensively in order to avoid serious accidents and disasters in our society. PSE is one of candidates to manage the uncertainty in a relatively easy way<sup>[39]</sup>. The topic on the uncertainty is also discussed in this paper. There are many PSE examples studied so far. In the references of [17-20] and [25] one can also find the example PSEs. In the next section typical example PSEs are introduced.

### **3 PSE EXAMPLES**

#### **3.1 A program generation support PSE**

PSE studies [2-14] for partial differential equation (PDE) based problems have been extensively explored in order to support engineers and scientists to compute or simulate their problems and products on computers in e-Sciences and e-Productions. One of the major objectives in PSE researches is to help users compute or simulate their problems without heavy tasks, for example, without complete knowledge [11, 12] for computations or without a full programming [2-13].

In this subsection a program generation support PSE, called NCAS is presented. NCAS inputs partial differential equations (PDEs), the initial and boundary conditions, the discretization method and the algorithm, and outputs a C language program for the problem. The PDEs are automatically discretized and the program is generated mechanically. NCAS is a white box system, in which users can see and steer all the processes of the program generation. NCAS contains all the information for program generation, including the basic equations, the discretization schemes, the discretized equations, the boundaries and the initial conditions, the mesh structure, the program structure, and the definitions of all the variables and the constants. Therefore, a document for the corresponding program is also generated together with the program itself. In PSE for PDEs problems, one of problems, which should be addressed, is to develop huge PSE systems, including reusability of legacy PSE software. In order to solve this problem, a module-based PSE is proposed<sup>[9, 40]</sup>; each PSE module solves a part of PSE tasks, for example, a problem description interface, a discretization module, a scheme suggestion module, a program flow designer, a program generator, a data analyzer, a visualizer, and so on. If each module can be developed independently and works cooperatively and smoothly to solve one PSE job, the heavy work of PSE development may be drastically relaxed. In this subsection a distributed PSE, called NCAS, is introduced, which supports users to generate computer programs<sup>[1-4, 9, 26, 40]</sup>.

The PSE system of NCAS inputs a problem information including discretization and computation schemes, and outputs a program flow graph, a C language source code for the problem and also a document for the program and for the problem. On a host computer a user inputs his/her problem, and the host guides the user to solve the problem. The distributed PSE for PDEs consists of several modules: a problem description, a discretization, an equation manipulation, a program design, a program generation, documentation support, a module liaison and a job execution service. Each module is distributed on distributed computers, and all the information is described by the Extensible Markup Language (XML) including the Mathematical Markup Language (MathML). Each distributed module communicates with the host module by using XML documents, so that outputs from each module are visualized. Independent modules, which are developed by other engineers or users for one of the

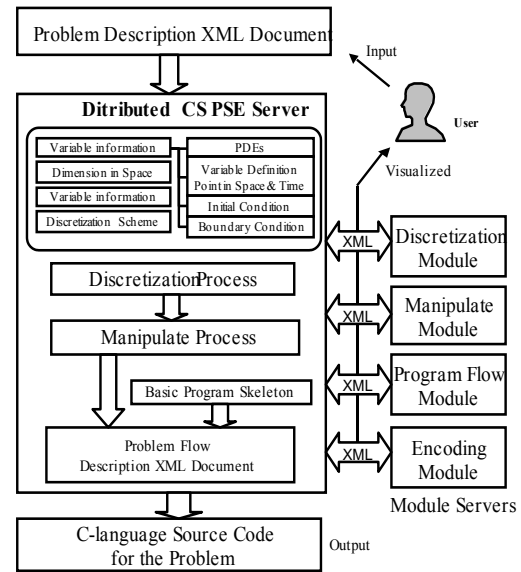


Fig. 2 Distributed-PSE: NCAS workflow.

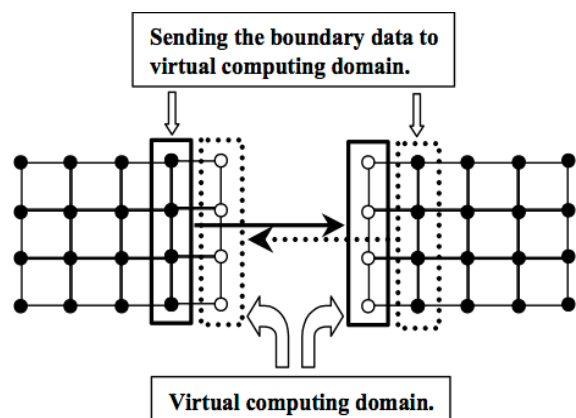


Fig. 3 Boundary data are communicated by the MPI functions in NCAS among domains decomposed. The MPI functions are automatically inserted into the program designed and generated in NCAS. The Finite Difference method (FDM) is employed in this example.

functions specified above can be also used after adjustments to the distributed PSE interface, if necessary. Therefore, the concept of the distributed PSE extends the potential of conventional PSE systems. The PSE contains all the information of the problem, PDEs, discretization scheme, mesh information, equation manipulation results, program design structure, variables and constant definitions and program itself. Therefore, the documentation support module also generates a document for the program generated and the problem itself in the PSE. The module liaison module generates an adapter module for the distributed PSE modules. The adapter module generated by the module liaison system inputs output data from preceding modules and/or external modules, and connects the data to the input data for the next module. The program generation PSE module provides a workflow shown in Fig. 2, and the user follows the workflow navigation for a problem generation.

The NCAS modules also help users generate MPI based parallel simulation programs based on partial differential equations (PDEs). The NCAS capability explores possibilities to visualize and steer the parallel program design process. At present NCAS supports a domain decomposition in a design of a parallel numerical simulation program, and the domain decomposition is designed or steered by users through a visualization window. After designing the domain decomposition, the parallel program itself is also designed and generated in NCAS, and the designed parallel program is visualized and steered by a PAD diagram. In NCAS, MPI functions are employed for message passing, and a SPMD (single program multiple data) model is supported. The visualization and steering capabilities provide users a flexible design possibility of parallel programming.

In the parallel program generation support in NCAS, for the data communication among the processors, the MPI functions are used. At least the boundary data for each domain decomposed are required to complete the computation in the adjacent processor (see Fig. 3). In NCAS the MPI functions are also automatically inserted to complete the parallel data communication programming. After specifying the domain decomposition information in NCAS, the parallel program is generated and provided to the users.

Figure 4 presents an example description of an input problem information, and Fig. 5 shows an example domain decomposition information. Through the NCAS visualization windows, for examples, shown in Figs. 4 and 5, one can check all the information and can also edit the information. In NCAS, after setting all the information for the problem description, the discretization information

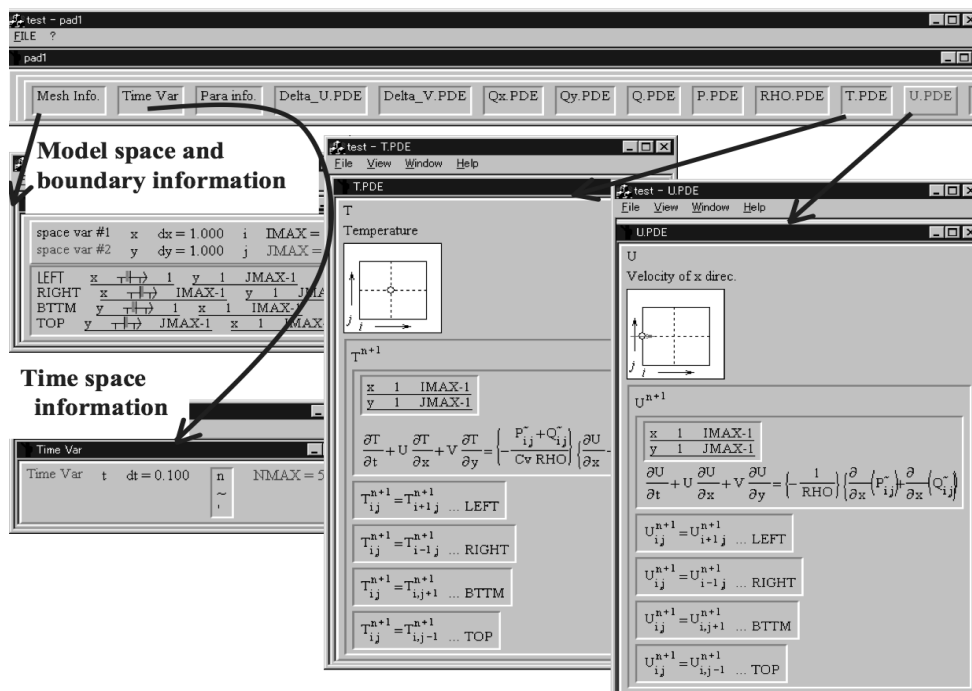


Fig. 4 An example PDE-problem description in NCAS. On each window users can edit the input description.

and the parallelization information through the NCAS windows, all the information is visualized to the users and the users can edit all the information through the windows. The discretization of each PDE is also performed automatically; depending on the discretization information which users input through the NCAS windows, the PDEs are discretized and manipulated appropriately according to the PDEs solving scheme. Then NCAS designs the parallel program for the problem, and outputs the parallel program and the corresponding document. Figure 6 shows an example MPI program automatically generated in NCAS.

In order to check the dynamic load balance function automatically generated by NCAS, during the computation an additional load was applied as shown in Fig. 7 (the left graph): by the additional load the computation time increases much in this specific case, if the static load balancing is used. When the dynamic load balancing method is selected in this example case, NCAS generates the functions, which measure the load balance of each machine dynamically, and according to the measured result each domain size is changed and adjusted dynamically to minimize the computation time. The right graph in Fig. 7 demonstrates the viability of the dynamic load balancing functions generated in NCAS, and the computation time reduction is significant in this case.

In the distributed PSE all the modules are distributed on network-linked computers. The information for the distributed modules and the computers are registered in a host computer. Newly developed modules by some users or scientists or so can be also registered in the host PSE server. The distributed PSE host server has the registered information for the modules oriented to one specific purpose, and users can obtain the information for each module and can select one of the modules to perform one task in all the PSE process.

The communication is accomplished through an interface using WWW server and Applet. The PSE server sends information described by XML to a module, and the module performs the task. The module sends the result based on the input XML information back to the PSE server. The result is visualized so that the user can check if the result is appropriate. After the successive processes, finally the NCAS generates a designed program flow and then a C program.

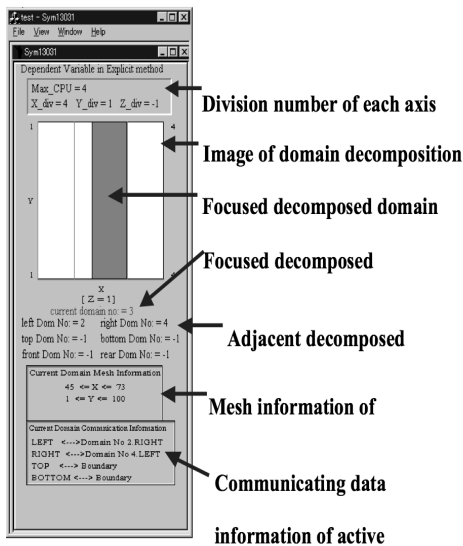


Fig. 5 Input and visualization of domain decomposition information.

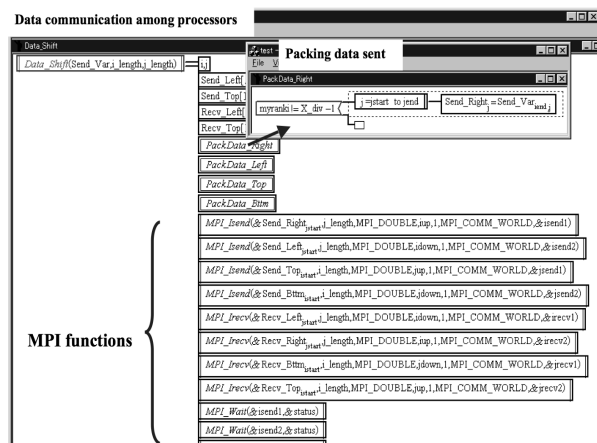


Fig. 6 Visualization of MPI functions designed for a domain decomposition information in NCAS.

### 3.2 An education support PSE

Network-based e-Learning is one of important education ways. In addition, the network-connected personal computers have become popular to schools and homes widely. In the network-based e-Learning, each learner can access education contents through the network anytime and anywhere. In an actual education, a network-based e-Learning system becomes popular in a long-distant learning and at the same time in a class-room education. Even inside class rooms, each computer is connected and can be used as a detecting device for the learners' progress and status. An e-Learning server may have facilities such as a user identification method or a file sharing tool in the network-based environment.

It would be difficult for teachers to know the learning state of students through each personal computer connected by a network. Without the detailed information of the students' achievement, it is difficult for the teachers to perform an appropriate guidance and education depending on the students' learning level. Therefore, the state of the students is important and required for the suitable guidance. The education-support PSE system, which provides teachers the student-achievement information, helps them in their teaching planning or the appropriate guidance.

The PSE concept was proposed to support the programming activity and also to provide integrated human-friendly computational facilities in e-Sciences and e-Productions<sup>[1-19]</sup>. In this subsection, an education and learning support PSE system: TSUNA-TASTE is introduced<sup>[32]</sup>.

The network education support system (TSUNA - TASTE) consists of four parts (see Fig. 8). The first part is an agent of student (Fig. 8(a)). It is a software, which always works on each personal computer of the student. The agent obtains the operation information of each student. The data are obtained from the operation information of the student through the OS with a resident software working on the personal computer of each student. The second part (Fig. 8(b)) is the education support server, that collects the data, which each student agent obtains via the network. The third part (Fig. 8(c)) is the database system. The database system stores the student profile data, the student personal data, the curriculum data and the teacher's personal data. The fourth part (Fig. 8(d)) is the WWW server displaying the information stored in the database. The WWW server (Servlet system) provides an interface to the TSUNA-TASTE handling.

The agent for each student resides on the memory of the personal computer of the student and performs the following three operations. Firstly the agent exchanges the messages with the education support server. The education support server transmits the messages to each agent. The student agent analyzes the messages, and obtains the process priority and the start time of the process described in the messages. The agent stores the message data in its task table. Secondly the agent

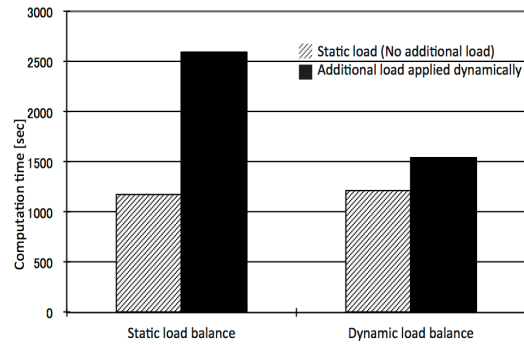


Fig. 7 A performance test result for a dynamic load balance. An additional load was applied during the computation, so that the computation time increases as shown in the left graph. When the dynamic load balancing function generated automatically by NCAS is used to this specific case, the domain size changes automatically depending on the machine load during the computation, and the result of the dynamic load balancing in the right graph shows the viability of

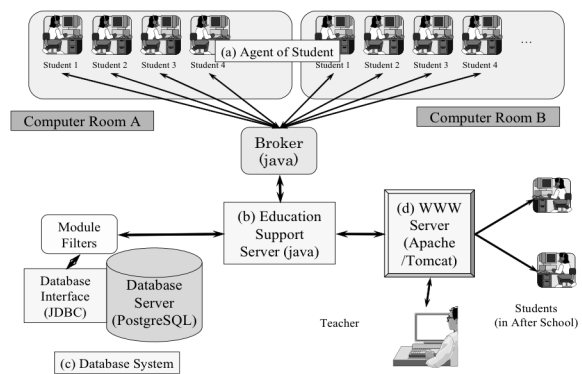


Fig. 8 Outline of the Computer assisted education support PSE: TSUNA-TASTE system.

manages the module program execution based on the task table. The module programs are small-size programs, which retrieve and output the student personal data from the student computers. The student personal data includes the achievement data, the operation data, the active window names and the process names. The third operation is a job to send back the data, which each module program collects, to the education support server. The module programs obtain the information of the student personal data from the OS of the student PCs. The module programs are implemented in the C++ language.

The module collects information about the student, however it does not store the raw data for security. It converts the raw data into statistics data. The transmission data are encoded and transferred. Furthermore, the personal information is not included in the data transmitted to the server. Thus, this system is robust for the electronic eavesdropping of data.

The education support server receives the operation data of the students through the student agent, and transmits the teacher's instructions to the students through the student agent. The education support server marks the students' absence, and identifies the students and their PCs. The education support server sends the messages of the data process demand to the agent of the student, and transmits the student personal data to the database server. The education support server also retrieves the student personal data requested by the teachers through the WWW server, and sends them back to the WWW server (see Fig. 8(d)) in the TSUNA-TASTE. The education support server is built using the Java language.

The data, which the education support server receives, are stored in the database. The database includes the private information of each student and teacher. The data contains the private information such as college student registration numbers, mail addresses and so on. These unchanged data are stored in the database together with the temporal data like the site of the student PCs. The server can receive the data from about 120 personal computers at the same time.

The WWW server system provides the user interface of the TSUNA-TASTE system. The teachers can obtain the state data of the students from the WWW system. The WWW server system presents the student achievement data, the learning progress and error occurrences situation during the programming exercises. The WWW system also provides an input interface to control the action of the TSUNA-TASTE: Through the WWW system, teachers can send a data gathering command, monitor the students' present usage of applications, and kill the unnecessary application processes on the students' PCs. The TSUNA-TASTE may open a new helpful e-Learning world.

### 3.3 Job execution support PSE on GRID

It is difficult for users to submit jobs to distributed computers on Cloud /Grid and to retrieve calculation data from them in scientific computing. In this subsection, a robust job execution service system is introduced in a closed distributed computer system<sup>[28, 29, 41]</sup>. The job execution service system consists of a dynamic system management servers, execution servers and data servers as shown in Fig. 9. The dynamic system management server is duplicated in order to keep the system robust, and has an assistant management server. The dynamic system management server has a function of the job execution system management, including software deployment, program compilation, job execution, job status retrieval and computing data retrieval. This system does not require special middleware for Cloud /Grid. Users access the WWW page on the dynamic system management server, and the clients submit jobs.

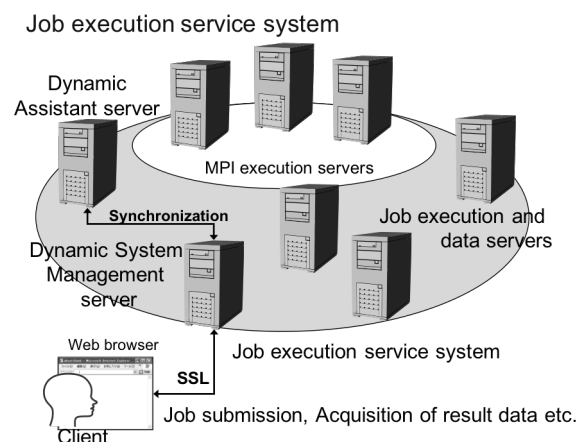


Fig. 9 Job execution service on distributed computers n Cloud / Grid.

After the submitted job finishes, the dynamic system management server collects the information from other distributed computers. When the present servers become busy, the dynamic management server and its assistant server move dynamically to new servers. The dynamic system management server also demands the execution server to transfer the result data to the optimal data server. The dynamic system management server copies the computing data and sends the compressed computing data to another optimal data server in order for a robust data storage system. The clients can deploy their programs, execute jobs and retrieve the result data by accessing only the WWW page in the job execution service system. This job execution management server also has a function of automatic system construction, so that the users can manage the setup of the job execution management system easily on their closed distributed computers.

Users access the WWW page on the dynamic system management server, and the clients submit jobs. After the submitted job finishes, the dynamic system management server collects the information from other distributed computers on Cloud / Grid. The clients can deploy their programs, execute jobs and retrieve the result data by accessing only the WWW page in the dynamic system management server.

The job execution service system acquires necessary resource information for servers for job execution and for data retrieval and storage. The resource information contains CPU architecture name, CPU operation frequency, total memory, memory in use, unused memory, load average and unused capacity of hard disk. The system sorts the resources in order for effective job execution. The users can find the resource information on the job execution service system WWW page.

Clients access the dynamic system management server through the WWW page of the system, and perform computing. Through the WWW page, the clients can up-load source files or executables to the dynamic system management server, select computing servers from among resources recommended by the system, and set execution environment. When two or more files are required for one job, the client should compress those files. When MPI jobs are executed, computing servers, on which MPI is installed, are recommended to the clients.

The compilation command, the execution method, the comment and the server name for job execution are specified by clients. The clients can also specify the storage location of the result data of the job. When the clients do not especially specify the storage data server, the system forwards the result data to the best data server. When input information is not sufficient, the job execution service system displays an error message, and advises to input the required input data. The clients can select the execution methods, or make scripts for the execution on the WWW page in a compressed file format.

When the job setting ends, the job execution service system forwards the job to a pertinent server or a server set based on the setting information. The setting file is described in XML, and contains the computing server information, the compilation command, the execution information and the data storage server information. When a compressed file, which contains source files/binaries and a make file, is sent to the computing servers, the compressed file is decompressed and the decompressed information is sent to the dynamic system management server, so that the clients can check if the file decompression is succeeded. When the compilation or the execution errors appear, the computing server notifies them to the dynamic management server. When the execution server specified is occupied by another job, the job is scheduled by the dynamic system management server.

When a job ends, the job execution server forwards the result data to a pertinent server based on the setting information. In addition, its compressed result data is stored in another data server. The result data duplication makes the data server robust and fault tolerant. When no data server is specified in the setting information, the computing server asks the dynamic system management server about the data storage servers. Based on the unused hard disk capacity, the better two data storage servers are selected from among the servers, on which no jobs run. One is for the result data uncompressed and the other is for the compressed backup data. When the result data is stored on the data servers specified, the data server locations are notified to the dynamic system management server. The client can refer to and can download the data from the WWW page on the dynamic

system management server.

## 4 CONCLUSIONS

The PSE has been extensively explored over the past few decades. The explorations have been supported by the reinforced computer power and algorithm power. PSE will boost up the programming power, and will enrich our e-Life and e-Science. In the near future of the PSE development we should consider how to create a PSE. To build up a PSE is a very hard task and needs huge human efforts. Therefore, PSE researchers have still been meeting this difficulty. In this research issue meta PSE or PSE for PSE may play an important role to build up service-oriented PSEs. One example of the meta PSE is a PSE Park<sup>[39]</sup>, in which many modules, developed by PSE researchers / developers, are distributed. Each module has one function or may be a one PSE, and is developed by many independent researchers and developers. By connecting the modules, PSE researchers or users can construct a single-purpose PSE or so. The interface should be opened, so that each PSE connector can be easily developed by each user or researcher or developer. The module mediator / connector may come into play there. The module base PSE may open a new PSE World.

Another research issue in PSE is validation, validity and uncertainty. When a PSE gives a wrong result for users, it may cause some difficulties, errors and accidents, depending on target problems. The validation and verification mechanisms are essentially important as usual software.

## ACKNOWLEDGEMENTS

This work was supported partly by JSPS, MEXT and Japan Society of Computational Engineering and Science. The authors would like to extend their appreciations to Prof. J. Rice, Prof. E. Houstis, friends in IFIP WG2.5, and friends in the PSE research group in Japan including Prof. S. Hioki, Dr. Y. Miyahara, Prof. D. S. Han, Dr. S. W. Hwang, Prof. T. Teramoto, Dr. H. Usami, Dr. T. Maeda, Dr. Y. Manabe, Dr. H. Kobashi, Dr. Y. Hayase and our former students and friends contributed to the works relating to the paper.

## REFERENCES

- [1] Boonmee, C. and Kawata, S., Computer-Assisted Simulation Environment for Partial-Differential-Equation Problem: 2. Visualization and Steering of Problem Solving Process, *Trans. of the Japan Society for Computational Engineering and Science*, Paper No. 19980002, (1998).
- [2] Boonmee, C., Kawata, S., Fujii, S., Manabe, Y. and Tago, Y., Visual Steering of the Simulation Process in a Scientific Numerical Simulation Environment - NCAS -, in print, *Enabling Technologies for Computational Science*, edited by E.Houstis and J.Rice, Kluwer Academic Pub., (2000).
- [3] Fujio, H., & Doi, S. (1998). Finite Element Description System as a Mid-Layer of PSE. *Proceedings of Conference on Computation Engineering and Science*, 3(2), (pp. 441-444).
- [4] Fujita, A., Teramoto, T., Nakamura, T., Boonmee, C. and Kawata, S. (2000). Computer-Assisted Parallel Program Generation System P-NCAS from Mathematical Model-Visualization and Steering of Parallel Program Generation Process-. *Transaction of the Japan Society for Computational Engineering and Science*, Paper No. 20000037.
- [5] Gallopoulos, E., Houstis, E. and Rice, J.R., Future Research Directions in Problem Solving Environments for Computational Science, Technical Report CSRD Report No. 1259, *Report of a workshop on Research Direction in Integrating Numerical Analysis, Symbolic Computer, Computational Geometry, and Artificial Intelligence for Computational Science*, Washington DC, April 11-12, (1991).
- [6] Gallopoulos, E., Houstis, E. and Rice, J. R. (1994). Computer as Thinker/Doer: Problem-Solving Environments for Computational Science. *IEEE Computational Science and Engineering*, 1(2), 1-23.
- [7] Hirayama, Y., Ishida, J., Ota, T., Igai, M., Kubo, S. and Yamaga, S. (1988). Physical Simulation using Numerical Simulation Tool PSILAB, *Proc. 1st Problem Solving Environment Workshop*, pp. 1-7.
- [8] Houstis, E. N. and Rice, J. R., Parallel ELLPACK, a development environment and problem solving environment for high performance computing machines, edited by In P. Gaffney and E. N. Houstis, *Programming Environments for High-Level Scientific Problem Solving*, North-Holland, Amsterdam, (1992), pp. 229-241.
- [9] Kawata, S., Boonmee, C., Fujita, A., Nakamura, T., Teramoto, T., Hayase, Y., Manabe, Y., Tago, Y. and Matsumoto, M., *Visual Steering of the Simulation Process in a Scientific Numerical Simulation Environment -NCAS-*, *Enabling Technologies for Computational Science*, E. N. Houstis and J. Rice (Ed.), Kluwer, (2000), pp. 291-300.
- [10] Okochi, T., Konno, C. and Igai, M., High Level Numerical Simulation Language DEQSOL for Parallel Computers. *Trans. of Information Processing Society of Japan*, 35(6), (1994), 977-985.
- [11] Umetani, Y., DEQSOL A numerical Simulation Language for Vector/Parallel Processors, *Proc. IFIP TC2/WG22*, 5, (1985), pp. 147-164.
- [12] Rice, J. R. and Boisvert, R. F., *Springer Series in Computational Mathematics 2, Solving Elliptic Problems Using ELLPACK*,

- Springer-Verlag, New York, (1984).
- [13] Kawata, S., Computer Assisted Problem Solving Environment (PSE), *Encyclopedia of Information Science and Technology, Third Edition*, ed. Mehdi Khosrow-Pour, Chapter 119, (2014), pp. 1251-1260, IGI Global, Hershey, PA, USA.
- [14] Kawata, S., Computer Assisted Parallel Program Generation, *Encyclopedia of Information Science and Technology, Fourth Edition*, ed. Mehdi Khosrow-Pour, Chapter 398, (2017), IGI Global, Hershey, PA, USA.
- [15] Kawata, S. Review of PSE (Problem Solving Environment) Study, *J. Convergence Information Tech.*, 5 2010, pp. 204-215.
- [16] IFIP WG2.5 (International Federation for Information Processing, Working Group 2.5), IFIP WG2.5 homepage retrieved on June 12, (2017), <http://www.ifip.org/wg-2.5>
- [17] Ford, B. and Chatelin, F. (Ed.), *Problem Solving Environments for Scientific Computing*, North-Holland, (1987).
- [18] Gaffney, P. W., and Houstis, E. N. (Ed.), *Programming Environments for High-Level Scientific Problem Solving*, North-Holland, (1992).
- [19] Houstis, E. N., Rice, J. R., Gallopoulos, E. and Bramley, R. (Ed.), *Enabling Technologies for Computational Science, Framework, Middleware and Environments*, Kluwer Academic Publishers, (2000).
- [20] Gaffney, P. W. and Pool, J. C. T. (Ed.), *Grid-Based Problem Solving Environments*, Springer, (2007).
- [21] Dienstfrey, A. and Boisvert, R. (Ed.), *Uncertainty Quantification in Scientific Computing*, Springer, (2012).
- [22] JSCES (The Japan Society for Computational Engineering and Science), JSCES homepage retrieved on June 12, (2017), <http://www.jscs.org/>.
- [23] PSE Research Group in Japan, homepage retrieved on June 12, 2017, <http://www.jscs.org/activity/research/pse/>.
- [24] Rice, J. R. and Boisvert, R. F., *Solving Elliptic Problems Using ELLPACK*, Springer Series in Computational Mathematics 2, Springer, (1984).
- [25] Kawata, S., Tago, Y., Umetani, Y. and Minami, K. (Ed.), *PSE Book: Computer assisted Problem Solving Environment in computing science (Basic & Advanced) (in Japanese)*, Tokyo: Baifukan, (2005).
- [26] Inaba, M., Fujii, H., Kitamuki, R., Kawata, S. and Kikuchi, T., Computer-Assisted Documentation in a Problem Solving Environment (PSE) for Partial Differential Equation Based Problems, *Trans. of the Japan Society for Computational Engineering and Science*, 20040025, 2004.
- [27] Message Passing Interface Forum, MPI: A Message-Passing Interface Standard, *Technical Report*, University of Tennessee, Knoxville, Tennessee, (1994).
- [28] Fujii, H., Kawata, S., Sugiura, H., Saitoh, Y., Usami, H., Yamada, M., Miyahara, Y., Kikuchi, T., Kanazawa, H. and Hayase, Y., Scientific Simulation Execution Support on a Closed Distributed Computer Environment, *2nd IEEE International Conference on e-Science and Grid Computing*, (2006), 27340112.
- [29] Kanazawa, H., Itou, Y., Yamada, M., Miyahara, Y., Hayase, Y., Kawata, S. and Usami, H., Design and Implementation of NAREGI Problem Solving Environment for Large-Scale Science Grid, *2nd IEEE International Conference on e-Science and Grid Computing*, (2006), 27340105.
- [30] Globus, Globus Online. Retrieved June 12, (2017), <http://www.globus.org/>
- [31] UNICORE, UNICORE. Retrieved June, (2017), <http://www.unicore.eu/>
- [32] Teramoto, T., Okada, T., and Kawata, S., A Distributed Education-Support PSE System, *3rd IEEE International Conference on e-Science and Grid Computing*, (2007), pp. 516-520.
- [33] CMFVVUQ (Committee on Mathematical Foundations of Verification, Validation, and Uncertainty Quantification), *Assessing the Reliability of Complex Models: Mathematical and Statistical Foundations of Verification, Validation, and Uncertainty Quantification*, The National Academies Press, (2012).
- [34] Johnson, C. R., Top Scientific Visualization Research Problems. *IEEE Computer Graphics and Applications: Visualization Viewpoints*, 24(4), (2004), pp. 13-17.
- [35] Kahan, W., Desparately Needed remedies for the Undebuggability of Large Floating-point Computations in Science and Engineering, *paper presented at IFIP Working Conference on Uncertainty Quantification in Scientific Computing*, retrieved on June 12, (2017), <http://www.eecs.berkeley.edu/~wkahan/Boulder.pdf>
- [36] Rump, S. M., Verification methods: Rigorous results using floating point arithmetic. *Acta Numerica*, 19, (2010), 287-449.
- [37] Weimer, W. R., *Exceptional Situation and Program Reliability*, PhD Thesis, University of California, Berkeley, (2005).
- [38] Houstis, E. N., Gallopoulos, E., Bramley, E. and Rice, J. R., Problem-Solving Environment in Computational Science. *IEEE Computational Science & Engineering*, 4, (1997), pp. 18-21.
- [39] Kawata, S., Kobashi, H., Ishihara, T., Manabe, Y., Matsumoto, M., Barada, D., Hayase, Y., Teramoto, T. and Usami, H., *Scientific Simulation Support Meta-System: PSE Park - with Uncertainty Feature Information -*, *International Journal of Intelligent Information Processing*, 3, (2012), 66-76.
- [40] Teramoto T., Nakamura, T., Kawata, S., Matide, S., Hayasaka, K., Nonaka, H., Sasaki, E. and Sanada, Y., A Distributed Problem Solving Environment (PSE) for Partial Differential Equation Based Problems, *Trans. Jpn. Soc. Comp. Sci. Eng.*, Paper No. 20010018, (2001).
- [41] Kawata, S., Usami, H., Hayase, Y., Miyahara, Y., Yamada, M., Fujisaki, M., Numata, Y., Nakamura, S., Ohi, N., Matsumoto, M., Teramoto, T., Inaba, M., Kitamuki, R., Fujii, H., Senda, Y., Tago, Y. and Umetani, Y., A Problem Solving Environment (PSE) for Distributed Computing, *Int. J. High Performance Computing and Network*, Vol. 1, No.4, (2004), pp. 223-230.

## **A Computational Fluid Dynamic Investigation of the Obesity-altered Hemodynamics in Children and Adolescents**

Asimina Kazakidi\*

\*University of Strathclyde

### **ABSTRACT**

Childhood obesity has become one of the major challenges of our century, taking epidemic proportions. Obesity, mainly a dietary disease, is known to advance endothelial dysfunction [1], an early sign of atherosclerotic lesions underlying most cardiovascular diseases. Endothelial damage in high-risk paediatric patients can be clinically assessed with measurements of the aortic and carotid intima-media thickness (IMT), and flow-mediated dilatation (FMD) of the brachial, radial, and femoral arteries [2]. However, it is not yet clear how the haemodynamic environment is altered in this particular group of patients and which flow-related mechanisms contribute to early vascular changes. This work will discuss a computational model of an arterial conduit with compliant walls during FDM that attempts to clarify some of these aspects. Solutions to the time-dependent, incompressible Navier-Stokes equations are based on high-fidelity finite volume and hybrid Cartesian/immersed-boundary (HCIB) methods [3] that overcome several of the shortcomings of conventional computational fluid dynamic methods and provide increased spatial flow analysis. The codes have previously been validated and used extensively in various applications. Implementation of wall motion is particularly easy with HCIB methods, which are inherently capable of handling arbitrarily large body motions and allow for effective solutions of wall configuration. The model provides an evaluation of the haemodynamic shear stresses, a common indicator of early atherosclerotic lesion localisation. Future work will include multi-scale modelling that combines high-resolution 3D blood flow computations, with macroscopic and microscopic features of the vascular environment. Further haemodynamic metrics, such as the time-averaged wall shear stress (TAWSS), the oscillatory shear index (OSI), and the transverse WSS will also be assessed, in conjunction with patient data. Acknowledgements: This project has received funding from the European Union's Horizon 2020 research and innovation programme under the Marie Skłodowska-Curie grant agreement No 749185. References [1] Cali, A.M.G. et al. (2008). Clin Endocrinol Metab 93(11) pS31 [2] Meyer AA et al. (2006) Pediatrics 117 p1560 [3] Kazakidi A et al. (2015) Comp Fluids 115 p54

## **Computational Mechanics in Pediatric Medicine**

Asimina Kazakidi\*, Vittoria Flamini\*\*

\*Strathmore, \*\*NYU

### **ABSTRACT**

Introduction to the topic of Computational Mechanics in Pediatric Medicine

## Stress-Based Topology Optimization of Multi-Material Truss Lattice Structures

Hesaneh Kazemi<sup>\*</sup>, Ashkan Vaziri<sup>\*\*</sup>, Julián Norato<sup>\*\*\*</sup>

<sup>\*</sup>University of Connecticut, <sup>\*\*</sup>Northeastern University, <sup>\*\*\*</sup>University of Connecticut

### ABSTRACT

We present a framework for the stress-based topology optimization of truss lattice structures made of multiple materials for desired bulk properties. Each strut in the lattice can be made of one of several available materials. We aim to solve lattice design problems subject to stress constraints, such as maximizing the lattice bulk modulus subject to stress constraints under an applied far-field traction. We employ the geometry projection method to map the geometry of each strut smoothly onto a continuous density field over a fixed finite element grid for analysis. Following recent work by our group, we adapt strategies used in density-based topology optimization to the geometry projection framework. These strategies address known challenges in stress-based topology optimization, namely the onset of singular optima and the large number of constraints. These strategies include the definition of a suitable relaxed stress, the use of aggregation functions to condense elemental stress constraints into a single optimization constraint, and the use of adaptive constraint scaling to ensure the desired stress limit is tightly satisfied. To accommodate multiple materials, we employ a novel aggregation scheme to perform the union of struts made of different materials. A size variable per material is ascribed to each strut in the lattice. Subsequently, an effective density per material is defined at each point, and the effective properties at that point are thus a function of the properties of the multiple available materials. To define the weights that determine the contribution of each strut to the effective density of a material, we adapt the Discrete Material Optimization (DMO) method. A size variable of unity indicates that the strut is made of the corresponding material. Furthermore, all size variables can be zero for a strut, allowing the optimizer to remove the strut altogether from the lattice. To avoid intermediate size variables in the optimal design, we penalize the size variables so that they are either 0 or 1. As opposed to DMO method, which enforces the penalization directly through the weighting factors, we penalize the size variables via an inequality constraint in the optimization (a 'discreteness constraint'). Moreover, each strut should be made of at most one material. Therefore, we impose another optimization constraint to ensure each strut has no more than one size variable of unity (a 'mutual material exclusion' constraint). We demonstrate the effectiveness of our method via several numerical examples.

## Ductile Fracture Modelling Using Local Approaches, Application to Steel Welded Joints in Nuclear Components

Safwane Kebiri<sup>\*</sup>, Myriam Bourgeois<sup>\*\*</sup>, François Di Paola<sup>\*\*\*</sup>, Habibou Maitournam<sup>\*\*\*\*</sup>

<sup>\*</sup>DEN - Service d'Etudes Mécaniques et Thermiques (SEMT), CEA, Université Paris-Saclay, F-91191, Gif-sur-Yvette, France, <sup>\*\*</sup>DEN - Service d'Etudes Mécaniques et Thermiques (SEMT), CEA, Université Paris-Saclay, F-91191, Gif-sur-Yvette, France, <sup>\*\*\*</sup>DEN - Service d'Etudes Mécaniques et Thermiques (SEMT), CEA, Université Paris-Saclay, F-91191, Gif-sur-Yvette, France, <sup>\*\*\*\*</sup>IMSIA - UMR 9219 - Institut des Sciences de la mécanique et Applications industrielles

### ABSTRACT

The simulation of crack propagation in ductile materials using the finite element method requires appropriate models for describing the nucleation, growth and coalescence of voids in a robust way. Local models, such as Rousselier and Gurson-Tvergaard-Needleman are now available in the finite element softwares as Cast3m [3]. A large number of models of this kind can be found in the literature, but they suffer from numerical drawbacks. First, they often show a marked mesh dependency of the solution. Second, volumetric locking of the elements is common in elastoplastic damage models in near-incompressible conditions. These two major issues must be solved in order to insure the robustness of such approaches. Our goal is to propose a model which will be able to handle these two problems. The mesh dependency can be solved by using regularization techniques, such as implicit gradient enrichment of an internal variable [1]. The locking can be treated, either using selective integration techniques, or a mixed formulation [2], which adds the volume variation as a new variable in addition to the displacement. The proposed models, based on the existing Rousselier and GTN models in Cast3m [3], address both issues using an implicit-enriched gradient of damage, and include a mixed formulation in the local models to ensure the desired robustness. In this presentation, the new models and the implementation of the new models are first presented. In a second part, simulations of crack propagation using the proposed models for axisymmetric and compact-tensile specimens in 2D using the Cast3m finite element software [3] are used to illustrate the relevancy of the approach. References [1] Samal, M. K.; Seidenfuss, M.; Roos, E.; Dutta, B. K. & Kushwaha, H. S. Finite element formulation of a new nonlocal damage model *Finite Elements in Analysis and Design*, 2008 , 44 , 358-371 [2] Lorentz, E.; Besson, J. & Cano, V., Numerical simulation of ductile fracture with the Rousselier constitutive law, *Computer Methods in Applied Mechanics and Engineering*, 2008 , 197 , 1965-1982 [3] Cast3M. Finite Element software developed by the French Atomic Energy Center (CEA) [www-cast3m.cea.fr](http://www-cast3m.cea.fr), 2017

## Comparison of Immersed, Embedded, and Moving Domain Approaches for Coupled Air/Water/Granular Dynamics

Chris Kees<sup>\*</sup>, Yong Yang<sup>\*\*</sup>, Milad Rakhsha<sup>\*\*\*</sup>, Leo Nouveau<sup>\*\*\*\*</sup>, Guglielmo Scovazzi<sup>\*\*\*\*\*</sup>

<sup>\*</sup>US Army ERDC-CHL, <sup>\*\*</sup>US Army ERDC-CHL, <sup>\*\*\*</sup>University of Wisconsin, <sup>\*\*\*\*</sup>Duke University, <sup>\*\*\*\*\*</sup>Duke University

### ABSTRACT

There is a compelling need for accurate, efficient, and robust computational models of granular media dynamics with tight coupling to multiphase air/water flow. Understanding riverine and coastal bank, dune, and sediment dynamics are just a few areas where fundamental science can be advanced with a computational laboratory representing, among other things, granular collisions and friction, air/water/solid surface tension forces, and high-Reynolds number incompressible flow. Having already invested heavily in development of conservative level set finite element methods for multiphase flow, a natural extension of our existing tools is the application of level-set-based approximations of the Nitsche approach to weak enforcement of fluid/solid Dirichlet boundary conditions [4]. The need to represent large-scale floating structures and vessels, however, also drove the development of boundary-fitted arbitrary Lagrangian-Eulerian formulations [1]. In this work we present an inter-comparison of several level-set approaches to the fluid-solid moving boundary, including the recently developed shifted boundary method [5], with a more traditional boundary-fitted deforming domain method [1]. We compare these methods in the context of modeling rigid particles interacting with air/water flow. These approaches, though recent, are not in principle new. Indeed, coupling the Discrete Element Method for granular materials to Finite Element Method has been addressed by many (e.g. [2,3]). The novel aspects of the current work are the coupling of air/water multiphase flow, higher-order FEM with immersed and embedded methods, and the opportunity for learning from inter-comparison of existing methods. [1] Ido Akkerman, Y Bazilevs, DJ Benson, MW Farthing, and CE Kees. Free-Surface Flow and Fluid-Object Interaction Modeling with Emphasis on Ship Hydrodynamics. *Journal of Applied Mechanics*, 79(1):010905, 2012. [2] B Avci and P Wriggers. A DEM-FEM Coupling Approach for the Direct Numerical Simulation of 3D Particulate Flows. *Journal of Applied Mechanics*, 79(1):010901, 2012. [3] Marcus VS Casagrande, Jose LD Alves, Carlos E Silva, Fabio T Alves, Renato N Elias, and Alvaro LGA Coutinho. A Hybrid FEM-DEM Approach to the Simulation of Fluid Flow Laden with Many Particles. *Computational Particle Mechanics*, 4(2):213{227, 2017. [4] C.E. Kees, I. Akkerman, M.W. Farthing, and Y. Bazilevs. A Conservative Level Set Method Suitable for Variable-Order Approximations and Unstructured Meshes. *Journal of Computational Physics*, 230(12):4536{4558, 2011. [5] A. Main and G. Scovazzi. The Shifted Boundary Method for Embedded Domain Computations. Part I: Poisson and Stokes Problems. *Journal of Computational Physics*, 2017.

## Multiscale Computational Stability Analysis of Active Elastomers across Scales

Marc-Andre Keip<sup>\*</sup>, Daniel Vallicotti<sup>\*\*</sup>, Elten Polukhov<sup>\*\*\*</sup>

<sup>\*</sup>Institute of Applied Mechanics (CE), University of Stuttgart, <sup>\*\*</sup>Institute of Applied Mechanics (CE), University of Stuttgart, <sup>\*\*\*</sup>Institute of Applied Mechanics (CE), University of Stuttgart

### ABSTRACT

We discuss aspects of the microscopic and the macroscopic stability of coupled, active elastomers with periodic microstructure based on a computational approach. The effective properties of the microstructured materials are determined via finite-element based computational homogenization of representative volume elements [1,2]. In the framework of the computational approach, localization-type macroscopic instabilities are detected by checking the strong ellipticity of homogenized moduli [3]. At the microscopic level, we determine bifurcation-type instabilities by means of a finite-element based Bloch-Floquet analysis [4]. The latter allows us to find altered periodicities of microstructures as well as critical macroscopic loading points [5]. Representative numerical examples will demonstrate the applicability of the proposed scheme to the detection of multiscale instabilities occurring in active elastomers. References: [1] K. Danas, Effective response of classical, auxetic and chiral magnetoelastic materials by use of a new variational principle, *J. Mech. Phys. Solids* 105:25-53, 2017. [2] M.-A. Keip and M. Rambauser, Computational and analytical investigations of shape effects in the experimental characterization of magnetorheological elastomers, *Int. J. Solids Struct.* 121:1-20, 2017. [3] A. Goshkoderia and S. Rudykh, Stability of magnetoactive composites with periodic microstructures undergoing finite strains in the presence of a magnetic field, *Comp. B Eng.*, 128:19-29, 2017. [4] K. Bertoldi and M. Gei, Instabilities in multilayered soft dielectrics, *J. Mech. Phys. Solids* 59:18-42, 2011. [5] E. Polukhov, D. Vallicotti and M.-A. Keip, Computational stability analysis of periodic electroactive polymer composites across scales, *Comput. Mech. Appl. Mech. Eng.*, submitted, 2017.

## **Reflections on DPG Methods**

Brendan Keith\*

\*The Institute for Computational Engineering and Sciences

### **ABSTRACT**

I will speak on several notable developments of the DPG methodology which I have contributed to over the past few years. Topics will include duality, DPG\* methods, a posteriori error estimation, and connections to weighted least-squares problems.

## Plastic Instability of Rate-Dependent Materials - Consideration of Isothermal and Adiabatic Conditions in Dynamic Tensile Tests -

Christian Keller\*, Uwe Herbrich\*\*

\*Bundesanstalt für Materialforschung und –prüfung (BAM), Unter den Eichen 87, 12205 Berlin, Germany,

\*\*Bundesanstalt für Materialforschung und –prüfung (BAM), Unter den Eichen 87, 12205 Berlin, Germany

### ABSTRACT

During dynamic processes, a certain range of strain rates is often observed along loaded structures and components. For precise numerical simulations, it is necessary to determine rate-dependent properties in dynamic tests and to describe the material behavior correctly within an appropriate domain of strain rates including adiabatic heating effects at higher strain rates, typically higher than  $10 \text{ s}^{-1}$ . In principle, numerical simulations are compared to experimental results to verify the applied material models. For dynamic tensile tests considering ductile materials and large plastic deformation beyond uniform elongation, it is challenging to obtain comparable results due to plastic instability and necking of the specimen, e.g., [1]. Based on the strain gradient in a general tensile specimen, a theoretical criterion was derived describing the plastic instability in rate-dependent materials under isothermal conditions in [2]. It was applied to different multiplicative and additive constitutive relations and the analytical onset of necking was compared to results from numerical calculations of quasi-static and dynamic tensile tests. The simulations of a sheet-metal specimen with rectangular cross-section were carried out using the Finite Element Method and it was found that the numerically calculated and the theoretically predicted onset of plastic instability agree very well. The analytical criterion for instability holds even for specimens without geometrical or material imperfections and confirms that the onset of plastic instability must be considered a material characteristic. However, real dynamic problems with higher strain rates are not isothermal, the heat generated by plastic work is not dissipated to the surrounding and the temperature of the material increases significantly. Adiabatic heating and thermal softening must be considered within the constitutive relations of rate-dependent materials and the discussion of plastic instability. In this paper, an enhanced and more generalized approach for the description of the condition for stability is discussed and applied to phenomenological as well as more physical constitutive relations from the literature. This allows an individual assessment of the accuracy and verification of rate-dependent material models with respect to plastic instability. [1] Böhm, R. ; Feucht, M. ; Andrade, F. ; Du Bois, P. ; Haufe, A.: Prediction of dynamic material failure – Part I: Strain rate dependent plastic yielding. In: 10th European LS-DYNA Conference (Proceedings). Würzburg, Germany, 2015 [2] Keller, C. ; Herbrich, U.: Plastic Instability of Rate-Dependent Materials - A Theoretical Approach in Comparison to FE-Analyses. In: 11th European LS-DYNA Conference (Proceedings). Salzburg, Austria, 2017

## **Towards Airframe Static Stress Requirements Improvement Using Probabilistic Analyses**

Martin Kempeneers\*

\*AIRBUS France

### **ABSTRACT**

The sizing by analysis approach is the most commonly used mean to demonstrate the structural integrity of an airframe component. Such an approach requires to account for the effect of all the physical parameters having a significant impact on the static strength of the part. These parameters can be for example: the mechanical loads, the material properties, the thermal environment, the built stresses... For static justification, the usual sizing by analysis approach used is of the deterministic type supported by probabilities. It means that it consists in considering a priori selected values for the parameters driving the static strength in order to assess the latter in a simple deterministic allowable vs applied load comparison check. The selection of the deterministic values is then based on probabilistic conditions. For the most important parameters (i.e. the mechanical load level and the material properties), the acceptable probability of occurrence to be considered are clearly specified in the certification regulations. Each of the other additional parameters to be taken into account in the analyses has also its own statistical distribution and an associated probability of occurrence. Most of the time, for these parameters, the selection of the deterministic values is based on engineering judgement and a low probability event (or even sometimes the worst case) is selected without further analysis (no detailed analysis of the effect of the parameters on the static strength). The reasons for doing so are most of the time for the sake of simplicity or because of a lack of method and/or data to do it better. This can result in the combination of very penalizing and unrealistic conditions in sizing analyses, and consequently taking into account scenarios beyond what needs to be reasonably considered. Rationalization can be done by using probabilistic assessments. This is the purpose of the present communication which defines a general approach to build probabilistic analyses intended to support the definition of improved static stress requirements reducing the accumulated conservatism.

## Time Discretization Bi-Fidelity Modeling

Vahid Keshavarzzadeh<sup>\*</sup>, Mike Kirby<sup>\*\*</sup>, Akil Narayan<sup>\*\*\*</sup>

<sup>\*</sup>University of Utah, <sup>\*\*</sup>University of Utah, <sup>\*\*\*</sup>University of Utah

### ABSTRACT

For many practical simulation scenarios, modification of the time-step (large versus small) provides a simple low versus high fidelity scenario in terms of accuracy versus computational cost. Multifidelity approaches attempt to construct a bi-fidelity model having an accuracy comparable with the high-fidelity model and computational cost comparable with the low-fidelity model. In this talk, we present a bi-fidelity framework defined by the time discretization parameter that relies on the low-rank structure of the map between model parameters/uncertain inputs and the solution of interest. We show how this framework behaves on canonical examples, and we show real-world (practical) extensions of our methodology to molecular dynamics simulations.

## Topology Optimization under Uncertainty with Multi-Resolution Finite Element Models

Vahid Keshavarzzadeh\*, Robert Kirby\*\*, Akil Narayan\*\*\*

\*University of Utah, \*\*University of Utah, \*\*\*University of Utah

### ABSTRACT

Abstract We present a computational framework for parametric topology optimization with multi-resolution finite element (FE) models. We use our framework in a bi-fidelity setting where a coarse and a fine mesh corresponding to low- and high-resolution models are available [1]. The inexpensive low-resolution model is used to explore the parameter space and approximate the parameterized high-resolution model and its sensitivity where parameters are considered in both structural load and stiffness. Our analysis provides computable error estimates for the bi-fidelity FE approximation and its sensitivity at each design iterate. We demonstrate our approach on benchmark density-based compliance minimization problems where we show significant reduction in computational cost i.e. the number of fine-resolution simulations for expensive problems such as topology optimization under manufacturing (geometric) variability while generating almost identical designs to those obtained with single resolution mesh [2]. To show the effectiveness of our bi-fidelity approach in estimating challenging quantities we compute the parametric Von-Mises stresses for the generated designs and compare them with standard Monte Carlo simulations. References [1] Narayan A, Gittelsohn C, Xiu D. A Stochastic Collocation Algorithm with Multifidelity Models. *SIAM Journal on Scientific Computing*. 2014;36(2):495–521. [2] Keshavarzzadeh V, Fernandez F, Tortorelli DA. Topology optimization under uncertainty via non-intrusive polynomial chaos expansion. *Computer Methods in Applied Mechanics and Engineering*. 2017;318:120–147.

## **Parallel Adaptive Implicit Extrapolation Methods**

David Ketcheson\*

\*KAUST

### **ABSTRACT**

Implicit extrapolation methods were developed extensively in the last two decades of the 20th century, including several codes based on serial implementations. We investigate the efficiency of a parallel high-order adaptive implicit extrapolation solver for stiff problems.

## **Computational Design of Nanocellulose Materials for Better Mechanical Performance**

Sinan Keten\*

\*Northwestern University

### **ABSTRACT**

Natural and engineered structural (load-bearing) nanocomposites often try to exploit microstructural configurations that lead to achieve remarkable mechanical properties such as damage tolerance. However, the mechanical properties of these materials depend strongly on both the chemistry of the interfaces and the microstructure of the material system, which complicates their design. In this talk, a new computational materials-by-design approach based on coarse-grained molecular simulations for understanding physical phenomena occurring at such disparate scales will be presented. I will discuss several cases where the coupling between nanostructure and chemical structure will lead to intriguing features, specifically focusing on nanocellulose neat films and nanocomposites. Drawing an analogy between thin films and nanocomposites, I will illustrate how understanding thin film simulations help us design better load-bearing nanocomposites with nanocellulose fillers. I will conclude with an outlook on impact tolerant polymer nanocomposites and tough interfaces inspired from biological systems.

## **A Novel Combination of Isogeometric Analysis with Far-field Expansion Absorbing Boundary Conditions for Exterior Acoustic Problems**

Tahsin Khajah\*, Vianey Villamizar\*\*

\*University of Texas at Tyler, \*\*Brigham Young University

### **ABSTRACT**

We have devised a new method combining Isogeometric Finite Element Method (IGA-FEM) with Far-field Expansion Absorbing Boundary Conditions (FEABC) for time-harmonic exterior acoustic problems. The FEABC has been recently developed [1]. It constitutes an arbitrary accurate representation of the outgoing waves on a conveniently chosen artificial boundary. First, we derive a weak formulation of the corresponding boundary value problem that includes the FEABC in the FEM context. The construction of the FEABC is based on truncated series of the well-known Wilcox and Karp farfield expansions which are used for an exact representation of the outgoing waves in the exterior. As a result, the error of the combined method IGA with FEABC can be made as small as the error made in the interior of the computational domain by increasing the number of terms in the Karp's and Wilcox's expansions. Hence, it is possible to obtain extremely accurate numerical solutions with rather low discretization densities. Both the pollution and truncation errors are well controlled even for high frequency regimes. In fact, the accuracy of the solution on the artificial boundary and the farfield is limited by the computational resources. We will present some numerical experiments for moderate and high frequencies to show the effectiveness of our novel method. [1] Vianey Villamizar, Sebastian Acosta, Blake Dastrup, High order local absorbing boundary conditions for acoustic waves in terms of farfield expansions, Journal of Computational Physics, Volume 333, 2017, Pages 331-351, ISSN 0021-9991, <https://doi.org/10.1016/j.jcp.2016.12.048>. (<http://www.sciencedirect.com/science/article/pii/S0021999116307124>)

## Computational Tools for Data-driven Design of Soft Robots

Mohammad Khalid Jawed\*

\*University of California, Los Angeles

### ABSTRACT

We report a numerical simulation framework for the mechanics of soft robots comprised of slender structures, for application in data-driven structural design, material selection, and adaptive control. Owing to prohibitive computational cost, soft robots are often designed solely based on empirical laws through a tedious trial-and-error process with no quantitative guideline. Inspired by fast and efficient modeling of hair and clothes in the animation industry, we adapt algorithms for physically-based simulations from computer graphics. We extend the Discrete Elastic Rods method to develop a simulator for a wide class of robots comprised of multiple slender structures (rods or shells) with compliant joints. In parallel with computation, we perform experiments with biomimetic robots composed of soft thermal actuators and confirm the validity of the simulation tool. Given the large number of parameters and high degree of nonlinearity associated with the performance and functionality of soft robots, emergent machine learning techniques offer a promising avenue for their computational design and optimization. The robustness and speed of our simulation can enable data-driven analysis of a broad range of smart programmable structures beyond soft robots.

## High Fidelity Anisotropic Adaptive Finite Element Method for Multiphase Flows with Phase Change

Mehdi Khalloufi\*, Rudy Valette\*\*, Elie Hachem\*\*\*

\*MINES ParisTech, PSL - Research University - Computing and Fluids Research Group, \*\*MINES ParisTech, PSL - Research University - Computing and Fluids Research Group, \*\*\*MINES ParisTech, PSL - Research University - Computing and Fluids Research Group

### ABSTRACT

We propose in this work a novel numerical framework, which allows dealing with the cooling of an immersed 3D solid surrounded by turbulent boiling flows with evaporation at the liquid-gas interfaces. Indeed, while standard numerical methods may not be able to deal with these heat transfer interactions simultaneously: gas-liquid-solid interfaces, vapor formations and dynamics, and 3D cooling of a heated solid, therefore, we propose in this paper a novel Eulerian method to achieve this challenging task. The key-points to achieve these difficult simulations are the development of an adaptive Eulerian framework. It uses a Level Set method to separate each state and to track each phase. A Variational Multiscale solver for the Navier-Stokes equations, which can deal with turbulent multiphase flows, is extended with implicit treatment of the surface tension. The phase change is performed using the balance of heat fluxes at the interface without the use of conforming mesh. Instead, the use of an a posteriori error estimate leading to highly stretched anisotropic elements at the interface enables to drastically reduce the interface thickness. This avoids the need of interface reconstruction or interpolation procedure. Finally, in the numerical results section, a series of 2-D and 3-D problems are solved to verify the efficiency and accuracy of the proposed framework. The cooling of an immersed solid is also presented and shows good agreement with the experimental results.

## Determining the Parameters of Constitutive Laws of XFEM and CZM for Modeling Premature Failures in Plated RC Beams

Mohammad Arsalan Khan\*

\*Dept. of Civil Engineering, Z.H. College of Engineering and Technology, Aligarh Muslim University,  
Aligarh-202002, India

### ABSTRACT

Structures are strengthened with FRP or steel plates through external retrofitting. This technique has been in practice mainly for two reasons: ease of implementation and minimal aesthetic change in the structural component. However, RC beams strengthened with this technique suffer from premature failure(s); that is, a beam failing in undesirable modes of failure which are unpredictable and against which the beam is not initially designed. One critical mode of such failure is peeling, leading to a catastrophic failure by ripping off of the coverconcrete along the rebars and thereby further leaving the rebars exposed. Peeling usually starts from the end of the plate and propagates further depending on wide range of geometrical and material parameters. Debonding, which may also start from plate-end, has a different failure mechanism to peeling and so the defining parameters. However, in literature, both types of failure have largely been put in one category as a failure from plate-end; and solutions to the existing problem are largely limited to the mode-II debonding behaviour. This may be attributed to the complex nature of material behaviour, combined with geometrical non-uniformities under mixed-mode loading. Current study shows the suitability of XFEM and Cohesive Zone Model (CZM) models to respectively predict peeling and debonding failures in plated RC beams subjected to 4-point loading condition. XFEM model is utilised along with Concrete Damaged Plasticity model (CDP). Beams have been selectively picked from literature to cover a wide range of material and geometrical variables and the ones that are failing in peeling or debonding. NA series of numerical simulations are performed for different combinations of bond parameters and verified against experimental data to identify parameters of traction-separation constitutive models, defining peeling and debonding, in terms of key material properties. Considering a level of non-uniformity of result patterns associated with this problem, multiple regression analysis is performed to reach desired relations of bond parameters. Suitability of different bond-slip curves are then evaluated for CZM, where bilinear law is found to be a closest match with experimental observations. Suitability of the bond parameters, thus arrived, is demonstrated against the experimental data consisting of strain distribution, plate-end displacement, number of cracks, and load and mode of failure.

## Scale Transition from Discrete to Continuous Models for Drying of Capillary Porous Media

Abdolreza Kharaghani\*, Xiang Lu\*\*, Evangelos Tsotsas\*\*\*

\*Otto von Guericke University Magdeburg, \*\*Otto von Guericke University Magdeburg, \*\*\*Otto von Guericke University Magdeburg

### ABSTRACT

Drying of porous media is a central process in many environmental and engineering applications. The physical processes involved are two-phase flow in porous media as well as phase transition. Two main approaches have been used to derive mathematical models for the drying process: The first approach considers the partially saturated porous medium as a continuum and partial differential equations are used to describe the mass, momentum and energy balances of the fluid phases. The continuum-scale models obtained by this approach involve constitutive laws which require effective material properties, such as the permeability, diffusivity, and thermal conductivity which are often determined by laborious experiments. The second approach considers the material at the pore scale, where the void space is represented by a network of pores. Micro- or nanofluidics models used in each pore give rise to a large system of ordinary differential equations with degrees of freedom at each node of the pore network. The characteristic length scale of the pore network models is several orders of magnitude smaller than the practically relevant length scale. A straightforward upscaling of the micro-scale models by using large pore networks is computationally costly, but it can be used to assess the quality of any chosen continuum-scale model as well as to estimate the effective parameters. When reliable estimates for these parameters have been obtained as functions of the pore size distribution and other material properties, the computationally much cheaper continuum-scale model may be used in future simulations without the need for further micro-scale simulations or experimental measurements. In this work, we demonstrate this scale transition with a three-dimensional pore network model at the micro scale and with the one-dimensional moisture diffusion model at the continuum scale. This is a quasilinear parabolic partial differential equation for the moisture content in the porous medium, where the effective moisture diffusion coefficient depends on the moisture content. We estimate this effective parameter from the post-processing of the (isothermal) micro-scale simulation results for multiple realizations of the pore space geometry from a given probability distribution.

## On Relaxed Energy Potentials in Magnetomechanics

Bjoern Kiefer\*, Thorsten Bartel\*\*

\*TU Bergakademie Freiberg, Institute of Mechanics and Fluid Dynamics, \*\*TU Dortmund, Institute of Mechanics

### ABSTRACT

The prediction of the effective macroscopic behaviors of micro-heterogeneous materials by means of adequate homogenization concepts is a classical problem in solid mechanics. Such analysis relies on the knowledge of geometrical, distributional and constitutive properties of the involved phases. It is well-known that standard homogenization schemes in micromechanics, such as the Taylor/Voigt and Reuss/Sachs assumptions, can also be interpreted as energetic bounds. Furthermore, energy relaxation concepts have been established that determine stable effective material responses based on appropriate convex, quasi-convex and rank-one convex energy hulls for multi-phase materials characterized by non-convex energy landscapes, see [2,3], and the references therein. In this contribution we propose analogous relaxation-based homogenization approaches for magnetizable solids--in extension of variational methods of magnetomechanics established in prior work, cf. [1-3]. In particular, we introduce novel scalar and vector-valued magnetic potential perturbation schemes. These yield relaxed effective free energy/enthalpy densities which simultaneously satisfy magnetic induction and magnetic field strength compatibility requirements---i.e.~the magnetostatic Maxwell equations---at phase boundaries. It is shown that the relaxed vector potential scheme requires the additional setting of gauge conditions to avoid spurious solutions and thereby improve its convergence behavior. In this context, we also propose adequate choices of thermodynamic potentials and their implications on the theoretical framework for constitutive modeling as well as corresponding numerical treatments. Furthermore, the challenges of implementing homogenization schemes based on potentials that are simultaneously relaxed with respect to mechanical and magnetic degrees of freedom are discussed as part of on-going work. Finally, it must be emphasized that the established variational relaxation schemes are equally applicable to the modeling of multi-phase solids exhibiting electromechanical coupling. References [1] Miehe, C., Kiefer, B., Rosato, D., An incremental variational formulation of dissipative magnetostriction at the macroscopic continuum level, *International Journal of Solids and Structures*, 48(13):1846–1866, 2011. [2] Bartel, T., Menzel, A., Svendsen, B., Thermodynamic and Relaxation-based Modeling of the Interaction Between Martensitic Phase Transformations and Plasticity, *Journal of the Mechanics and Physics of Solids*, 59(5):1004-1019, 2011. [3] Kiefer, B., Buckmann, K., Bartel, T., Numerical Energy Relaxation to Model Microstructure Evolution in Functional Magnetic Materials, *GAMM-Mitteilungen*, 38(1): 171–196, 2015.

## Isogeometric Phase-field Description of Brittle Fracture in Plates and Shells

Josef Kiendl<sup>\*</sup>, Davide Proserpio<sup>\*\*</sup>, Marreddy Ambati<sup>\*\*\*</sup>, Laura De Lorenzis<sup>\*\*\*\*</sup>

<sup>\*</sup>Norwegian University of Science and Technology, <sup>\*\*</sup>Norwegian University of Science and Technology, <sup>\*\*\*</sup>TU Braunschweig, <sup>\*\*\*\*</sup>TU Braunschweig

### ABSTRACT

Phase-field modeling of brittle fracture is a modern promising approach that enables a unified description of complicated failure processes, including crack initiation, propagation, branching, and merging, as well as its efficient numerical treatment [1]. In this work, we apply the phase-field fracture approach to shell structures, describing both the structure and the phase field by surface models. For avoiding fracture in compression, we split of the deformation tensor in tension and compression terms as proposed in [1]. We show that this requires special attention in structural models like plates and shells, where bending deformation typically induces both tension and compression at opposite sides of the structure. We propose a new approach [2], which allows for a varying degradation through the thickness while the phase field is represented as a single two-dimensional field on the shell's middle surface. The numerical implementation is based on isogeometric analysis with a rotation-free Kirchhoff-Love shell formulation for structural analysis. We extended the NURBS-based implementation to locally refinable LR-NURBS enabling local and adaptive mesh refinement, which is a crucial aspect for computational efficiency considering that the phase-field approach requires very fine mesh resolution locally in the cracked areas. References: [1] C. Miehe, M. Hofacker, F. Welschinger. A phase field model for rate-independent crack propagation: robust algorithmic implementation based on operator splits. CMAME (2010). [2] J. Kiendl, M. Ambati, L. De Lorenzis, H. Gomez, A. Reali. Phase-field description of brittle fracture in plates and shells. CMAME (2016).

## A High-order Local Discontinuous Galerkin Scheme for Viscoelastic Oldroyd B Fluid Flow

Anne Kikker\*, Florian Kummer\*\*

\*Graduate School CE, Technische Universität Darmstadt, Germany/Chair of Fluid Dynamics, Technische Universität Darmstadt, Germany, \*\*Chair of Fluid Dynamics, Technische Universität Darmstadt, Germany

### ABSTRACT

In numerical simulations of viscoelastic flow a breakdown in convergence often occurs for different computational approaches at critically high values of the Weissenberg number. This is due to two major problems concerning stability in the discretization. First, we have a mixed hyperbolic-elliptic problem weighted by a ratio parameter between retardation and relaxation time of viscoelastic fluid. Second, we have a convection-dominated convection-diffusion problem in the constitutive equations. We introduce a solver for viscoelastic Oldroyd B flow with an exclusively high-order Discontinuous Galerkin (DG) scheme for all equations using a local DG formulation with penalized fluxes in order to solve the hyperbolic constitutive equations [1] and using a streamline upwinding formulation for the convective fluxes of the constitutive equations [2]. While the saddle point problem of the Navier-Stokes system is of elliptic type, the constitutive equations modelling the viscoelastic behaviour are hyperbolic. The viscous parts of the momentum equations and of the constitutive equations are weighted by a ratio parameter. So depending on that parameter a change of type from elliptic to hyperbolic can occur and the numerical solution becomes unstable [2]. We use a local DG formulation following [1] to stabilize the system of equations including the constitutive equations for Oldroyd B fluid. The DG method allows jumps in the boundary conditions and preconditioning at the elemental level, appropriate flux functions for the edges can be chosen and additional velocity-stress compatibility conditions can be easily satisfied [2]. So the DG method is a promising method for convection dominated problems and is often used in combination with streamline upwinding for the convective terms of the constitutive equations of viscoelastic flow whereas the other terms are discretized using a Finite Elements ansatz. The successful implementation of both schemes is presented in an hp convergence study and first results are shown for various benchmark problems for viscoelastic flow. References: [1] Owens, R. G., Phillips, T. N.: Computational Rheology. Imperial College Press, London, River Edge, NJ (2002). [2] Cockburn, B., Kanschat, G., Schötzau, D., Schwab, C.: Local Discontinuous Galerkin Methods for the Stokes System. SIAM J. Numer. Anal. 40 (1), 319-343 (2002). The work of A. Kikker is supported by the Excellence Initiative of the German Federal and State Governments and the Graduate School of Computational Engineering at Technische Universität Darmstadt. The work of F. Kummer is supported by the German DFG through Collaborative Research Centre 1194/B06.

## Viscoelastic behavior of natural rubber with coarse-grained molecular dynamics

Byungjo Kim<sup>\*</sup>, Junghwan Moon<sup>\*\*</sup>, Maenghyo Cho<sup>\*\*\*</sup>

<sup>\*</sup>Seoul National University, <sup>\*\*</sup>Seoul National University, <sup>\*\*\*</sup>Seoul National University

### ABSTRACT

In this work, the viscoelastic properties of natural rubber are thoroughly investigated using a coarse-grained (CG) molecular dynamics (MD) simulation method. Due to the limitation of time and length scales in the MD simulation environment, it is challenging to assess the nature of viscoelastic of polymer materials with a computational approach. In that regards, CG MD offers an equivalent system with reduced degree of freedom by replacing a group of atoms with a corresponding bead particle. To describe the interactions between beads consisting of the system, the iterative Boltzmann inversion (IBI) is used for obtaining bonded and non-bonded potential. Herein, the time dependent shear relaxation modulus is calculated using the stress autocorrelation, and dynamic modulus (storage and loss modulus) is further calculated with the Fourier transformation in a complex domain. The viscoelastic behavior of natural rubber is studied considering a chain length effect. Plus, the influence of vulcanization of rubber is taken into account. To investigate more detailed viscoelastic nature of rubber, a wide range of temperature is considered for the present study. With the present work, the viscoelastic nature of rubber is understood by employing CG MD simulations which can enhance the scale of computation in terms of length and time. Further, this work can be extended to examine more complex polymeric system regarding the long-term physical nature or thermodynamic property. Keywords: Coarse-grained molecular dynamics, Rubber, Viscoelastic behavior. Acknowledgement This work was supported by a grant from the National Research Foundation of Korea (NRF) funded by the Korea government (MSIP) (No. 2012R1A3A2048841)

## **Development of Electricity-harvesting Piezoelectric Polymer Beams Vibrating in a Wind Flow Around Running Electric Vehicles Using Topology Optimization**

Cheol Kim<sup>\*</sup>, Changmin Park<sup>\*\*</sup>, Jin-Young Yoon<sup>\*\*\*</sup>

<sup>\*</sup>Kyungpook National University, <sup>\*\*</sup>Kyungpook National University, <sup>\*\*\*</sup>Hyundai Motor Company

### **ABSTRACT**

An electric energy harvesting system that is installed on the surface of a vehicle has been developed in order to supply auxiliary electric power for EV (electric vehicles). The system consists of several thin piezoelectric polymer beams that are fixed at both ends and vibrating in an air stream around the running electric vehicle. The fluctuation of airflows around the harvesting beams attached to a car is analysed by using a CFD program. The characteristics of beam vibration and resulting generation of electricity are computed by using FEM. To maximize the amount of electricity generation from harvesting beams, the cross-sectional curvature and shape of a piezoelectric harvesting beam are optimized by the shape and topology optimization method. The structural vibration in a turbulent flow is considered during the optimization process simultaneously. For optimization, we develop a new electro-mechanical coupling coefficient and cost function for piezoelectric polymer. As results of analysis, a reasonable amount of electric power can be successfully harvested from passing airflow around a vehicle. The harvesting beam is fabricated and is installed on a car for validation tests. Real car driving tests for the harvesting system give good agreements with numerical predictions.

## Tailoring the Stiffness of Tubular Structures through Auxetic Patterns

Do-Nyun Kim<sup>\*</sup>, Kwang Je Lee<sup>\*\*</sup>, Dongsik Seo<sup>\*\*\*</sup>, Jeong Min Hur<sup>\*\*\*\*</sup>

<sup>\*</sup>Seoul National University, <sup>\*\*</sup>Seoul National University, <sup>\*\*\*</sup>Seoul National University, <sup>\*\*\*\*</sup>Seoul National University

### ABSTRACT

Auxetic materials are emerging mechanical metamaterials showing a negative Poisson's ratio that may have interesting geometrical and mechanical properties such as synclastic curvature in bending, high impact and indentation resistance, and tuneable dynamic properties for vibration isolation and wave control. While various deformation mechanisms and patterns have been proposed to achieve a negative Poisson's ratio, little attention has been paid to its link to the fundamental mechanical properties of structures such as the stiffness. Here, we present a novel method to tailor the bending and torsional stiffness values of tubular structures by imposing auxetic cutting patterns on the tube. It is demonstrated that rational design of these patterns enables us to obtain a wide range of bending and torsional stiffness values without changing the cross-sectional shape, the size, and the material used. To illustrate, auxetic patterns based on the rigid-rotating-unit mechanism are employed and implemented on a cylindrical hollow tube by engraving alternating slits that divide the tube into rigid-rotating-unit-like and hinge-like sub-domains. Parametric studies for the geometric parameters of these patterns performed using the finite element method reveal the primary geometric parameters governing the tube stiffness. We also measure the tube stiffness experimentally for a set of patterned tubes, validating the simulation results and our design principles for stiffness control.

# Auto Parameter Tuning in Topology Optimization Using Deep Reinforcement Learning

Dongjin Kim\*, Jaewook Lee\*\*

\*Gwangju Institute of Science and Technology, \*\*Gwangju Institute of Science and Technology

## ABSTRACT

In this research, a basic auto parameter tuner has been developed to generate the target number of holes in topology optimization results using deep reinforcement learning [1]. This work aims to support engineers who suffer from parameter decision in topology optimization using deep learning techniques. In topology optimization problems, the unique solution is not guaranteed. To relieve numerical instability problems, various techniques have been proposed [2]. These techniques require careful control of many parameters. If improper parameters are used, it is difficult to get satisfactory optimization results. The parameters have been determined heuristically by designer's intuition till now. Therefore, this work proposes an auto parameter tuner constructed using deep reinforcement learning [1]. The deep reinforcement learning can be used for improving a quantified performance without the supervision [1]. In this research, the quantified performance is declared as a difference between the target and designed number of holes in the result of topology optimization. Here, the number of holes are calculated by the connected-component labeling [3]. For constructing the auto parameter tuner, a python code is developed. As a result, the developed parameter tuner generates the optimization result satisfying target number of holes. [1] Minh, V., et al, Nature(2015) 518: 529. [2] Sigmund, O. & Maute, K. Struct Multidisc Optim (2013) 48: 1031. [3] Wu, K., Otoo, E. & Suzuki, K. Pattern Anal Applic (2009) 12: 117.

## Quantitative phase-field simulations for solidification microstructure with different preferred growth direction

Geunwoo Kim<sup>\*</sup>, Munekazu Ohno<sup>\*\*</sup>, Kiyotaka Matsuura<sup>\*\*\*</sup>, Tomohiro Takaki<sup>\*\*\*\*</sup>

<sup>\*</sup>Hokkaido University, <sup>\*\*</sup>Hokkaido University, <sup>\*\*\*</sup>Hokkaido University, <sup>\*\*\*\*</sup>Kyoto Institute of Technology

### ABSTRACT

Preferred growth direction of metallic materials is one of important factors that have a great influence on solidification structures since it determines growth direction of dendritic structures. It has been understood and/or supposed, in general, that the preferred growth direction is exclusively determined by type of crystal structure. For instance, as the preferred growth direction in cubic crystals such as fcc and bcc is  $\langle 100 \rangle$ . In recent years, however, it was revealed that the preferred growth direction of fcc alloy (Al-Zn binary alloy) changes from  $\langle 100 \rangle$  to  $\langle 110 \rangle$  by increasing concentration of the solute element.[1] The preferred growth direction of crystal is entirely determined by anisotropy of solid-liquid interfacial energy. The anisotropy of interfacial energy is described by two kinds of anisotropy strength,  $e_1$  and  $e_2$  that characterize  $\langle 100 \rangle$  growth and  $\langle 110 \rangle$  growth, respectively. The transition of preferred growth direction with alloy concentration indicates that  $e_1$  and  $e_2$  depend on the alloy concentration.[1] It is very important to understand the dependence of size and morphology of solidification microstructure on these parameters. However, details of morphological change and dependence on solidification conditions and alloy systems have not been clarified yet. Therefore, in this study, we investigated the morphological change of the isothermally- and directionally-solidified dendritic structures associated with transition phenomenon of the preferred growth direction. In this study, the simulation of isothermal and directional solidification in fcc binary alloys was conducted by using quantitative phase-field model[2] which can predict solidification structure with high accuracy. And the morphological change was investigated by changing  $e_1$  and  $e_2$  systematically. Effects of several parameters such as supersaturation, cooling rate, temperature gradient and alloy system, on the morphology were also investigated. [1] T. Haxhimali, A. Karma, F. Gonzales, and M. Rappaz, Nat. Mater., 5(2006), 660 [2] M. Ohno and K. Matsuura, Phys. Rev. E 79, 031603(2009).

## Crack Self-healing During the Relaxation

Hokun Kim\*, Sung Youb Kim\*\*

\*UNIST, \*\*UNIST

### ABSTRACT

Unexpected behaviors of materials are critical for designing the structures which can lead to undesirable results. Hence, it is important to understand the behaviors of materials. However, the mechanical responses of nanomaterials are different from those of bulk counterparts causing unexpected behavior. For examples, nanomaterial becomes flaw insensitive under the critical size [1], small enough nanowire undergoes a phase transformation [2], and the surface stress affects the instability of nanomaterials [3]. Therefore, identifying the unique behavior of nanomaterial is significant for nanotechnology. Using molecular dynamics simulations with embedded atom method (EAM), we observed that cracks are self-healed during the relaxation of surfaces. Crack surfaces are closed (re-bonded) without any external force applied, leaving crack tip as a dislocation. Centered and edged cracks were investigated with different sizes and aspect ratios with various materials that have different amount of surface properties. Other unexpected behaviors of nanoscale cracks are discussed specially emphasized on the effect of surface relaxation. 1. Gao, H., Ji, B., Jager, I. L., Arzt, E. & Fratzl, P. Materials become insensitive to flaws at nanoscale: lessons from nature. *Proc. Natl. Acad. Sci. U. S. A.* 100, 5597–5600 (2003). 2. Diao, J., Gall, K. & Dunn, M. L. Surface-stress-induced phase transformation in metal nanowires. *Nat. Mater.* 2, 656–660 (2003). 3. Ho, D. T., Park, S.-D., Kwon, S.-Y., Park, K. & Kim, S. Y. Negative Poisson's ratios in metal nanoplates. *Nat. Commun.* 5, 3255 (2014).

## Level-set Based Shape Optimization Using Polyhedral Elements

Hyun-Gyu Kim\*, Son Nguyen-Hoang\*\*

\*Seoul National University of Science and Technology, \*\*Seoul National University of Science and Technology

### ABSTRACT

In the level-set based shape optimization, the structural boundary is implicitly represented by the zero-level set of an level set function and a velocity field is computed based on a shape sensitivity analysis to iteratively update the new shape of the structures by mathematically solving the Hamilton-Jacobi equation. Most of level-set based shape optimization methods utilize a fixed regular mesh for both of the level set function evolution process and the structural domain analyses. Due to the inexactitude of a mesh for the structural model, the finite element method cannot be implemented directly for the structural analyses. In this study, the evolution of geometric shapes based on level-set based shape optimization is obtained by cutting a background hexahedral mesh. The zero isosurface of a level set function split a background hexahedral mesh. Polyhedral elements are generated at the boundaries of the split domains by the marching cube algorithm. The trimmed hexahedral meshes are partitioned into an interior domain with negative level set values and an exterior domain with positive level set values. In the level-set based shape optimization using trimmed hexahedral meshes, polyhedral elements at their boundaries play an important role for capturing the structural domain. We recently proposed an efficient scheme for constructing shape functions on polyhedral domains with non-planar faces by using MLS approximation. The polyhedral shape functions satisfy the required properties of conventional finite element method such as continuity within elements, partition of unity, linear completeness, inter-element compatibility and the Kronecker-delta property. The trimmed hexahedral meshes can provide an efficient and effective tool for level-set based shape optimization problems.

## Finding Nearest Helpers for Cardiopulmonary Resuscitation Using Defibrillators

Jaewon Kim\*, Dongsoo Han\*\*

\*KAIST, \*\*KAIST

### ABSTRACT

If patients in heart attack are fell down and unable to move by themselves, they should be rescued in a hurry. The brains of the heart-attacked patients are damaged unless appropriate action is taken within 5 minutes. To help the fast rescue activity, hundreds of thousands of defibrillators have been deployed in many places these days. Nevertheless, taking first-aid measures for cardiopulmonary resuscitation for heart-attacked patients within 5 minutes is not a simple task. This paper proposes a technique to rescue heart-attacked patient using nearby defibrillators. This paper assumes that a heart-attacked patient asks a rescue service to a remote service center which is located far away from the patient. The patient usually loses consciousness immediately after the rescue request. Then the remote service center has to identify nearby people or rescue service members to help the hear-attacked patient. First, it estimates the patient's location and requests nearby special purpose access points (APs) to capture probing signals from smartphones. Then a server fetches the captured probing signals and identifies devices with the probing signals. The server determines a person who can rescue the patient and sends a message to help the patient. An experiment performed on the 7th floor, N1 building, KAIST with ten specially purpose APs. The experiment revealed that the scenario could be effective if the special purpose APs were properly installed in a service area.

## **Stress Based Creep Life Evaluation of Super304H Using Small Punch Creep Test**

Jeong Hwan Kim<sup>\*</sup>, Uijeong Ro<sup>\*\*</sup>, Moon ki Kim<sup>\*\*\*</sup>

<sup>\*</sup>sungkyunkwan university, <sup>\*\*</sup>sungkyunkwan university, <sup>\*\*\*</sup>sungkyunkwan university

### **ABSTRACT**

Ultra-supercritical power plant operating at high pressure and high temperature has advantage of high-efficiency. The super-heater and the re-heater must endure such harsh operating conditions. Metals exposed to high temperature usually fail by creep. Therefore, it is important to understand the creep to design a safe power plant. Creep phenomenon shows a plastic deformation of material in time even when it is subjected to a low stress below macroscopic yield stress. The conventional uniaxial creep test was mainly used to evaluate the creep life of the material. However, it has shortcomings that a specimen cannot be taken from a plant in-service without damage. And also, it usually takes a long test time. Small punch creep test overcomes these shortcomings by using a small sheet of specimen which is 1/200 in size compared with uniaxial creep test specimens. For this reason, the specimen can be sampled from an in-service power plant. Also, it consumes relatively less time than the uniaxial creep test. However, it was neglected in the industrial field because it is difficult to evaluate the creep life using small punch creep test than uniaxial creep test. This is because conventional life evaluation method of small punch creep test must be preceded by uniaxial creep test. Considering the aforementioned advantages, a creep life evaluation method using only small punch creep test is needed in order to reduce cost and time. In this study, a creep life evaluation method of small punch creep test was proposed. Stress based creep life evaluation method can evaluate creep life only using small punch creep test result without uniaxial creep test. Super304H which is one of the main material of ultra-supercritical power plant was used as the test specimen. And small punch creep test was performed at 650 degrees of Celsius. Finally, the suggested method is verified through Larson-Miller model.

## **Modeling of 3D Printed Carbon Nanotube-Thermoplastic Polyurethane Composites for Piezoresistive Pressure Sensors**

Ji Hoon Kim<sup>\*</sup>, Jaebong Jung<sup>\*\*</sup>, Myoung-Seok Kim<sup>\*\*\*</sup>, Dae-Hyeong Kim<sup>\*\*\*\*</sup>

<sup>\*</sup>Pusan National University, <sup>\*\*</sup>Pusan National University, <sup>\*\*\*</sup>Pusan National University, <sup>\*\*\*\*</sup>Seoul National University

### **ABSTRACT**

In order to design flexible pressure sensors with high sensitivity, a multi-physics computational model for piezoresistivity was developed. The anisotropic change of piezoresistivity upon deformation was analyzed experimentally and numerically using a 3D resistive network model. Then a phenomenological piezoresistivity model was developed to represent the piezoresistive behavior of conductive polymer composites. Carbon nanotube-thermoplastic polyurethane (CNT-TPU) composites were produced using 3D printing and used for validation of the proposed model. The effect of processing conditions and heat treatment on sensitivity was analyzed.

## Correlation Between Microstructural Characteristics and Properties of Cement Paste with Variable Void Distributions

Ji-Su Kim\*, Tong-Seok Han\*\*

\*Yonsei University, \*\*Yonsei University

### ABSTRACT

Concrete is composed of void and solid phase with hydration products [1]. Porous material generally has a material response related to its porosity. For instance, the strength of concrete is well known for being proportional to cube of gel-space ratio (e.g., Powers' model). Microstructural characteristics of cement paste include connectivity and continuity of voids as well as the porosity, and the continuity of voids has a relation to the response of materials. In this study, the material properties are described as a function of porosity and void distribution of cement paste. The correlation between microstructural characteristics and material properties is investigated using cement paste specimens with various water/cement ratio. To prepare the specimens, five water cement ratios (w/c) of cement paste are designed as 0.3, 0.4, 0.5, 0.6, and 0.7. Each specimen has a different microstructural characteristic, e.g., porosity and void continuity. In order to characterize the microstructure of the material, micro-CT images are taken and binarized into voids and solid phases [2]. A three-dimensional finite element model is generated from CT images, and a lineal-path function is used to characterize the void continuity among low-order probability functions [3]. The area of the lineal-path function is used as a quantified parameter of the void continuity. The material properties of cement paste are evaluated for strength and stiffness through compression test and nanoindentation. The crack phase field model with input parameters obtained from the experiments is performed. From this study, the relations between microstructural characteristics and material responses of cement paste are suggested in a simple functional form. [1] Mindess, S., Young, J. F., & Darwin, D. (2003). Concrete. Prentice Hall. [2] Chung, S. Y., Han, T. S., & Kim, S. Y. (2015). Reconstruction and evaluation of the air permeability of a cement paste specimen with a void distribution gradient using CT images and numerical methods. Construction and Building Materials, 87, 45-53. [3] Torquato, S. (2013). Random heterogeneous materials: microstructure and macroscopic properties (Vol. 16). Springer Science & Business Media.

## **Design of a Honeycomb Panel for Protection of a Steel Columns Subjected to Vehicle Collision**

Jinkoo Kim\*, Hyungoo Kang\*\*

\*Sungkyunkwan University, \*\*Sungkyunkwan University

### **ABSTRACT**

**ABSTRACT** This study investigates the performance of aluminum honeycomb panels attached to the face of a steel column for reducing local damage caused by automobile collision. A method for estimating the dynamic plateau stress of honeycomb was proposed based on mass and velocity of the vehicle. In addition, the stress-strain histories were linearized to easily estimate the amount of energy absorbable by the honeycomb structure. To verify the impact energy absorption capability of the honeycomb panel designed with the proposed method, a vehicle collision analysis was carried out using an 8-ton truck. According to the analysis results, the honeycomb panel could be effective in decreasing the displacement of the structure due to vehicle collision. It was also shown that the energy absorption capacity of the honeycomb panel estimated by the proposed method was found to be quite similar to the value obtained from the collision analysis. Key words : Vehicle impact, FE analysis, Honeycomb panel  
**Acknowledgement** This research was supported by Basic Science Research Program through the National Research Foundation of Korea(NRF) funded by the Ministry of Education(NRF-2016R1D1A1B03932880)

## Free Vibration of Thin-Walled Beams with Discontinuously Varying Cross-Sections

Jun-Sik Kim<sup>\*</sup>, Gijun Lee<sup>\*\*</sup>

<sup>\*</sup>Kumoh National Institute of Technology, <sup>\*\*</sup>Kumoh National Institute of Technology

### ABSTRACT

We investigate the frequency variation due to the interface in thin-walled beams. In order to properly consider the interface effect, we calculate the warping functions of the interface by employing the constrained cross-sectional eigenvalue analysis. The formulation starts with an asymptotic formulation which is applied to the Koiter-Sanders' shell theory built upon the general tensor-based coordinate system. One-dimensional finite element analysis for the cross-section of thin-walled beams is set up first, and then it is extended to the interface between two different cross-sections. The formulation takes the form of an eigenvalue problem with Lagrange's multipliers that are used to enforce the displacement continuity, rigid-body constraint, and orthogonality conditions to the fundamental warping functions. The results obtained will be compared to those of commercial software and will be discussed in terms of the importance of interface warping functions.

## Numerical Simulation of Butt-welding Considering Metallic Phase Transformation

Kyu Won Kim<sup>\*</sup>, Moon Kyum Kim<sup>\*\*</sup>, Woo Yeon Cho<sup>\*\*\*</sup>

<sup>\*</sup>Yonsei University, <sup>\*\*</sup>Yonsei University, <sup>\*\*\*</sup>POSCO

### ABSTRACT

Residual stresses may occur the deterioration of steel structure, buckling strength and fatigue strength, and these may cause damage to the integrity of the structure. In addition, tensile residual stress occurred at the centerline of the welding part increases the crack propagation force and decreases the resistance of the structure to brittle failure. It greatly affects the fracture behavior of the welded structure. Therefore, the prediction and the evaluation of the residual strain and residual stress due to the welding are very important for the quality and life prediction of the steel structure. The distribution of residual stresses due to welding was affected by various factors such as welding parameters, types, sequence, component type, component materials and component size. The temperature variation of metallic material in the welding process causes a phase transformation of the metal. The martensitic transformation such as volumetric changes of austenitic and martensitic that caused by rapid cooling to room temperature causes significant volume changes and yield stress changes. This paper presents a coupled three-dimensional (3-D) thermal-mechanical finite element analysis to simulate residual stresses due to butt welding considering metallic phase transformation. The heat of the welding arc is modeled by a body heat flux with a double ellipsoidal distribution proposed by Goldak and Akhlagi (2012), and the moving heat source is implemented by the ABAQUS subroutine DFLUX model. In the numerical model, phase transformation plasticity is also taken into account.

## Universal Meshes for Domains with Piecewise C2-regular Boundaries

Kyuwon Kim<sup>\*</sup>, Adrian Lew<sup>\*\*</sup>

<sup>\*</sup>Stanford University, <sup>\*\*</sup>Stanford University

### ABSTRACT

The idea of a universal mesh is that a background mesh can be used to achieve conforming meshes for a family of domains, which allows it to be applicable for domains with evolving boundaries. Rangarajan introduced an algorithm to achieve conforming meshes for domains with C2-regular boundaries under certain conditions, but its application on domains with more general boundaries, such as with corners, has not been studied yet. One necessary condition to achieve a valid mesh is that the projection of positive edges onto the boundary must be guaranteed to be a homeomorphism. We introduce an algorithm to select positive edges for domains with piecewise C2-regular boundaries in a manner that their projection is a homeomorphism. We introduce a theorem which assures that the projection of positive edges is sure a homeomorphism, when certain restrictions are given on the mesh. In our approach, we use the closest point projection and focus on how to choose an appropriate set of positive edges. Instead of selecting positive edges for the whole curve, the boundary is divided into a finite number of C2-continuous curves and treated separately. The positive side and positive edges are chosen individually for each curve to guarantee the projection to be a homeomorphism. Given the local maximum curvature of the curve and the maximum angle of the mesh, we also introduce an upper bound for the meshsize to guarantee the algorithm to work for domains with piecewise C2-regular boundaries.

## Development of Particle Growth Model in a Taylor-Couette Crystallizer Using Immersed Boundary Method

Moon Ki Kim\*, Tae-Rin Lee\*\*, Jang Gyun Lim\*\*\*

\*SAINT, School of Mechanical Engineering, Sungkyunkwan Univ., Republic of Korea, \*\*Advanced Institutes of Convergence Technology, Seoul nat. Univ., Republic of Korea, \*\*\*SKKU Advanced Institute of Nano Technology (SAINT), Sungkyunkwan Univ., Republic of Korea

### ABSTRACT

Lithium ion battery has led the secondary battery market. It is also expected to be widely used from portable IT devices to high capacity applications such as energy storage system and electric vehicles in the near future. To satisfy future demands, Ni<sub>1/3</sub>Co<sub>1/3</sub>Mn<sub>1/3</sub>O<sub>2</sub> (NCM) has been suggested as an alternative anode material because of its high rate of discharge/charge and stability. Electrochemical performance of NCM is determined by small size with a narrow particle size distribution (PSD) and spherical morphology. Taylor-couette crystallizer (TCC) is a highly effective manufacturing device to prepare uniform NCM particles using Taylor vortex. However, controlling the quality of a product is still ambiguous because of a short reaction time and complex interactions between hydrodynamics and manufacturing parameters. To overcome this obstacle, computational fluid dynamics is employed based on population balance equations. The coupled numerical problem has been solved by standard method of moments, discretized population balance, Monte Carlo simulation, and quadrature method of moments. Each previous study is limited by size-independent coefficients, a lot of class requirement, difficulty in applying to a real reactor, and a monotonous PSD. In this paper, a new numerical approach for agglomeration/deagglomeration is introduced to predict the change of PSD with an individual particle in TCC. Firstly, based on immersed boundary method, a unit cell is prepared as a Taylor vortex to implement core mechanisms for particle growth. In the unit cell, each particle is transported by Brownian motion or shear flow resulting in collisions. Then, the state of each particle is determined by collision efficiency [1], maximum agglomerates diameter [2], and breakage potential function for the next increment. These coefficients are updated by taking into account hydrodynamic and particle characteristics. After that, multiple cases of average particle size are tried to predict final average size and PSD. As a result, the average particle size and PSD is obtained for various input cases. A growth rate induced by the change of average size indicates whether the dominant phenomenon of the system is agglomeration or deagglomeration. A positive value of the growth rate implies an increase of average particle size and vice versa. By finding the size with a growth rate of zero, the final particle size is predicted. This prediction result shows a good agreement with the experimental data. 1. Balakin B. et al., Chem. Eng. Sci. 68, 305, (2012). 2. Kim, J. M. et al., W.S., Colloid. and Surf. 385, 31, (2011).

## Statistical model calibration for multivariate responses of piezoelectric energy harvester

Saekyeol Kim<sup>\*</sup>, Tae Hee Lee<sup>\*\*</sup>, Tae Hyun Sung<sup>\*\*\*</sup>, Yewon Song<sup>\*\*\*\*</sup>, Jihoon Kim<sup>\*\*\*\*\*</sup>, Taehyeok Choi<sup>\*\*\*\*\*</sup>

<sup>\*</sup>Hanyang University, Seoul, Korea, <sup>\*\*</sup>Hanyang University, Seoul, Korea, <sup>\*\*\*</sup>Hanyang University, Seoul, Korea, <sup>\*\*\*\*</sup>Hanyang University, Seoul, Korea, <sup>\*\*\*\*\*</sup>Hanyang University, Seoul, Korea

### ABSTRACT

The use of computational model for predicting the performance of engineering products has been largely increased due to the fast growth in computing power. The accuracy of computational results from high-fidelity model is now a great concern for engineers. In order to improve the accuracy of computational models, uncertainty in various material properties has to be considered. To address such issues, statistical model calibration has been developed[1], which increases the predictive capability of computational models by identifying and determining the uncertainty of material properties based on the results from both the experiments and the computational models. This method, has been recently employed to improve the high-fidelity electromechanical model of piezoelectric energy harvester[2]. To the best of our knowledge, however, the multivariate responses in the statistical model calibration has never been considered, which can be an important factor to improve the accuracy of the computational model. This paper proposes a statistical model calibration method, which considers multivariate responses of piezoelectric energy harvester: natural frequency and output voltage. The proposed method is used to perform a probabilistic design of piezoelectric energy harvester and the results are compared with the results from the previous statistical model calibration.

## **Construction of ITZ Specimens with Functionally Graded Microstructure by Extended Stochastic Optimization and Evaluation of its Properties**

Se-Yun Kim\*, Tong-Seok Han\*\*

\*Yonsei University, \*\*Yonsei University

### **ABSTRACT**

Concrete can be divided into three phases which are aggregates, bulk cement paste and interfacial transition zone (ITZ). The ITZ is located between the aggregates and the bulk cement paste. The void phase of the ITZ has a gradient distribution depending on the distance away from the aggregate, which means the ITZ is not only a functionally graded material but also a critical section to determine properties of concrete. However, information on the ITZ microstructure is difficult to obtain compared with bulk cement paste microstructure. In this study, three kinds of the bulk cement paste are used to construct virtual ITZ specimens. The low-order probability functions are used to quantify the characteristics of the void distributions over the bulk cement paste specimens in three orthogonal directions [1]. The characteristic of the microstructure is subdivided into clustering, continuity and connectivity of void clusters, and all of the characteristics are used as resources to construct the virtual ITZ specimens using a stochastic optimization. The stochastic optimization is extended to incorporate the information of the void gradient, and the iteration process in the stochastic optimization is modified to minimize the computational resources. Using the microstructures reconstructed from the extended stochastic optimization method, the properties of the ITZ in concrete can be evaluated a virtual loading tool, e.g., a finite element method. The evaluated elastic modulus, heat conductivity and permeability in three orthogonal directions show the anisotropy of the ITZ and a good correlation between the properties and the void distribution gradient. [1] Torquato, S. (2013). Random heterogeneous materials: microstructure and macroscopic properties (Vol. 16). Springer Science & Business Media.

## Towards an Integrated Model Reduction Algorithm of Component Mode Synthesis

Soo Min Kim<sup>\*</sup>, In Seob Chung<sup>\*\*</sup>, Jin-Gyun Kim<sup>\*\*\*</sup>, K. C. Park<sup>\*\*\*\*</sup>, Soo-Won Chae<sup>\*\*\*\*\*</sup>

<sup>\*</sup>Department of Mechanical Engineering, Korea University, <sup>\*\*</sup>Department of Mechanical Engineering, Korea University, <sup>\*\*\*</sup>Mechanical Systems Safety Research Division, Korea Institute of Machinery and Materials, <sup>\*\*\*\*</sup>Department of Aerospace Engineering Sciences and Center for Aerospace Structures, University of Colorado, <sup>\*\*\*\*\*</sup>Department of Mechanical Engineering, Korea University

### ABSTRACT

In the computational approach, efficiency and accuracy are the main aims of reduced-order modeling (ROM). Numerous techniques have been studied for the last several decades, but those are still main issues. Based on the motivation, we here suggest an integrated model reduction algorithm of Craig-Bampton (CB) component mode synthesis (CMS) method [1], which is one of the widely used ROM techniques in structural dynamics society. The proposed algorithm consists of three phases: important mode selection, CB based model reduction and a posteriori error estimation. In this work, we use a priori mode selection scheme [2], which was recently developed to precisely rank dominant substructural modes. The mode selection scheme was derived by using a moment-matching approach and a consistent perturbation expansion [2]. To evaluate the accuracy of a reduced model, a posteriori error estimator recently developed by Kim et al. is also employed, which can accurately predict relative eigenvalue errors of a reduced model without any information of reference eigenvalues [3]. Combining the techniques, we propose an integrated model reduction algorithm, and demonstrate its feasibility through several numerical examples. [1]. Craig, R., &&&& Bampton, M. (1968). Coupling of substructures for dynamic analyses. AIAA journal, 6(7), 1313-1319. [2]. Kim, S. M., Kim, J. G., Park, K. C., &&&& Chae, S. W. (2018). A component mode selection method based on a consistent perturbation expansion of interface displacement. Computer Methods in Applied Mechanics and Engineering. 330, 578-597 [3]. Kim, J. G., Lee, K. H., &&&& Lee, P. S. (2014). Estimating relative eigenvalue errors in the Craig-Bampton method. Computers &&&& Structures, 139, 54-64.

## **Drag Effect on the Motions of Dislocations and Grain Boundaries in Nanoscale**

Soon Kim<sup>\*</sup>, Jaehyung Hong<sup>\*\*</sup>, Sung Youb Kim<sup>\*\*\*</sup>

<sup>\*</sup>Ulsan National Institute of Science and Technology, <sup>\*\*</sup>Ulsan National Institute of Science and Technology,  
<sup>\*\*\*</sup>Ulsan National Institute of Science and Technology

### **ABSTRACT**

It is well known that plastic behaviors of materials are governed by collective motion of dislocations and interactions of them with other defects. A mobility and reaction properties of the dislocation are decided by its core structure. The core makes the dislocation have nonlinear properties, which cannot be explained by classical linear elasticity theory. Furthermore, it has been reported that the core induces unexpected behaviors in nanoscale [1]. To understand the fundamentals of material plasticity, thus, it is necessary to characterize behaviors of the dislocation core by priority. Especially, in case of metallic materials, the motion of dislocations is significantly disturbed by grain boundaries, and their interactions increase ductility of the materials. In a sense that most metals used in industry are polycrystalline, the influence of grain boundaries on material plasticity must be emphasized. Despite of the importance of the grain boundaries, however, the researches of the grain boundary have been focused on phenomenological approaches rather than systematic analysis due to difficulty caused by large degree of freedom to define the grain boundaries. In this work, we employ both atomistic simulation and theoretical approach to describe motion of various low angle grain boundaries by expanding dislocation theory in nanoscale. Firstly, we observed unusual behavior that externally applied stress is reduced inside of nanoscale materials while single dislocation is in motion, which is defined stress-drop behavior [1]. By developing simple analytic equation based on discrete lattice dynamics theory, we can explain this unusual behavior. Furthermore, we also observed that the stress-drop behavior appears during motion of the grain boundaries under external stress. Unlike single dislocation, however, not only the stress-drop but also curvature of grain boundaries were observed during their motions. And our result proves that the curvature is maintained by phonon drag induced by scattering of external loading and interaction between dislocations which consist the grain boundary during its motion.

## Comparison between Various Approximations for Free Energy Calculation in Partitioned-Domain Methods

Woo Kyun Kim\*, Ellad Tadmor\*\*

\*University of Cincinnati, \*\*University of Minnesota

### ABSTRACT

Partitioned-domain methods are multiscale approaches that divide a system into an atomistic region where full-atomistic resolution is retained, and a continuum region represented by a coarse-grained finite element model with local constitutive relations. At finite temperature, the constitutive relation corresponds to the Helmholtz free energy of a strained infinite crystal. This study examines several approximation methods for free energy calculations used in variations of the quasicontinuum (QC) method: (1) The quasi-harmonic (QH) approximation in which the potential energy is expanded to second order and the free energy is integrated analytically; (2) the local-Harmonic (LH) approximation, which is similar to QH but with off-diagonal terms in the Hessian matrix neglected; (3) the maximum entropy (max-ent) formalism based on ideas from information theory. To test the accuracy of these methods, all three have been implemented within a single framework. The results for various problems including thermal expansion, simple shear, and a Lomer dislocation dipole will be presented. In addition, the effect of "ghost forces" (numerical artifacts appearing at the continuum-atomistic interface) in a hot-QC simulation is investigated. For static QC, ghost forces can be addressed using a dead-load correction. The effectiveness of this approach in hot-QC is tested.

## Multiscale Indentation and Bending Simulations of Mono-layered Graphene in Elastic Regime

Yongwoo Kim<sup>\*</sup>, Keonwook Kang<sup>\*\*</sup>

<sup>\*</sup>Department of Mechanical Engineering, Yonsei University, Republic of Korea, <sup>\*\*</sup>Department of Mechanical Engineering, Yonsei University, Republic of Korea

### ABSTRACT

In this study, we investigated mechanical behaviors of mono-layered graphene under indentation [1] and bending using molecular statics (MS) simulations and finite element analysis (FEA). We tested circular graphene sheet with the Adaptive Intermolecular Reactive Empirical Bond Order potential (AIREBO) [2]. Changing thickness of graphene in FEA, the force-indentation depth curve was compared with that in MS. And we found an effective thickness where both results match in elastic regime. Additionally, deflection curve and induced Cauchy stress in graphene sheet were compared, too. Presented results demonstrate that the proposed method could provide a valuable tool for studying the mechanical behavior of mono-layered graphene sheet using FEA. [1] Lee, C., Wei, X., Kysar, J. W., & Hone, J. (2008). Measurement of the elastic properties and intrinsic strength of monolayer graphene. *science*, 321(5887), 385-388. [2] Stuart, S. J., Tutein, A. B., & Harrison, J. A. (2000). A reactive potential for hydrocarbons with intermolecular interactions. *The Journal of chemical physics*, 112(14), 6472-6486.

## **Rigid-body Mechanism Synthesis by SBM (Spring-connected Rigid Block Model) Based Topology Optimization**

Yoon Young Kim\*, Seok Won Kang\*\*

\*Department of Mechanical and Aerospace Engineering, Seoul National University, \*\*Department of Mechanical and Aerospace Engineering, Seoul National University

### **ABSTRACT**

In spite of great success of the topology optimization in designing load-carrying structures, its use in synthesizing motion-generating rigid-body mechanisms is less active. There are several issues to be resolved to advance the topology optimization based mechanism synthesis, but in this presentation, we will be focused mainly on the ground modeling issue. Especially for numerically efficient gradient-based topology optimization based synthesis, there are two ground models available, the revolute joint-connected link model and the zero-length spring-connected rigid block model (SBM). Unlike the link ground model only allowing revolute joints, we will show that the SBM developed in [1,2] allows the presentation of revolute, prismatic, and other types of joints when the spring stiffness takes on its upper or lower bound value. Because the stiffness can be interpolated as a function of a real design variable, the use of a gradient-based optimizer is readily possible. After the underlying concept of the SBM suitable to represent only revolute joints, an alternative model method called, the double-spring connected rigid block model (D-SBM) will be presented in order to represent general joints. Also, a method to deal with revolute and prismatic joints only is presented and its successful application in the design of a robotic rehabilitation device by the SBM-based topology optimization method will be presented. [1] Y.Y. Kim, G.W. Jang, J.H. Park, J.S. Hyun, S.J. Nam, Automatic synthesis of a planar linkage mechanism with revolute joints by using spring-connected rigid block models, *J. Mech. Des.* 129 (2007) 930–940. [2] S.W. Kang, S. I. Kim, Y. Y. Kim, Topology optimization of planar linkage systems involving general joint types, *Mechanism and Machine Theory* 104 (2016) 130-160.

## **Extended Analytic Model of Staggered Platelet Structure and Its Application to 3D Printing Technology**

Youngsoo Kim\*, Seunghwa Ryu\*\*

\*Department of Mechanical Engineering, Korea Advanced Institute of Science and Technology (KAIST),

\*\*Department of Mechanical Engineering, Korea Advanced Institute of Science and Technology (KAIST)

### **ABSTRACT**

There have been many studies to understand and utilize the superior mechanical properties of nacre with moderate stiffness and high toughness. The load transfer mechanism in the unique 'brick and mortar' structure of the nacre has been intensively analyzed and its structural features has been mimicked by various manufacturing methods such as 3D printing. However, due to the limited applicability of most analytical models and the limitation in the 3D printers, it has been difficult to theoretically predict and design the propertyed 3D printed structures. In this study, we improve the analytic models to predict the effective elastic properties of the 'brick and mortar' structure for a wide range of constituent materials and geometric ratios by correctly accounting volume (Area for 2D) average concept. In addition, we also reveal the effect of the printing direction and thickness on the 3D printed composite materials. We show that our extended analytic model accurately predict the properties of 3D printed composite when using the manufacturing-condition-dependent material properties as input. Furthermore, we suggest a new possible design to increase the toughness of composites. Our studies reveals the origin of discrepancy between theory and 3D printed structures and enable a rational design of nacre-inspired structures.

## **Strain-rate Dependent Microplane Constitutive Model for Dynamic Fracturing and Comminution of Concrete during Projectile Impact**

Kedar Kirane\*, Zdenek Bazant\*\*

\*Stony Brook University, \*\*Northwestern University

### **ABSTRACT**

While numerous studies have dealt with dynamic crack propagation in concrete, they have not led to a macroscopic continuum model usable in FE analysis. Such a model was recently developed and is presented here. The model is based on the recently developed theory of comminution according to which comminution of concrete under high-rate impact loading is driven by the release of the local kinetic energy (rather than the strain energy) of the shear strain rate field. This theory yields expressions to calculate the particle size and the additional kinetic energy density that must be dissipated in finite-element codes. In previous research, it was dissipated by additional viscosity, in a model partly analogous to turbulence theory. Here it is dissipated by scaling up the material strength. Microplane model M7 is used and its stress-strain boundaries are scaled up by factors proportional to the  $2/3$  power of the effective deviatoric strain rate and its time derivative. The crack band model with a random tetrahedral mesh is used and all the artificial damping is eliminated. The scaled M7 model is seen to predict correctly the crater shapes and exit velocities of projectiles penetrating concrete walls of different thicknesses. The choice of the finite strain threshold for element deletion criterion, which can have a big effect, is also studied.

## Efficient Simplicial Finite Elements Via Bernstein Polynomials

Robert Kirby\*

\*Baylor University

### ABSTRACT

The mathematical power offered by high-order finite element methods is all-too often realized at a high computational cost, especially on simplicial meshes where basis functions lack tensor product structure. However, recent work on Bernstein polynomials has led to efficient algorithms for many fundamental finite element kernels. Algorithms that evaluate load vectors and the (action of) finite element matrices with optimal complexity are now known, including for  $H(\text{div})$  and  $H(\text{curl})$  spaces. Additionally, optimal algorithms for interpolation and polynomial projection in the Bernstein basis, which are also required at various stages, can be given in terms of block-structured linear algebra. This structure depends intricately on the details of Bernstein polynomials. Finally, the nonnegativity of the Bernstein basis has been suggested as a pathway to enforce positivity for higher-order bases in transport or other applications with hard constraints. This talk will summarize the state of the art for Bernstein polynomials and include numerical examples.

## **NO<sub>x</sub> Prediction of a Natural Gas and Hydrogen Mixed-combustion-type Gas Turbine Combustor**

Ryosuke Kishine<sup>\*</sup>, Nobuyuki Oshima<sup>\*\*</sup>, Kohshi Hirano<sup>\*\*\*</sup>, Takeo Oda<sup>\*\*\*\*</sup>

<sup>\*</sup>Hokkaido University, <sup>\*\*</sup>Hokkaido University, <sup>\*\*\*</sup>Kawasaki Heavy Industries, Ltd., <sup>\*\*\*\*</sup>Kawasaki Heavy Industries, Ltd.

### **ABSTRACT**

In pursuit of a reduction in environmental loading, gas turbine combustors that use a hydrogen-enriched fuel instead of pure natural gas have entered practical service. In such a new attempt, numerical simulation is very effective for more efficient development because it can easily perform parametric studies. In our previous study [1], a numerical analysis was performed on a natural gas and hydrogen mixed-combustion-type gas turbine combustor using large-eddy simulation and a multi-scalar flamelet approach. Three conditions were analyzed with different introduction amount of hydrogen, and the tendencies of the simulation results qualitatively agreed with the knowledge in the experiments. In the current study, we aim to investigate an applicability of the numerical method for the turbulent mixed-combustion field by comparing the simulation results of NO<sub>x</sub> emission with the experimental ones as a next step. The calculation object was the combustor of an L30A-DLE gas turbine, developed by Kawasaki Heavy Industries, Ltd. This combustor has a diffusion pilot burner, a premixed main burner, as well as a premixed supplemental burner and cooling air inlets. In order to conduct a quantitative evaluation, the reproducibility of the shape for the burners and the other parts was improved compared to our previous research. The number of elements therefore increased from about 20 million to 30 million. Calculations were conducted under two different operating conditions of the same load. The design fuel ratio of the two-type premixed burners were different in each case. Because NO<sub>x</sub> is considered as a passive scalar in combustion calculations, it can be predicted separately from combustion calculation by LES. This idea about NO<sub>x</sub> prediction is very effective in decreasing the calculation cost. The simulated distributions of the NO<sub>x</sub> production rate well captured the difference between the two conditions. These results suggest that by setting the higher fuel ratio of the supplemental burner, NO<sub>x</sub> emissions are reduced along with the decrease in the high temperature region. In our presentation, we will show the quantitative comparison results of simulated values and experimental ones about NO<sub>x</sub> emissions. At the same time, we are planning to examine the validity of this NO<sub>x</sub> prediction method by comparing it with the results of the normal prediction method. [1]Kishine, R., et al., 2017, "Application of Large-eddy Simulation and the Multi-scalar Flamelet Approach to a Methane-hydrogen Mixed-combustion-type Industrial Gas-turbine Combustor," Proceedings of the ASME 2017 Power and Energy Conference, PowerEnergy2017-3247.

## **The Influence of Binder Mobility to the Viral Entry Driven by the Receptor Diffusion**

Sandra Klinge<sup>\*</sup>, Tillmann Wiegold<sup>\*\*</sup>, Gerhard A. Holzapfel<sup>\*\*\*</sup>

<sup>\*</sup>TU Dortmund University, <sup>\*\*</sup>TU Dortmund University, <sup>\*\*\*</sup>Graz University of Technology, Norwegian University of Science and Technology

### **ABSTRACT**

The current presentation deals with the simulation of the viral entry into a cell. There are two dominant mechanisms typical of this process: the endocytosis and the fusion with the cellular membrane. However, we only focus on the first scenario. To this end, we consider a virus as a substrate with a constant concentration of receptors on the surface. Differently, the concentration of receptors of the host cell varies and these receptors are free to move over the membrane. When the contact with the cell surface has been achieved, the receptors start to diffuse to the contact (adhesion) zone. The membrane in this zone inflects and forms an envelope around the surface of the virus. This is the way the newly formed vesicle imports its cargo into the cell. In order to simulate the process described, we assume that the differential equation typical of the heat transport is suitable to simulate the diffusion of receptors. Additionally, we formulate two boundary conditions: First, we consider the balance of fluxes on the front of the adhesion zone. Here, it is supposed that the velocity is proportional to the gradient of the chemical potential. The second subsidiary condition is the energy balance equation depending on four different contributions: the energy of binding receptors, the free energy of the membrane, the energy due to the curvature of the membrane and the kinetic energy due to the motion of the front. The differential equation itself along with two boundary conditions forms a well-posed problem which can be solved by applying a direct method, for example the finite difference method. The talk also includes numerical examples showing the distribution of receptors over the membrane as well as the motion of the front of the adhesion surface. In particular, the influence of the mobility of receptors has been studied.

## **A Computational Framework for Scale-bridging in Multiscale Simulations and Its Applications to Modeling of Energetic Materials**

Jaroslav Knap<sup>\*</sup>, Kenneth W. Leiter<sup>\*\*</sup>, Richard Becker<sup>\*\*\*</sup>, Brian C. Barnes<sup>\*\*\*\*</sup>

<sup>\*</sup>U.S. Army Research laboratory, <sup>\*\*</sup>U.S. Army Research laboratory, <sup>\*\*\*</sup>U.S. Army Research laboratory, <sup>\*\*\*\*</sup>U.S. Army Research laboratory

### **ABSTRACT**

Over the last few decades, multiscale modeling has become a dominant paradigm in materials modeling and simulation. The practical impact of multiscale modeling depends, to a great extent, on its ability to utilize modern large-scale computing platforms. However, since there are no general numerical and computational frameworks for multiscale modeling, the vast majority of multiscale material models or simulations are developed on a case-by-case basis. We seek to formulate an adaptive computational framework for multiscale modeling. We do not intend to develop a specific method for multiscale simulations, but instead, aim to develop a broad and flexible computational framework for designing and developing such simulations. Our focus is primarily on new scalable numerical algorithms applicable to a wide range of multiscale modeling applications and, more specifically, to scale-bridging. These algorithms fall into one of the three areas: i) adaptive computational strategies for multiscale modeling, ii) algorithms for scale-bridging in multiscale modeling, and iii) algorithms for development of surrogate models to reduce the computational cost associated with multiscale models. We present a formulation of our computational framework and describe our progress towards development of a two-scale model of an energetic material utilizing it.

## **Modeling Intragranular Misorientation, Grain Fragmentation, and Associated Effects on Mechanical Fields and Texture Evolution in Polycrystals Using the Viscoplastic Self-Consistent Framework**

Marko Knezevic<sup>\*</sup>, Rodney McCabe<sup>\*\*</sup>, Miroslav Zecevic<sup>\*\*\*</sup>, Ricardo Lebensohn<sup>\*\*\*\*</sup>

<sup>\*</sup>University of New Hampshire, <sup>\*\*</sup>Los Alamos National Laboratory, <sup>\*\*\*</sup>University of New Hampshire, <sup>\*\*\*\*</sup>Los Alamos National Laboratory

### **ABSTRACT**

In recent works, we reported the methodology to calculate intragranular fluctuations of the instantaneous lattice rotation rates (Lebensohn et al., 2016) and associated misorientation distributions developing inside each grain representing a polycrystalline aggregate within the mean-field viscoplastic self-consistent (VPSC) homogenization (Zecevic et al., 2017). The methodology is based on the second moment of intragranular stresses calculated by the VPSC model. This paper advances the methodology to incorporate the effect of the intragranular misorientations on stress fluctuations. Furthermore, the fluctuations of plastic spin are defined as a function of not only the stress fluctuations but also the intragranular misorientations. These advances facilitated the development of a grain fragmentation (GF) model within VPSC, which is conceived within the crystal orientation space. The overall model is termed GF-VPSC. Case studies including simple tension and plane-strain compression of face-centered cubic polycrystal deformed to large strains are used to illustrate the utility of the developed model. The predictions of intragranular misorientation distributions and texture evolution are compared with full-field calculations and experiments. Good agreement is obtained for the intragranular misorientation distributions and, as a result, more accurate modeling of texture evolution is facilitated by the new model relative to the standard VPSC. Since the developed intragranular misorientations act as driving forces for recrystallization, the novel GF-VPSC is shown to enable coupled modeling of microstructure evolution during deformation and recrystallization in a computationally efficient manner. Lebensohn, R.A., Zecevic, M., Knezevic, M., McCabe, R.J., 2016. Average intragranular misorientation trends in polycrystalline materials predicted by a viscoplastic self-consistent approach. *Acta. Mater.* 104, 228-236. Zecevic, M., Pantleon, W., Lebensohn, R.A., McCabe, R.J., Knezevic, M., 2017. Predicting intragranular misorientation distributions in polycrystalline metals using the viscoplastic self-consistent formulation. *Acta. Mater.* 140, 398-410.

## **Butterflies in Layered Media**

Nicholas Knight\*, Michael O'Neil\*\*

\*NYU-Courant, \*\*NYU-Courant

### **ABSTRACT**

We present an algorithm for electromagnetic scattering calculations in layered media by use of butterfly-accelerated Sommerfeld integrals. In the time-harmonic setting, representing electromagnetic fields by generalized Debye sources (and their Fourier transforms) along layered media interfaces efficiently decouples several unknowns, and leads to a representation whose evaluation is amenable to acceleration via a butterfly algorithm. When coupled with an iterative solver, the corresponding integral equation formulation can be efficiently solved.

## **A Shell Model with Variationally Embedded Interlaminar Stresses for the Calculation of Layered Composite Structures and Delamination Effects**

Gregor Knust<sup>\*</sup>, Friedrich Gruttmann<sup>\*\*</sup>

<sup>\*</sup>Solid Mechanics, Darmstadt University of Technology, Frankziska-Braun-Str. 7, 64287 Darmstadt, Germany,

<sup>\*\*</sup>Solid Mechanics, Darmstadt University of Technology, Frankziska-Braun-Str. 7, 64287 Darmstadt, Germany

### **ABSTRACT**

The computation of interlaminar stresses is essential for the design of layered composite structures. While solid elements are able to compute these stress states, they represent a numerically expensive approach. This work deals with layered shells subjected to static loading for prediction of interlaminar stresses. The underlying shell theory is based on the Reissner-Mindlin kinematics with an inextensible director field. Additional degrees of freedom for in-plane warping and relative displacements in thickness direction are introduced. These displacements are interpolated with layerwise cubic functions, which are constant within one element and discontinuously over its boundaries. The resulting shell element is applicable for geometrically and physically nonlinear problems. Further a multifield functional based on the Hu-Washizu functional is introduced. Here the associated Euler-Lagrange equations include the usual global shell equations in terms of stress resultants, the local equilibrium in terms of stresses, the geometric field equations and the constitutive equations. In addition the functional contains a constraint, which enforces the correct shape of the warping function through the thickness [1]. The finite element formulation is based on the isoparametric concept for four-node quadrilateral shell elements. The elimination of independent stresses, warping and Lagrange parameters on element level leads to a mixed hybrid shell element with the standard 5 or 6 degrees of freedom per node. This is a fundamental characteristic, since it is possible to use standard geometrical boundary conditions. Therefore the element can be applied to complex geometrical problems. The transverse stresses are continuous at layer boundaries for linear elastic problems. An interface to three-dimensional material laws is part of the element formulation, too [2]. This allows together with the determination of thickness normal stresses the computation of delamination effects of layered laminates. Results of several examples will be shown and compared to reference solutions. Here geometrically nonlinearity, as well as physically nonlinear material behavior is considered. In comparison to 3d models, the present shell element needs only a fractional amount of computing time. References: [1] F. Gruttmann, W. Wagner, G. Knust (2016) A Coupled Global-Local Shell Model with Continuous Interlaminar Shear Stresses. *Computational Mechanics* 57:237-255. [2] F. Gruttmann, G. Knust, and W. Wagner (2017) Theory and numerics of layered shells with variationally embedded interlaminar stresses. *Computer Methods in Applied Mechanics and Engineering* 326:713-738

## Three-dimensional Geometrical Characterization of Aneurysmal Location and Surface

Masaharu Kobayashi<sup>\*</sup>, Marie Oshima<sup>\*\*</sup>, Katsuyuki Hoshina<sup>\*\*\*</sup>, Shu Takagi<sup>\*\*\*\*</sup>, Masaaki Shojima<sup>\*\*\*\*\*</sup>

<sup>\*</sup>the Graduate School of Interdisciplinary Information Studies, The University of Tokyo, <sup>\*\*</sup>Interfaculty in Information Studies/Institute of Industrial Science, The University of Tokyo, <sup>\*\*\*</sup>Division of Vascular Surgery, Department of Surgery, Graduate School of Medicine, The University of Tokyo, <sup>\*\*\*\*</sup>Department of Mechanical Engineering, The University of Tokyo, <sup>\*\*\*\*\*</sup>Department of Neurosurgery, The University of Tokyo Hospital

### ABSTRACT

Rupture of a cerebral aneurysm often leads to a devastating event with high mortality and long term disability. In the abdominal artery, celiac trunk stenosis tends to generate multiple pancreaticoduodenal arcade aneurysms. Hemodynamic factors play an important role in aneurysmal formation, growth, and rupture. Hemodynamic simulations with patient-specific arterial geometry have been performed to calculate hemodynamic forces such as wall shear stress (WSS) and WSS gradient. The three-dimensional (3D) arterial bend can be characterized as curvature and torsion along arterial centerline. Lauric et al. [1] investigated the relationship between the curvature along internal carotid artery (ICA) with aneurysm and hemodynamic forces. On the other hand, concavity and convexity on aneurysmal surface can be characterized as Gaussian and mean curvatures. The purpose of this study is to characterize both vascular geometry of peri-aneurysmal environment and aneurysmal geometry. We have been developing an image-based 3D geometrical modeling system, V-Modeler [2], to investigate quantification of arterial morphological changes. The modeling system consists of five functions: 1) segmentation of arterial lumen; 2) extraction of arterial centerlines; 3) surface reconstruction; 4) calculation of geometric parameters; and 5) tracking of arterial geometry. The centerline and surface are represented as spline functions in order to remove influence of noise in medical images. Curvature and torsion along the centerline are calculated from the spline function. In addition, we develop a spline surface fitting method using correspondence between arterial centerline and surface. The method consists of: - Triangular spline surface representation [3] considering topological changes in arterial bifurcation and aneurysm, - Construction of 1-to-N index corresponding table between centerline and surface based on boundary representation, - Arterial surface smoothing based on triangular spline surface fitting with the corresponding table, - Calculation of Gaussian and mean curvatures based on spline surface function. The method is applied to arterial geometries extracted from medical images with pancreaticoduodenal arcade and ICA aneurysms. [1] A. Lauric et al., "Curvature effect on hemodynamic conditions at the inner bend of the carotid siphon and its relation to aneurysm formation." J Biomech. 2014 Sep 22;47(12):3018-27. [2] M. Kobayashi et al., "Development of an image-based modeling system to investigate evolutionary geometric changes of a stent graft in an abdominal aortic aneurysm," Circ. J., vol.79, no.7, pp. 1534-1541, 2015. [3] S. Harmann et al, "Triangular G1 interpolation by 4-splitting domain triangles", Computer Aided Geometric Design, Elsevier, vol. 17, pp. 731-757, 2000

## Computational Generation of High Quality Quad Layouts

Leif Kobbelt\*

\*RWTH Aachen University

### ABSTRACT

The conversion of raw geometric data (that typically comes in the form of unstructured triangle meshes) to high quality quad meshes is an important and challenging task. The complexity of the task results from the fact that quad mesh topologies are subject to global consistency requirements which cannot be dealt with by local constructions. This is why recent quad meshing techniques formulate the mesh generation process as a global optimization problem. By adding hard and soft constraints to this optimization, many desired properties such as structural simplicity, principal direction alignment, as well as injectivity can be guaranteed by construction. An even more challenging problem is the computation of quad layouts, where a coarse segmentation of the input surface into essentially rectangular patches is sought which also satisfies global consistency and shape quality requirements. While being structurally related, both problems need to be addressed by fundamentally different approaches. In my talk I will present some of these approaches and demonstrate that they can generate high quality quad meshes and quad layouts with a high degree of automation but that they also allow the user to interactively control the results by setting boundary conditions accordingly.

## **Instability Problems of Implicit FEM Solution Procedures for Fast Rotating Structures – Instability Sources and Solutions**

Markus Kober<sup>\*</sup>, Arnold Kühhorn<sup>\*\*</sup>, Akin Keskin<sup>\*\*\*</sup>

<sup>\*</sup>Brandenburg University of Technology Cottbus - Senftenberg, <sup>\*\*</sup>Brandenburg University of Technology Cottbus - Senftenberg, <sup>\*\*\*</sup>Rolls-Royce plc

### **ABSTRACT**

For the solution of dynamic FEM problems in the time domain in general two possibilities exist. The first one is to solve the equations of motion with an explicit time-integration scheme, which has the advantage of being very fast but on the other hand the time-steps have to be very small for stability reasons. The second possibility is to use an implicit time-integration scheme in combination with a Newton or Quasi-Newton algorithm, which is computationally more expensive but allows for much bigger time-steps. It is well known that implicit solution procedures tend to become instable for the simulation of elastic rotating structures [1,2]. But if the simulation time of complex real-world structures is bigger than a few milliseconds explicit time-integration is too inefficient due to the small time-steps and an implicit time-integration scheme has to be used. We will demonstrate the appearance of instabilities during the implicit FE simulation of elastic rotating structures at the example of simple academic problems. If the time-step size is small enough to consider the boundary value problem to be linear in one time-step, stability maps for the time-integration algorithm can be computed [3]. Surprisingly, the described instabilities appear although the time-integration algorithm (e.g. Newmark scheme) is unconditionally stable with respect to the stability map. With the help of a simple elastic rotating pendulum we will derive the sources of the instabilities and discuss this problem in detail. It will be shown that the Newton algorithm for the solution of the nonlinear system of equations and especially the models stiffness and the used time-step size have a direct impact to the stability. These results are then transferred to the presented FE examples and a general solution for the described problems is presented. Finally, results of the transient implicit simulation of a realistic aero-engine model, rotating at 10.000 rpm and using the derived concept for stability, are shown. References [1] D. Kuhl and M.A. Crisfield, Energy-conserving and Decaying Algorithms in Non-linear Structural Dynamics, International Journal for Numerical Methods in Engineering, 1999, 45, pp. 569-599. [2] K.J. Bathe and M.M.I. Baig, On a composite implicit time integration procedure for nonlinear dynamics, Computers and Structures, 2005, 83, pp. 2513–2524. [3] K.J. Bathe and E.L. Wilson, Stability and Accuracy Analysis of Direct Integration Methods, Earthquake Engineering and Structural Dynamics, 1973, 1, pp. 283-291.

## A Coupled FEM-SPH Approach for Investigating the Influence of a Fluid on the Vibration Behavior of an Oil Pan

Sebastian Koch<sup>\*</sup>, Sascha Duczek<sup>\*\*</sup>, Elmar Woschke<sup>\*\*\*</sup>

<sup>\*</sup>Otto-von-Guericke-University Magdeburg, <sup>\*\*</sup>Otto-von-Guericke-University Magdeburg,

<sup>\*\*\*</sup>Otto-von-Guericke-University Magdeburg

### ABSTRACT

Already in an early stage of the design process the manufacturer has to be enabled to estimate the performance of new products. Thus, the design of the first draft can be favorably adjusted in order to reach specific goals. Furthermore, expensive prototypes are only required for the final testing. The aim of this contribution is to improve a previously developed holistic simulation approach for the evaluation of the acoustic behavior. Here, a combustion engine is used as an automotive example [1]. An experimental investigation on an engine test bench shows significant differences between the measured and predicted results in the area of the oil pan. These differences can be traced back to the oil, which leads to a frequency shift and smaller amplitudes. Until now the oil was only taken into account as an additional mass. To improve the results, a particle-based approach is coupled with the Finite Element Method (FEM). For this a higher order FEM code [2] and the open source Smoothed Particle Hydrodynamic (SPH) program SPHysics are used. Initially, a co-simulation is performed and validated with typical benchmark examples. The interface region coincides with the surface of the solid structure and features FE nodes as well as the first row of SPH boundary particles. The pressure of the fluid particles is applied to the FE structure as an external load, which causes a deformation of the solid and consequently leads to displacements and velocities of the boundary particles. The coupling nodes and particles do not need to be conformal, as the required displacement and velocity values can be computed at any point in the interface by means of the shape functions. In a last step, the proposed method for the acoustical simulation of an oil pan is validated based on a 2D academic benchmark test. The influence of the fluid in the oil pan is quantified by a transient simulation and an inspection of the frequency spectrum computed by Fourier transformation of the results. For future applications more sophisticated coupling techniques are implemented to further improve the quality of the numerical simulation. [1] F. Duvigneau, S. Nitzschke, E. Woschke, U. Gabbert, "A holistic approach for the vibration and acoustic analysis of combustion engines including hydrodynamic interactions", *Archive of Applied Mechanics*, 86, (2016). [2] S. Duczek, *Higher Order Finite Elements and the Fictitious Domain Concept for Wave Propagation Analysis*, VDI-Verlag, VDI-Fortschritt-Berichte Reihe 20 Nr 458, (2014), url: <http://edoc2.bibliothek.uni-halle.de/hs/content/titleinfo/39725>.

## Multiscale Thermomechanical Analysis of Composites Containing Phase Change Materials

Kossi-Mensah Kodjo<sup>\*</sup>, Julien Yvonnet<sup>\*\*</sup>, Karam Sab<sup>\*\*\*</sup>, Mustapha Karkri<sup>\*\*\*\*</sup>

<sup>\*</sup>Université Paris-Est, Laboratoire Modélisation et Simulation Multi Échelle, MSME UMR 8208 CNRS., <sup>\*\*</sup>Université Paris-Est, Laboratoire Modélisation et Simulation Multi Échelle, MSME UMR 8208 CNRS., <sup>\*\*\*</sup>Université Paris-Est, Laboratoire Navier, CNRS UMR 8205, ENPC, IFSTTAR., <sup>\*\*\*\*</sup>Université Paris Est, Centre d'Études et de Recherche en Thermique, Environnement et Systèmes, CERTES - EA 3481.

### ABSTRACT

This work presents a concurrent multiscale method for thermomechanical properties of composite structures containing Phase Change Materials (PCM) particles at microscale. The PCM inclusions change from solid to liquid phase and lead to significant modifications of the macroscopic thermal behavior. The FE2 method [1] is extended to take into account phase change effects on the macroscale thermal heat conduction. For the mechanical behavior, a classical homogenization is performed on the same Representative Volume Element used in the FE2 procedure. The thermal behavior with phase change at microscale is strongly nonlinear and involves coupling with fluid flow in the liquid phase. An apparent heat capacity method proposed in [2] is used to model the thermal phase change in the inclusions. Thermal phase changes occur at almost constant temperature and the latent heat stored (or released) is largely higher than the energy exchanged by temperature variation. Thus, PCMs with phase change in range of room temperature have a great potential in building applications: improvement of thermal inertia of civil engineering constructions and reduction of energy consumption due to air conditioning. The method is applied to concrete including encapsulated paraffin wax. The results show that the macroscale temperature's fluctuations are smoothed as compared to concrete alone. In addition, the macroscopic temperature peaks are delayed in time. Furthermore, a comparison with a direct Finite Element analysis shows the ability of the proposed strategy to predict accurately the fully nonlinear thermal behavior of PCM based composites. Keywords: Phase Change Material, Heat conduction, Computational homogenization, Multi-scale modeling, FE2 method. References [1] F. Feyel. Multiscale FE2 elastoviscoplastic analysis of composite structures, *Computational Materials Science*, (1999) 16(1-4):344—354. [2] M. Aadmi, M. Karkri, M. E. Hammouti. Heat transfer characteristics of thermal energy storage of a composite phase change materials: Numerical and experimental investigations, *Energy*, Volume, (2014), (72):381 – 392.

## **Composite Crashworthiness Prediction for Bumper and Crush Can Assembly**

Ravi Kodwani\*, John Brink\*\*, Rogerio Nakano\*\*\*

\*Mr., \*\*Mr., \*\*\*Mr

### **ABSTRACT**

The United States Automotive Materials Partnership (USAMP) approached Altair with the goal of predicting the automotive crash behavior of composite laminates subjected to 6 different test configurations. Coupon and generic component level test data were supplied to help with the development of material models. Material characterization process and determination of failure parameters using DOE are detailed in the presentation. Final correlation was to a series of "blind" sled tests completed on a woven ply composite bumper with SMC over-molded ribs and woven ply crush cans. Altair submitted the RADIOSS predictions to USAMP and USAMP shared the test data shared after that. Apart from this prediction, presentation also discusses delamination failure criteria using macro shell models and comparison with and without them.

## System and Parameter Identification via Correlated Multifield Analysis.

Carsten Koenke<sup>\*</sup>, Long Nguyen-Tuan<sup>\*\*</sup>, Tom Lahmer<sup>\*\*\*</sup>, Volker Bettzieche<sup>\*\*\*\*</sup>

<sup>\*</sup>Institute off STructiral Mechanics, Bauhaus-Universität Weimar, <sup>\*\*</sup>Institute off STructiral Mechanics, Bauhaus-Universität Weimar, <sup>\*\*\*</sup>Institute off STructiral Mechanics, Bauhaus-Universität Weimar, <sup>\*\*\*\*</sup>Ruhrverband Essen

### ABSTRACT

System and parameter identification using methods of inverse analysis is a common problem in several engineering disciplines. In civil engineering applications the safety assessment of existing structures which often is the base for life-time predictions need system and parameter estimations for the investigated existing structures. Therefore inverse techniques are applied using sensor data from different physical fields, e.g. deformation data or temperature data. Usually only data from one physical field is used for the identification of system parameters at one time. Therewith the interaction effects between different physical fields are usually not taken into account. As an example for this interaction effects the correlation between pores, damage and cracks driven by mechanical or temperature loading and the permeability of solids can be seen. Using data from deformation measurements and superimposing this data with measurements from the hydraulic head field leads to improved identification results for the material parameters and their distribution in the domain for both fields. Inverse analysis based on correlated multifield data allows a much more robust identification of essential system parameters. The paper will present an approach in which a thermo-mechanical-hydraulic analysis will be used for the material parameter identification in masonry dam structures, i.e. to identify regions of local damage in large scale structures. Uncertainty of measured data is taken into account and leads to an information about the probability distribution of the damage zone. Issues such as correlation parameters and influence of noisy measurement data will be discussed in the presentation. The presented approach has been applied for parameter identification of existing masonry dam structures in Germany, which are in operation for already 100 years.

## The Conforming Reproducing Kernel Method for an Agile Design-to-Simulation Process

Jacob Koester\*, J.S. Chen\*\*, Michael Tupek\*\*\*, Scott Mitchell\*\*\*\*, Joe Bishop\*\*\*\*\*

\*Sandia National Laboratories and the University of California, San Diego, \*\*University of California, San Diego,  
\*\*\*Sandia National Laboratories, \*\*\*\*Sandia National Laboratories, \*\*\*\*\*Sandia National Laboratories

### ABSTRACT

Efficient model development for complex systems remains a challenge. Generating a mesh of sufficient quality for the Finite Element Method (FEM) can take months [1]. Research in agile design-to-simulation processes seeks to alleviate this bottleneck by taking on the difficult task of pairing automatic discretization techniques with numerical methods that are capable of producing satisfactory results. In this work, we present the Conforming Reproducing Kernel (CRK) numerical method. In this new approach, approximation functions are constructed using the reproducing kernel method with kernel functions created using Bernstein-Bezier splines on local geometry subdivisions. Meshfree methods, such as the Reproducing Kernel Particle Method (RKPM) [2], have an advantage over FEM as a high-quality mesh is not required. However, this flexibility in the construction of shape functions does present new challenges. Domain integration must be reformulated in order to maintain high accuracy and efficiency [3]. Concave geometries require special consideration so concavities are preserved. Material interfaces call for special attention so that weak discontinuities can be captured. Unlike traditional meshfree methods, CRK uses subdivisions to guide the construction of approximation functions. This allows CRK to better represent domain boundaries, especially nonconvex geometries. Also, the underlying reproducing kernel method gives CRK the flexibility to blend approximations over low quality subdivisions or handle non-contiguous meshes, making it compatible with automatic discretization processes that produce may produce low quality meshes. Previous work focused on developing the concept in two dimensions using  $C^1$  splines on triangulations. In this presentation, the method is extended to three dimensions and kernels are constructed using tetrahedral subdivisions. Examples utilizing the conforming kernels are shown and results are compared to predictions using FEM and RKPM. [1] M. Hardwick, R. Clay, P. Boggs, E. Walsh, A. Larzelere and A. Altshuler, DART system analysis, SAND2005-4647, Sandia National Laboratories, Albuquerque, NM, 2005. [2] W.K. Liu, S. Jun and Y.F. Zhang, Reproducing kernel particle methods, International Journal for Numerical Methods in Fluids, 20, 1081-1106, 1995. [3] J.S. Chen, M. Hillman and M. Rüter, An arbitrary order variationally consistent integration for Galerkin meshfree methods, International Journal for Numerical Methods in Engineering, 95, 387-418, 2013. \*Sandia National Laboratories is a multimission laboratory managed and operated by National Technology and Engineering Solutions of Sandia, LLC., a wholly owned subsidiary of Honeywell International, Inc., for the U.S. Department of Energy's National Nuclear Security Administration under contract DE-NA-0003525.

## Modification of Response Surface Single Loop Method in Reliability-Based Optimization

Nozomu Kogiso\*, Hiroaki Tanaka\*\*

\*Osaka Prefecture University, \*\*Osaka Prefecture University

### ABSTRACT

This study proposes an improvement method of the response surface single loop method (RSSL) [1] for the reliability-based optimization. The RSSL achieves computational efficiency with high approximation accuracy by directly evaluating the failure probability using the Hermite polynomial and the second-order approximated limit state function. Since the method does not require the most probable point (MPP) searching, the single loop reliability-based optimization is achieved, once the second-order approximation of the limit state function is established. However, we found from our experiment of application to several example problems that the RSSL method does not always have a sufficient accuracy. Especially when the approximation point of the limit state function is apart from the MPP, the approximate accuracy is deteriorated. While, the accuracy is sufficient, if the approximation point is closed to the MPP. For the purpose, we introduce an approximation point updating process in the optimization loop that utilizes an idea of the Single Loop Single Vector (SLSV) method [2] and the modified SLSV method [3]. It means that the second-order approximation point of the limit state function is updated to the approximated MPP by the SLSV method in each optimization step. Since the RSSL does not require the MPP to evaluate the failure probability, the failure probability approximation accuracy is sufficient for roughly approximated MPP. Through several numerical examples, the validity of the proposed method is illustrated by comparing between the proposed method, the original RSSL and also the SLSV. [Reference] 1. R. Mansour and M. Olsson, Response surface single loop reliability-based design optimization with higher-order reliability assessment, *Str. Multidiscip. Opt.*, 54 (2016), 63-79. 2. X. Chen, et al., Reliability based structural design optimization for practical applications, (1997), AIAA-97-1403. [3] N. Kogiso, et al., Modified single-loop-single-vector method for efficient reliability-based design optimization, *J. Adv. Mech. Des. Sys. Manuf.*, 6(7) (2012), pp. 1206-1221.

## Characteristics of Singular Electric Displacement Fields at the Vertex of Interface in Piezoelectric Joints

Hideo Koguchi\*, Hiromi Sato\*\*

\*Niigata Institute of Technology, \*\*Tsugami Corporation

### ABSTRACT

Singular fields of stress and electric displacement occur at the vertex of interface in piezoelectric joints under an external loading and the input of voltage<sup>1)</sup>. Until now, singular stress fields are intensively investigated for relating to the reliability of joints. It can be expected that concentrated electric displacements causes large electric fields in an adjacent space (air) and electric potential will be induced on the surface of electrode when the electrode approaches to the electric field. In the present paper, a piezoelectric joint which four blocks of piezoelectric material are bonded using an insulated resin is analyzed. In this joint, singular fields occur around a center gathering four vertexes in blocks and the intensity of singularity in electric displacements around the center of cross section in the joint may be four times larger. The intensity of singularity in electric displacements is numerically investigated using a conservative integral method to pursue the possibility of application of the singular fields. It is shown that when piezoelectric materials with large piezoelectric constant are used, electric displacements are amplified. Electric fields in air near the vertex of interface have also a singularity. In this study, a singular field of electricity in air is investigated using a commercial finite element program. The order of singularity in air is a little bit different from that in the joints. The influence of thickness of resin on the electric field in air is investigated. When the thickness of the resin increases, the intensity of singularity also increases. However, when the resin becomes thick, the singular fields do not influence on electric fields at the center region of cross section in the joint. Hence, a suitable thickness of the resin exists for amplifying the electric field in air. Next, a generated voltage in the joints and in a single phase piezoelectric material for loading on the side surface is investigated in experiment. Voltage in the joints is 1.5 times as large as that in the single phase material. It is supposed that this is attributed to the singular fields in electric displacement. Reference 1) H. Koguchi, H. Sato, T. Maekawa and C. Luangarpa, Investigation on singular fields in piezoelectric joints and its application, Trans. JSME (in Japanese), Vol. 83, No. 853, 2017, DOI: 10.1299/transjsme.17-00198.

## Numerical Simulation of Multi-Pass Electron Beam (EB) Scanning Process for Controlling Microstructure of Alloy 718 in EB-Powder Bed Fusion (EB-PBF)

Yuichiro Koizumi<sup>\*</sup>, Xiao Ding<sup>\*\*</sup>, Kenta Yamanaka<sup>\*\*\*</sup>, Kenta Aoyage<sup>\*\*\*\*</sup>, Yufang Zhao<sup>\*\*\*\*\*</sup>,  
Akihiko Chiba<sup>\*\*\*\*\*</sup>

<sup>\*</sup>Tohoku University, <sup>\*\*</sup>Tohoku University, <sup>\*\*\*</sup>Tohoku University, <sup>\*\*\*\*</sup>Tohoku University, <sup>\*\*\*\*\*</sup>Tohoku University,  
<sup>\*\*\*\*\*</sup>Tohoku University

### ABSTRACT

Electron beam melting (EBM) is a powder bed fusion (PBF) -type additive manufacturing (AM) process using electron beam (EB) as power source for fusing metal powder particle to fabricate metal parts. The most characteristic aspects of EBM process, compared with other metal AM process, such as selective laser melting (SLM) laser beam-PBF, are the high beam power and high scanning speed of electron beam (EB). These characteristics are believed to be beneficial for controlling the solidification condition and resultant microstructure with a large degree of freedom since they allow us to control temperature distribution variously. In this study, multi pass EB scanning process under various process conditions have been investigated by finite element method (FEM) using surface Gaussian heat source. Temperature gradient (G) and solidification rate (R) were calculated from the temporal change of simulated temperature distribution, and they were plotted on solidification map to predict microstructure. The predicted microstructures were compared to the experimentally observed microstructure to examine the validity of the scheme for predicting the microstructure of EBM-built parts. Simulated melt pool size is consistent with experimental results. With increasing heat input, predicted microstructures change from columnar to equiaxed grains. The columnar-to-equiaxed transition (CET) established for casting process is not applicable for EBM process. Peak temperature increases as pass number increases, and it will be kept constant after several passes. Melt pool width and depth increased at first and then reach stable status. Finally, a large melt pool of trapezoidal shape forms. Temperature gradient, solidification rate and cooling rate all decrease with increasing pass number. This suggests that the high scanning speed of EB can be utilized to control solidification condition precisely by controlling the local temperature gradient and solidification dynamically to obtain desired properties.

## Bi-penalty Stabilized Explicit Finite Element Algorithm for Contact-impact Problems: One Dimensional Case

Radek Kolman<sup>\*</sup>, Jose Gonzalez<sup>\*\*</sup>, Sang Soon Cho<sup>\*\*\*</sup>, K.C. Park<sup>\*\*\*\*</sup>, Jan Kopacka<sup>\*\*\*\*\*</sup>, Anton Tkachuk<sup>\*\*\*\*\*</sup>, Dusan Gabriel<sup>\*\*\*\*\*</sup>

<sup>\*</sup>Institute of Thermomechanics, Czech Academy of Sciences, <sup>\*\*</sup>Universidad de Sevilla, <sup>\*\*\*</sup>Korea Atomic Energy Research Institute, <sup>\*\*\*\*</sup>University of Colorado Boulder, <sup>\*\*\*\*\*</sup>Institute of Thermomechanics, Czech Academy of Sciences, <sup>\*\*\*\*\*</sup>University of Stuttgart, <sup>\*\*\*\*\*</sup>Institute of Thermomechanics, Czech Academy of Sciences

### ABSTRACT

An explicit time integration scheme for finite element solution of contact-impact problems with stabilization of contact forces using a bi-penalty formulation in finite element method for one dimensional case is presented [1]. The penalty approach for enforcing of contact constraints can be applied not only to the stiffness term but also to the inertia of the contact boundary condition. This technique is known as the bipenalty method [2]. By means of adding the bi-penalty terms (additional mass and stiffness terms concurrently) into the equations of motion corresponding to the contact pairs, we obtain a modified local dynamic system. In principle, we attune a frequency character of these equations of motion corresponding to the nodes for which contact conditions apply. The stability limit for an un-penalized/contact-free system is preserved by a special choice of mass and stiffness penalty parameter ratio. For time integration, the explicit time integration scheme is based on splitting of bulk and contact accelerations [3]. Dynamic situation in a bar without respecting contact forces is computed by pull-back time integration [4] with the critical time step size. Moreover, the time stepping process produces stable results for a large range of the stiffness penalty parameter. Behavior of the presented method is shown on impact problems of heterogeneous bars. The special attention is paid to study spurious oscillations of contact forces in one-dimensional contact-impact problem of bars. Acknowledgements to projects: CSF 17- 12925S (Kolman), CSF 16-03823S (Kopa?ka) and MEYS CZ.02.1.01/0.0/0.0/15\_003/0000493 (Gabriel) under AV0Z20760514. References [1] KOLMAN, R. - KOPA?KA, J. - TKACHUK, A. - GABRIEL, D. - GONZALEZ, J. A robust explicit finite element algorithm with bipenalty stabilization for contact-impact problems, International Journal for Numerical Methods in Engineering, in preparation, 2018. [2] KOPA?KA, J. - Tkachuk, A. - Gabriel, D. - Kolman, R. - Bischoff, M. - Plešek, J. On stability and reflection-transmission analysis of the bipenalty method in impact-contact problems: a one-dimensional, homogeneous case study, International Journal for Numerical Methods in Engineering, online, 2017, DOI: 10.1002/nme.5712. [3] S. R. Wu. A priori error estimates for explicit finite element for linear elasto-dynamics by Galerkin method and central difference method. Computer Methods in Applied Mechanics and Engineering, 192(51), p. 5329 -5353, 2003. [4] KOLMAN, R. - CHO, S.S. - PARK, K.C. Efficient implementation of an explicit partitioned shear and longitudinal wave propagation algorithm, International Journal for Numerical Methods in Engineering, 2016, vol. 107, no. 7, p. 543-579.

## Phase-field Simulation of the Formation of Plate-like Precipitates on Basal Plane and its Effect on the Critical Resolved Shear Stress in Magnesium-based Alloys

Kentaro Komiya<sup>\*</sup>, Yuhki Tsukada<sup>\*\*</sup>, Toshiyuki Koyama<sup>\*\*\*</sup>

<sup>\*</sup>Nagoya University, <sup>\*\*</sup>Nagoya University, <sup>\*\*\*</sup>Nagoya University

### ABSTRACT

The Mg-Ca binary alloys microalloyed with Al and Zn show precipitation hardening by aging because plate-like precipitates (or Guinier-Preston zones) are formed on the (0001) plane (basal plane). Furthermore, an indium addition is effective for enhancing age hardening behavior because it changes the habit plane of precipitates from the basal plane to {01-10} or {2-1-10} planes (prismatic planes) [1]. Fundamental knowledge on the formation process of precipitates and the relationship between the microstructure and mechanical properties is essential for microstructure design of Mg-based alloys. In this study, the formation process of plate-like precipitates on the basal plane is simulated by three-dimensional (3D) phase field simulations, where the elastic strain energy derived from the precipitation is explicitly considered based on the phase-field microelasticity theory. It has been simulated that the volume fraction of precipitates increases with time while the number density of precipitates decreases with time. Furthermore, by using the simulated 3D two-phase microstructure, the motion of a dislocation on the (0001) slip plane is simulated under an external shear stress in order to elucidate the influence of precipitates on the dislocation dynamics. Simulation results show that the existence of precipitates delays the dislocation motion even if the dislocation does not encounter any precipitates. It has been found that the dislocation motion is influenced by the elastic interaction between the dislocation and precipitates. The dislocation dynamics simulations are performed with varying the magnitude of external shear stress and the value of critical resolved shear stress (CRSS) is estimated. It has been simulated that during the aging process, the value of CRSS increases with time in the initial stage of precipitation while the value of CRSS decreases with time in the later stage of precipitation. The simulated change in the CRSS value with time is assumed to correspond to the precipitation hardening curve. It has been shown that plate-like precipitates on the basal plane are effective for precipitation hardening, and the elastic interaction between a dislocation and precipitates has a great influence on the mechanical properties of magnesium alloys. Reference: [1] C.L. Mendis et al., Metall. Mater. Trans. A 43 (2012) 3978-3987.

## Effects of Turbulence on Ignition of Fully Premixed Mixtures with Hydrocarbon Fuels

Takahiro Konagamitsu<sup>\*</sup>, Masayasu Shimura<sup>\*\*</sup>, Yuki Minamoto<sup>\*\*\*</sup>, Mamoru Tanahashi<sup>\*\*\*\*</sup>

<sup>\*</sup>Tokyo Institute of Technology, <sup>\*\*</sup>Tokyo Institute of Technology, <sup>\*\*\*</sup>Tokyo Institute of Technology, <sup>\*\*\*\*</sup>Tokyo Institute of Technology

### ABSTRACT

In order to realize a highly efficient spark ignition engine, establishment of combustion technology using low equivalent ratio, high turbulence intensity, high exhaust recirculation rate and the like is required. Under such conditions of combustion, however, ignition is difficult and the ignition characteristics are unknown, so it is necessary to clarify ignition characteristics such as the ignition criteria and ignition delay time. In this study, to determine the ignition criteria and effects of turbulence on the localized ignition delay time, direct numerical simulations (DNS) of forced ignition of lean fully premixed mixtures have been performed for hydrocarbon fuels such as methane and n-heptane with a high exhaust gas recirculation rate at high pressure. In the present DNS, the domain is initially filled with a fully premixed mixture at a uniform preheated temperature. As combustion conditions, equivalence ratio of the mixture, initial pressure, initial exhaust gas recirculation rate and uniform preheated temperature are set to be 0.5, 1.0 MPa, 20 % and 700 K for all fuels cases. A high-temperature kernel is used as an initial ignition kernel, and one-dimensional DNS are preliminary performed to determine the ignition criteria in terms of the ignition source energy and the thermal conduction from the ignition kernel during the induction period. Subsequently, two-dimensional DNS are performed with an initial kernel size and temperature which yields successful ignition for the one-dimensional laminar cases, to clarify the influence of the turbulent strain rate on the ignition delay time. It is found that the turbulent strain rate in the high-temperature region influences the ignition delay time. The ignition delay time increases proportionally to the square of strain rate averaged in the high concentration region of intermediate species during the induction period. This suggests that the ignition in a turbulent field is based on the balance between the influence of the local strain rate in the preheating region and the chemical time scale. Based on these observations, a simple relationship for the ignition delay time was considered based on the mean strain rate in the high concentration region of intermediate species during the induction period. The local ignition delay times predicted by this relationship, normalized using a corresponding laminar flame speed, flame thermal thickness and laminar ignition delay time, yields similar ignition trends for different fuels considered.

## **Gas-liquid Two-phase Flow Calculation Using Moving Particle Full-Implicit (MPFI) Method**

Masahiro Kondo\*

\*University of Tokyo

### **ABSTRACT**

Gas-liquid two phase flow emerges in various industrial processes like boiling, mixing, washing, bubble behavior and so on. To calculate gas-liquid two phase flow, numerical stability is very important because the large density ratio of the two fluid may easily result in instability. It is also the case in particle methods, and empirical relaxations were taken to avoid instability such as particle scattering. To achieve the numerical stability, MPFI (Moving Particle Full-Implicit) method took the approach based on the analytical mechanics, where the monotonic decrease of mechanical energy is assured. Therefore it is thought that the instability like particle scattering does not occur even in a gas-liquid system. In this study, gas-liquid two phase calculations are tested using the MPFI method to check the ability to run the calculations stably.

## A Numeric Algorithm for Solving Kinetic Equations Across All Flow Regimes

Bo Kong\*, Rodney Fox\*\*

\*Ames Lab-USDOE, \*\*Department of Biological and Chemical Engineering , Iowa State University

### ABSTRACT

In nature and many engineering applications, the particle volume fraction in fluid-particle flows often exhibits large variations. In other words, the particles can be closely packed in some locations, and very dilute in other locations at the same time, such as in circulating fluidized bed reactors. Traditionally, a hydrodynamic description of particle phase is often used to simulate fluid-particle flows, which has been shown to be inaccurate for dilute flow regions when particle-particle collisions are infrequent. On the other hand, quadrature-based moment methods (QBMM), which use Gauss quadrature to approximate particle velocity distribution, have been shown to be able to provide accurate solutions for the kinetic equation. However, in dense regions, the explicit nature of QBMM makes it highly inefficient compared to hydrodynamic solvers, in which the implicit methods can be used for spatial fluxes. To accurately simulate all fluid-particle flow regions, a novel algorithm, based on splitting the kinetic flux dynamically and locally in the flow, is proposed in this work. In it, a traditional hydrodynamic solver is employed in the dense region, while in dilute to very dilute regions a kinetic-based finite-volume QBMM solver is used. This algorithm was implemented in OpenFOAM, an open-source CFD package, for particle velocity moments up to second order. Three different flow conditions, fluidized bed, wall-bound channel flow, and homogeneous cluster-induced turbulence flow, are used to test the accuracy and robustness of the proposed flux-splitting algorithm. By varying the average particle volume fraction in the flow domain, it is demonstrated that this algorithm can handle seamlessly all flow regimes present in any particular application. In this talk, we will also briefly introduce a new algorithm for simulating polydispersed dense particle flows based on QBMM.

## **Structural Optimization for Mechanical Structure under Linear and Nonlinear Geometry by Using Topological Technique**

Suphanut Kongwat\*, Hiroshi Hasegawa\*\*

\*Shibauara Institute of Technology, Japan, \*\*Shibauara Institute of Technology, Japan

### **ABSTRACT**

Structural optimization is a one technique to determine an optimal value which becomes a powerful technique for engineering design problem. There are three main types of structural optimization methods i.e. size optimization, shape optimization and topology optimization. According to the best outcome, the topology optimization is considered as a complex method. This is because the optimal size and shape of the initial layout are not taken into consideration. Almost of topology optimization problems are concerned to linear behavior of material by assuming a small displacement for structure. However, when the external load is applied to the structure and causes large deformation, this case is necessary to consider the problem into nonlinearity. The nonlinearities of mechanical structure are related to three main types of problem include behavior of the material, geometry and contact and friction. So, the aim of this research is to investigate the difference of optimal layout between linear and nonlinear material geometry for mechanical structure by employing the topology optimization method. For performing an optimization problem, pre-processing and post-processing of the finite element method (FEM) are required to support the optimization processes. The problem is defined into the simple mechanical structure which created in three-dimensional model (3D) by Salome-Meca. A topology optimization is formulated based on Simplified Isotropic Material with Penalization method (SIMP). The objective for optimization process is to minimize the compliance of structure by corresponding to volume fraction constraint. As the Salome-Meca is open source software, user has to write python script for any problem which is more complicated than the common feature of this software. Absolutely, the optimization process is more complicated than the common feature of Salome-Meca, all of optimization algorithm has to be written with python script by user and combine to the software for computation process. For linear optimization, this is a simple computation by requiring material properties into elasticity, boundary conditions and optimization algorithm. The optimization under nonlinear geometry is more complex than linear optimization by requiring stress-strain relation in plasticity. Moreover, time-step control is also required under nonlinear optimization to control a convergence of results. Finally, the optimal layout of optimization process under linear and nonlinear conditions is obtained and the comparison results of the optimal shape between two cases are completely different. So, the effect of nonlinearities should be concerned into optimization process for suitable results of nonlinear problem.

## A Recursive Multilevel Trust Region Method for Phase-field Models of Fracture

Alena Kopanicakova\*, Rolf Krause\*\*

\*Università della Svizzera italiana, \*\*Università della Svizzera italiana

### ABSTRACT

A state of the art strategy for predicting crack propagation, nucleation and interaction is the phase-field approach. In this approach a damage variable is introduced, which characterizes the state of the material between the unbroken and the broken state. However, phase-field methods require the solution of strongly nonlinear coupled systems of equations at each time-step. This is computationally challenging due to huge number of unknowns and the ill conditioning caused by local changes in the damage variable. As a consequence, the design of efficient solution methods becomes an important task. Two popular solution strategies are monolithic and staggered schemes. In the monolithic approach a fully-coupled non-linear system is solved in each loading step/ time-step, whereas in the staggered approach the evolution operator is split algorithmically into the phase field and the displacement field. Then, in each time step, it is successively solved for both quantities. Numerical evidence shows that the staggered approach is more robust than the monolithic one, but it often underestimates the speed of the crack evolution. For this reason, small time-steps are usually required. On the other hand, the monolithic approach allows for bigger time-steps, but it results in highly ill-conditioned coupled system of equations to be solved. In this work, we employ a recursive multilevel trust region (RMTR) algorithm for the monolithic approach. The method tackles the nonlinearity directly on each level. This is done by introducing level dependent nonlinear objective functions, whose minimization can yield good coarse level corrections for the fine level problem. In contrast to the standard approaches, our approach makes use of both the monolithic and the operator splitting approach. On the fine level, the RMTR solution strategy operates directly on the coupled systems of equations. On the coarse levels, the models are built by using operator splitting techniques. The numerical examples will show that presented optimization technique leads to highly efficient solution strategy. The efficiency will be demonstrated by analyzing convergence behaviour and performing comparison to the commonly used nonlinear solvers.

## A Fully Compressible Multiphase SPH Scheme for Hypervelocity Impacts

Barry Koren<sup>\*</sup>, Iason Zisis<sup>\*\*</sup>, Bas van der Linden<sup>\*\*\*</sup>

<sup>\*</sup>Eindhoven University of Technology, The Netherlands, <sup>\*\*</sup>Praxis Software, Greece, <sup>\*\*\*</sup>LIME B.V, The Netherlands

### ABSTRACT

In Smoothed Particle Hydrodynamics (SPH) for weakly compressible flows, particles of unequal masses are typically employed. In this approach, the mass ratio of the particles determines the density ratio of the different phases. For fully compressible flows, particles of equal masses are advised [1], where the smoothing length needs to adapt to large variations in density. Here, the ratio of initial densities dictates the discretization length per phase, which implies computational and geometrical restrictions [2,3]. Schemes based on number-density can accommodate particles of unequal masses and can offer a robust alternative. The present study presents and validates a number-density SPH scheme, using particles of unequal masses. Test cases considered are: (i) a one-dimensional gas-liquid shock-tube problem with known analytical solution, (ii) two classical two-phase shock-bubble-interaction experiments, and (iii) an aluminum-lead hypervelocity impact experiment, in which the aluminum and lead objects are subjected to plastic deformation, liquefaction and even sublimation. It is found that the above scheme can accurately simulate the propagation of shocks and yields improved results in the simulation of hypervelocity impacts of solids. 1. D.J. Price. Smoothed Particle Hydrodynamics and magnetohydrodynamics. *Journal of Computational Physics*, 231:759–794, 2012. 2. I. Zisis, B. van der Linden, B. Koren, and C. Giannopapa. On the derivation of SPH schemes for shocks through inhomogeneous media. *International Journal of Multiphysics*, 9:83–99, 2015. 3. I. Zisis, R. Messahel, B. van der Linden, A. Boudlal, and B. Koren. Validation of robust SPH schemes for fully compressible multiphase flows. *International Journal of Multiphysics*, 9:225–234, 2015.

## Higher Order Total Variation for Regularizing Partial Differential Equations

Adeline Kornelus<sup>\*</sup>, Rodrigo Platte<sup>\*\*</sup>

<sup>\*</sup>Arizona State University, <sup>\*\*</sup>Arizona State University

### ABSTRACT

One of the main difficulties in solving the incompressible Navier-Stokes equations in fluid dynamics is the transfer of kinetic energy from coarse spatial scale to finer spatial scale, resulting in finite time singularities in the solution. In Fourier analysis, this phenomenon is described by the energy cascade from low modes to high modes. When these equations are discretized, the energy in high modes are usually lost, and as a result, spurious oscillations appear near discontinuities. In this talk, we propose using regularization techniques such as higher order total variation (HOTV), often used in image processing, to improve the numerical solution of such problems. We illustrate the accuracy of the proposed schemes using Burgers's and Euler's equations. The main idea is to penalize spurious oscillations using the polynomial annihilation and L1 minimization techniques. We treat the partial differential equation residual as the fidelity term. In particular, we show these regularized methods lead to better stability and accuracy. We apply HOTV regularization to numerical methods such as Fourier, Finite Differences and Discontinuous Galerkin. We observe that regularization properties of the solution on large scale and small scale depend on the numerical method used to discretize the equations. We also show how different number of elements and/or order of the method affects the quality of the solution. Finally, comparisons with other smoothing techniques such as entropy viscosity and essentially non-oscillatory methods are also provided.

## **Fluid-Structure Interaction Framework for Compressible and Incompressible Flows: Application to Aerospace and Marine Engineering**

Artem Korobenko\*

\*University of Calgary

### **ABSTRACT**

A Fluid-Structure Interaction (FSI) framework for compressible and incompressible flows is presented. The framework is composed of stabilized methods for fluid mechanics and thin-shell structural mechanics formulation. The key constituents of the framework are presented, including the coupling strategies, in a context of various aerospace and marine engineering applications.

## From Images to Material Characterization of Additively Manufactured Micro-architected Structures

Nina Korshunova<sup>\*</sup>, Alexander Düster<sup>\*\*</sup>, Daniel Reznik<sup>\*\*\*</sup>, Stefan Kollmannsberger<sup>\*\*\*\*</sup>, Ernst Rank<sup>\*\*\*\*\*</sup>, John Jomo<sup>\*\*\*\*\*</sup>

<sup>\*</sup>Chair for Computation in Engineering, Technical University of Munich, <sup>\*\*</sup>Numerical Structural Analysis with Application in Ship Technology (M-10), Hamburg University of Technology, <sup>\*\*\*</sup>Research and Technology Center, Siemens AG, Corporate Technology, <sup>\*\*\*\*</sup>Chair for Computation in Engineering, Technical University of Munich, <sup>\*\*\*\*\*</sup>Chair for Computation in Engineering, Technical University of Munich, <sup>\*\*\*\*\*</sup>Chair for Computation in Engineering, Technical University of Munich

### ABSTRACT

Key words: Additive manufacturing, CT Scans, Numerical homogenization, Window method Recent developments in additive manufacturing have provided a unique possibility to create complex structures with porosity on micro- and meso-structural levels. Such designs can outperform conventional materials in specific industrial applications, e.g. turbine blades with a transpiration cooling. However, the high flexibility of the input parameters for the 3D printers, such as the laser diameter, hatch distance etc., challenges a reliable estimation of the mechanical behavior of the final parts. Moreover, a high variation of porosity in all of the material directions limits the application of analytical bounds based on the void fraction ratio. Numerical homogenization is an efficient and robust alternative to perform a non-destructive evaluation of the material characteristics based on high-resolution 3D images of produced specimens. The conventional Finite Element Method applied to numerical homogenization leads to a labor-intensive meshing procedure to extract the representative volume elements that makes it impractical from the industrial point of view. Furthermore, non-symmetric micro-architected structures make it difficult to apply correct boundary conditions for the solution of the microstructural boundary value problem. To address these issues, in the scope of the presented work the Finite Cell Method [1] is employed in combination with the window method [2],[3]. A road map is presented for the automatized numerical computation of the homogenized elasticity tensor of additively manufactured steel structures using 3D images. The computational results are verified with the direct finite cell computation of a given produced specimen. Validation of the proposed model is performed comparing the numerical results with the results stemming from experimental tests. REFERENCES [1] Düster, A., Parvizian, J., Yang, Z. and Rank, E. The finite cell method for three-dimensional problems of solid mechanics. *Computer Methods in Applied Mechanics and Engineering*, 197(4548):3768 – 3782, (2008). [2] Heinze, S., Joulaiian, M. and Düster, A. Numerical homogenization of hybrid metal foams using the finite cell method. *Computers & Mathematics with Applications*, 70(7):1501 – 1517, (2015). [3] Hain, M. and Wriggers, P. Numerical homogenization of hardened cement paste. *Computational Mechanics*, 42(2):197 – 212, (2008).

## **Solution of PDE Constrained Inverse Problems from a Machine Learning Perspective**

Maximilian Koschade<sup>\*</sup>, Phaedon-Stelios Koutsourelakis<sup>\*\*</sup>

<sup>\*</sup>Technical University of Munich, <sup>\*\*</sup>Technical University of Munich

### **ABSTRACT**

The increasing interest in probabilistic methods for uncertainty quantification as well as PDE constrained problems typically relies on deterministic black-box solvers embedded within iterative algorithms such as Markov Chain Monte Carlo. While enabling the utilization of well-established and capable algorithms such as for instance the Finite Element Method, this approach obscures the underlying physical laws and state variables from the machinery of probabilistic inference. We advocate for an intrusive, fully probabilistic approach which constructs a probability distribution over all state variables of the PDE, which are constrained or mutually entangled by underlying physical laws. As such this method foregoes the explicit solution of the forward-model in a conventional sense and yields what can be considered a probabilistic white-box model, where forward solution and probabilistic inference no longer exist as decoupled entities. We demonstrate the applicability of this approach for the adjoint-free solution of a nonlinear, elliptic PDE constrained inverse problem, where we exploit the cheap availability of curvature information inherited from the Finite Element Method to conduct second order inference on our joint posterior over all state variables and unknown quantities simultaneously.

## Condition Assessment and Prognosis in Fluid-Structure Interaction through a Data-Driven Proxy Model Inversion Framework

Justyna Kosianka<sup>\*</sup>, Christopher Earls<sup>\*\*</sup>

<sup>\*</sup>Cornell University, <sup>\*\*</sup>Cornell University

### ABSTRACT

It is essential to identify damage within a structure as early as possible in order to propose corrective measures to prevent mechanical failure – ultimately extending service life. Such damage detection can be effected through non-destructive means that employ the updating of a physics model describing the system of interest. The resulting inverse problem is concerned with locating and characterizing the damage, by considering the structural dynamic response, before and after the onset of damage. Such model-based approaches also afford prognosis potential; as a calibrated physics model is subsequently available for the damaged system. In this work, a partitioned fluid-structure forward modeling capability is developed from combining an open source CFD tool (OpenFOAM) with an open source CSD solver (CU-BEN) in a tightly coupled framework that affords stable solutions. However, such high fidelity, coupled-physics forward modeling is prohibitive for use in solving model-based inverse problems, where the forward model must be called repeatedly; thus necessitating the consideration of reduced-order modeling methods. Within the context of inversion, the high-fidelity FSI forward model is evaluated on a series of plausible (physically inspired) “damaged” states to create an offline library of modeled damaged responses. These responses are expressed in compressed form through proper orthogonal bases (e.g. obtained via proper orthogonal decomposition) and subsequently represented as points on a certain Riemannian manifold. From this off-line library of compressed response representations from the FSI model, a proxy model is constructed, by “manifold interpolation,” on the nonlinear Riemannian manifold to “fill in the gaps” for damage contexts not explicitly contained within the library, but required as part of the inversion. This subsequent online inversion is effected as a non-convex optimization problem, employing a genetic algorithm to arrive at a plausible reduced order modeling instance that conforms to observations within some prescribed limits. An exploration of spatial decomposition methods (e.g. POD vs DMD) and data sampling schemes is presented for a simple test problem of an elastic cantilever oscillating in a bluff body flow with simulated erosion damage. The framework is scaled up for use on a marine structural element, such as propellers and basic ship hull components.

## Dynamic Failure of High Energy Materials

Marisol Koslowski<sup>\*</sup>, Nicolo Grilli<sup>\*\*</sup>, Camilo Duarte Cordon<sup>\*\*\*</sup>

<sup>\*</sup>Purdue University, <sup>\*\*</sup>Purdue University, <sup>\*\*\*</sup>Purdue University

### ABSTRACT

Polymer bonded explosives consist of high energy particles in a polymeric binder. When these composites are subjected to heat, impact, or other stimulus they undergo a rapid chemical change. The sensitivity to initiation depends on the amount of energy available in the system and on the rate at which it is released. This process is controlled by the formation of high temperature localized regions known as "hot spots". The mechanisms of hot spot nucleation are controlled by the microstructure, for example in the same sample some particles ignite while others do not. Finite element simulations that explicitly describe particles, are performed to study the sensitivity of the microstructure to initiation and to identify the mechanisms of hot spot formation under a range of mechanical stimulus. The finite element model incorporates plasticity, fracture and heat transport using a phase field approach. Different microstructures with initial defects, including cracks, debonding and voids are analyzed. Our work suggests that heat generated by friction at preexisting microcracks and at particle binder interfaces are of key importance for hot-spot formation.

## A Spatial Correlation Analysis of Tsunami Risk among Multiple Coastal Cities

Takuma Kotani<sup>\*</sup>, Shuji Moriguchi<sup>\*\*</sup>, Shinsuke Takase<sup>\*\*\*</sup>, Kenjiro Terada<sup>\*\*\*\*</sup>, Yu Otake<sup>\*\*\*\*\*</sup>, Yo Fukutani<sup>\*\*\*\*\*</sup>, Masaaki Sakuraba<sup>\*\*\*\*\*</sup>, Kazuya Nojima<sup>\*\*\*\*\*</sup>

<sup>\*</sup>Tohoku University, <sup>\*\*</sup>Tohoku University, <sup>\*\*\*</sup>Hachinohe Institute of Technology, <sup>\*\*\*\*</sup>Tohoku University, <sup>\*\*\*\*\*</sup>Niigata University, <sup>\*\*\*\*\*</sup>Kanto Gakuin University, <sup>\*\*\*\*\*</sup>Nippon Koei Co., Ltd., <sup>\*\*\*\*\*</sup>Nippon Koei Co., Ltd.

### ABSTRACT

This study presents a framework to evaluate the spatial correlation of tsunami risks among multiple coastal cities. The proposed framework consists of the three processes. First, response surfaces of the tsunami heights at selected multiple coastal cities are obtained from a series of numerical simulations in consideration of conceivable uncertainties of a tsunami hazard. Here, highly developed numerical simulations are extensively and efficiently utilized to obtain reliable data of tsunami heights under a certain scenario. Second, the statistical data sets of the tsunami height are calculated from the obtained response surfaces with the help of the Monte-Carlo simulation (MCS) [1]. Here, the use of the response surfaces, which are regarded as surrogate models, allows us to significantly reduce the calculation costs, as well as to study tendencies of simulated results against input parameters and calculation conditions [2]. In this procedure, a probability density distribution of the tsunami height is also analyzed to characterize the variability in each city. Third, the principal component analysis (PCA) is performed using the covariance matrix that can be obtained from the results of the MCS. Finally, the low risk correlation of the tsunami heights among the selected coastal cities is analyzed based on the result of PCA. Selecting the 2011 off the Pacific coast of Tohoku Earthquake as a target scenario for our tsunami risk evaluation, we present a numerical example to assess the appropriateness of the suggested framework. In specific variabilities of a few fault parameters are considered in this numerical example, and the modeling error of the numerical scheme is also considered as one of the uncertainties. Response surfaces of the coastal cities in Tohoku area are obtained from the results of several sets of tsunami simulations, then spatial correlation among the cities is analyzed. Based on the obtained results, the effectiveness and potential in providing against forthcoming tsunami hazards are discussed, and a characteristic of tsunami risk in Tohoku area is also mentioned. References [1] Honjo, Y., "Challenges in Geotechnical Reliability Based Design", proceedings of 3rd International Symposium on Geotechnical Safety and Risk, pp.11-27, 2011. [2] T. Kotani, S. Takase, S. Moriguchi, K. Terada, Y. Fukutani, Y. Otake, K. Nojima, M. Sakuraba: Numerical-analysis-aided probabilistic tsunami hazard evaluation using response surface, Journal of Japan Society of Civil Engineers, Ser. A2, Vol. 72, No. 1, pp. 58-69, 2016 (in Japanese).

## A Nitsche Based Extended Finite Element (XFEM) Approach to Embedded Contact Interfaces

Hardik Kothari\*, Rolf Krause\*\*

\*Università della Svizzera italiana, \*\*Università della Svizzera italiana

### ABSTRACT

Interface problems occur in many applications in physics. For these problems, it is important to capture discontinuous behavior in order to obtain a good approximation. The extended finite element method (XFEM) allows us to model the evolution of an interface without remeshing as the interface evolves. The XFEM approach captures the discontinuities along interfaces by enriching the standard finite element solution space. The interfaces are represented, implicitly in this case, using Heaviside functions. In the case of fracture mechanics, after the initial crack propagation the newly created surfaces could also come in contact, which would give rise to self contact. The XFEM framework is well suited to model interfaces, but it becomes complicated to model contact interfaces. This is due to the fact that the contact boundaries are not explicitly represented by the nodes or the element edges. In this work, we employ Nitsche's method to weakly compute the contact constraints over these implicit interfaces. Thus, we present a unified framework for fracture and contact mechanics problems, where crack propagations and contact problems are solved on the same mesh. As a crack propagates through the mesh, it is quite likely that the newly created crack passes very close to the nodes or the element edges. Due to this, some elements are fragmented into very small and into very large fractions, which gives rise to a highly ill-conditioned linear system. Such ill-conditioned systems require special solvers and preconditioners. In our work we present a variation of a multigrid method, known as a semigeometric multigrid as a technique to reduce computational complexity. This method uses pseudo-L2 projection based prolongation and restriction operators to transfer the information between the non-nested mesh hierarchies. We demonstrate the robustness and the efficiency of this method as a solver and as a preconditioner in a series of numerical examples. [1] R. Becker, P. Hansbo and R. Stenberg. A finite element method for domain decomposition with non-matching grids, *ESAIM-MMNA*, 37 (2), 209-226 (2003) [2] P. Krause and P. Zulian. A parallel approach to the variational transfer of discrete fields between arbitrarily distributed unstructured finite element meshes, *SIAM Journal on Scientific Computing*, 38(3), C307-C333 (2016) [3] A. Hansbo and P. Hansbo. An unfitted finite element method, based on Nitsche's method, for elliptic interface problems, *Computer methods in applied mechanics and engineering*, 191 (47), 5537-5552 (2002) [4] T. Dickopf and R. Krause. Evaluating local approximations of the L2 orthogonal projections between non-nested finite element spaces, *Numerical Mathematics*, 7(03), 288-316 (2014)

## Stochastic Response Determination of Nonlinear Systems with Singular Diffusion Matrices via a Wiener Path Integral Based Technique

Ioannis A. Kougioumtzoglou<sup>\*</sup>, Apostolos F. Psaros<sup>\*\*</sup>, Ioannis Petromichelakis<sup>\*\*\*</sup>

<sup>\*</sup>Columbia University, <sup>\*\*</sup>Columbia University, <sup>\*\*\*</sup>Columbia University

### ABSTRACT

In many random vibration problems including stochastically excited multi-degree-of-freedom (MDOF) systems subjected to forces applied to only few of the DOFs, as well as a certain class of coupled electro-mechanical energy harvesters, the solution of a system of Stochastic Differential Equations (SDEs) involving singular diffusion matrices is required. This problem can be viewed, alternatively, as a set of SDEs, in conjunction with a set of homogeneous ODEs. In the present work, the Wiener Path Integral (WPI) technique, developed in \cite{koug2} to treat systems with non-singular diffusion matrices, is extended to account for coupled SDEs with singular diffusion matrices. Specifically, the WPI technique determines the response transition PDF of a system of SDEs, based on a variational argument and the solution of the corresponding variational problem. For the herein considered problem, the set of homogeneous ODEs is identified as a set of constraints imposed on the response of the SDEs; thus, leading to a constrained variational problem. Next, relying on \textit{Calculus of Variations} tools, two distinct solution methodologies are proposed. The first, more general one, treats the constraints by utilizing the Lagrange multiplier technique, while the second, which is limited to problems where the set of ODEs forms a linear system (linear constraints), takes advantage of the direct Ritz method and the properties of the nullspace of the constraint matrix, similarly to \cite{antoniou2017}. In this manner, the constrained variational problem is reduced to an unconstrained optimization problem. It is noted that the proposed framework can readily account for additional, physically imposed constraints as well, and thus, address constrained dynamics problems also. The versatility of the technique is demonstrated through diverse numerical examples, while its accuracy is validated by comparisons with pertinent Monte Carlo simulation (MCS) data.

## **Collapse Resilience of Reinforced Masonry Structures Under Seismic Loads**

Andreas Koutras\*, P. Benson Shing\*\*

\*University of California San Diego, \*\*University of California San Diego

### **ABSTRACT**

Reinforced masonry is widely used for low-rise construction in North America, including regions of high seismicity. Under extreme seismic forces, reinforced masonry buildings designed to comply with current codes are expected to have a low probability of collapse. Nevertheless, prior studies using simplified analytical models have shown that low-rise short-period buildings, including those constructed of reinforced masonry might not meet this expectation of the codes. This could be largely attributed to the overly conservative simplified models that were used for such analyses. To provide a more realistic assessment of the collapse potential, this paper presents a refined finite-element analysis scheme to model the inelastic behavior of reinforced masonry structures. In this scheme, smeared-crack shell elements are combined with cohesive discrete crack interface elements to model the compressive crushing and tensile fracture of masonry. The cohesive interface elements allow for a more precise representation of crack opening and closing as well as shear sliding across cracks. Reinforcing bars are modeled with beam elements that have geometric and material nonlinearities to capture bar buckling and fracture. The bar elements are connected to the masonry elements through interface elements to represent the bond-slip and dowel-action behaviors. To enhance the robustness and accuracy of the numerical solution, an element removal scheme is introduced so that the weakly restrained nodes and associated elements resulting from bar fracture or masonry crushing are removed. The material models and the interface elements have been implemented in the commercial software LS-DYNA. The modeling scheme is validated with data from quasi-static cyclic tests performed on flexure- and shear-dominated reinforced masonry walls, as well as with results of shake-table tests of reinforced masonry building systems with earthquake ground motions. Furthermore, the modeling scheme is applied to the time-history analyses of several reinforced masonry building archetypes that have been designed according to current code provisions. The buildings are subjected to bi-directional base excitation to evaluate their seismic performance through collapse.

## Physics-constrained, Data-driven Discovery of Coarse-grained Dynamics

Phaedon-Stelios Koutsourelakis\*, Lukas Felsberger\*\*

\*Technical University of Munich, \*\*Technical University of Munich

### ABSTRACT

This paper is concerned with the discovery of data-driven, dynamic, stochastic coarse-grained models from fine-scale simulations with a view of advancing multiscale modeling. Many problems in science and engineering are modeled by high-dimensional systems of deterministic or stochastic, (non)linear, microscopic evolution laws (e.g. ODEs). Their solution is generally dominated by the smaller time scales involved even though the outputs of interest might pertain to time scales that are greater by several orders of magnitude. The combination of high-dimensionality and disparity of time scales has motivated the development of coarse-grained (CG) formulations. These aim at constructing a much lower-dimensional model that is practical to integrate in time and can adequately predict the outputs of interest over the time scales of interest. The Mori-Zwanzig (MZ) formalism provides a rigorous mathematical foundation for constructing such an effective model. Apart from the largely unsolved computational challenges associated with finding the terms in the Generalized Langevin Equation (GLE) prescribed by MZ, it does not address the issue of finding a good set of CG state variables. Furthermore, even if the evolution equations for the variables selected were perfectly known, it is difficult (without additional assumptions such as the prescription of a lifting operator) to reconstruct or infer the evolution of the full, fine-scale system. Hence if the observables one is interested in predicting, do not exclusively depend on the coarse variables selected, the CG model constructed is not useful. In this paper, we treat the CG process with a probabilistic state-space model where the transition law dictates the evolution of the CG state variables and the emission law the coarse-to-fine map. The directed probabilistic graphical model implied, suggests that given values for the FG variables, probabilistic inference tools must be employed to identify the corresponding values for the CG states and to that end, we employ Stochastic Variational Inference. Naturally, one of the most critical questions pertains to the form of the CG evolution law which poses a formidable model selection issue. We advocate a sparse Bayesian learning perspective based on Automatic Relevance Determination (ARD) which induces sparsity in the solutions identified, avoids overfitting and reveals qualitative features of the CG evolution. The formulation advocated enables the quantification of a crucial, and often neglected, component in the CG process, i.e. the predictive uncertainty due to information loss that unavoidably takes place and manifests itself in uncertainty in the predictions.

## Multi-scale Modelling of Linear and Non-linear Locally Resonant Metamaterials

Varvara Kouznetsova<sup>\*</sup>, Ashwin Sridhar<sup>\*\*</sup>, Priscilla Silva<sup>\*\*\*</sup>, Tim van Nuland<sup>\*\*\*\*</sup>, Marc Geers<sup>\*\*\*\*\*</sup>

<sup>\*</sup>Eindhoven University of Technology, <sup>\*\*</sup>Eindhoven University of Technology, <sup>\*\*\*</sup>Eindhoven University of Technology, <sup>\*\*\*\*</sup>Eindhoven University of Technology, <sup>\*\*\*\*\*</sup>Eindhoven University of Technology

### ABSTRACT

Locally resonant metamaterials are a relatively new class of metamaterials targeting manipulation of acoustic (and more generally mechanical) waves at subwavelength frequencies. The microstructure of these metamaterials is specifically designed to provoke interaction between propagating mechanical waves and fine scale micro-inertia mechanisms, leading to exotic emerging phenomena, such as band gaps, i.e. frequency ranges in which waves do not propagate or highly attenuated, negative refraction index etc. Pushing the material behavior into a non-linear regime opens even more possible applications, e.g. tunable waveguides, adaptive passive vibration control, superdamping, acoustic diodes, cloaking, noise insulation and (vibro-acoustic) energy harvesting. The development and design of such materials and devices made thereof, requires advanced modelling techniques, capable, on one hand, to deal with complex geometries, boundary conditions and excitations, and on the other hand be computationally more efficient than direct numerical simulations. In this work, a novel computational homogenization approach will be presented for multi-scale modelling of locally resonant materials. Originating from the classical computational homogenization technique, well established for quasi-static problems, an extension to transient problems has recently been developed [1]. For linear problems, the static-dynamic decomposition can be used to derive the closed form homogenized equations representing an enriched micromorphic continuum, in which additional kinematic degrees of freedom emerge to account for micro-inertia effects [2]. In non-linear case, fully coupled two scale transient computational homogenization is used to study the wave dispersion in finite size macroscopic structures, demonstrating various phenomena emerging due to the presence of non-linearities, e.g. amplitude dependent attenuation response and higher-order harmonics generation. A new design of a vibro-diode, allowing wave propagation in one direction only, has been proposed based on the combination of the linear and non-linear local resonators. Acknowledgements: The research leading to these results has received funding from the European Research Council under the European Union's Seventh Framework Programme (FP7/2007-2013) / ERC grant agreement n°[339392]. The support from 4TU Research Center High Tech Materials (4TU.HTM) is also gratefully acknowledged. References: [1] Pham, N.K.H., Kouznetsova, V.G. and Geers, M.G.D. Transient computational homogenization for heterogeneous materials under dynamic excitation. *Journal of the Mechanics and Physics of Solids* (2013) 6: 2125-2146. [2] Sridhar, A., Kouznetsova, V.G., and Geers, M.G.D. Homogenization of locally resonant acoustic metamaterials towards an emergent enriched continuum. *Computational Mechanics* (2016) 57: 423-435.

## Microstructure-Property Analysis Accelerated by Machine Learning Technique with Phase-field Method and Image-based Property Calculations

Toshiyuki Koyama\*, Yuhki Tsukada\*\*

\*Nagoya University, \*\*Nagoya University

### ABSTRACT

Recently, the phase-field (PF) method has been becoming the de facto standard simulation method for calculating various types of phase transformations and microstructure developments in real materials. Since the inhomogeneous microstructure data are available from the simulation, the materials properties are estimated based on the image-based calculation in which the inhomogeneous microstructure data obtained from PF simulation is utilized as a boundary condition for calculation. In this study, we focus on the mechanical property, i.e., the stress-strain (S-S) curve of dual-phase steels. Firstly, various morphologies of microstructure observed during spheroidization process from lamella structure are prepared by conventional PF method. Secondly, the S-S curves corresponding to each calculated microstructure are evaluated by the modified secant method [1], where the matrix and inclusion phases are assumed to be ferrite and martensite, respectively. As a consequence, the dataset composed of "microstructure data" and "S-S curve" is generated. From the microstructure data, we extract the following feature amount: volume fraction, interfacial area, genus, connectivity, variance of mean curvature and variance of Gaussian curvature. In order to understand the quantitative relationship between the S-S curves and the microstructure morphologies, the neural network machine learning technique is employed. Input data to the neural network are not only the feature amount above mentioned but also the true strain in the S-S curve, on the other hand, the output data for neural network training is the true stress only. In the current work, 145 pairs of "microstructure data" and "S-S curve" were applied to optimize the neural network system, then the trained neural network which can describe the relation between microstructure and mechanical property was constructed. By using the trained neural network, the sensitivity of each feature amount to S-S curve was estimated, and the following conclusions were obtained: The final stress level of S-S curve is determined mainly by the volume fraction. It is quite interesting that the stress level at the initial rise up stage of S-S curve depends strongly on the connectivity parameter. The connectivity means the spatial continuity of martensite phase. Therefore, the optimization of martensite morphology is a key point for improving the mechanical property of dual-phase steels. [1] T. Koyama, ISIJ International, 52 (2012) 723-728.

## Primary Blast Loading Effects on Axonal Deformation

Reuben Kraft<sup>\*</sup>, Harsha Garimella<sup>\*\*</sup>, Andrzej Przekwas<sup>\*\*\*</sup>

<sup>\*</sup>Penn State University, <sup>\*\*</sup>CFDRC, Inc., <sup>\*\*\*</sup>CFDRC, Inc.

### ABSTRACT

Subject-specific computer models (male and female) of the human head were used to investigate the possible axonal deformation resulting from the primary phase blast-induced skull flexures. The corresponding axonal tractography was explicitly incorporated into these finite element models using a recently developed technique based on the embedded finite element method. These models were subjected to extensive verification against experimental studies which examined their pressure and displacement response under a wide range of loading conditions. Once verified, a parametric study was developed to investigate the axonal deformation for a wide range of loading overpressures and directions as well as varying cerebrospinal fluid (CSF) material models. This study focuses on early times during a blast event, just as the shock transverses the skull (&lt; 5 milliseconds). Corresponding boundary conditions were applied to eliminate the rotation effects and the corresponding axonal deformation. A total of 138 simulations were developed - 128 simulations for studying the different loading scenarios and 10 simulations for studying the effects of CSF material model variance - leading to a total of 10,702 simulation core hours. Extreme strains and strain rates along each of the fiber tracts in each of these scenarios were documented and presented here. The results suggest that the blast-induced skull flexures result in strain rates as high as 150-378 s<sup>-1</sup>. This rapid deformation of the axonal fiber tracts, caused by flexural displacement of the skull, suggests the possibility of rate-dependent micro-structural axonal damage according to the published experimental studies.

## **Stabilization of Reduced-order Flow Models through Learning-based Closure Modeling**

Boris Kramer<sup>\*</sup>, Mouhacine Benosman<sup>\*\*</sup>, Omer San<sup>\*\*\*</sup>, Jeff Borggaard<sup>\*\*\*\*</sup>

<sup>\*</sup>Massachusetts Institute of Technology, <sup>\*\*</sup>Mitsubishi Electric Research Labs, <sup>\*\*\*</sup>Oklahoma State University,  
<sup>\*\*\*\*</sup>Virginia Tech

### **ABSTRACT**

In this talk, we present a learning-based method for stabilization of reduced-order models (ROMs) for thermal fluids, which are challenging multi-physics systems. The stabilization of the reduced-order model is achieved by using Lyapunov robust control theory to design a new closure model. Furthermore, the design parameters in the proposed ROM stabilization method are optimized using a data-driven multi-parametric extremum seeking (MES) algorithm. We show the advantages of the proposed method on numerically challenging test-cases by using the 2D and 3D Boussinesq equations. The results illustrate that closure models can be extended to multi-physics systems, by using multiple design parameters.

## Higher Order 2D Virtual Elements for Elastic Materials at Finite Strains

Alex Kraus<sup>\*</sup>, Peter Wriggers<sup>\*\*</sup>

<sup>\*</sup>Leibniz Universität Hannover, Institute for Continuum Mechanics, <sup>\*\*</sup>Leibniz Universität Hannover, Institute for Continuum Mechanics

### ABSTRACT

The recently developed Virtual Element method shows promise as an alternative to finite element formulations and has gained a lot of attention in the last years due to its flexibility using meshes with convex and non-convex elements. However, for large strain applications this discretization technique has not been established as a standard engineering tool. This is mainly due to the need to stabilize this formulation. Based on the stabilization method proposed by Wriggers et al. 2017, a new method for the evaluation of the stabilizing term for a virtual element formulation was developed in this approach. Furthermore, a higher order formulation for finite deformations was developed.

## A 3D Discontinuous Galerkin Cut Cell Immersed Boundary Method: Results and a View on Parallel Efficiency

Dennis Krause\*, Florian Kummer\*\*

\*TU Darmstadt, \*\*TU Darmstadt

### ABSTRACT

In the past, we developed an immersed boundary solver in a cut cell context based on a cut cell (extended, unfitted) Discontinuous Galerkin (DG) discretization. To overcome the difficulty of quadrature on cut cells, we use the hierarchical moment fitting quadrature technique proposed by Müller et al. [1]. For coupled motion we use a simple Lie-Splitting approach for the moving domain. Furthermore, the boundary conditions at the interface are represented by Dirichlet values for velocity in the weak form of the discretization. In first two dimensional calculations we could proof very good agreement with other works in the field of immersed boundary methods for moving body flows. This can be shown for simple static boundary test cases as well as for typical fluid-structure interaction problems like an oscillating cylinder or coupled problems like a disk separating in a vertical channel due to gravity forces. Additionally, the crucial benefit is the save of total degrees of freedom comparing with particulate flow literature. However, also a dependence of the calculated forces on the penalty parameter chosen was discovered. All results mentioned have already been published [2]. For large 3D calculations, it became apparent, that two main topics had to be addressed, in order to reach the aforementioned goal: First, the direct solver MUMPS had been substituted by an iterative solver, i.e. GMRES with a suitable Preconditioning. Second, the total parallel efficiency of the solver had to be increased. Additionally, a dynamic load balancing approach had to be implemented in case of moving boundaries. The presentation will shortly introduce the method. After that, we will focus on suitable preconditioning for the linear equations systems and analyse the bottlenecks of performance arising from large 3D calculations. Acknowledgement: The work of D. Krause is supported by the Excellence Initiative of the German Federal and State Governments and the Graduate School of Computational Engineering at Technische Universität Darmstadt. The work of F. Kummer is supported by the German DFG through Collaborative Research Centre 1194/B06. [1] B. Müller, F. Kummer and M. Oberlack. "Highly Accurate Surface and Volume Integration on Implicit Domains by Means of Moment-Fitting.", *Int. J. f. Num. Meth. in Engng.*, 96, no. 8 (2013): 512–528. [2] D. Krause and F. Kummer. "An Incompressible Immersed Boundary Solver with Applications to Moving Body Flows using a Cut Cell Discontinuous Galerkin Method.", *Comput. Fluids* 153 (2017): 118–29.

## Parallel Multigrid Methods for Interface Problems

Rolf Krause<sup>\*</sup>, Patrick Zulian<sup>\*\*</sup>, Maria Nestola<sup>\*\*\*</sup>, Cyrill von Planta<sup>\*\*\*\*</sup>

<sup>\*</sup>Institute of Computational Science, USI, <sup>\*\*</sup>Institute of Computational Science, USI, <sup>\*\*\*</sup>Institute of Computational Science, USI, <sup>\*\*\*\*</sup>Institute of Computational Science, USI

### ABSTRACT

In this talk, we discuss the design of efficient parallel multigrid methods for contact and interface problems. Contact and interface problems pose particular challenges for the development of efficient parallel solution methods. On the one hand, the presence of the strongly local non-linearities, which are associated to the interface, requires a global convergence control strategy. On the other hand, in particular for the case of multi-body contact or embedded interfaces, the discretization of the interface itself and of the (non-penetration) constraints at the interface will give rise to additional communication between the different processors. Thus, standard parallelization strategies for standard linear multigrid methods can not be applied directly to contact and interface problems. In this talk, we discuss the difficulties related to global convergence control for the case of parallel multigrid methods. We present different convergence control strategies, which are based on successive energy minimization in parallel and exploit the fact that contact problems can be viewed as constrained minimization problems. Our strategies can be applied in the case of linear as well as non-linear material laws. We furthermore discuss how to build efficiently a parallel and inherently non-linear multilevel method for contact problems. Finally, we explain how to compute in parallel the inter-mesh dependencies at contacting or embedded interfaces. We will treat the case of non-overlapping (contact) as well as of overlapping (embedded interfaces) decompositions. Examples from geo-sciences and from fluid-structure interaction in cardiovascular applications will illustrate our findings.

## Generation of Reliable Input Data for a Damage Model Taking Use of a Closed CAE-Chain Containing Material Interfaces

Constantin Krauss\*, Siegfried Galkin\*\*, Luise Kaerger\*\*\*

\*Karlsruhe Institute of Technology (KIT), Institute of Vehicle System Technology (FAST), Part Institute of Lightweight Technology, \*\*Karlsruhe Institute of Technology (KIT), Institute of Vehicle System Technology (FAST), Part Institute of Lightweight Technology, \*\*\*Karlsruhe Institute of Technology (KIT), Institute of Vehicle System Technology (FAST), Part Institute of Lightweight Technology

### ABSTRACT

Due to their high specific strength and stiffness, continuous fiber-reinforced polymers (CoFRP) are ideal lightweight materials for high performance structural components in the automotive sector. In addition, demands regarding economics, robustness and cycle times of the manufacturing processes are even higher in order to be able to compete with the commonly used metallic materials in large batch production. Such processes, for instance the Resin Transfer Molding, are further divided into a sequence of several sub processes containing draping, infiltration and curing steps. Developing and extending simulation models for these processes has been topic of numerous investigations in the past and present time and are quite well understood. Since in the field of composites, both the material and the actual part are results of the manufacturing, the material's history is crucial for the final structural performance. Occurring changes in fiber orientation, fiber volume content and additional effects such as fiber undulation or wrinkle formation and also remaining residual stresses need to be taken into account to avoid oversized or defective structures. Since material constitutive behavior, physics or reasonable mesh topology and size typically vary, different specialized software for each of the process steps is usually used. Therefore, the virtual interfaces between the individual simulation steps are going to play a key role in the future. Within these interfaces the exchange and transfer of relevant geometric and material data is managed. In the present moment, significant effort is required to develop and implement such interfaces, which are usually tailor-made for the current problem and not applicable to new cases. Within the EU research project ITEA-VMAP this issue is addressed by creating a new interface standard for virtual material modelling. The aim of this concept is to ease and accelerate the building of virtual process chains and thus of reducing the product's TTM. In this work, the virtual manufacturing route of an exemplary composite structure based of unidirectional non-crimp fabric reinforcement is presented. Hereby, the main focus is on the interface formulation and realization. It is demonstrated how the information flow within the CAE-chain is accomplished and how draping effects affect e.g. permeability, thermal expansion and strength. Eventually, a newly developed damage model is fed with the provided parameters resulting from the previous simulation steps. The main goal is to assess the impact on the load bearing capacity compared to computations neglecting the material's prehistory.

## Adaptive Direct FEM Simulation

Ezhilmathi Krishnasamy<sup>\*</sup>, Johan Jansson<sup>\*\*</sup>, Massimiliano Leoni<sup>\*\*\*</sup>, Niclas Jansson<sup>\*\*\*\*</sup>, Johan Hoffman<sup>\*\*\*\*\*</sup>

<sup>\*</sup>Computational Science and Technology, CSC, KTH, SE-10044 Stockholm, Sweden and BCAM - Basque Center for Applied Mathematics, Bilbao, Spain, <sup>\*\*</sup>Computational Science and Technology, CSC, KTH, SE-10044 Stockholm, Sweden and BCAM - Basque Center for Applied Mathematics, Bilbao, Spain, <sup>\*\*\*</sup>Computational Science and Technology, CSC, KTH, SE-10044 Stockholm, Sweden and BCAM - Basque Center for Applied Mathematics, Bilbao, Spain, <sup>\*\*\*\*</sup>Computational Science and Technology, CSC, KTH, SE-10044 Stockholm, Sweden, <sup>\*\*\*\*\*</sup>Computational Science and Technology, CSC, KTH, SE-10044 Stockholm, Sweden

### ABSTRACT

We present efficient way of solving incompressible Navier-Stokes Equations (NSE) for industrial applications involving turbulence modelling[1]. We named our methodology as Direct FEM Simulation (DFS)[2] which is based on the General Galerkin (G2); and it is defined by finite element method (FEM) with piecewise linear approximation in space and time, and with numerical stabilization in the form of a weighted least squares method based on the residual. The incompressible Navier-Stokes Equations (NSE) are discretized directly, without applying any filter. Thus, the method does not result in Large Eddy Simulation (LES) filtered solutions, but is instead an approximation of a weak solution satisfying the weak form of the NSE. This means no explicit turbulence model is used, and the effect of unresolved turbulent boundary layers is modeled by a simple parametrization of the wall shear stress in terms of a skin friction. Which leads to getting small skin friction on the boundary for the higher Reynolds number (in particular turbulence modelling) thus favors the slip boundary condition, and it requires not having solved costly (computationally expensive) boundary layer resolution. And another main advantage with our methodology is that adaptivity, which is achieved by doing posteriori error estimation using adjoint techniques[2], and it is defined as a goal functions, for example, lift and drag. This minimizes effort of computational domain manual mesh refinement. Our approach and methodology has been well tested against typical scientific and industrial benchmark models[2,3,4], in particular we have previously participated in HiLiftPW-2, HiLiftPW-3 and HiOCFD5 (tandem sphere test case). For example, even how one can get benefit (computational cost) using our methodology over higher order methods. And also we present parallel post processing based on the task parallelization using the VisIt[5] visualization tool. [1] FEniCS (2003), 'Fenics project', <http://www.fenicsproject.org>. [1] Hoffman, J. & Johnson, C. (2007), Computational Turbulent Incompressible Flow, Vol. 4 of Applied Mathematics: Body and Soul, Springer. [2] Hoffman, J. (2005), 'Computation of mean drag for bluff body problems using adaptive dns/les', SIAM J. Sci.Comput. 27(1), 184–207. [3] Hoffman, J. (2006), 'Adaptive simulation of the turbulent flow past a sphere', J.Fluid Mech. 568, 77–88. [4] Hoffman, J. (2009), 'Efficient computation of mean drag for the subcritical flow past a circular cylinder. [5] VisIt, <https://wci.llnl.gov/about-us>.

## Modeling of Damage and Crack Growth in Semi-Crystalline Polymers

Martin Kroon\*, Eskil Andreasson\*\*

\*Linnaeus University, \*\*Blekinge Technical University

### ABSTRACT

Crack growth in semi-crystalline polymers, represented by polyethylene, is considered. The material considered comes in plates that had been created through an injection-molding process. Hence, the material was taken to be orthotropic. Material directions were identified as MD: molding direction, CD: transverse direction, TD: thickness direction. Uniaxial tensile testing was performed in order to establish the direction-specific elastic-plastic behaviour of the polymer. In addition, the fracture mechanics properties of the material was determined by performing fracture mechanics testing on plates with side cracks of different lengths. The fracture mechanics tests were filmed using a video camera. Based on this information, the force vs. load-line displacement could be established for the fracture mechanics tests, in which also the current length of the crack was indicated, since crack growth took place. The crack growth experiments were then simulated using Abaqus, where crack growth was enabled by use of a cohesive zone. The force-displacement-crack length data from the experiments could be well reproduced in the simulations, where different model parameters for the cohesive zone were explored. Furthermore, the direction-specific work of fracture had been established from the experiments and these energies could be compared to the values of the J-integral from the simulations for the different crack lengths.

## **Mesh Generation Techniques for Converting Triangular Meshes to Quadrilateral and Mixed-element Meshes with Applications to Shallow Water Flow**

Ethan Kubatko<sup>\*</sup>, Dominik Mattioli<sup>\*\*</sup>, Dylan Wood<sup>\*\*\*</sup>

<sup>\*</sup>The Ohio State University, <sup>\*\*</sup>The University of Iowa, <sup>\*\*\*</sup>The Ohio State University

### **ABSTRACT**

In this talk, we discuss the development and implementation of a new, simple indirect methodology for producing high-quality quadrilateral (quad) and quad-dominant meshes from any pre-existing, unstructured triangular mesh. One of the primary motivations for this work is to provide a tool for generating meshes that can be used within a discontinuous Galerkin (DG) finite element framework for modeling shallow water flow — a setting where meshes of mixed-element composition can be easily accommodated and where the computational advantages of using quad elements have been demonstrated [1]. Employed techniques include: A strategic merging sequence of neighboring triangular element pairs to form quads, several topological operators designed to improve the quality of the resulting quad elements and a direct (i.e., non-iterative) smoothing method to improve overall mesh quality. When paired with an existing triangular-element mesh generator, ADMESH+ [2], this new methodology results in a mesh generation tool capable of automatically producing high-quality triangular, quad and mixed-element meshes within one framework. Several example quad and quad-dominant meshes produced from the mesh generation tool will be presented, and numerical results of shallow water simulations obtained from the quad and quad-dominant meshes will be compared to the results obtained from their parent triangular meshes in terms of overall accuracy and efficiency. [1] Wirasaet, D., Kubatko, E.J., Michoski, C.E., Tanaka, S., Westerink, J.J., and Dawson C., Discontinuous Galerkin methods with nodal and hybrid nodal/nodal triangular, quadrilateral, and polygonal elements for nonlinear shallow water flow *Computer Methods in Applied Mechanics and Engineering*, 270, pp. 113–149, 2013. [2] Conroy, C., Kubatko, E.J., and West, D., ADMESH: An advanced, automatic unstructured mesh generator for shallow water models, *Ocean Dynamics*, 62 (10), pp. 1503–1517, 2012.

## Meshless Remap for Earth System Models

Paul Kuberry<sup>\*</sup>, Pavel Bochev<sup>\*\*</sup>, Kara Peterson<sup>\*\*\*</sup>

<sup>\*</sup>Sandia National Laboratories, <sup>\*\*</sup>Sandia National Laboratories, <sup>\*\*\*</sup>Sandia National Laboratories

### ABSTRACT

Global Earth System Models comprise multiple components, representing a diverse set of physical phenomena and employing different types of discretizations adapted to the particular scales and features of the underlying physical phenomena. As a result, the coupling of these components requires information exchanges (remap) between codes, which involve fields defined on different types of meshes and possibly having different representations, e.g., finite element vs. finite volume, or node-centered vs. cell-centered. Typically, the coupling takes place over a shared subdomain boundary, resulting in interface discretizations that are generally mismatched. For such couplings, a mesh-free approach to data transfer offers an attractive alternative to traditional, mesh-based remap. In this talk we present a flexible data transfer tool, employing Generalized moving least squares (GMLS), and which can handle a wide range of "native" field representations. GMLS is a meshless reconstruction technique for approximating a target functional from nearby neighbor information, which makes it particularly well-suited for our purposes. The GMLS data transfer tool is based on the recently developed Compadre meshless toolkit, which provides a wide range of utilities for mesh-free discretizations of PDEs. Compadre utilizes the Trilinos software stack to balance workloads over processors, execute k-d tree searches, reconstruct functionals using GMLS, and to provide many additional capabilities for meshfree PDE discretizations. The talk will highlight the ability of the toolkit to also support coupling codes such as components of Earth system models, by allowing for processor assignment of coordinates or sites where information is needed from the peer program. This information is constructed using neighbor information in the peer program and then transferred back. Transfer in this way allows for completely independent distributions of field data in each code being coupled. Numerical results will be presented demonstrating exact transfer of specific orders of polynomial solutions on the sphere, as well as the approximation error introduced when the solution being transferred is not within the span of the basis for the reconstruction.

## BLADE TIP-TIMING SENSORS CALIBRATION AND ITS USAGE UNDER LOW LOAD CONDITION

Zdenek Kubin <sup>\*,†</sup>, Tomas Misek <sup>†</sup>, Jindrich Liska <sup>\*</sup>

<sup>\*</sup> Faculty of Applied Sciences,  
UWB in Pilsen, Univerzitní 22, Plzeň  
306 14, Czech Republic  
zdenek.kubin@doosan.com

<sup>†</sup> Doosan Skoda Power s.r.o.,  
Tylova 1/57, Plzeň  
301 28 Czech Republic

**Key words:** Blade Tip-Timing, Sensors, Calibration, Steam turbine, Vibration limits

**Abstract.** Blade Tip-Timing measurement becomes more and more valuable because power generation market is changing to the peak-load market. Today steam turbines have to full-fill high efficiency and reliability demand as well as increasing of number of cycles or operating under wide operational range which include windage or low load operation. The higher level of blade vibration is more common for windage and other non-nominal regimes. Blade Tip-Timing measurement offer solution for long term monitoring and safety operation.

The new last stage steam turbine blades have been developed with state of the art design features. The last stage moving blades are designed with integral shroud, mid-span tie-boss connection, and fir-tree dovetail. The blades are continuously coupled by blade untwist due to centrifugal force, and thus decreased vibrations and increased structural damping are provided. Unfortunately measurement of shrouded blades is much more complicated and the sensor to blade calibration has to be performed.

The Blade Tip-Timing measurement and sensor calibration is described in the paper. The calibration of magnetoresistive, optical sensors and eddy-current sensors was performed. The induction and optical reflection phenomena is described with their impact to shroud edge detection. The detection of shroud edges and its angle seems to be important in terms of calibration between tip deflections to high air foil stress identification. The comparison between the individual types of sensors is presented as well as the real results from 270MW steam turbine operation in wide operational range. The motivation to use multiple sensors and provide their calibration is reduced uncertainty of Blade Tip-Timing which is presented in many publications.

## 1 INTRODUCTION

In 2009, a new 48“ steam turbine last stage blade (LSB) was developed by Doosan Skoda Power and in 2013 a new 42” LSB for 3000 RPM and high backpressure was developed with the application of new design features. Using modern computational instruments, airfoils with high flow efficiency were designed. Successful detuning of natural frequencies with respect to harmonics of rotational frequency has been achieved for both blades by using interconnecting elements near the mid-span and at the tip of the blades. Friction forces among the contact elements result from the constraint of blade untwist induced by centrifugal force. The mechanical properties of LSB were measured under rotation in a Campbell testing rig (vacuum chamber with rotating bladed disk and some source of blade excitation). Measurement proved that blades are out of synchronous resonances up to 7th harmonic frequency.

Synchronous excitation is the most common excitation in terms of the steam turbine blades. This excitation is closely related with circumferential asymmetry, blade passing and unbalance. On the other hand, resonances with non-synchronous excitation can occur as a result of aerodynamic excitation. Avoiding that is quite demanding task, because even very small aerodynamic excitation forces with wide frequency range can excite blades if the damping is insufficient. A big amplitudes of vibration during ventilation conditions was present several times as well as unstalled flutter observation during power output increase [5]. 3D unsteady CFD methodology under ventilation conditions was published by Megerle in 2012 [1]. Rotating aerodynamic excitation was measured and confirmed by CFD simulation, unfortunately there are still some unpredictable cell patterns. Previous study made by Shnee in 1974 [6] shows that there is a dynamic stress 2-3 times higher than the dynamic stresses at rated conditions in the range of 30 – 60 % of the nominal volume flow due to aerodynamic induced vibrations during ventilation.

From time to time customers want to operate the turbine in extraordinary conditions which can cause unpredictable blade excitations. These excitations have impact on dynamic stress of blades and reduced blade lifetime. Based on this, it was decided to measure blade vibration in a wide range of operation conditions in the power station and reduces mechanical stress of rotating blades thereby increasing their service life.

Damage of the blades causes changes in their frequency characteristics, which are measured using a contact or contactless method. The contact measurement by strain gauges provides direct information about the blade stresses during operation. However, this method is not suitable for long-term measurements, because the sensors service life is short in a corrosive environment. Furthermore, it is very difficult and expensive to monitor all blades of the bladed disc.

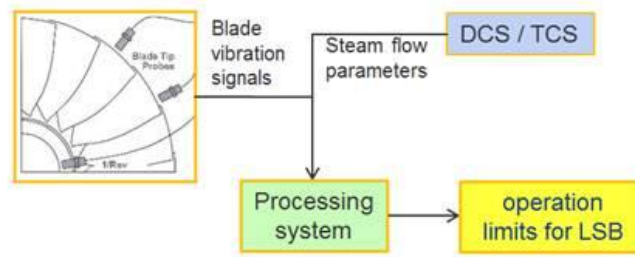


Figure 1 - Blade vibration monitoring system components

Noncontact measurement methods based on analysis of blade tip passing times are used for blade vibration measurement - blade tip-timing (BTT). The schematic description of BTT is shown on Figure 1. This method was used in 1970's for the first time. The manufacturers use abbreviations NSMS (Non- Intrusive Stress Measurement System), BSSM (Berührungslöse Schaufelschwingungsmessung) or usually Blade Tip Timing. BTT method is a cheaper alternative with a long-term instrumentation in comparison with strain gauges which offer a direct measurement of the blade stress but with a very short instrumentation lifetime. The BTT approach is based on sensors which are located circumferentially around bladed disk, radially mounted in the stator, watching tip of trailing edge [3, 4, 5]. This arrangement enables the measurement of blade tip passes. The system measures and analyses time differences of blades passing along the sensor position. The sensor itself is placed very close to the blade (order of ones-tens of millimetres depending on technology of the sensor), in order to guarantee fast response time and high sensitivity. The passing blade generates a trigger pulse which is captured by a high resolution time counter. All the data or timestamps are analysed and at the output of the system information on the blade vibration is provided.

It is important to monitor the blades frequency characteristics during turbine run-up, run-down and power changes. The measurement of vibrations provides information about blade deflection and blade residual lifetime. The long-term measurement of blade deflections is important for planning shutdowns and optimization of the maintenance cost and operation of the turbine.

Blade deflections are determined by differences between the real and expected passage times of the blades under the sensors. The deflection of the specific blade is sampled once per revolution. An antialiasing filter cannot be used in the measurement chain because the turbine rotation frequency is in fact the sampling frequency of the blade rotation movement and furthermore, the rotation speed changes. For these reasons, the vibrations of the specific blade are measured in a limited frequency range with lots of data mirrors at higher frequency and lower frequency resolution. Increasing the number of sensors does not often bring results adequate to expended resources.

Instead of single blade behaviour analysis, behaviour of the whole bladed disc could be analysed. The deflections are sampled by the passages of all blades. Then, the width of the frequency band is sufficient and aliasing doesn't manifest itself so much. The all-blade spec-

trum, which is the spectrum involving all blades of one disc, is calculated for each sensor from deflections measured for all blades passed under the sensor using short-time Fourier transform. Consequently, cross spectra are calculated from couples of the all-blade spectra from different sensors.

To obtain correct information about vibrations of shrouded blades, it was necessary to develop reliable measuring equipment for the shrouded blades. The key factor is to use adequate sensors [13, 14].

## 2 REQUIREMENTS FOR NON-CONTACT VIBRATION MEASUREMENTS ON SHROUDED BLADES

Observing the motion of rotating and vibrating blades in turbomachinery is a relatively demanding task. The sensors have to operate properly and precisely in a harsh environment characterized by temperatures up to 250°C and relative humidity of 100% (LP part of steam turbine). Concurrently, long-term stability, high accuracy and sensitivity of the sensors are required. Most present systems are therefore focused on the application of non-contact methods which can operate on a variety of principles. The limiting factor for non-contact measurement of blades vibration is the sampling frequency  $f_s$ . The sampling level has in BTT a significant influence on determining the vibration amplitude of the blades. Maximum resolution of the blade deflection is described by the following relation:

$$\Delta_a = \frac{2\pi \cdot r_{senz} \cdot f_{rot}}{f_s}, \quad (1)$$

where  $r_{senz}$  is the radius (measured from the center of the rotor) on which the sensor is placed.  $f_{rot}$  is the maximum rotational speed of the bladed disk in the measurements (typically 50 Hz). To illustrate the dependence between sampling rate and blade deflection amplitude resolution, the above relationship was used to provide the following table computed for rotation frequency of 50 Hz:

Table 1 - Resolution base on sampling frequency

$f_s$	blade 1220mm + 900mm rotor radius = 2120mm
100kHz (standard acquisition systems)	6660.2 $\mu\text{m}$
1MHz	666.0 $\mu\text{m}$
8MHz (oscilloscope standard)	83.2 $\mu\text{m}$
100MHz	6.6 $\mu\text{m}$
500MHz	1.3 $\mu\text{m}$

Table 1 shows the blade vibration resolution. It is clear that, for example, system resolution approaching units of microns should work with sampling frequencies of 500 MHz and

higher. Demand for a maximum resolution sensor should always be related to the largest bladed disk of the machine. For smaller diameters better resolution of measured deflection is always guaranteed, sampling frequency maintains.

The table above also shows that standard acquisition systems are not appropriate for BTT measurements (usually sampling frequency up to 100 kHz - 200 kHz). The biggest resolution of the measurement in such a case is in the order of millimetres, which is beyond the expected oscillatory behaviour of shrouded blades. For general diagnostic systems, which are able to monitor blades and evaluate their level of stress, it is necessary to use special hardware that allows the required sampling rate - hundreds of MHz. For the measurement of LSB, which is presented in this paper, the 200MHz system was used in combination with several types of sensors. This system seems to be sufficient to monitor LSB shrouded blades with vibration amplitudes 10 times under fatigue strength.

### 3 EDDY-CURRENT SENSOR CALIBRATION

The eddy-current sensors are most valuable in terms of robustness and cost. The principle is very simple see [13, 14]. There are magnet and coil in the sensor case. When the blade passes the sensor the eddy-current in the blade create magnetic field which induced the voltage in the sensor itself. The following equation describes the induced voltage in the sensor.

$$V = \frac{k \times \text{RPM} \times B(T) \times f(\text{RPM}, d_{\text{sensor}} \sqrt{[\mu\delta]_{\text{sensor}}(T)}) \times d_{\text{BLADE}} \sqrt{[\mu\delta]_{\text{BLADE}}(T)} \times T_{\text{sensor}}}{(\text{gap} + r)^6}, \quad (2)$$

where  $V$  is the blade pulse voltage, RPM is the rotor shaft speed,  $k$  is the calibration factor,  $B(T)$  is the permanent magnetic field, which varies with temperature. The term  $f(\cdot)$  describes the lowpass effect of the sensor signal due to eddy currents in the sensor itself, resisting the change in magnetic field. The frequency of the low pass effect is determined by the  $\mu\sigma$  product of the material in the sensor, which varies with temperature. The term  $d_{\text{BLADE}} \sqrt{[\mu\delta]_{\text{BLADE}}(T)}$  describes how the pulse amplitude increases with the  $\mu\sigma$  product and the thickness of the blade. The  $(\text{gap} + r)^6$  term relates how the pulse amplitude changes with changing gap. For the practical usage the equation 2 can be simplified as equation 3.

$$\text{gap} = K \left( \frac{\text{RPM}}{V - V_{\text{start}}} \right)^{1/6} - r, \quad (3)$$

To validate blade sensor model the computational model was created in ANSYS Maxwell – electromechanical FEM based simulation software. This model contained three blades (with cyclic symmetric condition), sensor and stator ring. The magnetic field around of the sensor is excited by a permanent magnet which is the part of the sensor. Magnetic flux lines are closing across the stator ring and blade shrouds. Changes in magnetic flux, caused by the shrouds rotation, are detected by the sensor coil.

By this model it was tried to cover the real conditions in a steam turbine. The blades rotate 50Hz that implies the tip speed 640m/s. This speed requires the simulation time and the simulation time step which had to be quite small.

For final evaluation the triggering algorithm was used. It was the same triggering algorithm which had been used for real BTT data. It is a very robust algorithm which contains high pass and low pass filtering, arm level which activates a trigger and finally the trigger which waits for a falling or rising edge going across the 0 level. (The algorithm was taken from HoodTech BTT acquire SW, because the authors have very good experience with it on-site).

This algorithm finally provides a time of arrival of individual blades which correspond to actual blade position. In next figure (Fig. 2) there are the times of arrival shown by cross markers (one cross for one axial position). It can be seen that these crosses correspond to outgoing edge of the shroud below the sensor coil.

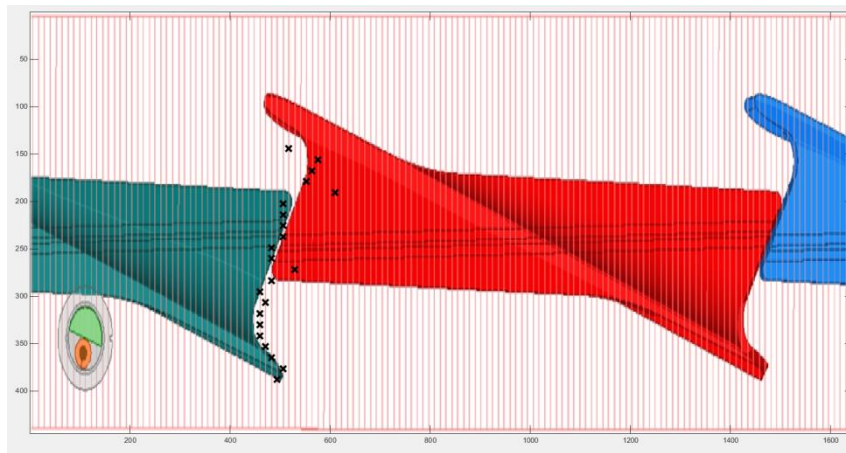


Figure 2 – Detection of the blade based on calculated signals and triggering algorithm

### 3.1 Experimental validation

The numerical calculation of the eddy-current sensor provides suitable solution. The next step was to verify the calculation by the measurement. The bladed disk was installed in to the Campbell machine. The Campbell machine is the vacuum chamber with rotor and one stage blade. The blades rotate in the vacuum with nominal speed and the vibration are excited by the electromagnets or oil jets.

The eddy-current sensors were installed into the vacuum chamber and used for measurement of time of arrival. The raw signals (before triggering algorithm usage) were recorded and then compared with calculation signals. The following figure 3 shows the comparison.

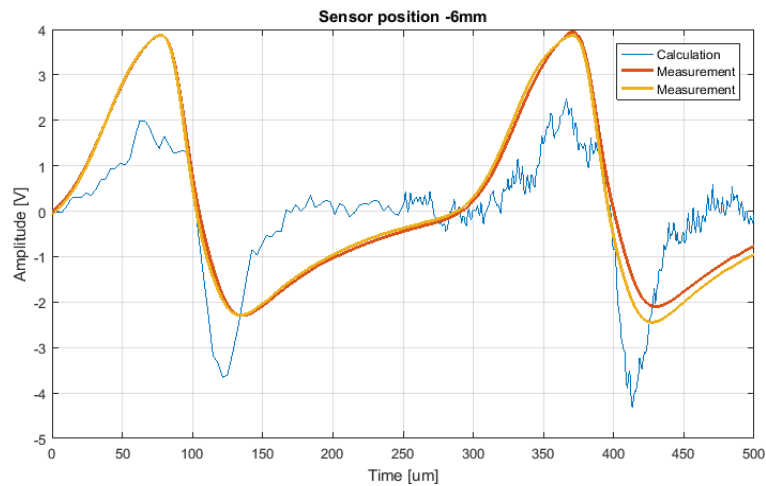


Figure 3 – Comparison of calculated signal (blue) and the measured signal from eddy-current sensor (red and yellow curves)

It is easy to see that calculated and real signals have same trends. The measured signals have lower noise than calculated one. The authors assume that the noise in the calculation is there because the 2 different meshes were used for the calculation – one for blades and second for electromagnetic surroundings. On the other hand the measured curve looks very smooth, it is happen because whole sensor system is behave like low pass filter.

#### 4 MEASUREMENT IN POWER STATION UNDER REAL AND SPECIAL OPERATIONAL CONDITIONS

The crucial task for blade monitoring is to determine blade vibration limits (BVL) which are basically dependent on blade mode shapes. In case of integrally coupled blading the nodal diameter also affects vibration limits.

BVL are evaluated base on blade material fatigue limit (Goodman diagram) and safety factors. When the safety factors are applied then two critical blade locations are distinguish: airfoil and dovetail.

Maximal allowable cyclic stress is defined as

$$\text{Airfoil} \quad \sigma_{max} = \frac{\sigma_F}{S_b S_e}, \quad (4)$$

$$\text{Dovetail} \quad \sigma_{max} = \frac{\sigma_F}{S_b S_e S_f} \quad (5)$$

Where:

$\sigma_F$	Fatigue strength reflecting mean stress preload ( Goodman diagram)
$S_b$	Basic safety factor
$S_e$	Safety factor for environment
$S_f$	Safety factor for fretting

Based on the FEM modal analysis the ratio R between dynamic cyclic stress at critical location and vibration amplitude of monitored tip location is determined for each mode shape and nodal diameter.

Maximal allowable vibration amplitude of the blade tip is determined as:

$$U_{max} = \frac{\sigma_{max}}{R}, \tag{6}$$

The BTT sensors monitor vibration only in circumferential direction therefore  $U_{max}$  has to be recalculated into proper direction in order to be used as BTT vibrational limits.

Figures 4 and 5 present typical  $U_{max}$  limits and BTT limits YC for the long LSB. Fatigue strength  $\sigma_F$  was determined based on the measured Wohler curve and Goodman diagram.

Figures 4 and 5 show that the most critical location from fatigue view is blade dovetail (root neck). This conclusion is also supported by the fact that the most cracks occur at the blade dovetails.

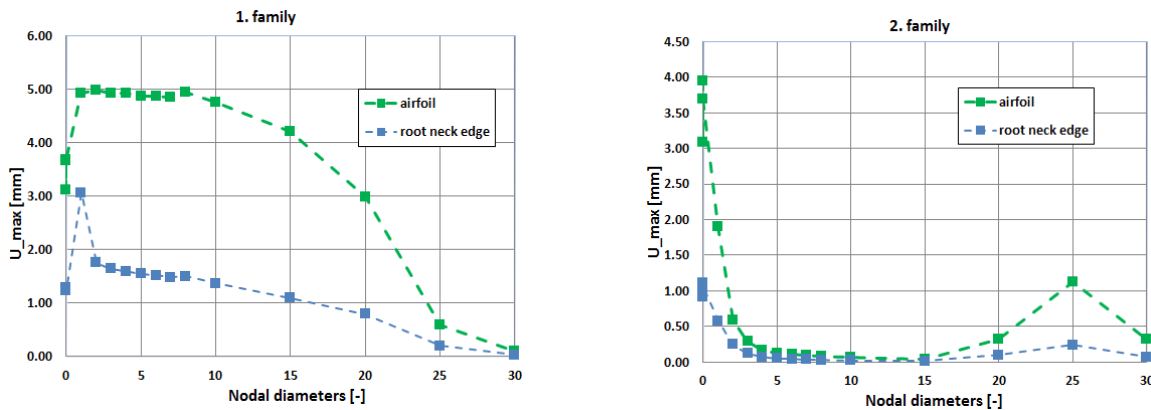


Figure 4 – Maximal allowable vibration amplitude at the blade tip for the first and second mode shape. Two critical locations are depicted

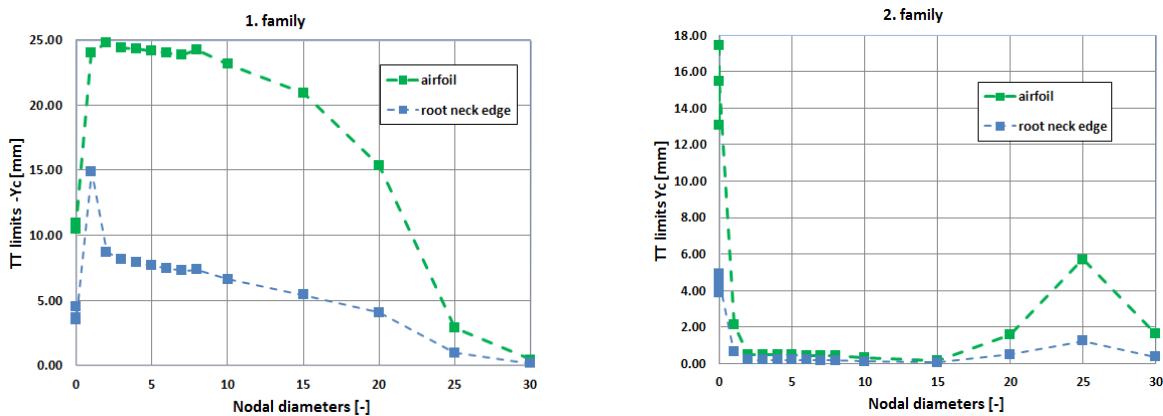


Figure 5 – BTT limits amplitude at leading edge for the first and second mode shape. Two critical locations are depicted

#### 4.1 Field vibration monitoring setup

In early 2013 biaxial magneto-resistive, standard eddy-current and green laser optical sensors were installed into the 270 MW steam turbine. The sensors were located in LP part and watched LSB tip trailing edge. Totally 18 sensors were installed non-uniformly around the half of bladed disk. There were 5 eddy-current sensors, 7 biaxial magneto-resistive sensors (2 pairs of 3 involved sensors and individual dual sensor) and 6 optical sensors. Blade tip timing system from Hoodtech was used with 200MHz sampling frequency and it was able to measure up to 32 channels. The system allows setting up a different trigger for each sensor which was necessary because the physical principle of the sensors were different. The differences between signals from optical and electrical based sensors are shown in Figure 6.

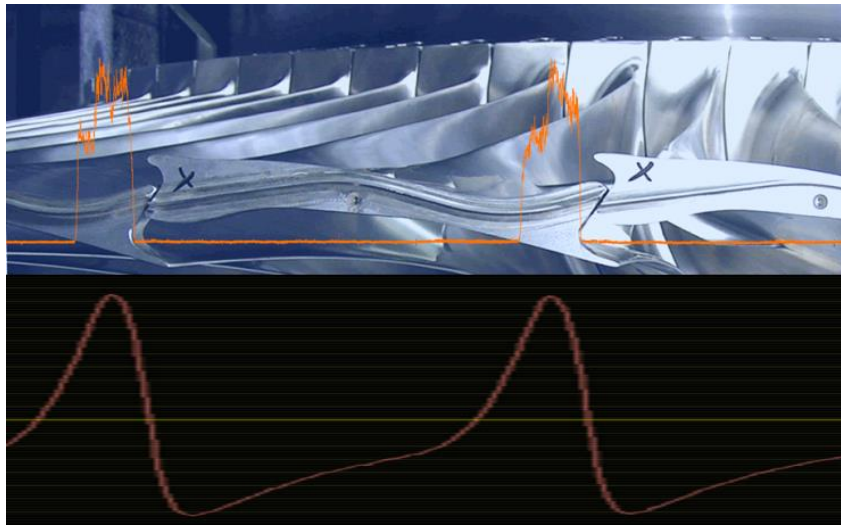


Figure 6 - different signal for triggering – upper picture represents optical signals and bottom picture is signal from eddy-current sensor

In 2016 on field blade monitoring was carried out at 135 MW steam turbine power plant. Seven different measuring runs were undertaken, see table 2. During the each run the back-pressure in condenser was gradually increasing from 10kPa to 42kPa. Both vacuum pumps were switched off one by one as required therefore vacuum drop control was limited however vacuum decay tendency (up to 2kPa/min) was still acceptable.

Table 2 - Measurement runs

1	1800rpm	Pre-heating of the turbine
2	3000rpm, 0MW	Large portion of steam was bypassed
3	20MW	Power control, certain portion of steam was bypassed
4	40MW	Power control, certain portion of steam was bypassed, LP regeneration switch on
5	65MW	Power control, LP regeneration switch on
6	90MW	Pressure control, not enough steam to maintain constant power
7	135MW	Pressure control, not enough steam to maintain constant power

Totally seven tests were done. Turbine reached seven different power outputs and then the back pressure was gradually changed (vacuum in condenser decrease from 0.05 up to 0.5 bar).

All measured data were evaluated by in-house code that was created for this purpose in MATLAB. It was found out that the blades vibrated under all operating regimes that were monitored:

- dominant vibration : 1st mode family, nodal diameters from 4 to 7 , ND5 – the most excited
- 2nd mode family was not observed

BTT vibration amplitudes were plotted in graphs with respect to nodal diameters see figures 7 to 8. Figures 9 show maximal BTT vibration amplitudes respectively.

Maximal vibrations in figure 9 are likely the most relevant amplitudes that should be focused on since they represent sum of all amplitudes but mostly those dominant related to ND4 to ND7. Even if the maximal vibration amplitudes are not presented continuously but only about 30% the total time a number of cycles related to these amplitudes are still sufficiently high in terms of high cycle fatigue (HCF).

The major output from the field monitoring of LSB is presented in the figures 7 to 9. It shows BTT amplitudes versus backpressure and volumetric flow. Red and black lines depict alarm and trip limits respectively. The colormap area in the above mentioned figures is limited by boiler capacity (mass flow) in other words the higher volumetric flow regimes for high backpressure than 42kPa are not reachable at this power plant.

After the evaluation of all data it became clear which type of sensor is the best. For operation with high steam parameters the laser sensor provides very accuracy signals without any electrical noise. On the other hand when the steam was wet and there were small water drops the signal was insufficient and it was not possible to measure blade vibration. Standard eddy-current sensors and newly developed magneto-resistive sensors [11] provided signals all the time. The differences between them could be shown only in all blade spectrums. The spectrum from biaxial magneto-resistive sensor is better in terms of signal to noise ratio. The 50 Hz and multiples of 50 Hz are very poor in spectrum of magneto-resistive sensor.

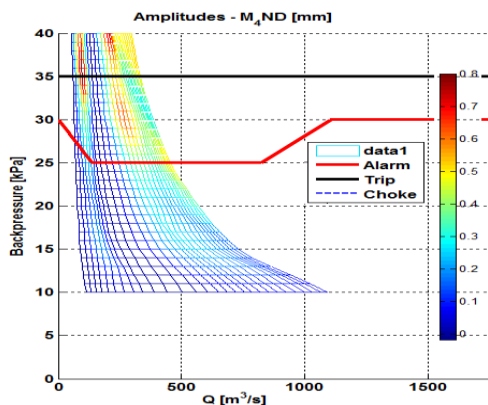


Figure 7 - TT vibration amplitudes (0-peak) for ND4

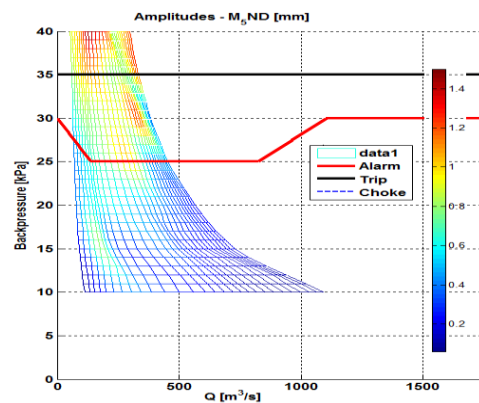


Figure 8 - TT vibration amplitudes (0-peak) for ND5

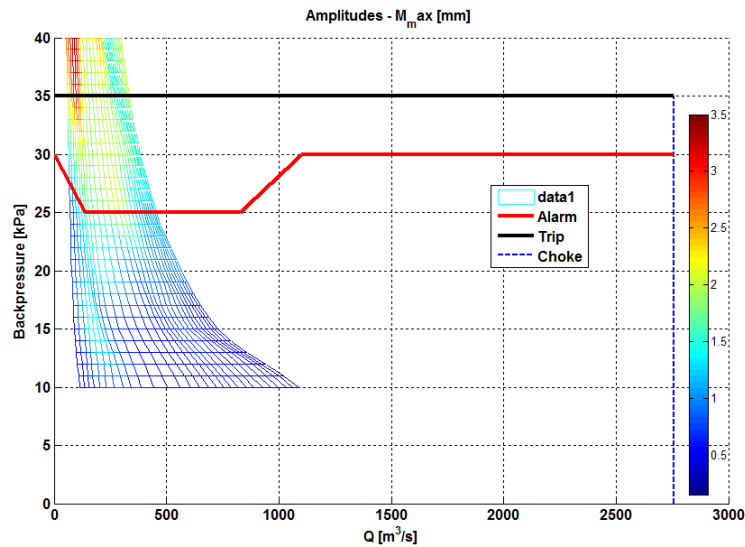


Figure 9 - BTT vibration amplitude - maximal from signal envelope (0-pk) versus backpressure and volumetric flow

## 5 CONCLUSION

The biaxial magnetolectric and optical sensors have proven successful in all installations. The sensors are designed for operation under a long-term temperature of 200°C and a short-term temperature of 250°C. Using permanent magnets in MR sensors as the source of the magnetic field simplified the sensor construction and increased its reliability. The most favourable properties of the group of magnetolectric sensors emphasized advantages of magneto-resistive sensors, which are characterized by high accuracy and sensitivity to displacement, wide frequency bandwidth (0 to 300 kHz) and a very important feature, which is the independence of the sensor output voltage magnitude on the speed of a blade passage. The advantage of this feature is that the sensors can be calibrated statically, for example using a positioning facility. The optical sensors with green laser source have been used in steam turbine with pretty good success. There are still some operational conditions in wet steam environment when the signal noise ratio is not good enough. Eddy-current sensors provide high quality signal as well and it was proven that it can be used for shrouded blades.

Several types of LSBs were measured under real and under special operational conditions. It was found out that the blades vibrated under all operating regimes that were monitored and the installed sensors were capable to identify the tip blade vibration.

It was proved that the blades can be operated in a wide range of operational conditions and they are resistant against high vibration.

The figures 7 - 9 proved Shnee hypothesis [7] that vibration in ventilation is 2-3 times higher. The windage condition are worst in terms of vibration which are 3 times higher than vibration at 100% volume even more the temperature increase dramatically.

## References

- [1] Benjamin Megerle, "Numerical and experimental investigation of the aerodynamic excitation of a model low-pressure steam turbine stage operation under low volume flow. ", GT2012-68384, Proceedings of ASME Turbo Expo 2012, June 11-15, 2012, Copenhagen, Denmark
- [2] Naoki Shibukawa, Yoshifumi Iwasaki, "A correlation between vibration stresses and flow features of steam turbine long blades in low load condition", GT2011-46368, Proceedings of ASME Turbo Expo 2011, June 6-10, 2011, Vancouver, British Columbia, Canada
- [3] M. Zielinski and G. Ziller, Noncontact Blade Vibration Measurement System for Aero Engine Application. MTU Aero Engines GmbH Engine Control and Testing Division 80995 München, German.
- [4] P. Beauseroy, R. Lengellé, Nonintrusive turbomachine blade vibration measurement system. System Modelling and Dependability Group - FRE CNRS 2848, Charles Delaunay Institute, Université de Technologie de Troyes BP2060 10010 TROYES Cedex, France
- [5] Y. Kadoy, M. Mase, Y. Kaneko, S. Umemura, T. Oda, M. C. Johnson, "Noncontact Vibrational Measurement Technology of Steam Turbine Blade", JSME International Journal, Vol. 38, No. 3, 1995.
- [6] Zdenek Kubin, Vaclav Cerny, Pavel Panek, Tomas Misek, Jan Hlous, Lubos Prchlik. "Determination of crack initiation on L-1 LP steam turbine blades, Part 1: Measurements on rotor train, material specimens and blades", GT2011 – 46203, Proceedings of ASME Turbo Expo 2011, June 6-10, 2011 Vancouver Canada
- [7] Y. Shnee, et al., "Influence of the operational factors on dynamic stresses in moving blades of a turbine stage", Teploenergetika, vol. 21, pp. 49-52, 1974
- [8] MISEK, T., Kubin, Z., Duchek, K., 2009, "Static and Dynamic Analysis of 48" Steel Last Stage Blade for Steam Turbine", Proceedings of ASME Turboexpo: Power for Land Sea and Air, Orlando, USA
- [9] PRCHLIK, L., Kubin, Z., Duchek, K., 2009, "THE Measurement of dynamic vibration modes and frequencies of a large LP bladed disc", Proceedings of ASME Turboexpo 2009: Power for Land, Sea and Air, Orlando, USA
- [10] Misek, T., et al., 2014. "Development of the New 54" Titanium Last Stage Blade", Power-Gen Europe, Cologne, Germany.
- [11] P. Procházka, and F. Vaněk, , "New Methods of Non-Contact Sensing of Blade Vibrations and Deflections in Turbomachinery", IEEE Trans. Instrum. Meas., vol. 63, p. 1583-1592, June 2014.
- [12] Kubín, Z., Liška, J., Mišek, T., Procházka, Pavel, "Application of non-contact vibration measurements on a 48" blade under low load condition", DYMAMESI 2017. Cracow (PL), 28.02.2017-01.03.2017, s. 45-54. ISBN 978-80-87012-62-8.
- [13] Zdenek Kubin, Tomas Misek, Jan Hlous, Tereza Dadakova, Josef Kellner, Tibor Bachorec, „CALIBRATION OF BLADE TIP-TIMING SENSOR FOR SHROUDED 40" LSB“, Mechanical Systems and Signal Processing, Volume 108, August 2018, Pages 88-98
- [14] Nidhal Jamia, Michael I Friswell, Sami El-Borgi, Ralston Fernandes, Simulating eddy current senso outputs for blade tip timing, Advances in Mechanical Engineering, 2018, Vol. 10(1) 1–12, DOI: 10.1177/1687814017748020

## A BASIC CELL MODELING METHOD FOR HOMOGENIZATION ANALYSIS OF PLAIN-WOVEN COMPOSITES WITH NESTING

G. KUBO\*, T. MATSUDA<sup>†</sup>, AND Y. SATO<sup>†</sup>

\*Affiliation

Department of Engineering Mechanics and Energy  
University of Tsukuba  
Tsukuba, Ibaraki, Japan  
Email address; s1730189@s.tsukuba.ac.jp

<sup>†</sup>Affiliation

Department of Engineering Mechanics and Energy  
University of Tsukuba  
Tsukuba, Ibaraki, Japan  
Email address; matsuda@kz.tsukuba.ac.jp

**Key words:** Plain-woven composite, Nesting, basic cell, Homogenization, Viscoplasticity.

**Abstract.** A basic cell modeling method is newly developed for the homogenization analysis of plain-woven composites with nesting. For this, based on the periodicity and point-symmetry of internal structures of plain-woven composites with nesting, a hexagonal prism-shaped basic cell and its boundary conditions are proposed. The basic cell and boundary conditions are then introduced into the homogenization theory for nonlinear time-dependent composites developed by the authors. Using the present method, elastic-viscoplastic behavior of a plain-woven glass fiber-reinforced plastic (GFRP) composite with nesting subjected to on- and off-axis loading is analyzed. In the analysis, the present method is successful in significantly reducing the analysis domain, and in achieving the modeling of a high volume fraction of fiber bundles caused by nesting. This cannot be attained if conventional cuboid cells are employed as analysis domains. Moreover, it is shown from the analysis results that the present method accurately predicts experimentally observed macroscopic elastic-viscoplastic behavior of the plain-woven GFRP composite with nesting.

### 1 INTRODUCTION

Plain-woven composites have many positive features, for example, high specific strength, high specific stiffness and good formability. Therefore, they have been used as primary structural members in many industrial fields such as the aerospace, auto and energy-related industries. Plain-woven composites are generally produced by stacking plain fabrics and impregnating them with polymer materials (Fig. 1). During this forming process, fabric layers are not necessarily

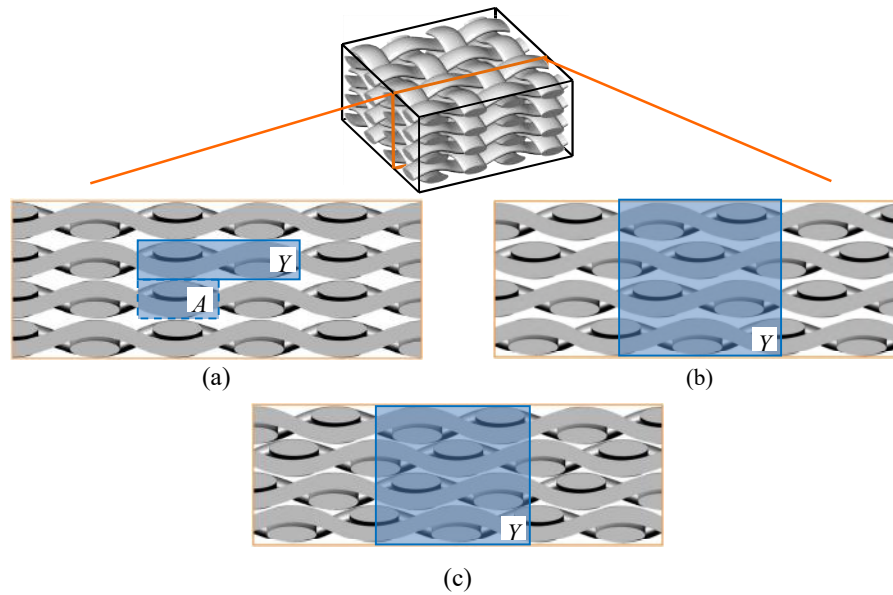


Fig. 1. Microstructures and unit cells of plain-woven laminates; (a) without misalignment, (b) with misalignment of  $1/4$  unit cell length, (c) with nesting.

aligned (Fig. 1(a)), but can be shifted in the in-plane directions (Fig. 1(b)), which will be referred to as "laminates misalignment". Moreover, compression in the forming process causes the fabric layers to press into each other in the stacking direction. Consequently, complicated internal structures as illustrated in Fig. 1(c), which are generally called "nesting", can occur in plain-woven composites [1-5]. It is known that the nesting can affect the mechanical properties of plain-woven composites, which is not limited to elastic properties such as initial stiffness [5-8], but extends to inelastic properties such as damage behavior and strength [9]. Therefore, we should consider the effects of nesting when analyzing the mechanical properties of plain-woven composites.

For such mechanical analysis of plain-woven composites with nesting, numerical unit cell analysis based on the finite element method (FEM) or homogenization theory [10] is considered as one of the most promising methods. This is because it can explicitly take into account the nesting structures in plain-woven composites. Such analysis, however, encounters two main difficulties. One is how we can easily generate unit cell geometries and FE meshes for unit cells of plain-woven composites with nesting. In general, the aforementioned complicated internal structures of plain-woven composites with nesting make it difficult and cumbersome to generate their unit cells and FE meshes. The second difficulty is that enormous computational costs are required for the analysis because unit cells with nesting basically become much larger than that without nesting due to the restriction of the periodic boundary condition (see the unit cells  $Y$  in Fig. 1). This can be a critical issue, especially for nonlinear analysis accompanied by incremental computation. For these reasons, the nesting has been ignored in many unit cell analyses [11-13] including our previous studies [14-16].

To overcome the above-mentioned difficulties, some researchers developed the methods to generate geometries and FE meshes of unit cells of woven composites with nesting using micro-computed tomography (CT) or scanning electron microscope (SEM) digital images [17-20]. These methods provided easier generation of realistic geometries for unit cells, e.g. shapes of

fiber bundles and degree of nesting. However, the number of elements in the unit cells became considerably large to obtain appropriate solutions, resulting in application of the methods only to two-dimensional or elastic analyses. In addition, it is difficult for the image-based modeling methods to guarantee the periodic connectivity of unit cells.

In this study, a basic cell modeling method is newly developed for the homogenization analysis of plain-woven composites with nesting, and is applied to an elastic-viscoplastic analysis of plain-woven glass fiber-reinforced plastic (GFRP) composites with nesting. For this, focusing on the periodicity and symmetry of internal structures of plain-woven composites with nesting, a novel basic cell and its boundary conditions are proposed. The basic cell and boundary conditions are introduced into the homogenization theory for nonlinear time-dependent composites developed by the authors [21-23]. The proposed method is then applied to an elastic-viscoplastic analysis of plain-woven GFRP composites with nesting subjected to on- and off-axis loading. Comparing the analysis results with experimental data, we validate the present method.

## 2 BASIC CELL FOR PLAIN-WOVEN COMPOSITES WITH NESTING AND HOMOGENIZATION THEORY

### 2.1 Introduction of the basic cell and properties of internal distributions

We consider a plain-woven composite with nesting on the Cartesian coordinates  $y_i$  ( $i=1, 2, 3$ ) as illustrated in Fig. 2, in which each plain fabric is assumed to possess the same degree of nesting in the  $y_3 - y_1$  plane. The composite is assumed to be subjected to a macroscopically uniform load, and to deform infinitesimally. Then, not a conventional cuboid cell [10-16] but a hexagonal prism cell shown in Fig. 2, which will hereafter be called "basic cell  $A$ ", is defined as an analysis domain. The boundary of  $A$ ,  $\Gamma$ , is divided into  $\Gamma_\alpha$  ( $\alpha=1, 2, \dots, 8$ ) as depicted in Fig. 3, where  $\Gamma_1 - \Gamma_4$  are sequentially numbered in the counterclockwise direction from the upper right to the front boundary facets as indicated in Fig. 3(a), and  $\Gamma_5 - \Gamma_8$  are also sequentially numbered in the counterclockwise direction from the lower left to the rear boundary facets as indicated in Fig. 3(b). It should be noted that  $A$  is much smaller than the unit cell  $Y$  [11, 13, 15] generally employed in the homogenization analysis on the basis of the so-called  $Y$ -periodic boundary condition.

Now, the microscopic velocity field  $\dot{u}_i(\mathbf{y}, t)$  in  $A$  is expressed as [10]

$$\dot{u}_i(\mathbf{y}, t) = \dot{F}_{ij}(t)y_j + \dot{u}_i^\#(\mathbf{y}, t), \quad (1)$$

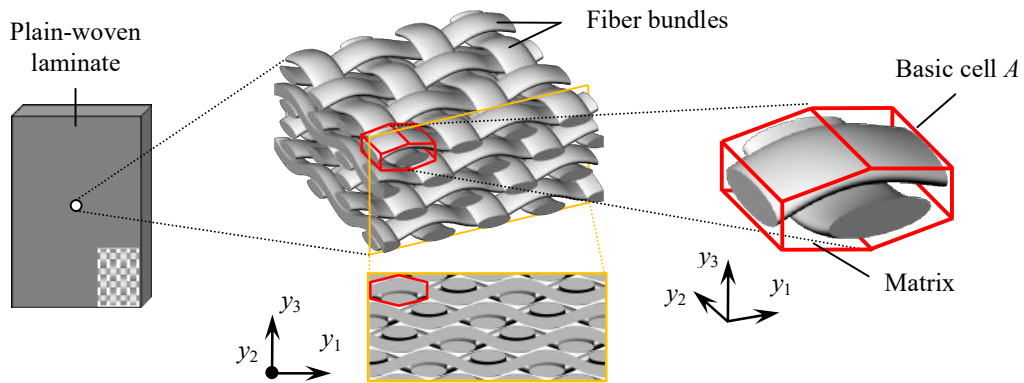
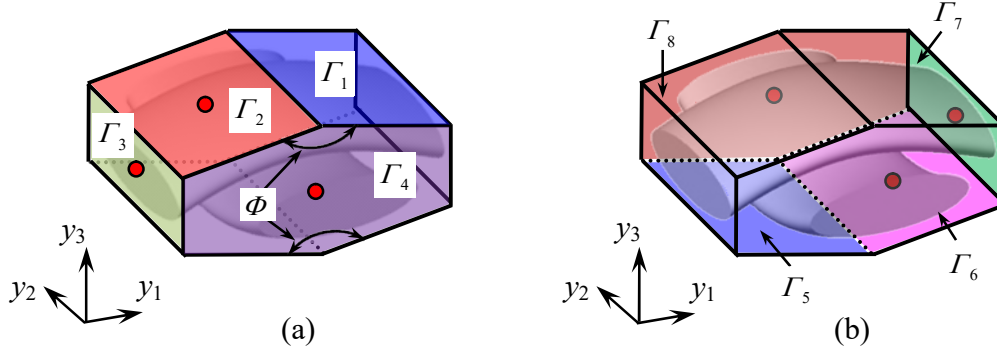


Fig. 2. Plain-woven composite with nesting in the  $y_3 - y_1$  plane and basic cell  $A$ .


 Fig. 3. Boundary facets of  $A$ ; (a)  $\Gamma_1 - \Gamma_4$ , (b)  $\Gamma_5 - \Gamma_8$ .

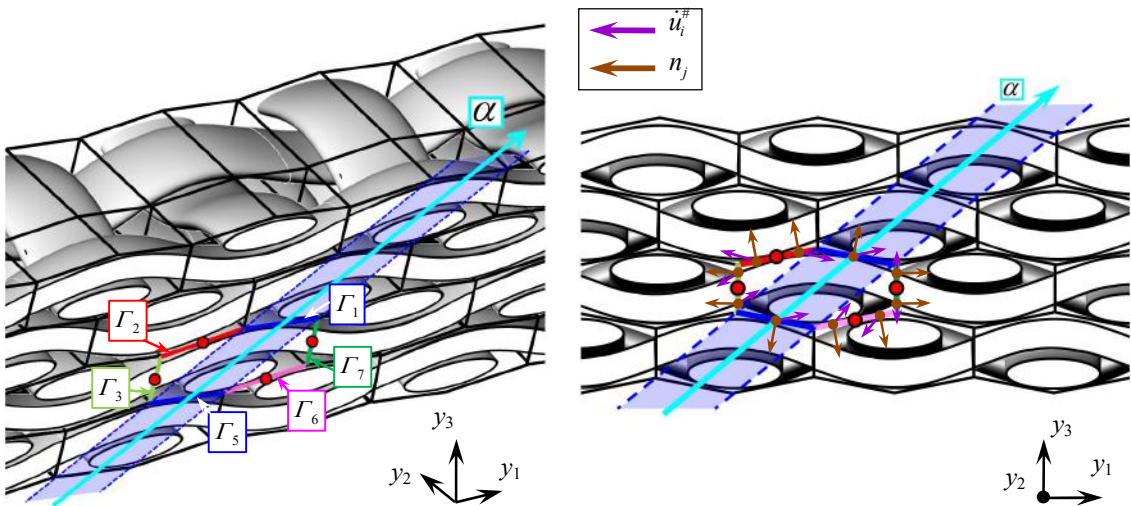
where  $(\cdot)$  indicates the differentiation with respect to  $t$ ,  $F_{ij}(t)$  is the macroscopic deformation gradient, and  $\dot{u}_i^\#(y, t)$  is the perturbed velocity. In the present nesting case, it is found from the cross-sectional view as illustrated in Fig. 4 that the microstructure possesses the periodicity in the  $\alpha$ -direction. Thus,  $\dot{u}_i^\#$  must be periodically distributed on  $\Gamma_1$  and  $\Gamma_5$ . Further, one can find that the microstructure possesses the point-symmetries with respect to the centers of  $\Gamma_2, \Gamma_3, \Gamma_6$  and  $\Gamma_7$ . In addition, such point-symmetries are satisfied with respect to the centers of  $\Gamma_4$  and  $\Gamma_8$ . This suggests that  $\dot{u}_i^\#$  on  $\Gamma_2 - \Gamma_4$  and  $\Gamma_6 - \Gamma_8$  should be point-symmetrically distributed with respect to these points (Fig. 4). It is clear that these periodicity and point-symmetries hold regarding the microscopic stress  $\sigma_{ij}$  and its rate  $\dot{\sigma}_{ij}$ .

## 2.2 Weak form of equilibrium of microscopic stress and its integral terms

The equilibrium of  $\sigma_{ij}$  in  $A$  can be expressed in a rate form as

$$\dot{\sigma}_{ij,j} = 0, \quad (2)$$

where  $(\cdot)_{,j}$  denotes the differentiation with respect to  $y_j$ . The integration by parts and the divergence theorem allow Eq. (2) to be transformed to a weak form:


 Fig. 4. Periodicity in the  $\alpha$ -direction and point-symmetries with respect to the centers of  $\Gamma_2, \Gamma_3, \Gamma_6$  and  $\Gamma_7$ , and perturbed velocity field  $\dot{u}_i^\#$  and unit normal vector  $n_i$  on each boundary facet.

$$\int_A \dot{\sigma}_{ij} v_{i,j} dA - \int_{\Gamma} \dot{\sigma}_{ij} n_j v_i d\Gamma = 0, \quad (3)$$

where  $v(\mathbf{y}, t)$  is an arbitrary variation of  $\dot{u}_i^{\#}$ , and  $n_j$  is the unit vector outward normal to  $\Gamma$ . It is noted that the boundary integral term in Eq. (3) can be expressed as

$$\int_{\Gamma} \dot{\sigma}_{ij} n_j v_i d\Gamma = \sum_{\alpha=1}^8 \int_{\Gamma_{\alpha}} \dot{\sigma}_{ij} n_j v_i d\Gamma. \quad (4)$$

On  $\Gamma_1$  and  $\Gamma_5$ , the periodicity of  $v_i$  and  $\dot{\sigma}_{ij}$  is satisfied as already described in the previous subsection, whereas  $n_j$  takes the opposite directions on these boundary facets (Fig. 4), leading to the following relationship:

$$\int_{\Gamma_1} \dot{\sigma}_{ij} n_j v_i d\Gamma + \int_{\Gamma_5} \dot{\sigma}_{ij} n_j v_i d\Gamma = 0. \quad (5)$$

On  $\Gamma_2 - \Gamma_4$  and  $\Gamma_6 - \Gamma_8$ , in contrast, the point-symmetries of  $v_i$  and  $\dot{\sigma}_{ij}$  with respect to the centers of these facets are satisfied, whereas  $n_j$  keeps the same direction on the facets (Fig. 4). Thus, the boundary integral terms with respect to these areas become zero, and we obtain

$$\int_{\Gamma_{\alpha}} \dot{\sigma}_{ij} n_j v_i d\Gamma = 0, \quad (\alpha=2-4, 6-8). \quad (6)$$

From Eqs. (4), (5) and (6), the second term on the left side of Eq. (3) vanishes, which enables Eq. (3) to be rewritten as

$$\int_A \dot{\sigma}_{ij} v_{i,j} dA = 0. \quad (7)$$

### 2.3 Homogenization

The constitutive equation of constituents in  $A$  is expressed in a rate form as

$$\dot{\sigma}_{ij} = c_{ijkl} (\dot{\epsilon}_{kl} - \beta_{kl}), \quad (8)$$

where  $c_{ijkl}$  and  $\beta_{kl}$  respectively denote the elastic stiffness and viscoplastic strain rate of the constituents, satisfying  $c_{ijkl} = c_{jikl} = c_{ijlk} = c_{klij}$  and  $\beta_{kl} = \beta_{lk}$ ,  $\dot{\epsilon}_{kl}$  indicates the microscopic strain rate. As already stated in the previous subsection, Eq. (7) has the same form as that of the original homogenization theory [10, 21, 22]. Therefore, according to the earlier works [21, 22], we can derive the following evolution equation of microscopic stress, and the relation between macroscopic stress rate  $\dot{\Sigma}_{ij}$  and macroscopic strain rate  $\dot{E}_{ij}$ :

$$\dot{\sigma}_{ij} = c_{ijpq} (\delta_{pk} \delta_{ql} + \chi_{p,q}^{kl}) \dot{E}_{kl} - c_{ijkl} (\beta_{kl} - \varphi_{k,l}), \quad (9)$$

$$\dot{\Sigma}_{ij} = \langle c_{ijpq} (\delta_{pk} \delta_{ql} + \chi_{p,q}^{kl}) \rangle \dot{E}_{kl} - \langle c_{ijkl} (\beta_{kl} - \varphi_{k,l}) \rangle, \quad (10)$$

where  $\delta_{ij}$  indicates the Kronecker's delta,  $\langle \# \rangle$  stands for the volume average in  $A$ , i.e.  $\langle \# \rangle = |A|^{-1} \int_A \# dA$ , where  $|A|$  signifies the volume of  $A$ . Moreover,  $\chi_p^{kl}$  and  $\varphi_k$  are the functions to be determined by solving the following boundary value problems for  $A$ :

$$\int_A c_{ijpq} \chi_{p,q}^{kl} v_{i,j} dA = - \int_A c_{ijkl} v_{i,j} dA, \quad (11)$$

$$\int_A c_{ijpq} \varphi_{p,q} v_{i,j} dA = \int_A c_{ijkl} \beta_{kl} v_{i,j} dA, \quad (12)$$

In general, the boundary value problems (11) and (12) are solved numerically to find  $\chi_p^{kl}$  and  $\varphi_k$  using the FEM. In this analysis, we impose the combination of the periodicity and point-symmetries already described in the previous subsections on  $\chi_p^{kl}$  and  $\varphi_k$  as the boundary conditions. It should be noted that the present modeling method, including the boundary conditions, enables us to substantially reduce the analysis domain for plain-woven composites with nesting compared with the previous methods mentioned in the introduction, which is eminently suitable for nonlinear analysis accompanied by incremental computation.

### 3 ELASTIC-VISCOPLASTIC ANALYSIS OF PLAIN-WOVEN GFRP COMPOSITES WITH NESTING

#### 3.1 Basic cell

To determine the geometry of the basic cell  $A$ , we performed SEM observation of cross-sections of the plain-woven GFRP composite. It is noted that, in the composite, nesting predominantly existed in the plane parallel to the warp-direction, whereas there was less nesting in the plane parallel to the weft-direction. We then measured the wavelength, shape, size and volume fraction of the fiber bundles, the fiber volume fraction in fiber bundles, and calculated their averaged values. Based on these observation results and averaged values,  $A$  with nesting in the  $y_3 - y_1$  plane with 69% volume fraction of fiber bundles was defined using the aforementioned hexagonal prism cell (Fig. 5), and was divided into eight-node isoparametric elements (1888 elements, 2329 nodes). It is noteworthy that the number of elements, 1888, is much smaller than in the preceding studies dealing with plain-woven composites with nesting [5, 17].

#### 3.2 Material properties

Fiber bundles were regarded as E-glass/epoxy unidirectional composites, and as transversely isotropic elastic materials. Their material properties were calculated using the homogenization theory on the assumption that the fiber volume fraction in fiber bundles was 72% in the accordance with the microscope observation, and that the fiber bundles had a hexagonal fiber array. The elastic constants of the E-glass fibers and epoxy used in the calculation were set as

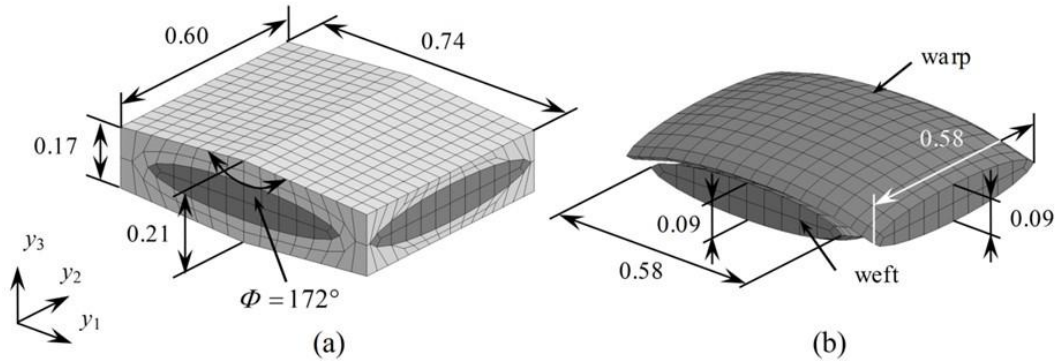


Fig. 5. Basic cell  $A$  of plain-woven GFRP laminates with nesting (1888 elements, 2329 nodes) with dimensions in mm; (a) full view, (b) fiber bundles (weft and warp) in  $A$ .

listed in Table 1. The epoxy matrix, on the other hand, was regarded as an isotropic elastic-viscoplastic material that obeyed the following constitutive equation [21-23]:

$$\dot{\epsilon}_{ij} = \frac{1+\nu_m}{E_m} \dot{\sigma}_{ij} - \frac{\nu_m}{E_m} \dot{\sigma}_{kk} \delta_{ij} + \frac{3}{2} \dot{\epsilon}_0^p \left[ \frac{\sigma_{eq}}{g(\bar{\epsilon}^p)} \right]^n \frac{s_{ij}}{\sigma_{eq}}, \quad (13)$$

where  $E_m$ ,  $\nu_m$  and  $n$  represent material constants,  $g(\bar{\epsilon}^p)$  stands for the exponential hardening function (Voce's hardening function) depending on the equivalent viscoplastic strain  $\bar{\epsilon}^p$  [19,24],  $\dot{\epsilon}_0^p$  signifies the reference strain rate,  $s_{ij}$  denotes the deviatoric part of  $\sigma_{ij}$ , and  $\sigma_{eq} = \left[ (3/2) s_{ij} s_{ij} \right]^{1/2}$ . In this study, no failure of the fiber bundles and epoxy, and no delamination between the fiber bundles and epoxy were considered.

### 3.3 Loading condition

The plain-woven GFRP composites were subjected to a macroscopically uniaxial tensile load at a constant strain rate of  $10^{-5} \text{ s}^{-1}$  at room temperature. Five kinds of off-axis angles, i.e.  $\theta = 0, 15, 30, 45$  and  $90^\circ$ , were considered.

### 3.4 Results of analysis

Figure 6 shows the macroscopic stress-strain relations obtained from the present analysis and the tensile tests of the plain-woven GFRP composite with nesting subjected to the uniaxial

Table 1 Material constants.

E-glass	$E_f = 80.0 \times 10^3$	$\nu_f = 0.22$	
Epoxy	$E_m = 3.5 \times 10^3$	$\nu_m = 0.35$	$\dot{\epsilon}_0^p = 1.0 \times 10^{-5}$
	$n = 30$	$g(\bar{\epsilon}^p) = 19 - 18 \times \exp(-190 \times \bar{\epsilon}^p)$	

MPa (stress), mm/mm (strain), s (time)

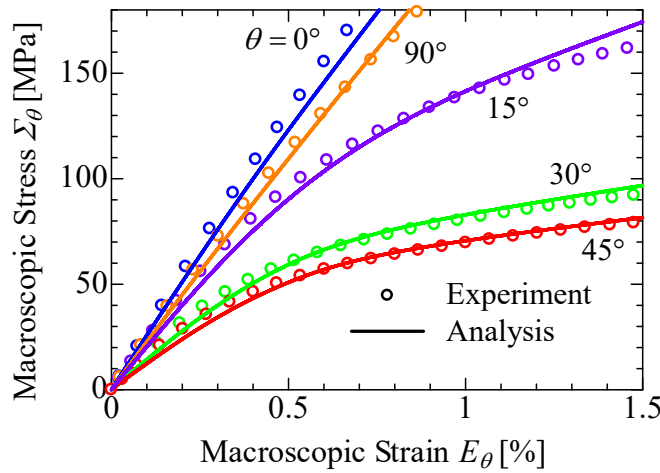


Fig. 6. Macroscopic stress-strain relations of plain-woven GFRP laminate with nesting at  $\theta = 0, 15, 30, 45$  and  $90^\circ$  at  $\dot{E}_\theta = 1.0 \times 10^{-5} \text{ s}^{-1}$ .

tension with  $\theta = 0, 15, 30, 45$  and  $90^\circ$ . In the figure, the analysis and the experimental results are respectively indicated by the solid lines and open circles. As seen from the experimental results in Fig. 6, the macroscopic stress-strain relations markedly depend on  $\theta$ , indicating that the plain-woven GFRP composite possesses remarkable elastic-viscoplastic anisotropy [13-15]. Comparing such experimental data with the analysis results, it is found that the present modeling method is successful in predicting the macroscopic behavior of the plain-woven GFRP composite.

#### 4 CONCLUSIONS

- The present method enabled us to substantially reduce the analysis domain for the homogenization analysis of plain-woven composites with nesting compared with the previous methods. This is eminently suitable for nonlinear analysis accompanied by incremental computation including the elastic-viscoplastic analysis performed in this study.
- High volume fraction of fiber bundles (69% in the present case) was achieved using the present modeling method. This could not be attained if conventional cuboid cells were employed. The present method therefore becomes significantly effective, especially in the case of the high volume fraction of fiber bundles caused by nesting as seen in the plain-woven GFRP composite dealt with in this study.
- Comparison between the analysis and the experimental results revealed that the present method was capable of accurately predicting the in-plane macroscopic elastic-viscoplastic behavior of the plain-woven GFRP composite with nesting.

#### ACKNOWLEDGMENTS

This presentation is based on results obtained from a project (P16010) commissioned by the New Energy and Industrial Technology Development Organization of Japan (NEDO). The presenter, G. Kubo, is grateful to the International Association for Computational Mechanics (IACM) for providing the IACM Scholarship covering his registration fee to participate in the 13th World Congress on Computational Mechanics (WCCM XIII) and the 2nd PanAmerican Congress on Computational Mechanics (PANACM II).

#### REFERENCES

- [1] Mesogitis, T.S., Skordos, A. and Long, A.C. Uncertainty in the manufacturing of fibrous thermosetting composites: A review. *Compos. Part A Appl. Sci. Manuf.* (2014) 57:67-75.
- [2] Yurgartis, S.W., Morey, K. and Jortner, J. Measurement of yarn shape and nesting in plain-weave composites. *Compos. Sci. Technol.* (1993) 46:39-50.
- [3] Saunders, R.A., Lekakou, C. and Bader, M.G. Compression and microstructure of fibre plain woven cloths in the processing of polymer composites. *Compos. Part A Appl. Sci. Manuf.* (1998) 29:443-454.

- [4] Hagiwara, K., Ishijima, S., Takano, N., Ohtani, A. and Nakai, A. Parameterization, statistical measurement and numerical modeling of fluctuated meso/micro-structure of plain woven fabric GFRP laminate for quantification of geometrical variability. *Mech. Eng. J.* (2017) 17-00053:1-12.
- [5] Lomov, S.V, Verpoest, I., Peeters, T., Roose, D. and Zako, M. Nesting in textile laminates: geometrical modeling of the laminate. *Compos. Sci. Technol.* (2003) 63:993-1007.
- [6] Naik, N.K. and Kuchibhotla, R. Analytical study of strength and failure behaviour of plain weave fabric composites made of twisted yarns. *Compos. Part A Appl. Sci. Manuf.* (2002) 33:697–708.
- [7] Ito, M. and Chou, T.W. An analytical and experimental study of strength and failure behaviour of plain weave composites. *J. Compos. Mater.* (1998) 32:2–30.
- [8] Olave, M., Vanaerschot, A., Lomov, S.V. and Vandepitte, D. Internal geometry variability of the stiffness. *Polym. Compos.* (2012) 33:1335-1350.
- [9] Olave, M., Vara, I., Husabiaga, H., Aretxabaleta, L., Lomov, S.V. and Vandepitte, D. Nesting effect on the mode I fracture toughness of woven laminates. *Compos. Part A Appl. Sci. Manuf.* (2015) 74:166-173.
- [10] Suquet, P.M. Elements of homogenization for inelastic solid mechanics. In: Sanchez-Palencia E., Zaoui, A., editors. *Homogenization techniques for composite media, lecture notes in physics, 272.* Berlin: Springer-Verlag; 1987.
- [11] Takano, N., Uetsuji, Y., Kashiwagi, Y. and Zako, M. Hierarchical modeling of textile composite materials and structures by the homogenization method. *Model. Simul. Mater. Sci. Eng.* (1999) 7:207-231.
- [12] Zako, M., Uetsuji. Y. and Kurashiki. T. Finite element analysis of damaged woven fabric composite materials. *Compos. Sci. Technol.* (2003) 63:507-516.
- [13] Carvelli, V., Poggi, C. A homogenization procedure for the numerical analysis of woven fabric composites. *Compos. Part A Appl. Sci. Manuf.* (2001) 32:1425-1432.
- [14] Matsuda, T., Nimiya, Y., Ohno, N. and Tokuda, M. Elastic-viscoplastic behavior of plain-woven GFRP laminates: Homogenization using reduced domain of analysis. *Compos. Struct.* (2007) 79:493-500.
- [15] Matsuda, T., Kanamaru, S., Yamamoto, N. and Fukuda, Y. A homogenization theory for elastic-viscoplastic materials with misaligned internal structures. *Int. J. Plast.* (2011) 27:2056-2067.

- [16] Matsuda, T., Kanamaru, S., Honda, N., Ohno, N. Macro/micro elastic-viscoplastic analysis of woven composite laminates with misaligned woven fabrics. *Adv. Struct. Mater.* (2013) 19:251-261.
- [17] Hivet, G. and Boisse, P. Consistent 3D geometrical model of fabric elementary cell. Application to a meshing preprocessor for 3D finite element analysis. *Finite. Elem. Anal. Des.* (2005) 42:25-49.
- [18] Faes, J.C., Rezaei, A., Paepegem, W. V. and Degrieck, J. Accuracy of 2D FE models for prediction of crack initiation in nested textile composites with inhomogeneous intra-yarn fiber volume fraction. *Compos. Struct.* (2016) 140:11-20.
- [19] Kim, J.H., Ryou, H., Lee, M., Chung, K., Youn, J.R. and Kang, T.J. Micromechanical modeling of fiber reinforced composites based on elastoplasticity and its application for 3D braided Glass/Kevlar composites. *Polym. Compos.* (2007) 28:722-732.
- [20] Potter, E., Pinho, S.T., Robinson, P., Lannucci, L. and McMillan, A.J. Mesh generation and geometrical modelling of 3D woven composites with variable tow cross-section. *Comp. Mater. Sci.* (2012) 51:103-111.
- [21] Ohno, N., Wu, X. and Matsuda, T. Homogenized properties of elastic-viscoplastic composites with periodic internal structures. *Int. J. Mech. Sci.*(2000) 42:1519-1536.
- [22] Ohno, N., Matsuda, T. and Wu, X. A homogenization theory for elastic-viscoplastic composites with point symmetry of internal distributions. *Int. J. Solids. Struct.*(2001) 38:2867-2878.
- [23] Matsuda, T., Ohno, N., Tanaka, H. and Shimizu, T. Effects of fiber distribution on elastic-viscoplastic behavior of long fiber-reinforced laminates. *Int. J. Mech. Sci.* (2003) 45:1583-1598.
- [24] Iltchev, A., Marcadon, V., Kruch, S. and Forest, S. Computational homogenisation of periodic cellular materials: Application to structural modeling. *Int J Mech. Sci.* (2015) 93:240-255.

## **A Control Volume Finite Element Approach for Modeling Molten Corium Spreading and Solidification**

Alec Kucala<sup>\*</sup>, Rekha Rao<sup>\*\*</sup>, Lindsay Erickson<sup>\*\*\*</sup>, David Noble<sup>\*\*\*\*</sup>

<sup>\*</sup>Sandia National Laboratories, <sup>\*\*</sup>Sandia National Laboratories, <sup>\*\*\*</sup>Sandia National Laboratories, <sup>\*\*\*\*</sup>Sandia National Laboratories

### **ABSTRACT**

When the core is breached during a severe nuclear accident, a molten mixture of nuclear fuel, cladding, and structural supports is discharged from the reactor vessel, which is often referred to as "corium". This scenario poses a difficult modeling problem due to the presence of large Peclet and Reynolds numbers, whereby the standard Galerkin based finite-element method (GFEM) technique is inadequate in suppressing the spurious oscillations in the mass, momentum, and energy equations. To address these oscillations, we implement a control volume finite element method (CVFEM) which allows for an upwinding treatment of the advection terms in the momentum and energy equations. Modeling the spreading of molten corium also requires a robust and accurate representation of the corium/air interface in two- and three-dimensions. To accomplish this, the conformal decomposition finite element method (CDFEM) is utilized to dynamically discretize the moving interface, allowing for the direct application of boundary conditions at the melt/air interface, such as surface tension and radiative energy transfer to the surrounding air. This CVFEM-CDFEM approach is used to model the spreading of molten corium in two- and three-dimensions, where the solidification of the melt is modeled using a temperature-dependent viscosity model. First, it is shown that the CVFEM technique is able to suppress spurious oscillations that GFEM cannot, where upwinding is introduced in the advection terms of the level set, momentum and energy equations. Our model is then compared directly with the FARO L26 corium spreading experiments and with previous numerical simulations in two- and three-dimensions. In these comparisons, good agreement is obtained with the evolution of the time-dependent corium spreading front.

## **Evaluation of Vehicle Aerodynamic Performance with Lane Change and Passing Using CFD and MBD**

Toshifumi Kudo\*

\*Altair Engineering

### **ABSTRACT**

Evaluation of aerodynamic performance using Wind Tunnels and CFD analysis conducted in each OEMs has great contribution to improve fuel consumption and performance of automobiles. The CFD has become more detail and has been able to solve a bigger scale problem in every year, a deviation between experimental and analysis results almost negligible and it is an effective tool for design and development process. However, is it enough to perform only Wind Tunnel experiments and CFD? Cross wind and air flow coming from various kind of other vehicles has a significant impact in actual driving. Furthermore, a vehicle posture changes due to the influence of air flow. That flow changes as the change of the vehicle attitude. Thus, in fact it is more complicated and fundamentally different from Wind Tunnel experiments. In principle, in order to better understand a physical phenomenon occurred, it is important to grasp a complex physical phenomenon rather than only solve a particular phenomenon. However, since governing equations vary in every physical phenomenon, it is important to couple each one. For this reason, this research aims to carry out analysis in a real condition and thus, the coupled analysis of mechanical and fluid is performed. As an example, we assume the following situation. Two cars are moving while receiving crosswinds, the latter vehicle changes its lanes and passing thru the front run vehicle. The vehicle has a steering and suspension system and the vehicle attitude changes as the change of the wind or lane. In order to carry out the simulation with taking all these conditions into consideration, the suspension and steering mechanism are included in Driver model of Multibody Dynamics analysis(MBD). It is then required to simulate the fluid flowing around the vehicle and to solve them simultaneously. In MBD we calculate displacement of the tire, steering, vehicle attitude, and store the displacement results to the CFD side. The CFD solver calculates the air flow using the calculated displacements obtained by MBD. At the end, force and moment are applied to the vehicle and we alternately performs this analysis through Multibody Dynamics analysis. Based on this simulation, it is now possible to estimate behavior of the vehicle which is not actually obtained by Wind Tunnel experiments including the influence of air flow from side wind, other vehicles. It is expected to be useful method in the product development process with higher accuracy and higher efficiency.

# ON NON-UNIFORM TORSION IN FGM BEAM STRUCTURES AND THE EXTRACTION OF RELEVANT STIFFNESS QUANTITIES BASED ON SAFE

STEPHAN KUGLER\*, PETER A. FOTIU\* AND JUSTIN MURIN†

\*University of Applied Sciences Wiener Neustadt,  
Department of Applied and Numerical Mechanics, Austria  
kugler@fhwn.ac.at; www.fhwn.ac.at

†Slovak University of Technology in Bratislava, FEI, Institute of Automotive Mechatronics,  
Department of Applied Mechanics and Mechatronics, Slovak Republic  
justin.murin@stuba.sk; www.stuba.sk

**Key words:** Non-uniform torsion; Vlasov's theory of torsion; Bescoter-related theory of torsion; Identification of stiffness parameters; SAFE

**Abstract.** All but axi-symmetric cross-sections warp during torsion, i.e. the cross-section deforms axially, and a warping or non-uniform theory of torsion has to be applied. Since the corresponding influence is severe in thin-walled open profiles much of the literature only covers thin-walled cross sections by Vlasov's theory of torsion. In this paper the classical Vlasov - theory is generalized to end up in a model similar to Bescoter's theory which is shown to be more accurate. A procedure to evaluate all arising stiffness quantities in arbitrarily shaped cross-sections accompanied with arbitrarily distributed constitutive parameters is proposed based on a reference beam problem in connection with semi-analytical finite elements. For the proposed theories of warping torsion effective finite beam elements are derived, and challenging benchmark-problems show the accuracy and the efficiency of the proposed formulations.

## 1 INTRODUCTION

Beam structures made of a Functionally Graded Materials (FGMs) show location dependent material parameters throughout their arbitrarily shaped cross-section. The load case of torsion introduces warping of the cross-section and a non-uniform theory of torsion has to be applied to achieve accurate solutions using one-dimensional finite elements. Starting with a suitable kinematic assumption where the cross-section rotates rigidly in its projection plane pivoting at the shear or drill center, the axial motion of a generic point is quantified based on an unknown warping function (depending

on the cross-section coordinates) multiplied with an axial field quantifying the amount of warping. The well-known and frequently applied Vlasov's theory of torsion [1] uses the first derivative of torsion angle  $\varphi'_x$  to quantify warping axially. This leads to two independent stiffness quantities (torsion stiffness and warping stiffness) which have to be identified in connection with one fourth order ordinary differential equation (ODE).

Alternatively, if the axial distribution of warping may be related to a yet unknown independent field rather than to the rate of twist, we end up with two coupled second order ODEs with four stiffness quantities. Such a calculation strategy is similar to the theory of Benscoter [3]. It can be shown by example that this theory leads to more accurate results compared to Vlasov's theory, especially for thick shafts. While the analytical evaluations regarding a set of two coupled ODEs are somewhat more involved very efficient finite beam elements can be derived based on linear shape functions. The evaluations of the related stiffness quantities can be carried out using a reference beam problem of arbitrary length in connection with three dimensional elasticity solutions where semi-analytical finite elements (SAFE) are applied. Due to SAFE and a specialized load case for the reference problem a true dimensional reduction is achieved and stress distributions, relevant cross-section parameters and stiffness quantities are accessible based on discretization of the cross-section only [2].

## 2 THEORY OF NON-UNIFORM TORSION

Under torsion any cross-section rotates about a specific location<sup>1</sup> with respect to the axial direction. The torsional angle  $\varphi_x(x)$  is found from a differential equation which is derived from suitable kinematic hypotheses, the strain displacement relations and the constitutive equations. The derivation is based on the principle of virtual work which is well suited to generate two-noded finite elements. If a cross-section warps during torsional loading the points of the cross-section undergo axial displacements  $u_x$ . The displacement field  $u_x(x, y, z)$  at a specific cross-section  $x$  is assumed in a multiplicative form,

$$u_x(x, y, z) = F(x)\omega(y, z), \quad (1)$$

where  $\omega(y, z)$  is the warping function. Figure 1 depicts the kinematics of torsion problems: There, we model an arbitrary cross-section with arbitrary material distributions in the  $y_m$ - $z_m$ , where the elastic center  $C$  (decoupling axial from bending deformations) and the shear center  $S$  (congruent with the drill center) is known (see [2]). The origin of the beam's coordinate system is located at  $C$  and the  $y$ - and  $z$ -axis is directed into the cross-sections principal directions. Any other orientation of the corresponding coordinate system might be possible without any further complexities for torsional loading, however, in light of shear force bending such an orientation is typically suggested. We then assume that the cross-section rotates rigidly about the shear (or drill) center  $S$  in terms of the torsional angle  $\varphi_x(x)$  and a generic point of the cross-section undergoes axial deformations,

---

<sup>1</sup>This specific location is called the drill center  $S$  and is congruent with the shear center of the cross-section which decouples torsion from shear force bending.

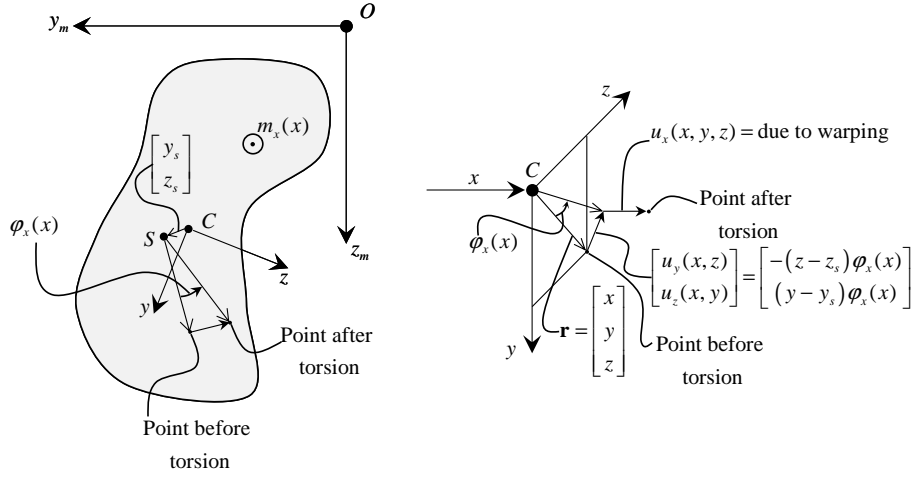


Figure 1: Kinematics of torsion

i.e. the cross-section is assumed to be rigid in its projection plane (any distortional deformations are neglected) but warps axially. According to the assumption (1) Vlasov assumes  $F(x) = \varphi'_x(x)$  while the Bencoter theory leaves  $F(x)$  to be determined. Hence, we have,

$$\text{Vlasov: } u_x(x, y, z) = \omega(y, z) \varphi'_x(x), \quad (2)$$

$$\text{Bencoter: } u_x(x, y, z) = \omega(y, z) F(x). \quad (3)$$

## 2.1 Vlasov's theory of torsion

According to Fig. 1 a generic point of the cross-section at  $x$  with the position vector  $\mathbf{r} = [x \ y \ z]^T$  displaces in the cross-section according to

$$u_y(x, z) = -(z - z_s) \varphi_x(x), \quad (4)$$

$$u_z(x, y) = (y - y_s) \varphi_x(x), \quad (5)$$

where  $\varphi_x(x)$  denotes the torsional angle and displaces out of that plane according to (2). Based on the above described kinematics we evaluate the strain fields according to the strain displacement relations,

$$\epsilon_{xx}(x, y, z) = \frac{\partial u_x(x, y, z)}{\partial x} = \omega(y, z) \varphi''_x(x), \quad (6)$$

$$\epsilon_{yy} = \frac{\partial u_y(x, z)}{\partial y} = 0, \quad \epsilon_{zz} = \frac{\partial u_z(x, y)}{\partial z} = 0, \quad (7)$$

$$\begin{aligned}\gamma_{xy}(x, y, z) &= \frac{\partial u_x(x, y, z)}{\partial y} + \frac{\partial u_y(x, z)}{\partial x} = \\ &= \left( \frac{\partial \omega(y, z)}{\partial y} - (z - z_s) \right) \varphi'_x(x) = (\omega_{,y} - (z - z_s)) \varphi'_x(x),\end{aligned}\quad (8)$$

$$\begin{aligned}\gamma_{xz}(x, y, z) &= \frac{\partial u_x(x, y, z)}{\partial z} + \frac{\partial u_z(x, y)}{\partial x} = \\ &= \left( \frac{\partial \omega(y, z)}{\partial z} + (y - y_s) \right) \varphi'_x(x) = (\omega_{,z} + (y - y_s)) \varphi'_x(x),\end{aligned}\quad (9)$$

$$\gamma_{yz} = \frac{\partial u_y(x, z)}{\partial z} + \frac{\partial u_z(x, y)}{\partial y} = -\varphi_x(x) + \varphi_x(x) = 0, \quad (10)$$

and the non-vanishing stress fields are found according to the constitutive relations,

$$\sigma_{xx}(x, y, z) = E(y, z)\epsilon_{xx}(x, y, z) = E(y, z)\omega(y, z)\varphi''_x(x), \quad (11)$$

$$\tau_{xy}(x, y, z) = G(y, z)\gamma_{xy}(x, y, z) = G(y, z)(\omega_{,y} - (z - z_s))\varphi'_x(x), \quad (12)$$

$$\tau_{xz}(x, y, z) = G(y, z)\gamma_{xz}(x, y, z) = G(y, z)(\omega_{,z} + (y - y_s))\varphi'_x(x), \quad (13)$$

where isotropy at each material point is understood (Young's modulus  $E$  and shear modulus  $G$ ). Using the principle of virtual work  $\delta W_a + \delta W_i = 0$  with prescribed kinematic boundary conditions at both beam ends ( $\delta\varphi_x(0) = \delta\varphi_x(l) = \delta\varphi'_x(0) = \delta\varphi'_x(l) = 0$ ) we have an external load due to a line moment  $m_x(x)$  [N],

$$\int_l m_x(x)\delta\varphi_x(x)dx - \int_V \sigma_{xx}\delta\epsilon_{xx}dV - \int_V \tau_{xy}\delta\gamma_{xy}dV - \int_V \tau_{xz}\delta\gamma_{xz}dV = 0, \quad (14)$$

and further,

$$\begin{aligned}\int_l m_x(x)\delta\varphi_x(x)dx - \int_l \underbrace{\int_A E(y, z)\omega^2(y, z)dA}_{=E_T C_\omega} \varphi''_x(x)\delta\varphi''_x(x)dx - \\ - \int_l \underbrace{\int_A G(y, z) [(\omega_{,y} - (z - z_s))^2 + (\omega_{,z} + (y - y_s))^2] dA}_{=G_T I_T} \varphi'_x(x)\delta\varphi'_x(x)dx = 0,\end{aligned}\quad (15)$$

where warping stiffness  $E_T C_\omega$  [Nm<sup>4</sup>] and the torsional stiffness  $G_T I_T$  [Nm<sup>2</sup>] are defined. Applying integration by parts,

$$\int_l m_x(x)\delta\varphi_x(x)dx - \int_l E_T C_\omega \varphi_x''''(x)\delta\varphi_x(x)dx + \int_l G_T I_T \varphi_x''(x)\delta\varphi_x(x)dx =$$

$$= \int_l \left( m_x(x) - E_T C_\omega \varphi_x''''(x) + G_T I_T \varphi_x''(x) \right) \delta \varphi_x(x) dx = 0, \quad (16)$$

delivers for arbitrary variations of the torsional angle the describing differential equation for warping torsion,

$$E_T C_\omega \varphi_x''''(x) - G_T I_T \varphi_x''(x) = m_x(x). \quad (17)$$

## 2.2 A Bencoter related theory of torsion

In Bencoter's theory [3] the kinematics are assumed according to (1)

$$u_x(x, y, z) = \omega(y, z) F(x), \quad (18)$$

and

$$u_y(x, z) = -(z - z_s) \varphi_x(x), \quad u_z(x, y) = (y - y_s) \varphi_x(x), \quad (19)$$

where axial warping deformations vary according to an unknown function  $F(x)$  along the beam's axis. This approach is also discussed in [4]. The non-vanishing strain fields read,

$$\epsilon_{xx}(x, y, z) = \frac{\partial u_x(x, y, z)}{\partial x} = \omega(y, z) F'(x), \quad (20)$$

$$\gamma_{xy}(x, y, z) = \frac{\partial u_x(x, y, z)}{\partial y} + \frac{\partial u_y(x, z)}{\partial x} = \omega_{,y} F(x) - (z - z_s) \varphi_x'(x), \quad (21)$$

$$\gamma_{xz}(x, y, z) = \frac{\partial u_x(x, y, z)}{\partial z} + \frac{\partial u_z(x, y)}{\partial x} = \omega_{,z} F(x) + (y - y_s) \varphi_x'(x), \quad (22)$$

and the stress fields are

$$\sigma_{xx}(x, y, z) = E(y, z) \epsilon_{xx}(x, y, z) = E(y, z) \omega(y, z) F'(x), \quad (23)$$

$$\tau_{xy}(x, y, z) = G(y, z) \gamma_{xy}(x, y, z) = G(y, z) \left( \omega_{,y} F(x) - (z - z_s) \varphi_x'(x) \right), \quad (24)$$

$$\tau_{xz}(x, y, z) = G(y, z) \gamma_{xz}(x, y, z) = G(y, z) \left( \omega_{,z} F(x) + (y - y_s) \varphi_x'(x) \right). \quad (25)$$

The principle of virtual work with the kinematic variables  $\varphi_x$  and  $F$  gives for prescribed kinematic variables at both beam ends ( $\delta \varphi_x(0) = \delta \varphi_x(l) = \delta F(0) = \delta F(l) = 0$ ),

$$\begin{aligned} & \int_l m_x(x) \delta \varphi_x(x) dx - \int_l \int_A E(y, z) \omega^2(y, z) dA F'(x) \delta F'(x) dx - \\ & - \int_l \int_A G(y, z) \omega_{,y}^2 dA F(x) \delta F(x) dx + \end{aligned}$$

$$\begin{aligned}
 & + \int_l \int_A G(y, z) \omega_{,y} (z - z_s) dA \left( F(x) \delta \varphi'_x(x) + \varphi'_x(x) \delta F(x) \right) dx - \\
 & - \int_l \int_A G(y, z) (z - z_s)^2 dA \varphi'_x(x) \delta \varphi'_x(x) dx - \int_l \int_A G(y, z) \omega_{,z}^2 dA F(x) \delta F(x) dx - \\
 & - \int_l \int_A G(y, z) \omega_{,z} (y - y_s) dA \left( F(x) \delta \varphi'_x(x) + \varphi'_x(x) \delta F(x) \right) dx - \\
 & - \int_l \int_A G(y, z) (y - y_s)^2 dA \varphi'_x(x) \delta \varphi'_x(x) dx = 0, \tag{26}
 \end{aligned}$$

which can be rewritten as,

$$\begin{aligned}
 & \int_l m_x(x) \delta \varphi_x(x) dx - \int_l \underbrace{\int_A E(y, z) \omega^2(y, z) dA}_{=E_T C_\omega} F'(x) \delta F'(x) dx - \\
 & - \int_l \underbrace{\int_A G(y, z) (\omega_{,y}^2 + \omega_{,z}^2) dA}_{=K_1} F(x) \delta F(x) dx - \\
 & - \int_l \underbrace{\int_A G(y, z) ((y - y_s) \omega_{,z} - (z - z_s) \omega_{,y}) dA}_{=K_2} \left( F(x) \delta \varphi'_x(x) + \varphi'_x(x) \delta F(x) \right) dx - \\
 & - \int_l \underbrace{\int_A G(y, z) ((y - y_s)^2 + (z - z_s)^2) dA}_{=K_3} \varphi'_x(x) \delta \varphi'_x(x) dx = 0, \tag{27}
 \end{aligned}$$

defining four stiffness quantities,  $E_T C_\omega$  and  $K_i$  for  $i = 1, 2, 3$ . Note, that (27) coincides with (15) if  $F(x) = \varphi'_x(x)$  is and

$$G_T I_T = K_1 + 2K_2 + K_3. \tag{28}$$

Integrating (27) by parts yields,

$$\begin{aligned}
 & \int_l m_x(x) \delta \varphi_x(x) dx + \int_l E_T C_\omega F''(x) \delta F(x) dx - \int_l K_1 F(x) \delta F(x) dx - \\
 & - \int_l K_2 \left( -F'(x) \delta \varphi_x(x) + \varphi'_x(x) \delta F(x) \right) dx + \int_l K_3 \varphi''_x(x) \delta \varphi_x(x) dx = 0, \tag{29}
 \end{aligned}$$

giving the Euler-Lagrange equations representing a system of coupled differential equations<sup>2</sup>,

$$m_x(x) + K_2 F'(x) + K_3 \varphi_x''(x) = 0, \quad (30)$$

$$E_T C_\omega F''(x) - K_1 F(x) - K_2 \varphi_x'(x) = 0. \quad (31)$$

Note that the strong form (30) (31) cannot be converted into the formulation (15) anymore and different results are expected.

### 3 EVALUATION OF STIFFNESS QUANTITIES AND STRESS DISTRIBUTIONS BASED ON SAFE

The identification of relevant stiffness quantities (warping stiffness  $E_T C_\omega$  and torsional stiffness  $G_T I_T$  (15) accompanied with  $K_i$  for  $i = 1, 2, 3$  (27)) is performed on a reference beam problem (modeled in the  $y_m$ - $z_m$  coordinate system) of arbitrary length  $l_{RB}$  which is analyzed by a three-dimensional elasticity formulation and the procedures discussed in [2]. The beam is assumed to rest on fork supports, i.e.  $\varphi_x = \sigma_{xx} = 0$  at both beam ends. Transverse volume forces  $f_i$  for  $i = y_m, z_m$  are applied (varying as a sine function with  $\alpha = n\pi/l_{RB}$ ,  $n = 1$ )

$$f_{y_m} = f_{y_{m0}} \sin(\alpha x_m) = (b_{y0} + b_{yy} y_m + b_{yz} z_m) E(y_m, z_m) \sin(\alpha x_m), \quad (32)$$

$$f_{z_m} = f_{z_{m0}} \sin(\alpha x_m) = (b_{z0} + b_{zy} y_m + b_{zz} z_m) E(y_m, z_m) \sin(\alpha x_m), \quad (33)$$

which are scaled by the location dependent Young's modulus  $E(y_m, z_m)$ . The constant quantities  $b_{uv} \neq b_{vu}$  with  $u = y, z$  and  $v = 0, y, z$  are unknowns at this stage, however, they can be identified by requiring that the reference beam problem has to react as shaft. Hence, we require

$$q_{y_{m0}} = \int_A f_{y_{m0}} dA = 0 \quad (34)$$

$$q_{z_{m0}} = \int_A f_{z_{m0}} dA = 0 \quad (35)$$

$$m_{x0} = \int_A (y_m f_{z_{m0}} - z_m f_{y_{m0}}) dA = 1 \quad (36)$$

We thus have three equations with six unknown parameters which can be solved by the Moore-Penrose pseudo-inverse. The mean torsional angle amplitude can be evaluated,

$$\bar{\varphi}_x = b_{y0} \bar{\varphi}_x^{b_{z0}} + b_{yy} \bar{\varphi}_x^{b_{zy}} + b_{yz} \bar{\varphi}_x^{b_{zz}} + b_{z0} \bar{\varphi}_x^{b_{z0}} + b_{zy} \bar{\varphi}_x^{b_{zy}} + b_{zz} \bar{\varphi}_x^{b_{zz}}, \quad (37)$$

<sup>2</sup>This formulation introduces four stiffness parameters, but it can be shown that  $K_1 = -K_2$  if the same warping function  $\omega$  is used for either Vlasov's theory or the Bencoter-related theory.

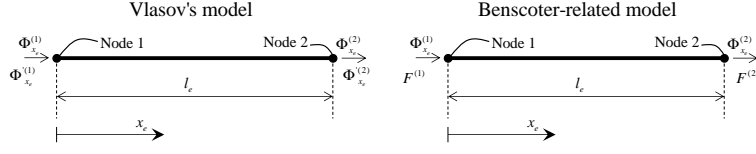


Figure 2: Two-noded beam finite element for Vlasov's and Benscoter's theory of torsion

where  $\bar{\varphi}_x^{b_{uv}}$  denote the mean value of torsional angle with respect to the cross-section's area evaluated from the reference beam problem due to the application of  $b_{uv}$  only (see [2] for additional details). According to Vlasov's theory the out of plane motion,

$$u_x(x, y_m, z_m) = \omega(y_m, z_m) \varphi'_x(x), \quad (38)$$

is proportional to  $\varphi'_x(x)$  and we find the nodal warping amplitudes  $\omega$  as

$$\omega = \frac{\mathbf{U}_x}{\alpha \bar{\varphi}_x} = \frac{\sum_{u=y}^z \sum_{v=0}^z b_{uv} \mathbf{U}_x^{b_{uv}}}{\alpha \bar{\varphi}_x}. \quad (39)$$

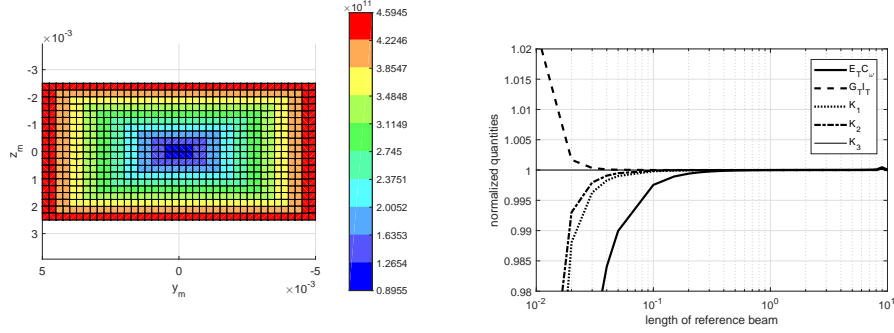
Once the warping distribution is at hand all stiffness properties can be evaluated. As a side product axial and shear stress distributions due to a unity torsional moment and unity bimoment  $M_\omega = \int_A \omega \sigma_{xx} dA$  are found without any additional effort. The reference beam problem is analyzed by semi-analytical finite elements (SAFE) (see [2, 5]) where only the cross-section of the beam has to be discretized since axial variations are assumed to be analytical functions. The only remaining free parameter of the reference problem is the length of the reference beam  $l_{RB}$ , where it can be shown that accurate solutions can be achieved for  $10r < l_{RB} < 500r$ , where  $r$  denotes a characteristic geometrical dimension of the actual cross-section. For  $l_{RB} < 10r$  beam theory is no longer accurate since cross-sectional distortions become important. For lengths  $l_{RB} > 500r$  some numerical problems regarding SAFE start to emanate.

#### 4 FINITE ELEMENT FORMULATIONS

In this section we present very briefly a two-noded beam finite element of length  $l_e$  for both theories (see Fig. 2). The nodal degrees of freedom are the torsional angle  $\Phi_x$  and either  $\Phi'_x$  or  $F$ . We use polynomial shape functions (cubic for Vlasov's theory and linear for Benscoter's model). This yields to the following equations

Vlasov:

$$\left\{ \frac{E_T C_\omega}{l_e^3} \begin{bmatrix} 12 & 6l_e & -12 & 6l_e \\ 6l_e & 4l_e^2 & -6l_e & 2l_e^2 \\ -12 & -6l_e & 12 & -6l_e \\ 6l_e & 2l_e^2 & -6l_e & 4l_e^2 \end{bmatrix} + \frac{G_T I_T}{30l_e} \begin{bmatrix} 36 & 3l_e & -36 & 3l_e \\ 3l_e & 4l_e^2 & -3l_e & -l_e^2 \\ -36 & -3l_e & 36 & -3l_e \\ 3l_e & -l_e^2 & -3l_e & 4l_e^2 \end{bmatrix} \right\} \begin{bmatrix} \Phi_{x_e}^{(1)} \\ \Phi_{x_e}^{\prime(1)} \\ \Phi_{x_e}^{(2)} \\ \Phi_{x_e}^{\prime(2)} \end{bmatrix} = \frac{m_{x0} l_e}{2} \begin{bmatrix} 1 \\ l_e/6 \\ 1 \\ -l_e/6 \end{bmatrix}. \quad (40)$$



(a) Distribution of Young’s modulus in rectangular FGM cross-section (b) Convergence characteristic for either parameters with respect to large variations of RB-lengths

Figure 3: Rectangular FGM cross-section

Benscoter:

$$\begin{bmatrix} \frac{K_3}{l_e} & -\frac{K_2}{2} & -\frac{K_3}{l_e} & -\frac{K_2}{2} \\ -\frac{K_2}{2} & \frac{K_1 l_e}{\chi_1} + \frac{E_T C_\omega}{l_e} & \frac{K_2}{2} & \frac{K_1 l_e}{\chi_2} - \frac{E_T C_\omega}{l_e} \\ -\frac{K_3}{l_e} & \frac{K_2}{2} & \frac{K_3}{l_e} & \frac{K_2}{2} \\ -\frac{K_2}{2} & \frac{K_1 l_e}{\chi_2} - \frac{E_T C_\omega}{l_e} & \frac{K_2}{2} & \frac{K_1 l_e}{\chi_1} + \frac{E_T C_\omega}{l_e} \end{bmatrix} \begin{bmatrix} \Phi_{x_e}^{(1)} \\ F^{(1)} \\ \Phi_{x_e}^{(2)} \\ F^{(1)} \end{bmatrix} = \frac{m_{x0} l_e}{2} \begin{bmatrix} 1 \\ 0 \\ 1 \\ 0 \end{bmatrix} \quad (41)$$

The constants  $\chi_1$  and  $\chi_2$  in equation (40) depend on the order of integration,

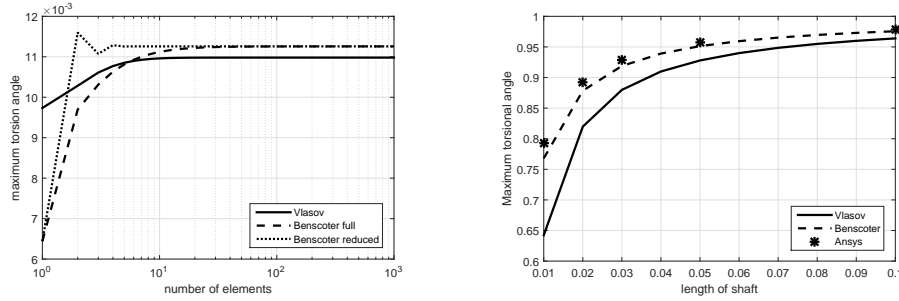
$$\text{Full integration (2 Gauss-points) : } \chi_1 = 3, \chi_2 = 6, \quad (42)$$

$$\text{Reduced integration (1 Gauss-point) : } \chi_1 = \chi_2 = 4. \quad (43)$$

It can be shown by example that the selectively reduced formulation converges much faster since locking effects are resolved.

## 5 EXAMPLE, RESULTS AND DISCUSSION

For sake of space only one example can be described here where we consider a rectangular cross-section (height  $h = 5 \cdot 10^{-3}$ , width  $w = 10 \cdot 10^{-3}$ ) which is made from pure aluminum (Al6061-TO,  $E = 69\text{GPa}$ ,  $\nu = 0.33$ ) in the core and pure titancarbid (TiC,  $E = 480\text{GPa}$ ,  $\nu = 0.33$ ) at the outer surfaces. Due to Murin et al. [8] the variation of the material properties is assumed to be linear in both transverse directions (see Fig. 3a where ten layers are used to approximate the continuous distribution). The mesh density defines the model of the continuous variation of Young’s modulus, i.e. the continuous variation is approximated by layers of one element horizontally and two elements vertically. It is shown in [8] that the application of ten layers delivers good accuracy regarding the stiffness quantities which are evaluated using a completely different procedure compared to



(a) Convergence of the herein proposed elements for torsion  $l = 0.05$ , prevented warping at  $x = l$ ,  $M_x = 10$  (b) Maximum torsion angle at the location of the load (warping is prevented at  $x = l$ ) for different shaft lengths ( $M_x = \frac{G_T I_T}{l}$ )

Figure 4: Results in a clamped shaft

the present one. The stiffness quantities are found using the proposed procedure and  $l_{RB} = 1$  as the length of the reference beam ( $E_T C_\omega = 1.3727e - 04$ ,  $G_T I_T = 42.2540$ ,  $K_1 = 35.3680$ ,  $K_2 = -35.3681$  and  $K_3 = 77.6221$ ). The convergence characteristic over a wide range of reference beam lengths is shown in Fig. 3b which indicates a relative error of less than two percent within an interval of  $0.04 < l_{RB} < 5$  (all quantities are normalized to the corresponding ones using  $l_{RB} = 1$ ).

Using these stiffness parameters we analyze the torsional behavior of a shaft of length  $l$  which is clamped at  $x = 0$  ( $\varphi_x = 0$  and  $u_x = 0$ ) and loaded with a torsion moment  $M_x$  at  $x = l$ . Reference solutions are found using Ansys (regular mesh of linear brick elements with enhanced strain formulation, edge length:  $0.25 \cdot 10^{-3}$ ) where the load is applied using a rigid contact with pilot (RBE2 element) and a concentrated torsional moment on the pilot node. The application of the load using an RBE2 element causes restrained warping at  $x = l$ . The corresponding outcome indicates good agreement of both theories of torsion compared to Ansys. Nevertheless, Vlasov’s theory of torsion delivers a relative error of three percent while Benscoter’s theory leads to 0.6 percent relative error for  $l = 0.1$  and  $l = 0.05$ . This indicates that Benscoter’s theory is slightly more predictive in that problem. The convergence characteristic of the proposed finite beam elements regarding a shaft length of  $l = 0.05$  for Vlasov’s cubic element, Benscoter’s fully integrated linear element and Benscoter’s reduced integrated linear element are shown in Fig. 4a, where accurate results are indicated for more than ten elements (Benscoter’s fully integrated linear element shows the worst convergence characteristic indicating two percent error for ten elements). The maximum torsional angle at the location of the load due to  $M_x = \frac{G_T I_T}{l}$  is shown in Fig. 4b for different shaft length and compared to Ansys. As expected all results converge to  $\varphi_x^{max} = 1$  for rather long shafts where warping is not important anymore (St. Venant problem), however, the system becomes stiffer in case of short shafts due to non-negligible warping effects. It turns out that the results due to the Benscoter-related model are much more accurate compared to Vlasov’s model in the problem of short shafts.

## 6 ACKNOWLEDGMENT

This work has been supported by Grant Agency VEGA(Grant No. 1/0102/18).

## References

- [1] V. Vlasov, Thin walled elastic beams, National Science Foundation, Washington, 1961.
- [2] S. Kugler, P. Fotiu, J. Murin, The application of safe to extract relevant stiffness quantities for efficient modelling of fgm beam structures - axial deformations and shear force bending, 13th World Congress on Computational Mechanics (WCCM XIII) and 2nd Pan American Congress on Computational Mechanics (PANACM II), July 22-27, 2018, New York City, NY, USA.
- [3] S. Benscoter, A theory of torsion bending for multicell beams, *Journal of Applied Mech* (1954) 25–34.
- [4] K. Saade, Finite Element Modeling of Shear in Thin Walled Beams with a Single Warping Function, PhD Thesis University of Bruxelles, 2004.
- [5] O. C. Zienkiewicz, R. L. Taylor, *Finite Element Method: Volume 2, Solid Mechanics (Finite Element Method)*, Butterworth-Heinemann, 2000.
- [6] E. Onate, *Structural Analysis with the Finite Element Method - Linear Statics - Volume 1: Basis and Solids*, Springer, 2009.
- [7] E. Dvorkin, D. Celentano, A. Cuitino, G. Gioia, A vlasov beam element, *Computers & Structures* 33 (1989) 187–196.
- [8] J. Murin, M. Aminbaghai, J. Hrabovsky, R. Gogola, S. Kugler, Beam finite element for modal analysis of FGM structures, *Engineering Structures* (2016) 1–18.

## Phase Field Modeling of Cracks in Heterogeneous Materials

Charlotte Kuhn\*, Ralf Müller\*\*

\*University of Kaiserslautern, \*\*University of Kaiserslautern

### ABSTRACT

One of the reasons why the phase field approach has become very popular for modeling fracture processes is that therein the entire evolution of fracture follows from energetic principles without the need for different criteria for crack initiation, nucleation, kinking or branching. Furthermore, these models allow for a straightforward numerical implementation with standard finite elements, since displacement jumps and stress singularities are avoided in these models. Consequently, phase field fracture models are now also used to model and simulate fracture of heterogeneous materials such as composites, where cracks may be arrested, deflected or bifurcated at interfaces between the different components of the composite material, resulting in complicated crack patterns. The crack propagation is not only controlled by the elastic and fracture properties of the bulk phases of the material but also by the properties of the interfaces in between. Thus, it is crucial to take these interface properties into account, and there are conceptually different approaches on how to integrate them into phase field fracture models. In [1] interfaces are modeled as zones of finite width with appropriately adjusted fracture parameters. Contrary, a combination with a cohesive type of modeling interface fracture is proposed in [2]. Another approach, which makes use of a new energetic formulation mixing bulk and cohesive surface energies, is proposed in [3]. In this work, interfaces are equipped with a fracture energy corresponding to the phase field fracture energy of the bulk phases in order to model the interface fracture properties. In the finite element implementation, the interfaces are modeled by means of surface elements without introducing additional degrees of freedom. The convergence behavior of the proposed model with respect to the sharp interface limit of the phase field fracture model as well as energy release rates during crack propagation are analyzed in numerical studies in order to verify the model. [1] A.C. Hansen-Dörr, P. Hennig, M. Kästner, K. Weinberg: A numerical analysis of the fracture toughness in phase-field modelling of adhesive fracture. Proc. Appl. Math. Mech. (submitted), 2017. [2] C.V. Verhoosel, R. de Borst: A phase-field model for cohesive fracture. Int. J. Numer. Meth. Engng 2013, 96:43-62 [3] T.T. Nguyen, J. Yvonnet, Q.-Z. Zhu, M. Bornert, C. Chateau: A phase-eld method for computational modeling of interfacial damage interacting with crack propagation in realistic microstructures obtained by microtomography. Comput. Methods Appl. Mech. Engrg. 2015, 312: 567-595

## **Augmented Total-FETI Algorithm for Computationally Efficient Micromechanical Analysis of a Representative Volume Element**

Nagesh Kulkarni\*, BP Gautham\*\*, Salil Kulkarni\*\*\*

\*TCS Research, Tata Consultancy Services Ltd. India, presently pursuing PhD at Mechanical Engineering Dept. IIT Bombay, India, \*\*TCS Research, Tata Consultancy Services Ltd., India, \*\*\*Mechanical Engineering Dept., IIT Bombay, India

### **ABSTRACT**

Representative Volume Element (RVE) is the smallest material volume that represents the material in terms of effective properties of interest. Analysis of a RVE is typically carried out to obtain response of material as a function of its underlying microstructure for a given load path. Periodic boundary conditions, which simulate the effect of embedding the RVE in a spatially infinite periodic structure, are commonly used in the analysis. They do not necessarily provide a good estimate of the effective properties if the size of the RVE is not very small as compared to the overall dimensions of the structure. The aim of this work is to develop an accurate and computationally efficient algorithm that effectively utilizes the principle of domain decomposition methods in a novel and natural way for estimating the effective properties of a periodic microstructure which is spatially finite in extent. The microstructure is assumed to be composed of a basic unit called cell which is spatially repeating. Instead of assuming the cell to be a RVE and applying periodic boundary conditions, the RVE is assumed to be composed of multiple identical cells glued together. It is then subjected to either uniform traction or uniform displacement boundary conditions as these are more representative of the actual boundary conditions in such case. A domain decomposition method called Total Finite Element Tearing and Interconnection (TFETI) method is used to perform the analysis. The proposed method of enlarging the size of the RVE using identical copies of the base cell and then using TFETI to computationally solve the problem is referred to as the Augmented TFETI method. Here subdomain level computations for the unit cell are directly used while performing calculations using the RVE. To demonstrate the applicability of the method, sample problem of finite size and having periodic microstructure is solved using the Augmented TFETI. It consists of a cell which has an eccentric hole embedded in an isotropic matrix. Uniform displacements are applied to the RVE's of increasing size. It is seen that the results obtained using RVE's of different sizes converge as the sizes of the RVEs increase. In addition the computational performance of the propose method is compared to that of using the standard finite element to solve problem with increased RVE size. It was also observed that the augmented TFETI is 50% computationally more efficient than the standard FEM applied to the RVE's with increased size.

# EFFECT OF MICRON-SCALE CONSTITUTIVE AND DAMAGE MODELING ON MULTISCALE CRACK PREDICTION IN POLYMER-MATRIX COMPOSITE LAMINATES

Yuta Kumagai<sup>a</sup>, Yoshiteru Aoyagi<sup>b</sup>, and Tomonaga Okabe<sup>a</sup>

<sup>a</sup>Department of Aerospace Engineering, Tohoku University  
6-6-01, Aramaki-Aza-Aoba, Aoba-ku, Sendai, Miyagi 980-8579, Japan  
kumagai@plum.mech.tohoku.ac.jp

<sup>b</sup>Department of Finemechanics, Tohoku University  
6-6-01, Aramaki-Aza-Aoba, Aoba-ku, Sendai, Miyagi 980-8579, Japan

**Key words:** Multiscale Modeling, Polymer-Matrix Composites, Failure Prediction

**Abstract.** Damage accumulation on the fiber-diameter scale causes failure of carbon fiber-reinforced plastics (CFRPs). Therefore, microscopic damage prediction is important to evaluate structural safety of composite structures made from CFRPs. In this study, effect of matrix modeling on the fiber-diameter scale is investigated using a multiscale approach that consists of macroscopic and microscopic analyses. On the macroscopic analysis, laminate-scale finite-element analysis assuming each lamina to be a homogeneous body is conducted to obtain strain histories at failure-expected points. On the microscopic analysis, periodic unit-cell (PUC) analysis considering heterogeneity of materials is performed to predict initiation of crack in the matrix phase of CFRP, based on strain histories obtained from macroscopic analysis. Two constitutive models and four sets of failure criteria are applied to the matrix phase on the PUC analysis, and compared with each other to evaluate important factors in multiscale failure prediction of CFRP laminates.

## 1 INTRODUCTION

Carbon fiber reinforced plastics (CFRPs) have been widely applied to aircraft structures because of their excellent mechanical properties. In the structures made of CFRPs, the initial cracking strain has been utilized as one of the design criteria of structures. However, it is difficult to accurately predict the initial cracking strain due to structural features of CFRP laminate, such as stacking sequence, free surface, ply drop-off, and heterogeneous microscopic

structure. These structural features cause inhomogeneous stress fields in laminate, and affect fiber-diameter scale crack formation. Therefore, development of accurate multiscale analysis methods that can consider both macroscopic deformation behavior and microscopic material structure is desired.

Thermosetting or thermoplastic resin used for polymer-matrix composites exhibits nonlinear inelastic behavior with damage evolution<sup>1,2</sup>. To predict such nonlinear deformation and damage evolution of polymers, various constitutive and damage models have been developed<sup>1,3-7</sup>, and implemented into the fiber-diameter scale unit-cell analysis<sup>4,7-9</sup>. These studies provide good understanding of micron-scale failure events in polymer-matrix composites. However, comprehensive evaluation of constitutive and damage models for the matrix phase of composites under practical loading conditions is still limited.

In this study, influence of constitutive models and failure criteria applied to matrix resin on crack prediction capability of multiscale analysis is investigated. Multiscale analysis, which consists of macroscopic finite-element (FE) analysis and microscopic periodic unit-cell (PUC) analysis, is developed. Two constitutive models and four sets of failure criteria are implemented to PUC analysis, and simulated results are compared with experiment in the previous studies to evaluate factors that need to consider for initial crack prediction in CFRP laminate.

## **2 SIMULATION METHOD**

In this study, in order to evaluate important factors in failure criteria for the matrix phase of CFRP, constitutive models and failure criteria for microscopic crack prediction are examined through the comparison of simulated results with experiment data in the previous studies<sup>10</sup>. In this section, macroscopic FE analysis and microscopic PUC analysis are explained, and then two-scale simulation procedure is described.

### **2.1 Macroscopic FE analysis of unidirectional laminates**

Unidirectional CFRP laminates under off-axis loading exhibit nonlinear stress-strain behavior because of plastic deformation of matrix resin. To reproduce this nonlinear behavior, macroscopic analysis is conducted based on an anisotropic elasto-plastic constitutive law proposed by Yokozeki et al.<sup>11</sup>. Implementation of the constitutive law in multiscale analysis is described in the literature<sup>12</sup>. The material properties used in the macroscopic analysis are listed in Table 1.

A schematic view of the computational model is presented in Fig. 1. The fiber angles of

Table 1 Elastic properties of unidirectional laminates used in macroscopic FE analysis.

Longitudinal Young's modulus $E_1$	151 GPa
Transverse Young's modulus $E_2, E_3$	9.16 GPa
Shear modulus $G_{12}, G_{13}$	4.62 GPa
Shear modulus $G_{23}$	2.55 GPa
Poisson's ratio $\nu_{12}, \nu_{13}$	0.302
Poisson's ratio $\nu_{23}$	0.589

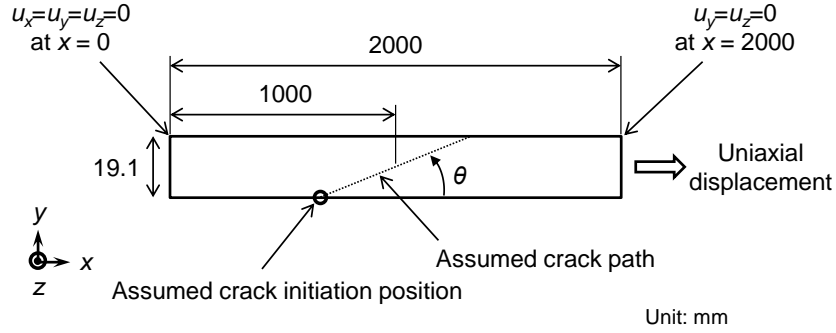


Fig.1 Schematic view of macroscopic FE analysis model.

unidirectional laminates are  $10^\circ$ ,  $20^\circ$ ,  $25^\circ$ ,  $30^\circ$ ,  $35^\circ$ ,  $40^\circ$ ,  $45^\circ$ , and  $90^\circ$ . The length of the computational model and the assumed initial cracking site are determined based on the literature<sup>12, 13, 14</sup>. Incremental uniaxial displacement is applied to the edge of the analysis model with the displacement rate of 0.01 mm/s.

## 2.2 Microscopic periodic unit-cell analysis

To predict crack initiation under several loading conditions, a three-dimensional unit-cell model, which consists of five carbon fibers and matrix resin, is utilized. A FE model used for microscopic analysis is shown in Fig. 2. The carbon fiber is modeled as an orthotropic elastic body, and the matrix resin is modeled as an isotropic inelastic body explained later. The fiber diameter is 5  $\mu\text{m}$ , and the fiber volume fraction is 56%. In this study, the interface between fiber and matrix resin is assumed to be perfectly bonding to focus on only matrix cracking. In addition, the periodic boundary condition is imposed on the unit-cell model. Material properties used in the PUC analysis are listed in Table 2.

To evaluate the effect of matrix constitutive modeling on two-scale FE analysis, two constitutive models were applied to matrix resin of PUC analysis. First one is an elastoviscoplastic model<sup>3</sup> proposed to reproduce mechanical responses of ductile polymers. This

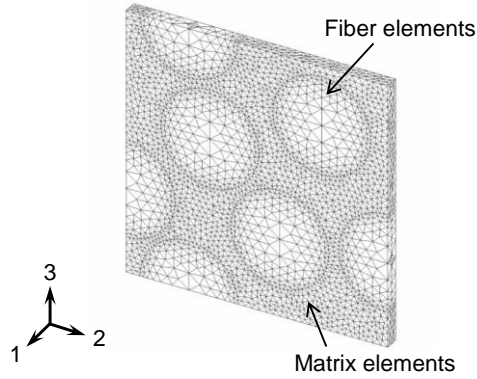


Fig.2 FE model for microscopic PUC analysis.

Table 2 Material properties of carbon fiber and epoxy resin used in the PUC analysis.

Fiber longitudinal Young's modulus $E_L$	294 GPa
Fiber transverse Young's modulus $E_T$	19.5 GPa
Fiber longitudinal Poisson's ratio $\nu_L$	0.17
Fiber transverse Poisson's ratio $\nu_T$	0.46
Fiber's coefficient of thermal expansion for the longitudinal direction $\alpha_L$	$-1.1 \times 10^{-6}/K$
Fiber's coefficient of thermal expansion for the transverse direction $\alpha_T$	$10 \times 10^{-6}/K$
Matrix Young's modulus $E_m$	3.2 GPa
Matrix Poisson's ratio $\nu_m$	0.38
Matrix's coefficient of thermal expansion $\alpha_m$	$60 \times 10^{-6}/K$

model includes a one-parameter damage variable based on the hypothesis of strain equivalence.

$$\dot{\boldsymbol{\sigma}} = (1 - \omega) \mathbf{C}_m^e : \dot{\boldsymbol{\varepsilon}} - (1 - \omega) \frac{3\mu \dot{\bar{\varepsilon}}^P}{\bar{\sigma}} \boldsymbol{\sigma}' - \frac{\dot{\omega}}{1 - \omega} \boldsymbol{\sigma} \quad (1)$$

Here,  $\boldsymbol{\sigma}$  is the stress tensor,  $\mathbf{C}_m$  is the elastic stiffness tensor for the matrix resin,  $\boldsymbol{\varepsilon}$  is the strain tensor,  $\mu$  is the Lamé constant,  $\bar{\varepsilon}^P$  is the equivalent plastic strain,  $\bar{\sigma}$  is the von Mises stress,  $\boldsymbol{\sigma}'$  is the deviatoric stress tensor, and  $\omega$  is the scalar variable that gives the stiffness degradation rate. The equivalent plastic strain rate  $\dot{\bar{\varepsilon}}^P$  is determined by the following equation used by Matsuda et al.<sup>15</sup>, including hydrostatic stress dependence<sup>9</sup>:

$$\dot{\bar{\varepsilon}}^P = \dot{\varepsilon}_r \left( \frac{\bar{\sigma} + \beta \sigma_m}{g(\bar{\varepsilon}^P)} \right)^{\frac{1}{m}}, \quad (2)$$

$$\mathbf{g}(\bar{\boldsymbol{\varepsilon}}^p) = \mathbf{g}_1(\bar{\boldsymbol{\varepsilon}}^p)^{g_2} + \mathbf{g}_3. \quad (3)$$

Here,  $\dot{\boldsymbol{\varepsilon}}_r$  is the reference strain rate;  $\sigma_m$  is hydrostatic stress;  $m$  is an exponent regarding strain-rate sensitivity;  $\beta$  is hydrostatic stress sensitivity; and  $g_1$ ,  $g_2$  and  $g_3$  are material constants.

The second model is an inelastic constitutive model<sup>1</sup> that accounts for the effect of free volume variation in polymer on mechanical responses.

$$\dot{\boldsymbol{\sigma}} = \mathbf{C}_m^e : \dot{\boldsymbol{\varepsilon}} - \frac{\sqrt{2}}{\tau} \dot{\gamma}^p \boldsymbol{\sigma}', \quad (4)$$

where

$$\dot{\gamma}^p = \dot{\gamma}_0 \int_0^\infty \psi(\Delta F) \left[ \exp\left\{-\frac{\Delta F - \tau \Delta v_\tau^*}{k_B T}\right\} - \exp\left\{-\frac{\Delta F + \tau \Delta v_\tau^*}{k_B T}\right\} \right] \exp\left\{-\frac{\Delta F}{k_B T}\right\} d\Delta F. \quad (5)$$

Here,  $\dot{\gamma}_0$  is macroscopic inelastic strain rate,  $\Delta F$  is an activation energy for transformation,  $\psi$  is a probability density function of activation energy,  $\tau$  is equivalent shear stress,  $T$  is temperature,  $\Delta v_\tau^*$  is shear activation volume,  $k_B$  is the Boltzmann constant, and  $\Delta F$  is local transformation strain energy. Detailed expressions of variable's evolution laws are described in the literature<sup>1</sup>.

Material parameters used for each constitutive model were identified through the comparison of neat-resin FE analysis with neat-resin experiment of Fiedler et al.<sup>2</sup>. We employed  $\dot{\boldsymbol{\varepsilon}}_r = 1.0 \times 10^{-5}$ ,  $m = 1/35$ ,  $\beta = 0.2$ ,  $g_1 = 90$  MPa,  $g_2 = 0.08$ , and  $g_3 = 20$  MPa for Eqs. (2) and (3); and  $\dot{\gamma}_0 = 1.51 \times 10^7$  1/s,  $T = 297$  K, and  $\Delta v_\tau^* = 1.24 \times 10^{-18}$  mm<sup>3</sup> for Eq. (5).

To investigate important factors in failure criteria of composites, four sets of failure criteria are applied to matrix resin individually. Three criteria predict crack initiation based on the tensile and compressive strengths of matrix. Another criterion models crack initiation under elastic and plastic deformation, using two failure models.

The first criterion is von Mises criterion, expressed by the following equation.

$$\frac{1}{2} \left[ (\sigma_{11} - \sigma_{22})^2 + (\sigma_{22} - \sigma_{33})^2 + (\sigma_{33} - \sigma_{11})^2 \right] + 3(\sigma_{12}^2 + \sigma_{23}^2 + \sigma_{31}^2) \leq \sigma_t^2 \quad (6)$$

Here,  $\sigma_i$  is the stress component with respect to material principal axis, and  $\sigma_t$  is tensile strength of matrix resin.

The second criterion is Drucker-Prager criterion<sup>16</sup>, which includes the hydrostatic stress

effect on yielding behavior.

$$\frac{3}{2}\left(\frac{1}{3}-\frac{1}{3}\right)\sigma_m + \frac{1}{2}\left(\frac{1}{3}+\frac{1}{3}\right)\bar{\sigma} \leq 1 \quad (7)$$

Here,  $\bar{\sigma}$  is compressive strength of matrix resin.

The third criterion is Christensen's failure criterion<sup>5</sup>, which considers brittle failure under elastic deformation as well as ductile failure under plastic deformation.

$$3\left(1-\frac{1}{3}\right)\hat{\sigma}_m + \hat{\sigma}^2 \leq - \quad (8)$$

Here,  $\hat{\sigma}_m$  and  $\hat{\sigma}$  are hydrostatic and equivalent stresses normalized by compressive strength  $\bar{\sigma}$ , respectively. On the PUC analysis with Eq. (7), (8), or (9),  $\bar{\sigma}$  in Eq. (1) is set at zero to independently evaluate each failure criterion, and a matrix crack is assumed to occur when the stress state in an element satisfies each equation.

The fourth criterion is the combined criterion<sup>12</sup> that consists of two failure models to predict brittle failure under elastic deformation and ductile failure under plastic deformation. The first model is the dilatational energy density criterion, proposed by Asp et al.<sup>6</sup>. The dilatational energy density of a linear elastic body,  $U_v$ , is given by

$$U_v = \frac{3(1-2\nu)}{2E}\sigma_m^2 \quad (9)$$

where  $\nu$  is Poisson's ratio and  $E$  is Young's modulus. A matrix crack is assumed to occur when  $U_v$  reaches a critical value,  $U_v^{\text{crit}}$ , under elastic deformation. We employ  $U_v^{\text{crit}} = 0.9$  MPa, referring to the literature<sup>12</sup>. The second model is based on the damage parameter,  $D$ , calculated by the following evolutionary equation<sup>7</sup>, which is based on the Gurson-Tvergaard-Needleman model<sup>17, 18</sup>.

$$\dot{D} = H(\bar{\sigma} - \sigma_Y)(1 - D) \langle \dot{\epsilon}_m^p \rangle + (D_0 + D_1) \dot{\epsilon}^p. \quad (10)$$

Here,

$$\langle \dot{\epsilon}_m^p \rangle = \left[ \left( \frac{\langle \sigma_m \rangle}{\hat{\sigma}} \right)^2 \right]^{\bullet} \quad (11)$$

The first term on the right-hand side in Eq. (10) represents void growth caused by mean plastic vertical strain, and the second term indicates damage evolution caused by shear deformation. Here,  $H$  is the Heaviside function,  $\hat{\sigma}$  is the reference stress,  $\sigma_Y$  is the linearity limit of the matrix resin, and  $D_0$ ,  $D_1$  and  $D_2$  are non-dimensional constants. We employ  $\hat{\sigma} = 73$

MPa,  $\sigma_0 = 1.5$ ,  $\sigma_c = 0.6$ , and  $\sigma_1 = 0.6$ , referring to the literature<sup>12</sup>.  $\sigma^*$  is introduced to include the effect of the rapid evolution of damage due to the coalescence of micro voids<sup>18</sup>.

$$\sigma^* = \begin{cases} \sigma & (\sigma < \sigma_c) \\ \sigma_c + \frac{\sigma_{crit}^* - \sigma_c}{\sigma_{crit} - \sigma_c} (\sigma - \sigma_c) & (\sigma \geq \sigma_c) \end{cases} \quad (12)$$

Rapid damage evolution starts when  $\sigma$  reaches the threshold value  $\sigma_c$ . Here,  $\sigma_{crit}$  is the critical value of  $\sigma$ , and  $\sigma_{crit}^*$  is the critical value of  $\sigma^*$ . A matrix crack is assumed to occur when  $\sigma$  reaches the critical value,  $\sigma_{crit}$ , under plastic deformation. We utilize  $\sigma_c = 0.08$ ,  $\sigma_{crit} = 0.25$ , and  $\sigma_{crit}^* = 1/1.5$ , referring to the literature<sup>19</sup>. Furthermore, to avoid the mesh dependence of matrix damage, the nonlocalization of the variables that relate to failure criteria is conducted according to the literature<sup>20</sup>.

### 2.3 Computational procedure

To consider microscopic structure of composites and macroscopic deformation behavior of laminate simultaneously, multiscale analysis that consists of microscopic PUC analysis and macroscopic FE analysis is carried out. The computational procedure of the multiscale analysis is summarized as follows.

- 1) On the macroscopic scale, displacement-controlled tensile test analysis is performed to predict strain fields in laminate. The strain history is extracted at the assumed crack initiation point presented in Fig. 1.
- 2) On the PUC analysis, temperature decrease analysis is carried out to calculate thermal residual stress generated in the manufacturing process. Through the analysis, temperature is decreased by 150 K, which corresponds to the difference from curing temperature to room temperature. Macroscopic strain increment, which is uniformly applied to whole unit-cell, is controlled in order that volume-averaged stress of unit-cell will be zero, which reproduces the thermal shrinkage of laminate. Stress and strain fields obtained from this calculation are defined as initial states of laminate.
- 3) Macroscopic strain increment based on the strain history obtained from procedure 1) is applied to unit-cell to predict crack initiation in laminate subjected to tensile loading. Initial cracking strain is defined as the applied strain of the laminate when the failure criterion described in the section 2.2 is firstly satisfied in an element.

### 3 RESULTS AND DISCUSSION

Firstly, the effect of matrix constitutive modeling on laminate nonlinear response prediction was examined. Figure 3 shows the comparison of simulated results obtained from PUC analysis with experiment data of Yoshioka et al.<sup>10</sup>. The horizontal axis indicates applied strain, and the vertical axis represents volume-averaged stress over the unit cell. Multiscale predictions with both constitutive models reproduced inelastic stress-strain relationship of laminate. In the case of unidirectional laminate under off-axis loading, appropriate constitutive modeling, which is established based on experiment data, provides reasonable prediction of nonlinear stress-strain response.

Failure criteria were compared with each other, using the constitutive model of Eq. (1). Parameters  $\sigma_c$  and  $\epsilon_c$  were identified through the comparison of simulated cracking strains with experiment results of unidirectional off-axis tensile tests conducted by Yoshioka et al.<sup>10</sup>. Figure 4 shows simulated failure strains obtained from multiscale analysis with each failure criteria, using identified parameters. Except for von Mises criterion, simulated results qualitatively agree with experiment data. The identified parameters  $\sigma_c$  and  $\epsilon_c$  shown in Fig. 4 are feasible because these values are in the range of experimentally measured strength<sup>2, 21</sup>.

For more detailed evaluation, initial cracking sites obtained from each failure criterion were compared. Figure 5 shows the initial cracking sites predicted by each failure criterion in the 30° off-axis test. The hydrostatic and equivalent stress distributions obtained from the PUC analysis with the combined criterion are also shown in Fig. 5. In this case, initial crack was initiated

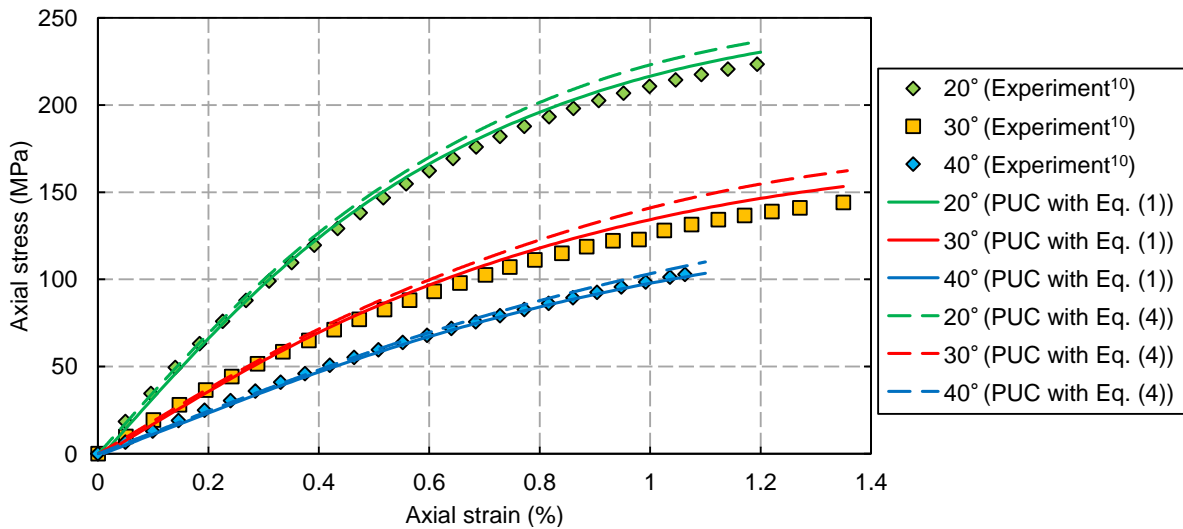


Fig. 3 Comparison of simulated off-axis tensile response of laminate with experiment data.

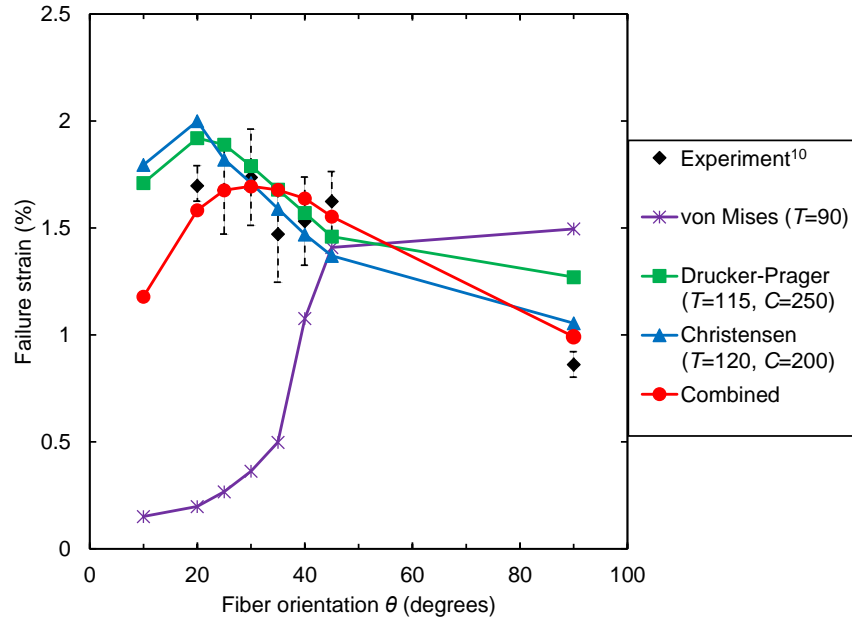


Fig. 4 Comparison of initial cracking strains obtained from multiscale analysis with experiment.

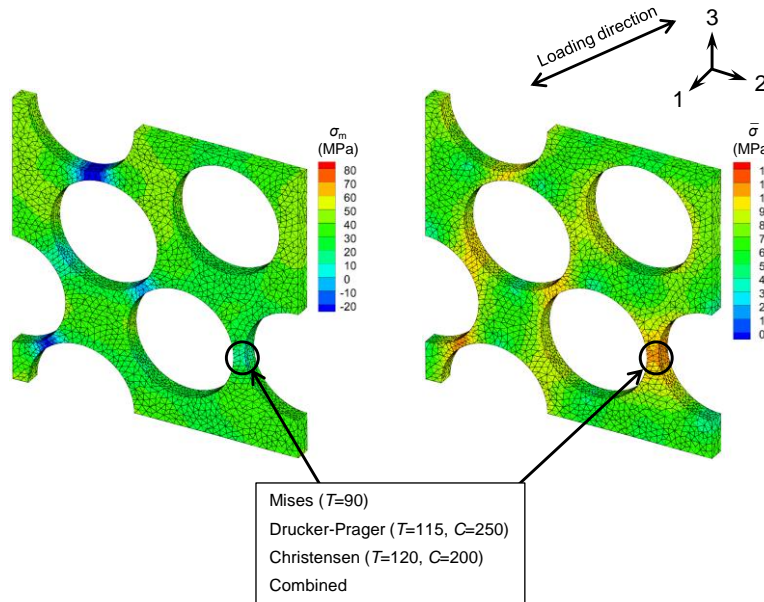


Fig. 5 Initial cracking sites predicted by each failure criterion and hydrostatic and equivalent stress distribution obtained from 30° off-axis analysis with combined criterion.

between fibers where large equivalent stress occurs. This large equivalent stress was caused by the shear deformation of laminate, and it led to crack formation under plastic deformation.

Figure 6 shows the initial cracking sites predicted by each failure criterion in the transverse

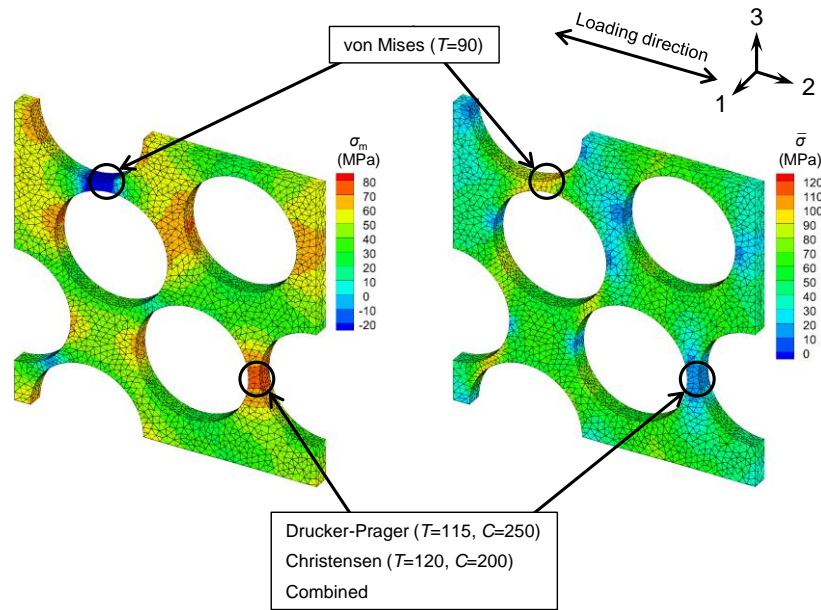


Fig. 6 Initial cracking sites predicted by each failure criterion and hydrostatic and equivalent stress distribution obtained from 90° off-axis analysis with combined criterion.

tension test. Figure 6 also shows the hydrostatic and equivalent stress distributions obtained from the PUC analysis with the combined criterion. In the case of the Drucker-Prager, Christensen and combined criteria, the initial crack occurred between fibers that are aligned parallel to the loading direction. These results agree well with previous experimental work<sup>21</sup> and numerical results<sup>8,9</sup>. On the other hand, in the case of von Mises criterion, the initial crack was initiated between fibers that are aligned perpendicular to the loading direction. The von Mises criterion cannot reproduce the initial cracking site under transverse loading because this criterion does not consider the hydrostatic stress effect that causes cavitation-induced brittle failure reported by Asp et al.<sup>6,8</sup>. These results indicate that a failure criterion for matrix resin should include not only the distortional component that causes ductile failure but also the dilatational component that induces brittle failure to predict initial failure under practical loading conditions.

#### 4 CONCLUSIONS

In this study, the effect of constitutive and failure modeling of matrix resin on crack prediction capability of multiscale analysis is investigated. Two constitutive models were applied to matrix resin of PUC analysis to examine their influence on nonlinear stress-strain

response prediction of CFRP laminate. For unidirectional laminate, inelastic constitutive models with experimentally identified parameters provided reasonable multiscale prediction of material nonlinearity. Four sets of failure criteria were implemented to microscopic PUC analysis to evaluate factors that need to predict crack initiation in composite laminate. Except for von Mises criterion, simulated results qualitatively agreed with experiment data. This is because von Mises criterion does not consider the hydrostatic stress effect on crack formation. These results imply that a failure criterion for matrix resin ought to take account for not only the distortional effect that leads to ductile failure but also the dilatational effect that induces brittle failure to predict crack formation. We will conduct multiscale matrix modeling evaluation with practical laminate to develop matrix modeling strategy for multiscale failure prediction, which is capable under more complex loading conditions.

## REFERENCES

- [1] Hasan, O. A., and Boyce, M. C., A constitutive model for the nonlinear viscoelastic viscoplastic behavior of glassy polymers, *Poly. Eng. Sci.* (1992) 35:331-344.
- [2] Fiedler, B., Hojo, M., Ochiai, S., Schulte, K., and Ando, M., Failure behavior of an epoxy matrix under different kinds of static loading, *Compos. Sci. Technol.* (2001) 61:1615-1624.
- [3] Kobayashi, S., Tomii, D., and Shizawa, K., A modelling and simulation on failure prediction of ductile polymer based on craze evolution and annihilation, *Trans. Jpn Soc. Mech. Eng. Ser. A* (2004) 70:810-817. (in Japanese).
- [4] Bai, X., Bessa, M. A., Melro, A. R., Camanho, P. P., Guo, L., and Liu, W. K., High-fidelity micro-scale modeling of the thermo-visco-plastic behavior of carbon fiber polymer matrix composites, *Compos. Struct.* (2015) 134:132-141.
- [5] Christensen, R. M., *The Theory of Materials Failure*, Oxford University Press (2013).
- [6] Asp, L. E., Berglund, L. A., and Talreja, R., A criterion for crack initiation in glassy polymers subjected to a composite-like stress state, *Compos. Sci. Technol.* (1996) 56:1291-1301.
- [7] Nishikawa, M., *Multiscale modeling for the microscopic damage and fracture of fiber-reinforced plastic composites*, Dr. Eng. Thesis, The University of Tokyo (2008). (in Japanese).
- [8] Asp, L. E., Berglund, L. A., and Talreja, R., Prediction of matrix-initiated transverse failure in polymer composites, *Compos. Sci. Technol.* (1996) 56:1089-1097.
- [9] Okabe, T., Nishikawa, M., and Toyoshima, H., A periodic unit-cell simulation of fiber

- arrangement dependence on the transverse tensile failure in unidirectional carbon fiber reinforced composites, *Int. J. Solids Struct.* (2011) 48:2948-2959.
- [10] Yoshioka, K., Kumagai, Y., Higuchi, R., Lee, D., and Okabe, T., Multiscale Modeling of Failure Strain in Off-Axis Tensile Testing of UD-CFRP, *Mater. Sys.* (2016) 34:7-13. (in Japanese).
- [11] Yokozeki, T., Ogihara, S., Yoshida, S., and Ogasawara, T., Simple constitutive model for nonlinear response of fiber-reinforced composites with loading-directional dependence, *Compos. Sci. Technol.* (2007) 67:111-118.
- [12] Sato, Y., Okabe, T., Higuchi, R., and Yoshioka, K., Multiscale approach to predict crack initiation in unidirectional off-axis laminates, *Adv. Compos. Mater.* (2014) 23:461-475.
- [13] Pipes, R. B., and Gosse, J. H., An Onset Theory for Irreversible Deformation in Composite Materials, in: *17th International Conference on Composite Materials* (2009).
- [14] Tran, T. D., Kelly, D., Prusty, B. G., Gosse, J. H., and Christensen, S., Micromechanical modelling for onset of distortional matrix damage of fiber reinforced composite materials, *Compos. Struct.* (2012) 94:745-757.
- [15] Matsuda, T., Ohno, N., Tanaka, H., and Shimizu, T., Homogenized in-plane elastic-viscoplastic behavior of long fiber-reinforced laminates, *JSME Int. J. Ser. A* (2002) 45:538-544.
- [16] Drucker, D., and Prager, W., Soil Mechanics and Plastic Analysis or Limit Design, *Quart. Appl. Math.* (1952) 10:157-165.
- [17] Gurson, A. L., Continuum theory of ductile rupture by void nucleation and growth: Part I- Yield criteria and flow rules for porous ductile media, *J. Eng. Mater. Technol.* (1977) 99:2-15.
- [18] Tvergaard, V., and Needleman, A., Analysis of the cup-cone fracture in a round tensile bar, *Acta Metall.* (1984) 32:157-169.
- [19] Tvergaard, V., and Needleman, A., Effects of nonlocal damage in porous plastic solids, *Int. J. Solids Struct.* (1995) 32:1063-1077.
- [20] Bažant, Z. P., and Pijaudier-Cabot, G., Nonlocal continuum damage, localization instability and convergence, *J. Appl. Mech.* (1988) 55:287-293.
- [21] Hobbiebrunken, T., Hojo, M., Adachi, T., De Jong, C., and Fiedler, B., Evaluation of interfacial strength in CF/epoxies using FEM and in-situ experiments, *Compos. Part A* (2006) 37:2248-2256.

## Hydrodynamics and Nutrient Transport Inside a Cell-Seeded Hollow Fibre Membrane Bioreactor

Prakash Kumar\*, Raja Sekhar G. P.\*\*

\*Indian Institute of Technology Kharagpur, India 721302, \*\*Indian Institute of Technology Kharagpur, India 721302

### ABSTRACT

Introduction Biodegradable extracellular matrix (ECM), also termed as the scaffold, are manufactured using natural materials such as collagen, glycosaminoglycan, and chitosan. In addition to natural materials, artificially synthetic polymers like polyglycolic acid (PGA), polylactic acid (PLA), and polycaprolactone (PCL) have also been used; moreover, most of the products used are deformable in nature [1]. The objective of this study is to provide a mathematical model of HFMB bioreactor along with deformable scaffold so that a uniform distribution of nutrient concentration can be supplied to each part of the bioreactor. Methods In order to deal with deformation of the solid phase and movement of the fluid phase, we adopt biphasic mixture theory equations [2]. The flow inside the lumen is governed by Stokes equation. We close the model using the appropriate boundary conditions at the wall and the interphase of the bioreactor. The flow inside the bioreactor is assumed to be unidirectional and the advection-diffusion-reaction equation is used to get the momentum balance of the nutrient in scaffold and lumen region. We use asymptotic methods to reduce the system (lubrication approximation) to obtain leading order nutrient concentration. This leads to a coupled system of partial differential equations (PDEs) with time-dependent variables. Laplace transformation is used to deal with time-dependent terms and Durbin's algorithm was used to retrieve time dependency. Results The effect of fluid velocity and the solid displacement is analyzed with respect to varying pressure gradient, porosity, the permeability of the scaffold region. The convection in the nutrient balance equation is affected by the composite velocity inside the scaffold region. The reaction rate of different cells based on available experimental data is used to study the effect on nutrient concentration. The factors affecting the nutrient concentration are lumen radius, porosity, and permeability of the scaffold, Thiele modulus, pressure gradient etc. Total mass transfer rate is computed to analyze the movement of nutrient supply in each cross-section of the bioreactor. Nutrient concentration inside the bioreactor increases with increase in the thickness of the lumen whereas porosity and permeability have significant role in the uniformity of nutrient concentration. Nutrient concentration decreases with higher Thiele modulus and the mass transfer increases with the increase in the thickness of scaffold region. References 1. P. Chumtong, et al. Mechatronics and Automation (ICMA), 2014 IEEE International Conference on. IEEE, 2014. 2. K. R. Rajagopal, Mathematical Models and Methods in Applied Sciences 17.02 (2007): 215-252.

## **A C 0 Interior Penalty Discontinuous Galerkin Method for Fourth Order Total Variation Flow**

Rahul Kumar<sup>\*</sup>, Chandi Bhandari<sup>\*\*</sup>, Ronald H.W Hoppe<sup>\*\*\*</sup>

<sup>\*</sup>Basque Center for Applied Mathematics (BCAM), Bilbao, Spain, <sup>\*\*</sup>University of Houston, Houston, <sup>\*\*\*</sup>University of Houston, Houston, USA

### **ABSTRACT**

We consider the numerical solution of the regularized fourth order total variation flow problem based on an implicit discretization in time and a C 0 Interior Penalty Discontinuous Galerkin (C 0 IPDG) method in space. In particular, we prove coerciveness and boundedness of the associated C 0 IPDG form with respect to a mesh dependent C 0 IPDG-norm of the underlying function space. The main result is an a priori error estimate of the global discretization error in the mesh dependent C 0 IPDG-norm. The derivation of the error estimate requires an Aubin-Nitsche type argument by considering an appropriate boundary value problem for the adjoint of the linearized partial differential operator. Numerical results are also provided illustrating the performance of the C 0 IPDG method and confirming the theoretical findings. Finally documentation of applications to medical imaging will be produced.

## Enhanced Local Maximum Entropy Approximation for Stable Meshfree Simulations

Siddhant Kumar<sup>\*</sup>, Dennis Kochmann<sup>\*\*</sup>, Kostas Danas<sup>\*\*\*</sup>

<sup>\*</sup>California Institute of Technology, <sup>\*\*</sup>ETH Zürich, <sup>\*\*\*</sup>École Polytechnique

### ABSTRACT

We propose an improved meshfree approximation scheme which is based on the local maximum-entropy strategy as a compromise between shape function locality and entropy in an information-theoretical sense. The improved version is specifically designed for severe, finite deformation and offers significantly enhanced stability as opposed to the original formulation. This is achieved by (i) formulating the quasi-static mechanical boundary value problem in a suitable updated-Lagrangian setting, (ii) introducing anisotropy in the shape function support to accommodate directional variations in nodal spacing with increasing deformation, (iii) spatially bounded shape function support to restrict the domain of influence and increase efficiency, (iv) truncating shape functions at interfaces in order to stably represent multi-component systems like composites or polycrystals. The new scheme is applied to benchmark problems of severe elastic deformation that demonstrate its performance both in terms of accuracy (as compared to exact solutions and, where applicable, finite element simulations) and efficiency. Importantly, the presented formulation overcomes the classical tensile instability found in most meshfree interpolation schemes, as shown for stable simulations of, e.g., the inhomogeneous extension of a hyperelastic block up to 300% or the torsion of a hyperelastic cube by 270 degrees – both without the need for remeshing.

## A Cluster-based Microstructural Topology Optimization

Tej Kumar\*, Krishnan Suresh\*\*

\*University of Wisconsin, Madison, \*\*University of Wisconsin, Madison

### ABSTRACT

The advent of 3D printing has enabled the possibility of custom designed microstructures for demanding applications. Microstructures were initially employed in structural optimization to create repeating structures using a single set of microstructural design variables. Later, macro-structural variables were included together with a local volume constraint to achieve a two-level optimization [1, 2]. The local volume constraint was found to be essential to avoid completely degenerate (entirely solid, or entirely void) microstructures. However, this additional constraint inhibited the design from achieving peak performance. Here, we propose to get rid of both the macro-structural variables, as well as the local volume constraint. Instead, we directly impose a volume constraint via the microstructural variables. This leads to spatially varying, and optimal, microstructures. To address the computational cost, we generalize the grid-based clustering strategy proposed in Sivapuram et al. [1]. In particular, we propose several alternate clustering strategies that lead to significant improvement in performance, without significantly affecting the computational cost. Clusters are allowed to remain fixed or can adapt, during optimization. The clustering strategies are developed based on the well-known k-clustering algorithm, using multiple metrics. The effectiveness of these strategies is demonstrated through several examples. Associated computational cost and performance are studied with varying number of clusters. [1] Sivapuram, R., Dunning, P. D., Kim, H. A. (2016). Simultaneous material and structural optimization by multiscale topology optimization. *Structural and Multidisciplinary Optimization*, 54(5), 1267–1281. <https://doi.org/10.1007/s00158-016-1519-x> [2] Chen, W., Tong, L., & Liu, S. (2017). Concurrent topology design of structure and material using a two-scale topology optimization. *Computers and Structures*, 178, 119–128. <https://doi.org/10.1016/j.compstruc.2016.10.013>

## Numerical Modeling of Contact Friction Problems Using Phase-Field Model of Fracture

Vivek Kumar\*, Maurizio Chiaramonte\*\*

\*Civil and Environmental Engineering Dept, Princeton, NJ, \*\*Civil and Environmental Engineering Dept, Princeton, NJ

### ABSTRACT

Correctly predicting the behavior of faults and fissures in rocks or concrete-to-concrete sliding in civil engineering structures is important to prevent structural failure. These essentially turn into solving contact problems between fractured surfaces. Earlier approaches to solve contact problems based on extended finite element method (X-FEM) suffer from numerical instability and the contact pressure so obtained between cracked surfaces show spurious oscillations. Moreover, these oscillations persist or become worse with mesh refinement. Hence, various stabilization techniques had to be employed to overcome the numerical instability. Some of the commonly employed stabilization techniques are Nitsche's stabilization, bubble stabilization, reduced Lagrange methods and polynomial pressure projection. In this article we discuss a new method for solving frictional contact problems which do not suffer from such issues. In this work, we develop a phase-field model of fracture for solving frictional contact problems. Phase field model is a diffusive model of fracture based on the introduction of an auxiliary field called phase field. The phase-field model used in this article is based on the work of Miehe et. al [Miehe C, Hofacker M, Welschinger F. A phase field model for rate-independent crack propagation: Robust algorithmic implementation based on operator splits. *Computer Methods in Applied Mechanics and Engineering*. 2010 Nov 15;199(45):2765-78.]. We detail the mathematical formulation for extending the use of phase-field for frictional contact problems and implement the scheme using FEniCS, an open source computing platform for solving partial differential equations. Benchmark problems involving both frictionless and frictional contact are solved to demonstrate the advantages of this new method. Finally, the above method is used to simulate the crack growth when surfaces with frictional contact move past each other, and the results are compared with those found in literature.

## On the Combination of Extended Galerkin Methods with Mesh Adaptation

Florian Kummer\*

\*TU Darmstadt/Fluid Dynamics

### ABSTRACT

Over the past years, we developed a high-order numerical method for multi-phase flow problems, such as droplets or bubbles, which employs a sharp interface representation by a level-set and an extended discontinuous Galerkin (XDG) discretization for the flow properties. The shape of the XDG basis functions is dynamically adapted to the position of the fluid interface, so that the spatial approximation space can represent jumps in pressure and kinks in velocity accurately. By this approach, the high-order convergence property of the discontinuous Galerkin (DG) method can be preserved for the low-regularity, discontinuous solutions, such as those appearing in multi-phase flows. However, in realistic droplet setups one observes length scales which may cover several magnitudes. While extended methods are well suited to embed arbitrary interfaces or surfaces on (e.g. Cartesian) background meshes they lack the capability to adapt to different length scales. Therefore, an extended method has to be combined with techniques like adaptive mesh refinement. This refinement can be feature-based, e.g. controlled by the local curvature of the fluid interface. Our presentation will focus on some of the critical building-blocks of the method and their integration in the full solver.

## The Lie Symmetries of Forced Duffing Type Oscillators

Bidisha Kundu\*, Ranjan Ganguli\*\*

\*Ph.D Student, \*\*Professor

### ABSTRACT

In the era of advanced computation techniques and tools, still, the researchers are interested in inventing new ways of calculation. Their interests lie in searching analytical solutions, exact or closed form of the solutions to save the computation time. The Lie symmetry method is the most famous and successful among them for applying on different types of differential equations. The Norwegian mathematician Sophus Lie (1842-1899) first introduced this technique and later it was developed more and employed in several problems [1]. This method is the mixture of two branches of mathematics- algebra and analysis. There are various kinds of motivations for studying the Lie method such as to find the symmetries of the system, an equivalent form of the equation by reducing the order of the equation or linearize the nonlinear equation, and the invariant solutions which are in exact or closed form in most of the cases. In this work, we mainly concentrate on the nonlinear damped spring-mass system with external force. Due to nonlinear restoring force (Duffing oscillator), or for the damping (van der Pol oscillator), the nonlinearities appear. In [2], the general Liénard type equations were studied but without forcing effect. We follow the Lie symmetry procedure to understand the symmetries and try to find the similarity transformation dependent on the damping coefficient, force etc. Duffing type oscillators with external force effect are studied here. So, time variable is explicitly present in the equation, and the equation is nonautonomous. In this case, the Lie method will help us to investigate this system to get the invariant solution, and it may also linearize the equation. In this presentation, at first, I will discuss the fundamental theories and background of the Lie method and the application procedure. The primary challenge is to solve the determining equations which provide the transformations. We have solved them analytically and found a relationship between the damping coefficient, stiffness nonlinearity and the force. We hope we can extract more information and extend our work to coupled Duffing type oscillators. References: [1] Olver P. J., Applications of Lie Groups to Differential Equations, vol. 107 (Springer Science & Business Media, New York, 2012). [2] Pandey, S.N., Bindu, P.S., Senthilvelan, M., Lakshmanan, M., J. Math. Phys. 50, 082702 (2009).

## Particle Image Velocimetry-based Validation of a CFD Model for the Treatment of Intracranial Aneurysms Using a Shape Memory Polymer Embolization Device

Robert Kunkel<sup>\*</sup>, Devin Laurence<sup>\*\*</sup>, Donnie Robinson<sup>\*\*\*</sup>, Joshua Scherrer<sup>\*\*\*\*</sup>, Aichi Chien<sup>\*\*\*\*\*</sup>,  
Bradley Bohnstedt<sup>\*\*\*\*\*</sup>, Yi Wu<sup>\*\*\*\*\*</sup>, Yingtao Liu<sup>\*\*\*\*\*</sup>, Ching-Hao Lee<sup>\*\*\*\*\*</sup>

<sup>\*</sup>University of Oklahoma, <sup>\*\*</sup>University of Oklahoma, <sup>\*\*\*</sup>University of Oklahoma, <sup>\*\*\*\*</sup>University of Oklahoma,  
<sup>\*\*\*\*\*</sup>University of California Los Angeles Medical School, <sup>\*\*\*\*\*</sup>The University of Oklahoma Health Sciences Center,  
<sup>\*\*\*\*\*</sup>University of Oklahoma, <sup>\*\*\*\*\*</sup>University of Oklahoma, <sup>\*\*\*\*\*</sup>University of Oklahoma

### ABSTRACT

Intracranial aneurysms (ICAs) are localized dilations of blood vessels in the brain caused by weaknesses in the vessel walls. ICAs have a prevalence of 0.5% - 6% in adults. While the aneurysm itself is typically asymptotic, incidental rupture of an ICA produces subarachnoid hemorrhage (SAH), leading to 5% of all strokes and the death of roughly 10% of patients before receiving medical attention [1]. Computational fluid dynamic (CFD) modeling of the hemodynamics of ICAs can be used by physicians to inform the treatment process once an aneurysm has been diagnosed. The objective of this study is to develop a CFD model for simulating the velocity patterns within ICAs, and eventually for accommodating a novel endovascular treatment method utilizing an aliphatic urethane shape memory polymer. The CFD model will be developed from patient-specific brain computed tomography (CT) angiography in ANSYS Fluent. The model will be validated using in-house particle image velocimetry (PIV) analysis of patient-specific aneurysm phantoms under pulsatile flow conditions. The current clinical practice includes two main treatment methods for ICAs— a clipping device that is surgically attached around the outer neck of the aneurysm and an endovascular embolization method that uses an intravenous delivery device to coil flexible wire within aneurysm sac [2]. We are developing a novel treatment using patient-specific shape memory polymer (SMP) inserts for an endovascular embolization technique capable of achieving a higher volume fill rate and providing more permanent occlusion. CFD is used to evaluate which treatment method will result in the most favorable flow conditions once implemented. For our innovative therapeutics, we plan to use a stereolithographic 3D printer to cure SMP in geometries based on CT scan image data from individual patients. The SMP will then be deformed into a thin filament capable of being delivered intravenously, and will be thermally activated to revert to its original geometry once arriving at the aneurysm. To properly demonstrate the feasibility of this treatment, the developed CFD model will need to accurately predict the velocity patterns within the untreated aneurysm, and account for interactions between the blood flow and the boundary of the SMP device. The developed CFD-based aneurysm treatment simulation platform will provide a useful tool for predicting the effectiveness of SMP based occlusion in patient-specific scenarios. References: [1] S. Yu and J. Zhao, *Medical Engineering &amp;amp;amp;amp;amp;amp;amp;amp;amp; Physics* 1999, 21(3): 133–141. [2] Y. Hoi, *Journal of Biomechanical Engineering*, 2006, 128(6): 844.

## Micro-FE Modeling for Multiscale Coupled Analysis of Resistance Spot Welding

Hiroyuki Kuramae<sup>\*</sup>, Tomoya Niho<sup>\*\*</sup>, Tomoyoshi Horie<sup>\*\*\*</sup>

<sup>\*</sup>Osaka Institute of Technology, <sup>\*\*</sup>Kyushu Institute of Technology, <sup>\*\*\*</sup>Kyushu Institute of Technology

### ABSTRACT

Since electrical contact resistance is an important property in the numerical simulations for resistance spot welding, a multiscale coupled finite element (FE) procedure for resistance spot welding is proposed to evaluate the high accuracy of the electrical contact resistance. This analysis consists of macroscopic coupled FE analysis for the resistance spot welding and microscopic the electrical contact resistance analysis using three-dimensional (3D) thermal elasto-plasticity contact FE simulation. The multiscale analysis is based on coupled FE procedure among structural deformation, electric current and temperature distributions to evaluate a nugget growth by Joule heating in the macro-scale analysis, and to calculate the electrical contact resistance in the micro-scale analysis. Temperature-dependent material properties such as yield stress, work hardening rate and resistivity are considered in both scale analyses. A rigid plate is contacted to the micro-FE model with contact pressure and temperature that are obtained by macro-analysis, to calculate electrical contact resistance by elast-plasticity contact FE analysis including large deformation theory combined with electric FE analysis based on the phi-method. The micro-scale analysis is a very computationally expensive process because of evaluation of electrical contact resistance distribution on the macro-contact surface every time step. A micro-FE model, which corresponds to statistically similar representative volume element (SS-RVE), was constructed based on a surface roughness measurement of a steel sheet using laser microscope apparatus with 0.139 micrometers interval. In this study, an optimum size of SS-RVE in-plane was determined based on correlational analyses between frequency distribution of the microscopic surface roughness between measured 284.7×213.5 square micrometers and various sampling size. The optimum size of SS-RVE was determined as 100×100 square micrometers in-plane. Resolution of 3D FE mesh in-plane is also examined by the micro-scale electrical contact resistance analyses. In addition, to analyze realistic electrical contact resistance of steel plate contact in the micro-scale analysis, an oxide film FeO on the surface is considered. The oxide film is 3nm thickness and is introduced into the surface of the micro-FE model. The electrical contact resistance with the oxide film was higher accuracy than without one.

## Comparison of Fracture Behavior in Concrete between FEM and DIC

Mao Kurumatani<sup>\*</sup>, Yusuke Koakutsu<sup>\*\*</sup>, Kazuya Hashiguchi<sup>\*\*\*</sup>

<sup>\*</sup>Ibaraki University, <sup>\*\*</sup>Ibaraki University, <sup>\*\*\*</sup>Ibaraki University

### ABSTRACT

We present a comparison of fracture behavior in reinforced concrete between simulation and experiment toward the V&amp;V analysis which has recently been required in the field of computational mechanics. Particularly, the V&amp;V for the fracture simulation in concrete seems to be difficult because many studies still have been made on the numerical methods for crack propagation for a long time. In this study, the FEM with a damage model is applied to simulate the fracture behavior with cracking in concrete. The damage model is based on fracture mechanics for concrete in consideration of cohesive zone in the fracture process, which is equivalent to a kind of energy balance approach in terms of fracture energy. The modified von-Mises criterion is introduced into the damage model to evaluate the cracking in concrete while the von-Mises plasticity is applied to model the plastic behavior of steel-reinforcements. To measure the crack propagation in concrete, we employ the digital image correlation (DIC) method which has been developed in our laboratory. A numerical simulation with the FEM and experimental measurement with the DIC are performed for 4-point bend test of RC beams with different shear reinforcements. The quantitative comparison of crack propagation between the numerical and experimental results offer valuable insight into the V&amp;V for the fracture simulation of concrete and reinforced concrete.

## Autonomous Materials Research Systems: Phase Mapping

A. Gilad Kusne<sup>\*</sup>, Brian DeCost<sup>\*\*</sup>, Jason Hattrick-Simpers<sup>\*\*\*</sup>, Ichiro Takeuchi<sup>\*\*\*\*</sup>

<sup>\*</sup>National Institute of Standards & Technology, <sup>\*\*</sup>National Institute of Standards & Technology, <sup>\*\*\*</sup>National Institute of Standards & Technology, <sup>\*\*\*\*</sup>University of Maryland

### ABSTRACT

The last few decades have seen significant advancements in materials research tools, allowing researchers to rapidly synthesize and characterize large numbers of samples - a major step toward high-throughput materials discovery. Machine learning has been tasked to aid in converting the collected materials property data into actionable knowledge, and more recently it has been used to assist in experiment design. In this talk we demonstrate the next step in machine learning for materials research - an autonomous materials measurement system. The software system controls X-ray diffraction measurement systems both in the lab and at the beamline to identify composition-temperature phase maps from composition spreads with a minimum number of measurements. The algorithm also capitalizes on prior knowledge in the form of physics theory and external databases, both theory-based and experiment-based, to more rapidly hone in on the optimal results. Materials of interest include Fe-Ga-Pd, TiO<sub>2</sub>-SnO<sub>2</sub>-ZnO, and Mn-Ni-Ge.

## FINITE BEAM ELEMENT WITH PIEZOELECTRIC LAYERS AND FG MATERIAL OF CORE

VLADIMÍR KUTIŠ\*, JUSTÍN MURÍN†, JURAJ PAULECH† AND  
GABRIEL GÁLIK†

\*†Department of Applied Mechanics and Mechatronics  
Institute of Automotive Mechatronics  
Faculty of Electrical Engineering and Information Technology  
Slovak University of Technology  
Ilkovičova 3, 812 19 Bratislava  
Slovak Republic

[vladimir.kutis@stuba.sk](mailto:vladimir.kutis@stuba.sk)  
[justin.murin@stuba.sk](mailto:justin.murin@stuba.sk)  
[juraj.paulech@stuba.sk](mailto:juraj.paulech@stuba.sk)  
[gabriel.galik@stuba.sk](mailto:gabriel.galik@stuba.sk)

**Key words:** Beam Element, FEM, Piezoelectric Analysis, State Space Model.

**Abstract.** New smart materials have been developed in material science, that are suitable for broad mechatronic applications. Modern mechatronic systems are focusing on minimizing size, active control and low energy consumption. To improve performance of such systems, new materials and technologies are developed – one of them, which found broad application usage in mechatronics is Functionally graded material (FGM). Connection of FGM beam with piezoelectric layers can be considered as suitable smart material composition for mechatronics. In the contribution, finite element beam with thick FGM core and thin piezoelectric layers is presented. FGM finite element beam with piezolayers has 6 structural degree of freedom and 4 electric degree of freedom. Stiffness matrix and mass matrix of beam element is computed using transfer functions and transfer constants, where the homogenization process of FGM core and piezoelectric layers is applied.

### 1 INTRODUCTION

Smart structures are widely used in modern engineering applications. They can combine the progress in material science, control theory, electronics and informatics. The best way how to examine such structures before their production is to create their mathematical model. Finite element method is dominant mathematical tool to analyzed such structures and with combination with control can be able to create model of smart structure.

In the presented paper, beam element with core made of functionally graded material in

transversal and longitudinal direction and with piezoelectric layers is presented. The goal is to create dynamic representation of beam structures with active parts made from piezoelectric layers, which can be also used for model of control of the structure.

## 2 HOMOGENIZED MATERIAL PROPERTIES OF BEAM

Let us consider straight sandwich beam with core made from functionally graded material (FGM) and top and bottom layers made from piezoelectric material with constant material properties – Fig. 1. Cross-section of FGM core has height  $h_{FGM}$  and depth  $b$ , one piezoelectric layer has height  $h_p$  and depth  $b$ .

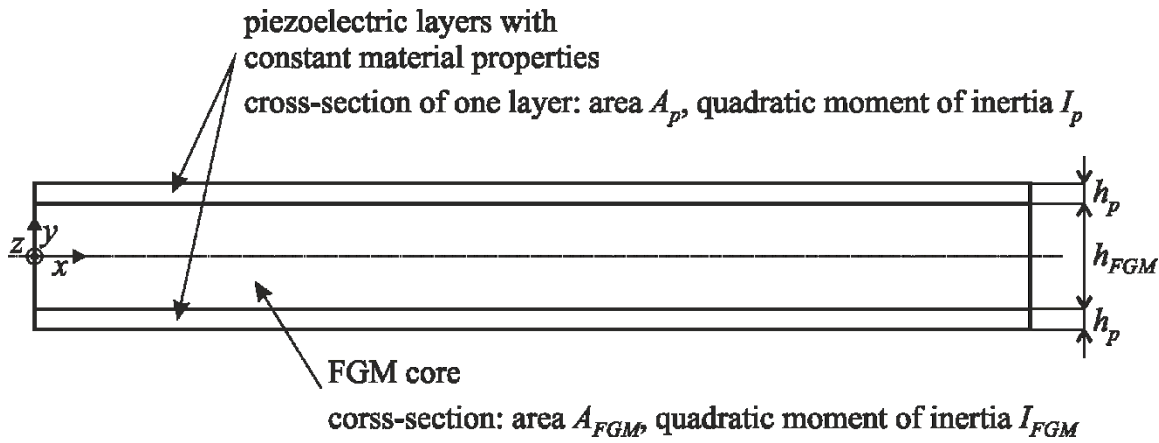


Fig. 1: Piezoelectric beam with core made from FGM material

The composite material of the FGM core arises by mixing two components (matrix and fibers) that are approximately of the same geometrical form and dimensions.

Both the fiber volume fraction  $v_f(x, y)$  and matrix volume fraction  $v_m(x, y)$  are chosen as a polynomial function of longitudinal position  $x$ , and with continuous and symmetrical variation through its height  $h$  with respect to the neutral plane of the FGM core. The volume fractions are assumed to be constant through the cross-section depth  $b$ . At each point of the FGM core it holds:  $v_f(x, y) + v_m(x, y) = 1$ .

Young modulus of the constituents (fibers -  $E_f(x, y)$  and matrix -  $E_m(x, y)$ ) can analogically vary as it is stated by the variation of volume fractions. For effective Young's modulus  $E_{FGM}(x, y)$  of FGM core we can write [1,2]

$$E_{FGM}(x, y) = v_f(x, y)E_f(x, y) + v_m(x, y)E_m(x, y) \quad (1)$$

## 2.1 Homogenized properties of FGM core

Homogenized Young's modulus for axial loading  $E_{FGM}^{HN}(x)$  and bending  $E_{FGM}^{HM}(x)$  of FGM core with cross-section  $A_{FGM}$  (height  $h_{FGM}$  and depth  $b$ ) and quadratic moment of inertia  $I_{FGM}$  can be expressed in form

$$E_{FGM}^{HN}(x) = \frac{\int_{-h_{FGM}/2}^{h_{FGM}/2} b E_{FGM}(x,y) dy}{A_{FGM}} \quad (2)$$

$$E_{FGM}^{HM}(x) = \frac{\int_{-h_{FGM}/2}^{h_{FGM}/2} b y^2 E_{FGM}(x,y) dy}{I_{FGM}} \quad (3)$$

Both homogenized Youngs' moduli of FGM core are dependent only on axial location  $x$  and not on transversal location  $y$ .

## 2.2 Homogenized properties of beam with FGM core and piezoelectric layers

Homogenized Young's modulus for axial loading  $E^{HN}(x)$  and bending  $E^{HM}(x)$  of beam with FGM core and piezoelectric layers can be expressed in form

$$E^{HN}(x) = \frac{A_{FGM}}{A} E_{FGM}^{HN}(x) + \frac{2A_p}{A} E_p \quad (4)$$

$$E^{HM}(x) = \frac{I_{FGM}}{I} E_{FGM}^{HN}(x) + \frac{2I_{pz}}{I} E_p \quad (5)$$

where  $A$  is total cross section ( $A = A_{FGM} + 2A_p$ ),  $I$  is total quadratic moment of inertia and  $I_{pz}$  is quadratic moment of inertia of piezolayer to global axis  $z$ .

Both homogenized Youngs' moduli of beam with FGM core and piezoelectric layers are dependent only on axial location  $x$ .

## 3 PIEZOELECTRIC BEAM FINITE ELEMENT EQUATIONS

### 3.1 Piezoelectric constitutive equations

Piezoelectric constitutive equations describe the relation between mechanical and electrical quantities. The form of the constitutive equations depends on chosen mechanical and electrical quantities and can be expressed in two basic configurations. The first configuration is expressed by stress tensor components  $\sigma_{kl}$  and vector components of electric intensity  $E_k$  and has form

$$\begin{aligned} \varepsilon_{ij} &= d_{ijk} E_k + s_{ijkl}^E \sigma_{kl} \\ D_i &= \epsilon_{ik}^\sigma E_k + d_{ikl} \sigma_{kl} \end{aligned} \quad (6)$$

where  $\varepsilon_{ij}$  are strain tensor components,  $D_i$  are components of electric displacement vector,  $d_{ijk}$  are tensor components of piezoelectric constants,  $\epsilon_{ik}^\sigma$  are components of permittivity tensor on conditions constant mechanical stress and  $s_{ijkl}^E$  are components of compliance tensor on conditions constant electric intensity [3].

The constitutive equations can be also expressed by strain tensor components  $\varepsilon_{kl}$  and vector components of electric intensity  $E_k$  and has form

$$\begin{aligned}\sigma_{ij} &= c_{ijkl}^E \varepsilon_{kl} - e_{ijk} E_k \\ D_i &= e_{ikl} \varepsilon_{kl} + \epsilon_{ik}^\varepsilon E_k\end{aligned}\quad (7)$$

where new quantities are components of stiffness tensor  $c_{ijkl}^E$  and components of piezoelectric modulus tensor  $e_{ikl}$ .

The other equations, which play important role, are relation between the components of strain tensor  $\varepsilon_{ij}$  and components of deformation  $u_i$  and relation between vector components of electric intensity  $E_i$  and electric potential  $\varphi$ . These relations can be expressed as

$$\begin{aligned}\varepsilon_{ij} &= 1/2 (u_{i,j} + u_{j,i}) \\ E_i &= -\varphi_{,i}\end{aligned}\quad (8)$$

Tensor equations (6) and (7) can be expressed in matrix forms, which is more suitable for finite element formulations, using symmetry of mechanical and electrical quantities as well as material properties. Matrix formulations of constitutive equations (7) can be expressed as

$$\begin{aligned}\boldsymbol{\sigma} &= \mathbf{c}^E \boldsymbol{\varepsilon} - \mathbf{e}^T \mathbf{E} \\ \mathbf{D} &= \mathbf{e} \boldsymbol{\varepsilon} + \boldsymbol{\epsilon}^\varepsilon \mathbf{E}\end{aligned}\quad (9)$$

where  $\boldsymbol{\sigma}$  is vector (in mathematical meaning) of 6 stress tensor components,  $\mathbf{D}$  is vector of 3 electric displacement vector components,  $\boldsymbol{\varepsilon}$  is vector of 6 strain tensor components,  $\mathbf{E}$  is vector of 3 electric intensity vector components,  $\mathbf{c}^E$  is 6x6 matrix of mechanical properties,  $\boldsymbol{\epsilon}^\varepsilon$  is 3x3 matrix of electrical properties and  $\mathbf{e}$  is 3x6 matrix of piezoelectric properties.

### 3.2 Piezoelectric FEM equations

Piezoelectric governing equations for dynamic problems can be obtain by Hamilton's principle, which can be written in form

$$\int_{t_1}^{t_2} (\delta L + \delta W) dt = 0 \quad (10)$$

where  $L$  is Lagrangian,  $W$  is work of external mechanical and electrical forces and  $t_1$  and  $t_2$  defined considered time interval. Lagrangian of piezoelectric structure is given by

$$L = T - U + W_e \quad (11)$$

where  $T$ ,  $U$  and  $W_e$  is kinetic energy, potential energy and electric energy of investigated structure, respectively. They can be expressed as

$$\begin{aligned} T &= \int_{(V)} \frac{1}{2} \rho \dot{\mathbf{u}}^T \dot{\mathbf{u}} dV \\ U &= \int_{(V)} \frac{1}{2} \boldsymbol{\varepsilon}^T \boldsymbol{\sigma} dV \\ W_e &= \int_{(V)} \frac{1}{2} \mathbf{E}^T \mathbf{D} dV \end{aligned} \quad (12)$$

where  $\dot{\mathbf{u}}$  is velocity vector with 3 components. Virtual work of external mechanical and electrical forces can be expressed as

$$\delta W = \sum \delta \mathbf{u}^T \mathbf{F} - \sum \delta \phi Q \quad (13)$$

where  $\mathbf{u}$  is displacement vector with 3 components,  $\mathbf{F}$  is force vector with 3 components,  $\phi$  is electric scalar potential and  $Q$  is electric charge.

Hamilton's principle (10) can be using equations (12), (13) and constitutive equation (9) expressed in following form

$$\int_{t_1}^{t_2} \left[ - \int_{(V)} \rho \delta \mathbf{u}^T \dot{\mathbf{u}} dV - \int_{(V)} \delta \boldsymbol{\varepsilon}^T \mathbf{c}^E \boldsymbol{\varepsilon} dV + \int_{(V)} \delta \boldsymbol{\varepsilon}^T \mathbf{e}^T \mathbf{E} dV + \int_{(V)} \delta \mathbf{E}^T \mathbf{e} \boldsymbol{\varepsilon} dV + \int_{(V)} \delta \mathbf{E}^T \boldsymbol{\varepsilon}^E \mathbf{E} dV + \sum \delta \mathbf{u}^T \mathbf{F} - \sum \delta \phi Q \right] dt = 0 \quad (14)$$

Relationship between displacement of point and nodal displacement of finite element and between scalar electric potential of point and nodal scalar electric potential of finite element can be expressed by shape functions of element

$$\begin{aligned} \mathbf{u} &= \mathbf{N}_u \mathbf{u}^e \\ \phi &= \mathbf{N}_\phi \phi^e \end{aligned} \quad (15)$$

$\mathbf{N}_u$  and  $\mathbf{N}_\phi$  are matrices with shape functions. Relationship between components of strain and components of nodal displacements and relationship between components of electric intensity and nodal electric scalar potential have forms

$$\begin{aligned}\boldsymbol{\varepsilon} &= \mathbf{B}_u \mathbf{u}^e \\ \mathbf{E} &= -\mathbf{B}_\phi \boldsymbol{\phi}^e\end{aligned}\quad (16)$$

$\mathbf{B}_u$  and  $\mathbf{B}_\phi$  are matrices with derivative of shape functions. Hamilton's principle (10) can be rewritten by equations (15) and (16) into form

$$\begin{aligned}& \int_{t_1}^{t_2} \delta(\mathbf{u}^e)^T \left[ - \left( \int_{(V)} \mathbf{N}_u^T \rho \mathbf{N}_u dV \right) \ddot{\mathbf{u}}^e - \left( \int_{(V)} \mathbf{B}_u^T \mathbf{c}^E \mathbf{B}_u dV \right) \mathbf{u}^e - \left( \int_{(V)} \mathbf{B}_u^T \mathbf{e}^T \mathbf{B}_\phi dV \right) \boldsymbol{\phi}^e + \right. \\ & \left. + \Sigma \mathbf{N}_u^T \mathbf{F} \right] dt + \int_{t_1}^{t_2} \delta(\boldsymbol{\phi}^e)^T \left[ - \left( \int_{(V)} \mathbf{B}_\phi^T \mathbf{e} \mathbf{B}_u dV \right) \mathbf{u}^e + \left( \int_{(V)} \mathbf{B}_\phi^T \boldsymbol{\varepsilon}^E \mathbf{B}_\phi dV \right) \boldsymbol{\phi}^e - \right. \\ & \left. \Sigma \mathbf{N}_\phi^T Q \right] dt = 0\end{aligned}\quad (17)$$

FEM equations of individual element can be derived from (17) in form

$$\begin{bmatrix} \mathbf{M}_{uu}^e & \mathbf{0}^e \\ \mathbf{0}^e & \mathbf{0}^e \end{bmatrix} \begin{bmatrix} \ddot{\mathbf{u}}^e \\ \ddot{\boldsymbol{\phi}}^e \end{bmatrix} + \begin{bmatrix} \mathbf{K}_{uu}^e & \mathbf{K}_{u\phi}^e \\ \mathbf{K}_{\phi u}^e & \mathbf{K}_{\phi\phi}^e \end{bmatrix} \begin{bmatrix} \mathbf{u}^e \\ \boldsymbol{\phi}^e \end{bmatrix} = \begin{bmatrix} \mathbf{F}^e \\ \mathbf{Q}^e \end{bmatrix}\quad (18)$$

The equation (18) represents dynamic behavior of piezoelectric material without mechanical damping. If the damping is considered, then the equation (18) has form

$$\begin{bmatrix} \mathbf{M}_{uu}^e & \mathbf{0}^e \\ \mathbf{0}^e & \mathbf{0}^e \end{bmatrix} \begin{bmatrix} \ddot{\mathbf{u}}^e \\ \ddot{\boldsymbol{\phi}}^e \end{bmatrix} + \begin{bmatrix} \mathbf{C}_{uu}^e & \mathbf{0}^e \\ \mathbf{0}^e & \mathbf{0}^e \end{bmatrix} \begin{bmatrix} \dot{\mathbf{u}}^e \\ \dot{\boldsymbol{\phi}}^e \end{bmatrix} + \begin{bmatrix} \mathbf{K}_{uu}^e & \mathbf{K}_{u\phi}^e \\ \mathbf{K}_{\phi u}^e & \mathbf{K}_{\phi\phi}^e \end{bmatrix} \begin{bmatrix} \mathbf{u}^e \\ \boldsymbol{\phi}^e \end{bmatrix} = \begin{bmatrix} \mathbf{F}^e \\ \mathbf{Q}^e \end{bmatrix}\quad (19)$$

where individual submatrices are defined as follows:

$$\mathbf{M}_{uu}^e = \int_{(V)} \mathbf{N}_u^T \rho \mathbf{N}_u dV; \mathbf{K}_{uu}^e = \int_{(V)} \mathbf{B}_u^T \mathbf{c}^E \mathbf{B}_u dV; \mathbf{K}_{u\phi}^e = \int_{(V)} \mathbf{B}_u^T \mathbf{e}^T \mathbf{B}_\phi dV;$$

$$\mathbf{K}_{\phi u}^e = \int_{(V)} \mathbf{B}_\phi^T \mathbf{e} \mathbf{B}_u dV; \mathbf{K}_{\phi\phi}^e = \int_{(V)} \mathbf{B}_\phi^T \boldsymbol{\varepsilon}^E \mathbf{B}_\phi dV; \mathbf{C}_{uu}^e = \alpha \mathbf{M}_{uu}^e + \beta \mathbf{K}_{uu}^e$$

$\mathbf{F}^e$  and  $\mathbf{Q}^e$  represent nodal forces and nodal charges on considered element.

For whole structure we can formally write

$$\begin{bmatrix} \mathbf{M}_{uu} & \mathbf{0} \\ \mathbf{0} & \mathbf{0} \end{bmatrix} \begin{bmatrix} \ddot{\mathbf{u}} \\ \ddot{\boldsymbol{\phi}} \end{bmatrix} + \begin{bmatrix} \mathbf{C}_{uu} & \mathbf{0} \\ \mathbf{0} & \mathbf{0} \end{bmatrix} \begin{bmatrix} \dot{\mathbf{u}} \\ \dot{\boldsymbol{\phi}} \end{bmatrix} + \begin{bmatrix} \mathbf{K}_{uu} & \mathbf{K}_{u\phi} \\ \mathbf{K}_{\phi u} & \mathbf{K}_{\phi\phi} \end{bmatrix} \begin{bmatrix} \mathbf{u} \\ \boldsymbol{\phi} \end{bmatrix} = \begin{bmatrix} \mathbf{F} \\ \mathbf{Q} \end{bmatrix}\quad (20)$$

### 3.3 FEM equations of FGM beam with piezoelectric layers

2D beam element with piezoelectric layers and FGM core with degree of freedom is shown in Fig. 2.

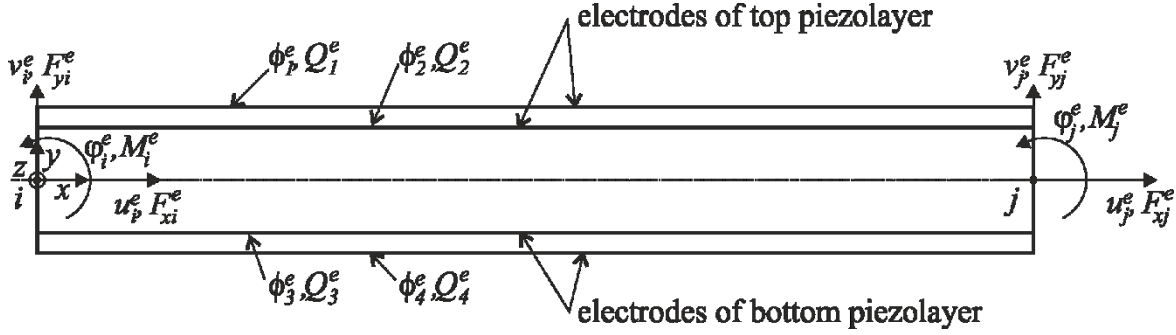


Fig. 2: 2D beam element with piezoelectric layers – degree of freedom and internal forces

Length of beam element is  $L^e$ , cross-section of FGM core is  $A_{FGM}$  and cross-section of piezolayer is  $A_p$ . Homogenized Youngs' moduli for axial loading and bending are computed according equations (4) and (5). Mechanical degree of freedom of element are displacements and rotations in both nodes  $(u_i^e, v_i^e, \phi_i^e, u_j^e, v_j^e, \phi_j^e)$ , electrical degree of freedom are electric potential on all 4 electrodes of both piezoelectric layers  $(\phi_1^e, \phi_2^e, \phi_3^e, \phi_4^e)$ . Internal element mechanical loads are forces and moments in both nodes  $(F_{xi}^e, F_{yi}^e, M_i^e, F_{xj}^e, F_{yj}^e, M_j^e)$ , internal element electric loads are electric charge on all 4 electrodes of both piezoelectric layers  $(Q_1^e, Q_2^e, Q_3^e, Q_4^e)$  [4].

FEM equation of 2D piezoelectric beam with FGM core has formally the same equation as equation (20), but individual stiffness submatrices have different form, because they are using transfer constant and not classical shape functions. Mass submatrix  $\mathbf{M}_{uu}^e$  can be constructed by classical shape functions.

The structural submatrix for the beam element with piezoelectric layers can be expressed in a form

$$\mathbf{K}_{uu}^e = \begin{bmatrix} k'_u & 0 & 0 & -k'_u & 0 & 0 \\ 0 & k'_{v2} & k'_{v3} & 0 & -k'_{v2} & k_{v2} \\ 0 & k'_{v3} & k'_{v33} & 0 & -k'_{v3} & k_{v3} \\ -k'_u & 0 & 0 & k'_u & 0 & 0 \\ 0 & -k'_{v2} & -k'_{v3} & 0 & k'_{v2} & -k_{v2} \\ 0 & k_{v2} & k_{v3} & 0 & -k_{v2} & k_{v23} \end{bmatrix} \quad (21)$$

Computation of individual components of the structural submatrix contains the influence of FGM core and piezoelectric layers, where homogenized material properties of beam is considered. The computation is performed numerically using concept of transfer constants.

The electrical submatrix for the beam element with piezoelectric layers can be expressed in a form

$$\mathbf{K}_{\phi\phi}^e = \begin{bmatrix} -\frac{A_p L \epsilon^\varepsilon}{h_p^2} & \frac{A_p L \epsilon^\varepsilon}{h_p^2} & 0 & 0 \\ \frac{A_p L \epsilon^\varepsilon}{h_p^2} & -\frac{A_p L \epsilon^\varepsilon}{h_p^2} & 0 & 0 \\ 0 & 0 & -\frac{A_p L \epsilon^\varepsilon}{h_p^2} & \frac{A_p L \epsilon^\varepsilon}{h_p^2} \\ 0 & 0 & \frac{A_p L \epsilon^\varepsilon}{h_p^2} & -\frac{A_p L \epsilon^\varepsilon}{h_p^2} \end{bmatrix} \quad (22)$$

where  $\epsilon^\varepsilon$  is permittivity of piezoelectric layer under constant strain.

Submatrices of piezoelectric coupling can be expressed in following forms

$$\mathbf{K}_{u\phi}^e = \begin{bmatrix} -\frac{A_p d_{21} E_p}{h_p} & \frac{A_p d_{21} E_p}{h_p} & -\frac{A_p d_{21} E_p}{h_p} & \frac{A_p d_{21} E_p}{h_p} \\ 0 & 0 & 0 & 0 \\ \frac{A_y d_{21} E_p}{h_p} & -\frac{A_y d_{21} E_p}{h_p} & \frac{A_y d_{21} E_p}{h_p} & -\frac{A_y d_{21} E_p}{h_p} \\ \frac{A_p d_{21} E_p}{h_p} & -\frac{A_p d_{21} E_p}{h_p} & \frac{A_p d_{21} E_p}{h_p} & -\frac{A_p d_{21} E_p}{h_p} \\ 0 & 0 & 0 & 0 \\ -\frac{A_y d_{21} E_p}{h_p} & \frac{A_y d_{21} E_p}{h_p} & -\frac{A_y d_{21} E_p}{h_p} & \frac{A_y d_{21} E_p}{h_p} \end{bmatrix} \quad (23)$$

$$\mathbf{K}_{\phi u}^e = \begin{bmatrix} -\frac{A_p e_{21}}{h_p} & 0 & \frac{A_y e_{21}}{h_p} & \frac{A_p e_{21}}{h_p} & 0 & -\frac{A_y e_{21}}{h_p} \\ \frac{A_p e_{21}}{h_p} & 0 & -\frac{A_y e_{21}}{h_p} & -\frac{A_p e_{21}}{h_p} & 0 & \frac{A_y e_{21}}{h_p} \\ -\frac{A_p e_{21}}{h_p} & 0 & \frac{A_y e_{21}}{h_p} & \frac{A_p e_{21}}{h_p} & 0 & -\frac{A_y e_{21}}{h_p} \\ \frac{A_p e_{21}}{h_p} & 0 & -\frac{A_y e_{21}}{h_p} & -\frac{A_p e_{21}}{h_p} & 0 & \frac{A_y e_{21}}{h_p} \end{bmatrix} \quad (24)$$

where  $A_y = \frac{1}{2} A_p (h_{FGM} + h_p)$ ,  $d_{21}$  and  $e_{21}$  are piezoelectric constants.

#### 4 STATE SPACE EQUATIONS OF PIEZOELECTRIC BEAM FINITE ELEMENT

Smart structures made from piezoelectric material, are usually connected to controller in order to have required behavior of structure. For this purpose, FEM equations are transformed to state space equations [5].

The voltage actuation and charge sensing are considered. Actuation is done by imposing a voltage on the actuators and sensing by imposing a zero voltage and measuring the electric

charges appearing on the sensors. Vector of nodal displacement of the structure  $\mathbf{u}$  can be expressed by truncated modal decomposition

$$\mathbf{u} = \mathbf{Z}\mathbf{x} \quad (25)$$

where  $\mathbf{Z}$  represents chosen  $n$  modal shapes of structure and  $\mathbf{x}$  represents modal amplitudes. Using equation (25) can be FEM equation of whole structure (20) rewritten to form

$$\mathbf{M}_{uu} \mathbf{Z}\ddot{\mathbf{x}} + \mathbf{C}_{uu} \mathbf{Z}\dot{\mathbf{x}} + \mathbf{K}_{uu} \mathbf{Z}\mathbf{x} + \mathbf{K}_{u\phi} \boldsymbol{\phi} = \mathbf{0} \quad (26)$$

$$\mathbf{K}_{\phi u} \mathbf{Z}\mathbf{x} + \mathbf{K}_{\phi\phi} \boldsymbol{\phi} = \mathbf{Q} \quad (27)$$

Using orthogonality property of mode shapes

$$\mathbf{Z}^T \mathbf{M}_{uu} \mathbf{Z} = \text{diag}(\mu_k) \quad (28)$$

$$\mathbf{Z}^T \mathbf{K}_{uu} \mathbf{Z} = \text{diag}(\mu_k \omega_k^2) \quad (29)$$

$$\mathbf{Z}^T \mathbf{C}_{uu} \mathbf{Z} = \text{diag}(2\xi_k \mu_k \omega_k) \quad (30)$$

equations (26) and (27) can be rewritten into form

$$\boldsymbol{\mu} \ddot{\mathbf{x}} + 2 \boldsymbol{\xi} \boldsymbol{\mu} \boldsymbol{\omega} \dot{\mathbf{x}} + \boldsymbol{\mu} \boldsymbol{\omega}^2 \mathbf{x} + \mathbf{Z}^T \mathbf{K}_{u\phi} \boldsymbol{\phi} = \mathbf{0} \quad (31)$$

$$\mathbf{K}_{\phi u} \mathbf{Z}\mathbf{x} + \mathbf{K}_{\phi\phi} \boldsymbol{\phi} = \mathbf{Q} \quad (32)$$

where matrices  $\boldsymbol{\mu}$ ,  $\boldsymbol{\omega}$  and  $\boldsymbol{\xi}$  represent matrix of modal masses, modal frequencies and modal damping ratios of structure, respectively. After some manipulation, we can from equation (31) obtain

$$\ddot{\mathbf{x}} = -2 \boldsymbol{\xi} \boldsymbol{\omega} \dot{\mathbf{x}} - \boldsymbol{\omega}^2 \mathbf{x} - \boldsymbol{\mu}^{-1} \mathbf{Z}^T \mathbf{K}_{u\phi} \boldsymbol{\phi} \quad (33)$$

Equation (33) and (32) can be rewritten into form

$$\begin{bmatrix} \dot{\mathbf{x}} \\ \ddot{\mathbf{x}} \end{bmatrix} = \begin{bmatrix} \mathbf{0} & \mathbf{I} \\ -\boldsymbol{\omega}^2 & -2 \boldsymbol{\xi} \boldsymbol{\omega} \end{bmatrix} \begin{bmatrix} \mathbf{x} \\ \dot{\mathbf{x}} \end{bmatrix} + \begin{bmatrix} \mathbf{0} \\ -\boldsymbol{\mu}^{-1} \mathbf{Z}^T \mathbf{K}_{u\phi} \end{bmatrix} \boldsymbol{\phi} \quad (34)$$

$$\mathbf{Q} = [\mathbf{K}_{\phi u} \mathbf{Z} \quad \mathbf{0}] \begin{bmatrix} \mathbf{x} \\ \dot{\mathbf{x}} \end{bmatrix} + \mathbf{K}_{\phi\phi} \boldsymbol{\phi} \quad (35)$$

Equations (34) and (35) represents state space model of structure with piezoelectric sensors and actuators and can be used to analyzed structure from control viewpoint.

## 5 CONCLUSION

The paper presents beam finite element with piezoelectric layers, where core of the beam can be made of FGM materials. Such combination of materials is very attractive for mechatronic applications, because material composition of FGM core can be optimized for design stress state and deformation can be controlled by voltages on electrodes. FEM equations are rewritten to state space equations using truncated modal decomposition. Such model of beam structure can be easily incorporated into control model.

## REFERENCES

- [1] Murín, J., Kutiš, V., Masný, M. Composite (FGMs) beam finite elements. In: Composites with Micro- and Nano-Structure. Edited by: V. Kompiš, Springer Science+Business Media B.V., (2008), ISBN 978-1-4020-6974-1, p. 209 – 239.
- [2] Kutiš, V., Murín, J., Belák, R., Paulech, J. Beam element with spatial variation of material properties for multiphysics analysis of functionally graded materials. *Computers & Structures*, (2011) 89:1192–1205.
- [3] Moheimani, S.O.R. and Fleming, A.J.. *Piezoelectric Transducers for Vibration Control and Damping*. Springer, (2006).
- [4] Bruant, I., Coffignal, G., Lene, F., Verge, M. Active control of beam structures with piezoelectric actuators and sensors: modeling and simulation. *Smart Material Structures* (2001), 10:404–408.
- [5] Piefort, V. *Finite Element Modeling of Piezoelectric Structures*, PhD Thesis, Université Libre de Bruxelles, (2001).

## Performance Engineering for Advanced Lattice Boltzmann Methods in CFD

Konstantin Kutscher<sup>\*</sup>, Manfred Krafczyk<sup>\*\*</sup>, Martin Geier<sup>\*\*\*</sup>, Martin Schönherr<sup>\*\*\*\*</sup>

<sup>\*</sup>TU Braunschweig, iRMB, <sup>\*\*</sup>TU Braunschweig, iRMB, <sup>\*\*\*</sup>TU Braunschweig, iRMB, <sup>\*\*\*\*</sup>TU Braunschweig, iRMB

### ABSTRACT

We report on techniques developed for and implemented in our research CFD code VirtualFluids which has been developed as a C++-library for massively parallel CFD simulation. Its modular structure includes the following functionality: hybrid block based tree type grid, generation based on geometric objects and/or CAD data, restart options for different parallel setups, D3Q27 Cumulant LBM kernel including a so-called Esoteric Twist approach to reduce memory requirements, second order accurate grid refinement, implicit turbulence model, a hybrid parallelization based on MPI and pthreads, restart/checkpointing based on MPI/IO as well as parallel In-situ visualization and output in Paraview parallel format. The code is developed using of object-oriented techniques and design patterns which foster support and functional extension. We will report on various massively parallel CFD benchmarks for real-world problems including examples running on GPGPUs and discuss future options for code extensions for usage of hybrid CPU/GPU clusters.

## Limiting Techniques and hp Adaptivity for Continuous High-order Bernstein Finite Element Approximations

Dmitri Kuzmin<sup>\*</sup>, Christopher Kees<sup>\*\*</sup>, Manuel Quezada de Luna<sup>\*\*\*</sup>

<sup>\*</sup>TU Dortmund University, <sup>\*\*</sup>US Army Engineer Research & Development Center, <sup>\*\*\*</sup>US Army Engineer Research & Development Center

### ABSTRACT

In this talk, we present three new approaches to blending a continuous high-order Bernstein finite element discretization with a monotone piecewise-linear approximation based on the same nodal points. The first approach is a predictor-corrector method which constrains the difference between the high and low-order solutions using a localized flux-corrected transport (FCT) algorithm. The second approach constrains the difference between the residuals of the underlying discretizations using nodal limiters to adjust monotonicity-preserving artificial diffusion coefficients. This correction leads to nonlinear algebraic systems which are solved iteratively. The third approach combines the high and low-order finite element bases using a continuous piecewise-linear limiter function. This low-level limiting strategy represents a new kind of hp adaptivity. The proposed method adjusts the local order of approximation in a continuous manner while keeping the number of degrees of freedom fixed. The pros and cons of each limiting technique for high-order finite elements will be discussed and results of numerical studies for 2D test problems will be presented.

## Reduced Order Models for Divergence-Conforming Isogeometric Flow Simulations

Trond Kvamsdal<sup>\*</sup>, Eivind Fonn<sup>\*\*</sup>, Harald van Brummelen<sup>\*\*\*</sup>, Adil Rasheed<sup>\*\*\*\*</sup>

<sup>\*</sup>Norwegian University of Science and Technology, <sup>\*\*</sup>SINTEF Digital, <sup>\*\*\*</sup>Eindhoven University of Technology,  
<sup>\*\*\*\*</sup>SINTEF Digital

### ABSTRACT

Repetitive solutions of parametrized flow problems can be quite demanding, each solution involving a million or more degrees of freedom, that takes hours or days of computational time. A promising methodology to reduce the (on-line) computational effort is the use of Reduced Order Modelling (ROM). ROM offers the possibility to balance loss of accuracy with gain in efficiency. We have tied ROM with a divergence-conforming isogeometric high-fidelity method for incompressible flow simulations and achieved (significant) additional speedup compared to non-conforming methods. The additional speedup is related to less computations related to the so-called supremizers needed for avoiding that the ROM model get a rank-deficient velocity-pressure block. We will illustrate the performance of the development method by doing high fidelity simulations of stationary Navier-Stokes were performed of flow around a NACA0015 airfoil where we varies the inflow velocity and the angle of attack.

## Performance Characteristics of a High-order Finite Element Application on a Modern High Performance Computing System – Blue Waters

JaeHyuk Kwack\*, Gregory Bauer\*\*

\*National Center for Supercomputing Applications / University of Illinois at Urbana-Champaign, \*\*National Center for Supercomputing Applications / University of Illinois at Urbana-Champaign

### ABSTRACT

Performance indices of high performance computing (HPC) systems poorly represent the performance of science and engineering applications on the HPC systems. The most popular performance index of HPC systems, the TOP500, relies on a traditional LINPACK benchmark that is very limitedly used for modern HPC applications. The HPC community has recently made significant efforts to include more general numerical algorithms to represent the performance of modern HPC applications. This study is one of our continued efforts to find out the most optimal way to represent the performance of HPC systems and HPC applications [1,2,3]. We employed a high-order finite element application optimized for modern HPC systems to analyze performance characteristics depending on several configurations such as the order of shape functions, employed linear algebra solvers and structure for MPI and OpenMP hybrid computing. We profiled the application in scale with Cray Performance Measurement and Analysis Tools (CPMAT) on Blue Waters at National Center for Supercomputing Applications (NCSA). We present collected hardware counter data for flops, flop-rates, L1/L2/L3 data cache accesses and memory access for several important routines. In addition, we discuss potential rooflines of the system performance by analyzing the performance characteristics of the crucial routines for the considered configurations. With the above analysis, we provide our recommendations to help scientists and engineers optimize their algorithms for science and engineering applications on modern HPC systems. [1] J. Kwack, G. Bauer, S.Koric, &quot;Performance Test of Parallel Linear Equation Solvers on Blue Waters - Cray XE6/XK7 system&quot;, Proceedings of the Cray Users Group Meeting (CUG2016), London, England, May 2016. [2] G. Bauer, V. Anisimov, G. Arnold, B. Bode, R. Brunner, T. Cortese, R. Haas, A. Kot, W. Kramer, J. Kwack, J. Li, C. Mendes, R. Mokos, C. Steffen, &quot;Updating the SPP Benchmark Suite for Extreme-Scale Systems&quot;, Proceedings of the Cray Users Group Meeting (CUG2017), Redmond, WA, May 2017. [3] J. Kwack and G. Bauer, &quot;HPCG and HPGMG benchmark tests on Multiple Program, Multiple Data (MPMD) mode on Blue Waters - a Cray XE6/XK7 hybrid system&quot;, Concurrency and Computation, Practice and Experience journal, 30(1), 10.1002/cpe.4298, 2017.

## **Numerical Simulation of Wave/Current-Induced Scour Below Pipelines Using RKPM Method**

On Lei Annie Kwok\*, Pai-Chen Guan\*\*, Chien-Ting Sun\*\*\*

\*National Taiwan University, \*\*National Taiwan Ocean University, \*\*\*National Taiwan Ocean University

### **ABSTRACT**

Stability of marine pipelines and marine cables can be significantly affected by the presence of scour due to repeated wave and current action. In this study, RKPM (reproducing kernel particle method)-based numerical framework is used to simulate this fluid-structure-soil interaction process. Semi-Lagrangian reproducing kernel incompressible fluid method is employed to model the ocean wave and tidal flow while the pipeline is analyzed by RKPM Mindlin plate formulation. A non-cohesive seabed sediment is considered and modeled by a semi-Lagrangian reproducing kernel method. A contact algorithm is used to handle the interaction between fluid (waves), structure (pipelines) and solid (soil sediment). This investigation focuses on the effect of pipeline embedment, water depth to pipeline diameter ratios and soil properties on the stability of submarine pipelines/cables.

## Method to Analyze Welding Deformation Based on a Visualization Model for Plant Construction

KiYoun Kwon\*

\*Kumoh National Institute of Technology

### ABSTRACT

The ship and offshore plant are designed by dividing it into several blocks which constitute the hull, and each block is constructed separately and assembled. Blocks are usually made by assembling small parts fabricated by machining steel plates, and the plant is constructed through the assembly of large blocks from the small blocks. During these process, welding deformation causes many problems [1]. In order to prevent welding deformation, FEA (finite element analysis) is widely used. In this paper, we propose a mesh generation method to enable welding analysis based on a visualization model. The visualization model is widely used for visualizing and sharing large cad data in PLM (product lifecycle management) [2]. This model is mainly composed of triangular elements to minimize the file size and improve rendering performance. The method proposed in this paper is as follows. The visualization model has no information about the welding line. First, boundary curves are restored from the triangle elements of visualization model. After matching the connectivity of triangular elements, boundary element edges are extracted. Boundary curves are generated by connecting these boundary element edges. If the restored boundary curve lies on another part, it is classified as a welding line. Then, a polygon surface is created by using triangle elements constituting boundary curves for each plate, and a trim surface is created to include welding lines. The number of elements is given to the boundary curves and the welding lines, and a quadrilateral mesh is generated by using the domain decomposition method [3]. Finally, the welding line attribute information is added to the elements included in the welding line so that thermal deformation analysis is possible

References 1. Heo, H. and Chung, H, 2014, Stochastic assessment considering process variation for impact of welding shrinkage on cost of ship production, *International Journal of Production Research*, pp. 6076-6091 2. Ball, A., Ding, L. and Patel, M., 2007, Lightweight Formats for Product Model Data Exchange and Preservation, *PV 2007 Conference*, pp. 9-11. 3. Chae, S. W. and Kwon, K. Y., Quadrilateral Mesh Generation on Trimmed NURBS Surfaces, *KSME International Journal*, Vol. 15, pp. 592-601, 2001.

## Hygroelastic Multiscale Modeling of Epoxy-based Nanocomposites

Sunyong Kwon<sup>\*</sup>, Man Young Lee<sup>\*\*</sup>, Seunghwa Yang<sup>\*\*\*</sup>

<sup>\*</sup>Chung-Ang University, <sup>\*\*</sup>Agency for Defense Development, <sup>\*\*\*</sup>Chung-Ang University

### ABSTRACT

Hygroscopic aging occurs inevitably by consistent exposure to moisture in service condition of epoxy-based nanocomposites. Slow and steady process of aging causes swelling, plasticization, and degradation of mechanical and interfacial properties of epoxy-based nanocomposite eventually leading to the fast fracture of nanocomposites. Since the aging is a long-time process, experimental approach of hygroscopic aging is burdensome because it needs accelerated aging environment accompanied by time-to-time preparation of epoxy coupons for evaluation of properties. Therefore, in order to access hygroelastic behavior with computational mechanics, molecular dynamics (MD) simulation is firstly applied. To determine the aged structure-to-hygroelastic property relationship of epoxy-based nanocomposite, varying cross-linking and water contents of diglycidyl ether of bisphenol F (EPON862®)/ triethylenetetramine (TETA) epoxy system is studied. A defect-free single layer graphene is added in the nanocomposite structure as reinforcement. The dynamic cross-linking method is used to set the crosslinking ratio of epoxy from 30 to 70%. For each cross linking ratio, moisture weight fraction of 0, 2, 4 wt% is considered in each nanocomposite unit cell. Through the classical ensemble simulation incorporated with ab-initio parameterized PCFF forcefield, coefficient of moisture expansion (CME), diffusion coefficient of water, and elastic modulus and cohesive zone law of epoxy/graphene nanocomposite models are predicted. To efficiently diagnose and predict hygroscopic aging in real life conditions, establishing ternary correlation of aging time-micro structure- macro property is necessary. However, as MD simulation can only describe couple microseconds of material status, continuum scale computational analysis with well-established time dependent property analysis is essential to overcome the limitations of MD simulation in describing hygroscopic aging behavior of epoxy-based nanocomposites. Furthermore, hygroelastic and interfacial properties of epoxy/graphene nanocomposite calculated by MD simulation are essential element for implementing multi-scale analysis. Therefore, MD simulation incorporated with micromechanics theory and finite element method (FEM) is presented in this study. Thus, based on the previous calculation of hygroelastic and interfacial properties by MD simulation, moisture expansion elastic constitutive equation model and stress-strain behavior of moisture absorbed nanocomposite constitutive equation model approximation can be developed. Also, mapping of elastoplastic properties by connecting time dependent moisture concentration profile and Young's moduli of epoxy-based nanocomposite will be analyzed.

## Adaptive Isogeometric Analysis with Hierarchical B-Splines

Markus Kästner<sup>\*</sup>, Paul Hennig<sup>\*\*</sup>, Marreddy Ambati<sup>\*\*\*</sup>, Laura De Lorenzis<sup>\*\*\*\*</sup>

<sup>\*</sup>Institute for Solid Mechanics, TU Dresden, <sup>\*\*</sup>Institute for Solid Mechanics, TU Dresden, <sup>\*\*\*</sup>Institute for Applied Mechanics, TU Braunschweig, <sup>\*\*\*\*</sup>Institute for Applied Mechanics, TU Braunschweig

### ABSTRACT

The finite element discretisation of a large class of boundary value problems requires highly refined meshes to appropriately resolve, e.g., singularities in contact problems, shear bands in elasto-plasticity or steep local gradients in the field variables of phase-field models. If these domains evolve during the simulation, adaptive local mesh refinement and coarsening are essential for efficient computations. As Isogeometric Analysis (IGA) introduced by Hughes et al. [1] overcomes the disjunction between geometry and computational models it is the ideal discretisation technique to be combined with adaptive mesh refinement because already the coarsest mesh provides an exact geometry representation which is preserved during refinement. Tedious interactions with an underlying geometry during re-meshing, which is required to increase the accuracy of the geometry representation in standard FEM, are avoided. We present projection methods and transfer operations required for adaptive mesh refinement/coarsening in problems with internal variables at integration point level. By extending the results of Hennig et al. [2], we propose three different local and semi-local least squares projection methods for field variables and compare them to the standard global version. We discuss the application of two different transfer operators for internal variables. An alternative new operator inspired by superconvergent patch recovery [3] is also proposed. The presented projection methods and transfer operations are tested in benchmark problems and applied to phase-field modelling of spinodal decomposition and brittle and ductile fracture. REFERENCES [1] T. Hughes, J. Cottrell, Y. Bazilevs, Isogeometric analysis: CAD, finite elements, NURBS, exact geometry and mesh refinement, *Comput. Methods Appl. Mech. Eng.* Vol. 194, pp. 4135–4195, 2005. [2] P. Hennig, S. Müller, M. Kästner, Bézier extraction and adaptive refinement of truncated hierarchical NURBS. *Comput. Methods Appl. Mech. Eng.* Vol. 305, pp. 316 – 339, 2016. [3] M. Kumar, T. Kvamsdal, K. A. Johannessen, Superconvergent patch recovery and a posteriori error estimation technique in adaptive isogeometric analysis, *Comput. Methods Appl. Mech. Eng.* Vol. 316, pp. 1086 – 1156, 2017

## **Coupled Electro-Physiology, Mechanical and Fluid Structure Interaction for Heart Simulation Using LS-DYNA**

Pierre L&apos;Eplattenier<sup>\*</sup>, Sarah Bateau-Meyer<sup>\*\*</sup>, David Benson<sup>\*\*\*</sup>, Inaki Caldichoury<sup>\*\*\*\*</sup>,  
Facundo Del Pin<sup>\*\*\*\*\*</sup>, Attila Nagy<sup>\*\*\*\*\*</sup>

<sup>\*</sup>Livermore Software Technology Corporation, Livermore, CA, USA, <sup>\*\*</sup>Livermore Software Technology Corporation, CA, USA, <sup>\*\*\*</sup>Livermore Software Technology Corporation, Livermore, CA, USA, <sup>\*\*\*\*</sup>Livermore Software Technology Corporation, Livermore, CA, USA, <sup>\*\*\*\*\*</sup>Livermore Software Technology Corporation, Livermore, CA, USA, <sup>\*\*\*\*\*</sup>Livermore Software Technology Corporation

### **ABSTRACT**

Heart diseases are the leading cause of death in the western World. A deeper understanding of the heart functioning can provide important insights for medical doctors and clinicians in treating cardiovascular diseases but its extraordinary complexity represents a challenge for scientists and clinicians studying it. In this respect, some recent efforts have been made to be able to model the functioning of the heart along the entire heartbeat using the finite element commercial software LS-DYNA [1]. The model starts with Electro-Physiology (EP) which simulates the propagation of the wave of cell transmembrane potential in the heart. Different models, called "mono-domain" or "bi-domain", couple the diffusion of the potential along the walls of the heart with ionic equations describing the exchanges between the inner and the outer parts of the cells. These models give in particular the local intracellular calcium ion which provides the activation part of the heart muscle myofilament models, hence the input for the mechanical tissue models. The mechanical deformations of the heart are coupled with the hemodynamics using the Fluid and Structure Interaction (FSI) model of LS-DYNA. Benchmarks of the different parts of the model will be presented, followed by coupled multiphysics simulations of parts of the heart as well as an example of a full heart beat. The model will also be used to show the difference between a healthy heart and different heart diseases such as cardiac arrhythmia, in term of EP behaviors, mechanical deformations and pumped blood. [1] Hallquist, J.O., LS-DYNA Theory Manual. ISBN 0-9778540-0-0, LSTC, Livermore, CA, USA, 2006.

## **SIMNANO: A Highly Efficient Molecular Systems Energy Minimizer**

NIKOS LAGAROS\*, STAVROS CHATZIELEFTHERIOU\*\*

\*Institute of Structural Analysis & Antiseismic Research, School of Civil Engineering, National Technical University of Athens, \*\*Institute of Structural Analysis & Antiseismic Research, School of Civil Engineering, National Technical University of Athens

### **ABSTRACT**

In this study a new energy computationally highly efficient minimizer is presented, achieving excellent convergence properties; therefore, becomes suitable for dealing with large-scale molecular systems. SimNano relies on the analytical calculation of the gradient vectors and hessian matrices of the molecular systems by applying a computational modeling framework, possessed by the authors (J. Chem. Inf. Model. 2016, 56 (10), 1963-1978), that was inspired from structural mechanics and the finite element method. In order to present the efficiency of the proposed energy minimizer several test cases are examined and the results are compared with those obtained by one of the most popular molecular simulations software (LAMMPS). The comparative results indicate that the proposed minimizer depict superior convergence properties to those of the algorithms that are generally employed in the field. SimNano energy minimizer can be downloaded for free from the site: <http://users.ntua.gr/nlagaros/simnano.html>.

## **Optimization of Stiffened Composite Plate Using Artificial Neural Network-based Differential Evolution Algorithm**

THUAN LAM-PHAT\*, Son Nguyen-Hoai\*\*, Quan Nguyen-Anh\*\*\*

\*GACES, HCMC University of Technology and Education, Vietnam, \*\*GACES, HCMC University of Technology and Education, Vietnam, \*\*\*GACES, HCMC University of Technology and Education, Vietnam

### **ABSTRACT**

In this paper, a new algorithm called ABED (Artificial neural network Based Differential Evolution) is used to find the optimal design for the stiffened composite panel structure. This ABED algorithm is formed by the combination of an improved version of the Differential Evolution (DE) algorithm with the Artificial Neural Network technique and is adopted to look for suitable values of the fiber angle and the thickness of the stiffened composite plate. The ANN is used to compute the fitness of the object functions and evaluate the values related to the constraint conditions, meanwhile, the DE algorithm is used for optimization task. To verify the accuracy and the effectiveness of the algorithm, numerical solutions obtained from the proposed method are compared with those of other available approaches.

## **A Novel First-order Reliability Method Based on Performance Measure Approach for Highly Nonlinear Problems**

Gang LI<sup>\*</sup>, Bin Li<sup>\*\*</sup>, Hao Hu<sup>\*\*\*</sup>

<sup>\*</sup>Dalian University of Technology, <sup>\*\*</sup>Dalian University of Technology, <sup>\*\*\*</sup>Yancheng Institute of Technology

### **ABSTRACT**

The first-order reliability method (FORM) is widely used in structural reliability analysis for its simplicity and efficiency. When searching the MPP in traditional FORM, gradient-based algorithms may fail to converge due to oscillation or chaos if the performance function is highly nonlinear. Evolutionary algorithms could achieve convergence solutions even for highly nonlinear performance function, usually with expensive computational cost. To overcome their drawbacks, we propose a new reliability analysis method called PMA-IACC to search the most probable failure point (MPP). As the inverse reliability analysis and reliability analysis are reversible each other, the performance measure approach (PMA) of the inverse reliability analysis could be used for the reliability analysis based on the multi-objective optimization theory. With the iterative calculation of performance measure, the approximate MPP and reliability index would be gradually close to the true MPP and reliability index. Furthermore, the improved adaptive chaos control (IACC) method is also proposed to further improve the robustness and efficiency of inverse reliability analysis by updating and choosing suitable chaos control factors, without additional computational efforts at each iteration. And then, the IACC is integrated into the PMA reliability analysis strategy. The proposed PMA-IACC method has outstanding performance, which has been illustrated by five highly nonlinear examples with different dimensions, distributions and local optimal solution. Compared with some traditional reliability analysis methods, the proposed PMA-based reliability analysis methods (PMA-MCC, PMA-ACC, PMA-IACC) always show better accuracy and efficiency, among which the PMA-IACC is the best and is beneficial to the application in complex engineering problems. Furthermore, although it is hard to obtain the exact probability of failure currently by our proposed method in frame of FORM, our current work could be further used for higher-order reliability analysis based on the MPP-based DRM in the future study.

## **Multiscale Modeling of Soft Contact and Imulation of Cell Motility**

SHAOFAN LI\*

\*University of California-Berkeley

### **ABSTRACT**

Experimental observations have shown that the elasticity of the extracellular substrate has significant influence on cell motility and cell rotation. To explain such bio-physical or physiology phenomenon has been one of focuses of cell biology or cellular mechanobiology. In this work, we shall discuss multiscale modeling and simulations of soft matter contact and cell adhesion. In particular, our work is focused on modeling and simulation of contact and adhesion of cell on substrates with different rigidities and micro-structures. We have developed a soft matter cell model for actin filament aggregate, and a coarse-grained contact model that is based on a recently proposed multiscale adhesion model, which can take into account the long-range Van der Waals force, steric force, and colloidal interactions etc. By modeling the cell as an isotropic amphiphilic aggregate, it may be shown that under external stimulus the cell can change its microstructure, conformation, as well as configuration. We have used the soft matter cell model, the multiscale cell adhesive and contact model in conjunction with recently proposed Multiscale Moving Contact Line theory to successfully simulate cell motility in a virtual environment. In this presentation, we shall present our latest results on numerical simulations of cell contact, adhesion, spreading, and self-moving.

## **Multiscale Crystal Defect Dynamics (MCDD): Towards an Atomistically Determined Crystal Plasticity via Multiscale Dislocation Patter Dynamics**

SHAOFAN LI\*, Dandan Lyu\*\*

\*University of California-Berkeley, \*\*University of California-Berkeley

### **ABSTRACT**

In this work, we present the latest development of multiscale crystal defect dynamics (MCDD) for modeling of crystal plasticity by simulating crystal defect evolutions at small scales. The main novelties of the proposed MCDD are: (1) We use the dual-lattice tessellation to construct a process zone model that can represent dislocation patterns in single crystal; (2) We adopt a fourth-order (four scales) hierarchical strain gradient theory to model constitutive behaviors of various dislocation patterns, in which the atomistic-informed higher order Cauchy–Born rule is employed, and (3) We employ the Barycentric finite element technique to construct finite element shape functions for polygonal and polyhedral process zone elements. The proposed MCDD method provides an efficient and viable alternative to both molecular dynamics (MD) and dislocation dynamics (DD) in simulations of defect evolutions such as dislocation nucleation, and growth. In particular, MCDD offers a mesoscale description for dynamic lattice microstructure, defect microstructure, and their interactions. The method offers a possible solution for studying nanoscale and mesoscale crystalline plasticity. In this approach, coarse-grained models are adopted for both bulk media and material interphase or process zone. In bulk elements, the first order Cauchy-Born rule is adopted, so we can formulate an atomistic enriched continuum constitutive relation to describe the material behaviors. All the nonlinear deformation is assumed to be confined inside the process zone, and the process zone between the bulk elements is remodeled as a finite-width strip whose lattice constants and atomistic potential may be the same or different from those of the bulk medium. Inside the interphase zone, the higher order Cauchy-Born rules are adopted in process zones, and a higher order strain gradient-like coarse grain constitutive model is derived, which can capture the size-effect at the small scales. All interphase or process zones are constructed such that they are part (a subset) of slip planes in a lattice space. The multiscale crystal defect dynamics has been applied to simulate both dislocation motion and crack propagations in both single crystals and polycrystalline solids. Crack branching and void formation have been found possible for different element mesh stacking fault energies, which are dictated, by the effective lattice structure or microstructure in the process zone elements.

## **Modified Inherent Strain Theory for the Metal Additive Manufacturing Process with Experimental Validation Using Embedded Optical Fiber**

XUAN LIANG\*, Albert To\*\*

\*University of Pittsburgh, \*\*University of Pittsburgh

### **ABSTRACT**

Additive manufacturing (AM) has been paid increasing attention over the past few years, since usually arbitrarily-shaped parts can be manufactured through a bottom-up approach with little geometric limitation. However, residual stress and distortion have been the most critical issue for metal AM process. It is important to give an accurate prediction of residual stress and distortion in order to guarantee the quality of the printed metal parts. Usually thermomechanical simulation is employed to calculate the residual stress and strain; however, it is too time-consuming to simulate the printing process of a metal part containing thousands of layers. The inherent strain theory was established for solving residual stress and distortion for simple welding problem. It has been proved that the original theory is not accurate for calculating the residual stress and strain of the metal AM process. Therefore, the modified inherent strain theory is proposed in this work, taking the detailed physical process of metal AM into consideration. The modified method considers two different states in the metal AM process. On the one hand, an intermediate state is concerned where rapid solidification occurs, and the plastic strain is extracted correspondingly as the first part of the inherent strains. On the other hand, the increment of the elastic strains of the intermediate and final state is considered to be the other source of the inherent strain. This source of the inherent strain indicates the influence of the changing mechanical boundaries due to the new depositions in the multi-layer printing process. Based on the two different contributions, the modified inherent strains can be obtained. To capture the two important states in the metal AM process, the embedded optical fiber is used to measure the strain distribution in real time. Based on the measurement, the modified inherent strains can be calculated. Uniform averaged inherent strains are applied to a layer in a macroscale geometrical model as equivalent coefficients of thermal expansion. Meanwhile, variation of the inherent strains as a function of the distance to the deposition substrate will be employed in the layer depositing direction. After all the inherent strains are loaded, unit temperature change is applied to the model. Through a one-time full-body static analysis, the residual stress and distortion can be predicted in short time. Compared with the experimental measurement, good accuracy of the modified inherent strain method has been validated, which shows great potential for application to the metal AM field.

## INVESTIGATION ON VIBRATION CHARACTERISTICS OF THE HUMAN MIDDLE EAR AND APPLICATION FOR CLINICS IN TYMPANOPLASTY

Y. LIU\*, T. HIGASHIMACHI \*, AND R. TORIYA<sup>†</sup>

\*Department of Mechanical Engineering, Sojo University  
4-22-1 Ikeda, Nishi-ku, Kumamoto-shi, Kumamoto, JAPAN  
Email address: liu@mec.sojo-u.ac.jp

<sup>†</sup>Toriya ENT Clinic  
5-7-12 Kuhonji, Chuo-ku, Kumamoto-shi, Kumamoto, JAPAN

**Key words:** Human middle ear, Vibration characteristics, Auditory ossicles, Columella.

**Abstract.** In this paper, investigation on vibration characteristics of the human middle ear was carried out using the finite element harmonic vibration analysis. It was clarified that there is a relationship between hearing ability and stapes displacement including frequency characteristics. In tympanoplasty, the linkage of auditory ossicles may be reconstructed using the column article called the columella. It was also confirmed that stapes displacement changes according to the shape of columella or its mounting position to malleus. Then, a new method is proposed for estimating the hearing restoration effect prior to the tympanoplasty operation. That is, the hearing restoration effect can be estimated by a comparison of the differences in the stapes displacement between the reconstruction model and a healthy subject. In this study, as a part of the optimum design of the columella with the aim of better sound conduction efficiency, the correlation of columella junction area to the auditory ossicles and hearing restoration effect was clarified.

### 1 INTRODUCTION

In 2012, the World Health Organization (WHO) reported that there are 360 million persons in the world (5.3% of the world's population) with disabling hearing loss [1], which is one of the most severe problems in usual life activity of the human being. Conductive hearing loss is the most common case due to problems in the middle ear or the outer ear at times. A human middle ear which includes auditory ossicles (malleus, incus and stapes) and the tympanic membrane is a mechanical system. A key function of the mechanical system is to transmit sound energy from the air into the inner ear. The audition process begins in the tympanic membrane, which receives sound energy from outside and this causes the membrane to vibrate. Then the vibrations are amplified by the auditory ossicles while being transmitted through the malleus, incus and stapes. Finally, The stapes is responsible for transferring the vibrations into the cochlea fluid of the inner ear so that the hair cells in the inner ear can generate the neuronal signals. The conductive

hearing loss occurs when the middle ear is damaged by various ear diseases, and sounds hardly transfer through the ear canal to the eardrum and three ossicles. The chronic otitis media or middle ear cholesteatoma in which the ossicular chain in middle ear is damaged causes severe conductive hearing loss. The tympanoplasty operation is often carried out to reconstruct the damaged ossicular chain, and to improve the sound conduction efficiency. In the ossicular chain reconstruction, the columella is produced and used instead of incus which is generally broken. In this operation, the sound conduction efficiency changes by the variations in the shape, material and mounting position of the columella. Currently, the operation is carried out based on the workmanship and experience of the surgeon. Identification of the dynamic characteristics of the middle ear is very important in many areas including hearing aids, hearing loss evaluation, and design of middle ear prostheses. Many experimental measurements have been conducted in order to understand the dynamics of the middle ear. H. Wada et al. measured Young's modulus, thickness and damping ratio of the human eardrum by using measuring apparatus developed by themselves [2]. S. E. Voss et al. reported the measurements on human cadaver ears that describe sound transmission through the middle ear [3]. R. Aibara et al. measured the middle-ear pressure gain in 12 fresh human temporal bones for the 0.05 to 10 kHz frequency range [4]. However, experiments on live humans and cadavers are very limited. The dynamic characteristics of the middle ear exhibit a very complex behavior as well as individual variations. Several researchers on middle ear system use finite element analysis (FEA) in their study. The FEA is a powerful tool to analyze the vibration of a middle ear because the middle ear has a complicated shape. As for dynamics analysis on the middle ear system, a cat eardrum was firstly investigated by a finite element analysis on the curved conical eardrum by W. R. I. Funnell and C. A. Laszlo [5]. After that, H. Wada et al. made a three-dimensional FEM model of a human right middle ear, which included ossicles and the mechanical properties and boundary conditions of the middle ear were determined by a comparison between the numerical results obtained and the measurement results [6]. R. Z. Gan et al. performed a three-dimensional finite element analysis of the human ear that included the external ear canal, eardrum, ossicular bones, middle ear suspensory ligaments/muscles, and middle ear cavity [7] [8]. Q. Sun et al. proposed a practical and systematic method for reconstructing accurate computer and physical models of entire human middle ear [9]. T. Koike et al. performed the finite element analysis of the human middle ear and compared calculated results with measurement data [10]. Moreover, Liu et al. carried out a three-dimensional finite element analysis of human ear in order to analyze lesion of ossicular chain [11]. Computational modeling methodology of multi-body system was examined in order to simulate and study the middle ear mechanical response to acoustic stimulus by F. Bohnke et al. [12]. D. D. Greef et al. performed dynamics analysis on a new anatomically-accurate model composed of the tympanic membrane and malleus using the finite element method [13]. Lee, D. and Ahn, T. S. proposed statistical calibration framework effectively improves the middle ear FE model performance [14]. Nevertheless, there are few studies regarding clinical applications and aiming at improvement of the sound conduction efficiency in tympanoplasty. As mentioned upon, in the tympanoplasty operation, the shape, material and mounting position of the columella have been decided based on the workmanship and experience of the surgeon. In this paper, we introduce a new numerical approach using the finite element harmonic vibration analysis for estimating the hearing restoration effect prior to the tympanoplasty operation. This kind of approach makes it possible to propose a new medical treatment for the recovery of conductive or cochlear hearing loss. First of all, precise geometric models of the middle ear, including healthy type model and tympanoplasty type models, were

constructed on the basis of the computerized tomography (CT) scanning data. Then, frequency response characteristics of the stapes displacement in sound conduction were clarified using three-dimensional finite element harmonic vibration analysis. The vibration analysis was also carried out to investigate the effect on the frequency response characteristics caused by changes in the characteristics of the annular ligament and the division of the tympanic membrane. Based on the investigation results of vibration characteristics of the human middle ear, we proposed that the hearing restoration effect can be estimated by a comparison of the differences in the stapes displacement between the reconstruction model and the healthy subject. As an application for clinics in tympanoplasty, four kinds of models that change the mounting location of the columella were analyzed in order to investigate the difference of the displacement of the stapes basal plane. By comparing those analytical results with the result for a healthy model as a standard, the possibility of a clinical application of our method has been verified. Furthermore, as a part of the optimum design of the columella with the aim of better sound conduction efficiency, the correlation of columella junction area to the auditory ossicles and hearing restoration effect was clarified.

## 2 THE HUMAN MIDDLE EAR AND ITS FUNCTION

Figure 1 shows the structure of the ear. The middle ear is composed of the tympanic membrane, tympanic cavity, auditory ossicles and others. Auditory ossicles are behind the tympanic membrane in a small space (tympanic cavity), and they are composed of malleus, incus and stapes. The stapes basal plane connects with the inner ear through an oval window.

The tympanic cavity is a space filled with air. The inner wall of the tympanic cavity is covered with a mucous membrane. The air pressure of the tympanic cavity is controlled at the appropriate value by ventilation in order to keep the important function that is the sense of hearing. Furthermore, the tympanic cavity has a washing function that absorbs and removes bacterial waste by the secretion and reabsorption of the mucus. Each part of the auditory ossicles is connected with the joints. They are suspended by ligaments and muscles in the tympanic cavity. The vibration amount of the tympanic membrane is amplified about 17 times by the area ratio of the stapes basal plane and the tympanic membrane. In addition, the vibration amount of the tympanic membrane is amplified about 1.3 times by the lever motion of the auditory ossicles.

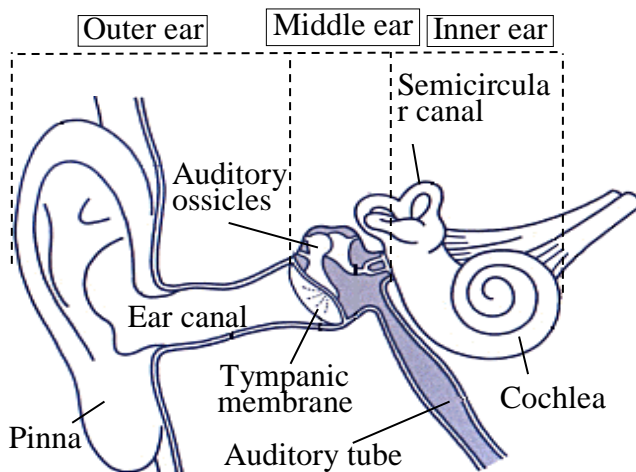


Fig. 1 Structure of the human ear

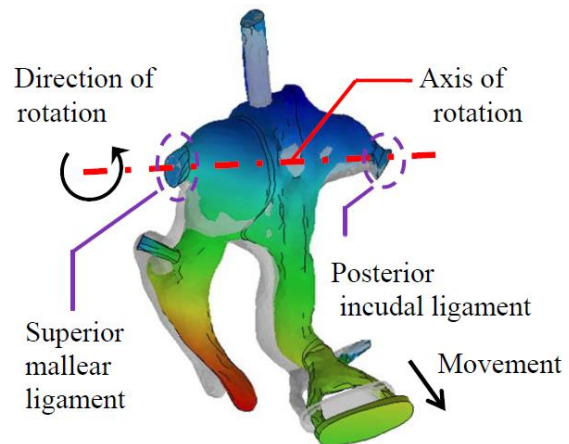


Fig. 2 Deformation of auditory ossicles

Figure 2 shows that the auditory ossicles turn about the axis connecting the superior ligament and the posterior incudal ligament [15]. By this rotary motion, the vibration of the tympanic membrane is efficiently converted into Z-direction (perpendicular to the stapes basal plane) movement of the stapes. The stapes vibration is transmitted to the labyrinthine fluid of the internal ear and converted to electrical signals, which are then recognized as sound in the brain. In this study, we consider that there is a certain relationship between hearing ability and the Z-direction displacement of the stapes.

### 3 GEOMETRIC MODELING OF THE MIDDLE EAR

The precise geometry of ossicles was obtained through CT scanning of the human head. As shown in Fig. 3, the two-dimensional slice images of the CT scanning data were transformed into three-dimensional solid geometries using a post-processing software and the region which contains the three ossicles was separated from the CT scanning data. Then, the 3D geometries were refined and converted to DICOM data, and further converted into STL data, which were imported into a general-purpose structure analysis software to create a FEM model. The geometric model for a healthy subject for finite element harmonic vibration analysis is shown in Fig. 4. This model is composed of the tympanic membrane, auditory ossicles, ligaments, joints, stapedial muscle and others.

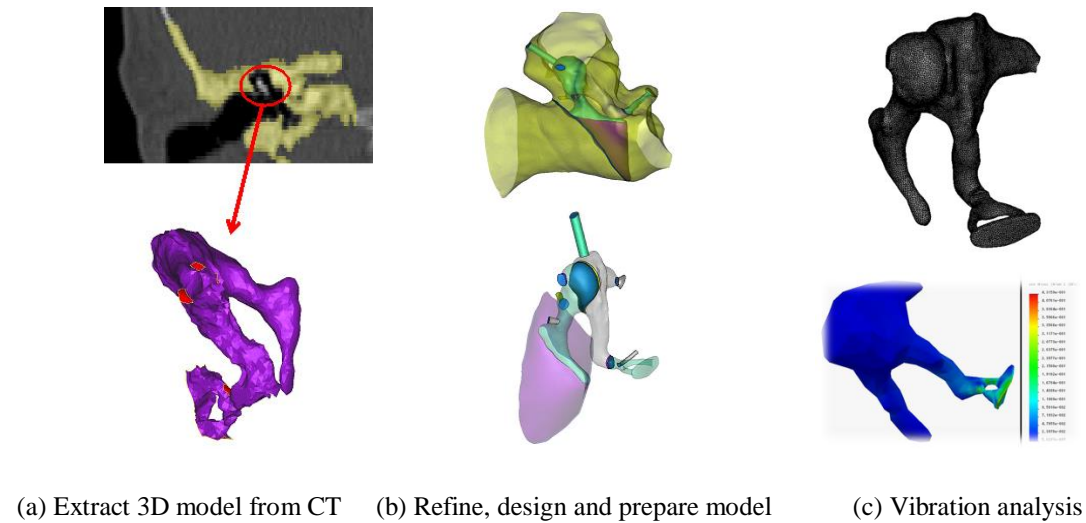
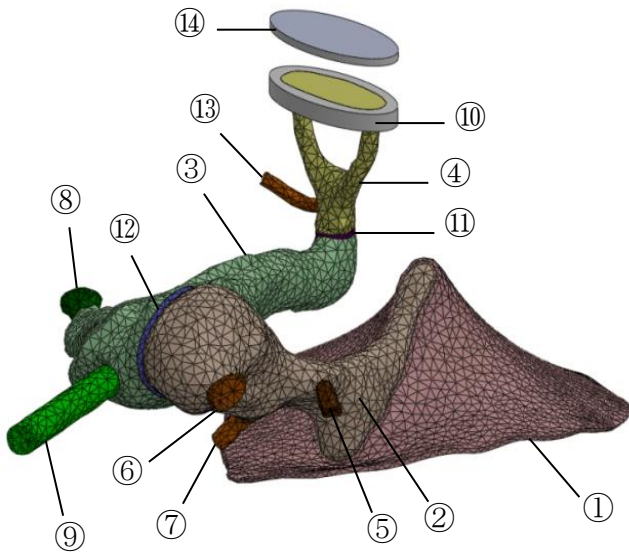


Fig. 3 Construction of a 3D model of human middle ear for vibration analysis

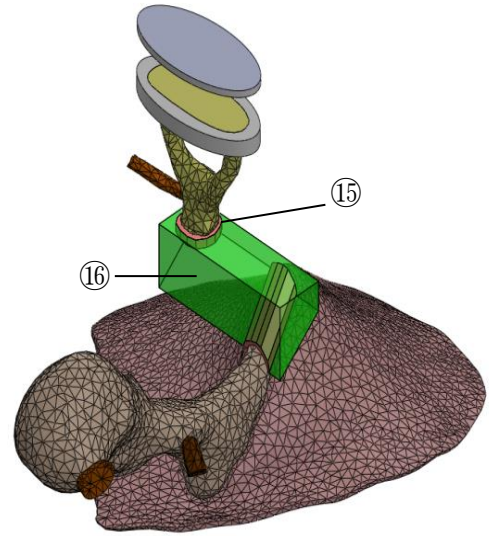
## 4 HARMONIC VIBRATION ANALYSES

### 4.1 Material data

Material data of the analysis model are shown in Table 1 [9] [10] [17]. The anatomical parts name number in the table corresponds to the number in Fig. 4. The base plate 14 is a virtual part for supporting the spring. Therefore, its Young's modulus can be assumed to be that of a rigid body.



(a) Healthy subject model of middle ear



(b) Operation model of middle ear

Fig. 4 Model of middle ear

Table 1 Material data

Anatomical name	Young's Modulus (MPa)	Density (kg/m <sup>3</sup> )	Poisson's ratio
① Tympanic membrane	33.4	1,200	0.3
② Malleus	13,436	4,350	
③ Incus			
④ Stapes			
⑤ Lateral malleolar ligament			
⑥ Superior malleolar ligament	21	2,500	
⑦ Anterior malleolar ligament			
⑧ Posterior incudal ligament			
⑨ Superior incudal ligament	0.65	1,200	
⑩ Stapedial annular ligament			
⑪ Incudostapedial joint	6	1,200	
⑫ Incudomalleolar joint			
⑬ Stapedial muscle	0.52	2,500	
⑭ Base plate	$1 \times 10^{10}$	-	
⑮ Columella (joint)	6	1,200	
⑯ Columella (Main body)	112,400	2,330	0.28

## 4.2 Boundary conditions

The tympanic membrane circumference, edges of ligament and muscle, and base plate were perfectly fixed in load conditions. A sound pressure of 90dB was converted into pressure using the equation (1) as load conditions.

$$L_p = 20 \log_{10}(P/P_0) \quad (1)$$

In Eq. (1),  $L_p = 90\text{dB}$  is the setting sound pressure (a relative noisy level) and  $P_0 = 20 \times 10^{-6}\text{Pa}$  a standard value (the lowest value of the sound intensity which is audible for humans). As a result, a pressure of  $P = 0.632\text{Pa}$  was obtained. However, in this analysis,  $P = 15.2\text{Pa}$  was given at the contact surface of the tympanic membrane and malleus. The ratio  $15.2/0.632$  equals the ratio of the total area of the tympanic membrane to the contact surface area of the tympanic membrane and malleus. A spring of  $40\text{N/m}$  spring constant was installed between the stapes and the base plate referring to the research of Gan et al [8]. Rayleigh damping was assumed and damping factors of  $\alpha = 0\text{s}^{-1}$ ,  $\beta = 7.5 \times 10^{-5}\text{s}$ .

## 4.3 Finite element analysis results of the healthy model

In this research, harmonic vibration analysis was done as a dynamic analysis using the finite element method. Fig. 5 shows the harmonic vibration analysis results for a healthy subject. The longitudinal axis shows the displacement of the stapes bottom in a perpendicular direction to the basal plane, and the lateral axis represents the frequency. In cases of a healthy subject, it is said that there is a resonance region of the middle ear at  $0.5\text{--}2\text{ kHz}$  in frequency, that is, conversation range. Average displacement of the stapes basal plane shows the peak of the resonance to be near  $1.3\text{ kHz}$  in frequency in the analytical results for a healthy subject. This displacement decreases gradually with an increase in frequency over  $2\text{ kHz}$ . It is possible to reproduce the resonance phenomena to some extent by our finite element model. Fig. 5 shows that the average displacement of the stapes base for the sound pressure of  $90\text{dB}$  is  $5.09 \times 10^{-6}\text{ mm}$ , which was used as a standard value in this study. If the change in this displacement is compared, the hearing restoration effect can be estimated prior to the tympanoplasty operation, in the case where the medical device, called columella, is substituted for the deficient auditory ossicles, or in the case of stiffening of the ligament. This kind of approach makes it possible to propose a new medical treatment for the recovery of conductive or cochlear hearing loss.

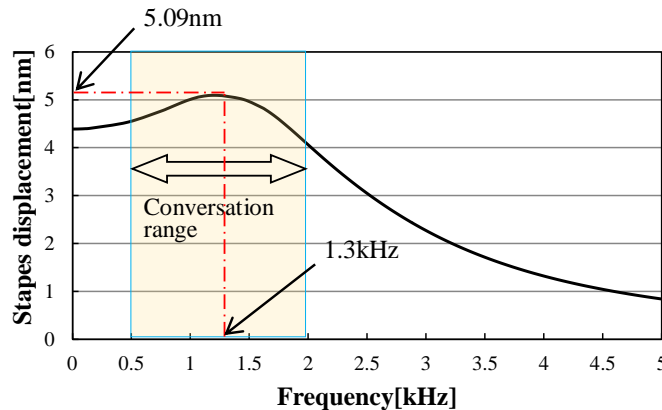
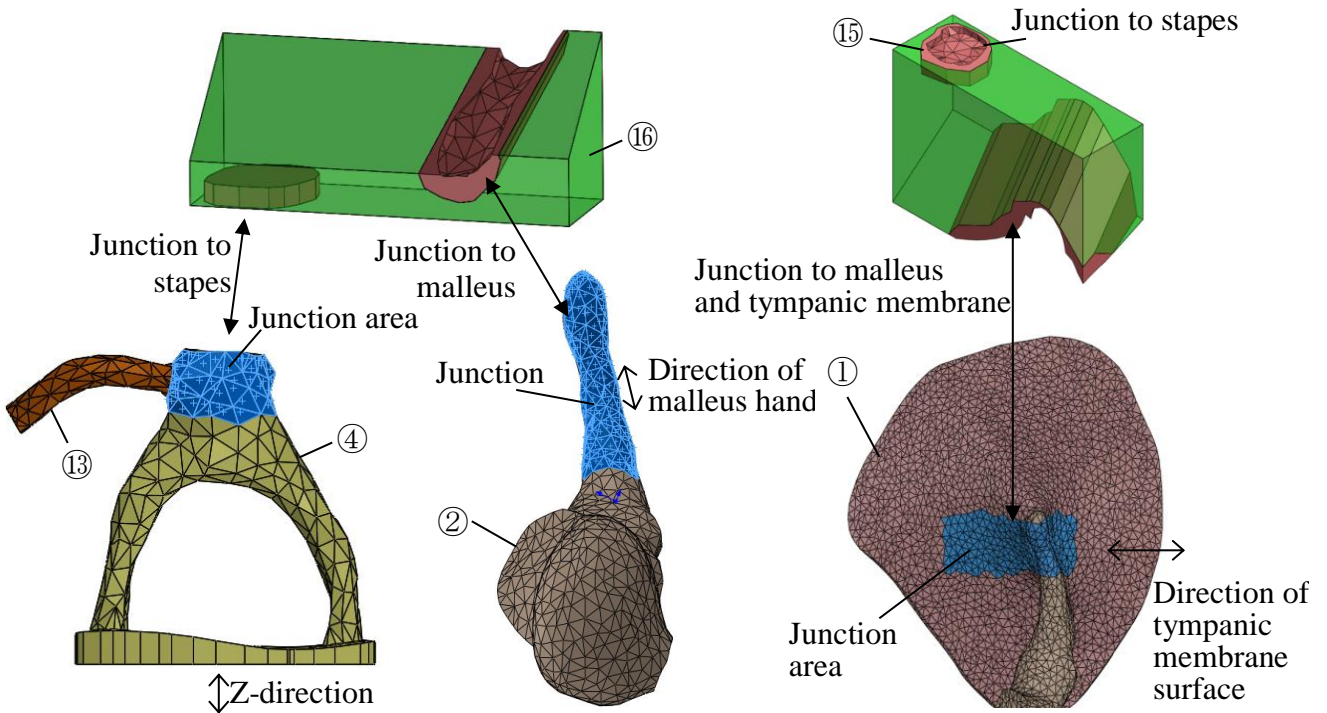


Fig. 5 Frequency response graph of healthy subject model

## 5 APPLICATION FOR CLINICS IN TYMPANOPLASTY

As mentioned in Section 1, the tympanoplasty operation is often carried out to reconstruct the damaged ossicular chain to improve the sound conduction efficiency when auditory ossicles were damaged for chronic otitis media, etc.. In the ossicular chain reconstruction, as shown in Fig. 4(b), the column article called columella is produced and used instead of incus which is generally broken. As a part of the optimum design of the columella with the aim of better sound conduction efficiency, the correlation of columella junction area to the auditory ossicles and hearing restoration effect was studied.



(a) Junction area for the stapes (b) Junction area for the malleus (c) Junction area for the tympanic membrane  
Fig. 6 Definition of the junction area

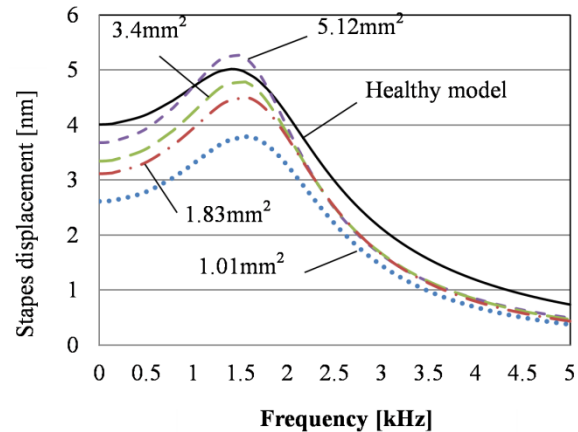
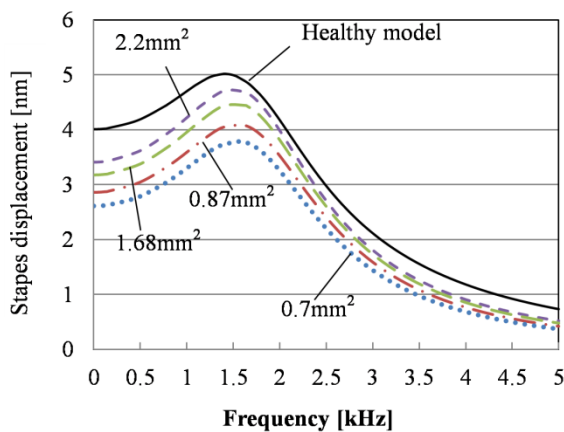


Fig. 7 Frequency response graph for the Fig. 6(a) model Fig. 8 Frequency response graph for the Fig. 6(b) model

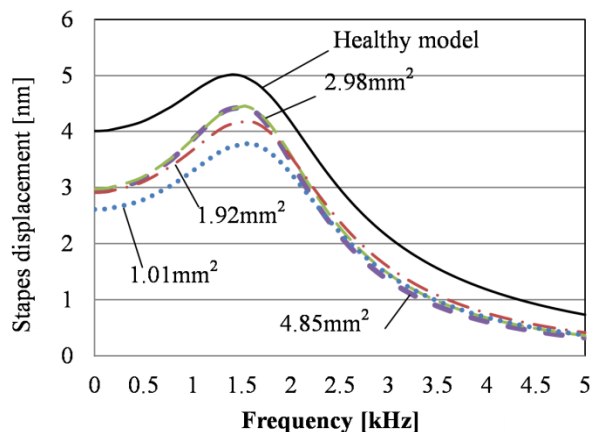


Fig. 9 Frequency response graph for the Fig. 6(c) model

The junction area is the contact area between a columella and malleus, stapes or tympanic membrane. The junction area is changed by the change of shape of the columella. A standard model of columella is shown in upside of Fig. 6. The junction area for the stapes side is shown in Fig. 6(a). In the case of stapes side, the shape of the columella is changed in the Z-direction, which is perpendicular to the basal plane of stapes. The junction area for the malleus side is shown in Fig. 6(b). In the case of malleus side, the shape of the columella is changed in the direction along the handle of malleus. The junction area for the tympanic membrane side is shown in Fig. 6(c). In the tympanic membrane side, the shape of the columella is changed in the direction along the tympanic membrane surface. The number of ①, ②, ④, ⑬, ⑮, ⑯ in Fig. 6 corresponds to the number in Fig. 4 and Table 1. The influence by the change of the junction area is examined, and the correlation of hearing restoration effect and junction area is clarified.

A frequency response graph obtained by the finite element analysis is shown in Fig. 7~9. These figures show the relation between the normal displacement of stapes bottom and frequency. Figure 7 shows the results in case the junction area for the stapes side changes. The solid line shows the result for a healthy subject, and the dotted line shows the result for the model where the junction area equals  $0.7\text{mm}^2$ . Moreover, the dashed and single-dotted line is the result for the model where the junction area is  $0.87\text{mm}^2$ . The long dashed line is the result for the model where the junction area is  $1.68\text{mm}^2$ . The short dashed line is the result for the model where the junction area is  $2.2\text{mm}^2$ .

Figure 8 shows the results in case the junction area for the malleus side changes. The solid line shows the result for a healthy subject. The dotted line shows the result for the model where the junction area equals  $1.01\text{mm}^2$ . The dashed and single-dotted line is the result for the model where the junction area is  $1.83\text{mm}^2$ . Long dashed line is the result for the model where the junction area is  $3.4\text{mm}^2$ . The short dashed line is the result for the model where the junction area is  $5.12\text{mm}^2$ .

Figure 9 shows the results in case the junction area for the tympanic membrane side changes. The solid line shows the result for a healthy subject. The dotted line shows the result for the model where the junction area equals  $1.01\text{mm}^2$ . The dashed and single-dotted line is the result

for the model where the junction area is  $1.92\text{mm}^2$ . The long dashed line is the result for the model where the junction area is  $2.98\text{mm}^2$ . The short dashed line is the result for the model where the junction area is  $4.85\text{mm}^2$ .

Figures 7 and 8 show that the stapes displacement increases with the increase of junction area between auditory ossicles (stapes or malleus) and the columella. By increasing the junction area, it is possible to more firmly connect the columella. Therefore, it seems to improve the transfer efficiency of sound. Fig. 9 shows that the stapes displacement increases with the increase of junction area between tympanic membrane and columella, but there is a limit in the increase. Tympanic membrane is not suitable to transmit the force, because the Young's modulus of the tympanic membrane is considerably lower than that of auditory ossicles as shown in Table 1. In previous research [16], we have obtained the same results in static analysis. The vibration of the tympanic membrane cannot sufficiently transmit to the stapes due to its low rigidity.

## 6 CONCLUSIONS

The vibration characteristics of the human middle ear were investigated in this paper and were applied to improve the sound conduction efficiency in tympanoplasty. We have proposed that the hearing restoration effect can be estimated by comparison of the displacement of stapes basal plane prior to the operation. The validity of our proposal was confirmed by analyzing various types of operation models using harmonic vibration analysis and compared with a healthy subject. Furthermore, as a part of the optimum design of the columella with the aim of better sound conduction efficiency, the correlation of hearing restoration effect and junction area of the auditory ossicles was clarified. It is possible and important to optimize the columella from the engineering viewpoint using the finite element method. This kind of approach makes it possible to propose a new medical treatment for the recovery of conductive or cochlear hearing loss.

## ACKNOWLEDGEMENT

This work was supported by JSPS KAKENHI Grant Number JP17K14581.

## REFERENCES

- [1] WHO global estimates on prevalence of hearing loss. WHO (2012).
- [2] Wada H, Kobayashi T, Nagamura H, Tashizaki H. Analysis of dynamic characteristics of eardrum : Young's modulus, thickness, and damping ratio of human eardrum. Transactions of the Japan Society of Mechanical Engineers Series C (1990) 56:1431–4.
- [3] Voss SE, Rosowski JJ, Merchant SN, Peake WT. Acoustic responses of the human middle ear. Hearing Research (2000)150:43 – 69.
- [4] Aibara R, Welsh JT, Puria S, Goode RL. Human middle-ear sound transfer function and cochlear input impedance. Hearing Research (2001)152:100 –9.

- [5] Funnell WRJ, Laszlo CA. Modelling of the cat eardrum as a thin shell using finite element method. *The Journal of the Acoustical Society of America* (1978) 63:1461–7.
- [6] Wada H, Metoki T, Kobayashi T. Analysis of dynamic behavior of human middle ear using a finite-element method. *The Journal of the Acoustical Society of America* (1993)92:3157–68.
- [7] Gan RZ, Dyer RK, Wood MW, Dormer KJ. Mass loading on the ossicles and middle ear function. *Annals of Otology, Rhinology & Laryngology* (2001)110:478–85.
- [8] Gan RZ, Feng B, Sun Q. Three-dimensional finite element modeling of human ear for sound transmission. *Annals of Biomedical Engineering* (2004) 32:847–59.
- [9] Sun Q, Gan RZ, Chang KH, Dormer KJ. Computer integrated finite element modeling of human middle ear. *Biomechanics and Modeling in Mechanobiology* (2002)1:109–22.
- [10] Koike T, Wada H. Modeling of the human middle ear using the finite element method. *The Journal of the Acoustical Society of America* (2002)111:1306–17.
- [11] Liu Y, Li S, Sun X. Numerical analysis of ossicular chain lesion of human ear. *Acta Mechanica Sinica* (2009) 25:241–7.
- [12] Frank Bohnke F, Bretan T, Lehner S, Strenger T. Simulations and measurements of human middle ear vibrations using multi-body systems and laser-doppler vibrometry with the floating mass transducer. *Materials* (2013) 6:4675–88.
- [13] Greef DD, Aernouts J, Aerts J, Cheng JT, Horwitz R, Rosowski JJ, et al. Viscoelastic properties of the human tympanic membrane studied with stroboscopic holography and finite element modeling. *Hearing Research* (2014) 312:69 – 80.
- [14] Lee D, Ahn TS. Statistical calibration of a finite element model for human middle ear. *Journal of Mechanical Science and Technology* (2015) 29:2803–15.
- [15] Higashimachi T, Shiratake Y, Maeda T, Toriya R. Three-dimensional finite element analysis of the human middle ear and an application for clinics for tympanoplasty. *Surface Effects and Contact Mechanics, XI, WIT Transactions on Engineering Sciences* (2013) 78:61–72.
- [16] Higashimachi T, Maeda T, Oshikata T, Toriya R. Finite element analysis of the human middle ear and an application for clinics for tympanoplasty (static and harmonic vibration analysis). In: *The 3rd International Conference on Design Engineering and Science, ICDES 2014* (2014).
- [17] Higashimachi T, Suga K, Sasahara H. Structural mechanical analysis and evaluation for extension of teeth lifetime. *Journal of Japanese Society of Precision Engineering* (2009)75:428–3.

## **Fracture Mechanism for Porous Single Crystals under Various Stress States**

ZHIGANG LIU\*

\*IHPC

### **ABSTRACT**

Void growth and coalescence are well known as the main mechanism of ductile fracture. While less effort has been devoted to investigating the process of void growth and coalescence in single crystal. This work examines the onset of void coalescence, the void behaviors that often precede eventual failure in ductile porous single crystal. The occurrences depends largely on the stress states in the solid, characterized by the stress triaxiality (T) and the Lode parameter (L). In employing a 3D unit cell simulation with crystal plasticity constitutive model, the strain at onsets of void coalescence behaviors can be operationally defined for different crystal orientation. Validated against known experimental and numerical works, we have demonstrated the stress state dependence of void coalescence. The crystal orientation and stress states on void coalescence are studied with five original single crystal orientations and two initial void volume fractions.

## Stochastic Geometric Nonlinear Analysis of Functionally Graded Circular Shallow Arches

Zhanpeng LIU<sup>\*</sup>, Wei GAO<sup>\*\*</sup>, Di WU<sup>\*\*\*</sup>, Guoyin LI<sup>\*\*\*\*</sup>

<sup>\*</sup>Centre for Infrastructure Engineering and Safety (CIES), School of Civil and Environmental Engineering, The University of New South Wales, Sydney NSW 2052, Australia, <sup>\*\*</sup>Centre for Infrastructure Engineering and Safety (CIES), School of Civil and Environmental Engineering, The University of New South Wales, Sydney NSW 2052, Australia, <sup>\*\*\*</sup>Centre for Infrastructure Engineering and Safety (CIES), School of Civil and Environmental Engineering, The University of New South Wales, Sydney NSW 2052, Australia, <sup>\*\*\*\*</sup>Department of Applied Mathematics, The University of New South Wales, Sydney NSW

### ABSTRACT

In this study, a stochastic geometric nonlinear analysis of functionally graded (FG) shallow arch is investigated. The constitutive material composition of the FG arch varies along the radial direction of the cross section, so the mechanical performance of the arch can be well controlled for various engineering design purposes. Based on the Euler-Bernoulli hypothesis, both geometric linear and nonlinear analytical solutions of the structural responses (i.e., displacements, axial compressive force and bending moment) of the FG arch subjected to uniform distributed load are derived by using the virtual work method. The boundary condition of the investigated FG arch is identified as pin-ended support at both ends. By adopting the derived analytical solution, the relationship between the structural response and the various FG material properties can be analysed efficiently. Once the analytical solutions of the deterministic structural responses of the FG arch are established, the stochastic analysis of the FG arch structure is performed by direct Monte Carlo simulation method. Both uncertain material properties and loading conditions can be incorporated within the simulative analysis framework. One numerical example is presented to demonstrate the applicability and effectiveness of the proposed nondeterministic analysis framework for the geometric nonlinear analysis of FG arch structures.

## Computational Investigation of Bio-inspired Composite Nano Rotor Blade

Zhen LIU\*, Chen BU\*\*, Shanyong ZHAO\*\*\*

\*State Key Laboratory for Strength and Vibration of Mechanical Structures, school of Aerospace, Xi'an Jiaotong University, \*\*State Key Laboratory for Strength and Vibration of Mechanical Structures, school of Aerospace, Xi'an Jiaotong University, \*\*\*State Key Laboratory for Strength and Vibration of Mechanical Structures, school of Aerospace, Xi'an Jiaotong University

### ABSTRACT

At ultra-low Reynolds number, the propulsive performance of nano rotor drops dramatically, which has a profound impact on the flight performance of NAV. The bio-inspired blade motion is introduced to improve the performance of nano rotor. However, the complex flow interacts with the flexible composite blade structure resulting in the variation of propulsion performance of nano rotor and the vibration of blade structure. In this paper, the nano-scale composite rotor with blade-pitching motion was studied computationally with a computational solvers based on a preconditioned compressible NS equations, Roe-scheme, LUSGS-?ts dual-time marching method coupling with a finite element solver. A non-contact modal experimental platform was established using sound excitation instrument and laser vibrometer. The structural characteristics of the composite nano rotor were measured. It was found that the natural frequencies are very close for the first two orders. The finite element model of composite rotor was created accordingly. The modal was studied computationally with FEM solver. It was found that the simulation results matched well with the experimental results which verified the correctness of the finite element model. The CFD model was established and the propulsive performance of nano rotor without bio-inspired motion was studied, respectively. The results showed that the computational results from Fluid-structure solver matched better than that for CFD solver. It is indicted that the fluid-structure method has a higher precision for nano rotor simulation. It is evident that it is necessary to consider the flexibility of the composite nano rotor when investigating the propulsion performance of bio-inspired nano rotor. Then the flow field of flexible nano rotor was also analyzed at different bio-inspired pitching frequency and the response of blade structure was also studied with the fluid-structure solver. Results showed that the propulsive performance for bio-inspired pitching rotor at different pitching frequency. It was found that the thrust and torque for the bio-inspired pitching rotor are higher than those for the rotor without bio-inspired motion. And it was also found that the propulsive performance for the nano rotor with bio-inspired pitching frequency of two times of that rotation frequency is higher than that with only one times pitching frequency. It is evident that the improvement enhanced with the increase of the pitching frequency. And the blade structure was also found vibrate with a small amplitude. In general, it was found that the bio-inspired pitching motion can improve the performance of nano rotor.

## Multibody Dynamics to Build a Reduced Ordered Model of a Car Crash Simulation

Tanguy LOREAU<sup>\*</sup>, Philippe SERRE<sup>\*\*</sup>, Laurent NOYELLE<sup>\*\*\*</sup>, Jean-Luc DION<sup>\*\*\*\*</sup>

<sup>\*</sup>QUARTZ EA 7393 - SUPMECA, <sup>\*\*</sup>QUARTZ EA 7393 - SUPMECA, <sup>\*\*\*</sup>GROUPE RENAULT, <sup>\*\*\*\*</sup>QUARTZ EA 7393 - SUPMECA

### ABSTRACT

Finite element models for vehicle crash studies are unsuited for upstream design: they have a large number of degrees of freedom and require precise information. Furthermore, their complexity implies high computational costs that make them unusable for short optimization loops. A way to overcome this complexity is to adapt results from another finite element simulation or crashtest of a vehicle close to the one to design. But this process uses only one part of the knowledge of the company, which restrains the new vehicle to be close to the previous one and requires a long time modeling and calculation making it a bad candidate for optimization. In this study, we aim to build a fast computing and robust model from all the knowledge of the company on crash simulation. A first approach is to apply a well suited and designed reduced ordered model method (POD, PGD, Deep Learning) on the simulation database. Yet these methods all have weaknesses that make them unusable for the crash reduction: either they need a quantity of data the company can't provide, or they are not adapted in contact detection, or the produced model needs parameters that are not available in upstream phases and, in all cases, these methods don't relate about physics so the model can't be so much extrapolated. A second approach, which is presented in this work, is to see a car during a crash as a rigid multibody system articulated with dissipative links (Carvalho &&& Ambrosio, 2011, Development of generic road vehicle multibody models for crash analysis using an optimization approach, International Journal of Crashworthiness). Indeed, an energetic analysis of a crash simulation shows that a very small quantity of parts explains most of the phenomenon. These parts can be modeled as sets of rigid bodies articulated with plastic links which localization and rheological parameters come from the finite element simulation. The method presented here proposes a way to read finite element simulations to soundly place sensors on finite element models and then, after a new simulation, to get rheological parameters and positions of links to build a multibody model from a finite element simulation. This new multibody model, after a well suited correlation and validation, will represent a car crash simulation.

## The Magneto-electric Coupling in Multiferroic Composites: Magnetostrictive Preisach and Ferroelectric Switching Model

Matthias Labusch\*, Jörg Schröder\*\*

\*University Duisburg-Essen, Germany, \*\*University Duisburg-Essen, Germany

### ABSTRACT

Multiferroic materials combine two or more ferroic properties and can exhibit an interaction between electric polarization and magnetization. This magneto-electric (ME) coupling can find applications in sensor technology or in magneto-electric data storage devices. Since most ME single-phase materials show such a coupling far below room temperature, the manufacturing of two-phase composites, consisting of a ferroelectric matrix with magnetostrictive inclusions, becomes important. Due to the interaction of both constituents the composites generate a strain-induced ME coupling at room temperature, where we distinguish between the direct and the converse ME effect. The direct effect characterizes magnetically induced polarization, where an applied magnetic field yields a deformation of the magnetostrictive phase, which is transferred to the ferroelectric phase. Due to the electro-mechanical properties of the matrix material the composite exhibit a change in polarization. On the other hand, the inverse ME effect characterizes electrically induced magnetization. The ME coupling significantly depends on the microscopic morphology and the ferroic properties of the individual constituents. In order to take both aspects into account, a finite element (FE<sup>2</sup>) homogenization approach is performed, which combines via a scale bridging the macro-and microscopic level [1]. Thereby, the microscopic morphology is characterized by representative volume elements and the ferroic properties of the phases are described by suitable material models. The typical ferroelectric hysteresis curves are modeled by considering the switching behavior of the spontaneous polarizations of barium titanate unit cells [2], whereas the magnetic hysteresis loops are described by a Preisach operator [3]. [1] J. Schröder, M. Labusch, and M.-A. Keip: Algorithmic two-scale transition for magneto-electro-mechanically coupled problems – FE<sup>2</sup>-scheme: Localization and homogenization. *Computer Methods in Applied Mechanics and Engineering* 302, 253 – 280 (2016). [2] S. Hwang, C. Lynch, and R. McMeeking: Ferroelectric/Ferroelastic interaction and a polarization switching model. *Acta metall. Mater.* 43, 2073-2084 (1995). [3] M. Kaltenbacher, B. Kaltenbacher, T. Hegewald, and R. Lerch: Finite Element Formulation for Ferroelectric Hysteresis of Piezoelectric Materials. *Journal of Intelligent Material Systems and Structures* (2010).

## **A Posteriori Estimation and Adaptivity for the Parabolic p-curl from Applied Superconductivity**

Marc Laforest<sup>\*</sup>, Andy T. S. Wan<sup>\*\*</sup>, Yann-Meing Law<sup>\*\*\*</sup>, Frédéric Sirois<sup>\*\*\*\*</sup>

<sup>\*</sup>École Polytechnique de Montréal, <sup>\*\*</sup>McGill University, <sup>\*\*\*</sup>École Polytechnique de Montréal, <sup>\*\*\*\*</sup>École Polytechnique de Montréal

### **ABSTRACT**

The optimal design in 3D of new electrical components from commercially available high-temperature superconductors pushes the limits of current computational tools. Strong currents develop near the envelope of the superconductor and under AC, the nonlinear resistance induces sharp fronts in the currents and in the magnetic field density. These are challenges for finite element approximations but they also introduce subtle regularity issues recently identified by our group. In this presentation, we discuss the a posteriori error estimation of the critical-state model from applied superconductivity, both with and without linearization. We also review our work on the generation of diffusion, and energy loss, at the front and its approximation by both FE approximation and non-oscillatory approximations using a relaxation formulation of the problem. Regularity issues at the boundary are further related to error estimation and modeling.

## Spectral Analysis of the Deflated Complex Shifted Helmholtz Operator

Domenico Lahaye\*, Kees Vuik\*\*

\*DIAM / TU Delft, \*\*DIAM / TU Delft

### ABSTRACT

The complex shifted Laplacian is widely recognized as a computationally very efficient preconditioner for the Helmholtz equation. It introduces a sequence of damped wave propagation problems. The linear systems that arise can efficiently be solved by for instance multigrid methods. This method can however be significantly accelerated by a procedure published in [1]. In this procedure, the preconditioner is multiplied with a deflation operator that employs multigrid vectors. The deflation operator thus accelerates the convergence of the preconditioner in a similar way that a coarse grid correction operator accelerates the convergence of a smoother in a multigrid method. The objective of this work is to analyze how damping influences the efficiency of the new hybrid method. We are especially interested in large amounts of damping that facilitates the approximate inversion of the preconditioner. Without the use of deflation operator, the converge of the outer Krylov method rapidly deteriorates with the amount of damping introduced. To study the influence of the deflation operator, we analyze the spectrum of the discrete Helmholtz operator preconditioned by a multiplicative combination of the first deflation operator and subsequently complex shifted Laplace preconditioner. We perform a Rigorous Fourier modal analysis of a one-dimensional model problem in which the Helmholtz equation with homogeneous Dirichlet boundary conditions discretized by a second order finite difference scheme on a uniform fine and coarse grid. With these choices, the discrete Helmholtz operator, the complex shifted Laplacian and the coarse grid operator share a set of eigenmodes. Our spectral analysis reveals that the inversion of the near-singular coarse grid operator causes the eigenvalues of the deflated operator spreads in tails along both sides of the real axis. The subsequent action of the preconditioner is to shrink, rotate and shift the set of eigenvalues. Unlike the case in which merely the preconditioner is employed, the smallest eigenvalue remains bounded away from zero for larger values of the damping parameter. Numerical results show that the eigenvalue distribution and the GMRES number of steps are well correlated. A much larger damping parameter than in algorithms without deflation can be used. This holds great promises for the future application of the new method. [1] A.H. Sheikh, D. Lahaye, L. Garcia Ramos, R. Nabben and C. Vuik, Accelerating the shifted Laplace preconditioner for the Helmholtz equation by multilevel deflation, *Journal of Computational Physics*, 322: 473--490, 2016.

## Phase Field Modelling of Brittle Fracture in Thin Shells Accounting for Cracks Partly Through the Thickness

Wenyu Lai<sup>\*</sup>, Jian Gao<sup>\*\*</sup>, Yihuan Li<sup>\*\*\*</sup>, Marino Arroyo<sup>\*\*\*\*</sup>, Yongxing Shen<sup>\*\*\*\*\*</sup>

<sup>\*</sup>University of Michigan-Shanghai Jiao Tong University Joint Institute, Shanghai Jiao Tong University, Shanghai, China, <sup>\*\*</sup>University of Michigan-Shanghai Jiao Tong University Joint Institute, Shanghai Jiao Tong University, Shanghai, China, <sup>\*\*\*</sup>University of Michigan-Shanghai Jiao Tong University Joint Institute, Shanghai Jiao Tong University, Shanghai, China, <sup>\*\*\*\*</sup>Laboratori de Calcul Numeric, Universitat Politecnica de Catalunya, Barcelona, Spain, <sup>\*\*\*\*\*</sup>University of Michigan-Shanghai Jiao Tong University Joint Institute, Shanghai Jiao Tong University, Shanghai, China

### ABSTRACT

In this work, we present a phase field fracture model for the brittle fracture of the Euler-Bernoulli beam theory and the Kirchhoff-Love shell theory under the principle of minimum potential energy. To account for transverse part-through cracks, we employ an ansatz for the phase field using two scalar fields within cross section, allowing variation of the phase field through the thickness. The problem then reduces to a one-dimensional nonlinear differential equation for the beam problem, or a two-dimensional nonlinear differential equation over the mid-surface for the shell problem, which can be solved with the finite element method. Combined with a phase field model discriminating tension and compression, this special treatment permits simulating fracture due to bending loads and to membrane loads. The continuous formulation then can be discretized using any standard numerical method allowing  $H^2$  continuity of the basis functions. In the presentation, we will talk about efficient simulation schemes for the numerical algorithm.

## **Modelling and Numerical Algorithm for Contact Problems with Frictional Heat Generation and Wear in Peridynamics**

Xin Lai\*, Lisheng Liu\*\*

\*Wuhan University of Technology, \*\*Wuhan University of Technology

### **ABSTRACT**

For multi-body contact problems, accurate modelling and numerical algorithm of the contact interaction between objects are very important to ensure the reliability of the numerical simulation. Especially, the frictional heat generated in the sliding and contacting progress, which is usually neglected, has great effect on the behavior of the material and the structure in material cutting, wearing, and impact problems. In such circumstances, the dramatic increasing of temperature caused by the frictional heat may change the physical properties, mechanical properties, or even the states of the material. Therefore, Frictional heat should be considered when dealing with high-speed contact problems. In this work, contact interactions including frictional heat has been modelling and numerically implemented in Peridynamic framework, which is recently widely used in impact damage problems. Numerical examples are carried out to validate the validity and accuracy of our algorithm. Comparisons have been made to show the influence of the material behavior affected by the frictional heat.

## **Dispersion, Spurious Reflections and Spurious Bifurcation of Flexural Waves**

José Laier\*

\*Engineering School of São Carlos USP

### **ABSTRACT**

Wave velocity dispersion, spurious bifurcation (numerical instability) and spurious reflections of the flexural wave model produced by numerical integration were investigated [1]. Classic cubic beam finite elements of two nodes with consistent mass matrix are taken into account [2]. The Newmark average acceleration integration method of single step is used for integration in time. The resultant system of difference equation is then analytically integrated in non-finite terms (numerical wave solution) using complex notation. Numerical results reveal that even for refined mesh the spurious reflections can be significant.

## **A Positive Asymptotic Preserving Scheme for Linear Kinetic Transport Equations**

M. Paul Lau<sup>\*</sup>, Martin Frank<sup>\*\*</sup>, Cory Hauck<sup>\*\*\*</sup>

<sup>\*</sup>Oak Ridge National Laboratory, <sup>\*\*</sup>Karlsruhe Institute of Technology, <sup>\*\*\*</sup>Oak Ridge National Laboratory

### **ABSTRACT**

We present a new positive and asymptotic preserving numerical scheme for solving linear kinetic transport equations. The proposed scheme is developed based on the standard spectral angular discretization and the classical micro-macro decomposition. The three main ingredients of the proposed scheme are a semi-implicit time discretization, a dedicated finite difference space discretization, and positivity limiters. We show that the proposed scheme is asymptotic preserving in the sense that when the mean free path of the particles goes to zero, the scheme achieves a correct numerical scheme for the limiting diffusion equation, without restrictive time step constraints. We also prove that the proposed scheme preserves positivity of the spatial particle concentration in the solution, which fixes a common defect of spectral angular discretizations. The proposed scheme is tested on two benchmark problems on a two-dimensional spatial domain, one with a single material and one with two types of material embedded as a checkerboard.

## An HPC Enhanced Agent Based System for Simulating Mass Evacuations

Maddegedara Lalith\*, Muneo Hori\*\*, Wasuwat Petprakob\*\*\*, Leonel Aguilar\*\*\*\*

\*Earthquake Research Institute, The University of Tokyo, \*\*Earthquake Research Institute, The University of Tokyo,  
\*\*\*Dept. of Civil Eng., The Univ. of Tokyo, \*\*\*\*Dept. of Humanities, Social and Political Sciences, ETH

### ABSTRACT

We present the details of implementation and applications of an HPC enhanced Agent Based Model (ABM) for simulating tsunami triggered evacuation of large coastal regions. In seeking various strategies to accelerate evacuation process, quantitative evaluation of their effectiveness, identifying unforeseen problems, etc., numerical simulations are invaluable to disaster mitigation authorities. Simple queue models with 1D networks are widely used for mass evacuations due to the ease of use, limited of computer resources, etc. These simplified models are inadequate for studying certain scenarios in congested urban regions which demand the use of accurate high resolution model of environment and complex models of individuals. Some of the scenarios requires best use of the available narrow spaces, debris, visibility in night time, pedestrian-vehicle interactions, etc. With the aim of simulating such demanding scenarios, we developed an ABM which includes a high resolution model of environment and sophisticated agents capable of perceiving the environment in high resolution [1, 2]. Environment is modeled as a hybrid of high resolution grid and a graph which contains the topological connectivity of accessible spaces in the grid. Each agent scans its surrounding in the grid in high resolution mimicking the eyes of an evacuee. This allows them to perceive dynamic changes in environment like progression of inundation and act accordingly. Agent store their experiences with reference to the topological graph and use those information in decision making. In order to meet the high computational demand of sophisticated agents in high resolution environment, we implemented MPI+OpenMP hybrid HPC extension. The heterogeneous nature of agents, the movements of agents from the domain of one CPU to other, etc. give rise to significant load imbalance among CPUs. To cope with this load imbalance, we implemented a dynamic load balancer using the measured execution time of each agent as a heuristic.

## **A Multiscale and Multiphase Model for the Description of Paracetamol-induced Hepatotoxicity Using the Example of the Human Liver**

Lena Lambers\*, Navina Waschinsky\*\*, Tim Ricken\*\*\*

\*Institute of Mechanics, Structural Analysis, and Dynamics; University of Stuttgart, \*\*Chair of Mechanics, Structural Analysis, and Dynamics; TU Dortmund University, \*\*\*Institute of Mechanics, Structural Analysis, and Dynamics; University of Stuttgart

### **ABSTRACT**

The liver is the most important human organ responsible for metabolic homeostasis. A further central task of the human liver is the detoxification of the blood since toxic substances or excessive medication can cause damage in the liver structure which can lead to acute liver failure. One example for a medicine which can cause hepatotoxicity is the analgesic Paracetamol (Acetaminophen). The toxic metabolites of the Paracetamol are normally bound by the internal Glutathione. When the concentration of Glutathione is exhausted, the metabolites react with cellular proteins causing liver necrosis. The detoxification capability of the liver can be affected by several liver diseases, e.g. the non-alcoholic fatty liver disease (NAFLD). The developed model is an extension of a previous published work, where a multicomponent, poro-elastic multiphase and multiscale function-perfusion approach based on the Theory of Porous Media (TPM), see [1], [2] has been presented, cf. [3]. Additionally, the decomposition of toxic metabolites causing cell damage is supplemented using the example of Paracetamol. Since the liver has a complex structure and different sizes, a scale bridging approach is requested. The total organ consists of liver lobules, where the toxic metabolites, just like other nutrients and substances, are initiated into the liver with an anisotropic blood flow via the sinusoids. As the structure of the lobules is extremely complex, we use a multicomponent mixture theory based on the Theory of Porous Media (TPM) see [1], [2] to describe the lobule scale. The computational model consists of a tetra-phasic component body, composed of a porous solid structure, fat tissue with the ability of growth, a liquid phase representing the blood and a solid phase, which characterizes the necrotic cells. The phases consist of a carrier phase, also called solvent, and solutes, representing microscopic components, solved in the solvent and consisting of the nutrients responsible for the liver metabolism. The metabolism takes place in the liver cells, which are located along the sinusoids. To calculate the metabolism processes on the cell scale, an embedded set of coupled ordinary differential equations (ODE) is used. [1] De Boer, R. [2002], „Theory of porous media: highlights in historical development and current state&apos;&apos;, Springer Science &amp; Business Media. [2] Ehlers, W. [2002], „Foundations of multiphase and porous materials“, Springer-Verlag Berlin, Heidelberg, New York., S. 3–86. [3] Ricken, T., et al. [2010], „A biphasic model for sinusoidal liver perfusion remodeling after outflow obstruction.&apos;&apos;, Biomech Model Mechanobiol, 9. Jg., Nr. 4, S. 435-450.

## **Deep Learning for Protein Structure Prediction and Protein Folding**

Guillaume Lamoureux\*

\*Concordia University

### **ABSTRACT**

I will be presenting our recent progresses on the development of deep neural networks for the prediction of the structure of a protein from its amino acid sequence. We are interested in neural network architectures that mimic the protein folding process and that learn not only the native structure of a protein but the shape of the folding funnel leading to it. In particular, we use neural networks designed to respect translational and rotational invariance, and to generate structures that obey the rules of molecular folding and assembly.

## **Coupled Thermal Mechanical Model of the LORELEI Experimental Device with Multiple Interactions and Heat Sources during Controlled Transients and Accident Scenarios**

Eran Landau<sup>\*</sup>, Hadas Shanha<sup>\*\*</sup>, Moran Ezra<sup>\*\*\*</sup>, Niv Moran<sup>\*\*\*\*</sup>, Avner Sasson<sup>\*\*\*\*\*</sup>

<sup>\*</sup>Rotem Industries LTD., <sup>\*\*</sup>Nuclear Research Center Negev, <sup>\*\*\*</sup>Rotem Industries LTD., <sup>\*\*\*\*</sup>Nuclear Research Center Negev, <sup>\*\*\*\*\*</sup>Rotem Industries LTD.

### **ABSTRACT**

A primary component within the LORELEI experimental device designed for single-rod Loss of Coolant Accident (LOCA) experiments in the French JHR research reactor, is a double-wall pressure flask with unique geometry and loading conditions containing the fuel rod and a peripheral heater. During the experiment sequence, the fuel power is controlled by moving the entire systems position relative to the reactor core. Heat transfer between the fuel, a surrounding heater (and instrumentation holder) and the double-wall flask result in significant axial and azimuthal temperature variations over the flask walls. The resulting temperatures are also influenced by the gamma heating of the structure materials, and the Zirconium cladding exothermal oxidation reaction and ballooning during the transient. In Addition, the system is also subjected to several notable external loads and constraints. Design-by-analysis initially relied on separate heat transfer and temperature-displacement analysis (uncoupled). This method however, produced relatively large displacements resulting in significant contact between the inner and outer flask walls, which in turn should have a strong effect over the resulting temperature field. For this reason, a fully coupled thermal and mechanical model of the LORELEI experiment device is developed, using a transient ABAQUS/Implicit solver with several tailored user-subroutines. The model employs a &quot;simplified&quot; approach for heat transfer over a gap (Radiation and Conduction/Convection) between cylindrical bodies using controlled (programmed) interactions, to accurately enable transient heat transfer between the deformable surfaces. Volumetric heat generation (nuclear, gamma, oxidation) is computed in user-subroutine HETVAL for each material model using several solution dependent variables (SDV&apos;s), Common block parameters and spatial functions, defined in user-subroutines USDFLD and UAMP. The device velocity, position, and the heater power are controlled by two independent PID controllers using temperature sensors on the cladding and heater hot-spots. The fully-coupled simulation displays notable differences in the temperature variation over the flask walls, and helps examine the influence of the existing pre-loads, cladding ballooning, added design features (such as centering pins) and the desired controller functions. LORELEI design calculations and safety analysis are based on qualified models. At this stage in development, the model is employed in evaluating safety margins and possible optimization that would result from future qualification of the model. In this presentation, special challenges in the development of the model and important findings will be discussed. [1] L.Ferry, D.Parrat, C.Gonnier, C.Blandin, Y.Weiss, A.Sasson. &quot;The LORELEI Test Device for LOCA Experiments in the Jules Horowitz Reactor&quot; WRFPM 2014

## Reduced-Order Models with Space-Adapted Snapshots

Jens Lang<sup>\*</sup>, Sebastian Ullmann<sup>\*\*</sup>

<sup>\*</sup>Technische Universität Darmstadt, Germany, <sup>\*\*</sup>Technische Universität Darmstadt, Germany

### ABSTRACT

Space-adaptive numerical methods have recently found their way into reduced-order modeling of parametrized PDEs [1, 2, 3]. Standard techniques assume that all snapshots are computed with one and the same spatial mesh, which is often not appropriate for multi-scale problems. Instead, we consider unsteady adaptive finite elements, where the spatial discretization varies over time or stochastic sampling. Our focus is on reduced-order models obtained by a Galerkin projection onto a proper orthogonal decomposition (POD) of solution samples. In this context, adaptive snapshot computations allow a reduction of computational complexity in the offline-phase of the reduced-order model. The following points will be discussed in the talk: (i) How can the effort for creating reduced-order models with space-adapted snapshots be minimized? (ii) How can the union of all snapshot meshes be avoided? (iii) What is the main difference between static and adaptive snapshots in the error analysis of Galerkin reduced-order models? Numerical test cases illustrate the convergence properties with respect to the number of POD basis functions. References: [1] M. Ali, K. Steih, and K. Urban. Reduced basis methods with adaptive snapshot computations. *Adv. Comput. Math.*, 43:257-294, 2017. [2] S. Ullmann, M. Rotkvic, and J. Lang. POD-Galerkin reduced-order modeling with adaptive finite element snapshots. *J. Comput. Phys.*, 325:244–258, 2016. [3] M. Yano. A minimum-residual mixed reduced basis method: exact residual certification and simultaneous finite-element reduced-basis refinement. *ESAIM: M2AN*, 50:163–185, 2016.

## **A Condensed Approach to Investigate Electromechanical Induced Phase Transitions in Lead Zirconate Titanate (PZT)**

Stephan Lange<sup>\*</sup>, Philip Uckermann<sup>\*\*</sup>, Andreas Ricoeur<sup>\*\*\*</sup>

<sup>\*</sup>University of Kassel, <sup>\*\*</sup>University of Kassel, <sup>\*\*\*</sup>University of Kassel

### **ABSTRACT**

Ferroelectric materials are used for a variety of technical applications, for example fuel injection or hearing devices. Despite containing lead, lead zirconate titanate (PZT) remains one of the most common actor materials because of its favorable electromechanical properties, particularly at the morphotropic phase boundary (MPB). PZT at the MPB consists of both tetragonal and rhombohedral unit cells. One of the most accepted theories for those properties is the existence of fourteen instead of six (tetragonal) or eight (rhombohedral) domain variants. The condensed method was developed to calculate e.g. hysteresis loops or residual stresses for polycrystalline materials without spatial discretization, resulting in low computational effort and large numerical stability [1]. It is suitable for efficient implementation of various constitutive behaviors, accounting for interactions of grains or different constituents of a material compound. Hitherto it has been applied to tetragonal ferroelectrics, ferromagnetics and multiferroic compounds [2] as well as to life time predictions in ferroelectrics [3]. In this research the approach is expanded towards transitions of tetragonal and rhombohedral phases. Therefore, the evolution law needs to be extended with respect these multiphase aspects. It contains energy barriers which can be reached by electrical or mechanical loads and distinguishes between phase transitions and domain wall motions. Some alternatives for modeling these barriers and the related consequences on material responses will be analyzed. Finally, the influences of the existence of two different types of unit cells and of phase transitions on properties of PZT at the MPB will be critically discussed. References [1] Lange, S. and Ricoeur, A., A condensed microelectromechanical approach for modeling tetragonal ferro- electrics, *International Journal of Solids and Structures* 54, 2015, pp. 100 – 110. [2] Ricoeur, A., Avakian, A. and Lange, S., Microstructured multiferroic materials: modelling approach towards efficiency and durability. In: Altenbach, H., Jablonski, F., Müller, W. H., Naumenko, K. and Schneider, P. (eds.), *Advances in Mechanics of Materials and Structural Analysis, Advanced Structural Materials*, 80, Springer 2017 (in press). [3] Lange, S. and Ricoeur, A., High cycle fatigue damage and life time prediction for tetragonal ferroelectrics under electromechanical loading, *International Journal of Solids and Structures* 80, 2016, pp. 181 – 192.

## Numerical Transition Behavior Modeling of High-Strength Low-Alloy Steels (HSLA) Extending a Gurson Model with a Modified Orowan Criterion

Julius Langenberg\*, Victoria Brinnel\*\*, Sebastian Münstermann\*\*\*

\*RWTH Aachen University, \*\*RWTH Aachen University, \*\*\*RWTH Aachen University

### ABSTRACT

Traditional design rules are hindering the usage of High-Strength Low-Alloy steels (HSLA) in constructions. Numerical studies performed by (1) on a modified Gurson-Tvergaard-Needleman model (GTN), prove that HSLA steels offer huge ductile resources. Yet, ductile as well as brittle failure properties are important to characterize the mechanical behavior of HSLA steels. The pure GTN model however is unable to simulate cleavage fracture. The aim of the presented study was therefore to combine the GTN model with a suitable cleavage fracture model to provide a tool for modelling the full transition behavior. Combinations of Gurson and Beremin models are widely used to characterize cleavage fracture (2). The probabilistic Beremin model bases on a threshold stress integrated in a test volume. Therefore, it may only be applied as a postprocessor computation. A prediction of the inverse transition behavior of ductile failure and cleavage fracture is thus not possible. Additionally, most Beremin models are not taking any stress triaxialities and plastic strains into account. A possible solution for this is an extended Orowan cleavage fracture criterion as proposed by (3), which defines failure in dependence of critical stress- and strain states for a single element. Such a single element formulation enables a prediction of transition zone behavior using interactive online coupling for the cleavage fracture and ductile failure mechanism. So far, the extended Orowan criterion is not combined with any Gurson model. This study focuses on numerical modeling of the transition behavior of HSLA steels by extending a Gurson model with a modified Orowan criterion. The extended Orowan cleavage fracture model proposed by (3) will be summarized and an overview on its implementation into the GTN model is given. Moreover, an experimental calibration scheme as well as the influence of stress triaxialities and plastic strains on cleavage fracture are discussed. The developed formulation of the GTN model helps to characterize transition behavior of high-strength steels. Thus, this study supports the structural application of HSLA steels by considering their combined ductile failure and cleavage fracture properties in design.

References 1. Brinnel, Victoria. 2017. Improved Limit State Definitions for Pressure Vessels by a Scalebridging Application of Damage Mechanics. Aachen 2. Pineau, Andre. 2008. Modeling ductile to brittle fracture transition in steels -micromechanical and physical challenges. International Journal of Fracture. 150: 129-156 3. He, Jinshan; Lian, Junhe; Golisch, Georg; Jie, Xiaodong; Münstermann, Sebastian. 2017. A generalized Orowan model for cleavage fracture. Engineering Fracture Mechanics. 186: 105-118

## Meshing Images with OOF3D

Stephen Langer\*, Andrew Reid\*\*

\*NIST, \*\*NIST

### ABSTRACT

The OOF project [1] at NIST develops software for analyzing materials with complex microstructures, starting with real or simulated micrographs. The OOF2 program reads and analyzes two dimensional micrographs, while OOF3D works in three dimensions. In both cases, the OOF user assigns continuum material properties to features in a micrograph, creates a finite element mesh, and performs virtual experiments on the mesh. An important step in the process is to match the finite element mesh to the microstructural geometry given by the micrograph. The crucial cpu-intensive part of matching the mesh is to compute the homogeneity of each element: the degree to which the 2D pixels or 3D voxels inside the element all have the same material properties. This requires the computation of the area or volume of the intersection of an element with a conglomeration of pixels or voxels (treating each pixel or voxel independently is too slow). In 2D this calculation is relatively straightforward, but in 3D it is complex and fraught with subtleties. If done incorrectly, microscopic round-off errors in the calculation of the position of an intersection can lead to macroscopically wrong answers. A new technique, based on Powell and Abel's "3d" graph clipping algorithm [2] is fast and robust. The boundary of a voxel set is represented by a planar graph, and the graph is clipped sequentially by each face plane of a finite element. The method depends only on the topology of the voxel set and round-off errors only lead to small changes in the final volume. I will discuss the algorithm, how to construct the graph efficiently, and modifications to the algorithm to handle concavities in the voxel set. [1] <http://www.ctcms.nist.gov/oof> [2] D. Powell and T. Abel, "An exact general remeshing scheme applied to physically conservative voxelization", *Journal of Computational Physics* 297 (2015) 340–356.

## Some Statistical Properties of the Frequency Response Functions of Random Systems

Robin Langley\*

\*University of Cambridge UK

### ABSTRACT

Professor Soize has made seminal contributions to the theory of random structures, and this paper considers some of the properties of the frequency response functions (FRFs) of such systems. Initially the properties of causal complex frequency response functions are discussed, and it is shown that under certain conditions these functions obey the Analytical Ergodicity (AE) condition, in that the average value of a function of the FRF is equal to the value of the function when evaluated using the average value of the FRF. This property can be used to derive simple expressions for power input to complex systems. Attention is then turned to the statistical properties of the energy FRFs of built-up systems. It is shown that by combining Statistical Energy Analysis (SEA) with random vibration theory, expressions can be obtained for the mean rate (as a function of frequency) at which an energy FRF crosses a critical level. Results are also derived for the probability that the FRF will cross a critical level at least once over a prescribed frequency range. The same analysis leads to results for the mean number of peaks in the FRF over a specified frequency range, and for the mean trough-to-peak height. The latter results are useful for auralisation (i.e. sound reconstruction) when using SEA: the averaging employed in SEA removed all detail from an FRF, and the present results provide metrics that should be met when reconstructing this detail.

## Meshfree Partition of Unity Radial Basis Function Methods

Elisabeth Larsson<sup>\*</sup>, Victor Shcherbakov<sup>\*\*</sup>, Alfa Heryudono<sup>\*\*\*</sup>

<sup>\*</sup>Uppsala University, <sup>\*\*</sup>Uppsala University, <sup>\*\*\*</sup>University of Massachusetts Dartmouth

### ABSTRACT

In this talk, we present how to build on radial basis function (RBF) approximation to obtain a numerical method for PDE solving that is high order accurate, numerically robust, and computationally efficient. Global RBF methods are too expensive for large scale problems, so the first step in achieving computational efficiency is to localize the approximations. We use a partition of unity approach, where local RBF approximations on overlapping patches are combined into a global approximation. Radial basis function methods are in general counted as meshfree methods, but there can still be sensitivity to the node layout. We avoid this by letting each patch have an identical optimized node layout. This introduces nodes outside of the computational domain, but we then use oversampling within the computational domain, and in the end perform a least squares fitting of the problem. This final ingredient also provides the numerical robustness for large scale problems.

## **A Two-scale Modeling Framework for Fracturing Solids Based on Smearred Macro-to-Micro Transitions of Discontinuities**

Fredrik Larsson\*, Erik Svenning\*\*, Martin Fagerström\*\*\*

\*Chalmers University of Technology, \*\*Chalmers University of Technology, \*\*\*Chalmers University of Technology

### **ABSTRACT**

In computational homogenization of solids, the effective response can be obtained from underlying simulations on, e.g., Statistical Volume Elements (SVEs). Although standard nowadays, such an approach leads to poor results when strain localization and fracture occurs in the material. Remedies to this problem exists in the literature, however, the proposed approaches all tend to focus on particular choices of constitutive models on the microscale. In the present work, we aim to circumvent the need for explicit fine-scale discontinuity tracking by developing a two-scale scheme for fracturing solids, where the eXtended Finite Element Method (XFEM) is chosen for representation of the macroscale discontinuities, see [1]. The formulation, which is based on Variationally Consistent Homogenization (VCH), leads to a weak problem of finding the (possibly discontinuous) displacement field. The macroscale weak equilibrium equations contains, in addition to the standard bulk contribution, a term of cohesive zone type and a novel correction term. The macroscale discontinuities are imposed on the microscale SVEs using weakly periodic boundary conditions that are aligned to the macroscale localization direction. A key feature is that the smearing width employed in the discontinuity transitions is related to the SVE size used for the fine scale analysis at the effective discontinuity. By combining the smeared discontinuity transitions with the strict ellipticity condition, we obtain a modeling framework that can be employed without restrictive assumptions on the constitutive models employed on the microscale. Numerical investigations are presented in two spatial dimensions. In particular, it is noted that the method does not result in pathological dependence on macroscale mesh-size, nor on the size of the SVE. References [1] E Svenning, F Larsson and M Fagerström: Two-scale modeling of fracturing solids using a smeared macro-to-micro discontinuity transition. Computational Mechanics 2017: 627–641.

## DEM-CFD Simulation of the Effect of Air on Powder Flow During Die Filling

Simon Larsson<sup>\*</sup>, Gustaf Gustafsson<sup>\*\*</sup>, Pär Jonsén<sup>\*\*\*</sup>, Hans-Åke Häggblad<sup>\*\*\*\*</sup>

<sup>\*</sup>Luleå University of Technology, <sup>\*\*</sup>Luleå University of Technology, <sup>\*\*\*</sup>Luleå University of Technology, <sup>\*\*\*\*</sup>Luleå University of Technology

### ABSTRACT

In the field of powder metallurgy (PM), complex components with complicated shapes can be manufactured. One important step in the PM process is the powder pressing process, where powder is consolidated during a forming operation into a desired shape, normally by applying pressure. During powder pressing, the mechanical properties of powder materials change dramatically. PM manufacturers tend to produce components with shapes of increasing complexity, requiring improved pressing equipment and methods. The most crucial aspect is to control the powder flow during die filling and the final powder density distribution after the filling stage, which has been shown to affect the strength of the final component significantly [1]. To investigate the non-homogeneity of the density of PM components, experimental studies combined with numerical simulations of the die filling stage are exploited. This work covers the numerical modelling and simulation of die filling. The discrete element method (DEM) [2] was used to model the powder, and computational fluid dynamics (CFD) to model the air. To study the effect of air on powder flow, the DEM was coupled to the CFD using a two-way coupling approach. Experimental measurements with digital speckle photography (DSP) from a previous study [3] were used for comparison with the numerical simulations. The comparison of the DSP measurements and the numerical simulations showed similar macroscopic flow characteristics. Thus, the adequacy of the proposed DEM-CFD model has been demonstrated in a metal powder die filling operation. The DEM-CFD method has been shown to be an effective method for the numerical simulation of the interaction between powder and air. References [1] Zenger, D. & Cai, H. (1997). Handbook of the Common Cracks in Green P/M Compacts. Metal Powder Industries Federation, MPIF. Worcester, USA. [2] Cundall, P. A., & Strack, O. D. (1979). A discrete numerical model for granular assemblies. *geotechnique*, 29(1), 47-65. [3] Larsson, S., Gustafsson, G., Jonsén, P. & Häggblad, H.-Å. (2016). Study of Powder Filling Using Experimental and Numerical Methods. In: World PM2016 Congress & Exhibition, Hamburg, October 9-13, 2016.

## Modelling of Red and White Thrombus Formation in Intracranial Aneurysms after Flow Diversion

Toni Lassila<sup>\*</sup>, Ali Sarrami-Foroushani<sup>\*\*</sup>, Mostafa Hejazi<sup>\*\*\*</sup>, Alejandro Frangi<sup>\*\*\*\*</sup>

<sup>\*</sup>University of Sheffield, <sup>\*\*</sup>University of Sheffield, <sup>\*\*\*</sup>University of Sheffield, <sup>\*\*\*\*</sup>University of Sheffield

### ABSTRACT

Treatment of intracranial aneurysms with flow-diverting stents is a highly successful minimally invasive technique. It typically results in the stable embolisation, endothelialisation, and complete elimination of the aneurysm. Computational fluid dynamics simulation of post-operative flow reduction inside the aneurysm has shown utility in predicting whether or not the procedure will be successful. However, in some cases the aneurysm fails to develop a stable clot or recurs even when sufficient levels of flow reduction are attained. It is not fully understood why some aneurysms fail to develop a stable clot. We believe that computational prediction of thrombus formation dynamics can help predict the post-operative response in these challenging cases. In this work, we propose a new model of thrombus formation inside intracranial aneurysms (Sarrami-Foroushani et al. 2018) that builds on previously proposed models of haemostatic thrombosis at the site of vascular injury (Wu et al., 2017). Our novel contributions are: 1) the initiation mechanism, where we modelled post-operative flow stasis as the thrombosis initiator, and 2) the combination of platelet activation and transport models with fibrin generation models that are key in characterising stable and unstable thrombus. The model is based on post-mortem observations of two types of thrombus inside aneurysms: red thrombus (erythrocyte- and fibrin-rich) can be found in unstable clots, while white thrombus (fibrin- and platelet-rich) can be found in stable clots. The thrombus generation model is coupled to 3-D CFD model developed in ANSYS CFX. The coupled flow and thrombus formation model is simulated until a steady state is reached, after which point the quality of the resulting thrombus is evaluated as a combination of platelet content and fibrin concentration within the aneurysm. Computational predictions of thrombus quality are validated against two idealised flow diversion scenarios. The first is an in vitro phantom study (Gester et al. 2016) of two flow-diverting stents with different sizings. We demonstrate that our model accurately predicts the lower thrombus stability that results in the oversized stent scenario. The second validation study explores the behaviour of the proposed thrombus quality indicator in a range of idealised sidewall aneurysms with variable aspect ratio and diameter. References Sarrami-Foroushani A, et al. A mathematical model of thrombus formation in intracranial aneurysms, *Biomech. Model. Mechanobiol.*, submitted, 2018 Wu, WT, et al. Multi-constituent simulation of thrombus deposition. *Sci.Rep.* 7: 42720, 2017 Gester K, et al. In vitro evaluation of intra-aneurysmal, flow-diverter-induced thrombus formation: a feasibility study. *Am. J. Neuroradiol.* 37.3:490-496, 2016

## Time-Independent Formulations for Growth and Remodeling of Soft Tissues

Marcos Latorre<sup>\*</sup>, Jay Humphrey<sup>\*\*</sup>

<sup>\*</sup>Yale University, <sup>\*\*</sup>Yale University

### ABSTRACT

Most biological soft tissues exhibit a remarkable ability to adapt to sustained changes in mechanical loads. These macroscale adaptations, including growth (changes in mass) and remodeling (changes in microstructure), are important determinants of physiological behaviors at a systems level and thus clinical outcomes. Necessarily, growth and remodeling (G&R) processes are time dependent due to the finite periods needed for material to be synthesized, deposited, degraded, and/or reorganized. Moreover, because soft tissues appear to have some material “memory” during G&R, hereditary integral formulations [1], as commonly used in viscoelasticity, have proven useful in describing and predicting evolving responses of soft tissues under diverse conditions. As frequently done in many areas of mathematical physics, however, these time-dependent models can be specialized to respective time-independent formulations that provide tremendous simplification and yet considerable insight. We present a new time-independent approach for modeling the evolution of soft tissue G&R [2] that arises from a general constrained mixture model. We discuss the mathematical conditions, in terms of ratios of characteristic times of tissue responses and external loading, that yield the particularized formulation. In these cases, integral-type evolution equations can be written in terms of an equivalent set of time-independent, algebraic nonlinear equations that can be solved efficiently. We show that the simplified theory captures well the predictions of a fully general constrained mixture theory at a fraction of the computational expense for problems defined by particular characteristic times. Additionally, with the present pre-integrated model at hand, we compute exactly the long-term outcomes of G&R processes in response to sustained external stimuli following a direct approach. The present formulation plays parallel roles as in Fung’s theory of pseudoelasticity to better understand complex G&R of soft tissues, in general, and of arteries, in particular. Indeed, simplified formulations of this type can serve as efficient tools for studies of parameter sensitivity, uncertainty quantification, and optimization, which tend to be even more demanding computationally. Acknowledgements US NIH: R01 HL105297, U01 HL116323, R01 HL128602, R01 HL134712. Spain: CAS17/00068, DPI2015-69801-R. UPM: “Ayudas al personal docente e investigador para estancias breves en el extranjero 2017”. References [1] JD Humphrey, KR Rajagopal (2002). A constrained mixture model for growth and remodeling of soft tissues. *Math Models Methods Appl Sci*, 12, 407-430. [2] M Latorre, JD Humphrey. Critical Roles of Time-Scales in Modeling Soft Tissue Growth and Remodeling. Invited. Under review.

## **Micropolar Crystal Plasticity Finite Element Models with Grain Shape Effects on Slip Resistance**

Marat Latypov<sup>\*</sup>, Jason Mayeur<sup>\*\*</sup>, Irene Beyerlein<sup>\*\*\*</sup>

<sup>\*</sup>University of California Santa Barbara, <sup>\*\*</sup>CFD Research Corporation, <sup>\*\*\*</sup>University of California Santa Barbara

### **ABSTRACT**

Emerging manufacturing routes for advanced materials (such as additive manufacturing) often result in complex microstructures at the mesoscopic length scale. These complex microstructures with features (e.g., grains) far from equiaxed shapes require advanced modeling approaches. In this contribution, we present size-dependent crystal plasticity finite element framework that explicitly accounts for grain shape effects. The intrinsic length scale and size dependence are captured at the single crystal constitutive level by the micropolar theory. This subclass of micromorphic higher-order continuum theory considers lattice rotations as generalized displacements and incorporates couple stresses that lead to kinematic hardening of slip systems originating from gradients of lattice rotations. The grain shape effect is accounted for at two levels: (i) at the slip system level where slip resistance for each grain is calculated according to the chord length along the slip direction and (ii) at the finite element model level where the actual grain shapes are constructed. Potential applications of the proposed framework include improved predictions of effective yield strength or high-cycle fatigue crack initiation of polycrystals.

## Binding to Glutamate Receptors: Follow the Yellow Brick Road

Albert Lau<sup>\*</sup>, Alvin Yu<sup>\*\*</sup>, Hector Salazar<sup>\*\*\*</sup>, Andrew Plested<sup>\*\*\*\*</sup>

<sup>\*</sup>Johns Hopkins University School of Medicine, <sup>\*\*</sup>Johns Hopkins University School of Medicine, <sup>\*\*\*</sup>Humboldt University Berlin, <sup>\*\*\*\*</sup>Humboldt University Berlin

### ABSTRACT

Ionotropic glutamate receptors (iGluRs) mediate neurotransmission at the majority of excitatory synapses in the brain. Little is known, however, about how the neurotransmitter glutamate reaches the recessed binding pocket in iGluR ligand-binding domains (LBDs). Here we report the process of glutamate binding to a prototypical iGluR, GluA2, in atomistic detail using both enhanced sampling and unbiased molecular dynamics simulations. Charged residues on the LBD surface are found to form pathways that facilitate glutamate binding by effectively reducing a three-dimensional diffusion process to a spatially-constrained two-dimensional one. Free energy calculations identify residues that metastably interact with glutamate and help guide it into the binding pocket. These simulations also reveal that glutamate can bind in an inverted conformation and also reorient while in its pocket. Electrophysiological recordings demonstrate that eliminating these transient binding sites slows activation and deactivation, consistent with slower glutamate binding and unbinding. These results suggest that binding pathways have evolved to optimize rapid responses of GluA-type iGluRs at synapses.

## **An Atomistic Study of the Microstructure and Mechanical Properties in Bamboo under Uniaxial Tension**

Devnid Lau\*, Huali Han\*\*

\*City University of Hong Kong, \*\*City University of Hong Kong

### **ABSTRACT**

There is an increasing requirement for lightweight materials that are able to be served in engineering such as transportation, buildings, and energy storage and conversion. The natural materials of hierarchical structures have low density and outstanding mechanical properties inspiring us to design and fabricate bio-materials with unprecedented combinations of stiffness, strength and toughness at low density by replicating their structures [1]. In this work, the bamboo is used as the example to study the structure-properties relationship for the bio-material design because bamboo has a greater stiffness-to-weight and strength-to-weight ratio than that of common wood, cast iron, aluminum alloy and structural steel. According to the experimental characterization of the bamboo, the bamboo fibers that are resource of the mechanical properties have lamellar structures where the cellulose microfibrils are embedded in the matrix of lignin and hemicellulose [2]. The dynamic evolution of the modeled constituents under uniaxial tension is observed with the help of the molecular dynamics simulations to disclose the role of the basic constituents in the mechanical behavior of bamboo fibers. It is found that the cellulose mainly provides the strength and the matrix is responsible for the load transformation. The interfacial interaction between the cellulose and the matrix of hemicellulose and lignin is also studied. The interaction of different constituents combining with the molecular conformation evolution of the individual constituents during the deformation enables us to figure out the relationship between the microstructure and mechanical performance of bamboo fibers and to understand the critical structural features for the outstanding mechanical properties in the bamboo. Our work provides a guideline for the design of synthetic materials by replicating the structural characteristics of their natural counterparts. Moreover, the computation methods used in our work can also be worked as an efficient way to synthesize novel compounds with improved performance. [1] U G.K. Wegst, H. Bai, E. Saiz, A.P. Tomsia and R.O. Ritchie. Bioinspired structural materials. *Nature Materials*, 14 (2015) 23-36. [2] M.K. Habibi, L-H. Tam, D. Lau, Y. Lu. Viscoelastic damping behavior of the structural bamboo material and its microstructural origins. *Mechanics of Materials*, 97 (2016)184-198.

## Development of a Multiscale Computational Modeling Framework for the Tricuspid Valve – Linking Valvular Interstitial Cell Mechanobiology with Organ-Level Function

Devin Laurence<sup>\*</sup>, Yi Wu<sup>\*\*</sup>, Chung-Hao Lee<sup>\*\*\*</sup>

<sup>\*</sup>The University of Oklahoma, <sup>\*\*</sup>The University of Oklahoma, <sup>\*\*\*</sup>The University of Oklahoma

### ABSTRACT

The tricuspid valve (TV) is located in the right side of the heart and prevents the retrograde blood flow between the right ventricle and right atrium during systole. Functional tricuspid regurgitation (FTR) occurs when the TV's three leaflets are unable to fully close, causing an undesired backflow into the right atrium as the right ventricle contracts to move blood through the pulmonary vascular system. Approximately 1.6 million Americans are affected by FTR annually with only 8,000 undergoing surgical repair; furthermore, there exists a disappointing recurrence rate (~20%) of FTR 10 years after the initial repair.<sup>1,2</sup> Recent investigations have demonstrated and quantified the multiscale behavior of the mitral valve (MV) under both physiological and pathophysiological conditions,<sup>3</sup> but no such extensive investigation has been performed for the TV. In this work, we are developing a multiscale computational framework of the TV to provide insight into the underlying mechanisms behind TR initiation and progression, which contains three anatomical scales: the tissue-level, the downscale cellular microenvironment, and the organ-level. First, the tissue-level model is developed by considering the underlying constituents (extracellular matrix, collagen, and elastin), which is validated against previously acquired biaxial tension data to accurately capture tissue's anisotropic behaviors. Then, the tissue-level deformation is prescribed as boundary conditions to the downscale microenvironment model (containing the ECM and heterogeneously dispersed valvular interstitial cells (VICs)) to provide insight into the VIC mechanobiology. Finally, the information obtained from the tissue-level and microenvironment models is combined with realistic valve geometry and heterogeneous mapping of leaflet constituents (i.e., collagen, elastin, and VICs) in high-fidelity organ-level finite element simulations of the TV. Our preliminary investigations have demonstrated the VIC's interaction with the surrounding ECM, specifically the VIC cytoplasm's key function in transferring mechanical stimuli from the ECM to VIC nucleus. The ongoing development will facilitate patient-specific modeling of the TV in healthy, diseased, and repaired states. Moreover, the developed model can be extended to provide objective recommendations to surgeons for repair timing and individual-optimized therapy to significantly increase the repair longevity. Acknowledgments AHA SDG (16SDG27760143) for CHL; OU UROP (2018) and MRF (2017-2018) for DL. References [1] Stuge O, et al., JTSC (2006). [2] Ballazhi F., et al., TCS (2016). [3] Ayoub S., et al., JRSI (2017).

## Gradient-Enhanced Parametric Optimization of Vibro-Acoustic Problem Using Xfem and a Dedicated Metamodel

Luc Laurent\*, Antoine Legay\*\*

\*Laboratoire de Mécanique des Structures et des Systèmes Couplés, Conservatoire National des Arts et Métiers, case 2D6R10, 2 rue Conté, 75003 Paris, France, \*\*Laboratoire de Mécanique des Structures et des Systèmes Couplés, Conservatoire National des Arts et Métiers, case 2D6R10, 2 rue Conté, 75003 Paris, France

### ABSTRACT

Noise reduction is a design constraint which is more and more taken into account. For instance, this constraint occurs in aircraft cabin design on which the noise propagation is minimized by finding the optimal arrangement. Classical design processes require many expensive numerical computations. In order to reduce the computation time, a new strategy is proposed based on two specific tools integrated in a dedicated optimization strategy: (1) a finite element solver which provides responses and gradients of the objective function to (2) a gradient-enhanced metamodel which interpolates both kinds of information. Solving the mechanical problem remains to solve a coupled problem composed of structural and fluid domains. The acoustic fluid problem is governed by the Helmholtz's equation. A porous material present in the acoustic cavity is modeled by the Biot-Allard's constitutive law. The structural problem corresponds to thin walls placed in the fluid and governed by elasto-dynamics equation. The air-structure problem is solved using xfem in order to be able to consider an arbitrary structure placed in the acoustic cavity. In order to reduce the computation time, a reduced model is built from the full coupled problem using a Craig-Bampton's approach. In addition to the resolution of the coupled problem, the calculation of the gradients with respect to the design parameters is proposed by considering an intrusive approach. Due to the fact that design parameters govern only the position of the structure in the acoustic cavity, the calculation of the gradients requires only calculation of gradients of the xfem's operators which can be done analytically. The global optimization based on this mechanical problem requires a large number of calls of the mechanical solver. Therefore a gradient-enhanced surrogate-based optimization is used. The approach is based on the Efficient Global Optimization composed of two phases: (1) a gradient-enhanced cokriging metamodel is built using only a few sample points and associated responses and gradients and (2) an iterative scheme using the expected improvement allows us to find the global minimum by adding smartly new sample points to the initial surrogate model. The whole strategy has been applied on some 2D and 3D cavity on which the position of a wall is determined in order to minimize the mean quadratic pressure in a control volume. Some examples will be presented for illustrating the performance of the proposed approach.

## Multilevel Monte Carlo for Inverse Problems

Kody Law\*

\*University of Manchester

### ABSTRACT

Uncertainty is recently becoming a requisite consideration in complex applications which have been classically treated deterministically. This has led to an increasing interest in recent years in uncertainty quantification (UQ). Another recent trend is the explosion of available data. Bayesian inference provides a principled and well-defined approach to the integration of data into an a priori known distribution. The posterior distribution, however, is known only point-wise (possibly with an intractable likelihood) and up to a normalizing constant. Monte Carlo methods have been designed to sample such distributions, such as Markov chain Monte Carlo (MCMC) and sequential Monte Carlo (SMC) samplers. Recently, the multilevel Monte Carlo (MLMC) framework has been extended to some of these cases, so that approximation error can be optimally balanced with statistical sampling error, and ultimately the Bayesian inverse problem can be solved for the same asymptotic cost as solving the deterministic forward problem. This talk will concern the recent development of multilevel Monte Carlo methods for inverse problems and data assimilation in the context of complex engineering applications. This class of algorithms are expected to become prevalent in the age of increasingly parallel emerging architecture, where resilience and reduced data movement will be crucial algorithmic considerations.

## ARCHITECTURAL LAYOUT DESIGN FOR RAILWAY STATION PLATFORMS TO MITIGATE PASSENGER HAZARD RISK DUE TO TERRORIST EXPLOSIONS

VIVIAN LAWRENCE\*, SAKDIRAT KAEWUNRUEN<sup>†</sup>, AND CHARALAMPOS BANIOTOPOULOS<sup>†</sup>

\* School of Engineering, The University of Birmingham  
52 Pritchatts Road  
Edgbaston B152TT United Kingdom  
Email address; VJL693@student.bham.ac.uk;

<sup>†</sup> School of Engineering, The University of Birmingham  
52 Pritchatts Road  
Edgbaston B152TT United Kingdom  
Email addresses: s.kaewunruen@bham.ac.uk (S. Kaewunruen); C.Baniotopoulos@bham.ac.uk (C. Baniotopoulos)

**Key words:** Passenger safety, explosive blast, physical and cyber threats, hazard risk, railway systems, platform layout design; layout optimization.

**Abstract.** The first priority in operating transportation and transit systems is public safety. Generally, operators are expected highly to assure the reliable and safe day-to-day journeys of public transports. However, based on recent factual evidences, extreme physical and cyber threats are no longer uncommon and these unpreventable measures are even more dangerous to the public's daily lives. Such clear examples are the terrorist attacks in Saint Petersburg in 2017, in London in 2017, in Stockholm in 2017, in Brussels in 2016, in Nice in 2016, and so many more. These examples have one thing in common. The transportation and transit system hubs are the clear target: either on rail, bus, car or truck, etc. This research establishes a novel and innovative development and optimization of architectural layout design on the railway platform in order to improve safety, manage risks, and mitigate uncertainties where perspectives from the humanities and the operations are fully considered. Computational multi-physics simulations have been used to simulate blast effects from terrorist attacks at a railway platform. Birmingham Grand Central railway station has been selected for case study modelling using LS-Dyna. A platform layout design as structural wave barriers has been used to illustrate the hazard risk mitigation for train passengers due to explosive blast pressures. The reflected air blast from a simulated terrorist bomb has been calculated using LS-Dyna CFD in comparison with the US Army guideline. The new insight will guide a new platform layout design to minimize damage and hazard risks to rail passengers. This research aligns with United Nation's Sustainable Development by creating novel engineering solutions enabling a safer built environment.

# 1 INTRODUCTION

Since the 1970's, terrorist attacks in Western Europe have remained a constant threat [1]. The number of attacks and fatalities can be seen in Figure 1. Therefore, it is of paramount importance to consider blast attack resistance in all design processes of new built environments and the assessment of existing ones in order to mitigate risks and minimise hazards to the public. To put the physical and cyber threats into context, areas of high importance and potential targets include train stations, airports, shopping centres, sport stadiums, malls, concert halls and theatres. In other words, anywhere that could have a large number of casualties or have a detrimental effect on transport and infrastructure networks or the economy [2].

There are currently no official standards governing the testing or specification of blast-resistant structures in Eurocodes [3]. However, there are accepted technical manuals for blast-resistant design, including but not limited to:

- EN 1990: Eurocode - Basis of structural design
- GSA-TS01-2003: US General Services Administration Standard Test Method for Glazing and Window Systems Subject to Dynamic Overpressure Loadings
- ASTM F2912 – 11: Standard Specification for Glazing and Glazing Systems Subject to Air blast
- UFC 3-340-02: Structures to resist the effects of accidental explosions.

Railway assets are a critical infrastructure that requires active monitoring and protection against man-made hazards (such as terrorist attack, severe vandalism, derailments, and human errors). The loading actions and design criteria are complex in nature with strict considerations for systemic and sub-systemic compatibility [3-7]. With the active engagement in overseas military missions, Europe's critical infrastructures remain at high risk of terrorist attack, especially at crowded railway stations as shown in Figure 2. Based on a critical literature review, most studies into blast effects are focussed on the damage on built environments or on building structures. In fact, the impact on passengers or human responses, especially at railway platforms, has not been thoroughly investigated. In this study, we pioneer a novel and innovative development in re-designing and optimising the railway platform layout in order to minimise blast damage to railway passengers. This type of development is highly in significant demand in this modernised but conflicted world.

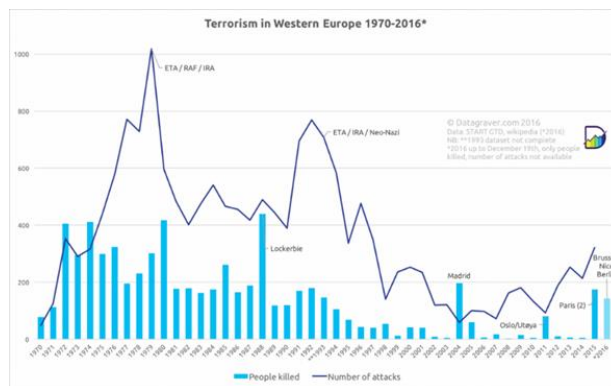


**Fig.1:** Terrorism in Western Europe [1]



**Figure2:** Birmingham Grand Central Station

It is important to note that only high explosives will be considered as a terrorist threat within this research project. The high explosives are often in solid form. TNT is used as a universal reference point for determining a scaled distance from the blast wave source, by converting the charge mass of an explosive into the equivalent mass of TNT. This is done by multiplying the charge mass by a conversion factor derived from the specific energy and charge mass of TNT [8].

An explosion is defined as a sudden release of energy, dissipated as shock waves, projecting missiles and thermal radiation [9]. The detonation of high explosives generates hot gases and high pressures, which rapidly expands, compressing a layer of air and forming a shock wave [10]. As shown in Figure 3, the shock wave instantaneously increases the surrounding pressure above ambient atmospheric pressure,  $P_o$ , to peak pressure,  $P_{so}$ . This deteriorates as the shockwaves expand outwards from the epicentre [11]. Once the wave front has passed, after a short period of time, the pressure may drop below the ambient air pressure, producing a partial vacuum. This, together with suction winds, can carry debris for long distances away from the centre of the explosion [11]. Pape et al. [10] also explains that the overpressure, which is any pressure above ambient atmospheric pressure, tapers off and goes below ambient pressure, later returning to equilibrium. It can also be seen in Figure 3 that the area of positive pressure is called the 'positive phase' and the area of negative pressure is called the 'negative phase'. Both the positive and negative phases can contribute to causing damage. The time-pressure curve seen in Figure 3 can usually be approximated using Friendlander's equation, seen in Eq.1:

$$p(t) = p_s \cdot \left(1 - \frac{t}{t_0}\right) \exp\left(-\frac{bt}{t_0}\right) \quad (1)$$

There are 3 types of explosion: unconfined explosions, confined explosions and explosions attached to the structure [12]. Unconfined explosions are categorised into two types; an air-burst and a surface-burst, which create shock waves that interact in different ways. Surface-bursts are often the most common type of burst when it comes to terrorist activities, as they usually occur in built-up areas, where devices are placed on or close to the ground surface [12]. Only a surface-burst will be considered for purposes of this study. A surface-burst is when detonation occurs on the near the ground surface, causing initial shockwaves to be immediately reflected and

amplified by the ground surface, forming a single wave front, from both the initial and reflected shockwaves [13-14].

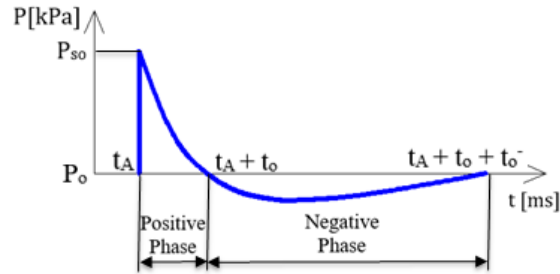


**Fig.3:** Shockwave pressure progression [6]

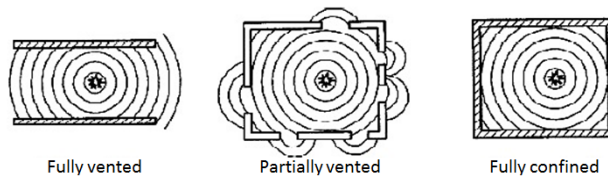


**Fig.4:** Degree of confinement [12]

The effects of an explosion inside a structure will need to be considered, which will depend on the degree of confinement, which in turn depends on the location of a blast. A confined explosion occurs where the initial peak pressures are very high, enhanced by refraction within the structure [13]. Examples of degrees of confinement can be seen below in Figure 4. Other factors that affect the amount of damage inflicted will include ventilation, temperatures, accumulation of gas pressure, blast characteristics, weight of the explosives and location of detonation [15].

## 2 RAILWAY STATION MODELLING

Birmingham Grand Central railway station has been re-developed and opened for multi-purpose uses in September 2015. As illustrated in Figure 5, Grand Central underwent a major overhaul as part of the New Street Station Gateway Plus redevelopment. The mall has been redesigned with a glass atrium roof as centrepiece, and is home to over 60 stores across 500,000 ft<sup>2</sup>. Many of the shops, restaurants and cafés are creating very vibrant and extremely crowded malls that are fully integrated to one of the UK busiest rail hubs, with 12 train platforms.

In this study, the chosen platform is an island platform with a width of 16m. There are several structural columns situated 12m apart. The columns are 3m high and 1m wide. Fig .6 shows the finite element modelling of the platform. Two types of blast protective barriers have been installed in the simulation at a symmetrical distance in order to measure the comparable impact. The meshing optimization was used to suit the analysis purpose [16-20]. The platform and columns are to be modelled as reinforced concrete. The function `CONSTRAINED_LAGRANGE_IN_SOLID` is a validated solution to model the rebar within the concrete mesh. The concrete material uses the function `MAT_CSCM_CONCRETE`. Through which C32/40 concrete properties are imputed. The rebar and steel barriers are both defined to be

MAT\_PLASTIC\_KINEMATIC. Transverse rebar is 16 millimetres diameter; longitudinal rebar is 10 millimetres diameter. The steel properties of the barrier are shown in Table 1.

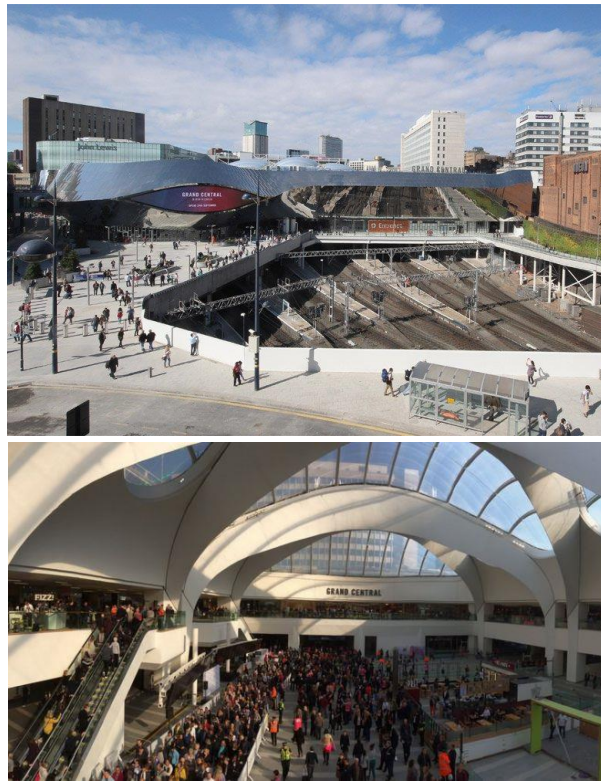


**Figure 5:** Birmingham Grand Central Station

**Table 1:** Steel Properties

Property	Value	Unit
Mass Density	7850	kg/m <sup>3</sup>
Young's Modulus	2.1 x 10 <sup>5</sup>	MPa
Poisson's Ratio	0.3	
Yield Stress	400	MPa

### 3 EXPLOSIVE BLAST MODELLING

The platform, one scenario of terrorist attacks is simulated, both using 15kg of TNT.

- The bomb is placed in a bag and left on the floor of the platform (0m above G.L).

The barrier design and orientations from the previous study were used [21], as shown in Fig. 6. LS-DYNA software was used to simulate the air blast created from TNT. LS-DYNA has an empirical function LOAD\_BLAST\_ENHANCED which computes to a high degree of calibration, the pressure exerted on a Lagrangian structure from an air blast. LS-DYNA calculates pressure by measuring the distance from segment to charge, and the angle of incidence from the segments normal. To identify the blast load criticality, the document Unified Facilities Criteria (UFC), Structures to Resist the Effects of Accidental Explosions [5] has been reviewed.

$$Z = \frac{R}{\sqrt[3]{W}} \quad (2)$$

where  $R$  is the distance between the point of the detonation and the structure,  $W$  is the weight of the charge.

The scaled distance is computed. `LOAD_BLAST_ENHANCED` uses both of these variables at every cycle to calculate the pressure. The pressure can also be calculated by hand using this formula to validate the pressure computed by LS-DYNA. `LOAD_BLAST_ENHANCED` enables the blast to be located at any point throughout the model. The function can allow for four different types of blast shape. This research uses the hemispherical blast with reflected waves, as well as a free air blast with reflective waves. The model was created through LS-DYNA Prepost and is based on Birmingham New Street Station as shown in Figure 6. The floor slab and roof slab were made completely rigid to simulate a blast underground.

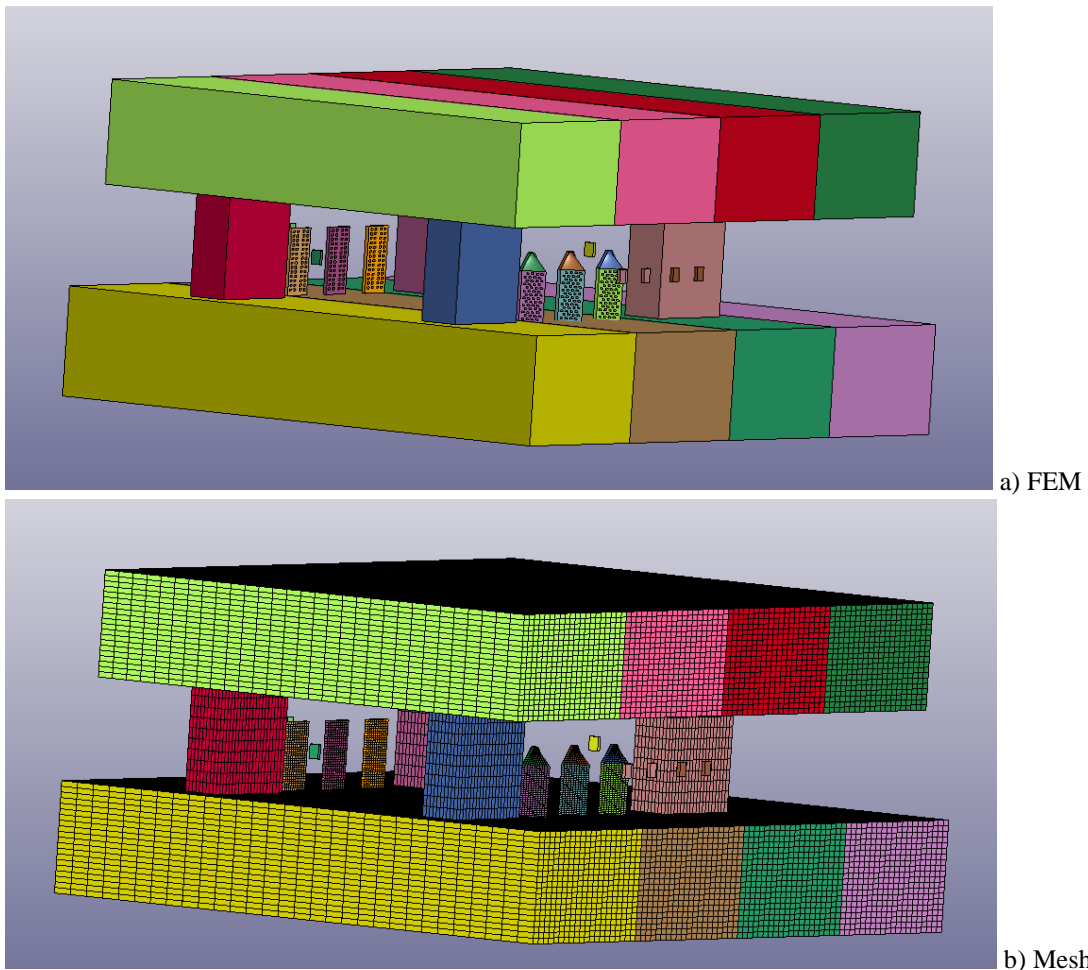


**Fig.6:** Platform modelling with blast protective barriers

The architectural barrier layout arrangements are presented in Figure 7. It can be seen that the different arrangements have been setup to evaluate the hazard risks to the rail passengers measured by sensors (at locations that affect human).

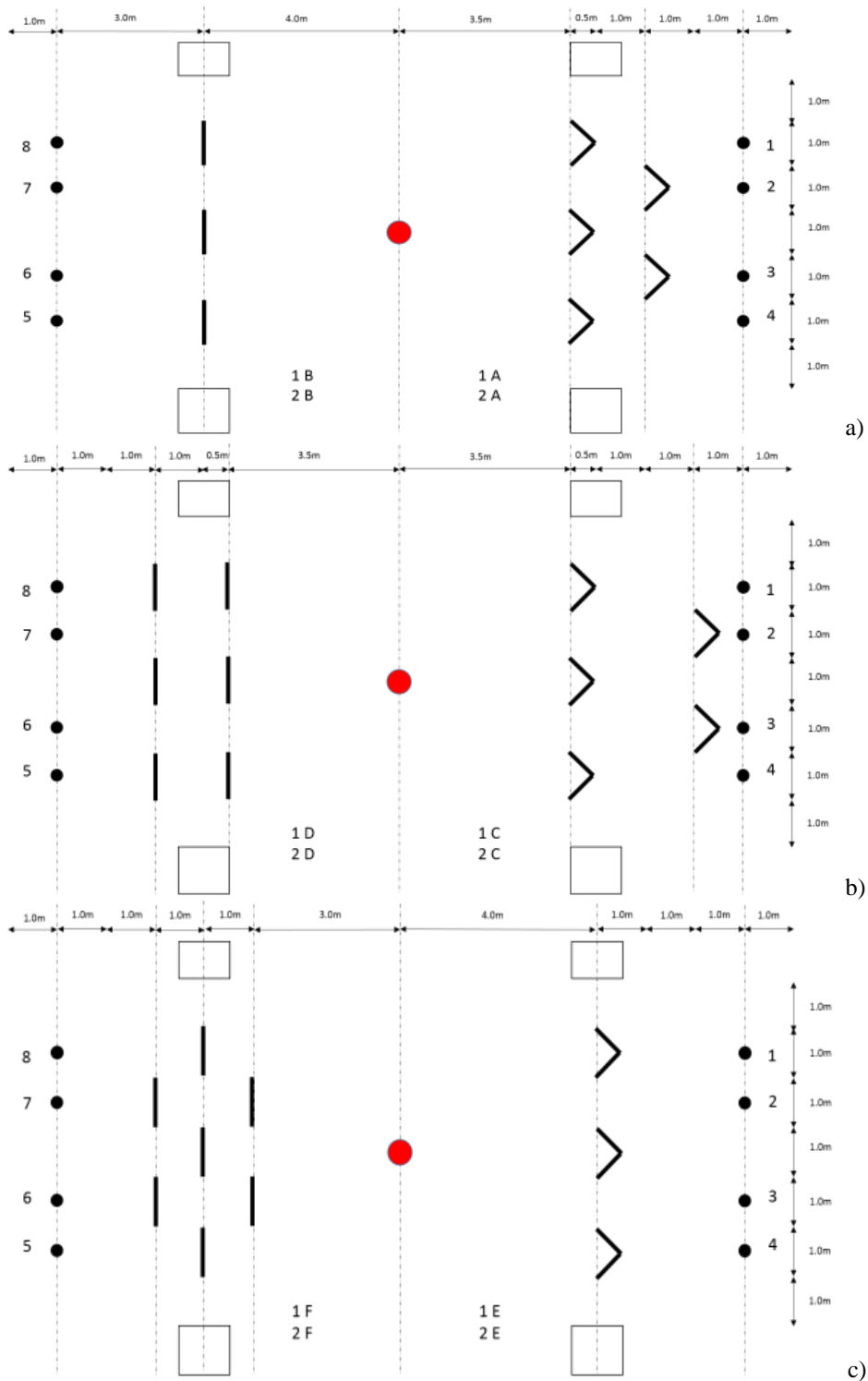


**Figure 7:** Layout optimization of architectural blast protective barriers

## 4 RESULTS AND DISCUSSION

Table 2 shows the pressure on the sensors due to near surface blast. When comparing the control sensor values with arrangements 1B and 1E the two central sensors have an increased pressure. The increased pressure is caused by the blast pressure reflecting and intensifying as it is transmitted through the barriers. It is noted that the flow of a shock wave expands directly after the barrier gap, resulting in the velocity of the wave intensifying [22]. The two external sensors of both arrangements were predicted to act the same due to the findings of recent study [21]. Concluding that the shape of the barriers placed in identical orientation has minimal effect on mitigating the blast wave. It is also concluded that a blast wave travels over a barrier, reforming a reduced pressure wave on the other side.

**Table 2:** Near surface blast pressure (kPa)

Sensor Number	1A	1B	1C	1D	1E	1F
1 & 8	254	289	238	248	289	211
2 & 7	279	339	276	315	339	237
3 & 6	279	339	276	315	339	237
4 & 5	266	305	250	261	305	221

Arrangement 1A and 1C were created to investigate this conclusion. Arrangement 1C is the same orientation as 1A but the barriers have a greater distance between them. From the results 1C reduced the overall pressure of the blast wave. The two external sensors of 1C both have a decreased pressure of 16 KPa than 1A. As found by [22], the reformed blast wave travels a longer distance until reaching the second row of barriers. Within this distance the wave is dissipating, thus reducing in force. However, the two central sensors show a very minimal decrease in pressure. The cause of both outcomes is as a result of the shape of the transmitted shock wave. As demonstrated in [22] the peak of a transmitted shock wave is created at the centre point between two barriers. The remaining transmitted wave travels in a ‘close to’ hemispherical shape, depending on the angular degree of barrier shape.

1C allows for the transmitted blast wave to dissipate and reduce more, before impacting the external sensors. The peak transmitted blast wave travels identically in both 1A and 1C resulting in minimal reduction at the central sensors. Arrangement 1F insured the two most vulnerable sensors (central) were protected from the peak transmitted blast wave. 1F increased the number and density of the barriers. Comparing the results with the other arrangements, 1F has significantly decreased the pressure over all sensors.

## 5 CONCLUSION

The safety in and within public transport is significantly paramount to every society globally. This study aligns with United Nation’s Sustainable Development by creating novel engineering solutions enabling a safer built environment. The project develops architectural layout design for protective blast barriers to mitigate primary and secondary dangers to train passengers and commuters at a railway platform. Considering recent factual evidences, extreme physical and cyber threats are no longer uncommon and these protective measures could be adopted to prevent damage and improve safety of the public’s daily lives.

Computational multi-physics simulations using LS-Dyna have been used to simulate blast effects from terrorist attacks at a railway platform. Birmingham Grand Central railway station has been selected for case study. A platform layout design as structural wave barriers has been used to illustrate the hazard risk mitigation for train passengers due to explosive blast pressures. The numerical three-dimensional simulations are in excellent agreement with empirical estimates developed by US Army. This study reveals that the layout of blast barriers does have an impact on the reduction of blast pressure. Increasing the amount of barriers between the explosion and target can increase the chance of survival. The results show that layouts 1F and 2F both had very successful effects compared with other layouts. In addition, this study is the first to demonstrate that the shape of the barrier provides minimal effect on the mitigation of blast pressure to rail passengers. The new insight will guide a new platform layout design to minimize damage and hazard risks to rail passengers.

## **ACKNOWLEDGEMENT**

The second author wishes to thank the Australian Academy of Science and Japan Society for the Promotion of Sciences for his Invitation Research Fellowship (Long term), Grant No. JSPS-L15701 at the Railway Technical Research Institute and The University of Tokyo, Tokyo Japan. The authors wish to gratefully acknowledge the financial support from European Commission for H2020-MSCA-RISE Project No. 691135 “RISEN: Rail Infrastructure Systems Engineering Network,” which enables a global research network that tackles the grand challenges in railway infrastructure resilience and advanced sensing under extreme events ([www.risen2rail.eu](http://www.risen2rail.eu)).

## **REFERENCES**

- [1] DataGraver, People killed by terrorism per year in western europe 1970-2015. [online]. Available from: <http://www.datagraver.com/case/people-killed-by-terrorism-per-year-in-western-europe-1970-2015> [Accessed 5 December 2016] (2016)
- [2] Remennikov, A. and Carolan, D., “Building vulnerability design against terrorist attacks.” In Stewart, M. and Dockrill, B. (1st ed.) Proceedings of the Australian Structural Engineering Conference 2005. Australia: Tour Hosts Pty Ltd. pp. 1-10, (2005).
- [3] Larcher, M., Arrigoni, M., Bedon, C., Van Doormaal, J. C. A. M., Haberacker, C., Hüsken, G., Millon, O., Saarenheimo, A., Solomos, G., Thamie, L., Valsamos, G., Williams, A. and Stolz, A., Design of blast-loaded glazing windows and façades: a review of essential requirements towards standardization. *Advances in Civil Engineering*, 1-14, (2016).
- [4] Kaewunruen, S., Sussman, J. M., and Matsumoto, A. Grand challenges in transportation and transit systems. *Frontiers in Built Environments*, 2:4, (2016) doi:10.3389/fbuil.2016.00004
- [5] Unified Facilities Criteria (UFC), Structures to Resist the Effects of Accidental Explosions, U. S. Army Corps of Engineers, Naval Facilities Engineering Command, Air Force Civil Engineer Support Agency, UFC 3-340-02, 5 December (2008).
- [6] Kaewunruen, S., Pompeo, G., Bartoli, G., “Blast simulations and transient responses of long-span glass roof structures: A case of London's railway station”, Proceedings of the 25th UKACM Conference on Computational Mechanics, 12–13 April 2017, University of Birmingham, Birmingham, U.K., (2017).

- [7] United States DoD. "UFC 3-340-02: Structures to resist the effects of accidental explosions". Washington D.C.: US Department of Defense (USDOD), (2008).
- [8] Draganić, H. and Sigmund, V., Blast loading on structures. *Technical Gazette*, 19 (3): 643-652, (2012).
- [9] Kinney, G. and Graham, K., Explosive shocks in air. 2nd ed. New York: Springer, (1985).
- [10] Pape, R., Mniszewski, K. R. and Longinow, A. "Explosion phenomena and effects of explosions on structures i: phenomena and effects". *Practice Periodical on Structural Design and Construction*, 15 (2): 135-140., (2010).
- [11] Ngo, T., Mendis, P., Gupta, A. and Ramsay, J. Blast loading and blast effects on structures – an overview. *EJSE Special Issue: Loading on Structures*, 2007: 76-91, (2007).
- [12] Koccaz, Z., Sutcu, F. and Torunbalci, N., Architectural and structural design for blast resistant buildings. The 14th World Conference on Earthquake Engineering. [online]. Available from: [http://www.iitk.ac.in/nicee/wcee/article/14\\_05-01-0536.PDF](http://www.iitk.ac.in/nicee/wcee/article/14_05-01-0536.PDF) [Accessed 5 December 2016]
- [13] Mali, P., Lokare, S. and Chitra, V. Effect of blast loading on reinforced concrete structures. *International Journal of Scientific Engineering Research*, 5 (12): 14-16, (2014).
- [14] Remennikov, A.M., Kaewunruen, S., A review on loading conditions for railway track structures due to wheel and rail vertical interactions. *Structural Control and Health Monitoring*, 15(2): 207-234, (2008).
- [15] Lawrence, V., Ngamkhanong, C., Kaewunruen, S. "An investigation to optimize the layout of protective blast barriers using finite element modelling", *International Conference on Mechanical Engineering*, 19-21 October 2017, University of Birmingham, Birmingham, U.K., (2017).
- [16] Griffin, D.W.P., Mirza, O., Kwok, K., and Kaewunruen, S., "Finite element modelling of modular precast composites for railway track support structure: A battle to save Sydney Harbour Bridge", *Australian Journal of Structural Engineering* 16 (2), 150-168, (2014).
- [17] Remennikov, A.M., "A review of methods for predicting bomb blast effects on buildings", *Journal of Battlefield Technology* 6 (3), 5, (2003).
- [18] Remennikov, AM and Kaewunruen, S, Simulating shock loads in railway track environments: experimental studies, *Proceedings of 14th International Congress on Sound and Vibration*, Cairns, Australia, 9-12 July 2007. Copyright 2007 Australian Acoustics Society, Australia, (2007).
- [19] Kaewunruen, S and Remennikov, AM, "An Experimental Evaluation of the Attenuation Effect of Rail Pad on Flexural Behaviour of Railway Concrete Sleeper under Severe Impact Loads." In E. F. Gad & B. Wong (Eds.), *Proceedings of the 2008 Australasian Structural Engineering Conference (ASEC)* (p. [10]), Melbourne, Australia, June 26-27, (2008).
- [20] Kaewunruen, S and Remennikov, AM, "Experimental simulation of the railway ballast by resilient materials and its verification by modal testing", *Experimental Techniques* 32 (4), 29-35, (2008).
- [21] Hajek R and Foglar M *Structures Under Shock and Impact XIII* **141** 265-275, (2015).
- [22] Berger S, Ben-Dor G. and Sadot O. *Journal of Fluids Engineering* **137** 41203-1-41203-11, (2015).

## Mesoscale Finite Element Modeling of Concrete Materials

William Lawrimore<sup>\*</sup>, Jameson.d.shannon@usace.army.mil Shannon<sup>\*\*</sup>, Mei Chandler<sup>\*\*\*</sup>,  
Stephen Akers<sup>\*\*\*\*</sup>, Charles Burchfield<sup>\*\*\*\*\*</sup>, Zackery McClelland<sup>\*\*\*\*\*</sup>, Robert Moser<sup>\*\*\*\*\*</sup>

<sup>\*</sup>US. Army Engineer Research and Development Center, <sup>\*\*</sup>US. Army Engineer Research and Development Center,  
<sup>\*\*\*</sup>US. Army Engineer Research and Development Center, <sup>\*\*\*\*</sup>US. Army Engineer Research and Development  
Center, <sup>\*\*\*\*\*</sup>US. Army Engineer Research and Development Center, <sup>\*\*\*\*\*</sup>US. Army Engineer Research and  
Development Center, <sup>\*\*\*\*\*</sup>US. Army Engineer Research and Development Center

### ABSTRACT

The topological complexity of concrete materials has been a barrier against the development of a high fidelity computational modeling methodology with which to analyze them. Hierarchical multiscale modeling methods have shown remarkable capacity to enhance the computational analyses in other material genomes. As a part of the multiscale hierarchy, this work is focused on efforts to model concrete materials at the mesoscale in order to harvest crucial deformation mechanism information to be used at higher scales in the multiscale modeling hierarchy. Two approaches using idealized topological representations of concrete are demonstrated herein. The first approach simplifies aggregate inclusions to be spherical within a cementitious matrix where the size distribution of the aggregate is prescribed from experimental data and the virtual topologies are built using the Virtual Composite Structure Generator (VCSG) method. The second approach utilizes microstructure data generated from the Virtual Cement and Concrete Testing Lab (VCCTL) as a source from which a voxel mesh is built for mesoscale finite element analysis. Both approaches feature Interface Transition Zones (ITZ) between the aggregate and cement matrix. Results from each approach are compared and discussed.

## Rate and Size Effects on Dynamic Tensile Strength of Quasibrittle Structures

Jia-Liang Le<sup>\*</sup>, Anna Gorgogianni<sup>\*\*</sup>, Josh Vievering<sup>\*\*\*</sup>, Jan Elias<sup>\*\*\*\*</sup>

<sup>\*</sup>University of Minnesota, <sup>\*\*</sup>University of Minnesota, <sup>\*\*\*</sup>University of Minnesota, <sup>\*\*\*\*</sup>Brno University of Technology

### ABSTRACT

In this study, we develop a rate-dependent finite weakest-link model of strength statistics of quasibrittle structures. The model involves a length scale influenced by the applied strain rate, which captures the transition from localized damage to diffused damage as the strain rate increases. The present model predicts that the probability distribution of the nominal tensile strength depends on both the specimen size and the strain rate. At low strain rates, the strength distribution varies from a predominantly Gaussian distribution to a Weibull distribution as the specimen size increases, whereas at high strain rates the strength distribution follows a Gaussian distribution and its variance decreases with an increasing specimen size. In parallel with analytical modeling, a set of stochastic simulations is performed to study the dynamic tensile fracture of aluminum nitride (AlN) specimens. The simulations use a stochastic discrete element model (DEM), which explicitly takes into account the randomness of both the microstructural geometry and the fracture properties of AlN. In the DEM, the fracture behavior of the grain boundary is described by a mixed-mode failure model, in which the tensile and shear strengths and mode-I and mode-II fracture energies are considered to follow some prescribed probability distributions. The dynamic equilibrium equations are solved by the implicit Newmark method. The model is applied to simulate the nominal tensile strengths of geometrically similar AlN square plates of different sizes subjected to a range of strain rates. The simulations indicate that, as the applied strain rate increases, the size dependence of the mean structural strength diminishes while the coefficient of variation (CoV) of the strength exhibits a strong size effect. This simulated rate dependence agrees well with the prediction by the rate-dependent finite weakest-link model. The rate and size effects on strength distribution have important implications for stochastic simulations of dynamic quasibrittle fracture.

## **A Force Treatment of Immersed Boundary Method for Light-weighted Structures Interacting with Fluids**

Trung Le\*

\*Medical College of Wisconsin

### **ABSTRACT**

Performing Fluid-Structure Interaction with immersed boundary method at high Reynolds numbers is challenging due to the spurious force oscillation (SFO) phenomenon on the fluid-solid interface. In this work, we present a new development of enforcing the incompressibility condition on the fluid-solid interface so that the SFO is limited. The application of the method is in the hydrokinetic turbine application. The hydrokinetic blade is simulated with a thin-walled beam model, which is derived for variable cross-section structures. The beam model does not require any priori definition of cross-sectional warping but compute it directly from the final solution. The deformation pattern is superimposed on the bending deformation described by Euler-Bernoulli beam theory. Due to the combination between the beam and finite element assumptions, all sectional properties are automatically incorporated in the analysis when the final system of equations is assembled. The resulted model is suitable to simulate the dynamics of wind/hydrokinetic turbine blade with low computational cost under the fluid-structure interaction (FSI) simulation. A number of test cases have been carried out to validate the structural model which shows good agreement between the computational results and analytical solutions. Finally, FSI simulation of a hydrokinetic blade under critical flow condition is carried out to exemplify the capability of the current FSI model in practice.

## State Health Monitoring of High-speed Train Suspensions by Bayesian Calibration Based on Gaussian Surrogate Modeling

David Lebel<sup>\*</sup>, Christian Soize<sup>\*\*</sup>, Guillaume Perrin<sup>\*\*\*</sup>, Christine Fünfschilling<sup>\*\*\*\*</sup>

<sup>\*</sup>Université Paris-Est, <sup>\*\*</sup>Université Paris-Est, <sup>\*\*\*</sup>CEA, <sup>\*\*\*\*</sup>SNCF

### ABSTRACT

The work presented here deals with the development of a state health monitoring method for high-speed train suspensions using in-service measurements by embedded accelerometers. Mathematically, it consists in solving a statistical inverse problem. A rolling train is a dynamic system excited by the track geometric irregularities. They consist of small displacements of the rails relatively to the theoretical track design. The suspension elements play a key role for the ride safety and comfort. The train dynamic response being dependent on the suspensions mechanical characteristics, information about the suspensions state can be inferred from acceleration measurements in the train. This information would allow for providing a more efficient maintenance. Track geometry is subject to damage caused by railway traffic and to maintenance operations. Consequently, it evolves through time. Because of the high sensitivity of the train dynamic response to the track geometric irregularities, their evolution must be taken into account through the use of train dynamics simulation. Because the system input (the track geometric irregularities) and output (the train dynamic response) are stochastic quantities, the inverse problem is solved in the Bayesian framework. The monitoring method thus consists in performing a Bayesian calibration of a simulation-based model using joint measurements of the system input and output. Its objective is to identify the posterior distribution of the model parameters describing the suspensions mechanical characteristics. Classical Bayesian calibration implies the computation of a likelihood function using a stochastic model and experimental data. This likelihood function is then used to estimate the posterior distribution of the model parameters. This step can be performed by Markov Chain Monte Carlo (MCMC) algorithms, which require numerous calls to the likelihood function. If the latter is expensive to compute, it may result in unaffordable computational costs, which is the case here. To address this issue, we propose to rely on surrogate models. They are usually used to provide an algebraic approximation of the system output. However, in the present case, the output is functional, which makes a surrogate model difficult to build. Instead, we propose a calibration method based on a Gaussian surrogate model of the scalar likelihood function. We present how such a random surrogate model can be used to estimate the model parameters distribution, how the new uncertainty it introduces can be taken into account to correctly evaluate the calibration accuracy, and the results of the method applied to our railway monitoring case.

## Numerical Modeling of the Propagation of Planar 3D Hydraulic Fracture in Material with Anisotropic Toughness

Brice Lecampion\*, Haseeb Zia\*\*

\*EPFL, \*\*EPFL

### ABSTRACT

Sedimentary rocks often exhibit a transverse isotropy due to fine scale layering. We investigate numerically the effect of the anisotropy of fracture toughness on the propagation of a planar 3D hydraulic fracture perpendicular to the isotropy plane: a configuration commonly encountered in sedimentary basins. We extend a fully implicit level set scheme for the simulation of hydraulic fracture growth to the case of anisotropic fracture toughness. We derive an analytical solution for the propagation of an elliptical hydraulic fracture in the toughness dominated regime - a shape which results from a particular form of toughness anisotropy. The developed numerical solver closely matches this solution as well as classical benchmarks for hydraulic fracture growth with isotropic toughness. We then quantify numerically the transition between the viscosity dominated propagation regime at early time -where the fracture grows radially- to the toughness dominated regime at large time where the fracture reaches an elliptical shape in the case of an elliptical anisotropy. The time scale at which the fracture starts to deviate from the radial shape and gets more elongated in the direction of lower toughness is in accordance with the viscosity to toughness transition time-scale for a radial fracture defined with the largest value of fracture toughness. Similarly, the toughness dominated regime is fully reached along the whole fracture front when the time gets significantly larger than the same transition time-scale defined with the lowest value of toughness. Using different toughness anisotropy functions, we also illustrate how the details of the complete variation of fracture toughness with propagation direction governs the final hydraulic fracture shape at large time. Our results highlight toughness anisotropy as a possible hydraulic fracture height containment mechanism as well as the need for its careful characterization beyond measurements in the sole material axes (divider and arrester) directions.

## **Elucidating Metal Powder Rheology via Discrete Element Simulations and Mechanically Stirred Powder Rheometry**

Jeremy Lechman<sup>\*</sup>, Dan Bolintineanu<sup>\*\*</sup>, Anne Grillet<sup>\*\*\*</sup>

<sup>\*</sup>Sandia National Laboratories, <sup>\*\*</sup>Sandia National Laboratories, <sup>\*\*\*</sup>Sanida National Laboratories

### **ABSTRACT**

Bulk solids composed of many discrete particles, i.e., grains and powders, are present in numerous engineering applications from mining to materials processing to energy storage to consumer products to food. In addition, particles are often added to materials to enhance their properties and subsequent performance in some fashion. Although particulate materials are ubiquitous, there remains a general lack of predictive understanding of their behavior; leading to a deficiency in effective, efficient control of the processing of such materials. At the core of this poor understanding is a shaky fundamental explanation of how the dynamics of individual particles, in ensemble, lead to the complicated dilative, yield stress, pressure dependent rheological behaviors of the bulk material. This challenge is particularly acute at low confining stresses for small, mildly cohesive particles. In this paper, we will present work to simulate, via the Discrete Element Method (DEM), the dynamics of individual particles of metal powders in a mechanically stirred powder rheometer. Our aim is to elucidate the connection between particle dynamics and powder rheology. In addition, we will assess the use of powder rheometry as a means of validating DEM models. Sandia National Laboratories is a multimission laboratory managed and operated by National Technology and Engineering Solutions of Sandia LLC, a wholly owned subsidiary of Honeywell International Inc. for the U.S. Department of Energy's National Nuclear Security Administration under contract DE-NA0003525.

## Primal Hybrid DG Finite Element Formulations for the Biot Consolidation Problem

Ismael Ledoino\*, Abimael Loula\*\*

\*LNCC/MCTIC, \*\*LNCC/MCTIC

### ABSTRACT

As a model problem we consider the linear Biot's consolidation problem in two space dimensions whose existence and uniqueness of solution are proved in [1]. It is well known that Finite element approximations for the Biot's consolidation problem based on the Continuous Galerkin method may present spurious oscillations in the pressure due to the incompressibility constraint on the displacement field in the beginning of the consolidation process, as analyzed in [2,3]. Some combinations of finite element interpolations, including equal order for both fields, are unstable due to the incompressibility constraint on the displacement field in the initial state, as analyzed in [2,3]. To gain more flexibility in the choice of stable finite element spaces and to improve stability and accuracy we propose here stabilized hybrid Discontinuous Galerkin finite element methods with Lagrange multipliers associated with the traces of the displacement and pore pressure fields. Stability of low order approximations are recovered including equal order for all fields. [1] A. Zenisek, The existence and uniqueness theorem in Biot's consolidation theory. *Aplik. Matem.*, 29 (1984), pp. 194-210. [2] M. A. Murad, A. F. D. Loula, Improved accuracy in finite element analysis of Biot's consolidation problema. *Comput. Methods Appl. Mech. Engrg.*, 95 (1992), pp. 359-382. [3] M. A. Murad, V. Thomee, A. F. D. Loula, Asymptotic Behavior of Semidiscrete Finite Element Approximations of Biot's Consolidation Problem. *SIAM Journal on Numerical Analysis*, Vol. 33, No. 3 (1996), pp. 1065-1083.

## Parallel Surface Mesh Adaptation for Manycore Architecture

Franck Ledoux<sup>\*</sup>, Hoby Rakotoarivelo<sup>\*\*</sup>, Franck Pommereau<sup>\*\*\*</sup>

<sup>\*</sup>CEA, DAM, <sup>\*\*</sup>CEA, DAM, <sup>\*\*\*</sup>IBISC, Université Paris-Saclay

### ABSTRACT

In this work, we design a dedicated process to adapt triangular meshes for the purpose of simulation codes on 3D CAD models in the HPC context where manycore architectures are used. Our technical contribution is to provide a standalone library that can be called from any C++ simulation code to adapt a surface mesh  $M$  while both preserving some surface geometric properties and taking into account some relevant data given by the simulation code. More precisely, the simulation code must give the expected number of points in the final mesh and either provide a scalar function  $F$  defined on the mesh  $M$  or directly specify the desired size and direction of elements everywhere in the computational domain. When function  $F$  is given, sizes and directions are derived from it. Formally, sizes and directions are encoded using a metric field that we will call a computational metric field. Another metric field, called geometric metric field, is used to represent surface properties. By combining computational and geometric metric fields, we drive the mesh adaptation process, which consists in iteratively applying several meshing kernels (edge swapping, triangle splitting, smoothing,) until getting the expected size and direction for each triangle on the surface. Several meshing techniques are used to achieve it: computational and geometric metric fields are intersected to preserve both the computational requirements and the surface geometry; gradation is computed to handle strong anisotropy; sharp features induce specific cases in each meshing kernel, ... In order to obtain good performances on modern manycore architectures, we follow a 3-steps schema for every kernel: (1) we build a task graph of the local operations that have to be done; (2) we extract an ordering set of independent tasks from this graph; (3) Extracted independent tasks are finally performed in parallel. Note that every step is done in a lock-free manner and the overhead induced by steps (1) and (2) is very low. Our solution has been tested and validated on different target architecture with up to several hundred of threads, different CAD models and input computational field. In practice good weak and strong scalings are obtained thanks to the 3-steps schema we apply and with dedicated mesh data structures.

## High-Dimensional Stochastic Sensitivity Analysis and Design Optimization for Dependent Random Variables

Dongjin Lee\*, Sharif Rahman\*\*

\*The University of Iowa, \*\*The University of Iowa

### ABSTRACT

Stochastic sensitivity analysis plays a central role in robust design optimization and reliability-based design optimization of complex systems. For calculating design sensitivities of a stochastic response of interest, the finite-difference method constitutes the most straightforward approach, but it mandates repeated stochastic analyses for different instances of design variables, rendering the method prohibitive for practical design optimization. The other prominent method, the score function method [1], has been used when the input random variables are independent with product-type probability measures, where both the stochastic response and its sensitivities are obtained from a single stochastic simulation. In reality, though, the random variables are often statistically dependent producing non-product-type probability measures, invalidating most available methods, including the existing score function method [1]. This paper presents a novel computational method for calculating design sensitivities of statistical moments and reliability of high-dimensional complex systems subject to dependent random variables with arbitrary, non-product-type probability measures. The method represents a novel integration of the referential dimensional decomposition (RDD) [2] of a multivariate stochastic response function and score functions adapted for dependent random variables. Applied to the statistical moments, the method provides mean-square convergent analytical expressions of design sensitivities of the first two moments of a stochastic response. For reliability analysis, the method exploits the combination of embedded Monte Carlo simulation of the RDD approximation and score functions. The statistical moments or failure probabilities and their design sensitivities are both determined concurrently from a single stochastic analysis or simulation. Numerical examples, including a 100-dimensional mathematical problem, indicate that the new method developed provides not only theoretically convergent, but also computationally efficient design sensitivities for dependent random variables. A practical example involving robust design optimization of a three-hole bracket illustrates the usefulness of the proposed method. [1] Rahman, S. and Ren, X., "Novel Computational Methods for High-Dimensional Stochastic Sensitivity Analysis," *International Journal for Numerical Methods in Engineering*, Vol. 98, 2014, pp. 881–916. [2] Rahman, S., "Approximation Errors in Truncated Dimensional Decompositions," *Mathematics of Computation*, Vol. 83, No. 290, 2014, pp. 2799-2819.

## Investigation of Transient Temperature of Pharmaceutical Tablets during Compaction Utilizing Infrared Thermography and Computational Modeling

Hwahsiung Lee<sup>\*</sup>, Bereket Yohannes<sup>\*\*</sup>, Alberto Cuitino<sup>\*\*\*</sup>

<sup>\*</sup>Rutgers University, <sup>\*\*</sup>Rutgers University, <sup>\*\*\*</sup>Rutgers University

### ABSTRACT

Compaction of pharmaceutical tablets from powders is always accompanied by the conversion of irreversible mechanical work of compaction into heat. The heat is generated due to friction between powder particles, particles and the die wall, plastic deformation of particles, bonding, and other irreversible processes. The resulting temperature increase could significant effect tablet's performance including mechanical properties, disintegration times, and drug release profiles. Temperature rise can also affects physiochemical properties of the medicinal substances, including chemical stability, crystallinity and polymorphous state. The temperature increase in the powder during compaction is detrimental to heat sensitive APIs with low heat conductivity, such as most organic materials used in pharmaceutical formulations. Therefore, it is important to understand the thermomechanical behavior of powders during compaction. Infrared thermography (IR) provides a useful tool to trace the temperature distribution evolution of the tablet surface after ejection from the tablet press in laboratory experiments but also during manufacturing, in particular as in-line process analytical technology (PAT) tool for quality control. In the present work, we show that utilizing infrared thermography as a nondestructive and noncontact PAT tool that allows accurate tablet surface temperature fields acquisition in real time to accuracy of  $\pm 0.1$  °C during tablet compaction. Heat transfer of particulate systems in pharmaceutical tablet manufacturing is important element to be considered, yet is not fully understood. In this study, we utilize computational tools based on particle-mechanics to describe the formation of networks during the consolidation process. These heterogeneous networks are subsequently used to simulate the heat transfer process after ejection. We demonstrate the computational modeling match well with experimental results from infrared measurement, which have not been previously reported.

## Unconditionally Energy Stable and High-Order Time Accurate Schemes for the Multi-Component System

Hyun Geun Lee<sup>\*</sup>, Jaemin Shin<sup>\*\*</sup>, June-Yub Lee<sup>\*\*\*</sup>

<sup>\*</sup>Kwangwoon University, <sup>\*\*</sup>Ewha Womans University, <sup>\*\*\*</sup>Ewha Womans University

### ABSTRACT

In contrast to the well-developed convex splitting schemes for gradient flows of two-component system, there were few efforts on applying the convex splitting idea to gradient flows of multi-component system, such as the vector-valued Cahn-Hilliard (vCH) equation. In the case of the vCH equation, one need consider not only the convex splitting idea but also a specific method to manage the partition of unity constraint (the sum of concentration fields must be unity) to design an unconditionally energy stable scheme. In this study, we propose a constrained convex splitting scheme for the vCH equation, which is based on a convex splitting of the energy functional for the vCH equation under the constraint. We show analytically that the scheme satisfies the constraint at the next time level for any time step thus is unconditionally energy stable. Note that the scheme is first-order accurate in time thus we extend it to high-order time accuracy by applying the recently developed scheme for gradient flows. We also show analytically that the high-order schemes are unconditionally energy stable. Numerical experiments are presented demonstrating the accuracy, energy stability, and efficiency of the proposed first-, second-, and third-order constrained convex splitting schemes.

## Verification and Validation of Bioprosthetic Heart Valve FSI Simulations

Jae Lee<sup>\*</sup>, Boyce Griffith<sup>\*\*</sup>, Alex Rygg<sup>\*\*\*</sup>, Brent Craven<sup>\*\*\*\*</sup>, Robert Hunt<sup>\*\*\*\*\*</sup>, Pierre-Yves Passaglia<sup>\*\*\*\*\*</sup>

<sup>\*</sup>University of North Carolina at Chapel Hill, <sup>\*\*</sup>University of North Carolina at Chapel Hill, <sup>\*\*\*</sup>U.S. Food and Drug Administration, <sup>\*\*\*\*</sup>U.S. Food and Drug Administration, <sup>\*\*\*\*\*</sup>University of North Carolina at Chapel Hill, <sup>\*\*\*\*\*</sup>University of North Carolina at Chapel Hill

### ABSTRACT

Every year, 300,000 heart valve repair/replacement procedures are performed worldwide in order to treat stenosis or regurgitation. This number continues to increase as these procedures become less invasive by using more transcatheter aortic valve replacement (TAVR) or by expanding access to cardiac surgery and interventional cardiology. Heart valves can be replaced with prosthetic or manufactured heart valves, but there are still difficulties with current prosthetic heart valves. Mechanical heart valves (MHVs) are durable but yield non-physical flow patterns that induce platelet activation, possibly causing other complications such as stroke, pulmonary embolism, or myocardial infarction. As a result, patients with MHVs need blood thinners for lifetime, which increases a risk of bleeding. Bioprosthetic heart valves (BHVs), which are made out of either bovine or porcine pericardium, are becoming increasingly popular because they yield hemodynamics flow patterns that are similar to the native valve, allowing patients to avoid complications from using MHVs. However, currently available BHVs require replacement after 10-15 years due to degradation of the tissue. A fluid-structure interaction (FSI) approach is necessary in modeling heart valves, which are thin elastic structures that interact with the blood flow. This presentation will describe ongoing work to develop computational models of prosthetic heart valve dynamics using extensions of the immersed boundary (IB) method. This work starts by evaluating the accuracy of the approach using benchmark problems associated with such modeling. The accuracy of the computational model is assessed by comparing with experimental measurements acquired in a left heart pulse duplicator system. This will ultimately lead to developing high-fidelity predictive models to perform simulations that can help answer challenging questions about optimal device performance, device selection, regulation for future cardiovascular devices, and surgical planning.

## **An Efficient Structural Optimization Strategy Based on a Parametric Reduced-Order Model Using the Selection and Interpolation of Substructural Modes**

Jaehun Lee<sup>\*</sup>, Maenghyo Cho<sup>\*\*</sup>

<sup>\*</sup>Kyungnam University, <sup>\*\*</sup>Seoul National University

### **ABSTRACT**

In this study, an efficient structural design optimization strategy is presented by combining the interpolation-based parametric reduced-order model (IB-PROM) with the component mode synthesis (CMS) in the finite element framework. In particular, to enhance the robustness of the IB-PROM combined with the CMS [1] for the structural design optimization, we employ a substructural mode selection method to the interpolation of the component mode. In general, for the ROMs that consist of off-line and on-line stages, the off-line sampling of a large-scale structure containing many parameters requires numerous computations to explore the parameter-dependency of a dynamical system. Therefore, we suggest to divide the structure into multiple subdomains to execute the sampling in the substructural level. Since one design variable does not usually change the whole mesh configuration of a structure, synchronizing design domains with substructures is possible, which should be done before the sampling. As a result, the computation time for sampling is greatly reduced compared with that using a full order model. For the CMS that is effective to solve the eigen-problem of a large-scale structure, we usually employ domain decomposition algorithms to divide the structure into nearly uniform substructures in size. Then we select a dominant substructural modes by the frequency cut-off method. However, the design variables of a large-scale system might not be uniformly distributed different from the subdomains divided automatically. Therefore, the substructural modes selected by the frequency cut-off might not be regarded as the optimum when we use the CMS to structural design problems. In addition, the selection of the important substructural mode can be changed depending on the value of the parameter. As a consequence, the ROM might lose its accuracy as the parameters vary over a wide range. Therefore, we employ the mode selection method to improve the accuracy of the ROM. Among the various mode selection methods, a moment matching-based method (CMS?, [2]) is applicable to the present method since it can be performed in near real-time. Numerical examples including the dynamic response optimization of large-scale system support the strength of the proposed method. [1] J. Lee and M. Cho, An interpolation-based parametric reduced order model combined with component mode synthesis, *Comput. Methods Appl. Mech. Engrg.*, Vol. 319, pp. 258-286, 2017. [2] B.-S. Liao, Z. Bai and W. Gao, The important modes of subsystems: A moment-matching approach, *Int. J. Numer. Meth. Engng.*, Vol. 70, pp. 1581-1597, 2007.

# COMPUTATIONAL ANALYSIS FOR DRY-ICE MIXED CO<sub>2</sub> JET IMPINGEMENT FLOW AND SUBLIMATION EFFECT

SONGMI KWAK\* and JAESEON LEE\*

\*Ulsan National Institute of Science Technologies (UNIST)  
Ulsan, S. Korea (ROK)  
JaeseonLee@unist.ac.kr

**Key words:** Jet impingement, carbon dioxide, sublimation, solid-gas multi-phase flow.

**Abstract.** The flow and heat transfer characteristics of a novel gas - solid two - phase impinging jet have been studied numerically. When the high pressure carbon dioxide (CO<sub>2</sub>) flow passes through a nozzle or orifice, it experiences the sudden expansion and the rapid temperature drop occurred by Joule-Thomson effect. This temperature drop causes the lower bulk jet fluid temperature than the CO<sub>2</sub> sublimation line, so dry-ice becomes formed. By using CO<sub>2</sub> gas-solid mixture as a working fluid of jet impingement, it is expected the heat transfer enhancement can be achieved due to the low bulk temperature and the additional phase change sublimation heat. In this study, 2D computational model is created to predict the cooling effect of gas-solid CO<sub>2</sub> jet. The gas-solid CO<sub>2</sub> flow is considered by Eulerian approach of mixed phase and the additional heat transfer module is embedded to account for the sublimation phenomena of the solid state CO<sub>2</sub>. The jet flow and heat transfer performance of gas-solid CO<sub>2</sub> jet is investigated by the variance of flow parameter like Reynolds number, solid phase concentration and jet geometries.

## 1 INTRODUCTION

An impinging jet is a flow in which a fluid accelerated through a nozzle or an orifice is projected onto a target surface. Such impinging jets can be used for a variety of engineering purposes, such as heating, cooling, drying or cleaning solid surfaces. This technique has been studied for decades in various heat transfer applications. Since high heat transfer rates can be obtained near the jet stagnation point, impinging jets are widely used in applications where tight area thermal management is required. Typical applications include processing glass or metal and cooling gas turbine or electronic components.

Numerous experimental and numerical studies of single-phase impinging jets have been performed and various methods to improve their heat transfer efficiency have been suggested. Caggese *et al.*<sup>1</sup> showed a change in the heat transfer enhancement of the confined jet with

varying nozzle spacing. The flow recirculation caused by a confined jet affects the wall jet flow streams over the target surface and the heat transfer performance. Behnia *et al.*<sup>2</sup> showed the differences in flow characteristics between confined and free jets.

Carbon dioxide has some advantages for impinging jet cooling process. First, carbon dioxide has a high Joule-Thomson coefficient. In the case of a gas jet, the source of the gas working fluid is generally in the form of a compressed gas in the vessel and the jet flow is generated by the pressure difference between this source and the environment. The pressurized gas expands over some steps and the state of gas is continuously changed during expansion. The final state of injected gas is affected by the condition of ambient, but it is obvious that the gas temperature should be changed during expansion. Especially the change of gas temperature in expansion process is related to Joule-Thomson coefficient. Due to the high Joule-Thomson coefficient of carbon dioxide, the temperature of injected carbon dioxide gas jet drops rapidly. Theoretically the temperature of carbon dioxide from highly pressurized source becomes lower than the sublimation temperature and solid carbon dioxide particle becomes to be formed. Thus, the created particle and cold carbon dioxide gas exits the nozzle and gas-solid mixture phase is made. If the gas-solid carbon dioxide mixture is used for impinging jet cooling and the jet is injected to ambient air, the temperature of ambient air and heat transfer from the target surface can cause the sublimation of solid carbon dioxide particles. Sublimation during jet cooling absorbs the heat energy and it may add the additional benefits of target surface of cooling. Recently, experimental studies have been reported to use these sublimation properties of carbon dioxide for cooling<sup>3-5</sup>.

In this study, jet impingement cooling with sublimation effect was investigated through computational analysis. There are two issues concerning numerical analysis of gas-solid multiphase flow including sublimation phenomena. One is a method for simulating a bulk gas-solid multiphase flow and the other is a method for simultaneously integrating a sublimation phenomenon to the bulk flow. To simulate the gas-solid mixture carbon dioxide jet, this study uses Euler-Euler method which considers solid particle flow as granular flow. This method assumes the solid particle phase as a kind of pseudo fluid. The method can simulate the bulk motion of solid particle flow but cannot show the state or condition of each individual particle in flow. Using Euler-Euler method, particle sublimation should be calculated by adjusting the phase fraction of particle flow in a cell. The rate of sublimation is assumed as the linear function of temperature. The Euler-Euler method is suitable for a relatively large number of solid particles in comparison to the volume of the gaseous phase. Considering the amount of dry ice that can be observed in high-pressure carbon dioxide jet experiments<sup>3</sup>, it seems to be the preferred approach

## 2 NUMERICAL STUDY

### 2.1 Eulerian multiphase slot jet model

Figure 1 shows the details of a 2-D single unconfined slot jet which is a computational domain of current study. Key boundary conditions are also shown in the figure. The nozzle width ( $w$ ) is 1 mm and the nozzle inlet condition is a velocity inlet. The origin of the coordinates is located at the center of the target heater block surface, and the  $x$  direction is set parallel to the surface of the heater block and the surrounding insulating material. The nozzle inlet conditions were 216.36 and 510 a, which is the result of carbon dioxide in the 5.5 MPa container first being depressurized by the regulator valve<sup>3</sup>. This temperature condition has already caused the sublimation of carbon dioxide and the nozzle inlet is a mixture of solid and gas. The jet cooling surface is a heated copper surface and the insulating material (G10) insulates everything but the jet exposed surface of the copper block. The properties of copper are  $\rho = 8978 \text{ kg/m}^3$ ,  $c_p = 381 \text{ J/kg} \cdot \text{K}$ ,  $k = 387.6 \text{ W/m} \cdot \text{K}$ . The properties of G10 are  $\rho =$

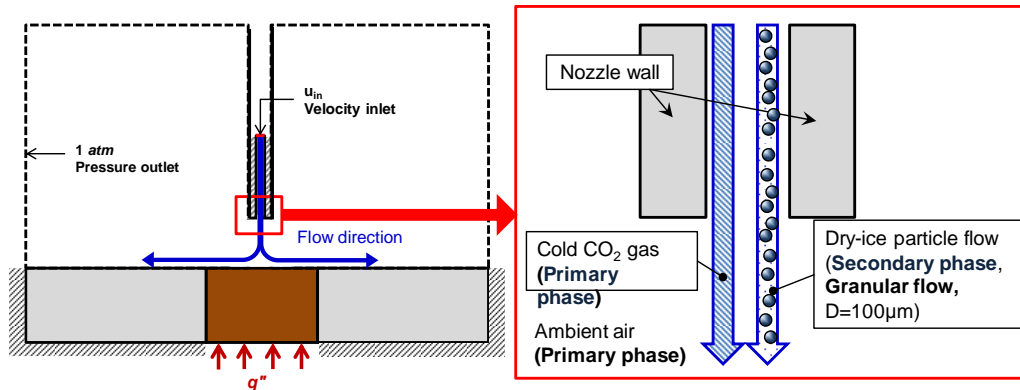


Figure 1 Details of boundary conditions and inlet flow for the linear sublimation model.

$1818 \text{ kg/m}^3$ ,  $c_p = 800 \text{ W/kg} \cdot \text{K}$  and  $k = 0.288 \text{ W/m} \cdot \text{K}$ . A constant heat flux is exerted on the bottom of the copper block. All the insulation surfaces that are not contact with jet flow are assumed to be adiabatic with a constant temperature. A species model is used to depict the carbon dioxide jet. As the jet is injected into the ambient air, a mixed gas state of carbon dioxide and air must be considered. The properties of the air are constant:  $\rho = 1.225 \text{ kg/m}^3$ ,

$c_p = 1006.43 \text{ J/kg} \cdot \text{K}$  and  $k = 0.0242 \text{ W/m} \cdot \text{K}$ .

Gas-phase carbon dioxide is considered as a compressible ideal gas. In the case of carbon dioxide, the gas properties are calculated using the ideal gas equation because the temperature and pressure changes are large. The properties of solid carbon dioxide (dry ice) are  $\rho =$

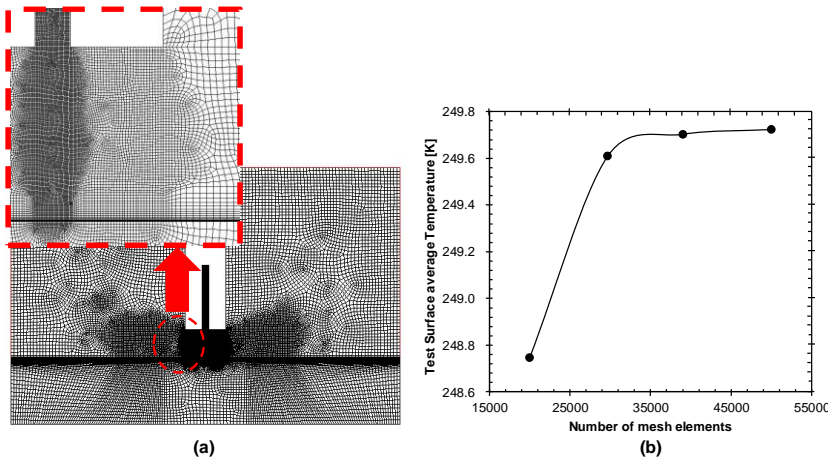


Figure 2 a Computational grid construction b Grid dependency test.

$1562 \text{ kg/m}^3$ ,  $c_p = 54.55 \text{ J/kg} \cdot \text{K}$  and  $k = 0.086 \text{ W/m} \cdot \text{K}$ .

A pressure-based steady solver using a coupled scheme for pressure-velocity coupling was applied and a second-order upwind scheme was used for the momentum, pressure, and energy equations. The realizable k- $\epsilon$  model was chosen for each gas phase turbulent flow model. A multiphase Eulerian model was chosen to account for the multiphase flow of mixed solid phase of carbon dioxide. The schematic of inlet flow and computational domain is described in Figure 1. The primary phase is the gaseous phase, the mixture of air and gas state carbon dioxide. The secondary phase is solid carbon dioxide (dry ice), a solid particle phase. There are few previous studies to quantitatively measure dry ice production by pressure and temperature drop. For this reason, it was assumed that the flow conditions at the nozzle inlet consisted of 90% carbon dioxide gas and 10% solid particulate carbon dioxide. The diameter of the carbon dioxide solid particles was also assumed to be a constant of 100 microns. This diameter is the size that can be observed with ordinary human eyes, and is considered a reasonable assumption based on experimental experience<sup>3</sup>.

The governing equations of the multiphase Eulerian model are summarized as follows<sup>6,7</sup>.

$$\frac{\partial}{\partial t}(\alpha\rho) + \nabla \cdot (\alpha\rho\vec{v}) = \frac{dm}{dt} \quad (2)$$

$$\frac{\partial}{\partial t}(\alpha\rho\vec{v}) + \nabla \cdot (\alpha\rho\vec{v}\vec{v}) = -\alpha\nabla p + \nabla \cdot \vec{\tau} + \alpha\rho\vec{g} + \vec{F} + \vec{R} \quad (3)$$

$$\frac{\partial}{\partial t}(\alpha_s\rho_s\vec{v}_s) + \nabla \cdot (\alpha_s\rho_s\vec{v}_s\vec{v}_s) = -\alpha_s\nabla p + \nabla p_s + \nabla \cdot \vec{\tau}_s + \alpha_s\rho_s\vec{g} + \vec{F}_s + \vec{R} \quad (4)$$

$$\vec{R} = K_s(\vec{v} - \vec{v}_s) \quad (5)$$

$$\frac{\partial}{\partial t}(\alpha\rho i) + \nabla \cdot (\alpha\rho\vec{v}i) = \alpha\frac{\partial p}{\partial t} + \vec{\tau}:\nabla\vec{v} - \nabla \cdot \vec{q} + \frac{dE}{dt} + Q \quad (6)$$

The continuity, momentum, and energy equations were solved for each phase.  $\vec{F}$  contains external body force, lift force, and wall lubrication force.  $\vec{R}$  is the phase interaction force that depends on the friction, pressure, cohesion, and other effects between phases. Equation (4) is the modified momentum equation for the solid phase and  $p_s$  is the solid pressure term. The phase interaction force term  $\vec{R}$  can be obtained by equation (5), where  $K_s$  is the interphase momentum exchange coefficient. The  $K_s$  value between the fluid and the solid phase is obtained by the Syamlal-O'Brien model<sup>18</sup>, which is already implemented in commercial CFD code FLUENT<sup>®</sup>. The  $Q$  and  $\frac{dE}{dt}$  terms of the energy conservation equation (6) represent the heat transfer amount between phases and the sublimation heat amount through sublimation, respectively. For the latter term, a more detailed description is provided in the next section. The multiphase Eulerian model recognizes that it is impossible for any phase to have both fluid and solid particle trajectories at the same time. The computational domain was constructed mainly with quadrilateral elements, as shown in Figure 2 (a). In the nozzle, core jet, and jet stagnation zones where complex flows exist, a finer grid is created. A fine grid was also added near the surface of the heater and the insulation where the wall jet flow was formed. Grid sensitivity tests were performed by examining the surface temperature of the heater block as the number of mesh elements increased. The average temperature of the block becomes almost constant when the number of mesh elements is above 40,000. Therefore, the current studies were conducted using a 40,000 elements quadrilateral grid.

## 2.2 Solid to gas phase change modeling

In conventional commercial CFD solvers, there is no way to analyze the phenomenon of phase change between gas and solid which is the main subject of this study. In this study, the internal code for considering the carbon dioxide sublimation process in the jet flow was embedded to the existing CFD solver. FLUENT<sup>®</sup>, the CFD solver used in this study, provides a melting and solidification module. The present sublimation model was applied in such a way that the melting and solidification model was modified by considering the physical exchanges in mass and energy during sublimation process. Because it was calculated by modifying the existing commercial code module, it is possible to use the existing variable name as it is in the explanation below (Ex.  $i_{liquid}$ ,  $i_{solid}$ , etc.). Among these parameters, the melting model parameters related to the liquid phase represent gas phase in the sense of the present study. The enthalpy of the material ( $i$ ) is calculated as the sum of the sensible enthalpy ( $i_s$ ) and the latent heat of sublimation material ( $I$ ).

$$i = i_s + I \quad (7)$$

$$i_s = i_{ref} + \int_{T_{ref}}^T c_p dT \quad (8)$$

$$I = \beta L \quad (9)$$

$\beta$  is the sublimation rate fraction and  $L$  is the latent heat.  $\beta$  is modeled to be varied by the material temperature in the mushy zone, which is the gas-solid two-phase region originated from the melting or solidification module<sup>6</sup>.  $\beta$  is defined as

$$\beta = 0 \quad \text{if } T < T_{solidus} \quad (10)$$

$$\beta = 1 \quad \text{if } T > T_{liquidus} \quad (11)$$

$$\beta = \frac{T - T_{solidus}}{T_{liquidus} - T_{solidus}} \quad \text{if } T_{solidus} \leq T \leq T_{liquidus}. \quad (12)$$

The sublimation rate is expected to vary depending on the difference between the dry ice particle and the ambient temperature. When the temperature increases, the sublimation rate also increases, but the rate will converge to a constant value. In this study, a simple carbon dioxide sublimation rate model is assumed. The assumption is that the sublimation rate is a linear function of temperature difference and all solid phase vanish when the environmental temperature becomes higher than the criterion temperature which is assumed as 10 higher than sublimation saturation temperature in this study. The setting of these 10 temperature differences in the current research phase is arbitrary. Since the sublimation heat is relatively small, it can be believed that the sublimation can be sufficiently completed within this setting value. However, it is a set value that needs to be supplemented through further future investigations.

$$\frac{dm}{dt} = -\frac{\rho \alpha_s}{\Delta} \frac{T - T_{sat}}{T_c - T_{sat}} \quad (13)$$

$$\frac{dE}{dt} = L_{CO2} \frac{dm}{dt} = -L_{CO2} \frac{\rho \alpha_s}{\Delta} \frac{T - T_{sat}}{T_c - T_{sat}} \quad (14)$$

$\Delta t$  is time step size of flow time for each individual cell and  $T_c$  is the criterion temperature at which the sublimation is finally completed.  $L_{CO_2}$  is the latent heat of sublimation of carbon dioxide (545 g at 194.67 ; Giauque<sup>9</sup>). From equation (13), the mass exchange rate is calculated in each cell. When the temperature of a solid carbon dioxide particle exceeds the criterion temperature, all the solid carbon dioxide particles in the cell are vanished. The equation for the rate of change of the energy is the product of the sublimation latent heat and the mass change rate. This equation plays an important role in the temperature change by adding the role of sublimation in the jet flow energy exchange with environment.

### 3 RESULTS OF ANALYSIS

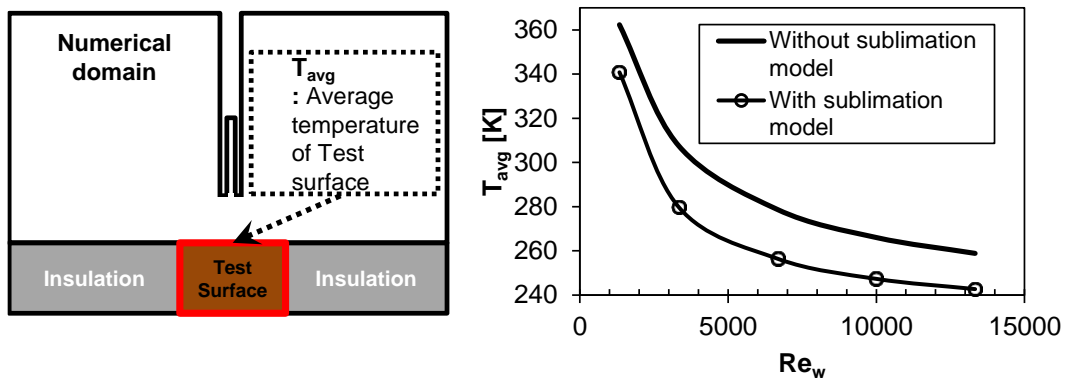


Figure 3 Average temperature of copper bloc test surface by the change of  $Re_w$   $q = 10 \text{ W}$ .

The distribution of the solid phase fraction of the jet flow varies greatly depending on whether the sublimation model is applied or not, and accordingly, the heat transfer characteristic changes. Reynolds number is used for the variable which describes inlet velocity and nozzle width is selected as characteristic length. Reynolds number ( $Re_w$ ) is defined as  $Re_w = \rho v w / \mu$  and  $v$  is velocity of inlet flow.  $\rho$  is density of gas phase and  $\mu$  is dynamic viscosity of gas phase. The different cases with  $Re_w$  variation from about 1,300 to 13,000 were analyzed and the results with and without applying the sublimation model were compared. Figure 3 shows the average change in temperature of the top surface of the heater block with variation in  $Re_w$ . A total heat of 10 W was applied to the heater. As in the case of the other jet flows, the surface temperature decreases as the Reynolds number increases. The analytical results with the sublimation model predict lower surface temperatures than those not included. The additional cooling effect by sublimation is effectively expressed in the results. It can be seen that the cooling effect for this sublimation is relatively weak at low Reynolds number flow. However, as the Reynolds number increases, a certain amount of sublimation cooling effect is maintained. Figure 4 shows the dry ice volume fraction and temperature distribution according to CFD analysis when the sublimation model is not applied. All the solid-phase carbon dioxide escapes from the computational domain of Fig. 4 without a large change in the volume fraction. The thickness of the solid phase volume fraction gradient becomes thinner as  $Re_w$  increases. Figure 4 (b) shows the temperature distribution with

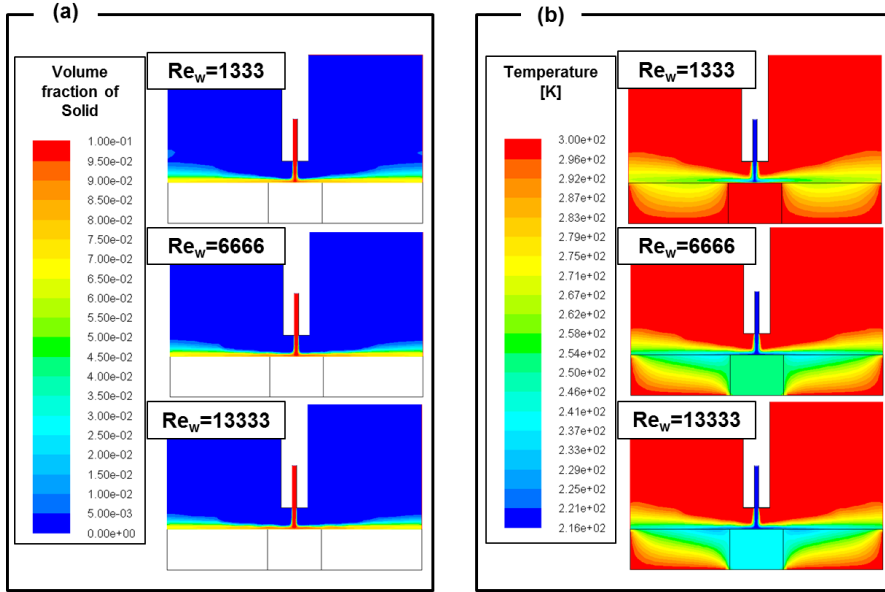


Figure 4 a Dry ice phase volume fraction contour variation and b Temperature distribution without the sublimation model.

variation in  $e_w$ . If the  $e_w$  is high due to the fast jet velocity, the jet flow will be kept cooler and the heater block will be maintained as colder temperature.

Figure 5 shows the results when the sublimation model is activated. The volume fraction of the solid carbon dioxide phase decreases when the solid carbon dioxide bulk temperature is

higher than the carbon dioxide saturation temperature in Figure 5 (a). Thus, application of the sublimation model changes the distribution of the solid phase volume fraction. In all cases, when the sublimation model is applied, the solid carbon dioxide phase disappears before reaching the domain outlet. As  $e_w$  increases, the point at which all the solid carbon dioxide phase disappears is delayed toward the downstream. The solid phase volume fraction contour

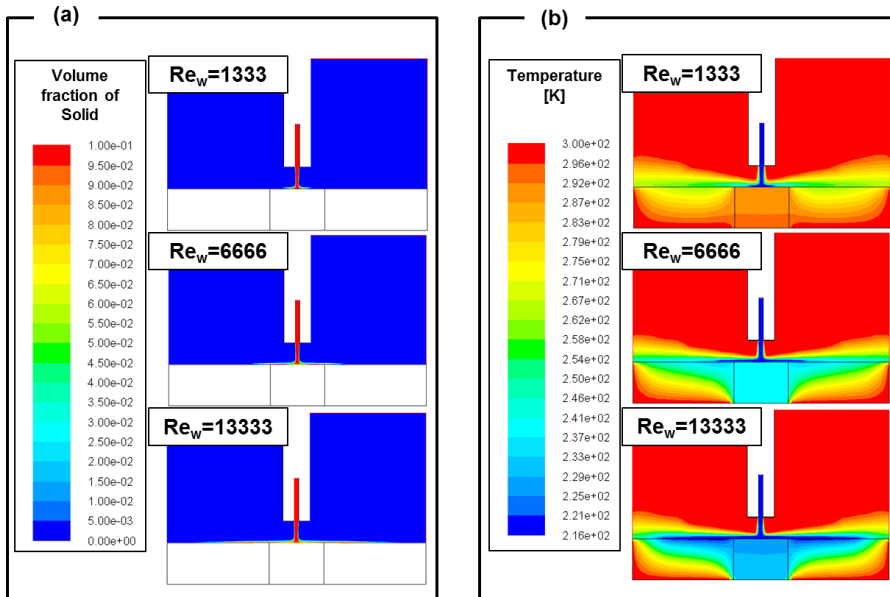


Figure 5 a Dry ice phase volume fraction contour variation and b Temperature distribution with the sublimation model.

almost coincides with the low temperature distribution of the temperature contour in Figure 5 (b).

The plots in figure 6 show the volume fraction of solid phase carbon dioxide along the x direction, which is the direction of the jet flow near the wall, and the y direction, which is the cross-sectional direction of the wall jet. The horizontal position of

the data is 0.5 mm above the test surface and figures 6 (a) and (b) show dry ice volume fraction variations when the sublimation model is not applied and when applied, respectively. The vertical location of the data is 2.5 mm from the center of the jet core and the vertical distribution results are represented in figure 6 (c). As all of the data are symmetrical with regard to the center of the jet core, the results represent only one side of the domain. The center of jet core represents the stagnation point of the impinging jet. When the sublimation model is not applied in the calculation, the volume fraction changes slightly along the  $x$  direction as shown in figure 6 (a). The reason that the volume fraction of solid carbon

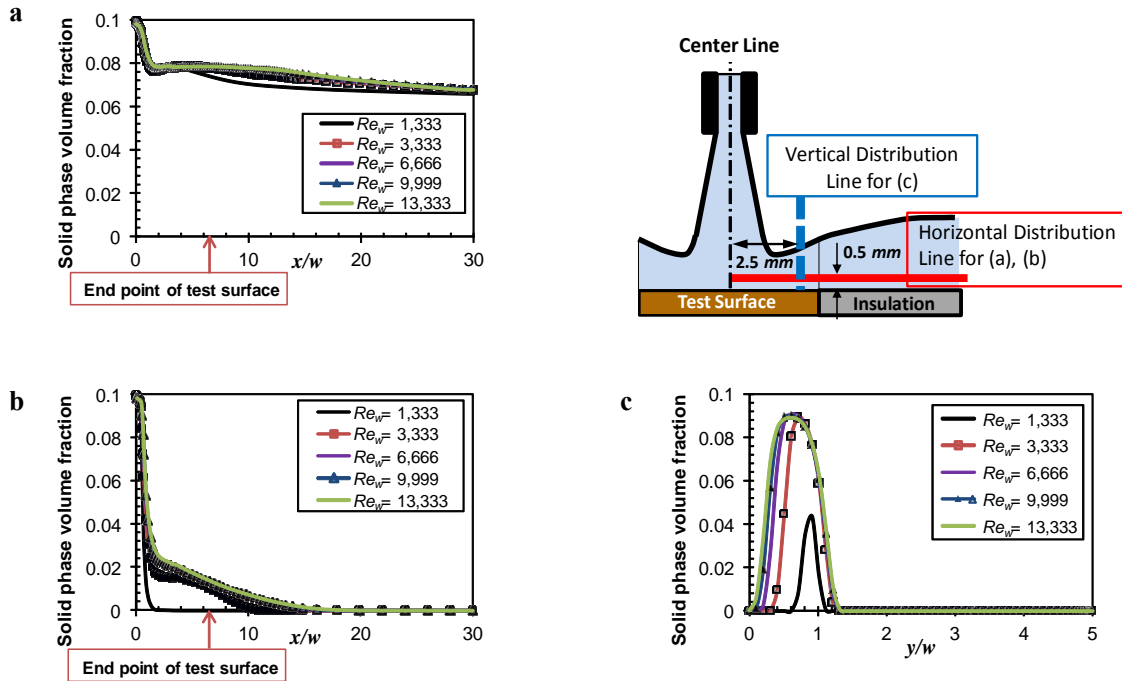


Figure Dry ice volume fraction distribution a without the sublimation model in horizontal direction b with the sublimation model in horizontal direction c with the sublimation model in vertical direction.

dioxide phase is reduced to a small amount is because the jet flow diffuses along the  $x$  direction even though sublimation is not considered. A greater change is observed when the sublimation model is applied, in figure 6 (b). All solid phase carbon dioxide disappears before the main jet flow escapes the domain outlet and the solid phase volume fraction lasts longer when the Reynolds number is higher as shown in figure 5 (a). Especially when  $e_w = 1,333$ , all of the solid phase carbon dioxide sublimates before the jet flow passes the end of the heater block. The low-temperature distribution corresponding to the solid carbon dioxide phase distribution is related to heat transfer enhancement and will be discussed below. Figure 6 (c) shows the vertical distribution of solid carbon dioxide volume fraction at the fixed horizontal location of  $x/w = 5$ . Sublimation is actively induced by the thermal energy supplied near the wall surface, so that the volume fraction of the solid phase is lowered and the maximum volume fraction is obtained at a constant height position. As the jet flow increases, that is, as the  $e_w$  number increases, the position of this maximum volume fraction approaches the wall

due to the momentum of the jet flow.

#### 4 CONCLUSIONS

Due to the high Joule-Thompson coefficient, carbon dioxide can be easily lowered below the sublimation point by the throttle effect, and the formation of dry ice can easily occur. In this study, numerical analysis on the enhancement of jet impingement heat transfer caused by sublimation and simultaneous collision of dry ice on cooling surface was performed. The jet flow of the gas-solid mixture was simulated by the Eulerian multiphase flow analysis method and mass and energy transfer equations for analyzing the phase change between dry ice gas-solid phase were added. The key conclusions are listed below.

- The analysis of the impinging jet flow with solid dry ice particle was performed by adding a module for the analysis of gas-solid phase change which is lacking from the conventional CFD code.
- The latent heat of dry ice sublimation keeps the jet bulk flow at low temperature. As the flow rate, or  $e_w$ , increases, the temperature of the jet bulk flow is maintained at a lower level for a longer period of time.
- When  $e_w$  is low, all solid carbon dioxide is sublimated before the jet flow reaches the end of the heater surface. Also, the low temperature jet bulk flow is not maintained on the near heater wall surface, so the heat transfer enhancement effect is limited to the minimum area of heater surface.
- As the jet flow rate or  $e_w$  increases, the effect of sublimation of a larger amount of solid dry ice appears on near the surface of the heater. The temperature of the impinging surface is reduced and the effect of the heat transfer enhancement occurs in a larger area.
- It can be seen that the heat transfer coefficient of the dry ice jet flow is greatly increased due to the absorption of the additional heat energy by sublimation above a certain flow rate condition.
- The proposed dry ice sublimation model is integrated with the existing Eulerian multiphase flow analysis to show that it can effectively describe the characteristics of dry ice impinging jet flow.

#### *Acknowledgement*

This material is based upon work supported by the research funding from Basic Science Research Program through the National Research Foundation of Korea (NRF) funded by the Ministry of Education (Grant No. NRF-2017R1D1A1B03029858) and Ulsan National Institute of Science and Technology (Grant No. 1.180038.01).

#### REFERENCES

- [1] O. Caggese, G. Gnaegi, G. Hannema, A. Terzis and P. Ott, "Experimental and numerical investigation of a fully confined impingement round jet", *International journal of heat and mass transfer*, vol. 65, 873-882, 2013.

- [2] M. Behnia, S. Parneix, Y. Shabany and P. A. Durban, "Numerical study of turbulent heat transfer in confined and unconfined impinging jets", *International journal of heat and fluid flow*, vol. 20, 1-9, 1999.
- [3] D. Kim and J. Lee, "Experimental investigation of CO<sub>2</sub> dry-ice assisted jet impingement cooling", *Thermal Engineering*, vol. 107, 927-935, 2016.
- [4] M. R. O. Panão, J. J. Costa, M. R. F. Bernardo, "Thermal assessment of sublimation cooling with dry-ice sprays", *International journal of heat and mass transfer*, vol. 118, 518-526, 2018.
- [5] Robert. S, "Carbon Dioxide Snow Cleaning", *Particulate Science and Technology*, Vol. 25, 37-57, 2007.
- [6] *ANSYS Fluent 15.0 Theory Guide, Fluent user's Guide*, Fluent Inc, Canonsburg, PA, 2013.
- [7] *ANSYS Fluent 15.0 UDF Manual, Fluent user's Guide*, ANSYS Inc, Canonsburg, PA, 2013.
- [8] M. Syamlal and T. J. O'Brien. "Computer Simulation of Bubbles in a Fluidized Bed", *AIChE J. Symp. Ser.*, 85, 22-31, 1989.
- [9] W. F. Giaque and C. J. Egan, "Carbon dioxide. The heat capacity and vapor pressure of the solid. The heat of sublimation. Thermodynamic and spectroscopic values of the Entropy", *Journal of chemical physics*, vol. 5, 45-54, 1937.

## Pattern Design of Permanent Magnet Segments using Topology Optimization

Jaewook Lee<sup>\*</sup>, Tsuyoshi Nomura<sup>\*\*</sup>, Ercan Dede<sup>\*\*\*</sup>

<sup>\*</sup>School of Mechanical Engineering, Gwangju Institute of Science and Technology (GIST), <sup>\*\*</sup>Toyota Central R&D Labs, <sup>\*\*\*</sup>Toyota Research Institute of North America

### ABSTRACT

In this work, the patterns of permanent magnet segments are designed using topology optimization. Specifically, the optimal border and magnetization directions of permanent magnet segments are designed using the topology optimization technique for the given design goal. For this, an orientation design variable in Cartesian coordinate system is assigned at each finite element. The orientation variable controls the magnetization direction of permanent magnets. Compared to the polar coordinate design variable, the variable in Cartesian coordinate is known to be beneficial to the optimization problem stability. To achieve the segmented permanent magnet arrays with discrete magnetization directions, a penalization scheme is applied. In this scheme, the strength of permanent magnet is controlled by the magnetization directions. The permanent magnet strength becomes weak where the magnetization direction is located between target discrete directions. Through this penalization, the design result composed of discrete target magnetization directions can be obtained. As a numerical example, a Halbach cylinder pattern is designed using topology optimization. The design result is compared with the analytical pattern design result derived by Halbach.

## Multiscale Modeling of Surface Functionalized Graphene-Polymer Nanocomposite

Jeong-ha Lee<sup>\*</sup>, Seunghwa Yang<sup>\*\*</sup>, Inseok Jeon<sup>\*\*\*</sup>

<sup>\*</sup>Chung-Ang University, <sup>\*\*</sup>Chung-Ang University, <sup>\*\*\*</sup>Chung-Ang University

### ABSTRACT

Graphene, a 2-dimensional single layered carbon nanostructure, is a promising material due to its excellent electrical, thermal and mechanical properties. Among the promising applications of the graphene, the reinforcement into a polymer nanocomposite (PNC) is one of the most well-known processes of strengthening polymer structure. However, restacking issue on dispersed graphene nanosheets [1] caused by the van der waals forces decrease PNCs mechanical and thermal properties. Moreover, weak van der waals interaction between polymer and graphene reduces their thermoelastic behavior and cohesive zone energy at the materials' interface. To improve the intrinsic weak interfacial strength between the graphene and polymer and to improve the dispersion state of the graphene in PNCs, several surface functionalization such as oxygen functionalization as well as covalent grafting have widely been applied to the nanocomposites. In this study, multiscale modeling approach for pristine and covalently functionalized graphene reinforced polypropylene (PP) nanocomposites is proposed. The representative molecular unit cells consisting of single layer graphene and PP matrix are modeled for molecular dynamics simulations with periodic boundary conditions. Direct covalent grafting between graphene and PP matrix are constructed via a dynamics cross linking method based on the cut-off methods. In molecular dynamics (MD) simulations, reactive forcefield is used for graphene including the grafted carbon-carbon covalent bond while classical potential model is used for the matrix phase. Through the statistical ensemble simulations, thermoelastic properties of PNCs are determined according to the grafting density at the interface. For equivalent continuum modeling to account for the effect of covalent grafting, the mean field micromechanics model [2] is incorporated to characterize the effect of covalent grafting on the interfacial and interphase properties of nanocomposites. Besides the interfacial point of view, contribution of the covalent grafting to the dispersion of graphene inside the polymer matrix is examined. [1] Dan LI, Marc B. Muller, Scott Gilje, Richard B. Kaner and Gordon G. Wallace, &quot;Processable aqueous dispersions of graphene nanosheets&quot;, Nature Nanotechnology, Vol 3, pp. 101-105, 2008. 02 [2]Seunghwa Yang, Maenghyo Cho, &quot;Scale bridging method to characterize mechanical properties of nanoparticle/polymer nanocomposites&apos;, Appl. Phys. Lett., 93, 043111, 2008. 07

## Root-Finding Absorbing Boundary Conditions for Wave Propagation Problems in Infinite Media

Jin Ho Lee\*

\*Pukyong National University

### ABSTRACT

The theory of wave propagation is the basis of understanding various physical phenomena in fields such as civil engineering, mechanical engineering, offshore engineering, seismology, meteorology, and oceanography. Because many wave propagation phenomena occur in extensive, unbounded or infinite media, it is required that the dynamic behaviors of such media is simulated accurately and efficiently. Wave propagation phenomena in infinite media can be simulated using computational treatments such as those based on the finite element method and the finite difference method. However, since these treatments were developed originally for problems in finite domains, it is necessary to use a special numerical or mechanical model that can precisely consider the energy radiation into infinity. Therefore, various models such as consistent transmitting boundaries, boundary elements, infinite elements, high-order absorbing boundary conditions (ABCs), and perfectly matched layers (PMLs) have been developed and used for various wave propagation problems in infinite media. Various nonlinear behaviors, for example, material nonlinearities, may occur in wave propagation phenomena. These can be addressed most conveniently in the time domain. Therefore, with infinite media, it is best to consider energy radiation into infinity directly in the time domain. Accuracy and efficiency depend on how well we can account for energy radiation into infinity in the time domain. Among the models mentioned above that can consider the influence of the infinite domain, the higher-order ABCs and PMLs can guarantee both accuracy and efficiency in the time domain and have been applied widely to wave propagation problems. Both approaches for time-domain applications entail their own advantages and disadvantages. The high-order ABCs approximate the dispersion equation of waves in the infinite region by rational expressions or a series of simple differential operators while the PMLs introduce artificial damping through complex transformations of the spatial coordinate system. Recently, a new absorbing boundary condition for scalar-wave propagation problems has been developed [1] on the basis of solutions of the dispersion equation using a root-finding algorithm such as the Newton-Raphson method. This boundary condition is referred to as a Root-Finding Absorbing Boundary Condition (RFABC). In this study, the RFABC is extended to elastic waves. The accuracy of the newly developed boundary condition is demonstrated by application to time-domain analysis of an elastic-wave propagation problem. References 1. Lee JH, Tassoulas JL. Absorbing boundary condition for scalar-wave propagation problems in infinite media based on a root-finding algorithm, *Computer Methods in Applied Mechanics and Engineering* 2018; 330: 207-219.

## Topology Optimization Considering Stress Constraint for Dynamic Load Using Response Filtering Method

Jongwook Lee\*, Gilho Yoon\*\*

\*Hanyang university, Seoul, Korea, \*\*Hanyang university, Seoul, Korea

### ABSTRACT

When a sudden collision, explosion or earthquake occurs, the stress wave from that region propagates to the surroundings. Since the propagating stress wave can cause unexpected failure, it is possible to design a safer structure considering the stress wave in the design stage. In this study, we focused on structural optimization techniques considering these stress waves. To consider the stress wave, the propagating stress is calculated numerically. However, when numerically calculating the stress wave, numerical inaccuracies appear [1-2]. Especially, undershoot and overshoot are found in numerical solutions, which cause ambiguity in the design of structures considering stresses. Therefore, we have developed a new filtering technique called RFM (Response Filtering Method) to eliminate these numerical errors. Numerical errors of propagating stress waves can be reduced by this method. In addition, accuracy was improved when compared with the exact solution. In addition, it is confirmed that the frequency characteristic is also similar to the exact solution in this research. Acknowledgement This work was supported by the National Research Foundation of Korea (NRF) grant funded by the Korea government (MEST) (NRF-2015R1A2A2A11027580). References [1] Cook, Robert D., et al., Concepts and applications of finite element analysis. New York: Wiley. 1974. [2] Daryl L. Logan., A first course in the finite element method, fifth ed., Thomsom, 2011.

## Development of a Three-Dimensional Parallel Volume Integral Equation Method

Jungki Lee\*

\*Hongik University, Sejong Campus

### ABSTRACT

A three-dimensional parallel volume integral equation method (PVIEM) is applied for the analysis of elastostatic problems in an unbounded isotropic matrix containing multiple anisotropic inclusions. It is necessary to use standard parallel programming, such as MPI (message passing interface), to speed up computation in the volume integral equation method (VIEM). It should be noted that this numerical method does not require the use of the Green's function for the anisotropic inclusion - only the Green's function for the unbounded isotropic matrix is needed. A detailed analysis of stress field at the interface between the isotropic matrix and the central anisotropic inclusion is carried out for simple cubic packing arrangements of multiple spherical inclusions. The effects of multiple anisotropic spherical inclusions on the stress field at the interface between the matrix and the central inclusion are investigated. The accuracy of the parallel volume integral equation method for the interfacial stress field is compared by the finite element method (FEM). The PVIEM is shown to be very accurate and efficient for solving general three-dimensional elastostatic and elastodynamic problems involving multiple anisotropic inclusions whose shape and number are arbitrary.[1-3] References [1] A volume integral equation technique for multiple inclusion and crack interaction problems - Journal of Applied Mechanics, Volume 64, Issue 1, March 1997, pp. 23-31. Jungki Lee, Ajit Mal. [2] Calculation of interfacial stresses in composites containing elliptical inclusions of various types - European Journal of Mechanics, A/Solids, Volume 44, 2014, pp. 17-40. Jungki Lee, Sangmin Oh, Ajit Mal. [3] Multiple scattering using parallel volume integral equation method: Interaction of SH waves with multiple multilayered anisotropic elliptical inclusions - Mathematical Problems in Engineering, Volume 2015, 2015, Article ID 809320, 48 pages. Acknowledgements This research was supported by the International Science and Business Belt Program through the Ministry of Science and ICT (2017K000451) and Korea Institute of Science and Technology Information (KISTI) supercomputing center through the strategic support program for the supercomputing application research (KSC-2017-C1-0004).

## Automated Framework for Efficient Surrogate Model Building with Machine Learning Techniques

Kyungeun Lee\*, ikjin Lee\*\*

\*Ph.D candidate, Mechanical Engineering, KAIST, \*\*Associate professor, Mechanical Engineering, KAIST

### ABSTRACT

Variable selection is needed not only to improve computational efficiency but also accuracy of the analysis by eliminating unnecessary variables and focusing on the relevant ones. Especially, variable selection is essential for surrogate modeling with high-dimensional problems because the number of required sampling for the model building highly depends on the size of dimension. However, in practical, there is a limit on the number of training samples provided because most experiments or analysis are cost or time-consuming. Even the current computational performance is greatly improved, many FEM solving still take long time according to the nonlinearities or amount of elements. That kinds of model needs surrogate modeling. However, many computations are spent in variable selection itself prior to build a surrogate model which aims to replace time-consuming calculations. Moreover, after variable selection, new samples for the surrogate modeling are often required because the orthogonality of the initial sample with selected sub-dimension is broken. Therefore, in this study, we suggest to perform variable selection and surrogate model building at the same time with as few samples as possible. The key point of this study is that subset selection and model accuracy evaluation are performed simultaneously and iteratively in every loop. Gaussian process regression (GPR) is selected as the surrogate modeling methodology for its stochastic property. GPR can handle the perturbation caused by dimensionality reduction with covariance function. The overall process is as follows. At first, initial sample is drawn carefully to preserve the orthogonality and space-filling property with the sub-dimension as possible, using maximum projection design. Next, initial surrogate modeling is performed and the marginalized maximum likelihood (ML) derived after hyperparameter optimization of GPR is used as a subset selection fitness. K-means clustering is utilized to classify the ML values into converged and non-converged groups. The best subset is chosen as the minimum-sized subset in the converged group to prevent the overfitting and remove redundant variables. Model accuracy is evaluated with Leave-One-Out cross validation. If the model is proved to be inaccurate or converged/non-converged groups are not discriminating, next sequential sample is chosen focused on the most recently selected subset dimension. By this process, when the algorithm is finished which means both model accuracy is validated and subset selection is converged, variable selection and surrogate model building is completed at the same time. This research suggests efficient stochastic surrogate modeling framework.

## **Flooding Simulation Method of Railway Infrastructure by Using Open Data Schema-based 3D Information Model**

Sang-Ho Lee<sup>\*</sup>, Young-Hoon Jang<sup>\*\*</sup>, Kyung-Wan Seo<sup>\*\*\*</sup>, Tae Ho Kwon<sup>\*\*\*\*</sup>

<sup>\*</sup>Yonsei University, <sup>\*\*</sup>Yonsei University, <sup>\*\*\*</sup>Yonsei University, <sup>\*\*\*\*</sup>Yonsei University

### **ABSTRACT**

The damage of railway infrastructure from flooding has been steadily increasing as a recent climate change. The predicting the particular damage situation can be one of the effective provisions for reducing the damage of structures. The flooding simulation totally depends on the structure's information, and the information of a railway infrastructure is the complex, tangled, and linked various application fields. It needs, therefore, multidisciplinary approach for the successful flooding simulation of the railway infrastructure. BIM is a new paradigm that can interoperably manage the lifecycle information on facility, it can effectively satisfy the requirements for flooding simulation of the railway infrastructure. Industry Foundation Classes (IFC) is the BIM standard open data schema developed by buildingSMART. The IFC, however, has limitations to represent the exact city information model including the railway infrastructure since it focuses on building structures. The CityGML is the open data schema to build a city model while IFC is developed for one specific facility. The IFC is a relatively detailed schema that can support the whole lifecycle of facility, whereas the CityGML is rough but can be considering the relationship between facilities. This study aimed to build an effective and detailed city information model focused on the railway infrastructure based on open data schema and to conduct flood damage assessment by 3D model-based simulation. For this procedure, the authors have been proposed the IFC-based extended data schema for the railway infrastructure and developed converting method from IFC-based model to CityGML-based model. The hydraulic analysis data were spread on terrain model and the flooding damage assessment was simulated through conflict check between 3D city object model and hydraulic analysis model. The damage assessment of flooding situation was categorized casualty, property damage estimation, and availability check of railway infrastructure. The simulating results of flood damages were stored in linked external database. By using this, it could be possible to capture semantic data by a query according to the condition of the flood occurrence. The authors have examined the proposed modeling and simulation method on the part of the real city and checked the feasibility of the methods.

&lt; Acknowledgement&gt; This research was supported by a grant (16RTRP-B104237-03) from Railroad Technology Research Program funded by Ministry of Land, Infrastructure and Transport (MOLIT) of Korean government.

## A Kernel-based Learning Approach for Mechanical Characterization of Soft Tissue

Sangrock Lee<sup>\*</sup>, FNU Rahul<sup>\*\*</sup>, Uwe Kruger<sup>\*\*\*</sup>, Suvranu De<sup>\*\*\*\*</sup>

<sup>\*</sup>Rensselaer Polytechnic Institute, <sup>\*\*</sup>Rensselaer Polytechnic Institute, <sup>\*\*\*</sup>Rensselaer Polytechnic Institute,  
<sup>\*\*\*\*</sup>Rensselaer Polytechnic Institute

### ABSTRACT

In recent years, elastography has emerged as a viable technique for non-invasive assessment of mechanical properties of tissue. Elastography techniques rely on imaging modalities, such as ultrasound imaging, to quantitatively assess changes in the elasticity of soft tissue in various pathologies, which is useful for diagnostic purposes [1]. However, these techniques require solving an inverse problem to identify the mechanical properties of soft tissue while under external load, which is computationally expensive particularly for tissues that exhibit nonlinear mechanical characteristics under finite deformation [2]. We propose a kernel-based machine learning approach for rapid assessment of mechanical properties of soft tissue based on a training dataset for which the deformation map represents the cause and the corresponding spatial distribution of material parameter, or elasticity map, is the response to be predicted. A nonlinear kernel-based partial least square (KPLS) regression model is employed to learn the relationship between the deformation map and corresponding elasticity map. KPLS is a chemometric tool that is particularly useful in situations where the number of cause variables exceeds the number of observations [3], which is often the case with clinical patient specific dataset. Hence, KPLS is chosen to directly address this problem of small elastography datasets. A Gaussian kernel is used to construct the nonlinear mapping for the KPLS model. The parameters of KPLS model, i.e. the latent variable sets and Gaussian kernel parameter, are obtained by n-fold cross-validation to guarantee an independent assessment of the model. The prediction error of the KPLS regression model is estimated by n-fold cross validation on a synthetic dataset. References [1] Sigrist, R.M., Liao, J., El Kaffas, A., Chammas, M.C., Willmann, J.K., 2017. Ultrasound Elastography: Review of techniques and clinical applications. *Theranostics*, 7, 1303-1329. [2] Dargar, S., Akyildiz, A.C., De, S., 2017. In situ mechanical characterization of multilayer soft tissue using ultrasound imaging. *IEEE Transactions on Biomedical Engineering*, 64, 2595-2606. [3] Rosipal, R., Trejo, L.J., 2001. Kernel partial least squares regression in reproducing kernel Hilbert space. *Journal of Machine Learning Research*, 2, 97-123.

## **Micromechanics-based Homogenization Method Applicable to a Wide Range of Interfacial Damage for Reinforced Composites Having Anisotropic Matrix**

Sangryun Lee<sup>\*</sup>, Jinyeop Lee<sup>\*\*</sup>, Seunghwa Ryu<sup>\*\*\*</sup>

<sup>\*</sup>Korea Advanced Institute of Science and Technology, <sup>\*\*</sup>Korea Advanced Institute of Science and Technology,  
<sup>\*\*\*</sup>Korea Advanced Institute of Science and Technology

### **ABSTRACT**

In this study, we study a micromechanics model to predict effective moduli of a reinforced composite having interfacial damage using linear spring model. We propose a modified Eshelby tensor of an anisotropic matrix which is applicable to the entire range of interfacial damage from perfect bonding to complete de-bonding. Then, we obtain a modified strain concentration tensor by decomposing the damaged interface problem of single inhomogeneity into three independent elasticity problems. Also, we derived exterior Eshelby tensor and exterior strain concentration tensor and validate our analytic model against finite element analysis (FEA) results. Combining the modified Eshelby tensor and strain concentration tensor in the Mori-Tanaka framework, we derive the effective moduli of a particle-reinforced composite having an anisotropic matrix and interfacial damage with correct upper bound (perfect bonding) and lower bound (porous medium). We study the effect of penetration at the interface because the micromechanics model can not account for contact behavior which is a highly nonlinear behavior. To study the effect of the penetration on the effective moduli of composite, we use FEA to compute the effective modulus of the composite having contact behavior at the interface and compare with the micromechanics model allowing penetration. Besides, we compute stress strain curve of the composite and stress state of each phase theoretically considering interfacial damage under uniaxial loading, which allows us to compute the ultimate strength of nanocomposites in a wide range of interfacial damage.

## Blood Flow Simulation from Cellular Interaction to Microvascular-network

Tae-Rin Lee<sup>\*</sup>, Seokjin Park<sup>\*\*</sup>, Ji-Ah Hong<sup>\*\*\*</sup>

<sup>\*</sup>Advanced Institutes of Convergence Technology, Seoul National University, <sup>\*\*</sup>Department of Mechanical Engineering, Ajou University, <sup>\*\*\*</sup>Department of Mechanical Engineering, Ajou University

### ABSTRACT

Blood flow in the microvasculature is a key component to understand various phenomena in the field of biomedical engineering, e.g. angiogenesis, tumor growth, metastatic cancer and etc. However, the nonlinear properties in hemodynamics make it difficult to precisely understand the blood flow. In this talk, we will introduce an immersed boundary method for simulating blood cells in microvessels and for quantifying hemodynamic properties at the microvascular-network level. Specifically, blood cells are modeled by material points with springs. The fluid-structure interaction (FSI) force is generated by using a direct-forcing technique. Based on the FSI method, we will estimate the plasma skimming effect in bifurcated microvessels for predicting the blood flow in the microvasculature. Here, the cellular level interaction for simulating blood flow in the microvasculature is limited in a few microvessels and thousands of cells. Therefore, it is required to develop an 1-D blood flow model for simplifying the complex blood flow in continuously bifurcating microvessels. We will computationally construct microvascular geometries and simulate the blood flow through them by using an extended 1-D blood flow model with plasma skimming effect. The suggested model will be compared with experimental data in rat mesentery and mouse cortex. Based on the simulation results, the linking between cellular model and network model is fully discussed.

## Improving the Accuracy of Consumer Preference Estimation Using Economic Simulation Model

Ungki Lee<sup>\*</sup>, Namwoo Kang<sup>\*\*</sup>, Ikjin Lee<sup>\*\*\*</sup>

<sup>\*</sup>Korea Advanced Institute of Science and Technology, <sup>\*\*</sup>Korea Advanced Institute of Science and Technology,  
<sup>\*\*\*</sup>Korea Advanced Institute of Science and Technology

### ABSTRACT

The research field of the design for market systems (DMS) gives insights to decision makers to find profit-maximized product design [1]. After estimating the consumer preferences toward the product attributes, product design can be formulated as a mathematical optimization problem, and the optimum design that maximizes the expected value can be achieved. Therefore, it is important to predict a market share of a product using product attributes and consumer preferences when designing a product [2]. To obtain individual level consumer preference, choice-based conjoint (CBC) study is executed to extract actual responses results of consumers collected from surveys. Then a hierarchical Bayesian (HB) approach is used to estimate the part-worths on product attributes which indicate preferences of consumers [3]. However, the number of people who can conduct a survey is limited, and the number of questionnaires per person should not be large. This influences the predictive capability of HB in estimating consumer preferences on product attributes. This paper introduces an approach to improve the accuracy of consumer preference estimation using a simulation model despite the small number of actual survey data. Based on the demographic data of consumers surveyed, each consumer's discount rate which shows how future income or expenditure is valued at present can be obtained using optimization technique, and an economic simulation model that can replace each individual's choice on product can be established. Then the economic simulation model conducts virtual surveys which consist of a combination of various product attribute levels, and the achieved simulation data is calibrated with actual survey data to improve predictive capability. Some of the actual survey data is used to estimate consumer preferences, while some are used to validate the estimated consumer preferences. Validation calculates how much the marketing model which is generated through the calibration of actual survey data and economic simulation model data can match the actual survey results. [1] Lewis, K. E., Chen, W., Schmidt, L. C., and Press, A., 2006, *Decision Making in Engineering Design*, ASME Press, New York. [2] Kang, N., Ren, Y., Feinberg, F. M., and Papalambros, P. Y., 2016, "Public Investment and Electric Vehicle Design: A Model-based Market Analysis Framework with Application to a USA-China Comparison Study," *Des. Sci.*, 2, p. e6. [3] Kang, N., Feinberg, F. M., and Papalambros, P. Y., 2017, "Autonomous Electric Vehicle Sharing System Design," *ASME J. Mech. Des.*, 139(1), 011402.

## Multiscale Analysis of the Domain Patterns in Ferroelectrics

Yi-Chien Lee\*, Nien-Ti Tsou\*\*

\*Dept. of Materials Science and Engineering, National Chiao-Tung University, Hsinchu, Taiwan, \*\*Dept. of Materials Science and Engineering, National Chiao-Tung University, Hsinchu, Taiwan

### ABSTRACT

Ferroelectric materials have been widely used in many applications of sensors, actuators and memory devices in recent decades. These materials have strong electrical, thermal, or mechanical coupling, giving an opportunity for crystals to sense the change of external loading or boundary conditions. The microstructure is the most important factor to determining the crystal properties. However, there are some limitations of typical microstructural modeling. For example, certain patterns of microstructure are assumed for sharp interface models, and the small calculation regions for phase field methods. Thus, the aim of this study is to develop a multiscale analysis scheme combining the merits of sharp interface and phase field models. Firstly, the microstructure pattern can be obtained by sharp interface model based on compatibility equations. Wherein the pattern is determined with the assumption of flat interfaces. Then, the pattern is set as the initial state of the phase field model, for further energy minimization to eliminate the flat interface assumption. The phase field algorithm is implemented by a commercial software COMSOL Multiphysics. Microstructures of the tetragonal and rhombohedral ferroelectrics crystal are both examined in order to demonstrate the validity of the current work. Interesting laminate structures, such as herringbone patterns and stripe patterns, are generated. Also the effect of depolarization energy, applied load and applied electric field will be examined. The current multiscale model eliminates the assumption of flat interfaces, and at the same time, has better efficiency for engineering purposes. Keywords: phase-field method, ferroelectric, compatible pattern, interfacial energy

## **Topology Optimization of Synthesized, Stochastic Microstructures**

Sylvain Lefebvre\*

\*INRIA

### **ABSTRACT**

In this presentation I will discuss recent work made within our team regarding the optimization of objects filled with microstructures that are synthesized from stochastic processes. I will present two different approaches. The first, inspired by example-based texture synthesis techniques from Computer Graphics, allows designers to specify the local shape of porosities by providing an example. A global optimizer distributes material such as to obtain globally rigid shapes, while locally the material form porosities resembling the ones in the exemplar. The second approach relies on stochastic processes to generate microstructures resembling foams. By controlling the statistics of the generation process, we show that it is possible to control the final average elastic behavior. These techniques can be used in two-scale topology optimization problems, where a shape is globally optimized at a coarse scale, while the random process quickly generates a fine scale foam having the desired homogeneous behavior.

## Qualitative and Quantitative Inverse Analysis of Layered Pavement Properties from Falling Weight Deflectometer Data Using Artificial Neural Networks

Marek Lefik\*, Marek Wojciechowski\*\*

\*Technical University of Lodz, Poland, \*\*Technical University of Lodz, Poland

### ABSTRACT

Falling Weight Deflectometer (FWD) is an instrument for “in situ” test, commonly used to evaluate mechanical parameters and to assess the quality of layered structures of road and airfield pavements. The deflection response of the pavement to an falling weight (measured in several points aligned on a rigid support) is used as an indicator of material properties, and structural performance of the pavement. Determination of the mechanical parameters of the layers is classically done by minimization of a distance between the measured and a theoretical deflection (function of parameters of the model). Slow convergence of this method is described in [2]. Using ANN, it is possible to approximate directly the inverse relation between the set of parameter of the FE model of the layered half space and the deflection of its upper surface, computed for this set of parameters. To do this, the input of the ANN is valued with the deflections and the output with the corresponding set of parameters of the model. FE model can be constructed for many qualitatively different hypotheses concerning the mechanics of the layers (see [1]). For example, the influence of a quality of interlayer junction is crucial for the behavior of asphaltic pavements. Novel algorithm of the stepwise identification that we propose starts with qualitative identification. It is possible to train the ANN with sets of deflections computed according to different qualitative models, such that the ANN computes at the output the integers labelling these models. Having the qualitative solution of the inverse problem, the ANN is retrained with samples computed in frame of the identified FE model and for a coarse sampling of the multidimensional space of parameters. If the error of the solution is not sufficiently small, in the next step a retraining of the ANN is performed again with some set of samples from a neighborhood of the parameters identified in the previous step. If the solution of the inverse problem exists and is ambiguous, this procedure converges. Our own FE code is used to generate solutions of the forward problem. [1] Maoyun Li, Hao Wang, Guangji Xu, Pengyu Xie. Finite element modeling and parametric analysis of viscoelastic and nonlinear pavement responses under dynamic FWD loading, *Construction and Building Materials*, 141 (2017) 23-35 [2] P. Ruta, B. Krawczyk, A. Szydło, Identification of pavement elastic moduli by means of impact test, *Engineering Structures*, 100 (2015) 201–211

## **A New FEM/DEM Multiscale Model to Solve Immersed Granular Flows Based on Suspension Drops Simulations**

Vincent Legat<sup>\*</sup>, Matthieu Constant<sup>\*\*</sup>, Jonathan Lambrechts<sup>\*\*\*</sup>, Frédéric Dubois<sup>\*\*\*\*</sup>

<sup>\*</sup>Ecole Polytechnique de Louvain (UCL/EPL), <sup>\*\*</sup>Ecole Polytechnique de Louvain (UCL/EPL), <sup>\*\*\*</sup>Ecole Polytechnique de Louvain (UCL/EPL), <sup>\*\*\*\*</sup>Université de Montpellier, France

### **ABSTRACT**

This paper is devoted to the study of an hybrid multiscale model for flows mixing fluid and grains. The grains are solved at a fine scale using a Lagrangian approach with the Discrete Element Method. It provides the trajectories and the force applied on the grains with an accuracy that is needed to describe small scales phenomena happening in these flows. The dynamics of the fluid is deduced from a continuous representation of the mixture between grains and fluid at the coarse scale. We present an hybrid multiscale model for immersed granular flows using the Finite Element Method to solve the fluid phase and a non-smooth grains model to solve the contacts. This model will be validated on two-dimensional simulations of the suspension drops that refers to cluster of grains settling in a viscous fluid. The challenging point of this method stays in the coupling of the two different representation scales. Applying this model to the well-known problem of suspension drops provides validation and insight in this kind of methodology. All the features of a swarm of grains settling in a viscous fluid can be found to validate the model and its generality provides easily simulations at regimes where inertia is dominant compared to Stokeslet or Oseenlet simulations usually encountered in literature. Just after the drop begins to move, some grains escape from the closed envelop and form a tail that grows in time until it separates from the swarm. The tail contains grains from the rear of the swarm as well as grains from inside because of the recirculation that leads grains outside the closed envelop. The rate of grains leakage is linked to the falling velocity of the swarm, the radius of the swarm and the radius of the grains. At some time the centre of the swarm contains not enough grains and the tail breaks up. The fluid can go through the center of the swarm and it changes into an open torus that destabilises during expansion and contraction phases to form two (or more) secondary droplets.

## Topology Optimization and Model Reduction of Elastomer Damping Devices

Antoine Legay<sup>\*</sup>, Sylvain Burri<sup>\*\*</sup>, Jean-François Deü<sup>\*\*\*</sup>

<sup>\*</sup>Structural Mechanics and Coupled Systems Laboratory, Conservatoire National des Arts et Métiers, 292 rue Saint-Martin, 75141 Paris Cedex 03, France, <sup>\*\*</sup>Structural Mechanics and Coupled Systems Laboratory, Conservatoire National des Arts et Métiers, 292 rue Saint-Martin, 75141 Paris Cedex 03, France, <sup>\*\*\*</sup>Structural Mechanics and Coupled Systems Laboratory, Conservatoire National des Arts et Métiers, 292 rue Saint-Martin, 75141 Paris Cedex 03, France

### ABSTRACT

Due to their damping properties, elastomer materials are commonly used in the industry to achieve anti-vibration junctions between mechanical subsystems. These links are usually made of various materials (metallic, composites and elastomers). Their geometries may be optimized in order to fulfill the needs of the specific targeted application. Moreover, in order to predict the dynamic behavior of these junctions in their environment, efficient numerical dynamic models have to be developed. These models should take into account the viscoelastic behavior of the elastomer and the material and geometric nonlinearity. Thus, the objective of this work is thus to develop methods to optimize flexible damping devices made of elastomer as well as to build efficient models for the prediction of their dynamic behavior. Firstly, a three-dimensional finite element code using viscoelasticity constitutive relations is developed for the numerical modeling of the elastomer junctions. A Zener fractional derivative of the viscous behavior is implemented. Secondly, a topology optimization [1] of the damping device is achieved in order to find the best geometry shape. The objective function is based on the dynamic compliance of the whole system (the structure and its damping devices) in the frequency domain. A dual method using Lagrange function is used to find the optimum of the objective function, under a volume constraint. Thirdly, a reduced order model is developed. It is based on a component mode synthesis method adapted to highly damped structures by using a multi-model approach [2]. The final reduced element representing the junction is obtained by a dynamic condensation on the external rigid faces in contact with the sub-structures for a total of 12 dofs (6 dofs per face) [3]. The presented application is a junction used to damp the transmitted vibrations from a vibrating base such as a space launcher to a CubSat satellite during takeoff. [1] M.P. Bendsoe, O. Sigmund. Topology Optimization. Theory, Methods, and Applications. Springer, 2004. [2] L. Rouleau, J.-F. Deü, A. Legay. A comparison of model reduction techniques based on modal projection for structures with frequency-dependent damping. Mechanical Systems and Signal Processing, 90, 110–125, 2017. [3] A. Legay, J.-F. Deü, B. Morin. Reduced order models for dynamic behavior of prestressed elastomer damping devices. Proceedings of the VII European Congress on Computational Methods in Applied Sciences and Engineering, the ECCOMAS Congress 2016, Hersonissos, Crete, Greece, June 5-10, 2016.

## **A Phase Field Model for Three-phase System with Tunable Interfacial Energy and Its Application to Solid Oxide Fuel Cell**

Yinkai Lei<sup>\*</sup>, Tianle Cheng<sup>\*\*</sup>, Youhai Wen<sup>\*\*\*</sup>

<sup>\*</sup>National Energy Technology Laboratory, Albany OR, <sup>\*\*</sup>National Energy Technology Laboratory, Albany OR,  
<sup>\*\*\*</sup>National Energy Technology Laboratory, Albany OR

### **ABSTRACT**

An improved phase field model has been developed to simulate the microstructure evolution in three-phase system. Detailed analysis reveals that a cross term between the gradient of order parameters is essential to make the interfacial energy tunable. We demonstrate that the ratio between the energy of grain boundary and interphase boundary (or surface) can be easily tuned in our model. We use this model to simulate the microstructure evolution in both the anode and cathode of solid oxide fuel cell. The results show that our model is well applicable to two different three-phase systems, i.e. Ni-YSZ-pore for anode and LSM-YSZ-pore for cathode.

## Stochastic Agent-based Modeling of Cell Death and Tissue Shrinkage

Emma Lejeune\*, Christian Linder\*\*

\*Stanford University, \*\*Stanford University

### ABSTRACT

Cell death, a process which occurs both naturally and in response to external factors, is both a complex and diverse phenomenon. A better understanding of how cell death manifests on the population and tissue scales is relevant to both morphogenesis and tumor response to treatment. Under certain conditions, dying cells actively contract, which causes neighboring cells to rearrange and maintain tissue integrity. Under other conditions, dying cells leave behind gaps, which results in tissue separation. Here we establish a computational framework to study the effects of cell death on population scale shrinkage. In order to better quantify model uncertainty and parameter interactions, we implement a recently developed technique for conducting a variance-based sensitivity analysis on a stochastic model. In particular, we define appropriate technique for prescribing stochastic model components and constructing a meta-model to make sensitivity analysis with a computationally expensive simulation feasible. With this framework, we explore cell death implemented in a peridynamics based mechanical model [1]. Peridynamics, a theoretical and computational framework designed to unify the mechanics of continuous and discontinuous media, is a promising tool for coupling mechanical and algorithmic biological behavior. In our model, algorithmic rules applied on the cellular level interact with mechanical behavior and emerge on the population scale where their effects are quantified. We find that parameters such as cell shrinkage during death are as important as the fraction of dying cells for determining population scale shrinkage. Looking forward, we anticipate that the methods and results presented here are a starting point for significant future investigation toward modeling and understanding cell death in multiscale and multiphysics settings. [1] Lejeune, E. & Linder, C. *Biomech Model Mechanobiol* (2017) 16: 1141.

## Modeling the Capillary Transport of Deformable Nanoconstructs and Cells via a Lattice Boltzmann Method

Pietro Lenarda<sup>\*</sup>, Alessandro Coclite<sup>\*\*</sup>, Marco Miali<sup>\*\*\*</sup>, Hilaria Mollica<sup>\*\*\*\*</sup>, Anna Lisa  
Palange<sup>\*\*\*\*\*</sup>, Paolo Decuzzi<sup>\*\*\*\*\*</sup>

<sup>\*</sup>Fondazione Istituto Italiano di Tecnologia, <sup>\*\*</sup>Fondazione Istituto Italiano di Tecnologia, <sup>\*\*\*</sup>Fondazione Istituto Italiano di Tecnologia, <sup>\*\*\*\*</sup>Fondazione Istituto Italiano di Tecnologia, <sup>\*\*\*\*\*</sup>Fondazione Istituto Italiano di Tecnologia, <sup>\*\*\*\*\*</sup>Fondazione Istituto Italiano di Tecnologia

### ABSTRACT

In the treatment and imaging of diseases, nanoconstructs and engineered cells are emerging as powerful tools for the tissue specific delivery of multiple agents. Generally, nanoconstructs and cells are injected systemically and could reach any site within the circulatory system as they are transported by the blood flow. In the case of nanoconstructs, the size, shape, surface properties and softness – 4S parameters – can be tailored during the synthesis process to enhance their specific accumulation within the diseased tissue. Similarly, stem cells, macrophages and other types of cell can be engineered ex-vivo to express specific surface receptors that would facilitate the recognition of the biological target. Given, the variety of independent parameters and the complexity of the biophysical problem, sophisticated computational tools to guide scientists in the rational selection of the most effective delivery strategy are urgently needed.[1] In this study, a computational framework based on coupling Lattice Boltzmann (LB) and Immersed Boundary (IB) methods is employed to predict the vascular transport and adhesion of nanoconstructs and cells in capillary flows. The fluid solver for the incompressible Navier-Stokes equations is based on the three dimensional D3Q19 Lattice-Boltzmann Method. The dynamics of deformable nanoconstructs and cells is simulated through a neo-Hookean membrane constitutive model coupled iteratively with the fluid. [2] Nanoconstructs and cells are decorated with ligand molecules interacting through probabilistic laws with receptors deposited along the blood vessel walls. The proposed numerical scheme is validated against known computational and experimental benchmarks. The vascular dynamics (margination) and adhesion of nanoconstructs and cells is predicted in terms of the 4S parameters – size, shape, surface and softness – and of vascular features – caliber, wall shear rate, receptor density and affinity. Numerical data are directly compared with experiments performed in microfluidic chips.[3] Implications on the rational design of nanoconstructs and efficiency of cell delivery are critically discussed. References 1. Decuzzi, P., Facilitating the Clinical Integration of Nanomedicines: The Roles of Theoretical and Computational Scientists. ACS Nano, 2016. 10(9): p. 8133-8. 2. Kruger, T., F. Varnik, and D. Raabe, Efficient and accurate simulations of deformable particles immersed in a fluid using a combined immersed boundary lattice Boltzmann finite element method. Computers & Mathematics with Applications, 2011. 61(12): p. 3485-3505. 3. Coclite, A., et al., Predicting different adhesive regimens of circulating particles at blood capillary walls. Microfluidics and Nanofluidics, 2017. 21(11): p. 168.

## Optimal Gear Design to Minimize Vibrations Through the Path Gear-Shaft-Bearing-Gearhousing

Jesson Xavier Leon-Medina\*, Henry Octavio Cortes-Ramos\*\*

\*Universidad Nacional de Colombia-Sede Bogotá, \*\*Universidad Nacional de Colombia-Sede Bogotá

### ABSTRACT

In this work, the dynamic behavior of a gearbox is optimized. We consider the interaction between the housing, the bearing, the shaft and the gears. We minimize the excitation sources generated by the meshing process, among which are included, the static transmission error-STE and the variation of the mesh stiffness. For the analysis of static transmission error, several methods have been generated, most of which are based on the finite element method for a set of successive positions of the driving wheel [1]. The STE is presented due to differences between ideal and real designs, such as deflections of teeth and manufacturing errors [2]. We seek to find the best gear profiles to reduce the vibrations present in a gearbox, taking into account the transmission effect involved in the interaction between gear, shaft, bearing and housing . This interaction can be modeled by two methods, the finite element method or the lumped mass method a hybrid method combining the advantages of the two methods can be employed to avoid some problems such as modeling error, time consuming and computing cost, etc. [3].  
References [1] Rigaud, E., & Barday, D. (1999). Modelling and analysis of static transmission error. Effect of wheel body deformation and interactions between adjacent loaded teeth. In 4th World Congress on Gearing and Power Transmission (pp. 1961-1972). [2] Carbonelli, A., Perret-Liaudet, J., Rigaud, E., & Le Bot, A. (2011). Particle swarm optimization as an efficient computational method in order to minimize vibrations of multimesh gears transmission. Advances in Acoustics and Vibration, 2011. [3] Gao, W., & Wang, L. (2015). Research on dynamic transmission characteristics of box-like structures based on a hybrid model method. In Advanced Intelligent Mechatronics (AIM), 2015 IEEE International Conference on (pp. 1190-1194). IEEE.

## Towards a Unified FSI and Multiphysics Heart Simulator for Clinical Applications

Massimiliano Leoni<sup>\*</sup>, Cem Degirmenci<sup>\*\*</sup>, Johan Jansson<sup>\*\*\*</sup>, Johan Hoffman<sup>\*\*\*\*</sup>

<sup>\*</sup>KTH Royal Institute of Technology and Basque Center of Applied Mathematics, <sup>\*\*</sup>Basque Center of Applied Mathematics, <sup>\*\*\*</sup>KTH Royal Institute of Technology and Basque Center of Applied Mathematics, <sup>\*\*\*\*</sup>KTH Royal Institute of Technology and Basque Center of Applied Mathematics

### ABSTRACT

We present our plan and latest developments on our unified framework for multiphysics simulation of a human heart. Our project is built on top of our Unified Continuum formulation for fluid-structure interaction, where we solve the conservation equations for the fluid and the solid parts in a unified computational framework based on a stabilized finite elements method [1]. The long-term idea is to be able to couple this model with various domain-specific model, ideally individually designed to simulate a specific clinical procedure or heart disease, in a modular and flexible way. As a first, intermediate milestone, we already developed a simulator, for radiofrequency ablation of cardiac tissue, that solves a coupled system consisting of fluid motion, heat conduction and electrical diffusion; we plan to couple this solver with our Unified Continuum model in order to get a more reliable simulator of radiofrequency ablation of a beating heart. As an additional option, we also plan to pair Unified Continuum's intrinsic adaptive formulation into our framework, allowing for adaptivity to increase the computational efficiency of the whole procedure. More than one option is possible in this direction: h-adaptivity, where refinement is performed at the end of a primal-dual solver run on the cells that most contribute to the error on the computation of some cost functional [2], or r-adaptivity, where the mesh is moved during the computation in order to follow characteristic features of the solution as it is being computed. Our software is implemented in the FEniCS-HPC software framework for automated finite elements simulations, which has proven records of parallel performance on modern supercomputers [3].

References [1] Hoffman, J., Jansson, J., Stöckli, M. (2011). Unified Continuum Modeling of Fluid-Structure Interaction. *Mathematical Models and Methods in Applied Sciences*. [2] Jansson, J., Degirmenci, N. C., Hoffman, J. (2016). Adaptive Unified Continuum FEM Modeling of a 3D FSI Benchmark Problem. *International Journal for Numerical Methods in Biomedical Engineering*. [3] Jansson, N., Hoffman, J., Jansson, J. (2012). Framework for Massively Parallel Adaptive Finite Element Computational Fluid Dynamics on Tetrahedral Meshes. *SIAM Journal on Scientific Computing*.

## **Nuclear Fuel Assembly Deformation, Reduced Mechanical Model Dedicated to FSI Simulation**

Bertrand Leturcq\*

\*CEA, DEN, DANS, DM2S, SEMT, LM2S, F-91191 Gif sur Yvette, France

### **ABSTRACT**

In the pressure vessel of a PWR the core is constituted of a number of fuel assemblies. Under operation, they all suffer from various phenomena, among them, initial trapped efforts, thermal expansion, irradiation growth, creeping, tightening relaxation and rod slipping. Each fuel assembly may develop contacts with its neighbors and strongly interacts with the fluid. It then undergoes vertical as well as lateral fluid forces, which are partly coupled with its instantaneous shape. As a consequence the fuel assembly tends to get distorted during and still after operation. The first concern is economic: at the end of a cycle, when changing the assembly position in the core, the contact interactions with its neighbors due to its distorted shape sometimes delay the handling. The second concern is that the shutdown rods have to slide into the deformed shape of the guide tube and might be slowed due to excessive friction forces. In order to precisely assess these situations it is necessary to simulate numerically a complete core, taking into account all of the previously mentioned phenomena. For that purpose, we propose a light but relevant reduced mechanical model of a fuel assembly, partially based on a POD analysis performed on a detailed fuel assembly model. We then show that a rather simple model, still based on classical finite elements can be used and simplifies the integration of the local nonlinear constitutive equations. We then compare both of the detailed and reduced model on typical situations and show excellent agreement. The CPU time ratio between them, for a full nonlinear simulation of a single fuel assembly under operation, is over 1000, which is competitive against separation of variables based reduced order methods such as POD, PGD and even APHR[1]. So, yet still with a simplified FSI approach, the drastic memory and CPU reductions obtained now enable us to complete a 3D core simulation representing at least 4 years under operation (4 cycles), with as much as 241 individual fuel assemblies, in a reasonable time of a few hours. [1] David Ryckelynck, Djamel Missoum-Benziane. Multi-level A Priori Hyper-Reduction of mechanical models involving internal variables. Computer Methods in Applied Mechanics and Engineering, Elsevier, 2010, 199, pp.1134-1142. <10.1016/j.cma.2009.12.003>. <hal-00461492>

## Microscale Phase Field Modeling of Phase Transformation and Its Interaction with Discrete Dislocation Plasticity

Valery Levitas\*, Ehsan Esfahani\*\*

\*Iowa State University and Ames Laboratory, \*\*Iowa State University

### ABSTRACT

A microscale phase field approach with strain softening is developed to model microstructure evolution during stress-induced multivariant martensitic phase transformations [1]. In contrast to traditional phase field models, the current model is applicable to scales larger than 100 nm and without an upper limit. Gradient energy terms is omitted, but rate-type of regularization is used. During phase transformation, strain softening and related strain localization lead to separated band-like multivariant martensitic regions. The volume fraction of the martensite is the order parameter; the volume fraction of each martensitic variant is just the internal variable, and interfaces between variants are not reproduced. The model is used to study the phase transformation of a single- and polycrystal cubic (B2) austenite to monoclinic (B19') multivariant martensite in nitinol shape memory alloy. All twelve martensitic variants are engaged during the simulation of NiTi, and anisotropic elasticity is assumed for both high and low-temperature phases. Finite element model was developed and implemented into code ABAQUS. Simulations based on the presented model are showing the formation of martensitic microstructures which are in qualitative agreement with experimental observations. The results are mesh-independent and are also weakly strain-rate dependent for small strain rates. The effect of crystal orientation, polycrystalline structure, number and location of nucleation sites, an athermal friction on the evolution of the morphology of the transformed regions and global stress-strain curves are investigated under cyclic loading. In addition, pressure and shear strain-induced phase transformations in a bicrystal of a model material at the evolving dislocations pile-up have been studied at the microscale, in contrast to our previous nanoscale studies [2]. Strong stress concentrator at the tip of the dislocation pile-up significantly increases the local thermodynamic driving force for the phase transformation, which drastically reduces transformation pressure in comparison with a hydrostatic loading. This allows us to explain reduction of the transformation pressure by an order of magnitude due to plastic shear in some experiments [2,3]. 1. Esfahani S.E., Ghamarian I., Levitas V.I., Collins P.C. Microscale Phase Field Modeling of the Martensitic Transformation During Cyclic Loading of NiTi Single Crystal. Submitted. 2. Javanbakht M. and Levitas V.I. (2016) Phase field simulations of plastic strain-induced phase transformations under high pressure and large shear. Physical Review B, 94, 214104. 3. Ji C., Levitas V. I., Zhu H., et al. (2012) Shear-Induced Phase Transition of Nanocrystalline Hexagonal Boron Nitride to Wurtzitic Structure at Room Temperature and Low Pressure. PNAS, 109, 19108-19112.

## Effect of Fibre and Sheetlet Distribution on Physiological Models for Heart Contraction

Francesc Levrero-Florencio\*, Ricardo Ruiz Baier\*\*, Alfonso Bueno-Orovio\*\*\*, Vicente Grau\*\*\*\*, Blanca Rodriguez\*\*\*\*\*

\*University of Oxford, \*\*University of Oxford, \*\*\*University of Oxford, \*\*\*\*University of Oxford, \*\*\*\*\*University of Oxford

### ABSTRACT

Cardiac disease is, according to the World Health Organization (2015), the first cause of death worldwide, making the study of its underlying mechanisms a priority. A current popular and non-invasive alternative to animal testing or clinical trials is multi-scale computational modelling, particularly that which takes into account the contraction mechanisms of the heart. The heart achieves its primary role of pumping blood through the circulatory system by means of active contraction of cardiomyocytes. Cardiomyocytes have a well-defined local fibre orientation. Moreover, during systole, myocytes slide over each other in compounds of sheetlets, leading to a wall thickening of &gt;25%. In order to reproduce physiological ranges of thickening, cardiac electro-mechanical models require to incorporate such sliding mechanisms in addition to realistic fibre and sheetlet architectures. Furthermore, conditions which affect the fibre orientation distribution, such as hypertrophic cardiomyopathy (fibre disarray) might also lead to contraction abnormalities if these mechanisms are not considered. The developed models include the description of multi-physics and spatial/temporal multi-scale mechanisms and consider the coupling between electrical activation, excitation-contraction coupling, and solid mechanics. The passive mechanical behaviour is modelled with an anisotropic and incompressible hyperelastic constitutive law; the active strain orthotropic model with sliding filaments from Rossi et al. (2014) is used to represent the active contraction; electrical propagation throughout the myocardium is modelled with the bidomain equations. At the single cell level, biophysical processes underlying electrophysiology, contraction and relaxation of cardiomyocytes are represented in the model through the coupling of two systems of ODEs: the O'Hara-Rudy model for cell electrophysiology and the Land et al. (2017) excitation-contraction coupling model. The biophysical detail of this multi-scale model enables simulation of microscopic mechanisms, such as disease-induced remodelling or pharmacological blocks of specific ionic currents. The impact of the model choices on the deformation obtained for different normal or abnormal sheetlet distributions (see e.g. Potse et al., 2006) is studied. We also address an additional application considering local fibre disarray, in which the obtained deformation is compared to the normal case. This study contributes to assessing the effect of healthy and diseased sheetlet distributions on the mechanical deformation during contraction of the ventricles, and it will serve to increase the predictive capabilities of electro-mechanical cardiac models, particularly during diseased conditions. References: - Rossi et al., 2014. Eur J Mech A Solids. - Potse et al., 2006. IEEE Trans Biomed Eng. - Land et al., 2017. J Mol Cell Cardiol.

## Probably Robust Directional Vertex Relaxation for Geometric Mesh Optimization

Adrian Lew<sup>\*</sup>, Ramsharan Rangarajan<sup>\*\*</sup>

<sup>\*</sup>Department of Mechanical Engineering, Stanford University, <sup>\*\*</sup>Department of Mechanical Engineering, Indian Institute of Science Ban- galore

### ABSTRACT

We introduce an iterative algorithm called directional vertex relaxation that seeks to optimally perturb vertices in a mesh along prescribed directions without altering element connectivities. Each vertex update in the algorithm requires the solution of a max-min optimization problem that is nonlinear, nonconvex and nonsmooth. With relatively benign restrictions on element quality metrics and on the input mesh, we show that these optimization problems are well posed and that their resolution reduces to computing roots of scalar equations regardless of the type of the mesh or the spatial dimension. We adopt a novel notion of mesh quality and prove that the qualities of mesh iterates computed by the algorithm are nondecreasing. The algorithm is straightforward to incorporate within existing mesh smoothing codes. We include numerical experiments which are representative of applications in which directional vertex relaxation will be useful and which reveal the improvement in triangle and tetrahedral mesh qualities possible with it.

## **Numerical Implementation of an Invariant-Based Model for Foamed Elastomers with Strain Softening and Nonlinear Time Dependent Response**

Matthew Lewis\*

\*Los Alamos National Laboratory

### **ABSTRACT**

A hyperelastic strain energy function (Lewis, 2017) has been developed to describe the mechanical response of elastomeric foams. The model for compression as the relative density (ratio of foam density to parent material density) approaches and even exceeds unity is based on the compaction of a spherical cavity in a compressible elastomer with a Neo-Hookean response and a logarithmic pressure- volume relationship. The relative volume is multiplicatively decomposed into a part resulting from the compressibility of the solid elastomer and a part resulting from isochoric deformation of this solid. Because of this formulation, even very low porosities and large compressions can be modeled using this strain energy function. A simplified continuum damage model was introduced to capture the strain softening effect in many foamed elastomers. Additionally, a nonlinear, viscous, inelastic response after the manner of Bergstrom and Boyce (1998) has been incorporated to introduce hysteresis and rate and time dependence into the model. Details of the numerical implementation of these aspects of the model and verification are presented. Lewis, M. "A Robust, Compressible, Hyperelastic Continuum Model for the Mechanical Response of Foamed Rubber," *Technische Mechanik* 36, 1-2 (2016), 88- 101. Bergstrom, J.S. and Boyce, M.C., "Constitutive modeling of the large strain time- dependent behavior of elastomers," *JMPS* 46, 5, (1998), 931-954.

## Simulation of Material Transport in Complex Geometry of Neurons Using Isogeometric Analysis

Angran Li<sup>\*</sup>, Xiaoqi Chai<sup>\*\*</sup>, Ge Yang<sup>\*\*\*</sup>, Yongjie Jessica Zhang<sup>\*\*\*\*</sup>

<sup>\*</sup>Carnegie Mellon University, <sup>\*\*</sup>Carnegie Mellon University, <sup>\*\*\*</sup>Carnegie Mellon University, <sup>\*\*\*\*</sup>Carnegie Mellon University

### ABSTRACT

Neurons exhibit strikingly complex and diverse geometry in their highly branched networks of neurites, i.e. axons and dendrites. The geometry is essential to function of individual neurons and formation of neural circuits. However, because material synthesis and degradation in neurons are carried out mainly in the cell body, neurons must constantly transport a wide variety of essential materials throughout the complex neurite network to survive and function. How material transport is carried out in the complex neuronal geometry remains a fundamental yet unanswered. Answering this question is critical to understanding the physiology and disease of neurons. To this end, we develop an isogeometric analysis (IGA) based solver to simulate the material transport in complex neurite networks of neurons. The material transport process is described by generalizing a one-dimensional motor-assisted transport model of intracellular particles to three dimensions. We start the modeling and simulation from a single neurite, a neurite bifurcation, to a simple neurite tree structure, which are the basic structural units of the complex neurite network in neurons. We use a skeleton sweeping method to construct hexahedral meshes for them. To solve the transport equations, we first develop a Navier-Stokes equation solver based on the variational multiscale method (VMS) to obtain the velocity field of material transport in neurons. Then, we develop the solver of the motor-assisted transport equations based on the streamline upwind/Petrov-Galerkin method (SU/PG). Finally, specific boundary conditions and initial conditions based on experiments are set to validate the simulations. Our simulation can reliably reproduce the spatiotemporal dynamics of material transport in neurons.

## Investigation of Dynamic Load Effect on LiCoO<sub>2</sub> Cathode of Lithium-ion Battery with Nanomechanical Raman Spectroscopy Analysis

Bing Li<sup>\*</sup>, Ryan Adams<sup>\*\*</sup>, Jafr Kazmi<sup>\*\*\*</sup>, Vikas Tomar<sup>\*\*\*\*</sup>, Vilas Pol<sup>\*\*\*\*\*</sup>, Tom Adams<sup>\*\*\*\*\*</sup>,  
William Kellerhals<sup>\*\*\*\*\*</sup>

<sup>\*</sup>Purdue University, <sup>\*\*</sup>Purdue University, <sup>\*\*\*</sup>United States Military Academy at West Point, <sup>\*\*\*\*</sup>Purdue University,  
<sup>\*\*\*\*\*</sup>Purdue University, <sup>\*\*\*\*\*</sup>Naval Surface Warfare Center, Crane Division, <sup>\*\*\*\*\*</sup>Purdue University

### ABSTRACT

For mechanical property and in service behavior analyze of material with complex composition and morphology, nano level mechanical tests including nano-impact have been proved successful for application on alloy and metallic powder[1]. For decades lithium-ion battery (LIB) has been accepted in energy storage industry as one of the most mature yet promising secondary batteries. However there are still safety flaws of LIB, one main hazard is dynamic impact generated defects in transportation, which could cause battery capacity drop. With most dynamic effect evaluation carried out at battery level, there exists need for evaluation of dynamic response of electrode excluding contribution of battery housing. Electrode material of LIB is typically in form of powder mixture consists of electroactive material, conductive agent and binder with particle diameter at level of micrometer. Considering composite composition and powder morphology nature, it is essential for battery design to obtain information of response and effect of dynamic load of electroactive material at nano level to reveal effect on electrode structure and influence on battery performance. Technique of nanomechanical Raman spectroscopy analysis developed by Interfacial Multiphysics group of Purdue University[2] was applied for investigation of dynamic response and corresponding structural change of LiCoO<sub>2</sub> cathode. Electrode was exposed to dynamic load for direct impact, with electrochemical structure evaluation carried out with analysis of impact history and nanomechanical Raman analysis, applied dynamic load was related with electrode structural response at nano level and battery electrochemical performance for first time. It was shown that direct dynamic impact is related with noticeable capacity drop of electrode which presented proportional relation with impact cycles. Change of electrochemical material structure was represented with positive Raman shift observed. [1]. Beake, B. D., et al. &quot;Investigating the correlation between nano-impact fracture resistance and hardness/modulus ratio from nanoindentation at 25–500° C and the fracture resistance and lifetime of cutting tools with Ti<sub>1-x</sub>Al<sub>x</sub>N (x= 0.5 and 0.67) PVD coatings in milling operations.&quot; Surface and Coatings Technology 201.8 (2007): 4585-4593. [2]. Gan, Ming, and Vikas Tomar. &quot;Surface stress variation as a function of applied compressive stress and temperature in microscale silicon.&quot; Journal of Applied Physics 116.7 (2014): 073502.

## Concurrent Multiscale Modeling of Ductile Failure Mechanisms in Metals

Bo Li<sup>\*</sup>, Hao Jiang<sup>\*\*</sup>

<sup>\*</sup>Case Western Reserve University, <sup>\*\*</sup>Case Western Reserve University

### ABSTRACT

We propose a high-performance computing based multiscale computational tool for the high fidelity prediction of ductile failure mechanisms in metals undergoing arbitrary deformations. A three-dimensional finite element model of the polycrystalline structure of metals at the mesoscale is reconstructed by incorporating the probability distribution functions (PDF) of grain sizes, orientation and misorientation angles from the experimental EBSD data. In particular, grain boundaries are explicitly represented by a thin layer of elements with non-zero misorientation angles. The behavior of the material at each finite element is obtained from a concurrent analysis of a representative volume element (RVE). Accordingly, we refer to the RVE as the packed hollow sphere (PHS) model and solved by a Ritz–Galerkin method based on spherical harmonics, specialized quadrature rules, and exact boundary conditions at the microscale. A single crystal plasticity model with the strain hardening law related to the local misorientation angle is employed at each quadrature point to predict the deformation of the hollow sphere and void growth in the RVE. The finite element at the mesoscale fails as the void of the representative hollow sphere grows beyond some critical size. As a result, the model predicts the strong coupling between polycrystal plasticity and void deformation to simulate the ductile failure mechanism in polycrystalline structures. The proposed method is validated in an example of spallation fracture in aluminum alloys under high velocity impact conditions.

## **A Micro-Mechanical Model of Saturated Granular Soils Using Discrete-Elements and a Lattice Boltzmann Form of the Averaged Navier-Stokes Equations**

Bo Li\*, Mourad Zeghal\*\*

\*Rensselaer Polytechnic Institute, \*\*Rensselaer Polytechnic Institute

### **ABSTRACT**

Saturated granular soils consists of grains forming a solid skeleton and water filling the pores. These soils exhibit a broad range of response patterns depending on the level of confining stresses and pore pressures, including granular flow, liquefaction, dilation and others. A number of studies were successfully conducted using a continuum-discrete approach to model the hydro-mechanical response of these soils. The solid phase is modeled using the Discrete Element method and the fluid phase is idealized using volume-averaged Navier Stokes (VANS) equations. The numerical solution of these equations is often tackled using the finite volume technique, which has limitation when used to solve complex-geometry problems. In this study, the lattice Boltzmann method (LBM) is modified and adapted to solve the VANS equations for incompressible pore fluid flow. This method employs fine lattice meshes and is highly effective in accommodated complex conditions. A new pressure correction term is introduced to resolve the solution inaccuracy and instability at the interface between zones of highly dissimilar permeabilities. A modified mass-source term is employed to ensure an accurate and stable solution to dynamic problems in which the porosity varies with time. A series of benchmark tests were preformed, and the proposed LBM scheme was found to agree well with analytical solutions.

## Correlation Analysis of Statistical Descriptors for Heterogeneous Materials

Chenfeng Li<sup>\*</sup>, SQ Cui<sup>\*\*</sup>, JL Fu<sup>\*\*\*</sup>

<sup>\*</sup>Swansea University, <sup>\*\*</sup>Swansea University, <sup>\*\*\*</sup>Swansea University

### ABSTRACT

Heterogeneous materials such as rock, concrete, composite often exhibit a random micro-structure, where two or more material phases distribute randomly through the medium. It is known that the mechanical, electrical, thermal properties of the heterogeneous material are closely related to the random morphology of micro-structure. For a specific heterogeneous material, a central requirement that is often raised is to predict the macro-scale properties from the morphological features of micro-structure. To achieve this goal, a number of statistical descriptors have been proposed in material science and computational mechanics to quantify the random morphology of heterogeneous materials. However, these statistical descriptors have very different mathematical formulation, and even worse some do not even have a closed form equation. As such, it is very difficult, if not impossible, to understand clearly the relationship between these statistical descriptors, which has long hampered the research progress of heterogeneous materials. This work address this challenge, by proposing a novel machine-learning base approach to quantitatively measure the correlation between various statistical descriptors. Furthermore, based on the correlation analysis, the statistical descriptors can be classified into different groups with similar descriptors grouped together. This classification not only helps to understand the characteristics of heterogeneous materials, but it also guide the researchers and engineers in material design and evaluation.

## Thermomechanical Extended Layerwise Method of Laminated Composite Plates

Dinghe Li\*, Jacob Fish\*\*

\*Civil Aviation University of China/Columbia University, \*\*Columbia University

### ABSTRACT

With accelerating use of aeronautic and aerospace composite structures in the high-temperature operating conditions, numerous research works were published on heat transfer and thermal stress analysis of laminated composite plates and shells during the last three decades. In order to uncouple heat transfer and thermal stress analyses, the thermomechanical dissipation was neglected in most of the existing analytical and numerical models. In addition, considerable research works were carried out under the steady-state assumption by considering the thermal effect as an additional term in the constitutive relationship. However, when the dynamic disturbances resulting from the heat flow are considered, the thermomechanical dissipation is of primary interest. Existing works mainly focus on the thermomechanical fracture problem of delamination or transverse cracking, but only few studies have been conducted on multiple delaminations and problems in which the delamination and transverse cracks interact. In the present work, a Thermomechanical Extended Layerwise Method (TELM) is developed for the laminated composite plates with multiple delaminations and transverse cracks. The discontinuity of displacements and temperature induced by multiple delaminations is simulated by strong discontinuous function while the discontinuity of strain and temperature gradient between dissimilar layers is modeled by a weak discontinuous function. Transverse cracks are modeled using classical Extended Finite Element Method (XFEM). The coupled thermomechanical variational principle is employed to derive the Euler equations and the discrete forms. Since the displacement and temperature fields are solved simultaneously, a fully coupled time integration method is developed based on the Newmark integration algorithm and Crank-Nicolson scheme. The strain energy release rate for multiple delamination fronts and stress intensity factors for transverse cracks are calculated by the Virtual Crack Closure Technique and the Interaction Integral Method, respectively. The proposed method is applied to the steady-state thermomechanical problems, elastic and thermomechanical dynamic problems for isotropic and composite plates with transverse cracks and multiple delaminations.

## **Development of Efficient Algorithms in the Design of Phononic Crystals / Acoustic Metamaterials**

Eric Li\*, ZC He\*\*

\*Teesside University, \*\*Hunan University

### **ABSTRACT**

The phononic crystals (PCs) / acoustic metamaterials (AMs) are periodic man-made composite materials. In this paper, a mass-redistributed finite element method (MR-FEM) is formulated to study the wave propagation within fluid PCs, solid/fluid PCs and fluid/solid PCs with fluid-structural interaction. With a perfect balance between stiffness and mass in the MR-FEM model, the dispersion error of longitudinal wave is minimized by redistribution of mass. In addition, the mathematical model to predict the upper and lower bounds of mechanical response of AMs with uncertainty parameters such as Young's modulus, Poisson's ratio and density, is established by the nonlinear interval perturbation hybrid node-based smoothed finite element method (NIPH-NS/FEM). One of the main features of NIPH-NS/FEM with a softened effect in the discretized model is capable to overcome the volumetric locking issue of incompressible rubber in the standard finite element method (FEM).

## **A Two-Scale Generalized FEM for the Evaluation of Stress Intensity Factors at Spot Welds in Large Structures**

Haoyang Li<sup>\*</sup>, Carlos Duarte<sup>\*\*</sup>

<sup>\*</sup>University of Illinois at Urbana-Champaign, <sup>\*\*</sup>University of Illinois at Urbana-Champaign

### **ABSTRACT**

Spot welds are commonly used to join thin gauge metallic structural components of automotive and aerospace vehicles. The failure of spot welds in these components may lead to the catastrophic loss of the structure. One of the common failure modes of spot welds is fatigue crack propagation through the surrounding material of the spot weld edge. Hence, resolving the local stress fields and extracting Stress Intensity Factors (SIFs) with high fidelity is rather important. The goal of this research is to simulate a large number of spot welds in representative aircraft panels and to calculate SIF variations at each weld with high accuracy and efficiency. This class of problem poses three major challenges. First, the disparate scales involved in a large structure with hundreds of spot welds prevent the discretization of all spot welds in a single FEM model. Second, a proper finite element (FE) approximation is needed to capture the singularity along spot weld edges. Third, an accurate extraction method is required to compute SIFs based on the FE solutions. In this presentation we report on a novel two-scale Generalized Finite Element Method with global-local enrichment (GFEMgl) to solve the target problem. This GFEMgl is a scale-bridging method which uses the solution of a local problem defined for each spot weld as enrichment functions for the structural-scale (global) model. This methodology allows the discretization of each spot weld independently of each other using fine meshes at the local scale, while keeping the global mesh fairly coarse. While solving local problems, a GFEM with singular function enrichments is deployed to capture the stress field along the crevice of each spot weld. With the help of the global-local enrichment, the localized phenomena can be accurately recovered in the global model. Finally, the Displacement Correlation Method (DCM) is adopted to evaluate SIFs along spot weld edges. Numerical experiments show that the proposed GFEMgl framework combined with the DCM can address all the aforementioned challenges and achieve comparable accuracy to the direct finite element simulation with the fine-scale features discretized in the global mesh. Furthermore, the proposed two-scale framework offers greater parallel efficiency in the simulation of structures with a large number of spot welds since local problem solutions are inherently parallel.

## Data Compression in Multiscale Analysis for Composite Materials

Hengyang Li<sup>\*</sup>, Jiaying Gao<sup>\*\*</sup>, Cheng Yu<sup>\*\*\*</sup>, Modesar Shakoor<sup>\*\*\*\*</sup>, Wing Kam Liu<sup>\*\*\*\*\*</sup>

<sup>\*</sup>Northwestern University, <sup>\*\*</sup>Northwestern University, <sup>\*\*\*</sup>Northwestern University, <sup>\*\*\*\*</sup>Northwestern University, <sup>\*\*\*\*\*</sup>Northwestern University

### ABSTRACT

Composite materials, such as fiber reinforced plastic, filled rubber, and composite laminates, are widely used in the industry. Their complex microstructures can be modeled at the scale of structures using multiscale analysis but with a huge computational burden. The discovery of efficient and accurate multiscale modeling methods is a challenge for researchers. Concurrent homogenization can be coupled to reduced order modeling techniques to efficiently generate material laws directly from the solution of Representative Volume Element (RVE) problems and use them in a finite element model of the structure. This presentation will present recent developments in concurrent multiscale modeling using data science to generate material laws. In particular, the recently proposed Self-consistent Clustering Analysis method [1][2][3] is used to solve RVE problems based on the assumption that material points of the RVE that have similar mechanical response can be associated to the same degrees of freedom. This association is generated automatically using data clustering techniques such as k-means, Self-organizing Map. The large RVE can be homogenized into a group of clusters. This will largely reduce the calculation cost in the following analysis. However, the influence of different data compression algorithms still needs more study. This presentation focusses on the accuracy and efficiency of different data science algorithms on data compression in multiscale analysis. Suggestion will be given based on comparison between difference data science algorithms. [1] Liu, Zeliang, M. A. Bessa, and Wing Kam Liu. &quot;Self-consistent clustering analysis: an efficient multi-scale scheme for inelastic heterogeneous materials.&quot; Computer Methods in Applied Mechanics and Engineering 306 (2016): 319-341. [2] Liu, Zeliang, Mark Fleming, and Wing Kam Liu. &quot;Microstructural material database for self-consistent clustering analysis of elastoplastic strain softening materials.&quot; Computer Methods in Applied Mechanics and Engineering 330 (2018): 547-577. [3] Bessa, M. A., et al. &quot;A framework for data-driven analysis of materials under uncertainty: Countering the curse of dimensionality.&quot; Computer Methods in Applied Mechanics and Engineering 320 (2017): 633-667.

## **A Multiphysics Model for Characterization of Responsive Performance of Urea-Sensitive Hydrogel**

Hua Li<sup>\*</sup>, K. B. Goh<sup>\*\*</sup>, K. Y. Lam<sup>\*\*\*</sup>

<sup>\*</sup>Nanyang Technological University, Singapore, <sup>\*\*</sup>Nanyang Technological University, Singapore, <sup>\*\*\*</sup>Nanyang Technological University, Singapore

### **ABSTRACT**

A remarkable feature of biomaterials is their ability to deform in response to certain external bio-stimuli. In this talk, a novel biochemo-electro-mechanical model is presented for the numerical characterization of the urea-sensitive hydrogel in response to the external stimulus of urea. Usually the urea sensitivity of the hydrogel is characterized by the states of ionization and denaturation of the immobilized urease, as such that the model includes the effect of the fixed charge groups and temperature coupled with pH on the activity of the urease. Therefore, a novel rate of reaction equation is proposed to characterize the hydrolysis of urea that accounts for both the ionization and denaturation states of the urease subject to the environmental conditions. After examination with the published experimental data, it is thus confirmed that the model can characterize well the responsive behaviour of the urea-sensitive hydrogel subject to the urea stimulus, including the distribution patterns of the electrical potential and pH of the hydrogel. The results point to an innovative means for generating electrical power via the enzyme-induced pH and electrical potential gradients, when the hydrogel comes in contact with the urea-rich solution, such as human urine.

## **Integrated Thermal-fluid-structural Analysis of Metallic Powder-substrate Interaction Using Phase Field Method**

Ji-Qin Li\*, Tai-Hsi Fan\*\*

\*Department of Mechanical Engineering, University of Connecticut, \*\*Department of Mechanical Engineering, University of Connecticut

### **ABSTRACT**

Selective laser melting of metallic powders is broadly applied in additive manufacturing process for building geometrically complicated parts. Understanding the underlying transport phenomena that control the fusion dynamics of the metallic powders is important to enhance the surface quality of the additive manufacturing parts and reduce their residual stress during the thermal manufacturing processes. Theoretical analysis focusing on resolving the small scale dynamics at the powder level, especially on the laser-powder-substrate interactions, is therefore critical on improving the process technology and product quality. Phase field method provides an excellent platform to develop new theoretical model that can combine thermal fluids, interfacial evolution, and elastic structural response into an integrated framework to simulate the process dynamics of metallic powders on various substrates. Here we present phase field formulation and simulation of the dynamics of single powder-substrate interactions driven by a pulsed laser beam. The entropy-based approach is applied in deriving the integrated model to ensure thermodynamical consistency of the deformable interfaces. Without the complication of evaporation from the liquid metal, this simplified 2D model describes fully coupled phenomena including melting, partially deforming interfaces, thermal capillary flow, and thermal expansion and elastic structure response during the heating and cool off processes. Thermal physical properties including thermal conductivity, viscosity of the liquid metal, and surface tension are considered temperature-dependent. The process dynamics is computationally resolved and characterized by the temperature distribution, interfacial evolution, thermal capillary pattern, thermal stress induced in the bulk substrate, and the overall morphology change after the pulse heating. The conceptual theoretical framework is important for further development on predicting complicated morphology involving many or hybrid powders, and for the prediction of void formation due to incomplete melting or fusion of metallic powders.

## Microstructural Analysis for the Nano-Indentation in Shape Memory Alloys by Using Molecular Dynamics Simulation

Ji-Ting Li<sup>\*</sup>, Nien-Ti Tosu<sup>\*\*</sup>

<sup>\*</sup>NCTU, <sup>\*\*</sup>NCTU

### ABSTRACT

Shape memory alloys (SMAs) have been widely used in medicine, aerospace and industry because of its superelasticity and shape memory effect. Many experimental measurements are used to study the origin of these two special properties, such as temperature-induced and stress-induced martensitic transformation. Nano-indentation is one of the stress-induced martensitic transformation way and particularly useful to characterize the properties of SMAs, such as hardness, elastic modulus, and the level of shape memory effect. However, only the macroscopic properties were considered and the discussion about the variants of microstructures due to the martensitic transformation is still limited. In recent years, Molecular Dynamics (MD) simulations opens an opportunity for SMA analysis. Most of these studies only focus on the crystal system after the martensitic transformation but mention the variants few. Typically, these methods identify limited sets of the crystal variants. The aim of this study is to develop a method to identify the variants in MD simulation, and then, apply to study the microstructures due to the martensitic transformation in NiTi SMAs. So far, this method had been successfully used in the temperature-induced martensitic transformation model. In this study, we focus on the microstructure evolutions of stress-induced martensitic transformation during the indentation process. The volume of each variant during the indentation process can be predicted. The interfaces between crystal variants are also examined by compatibility theory. Besides, the relationship between microstructure and mechanical properties are defined, such as hardness. Moreover, the curve features with the corresponding microstructures and the force-displacement distribution of the crystal are also discussed. It is expected to provide the design guidelines in current studies for the SMA applications. Keywords: Shape memory alloys, Molecular dynamics, Indentation, Crystal variants, Microstructure

## The Shifted Interface Method for Embedded Interface Computations

Kangan Li<sup>\*</sup>, Alex Main<sup>\*\*</sup>, Guglielmo Scovazzi<sup>\*\*\*</sup>

<sup>\*</sup>Duke University, <sup>\*\*</sup>Duke University, <sup>\*\*\*</sup>Duke University

### ABSTRACT

Based on the previous work on surrogate boundary method for embedded domain computations, we extend it to the embedded interface problems. The key idea of this approach is shifting the real interface to the surrogate interface. In order to preserve optimal convergence rate of the numerical solution, the shifted interface jump conditions are enforced weakly by using the minimum distance and Taylor expansions. From our view of point, this method is efficient and robust. We apply this concept here to the Poisson interface problems. In particular, we also present the numerical analysis and simulations for Poisson equations defined on complicated geometries.

## **Three-dimensional Finite Element Modeling of Dynamic BMP Gradient Formation in Zebrafish Embryonic Development**

Linlin Li<sup>\*</sup>, Xu Wang<sup>\*\*</sup>, Adrian Buganza Tepole<sup>\*\*\*</sup>, Tzu-ching Wu<sup>\*\*\*\*</sup>, David Umulis<sup>\*\*\*\*\*</sup>

<sup>\*</sup>Purdue University, <sup>\*\*</sup>Purdue University, <sup>\*\*\*</sup>Purdue University, <sup>\*\*\*\*</sup>Purdue University, <sup>\*\*\*\*\*</sup>Purdue University

### **ABSTRACT**

Bone Morphogenetic Proteins (BMPs) play a significant role in dorsal-ventral (DV) patterning of the early zebrafish embryo. BMP signaling is regulated by extracellular, intracellular, and cell membrane components. BMPs pattern the embryo during development at the same time that cells grow and divide to enclose the yolk during a process called epiboly. We developed a new three-dimensional growing finite element model to simulate the BMP patterning and epiboly process during the blastula stage. Quantitative whole mount RNA scope data of BMP2b and phosphorylated-SMAD data are collected and analyzed to precisely test the hypotheses of gradient formation in our model. We found that the growth model results in consistent spatially and temporally evolving BMP signaling dynamics within a range of biophysical parameters including a minimal rate of ligand diffusion.

## **Influence of Volume Fraction on the Effective Friction Law for Transient Granular Avalanche**

Liuchi Li\*, José Andrade\*\*

\*Caltech, \*\*Caltech

### **ABSTRACT**

We experimentally measure the dynamics of transient granular avalanche with two different types of grain in a rotating drum and for the first time carry out 3D soft particle simulations that are able to produce quantitatively comparable results, from which we discover a non-one-to-one relation of the widely used  $\mu_I$  law. We suggest that such phenomenon is caused by the relative dilation or contraction of granular material with respect to its steady state as transient flow develops and accordingly we propose a modification for  $\mu_I$  that can capture our major simulation observations. This finding provides important physical insight into understanding transient flow in comparison to steady flow by revealing the significance of volume fraction variation and its close connection with the effective friction coefficient, both of which can be key ingredients in accurately modeling the dynamics of transient flow that the current incompressible visco-plastic granular flow model fails to produce quantitative agreement with experimental measurements such as density variation and velocity evolution.

## Numerical Simulation of Sloshing Flows of Liquid Tanks in Waves

Qi Li\*, Decheng Wan\*\*

\*Shanghai Jiao Tong University, \*\*Shanghai Jiao Tong University

### ABSTRACT

The exploitation and the transportation of liquid natural gas energy is very challenging and dangerous in Ocean Engineering. In order to solve these problems, a new type of offshore unit FLNG (floating liquefied natural gas vessel) has been proposed. Among many problems that threatening the survival performance of FLNG, the liquid sloshing problem caused by partially filled LNG tanks has a significant coupling influence on FLNG motion. Different from the potential flow method in previous researches, computational fluid dynamics (CFD) method has its unique advantages, such as the consideration of fluid viscosity and the strong nonlinear phenomena. Using our in-house unsteady RANS solver, naoe-FOAM-SJTU, which is developed and based on the open source tool libraries of OpenFOAM, the sloshing coupled effect of a floating box which equipped with liquid tanks is simulated in numerical wave conditions in this paper. Firstly, the motions of the floating box with empty tanks in waves are simulated, the accuracy and effectiveness of the solver are validated by comparing its results with experiment results. Next, to clarify the sloshing influence on ship motion, several tank filling ratios (24.3%, 38.3%, 61.3%) are considered under the same incident wave frequency. The time histories of the corresponding motions are given and discussed, and the influence of the sloshing resonance frequency on sloshing phenomena is revealed and studied. Meanwhile, naoe-FOAM-SJTU solver can also calculate the moments on inside wall and outside wall of the liquid tank, so the coupling influence on the structure motion caused by sloshing and wave force can be studied individually. It is noticed that the amplitude of the rolling motion of the liquid tank has an obvious connection with the phase differences between sloshing moment and wave moment. All above results agree well with the experimental results, which shows that the naoe-FOAM-SJTU solver can effectively simulate the sloshing-motion coupling problem under the wave environment. Besides, on the basis of this study, further researches about other sloshing factors can be carried out in the future.

## Atomic-scale Investigation of Tensile Mechanical Properties of Nano-twinned Cu-Ag Multilayers

Qian Li<sup>\*</sup>, Yonggang Zheng<sup>\*\*</sup>, Hongwu Zhang<sup>\*\*\*</sup>, Hongfei Ye<sup>\*\*\*\*</sup>

<sup>\*</sup>Dalian University of Technology, P. R. China, <sup>\*\*</sup>Dalian University of Technology, P. R. China, <sup>\*\*\*</sup>Dalian University of Technology, P. R. China, <sup>\*\*\*\*</sup>Dalian University of Technology, P. R. China

### ABSTRACT

Understanding the mechanical properties and plastic deformation mechanisms of nano-twinned multilayered materials is essential to provide design parameter in the preparation of multilayer composites. Though extensive experiments and simulations conducted in recent years showed that the strength of nanoscale multilayered metallic materials is strongly dependent on the individual layer thickness, there is still a lack of a thorough understanding on the strengthening effect and underlying mechanism mediated by the hetero interface and twin boundary. In our recent work, we investigated the tensile mechanical properties and plastic deformation mechanisms of nano-twinned Cu//Ag multilayered materials based on molecular dynamics simulations. The simulation results show that, due to the different hetero interfacial configurations, the hetero-twin interfaces have a stronger resistance effect on the dislocation motion than that of the cube-on-cube hetero interfaces, the strength of hetero-twin multilayered materials is higher than that of the cube-on-cube samples. The strength increases with the increase of layer thickness of nano-twinned Cu//Ag multilayered materials with a constant twin spacing, while it decreases with the increase of layer thickness for twin-free ones, which is due to the stronger strengthening effect of the twin boundary than both the cube-on-cube and hetero-twin interfaces between Cu and Ag layers. The confined layer slip of dislocation is found to be the dominant plastic deformation mechanism for twin-free hetero-twin multilayered materials and the strengthening effect of twins follows the conventional Hall-Petch relationship in the nano-twinned multilayered composites. These results may provide guidelines to the fabrication of high strength nano-twinned multilayered metallic materials. References [1] Zheng, Y.; Li, Q.; Zhang, J.; Ye, H.; Zhang, H.; Shen, L. Hetero interface and twin boundary mediated strengthening in nano-twinned Cu//Ag multilayered materials. *Nanotechnology*. 2017, 28, 415705. [2] Zhang, J.; Zhang, H.; Ye, H.; Zheng, Y. Free-end adaptive nudged elastic band method for locating transition states in minimum energy path calculation. *J. Chem. Phys.* 2016, 145, 094104. [3] Zhang, J.; Zhang, H.; Ye, H.; Zheng, Y. Twin boundaries merely as intrinsically kinematic barriers for screw dislocation motion in FCC metals. *Sci. Rep.* 2016, 6, 22893.



## Analytic Modelling of Reactive Diffusion for Transient Electronics

Rui Li<sup>\*</sup>, Yonggang Huang<sup>\*\*</sup>, John A. Rogers<sup>\*\*\*</sup>

<sup>\*</sup>State Key Laboratory of Structural Analysis for Industrial Equipment, Department of Engineering Mechanics, and International Research Center for Computational Mechanics, Dalian University of Technology, <sup>\*\*</sup>Northwestern University, <sup>\*\*\*</sup>Northwestern University

### ABSTRACT

Transient electronics [1] is a class of technology that involves components which physically disappear, in whole or in part, at prescribed rates and at programmed times. Enabled devices include medical monitors that fully resorb when implanted into the human body (“bio-resorbable”) to avoid long-term adverse effects, or environmental monitors that dissolve when exposed to water (“eco-resorbable”) to eliminate the need for collection and recovery. Analytic models for dissolution of the constituent materials represent important design tools for transient electronic systems that are configured to disappear in water or biofluids [2, 3]. In this talk, solutions for reactive-diffusion are presented in both single- and double-layered structures, in which the remaining thicknesses and electrical resistances are obtained analytically. The dissolution time and rate are defined in terms of the reaction constants and diffusivities of the materials, the thicknesses of the layer, and other properties of materials and solution. These models are well validated by the experiments, and provide effective approaches to new designs of biofluid barriers for flexible electronic implants. Keywords: transient electronics, biofluid barrier, reactive diffusion, analytic model [1] S.-W. Hwang, H. Tao, D.-H. Kim, H. Cheng, J.-K. Song, E. Rill, M. A. Brenckle, B. Panilaitis, S. M. Won, Y.-S. Kim, Y. M. Song, K. J. Yu, A. Ameen, R. Li, Y. Su, M. Yang, D. L. Kaplan, M. R. Zakin, M. J. Slepian, Y. Huang, F. G. Omenetto, J. A. Rogers, *Science* 2012, 337, 1640. [2] R. Li, H. Cheng, Y. Su, S.-W. Hwang, L. Yin, H. Tao, M. A. Brenckle, D.-H. Kim, F. G. Omenetto, J. A. Rogers, Y. Huang, *Adv. Funct. Mater.* 2013, 23, 3106. [3] E. Song, Y. K. Lee, R. Li, J. Li, X. Jin, K. J. Yu, Z. Xie, H. Fang, Y. Zhong, H. Du, J. Zhang, G. Fang, Y. Kim, Y. Yoon, M. A. Alam, Y. Mei, Y. Huang, J. A. Rogers, *Adv. Funct. Mater.* 2017, 1702284.

## **A Novel Homogenisation-Aided Topology Optimisation Method for Fast Design of Graded Microstructures in Additive Manufacturing**

Shaoshuai Li<sup>\*</sup>, Yichao Zhu<sup>\*\*</sup>, Weisheng Zhang<sup>\*\*\*</sup>, Xu Guo<sup>\*\*\*\*</sup>

<sup>\*</sup>Dalian University of Technology, <sup>\*\*</sup>Dalian University of Technology, <sup>\*\*\*</sup>Dalian University of Technology, <sup>\*\*\*\*</sup>Dalian University of Technology

### **ABSTRACT**

Devices equipped with graded microstructures (GMs) whose constituting cells gradually deform in space have seen their vast engineering potentials in various industrial sectors, especially after the introduction of the 3D printing techniques. Given the fact that microscopic search for the optimal design of GMs is in general computationally unaffordable, homogenisation-aided topology optimisation (termed as "HATO") approaches provide numerous perspectives on fast design of additively manufacturable GMs. Up to now, however, a majority of existing HATO methods are dedicated for studying periodic lattice configurations. Here we present a novel homogenisation-aided topology optimisation approach (termed as "HATO plus"), where the originally multiscale optimisation problem gets asymptotically decomposed into two sub-problems concurrently taking place on different length scales. Compared to traditional HATO methods, HATO plus exhibits essential advantages which make it a suitable platform for the fast design of additively manufacturable GMs. Firstly, HATO plus stores GMs in a highly compressible manner. Under the HATO plus framework, a GM can be expressed with fewer design parameters. Secondly, existing common topology optimisation methods such as solid isotropic material with penalization (SIMP)/level-set approaches and moving morphological components (MMC)/voids (MMV) can be readily implemented within the HATO plus framework. Thirdly, HATO plus accommodates far more design freedom for GMs than traditional inverse-homogenisation-based schemes. Finally, the proposed HATO plus framework enjoys a diminishing FE-analytical scale compared to methods built on finer grid, while the abundance of its describable configurations is well maintained at the same time. Several simulation results will be presented to demonstrate the aforementioned advantage displayed by the HATO plus scheme.

## **Multi-scale and Multi-physics Simulations for Dusty Flows in Proto-Planetary Disks**

Shengtai Li\*

\*Los Alamos National Laboratory

### **ABSTRACT**

The recent observations from the ALMA telescope have revealed much detailed structures in many observed proto-planetary disks. The disks can be modeled as turbulent dusty gas motions around a central star with potential embedded planets. To simulate the formation of those disks and its interaction with embedded planets, we have developed a multi-scale and multi-physics numerical tool that can handle the interactions between gas and gas, gas and dust, dust and dust, disk and planets simultaneously. The dusty gas motion is solved as bi-fluid Navier-Stokes equations with the dust treated as the pressure-less flow. The stiff coupling between the dust and gas are solved by a semi-implicit method to improve the time step. The dust coagulation and fragmentation is treated using a partial equilibrium method. Numerical results are presented to demonstrate the effectiveness of our method.

## Multiscale Continuous Discontinuous Element Model and the Progressive Failure Rate

Shihai Li<sup>\*</sup>, Qindong Lin<sup>\*\*</sup>, Dong Zhou<sup>\*\*\*</sup>, Chun Feng<sup>\*\*\*\*</sup>, Yongbo Fan<sup>\*\*\*\*\*</sup>

<sup>\*</sup>Institute of Mechanics, Chinese Academy of Sciences, <sup>\*\*</sup>Institute of Mechanics, Chinese Academy of Sciences,  
<sup>\*\*\*</sup>Institute of Mechanics, Chinese Academy of Sciences, <sup>\*\*\*\*</sup>Institute of Mechanics, Chinese Academy of Sciences,  
<sup>\*\*\*\*\*</sup>Institute of Mechanics, Chinese Academy of Sciences

### ABSTRACT

The main features of the continuum discontinuum element method (CDEM), that is based on the generalized Lagrange equation, are introduced. The basic framework of this method is to express the variables in the continuous field and discontinuous field with the variables defined on discrete nodes, which are regarded as generalized variables of the generalized Lagrange equation. The unified expression for fluid, solids and discrete bodies can be obtained. A multi-scale calculation framework for the rock mass by CDEM is established. The physical meaning and the relationship of each scale are expressed, which including engineering scale for engineering problems, element scale for the numerical model, test scale for the continuous media model, micro particle scale for the continuous property and molecular scale for energy dissipation. The failure load on the microplanes within the representative volume element (RVE) is defined, that is the dot product of the stress intensity and the plane vector on microplane. On this basis, the concept of the progressive failure rate for heterogeneous media is proposed, which is defined as the ratio of the force on the microplane and the boundary force. The progressive failure rate represents the heterogeneity of the strength on the microplanes, which is equal to 1 when the strength of the microplanes are the same and will become higher when the loads on the microplanes are more inhomogeneous. The relationship between the force of the particle size and the Van Edward force between molecules is discussed. The progressive failure ratio can be also expressed as the ratio of the fracture force of the molecular bond and the load between particles. The results show that the progressive failure model on the molecular scale can describe the material properties of solids reasonably. When used as a constitutive model in the numerical computation, the influence of the mesh shape become much less, which could be an effective way to resolve the mesh dependence problem.

## Wrinkling of a Vesicle in Viscous Fluid

Shuwang Li\*

\*Illinois Institute of Technology

### ABSTRACT

We study the nonlinear, nonlocal dynamics of two-dimensional vesicles in a time-dependent, incompressible viscous flow at finite temperature. We focus on a transient wrinkling instability that can be observed when the surface tension becomes negative, e.g. the direction of applied flow is suddenly reversed. In the quasi-circular limit, we derive a Langevin type stochastic differential equation. Using a stochastic immersed boundary method with a biophysically motivated choice of thermal fluctuations, we find that thermal fluctuations actually have the ability to attenuate variability of the characteristic wavelength of wrinkling by exciting more wrinkling modes. Reference: Liu, Kai and Hamilton, Caleb and Allard, Jun and Lowengrub, John and Li, Shuwang, Wrinkling dynamics of fluctuating vesicles in time-dependent viscous flow, *Soft Matter*, 2016, 5663-5675.

## **Finite-element Analysis of Fracture Toughness of Bovine Cortical Bone: Effect of Osteonal Micro-morphology**

Simin Li<sup>\*</sup>, Mayao Wang<sup>\*\*</sup>, Vadim Silberschmidt<sup>\*\*\*</sup>

<sup>\*</sup>Loughborough University, <sup>\*\*</sup>Loughborough University, <sup>\*\*\*</sup>Loughborough University

### **ABSTRACT**

A crack-propagation process in cortical bone is difficult to comprehend using only in-situ experimental studies. A previous work [1] assessed quantitatively the fracture toughening mechanisms of cortical bone using a compact-tension experiment, characterising a linear rising fracture resistance curve, R-curve. Even though a final crack-propagation path could be observed with microscopy, the effect of osteonal morphology and their interaction with a surrounding matrix are still not documented properly. In this paper, a finite-element method employing a zero-thickness cohesive-element scheme was used to analyse the effect of micro-morphology of cortical bone on the crack-propagation process in a bone tissue. Microstructured models of cortical bone, incorporating statistical realisations of main features of the osteonal structure, consisting of osteons, cement lines and an interstitial matrix, were developed. They were based on osteonal morphometric parameters, acquired from experimental samples at posterior cortex of bovine cortical bone and used to simulate the process of crack propagation in the compact-tension experiment. The results of numerical simulations, validated experimentally, demonstrated that the suggested approach is an efficient method for investigation of the crack-growth process and fracture mechanics at micro-level. Observations from the experiments and simulation results indicated that the cement line acted as crack-inhibiting mechanism attracting surrounding cracks, while preserving the osteons. Crack-ligament bridging, another extrinsic toughening mechanism of cortical bone, happens for osteons with relatively large Haversian canals. Still, it is difficult to reduce the damage to osteons during a crack growth. Fracture mechanics, as shown in this paper, is influenced significantly by the micro-morphological parameters of osteons, and studying systematically such interplay between osteonal micro-morphology and crack propagation, one could gain an insight into individual fracture toughening mechanisms of cortical bone and their contribution towards tissue-level fracture resistance.

## Design and Simulation of a Nanomaterial-based Reverse Osmosis Device with an Intrinsic Anti-fouling Mechanism

Tiange Li\*, Shaofan Li\*\*

\*University of California, Berkeley, \*\*University of California, Berkeley

### ABSTRACT

A concept of the porous graphene membrane centrifuge is proposed aiming at fabrication of large scale, fouling free desalination machine with nanomaterial-based reverse osmosis (RO) modules. The concept as well as operation strategy of such porous rotating graphene membrane device is validated through molecular dynamics (MD) modeling and simulation of a nano-fluidic device in order to make a quantitative evaluation. One of the challenges in the development of such a device is the tendency of the ions to block the pores on the membrane wall, which is called the fouling problem in RO desalination. The fouling problem can be quantified in terms of ion concentration polarization or ion density distribution. The ion density distribution may become higher close the membrane wall, while the water density distribution becomes low. In order to investigate the distribution of ions, the ion density distribution as a result of the conducted MD simulations is plotted in the radial direction. It is observed that the ion density concentration is almost zero at the membrane wall, which implies that concentration polarization does not exist for the proposed nano-porous membrane centrifuge. Accordingly, it is demonstrated that the proposed desalination device has an intrinsic anti-fouling mechanism, which can be attributed to the presence of the Coriolis force along the tangential direction. After overcoming this significant challenge, several other aspects, related to the design and operation of the developed device, are investigated. First, an analytical formulation is derived for the critical angular velocity, above which the centrifugal force is able to counter-balance osmosis pressure, so that the RO desalination process can proceed. Moreover, energy efficiency and flux rate analyses are conducted for the proposed desalination device, and relationships are developed between fresh water flux rate and energy efficiency and several design parameters, such as the angular velocity, pore size and length of the device. Overall, it is demonstrated that the proposed desalination device can significantly improve desalination efficiency with its important features of the anti-fouling mechanism and adaptable design to achieve maximum efficiency.

## Hydraulic Fracture Modeling Based on Poromechanical Method

WANG Li\*, CAO yunxing\*\*

\*Henan Polytechnical University, \*\*Henan Polytechnic University

### ABSTRACT

Hydraulic fracturing(HF) is an important technique in enhancing the permeability of petroleum and gas reservoirs. The mechanisms of fracture propagation are well understood and involve the propagation of a fluid-driven fracture, inclusive of the effects of fluid transport and fluid lag at the tip. Where propagation is in fluid saturated porous media, the interaction of the fracturing fluid and the formation fluid are intimately coupled and may influence propagation. The complexity and nonlinearity of the principal physical interactions mean that numerical methods are the favored choice in representing response. And typically, domain methods such as finite element (FEM) and finite difference (FDM) methods are the preferred vehicles for solution as these enable nonlinear effects in the porous medium adjacent to the propagating fracture to be rigorously accommodated. The direct coupling is also referred to as strongly coupled or implicit, where the multiple physical field variables are taken as the unknown field variable vector and the final solution is recovered by solving the simultaneous equations. However, many engineering problems do not satisfy the conditions of strong coupling, especially for problems of damage-induced fracture - where it is difficult to ensure solution convergence. The load transfer method approaches a solution of the unknown field variables by successively solving the multi-physical field equations, in which one field variable is used as an input for the solution of another, and repeated through the sequence of couplings until a tolerance for an equilibrium solution is reached. We present a load transfer coupling finite element model (FEM) to represent hydraulic fracture propagation in porous media. The model represents: (1) poro-mechanical coupling of fluid and solid response for slightly compressible fluid; (2) damage localization, to calculate hydraulic fracture opening; (3) tensors of damage and permeability to denote the evolution of fracture-induced anisotropic properties; and (4) a loading scheme using full flow rate. The model is validated against a geometry of hydraulic fracture propagation in a three-layer reservoir. We demonstrate that the model returns the correct morphology of the evolving fracture zone and fluid pressure distribution and its variation with injection schedule. The simulation seamlessly follows four stages of fracture propagation (which are fracture nucleation, kinetic propagation, steady propagation and propagation termination) and represents the coupling between fracture tip and fluid front.

## Moment Closure for Radiative Transfer Based on Beta Distribution

Weiming Li<sup>\*</sup>, Ruo Li<sup>\*\*</sup>

<sup>\*</sup>Beijing Computational Science Research Center and Hong Kong University of Science and Technology, <sup>\*\*</sup>Peking University

### ABSTRACT

We present an approximation of the M2 model for radiative transfer in three-dimensional space based on a combination of beta distributions. It is an extension of the second-order extended quadrature method of moments (EQMOM) to multiple dimensions. Like the M2 closure, the ansatz of the new model can capture both isotropic and strongly peaked solutions. Also, the new model has fluxes in closed-form, making it cost-effective for numerical simulations. The rotational invariance, realizability, and hyperbolicity of the model are studied. We will also present numerical experiments testing the effectiveness of the new model.

## **An New Algebraic Subgrid-scale Model for Flow within Vegetation Canopies**

Weiyi Li<sup>\*</sup>, Marcelo Chamecki<sup>\*\*</sup>, Marc Parlange<sup>\*\*\*</sup>, Marco Giometto<sup>\*\*\*\*</sup>

<sup>\*</sup>Columbia University, <sup>\*\*</sup>University of California-Los Angeles, <sup>\*\*\*</sup>Monash University, <sup>\*\*\*\*</sup>Columbia University

### **ABSTRACT**

In flows over and within vegetation canopies, the presence of branches and leaves profoundly modifies the structure of turbulence, impacting transfer rates of energy, momentum and mass. In current Smagorinsky-type large-eddy simulations of such flow systems, the canopy-wake contributions to the subgrid-scale viscosity and diffusivity is not included. This flow feature is known to significantly affect scalar transfer rates deep within uniform dense canopies. In this contribution, an algebraic correction to the Smagorinsky model is proposed to encode the effect of the wake turbulence. The model is validated in neutrally-stratified pressure-driven atmospheric boundary-layer flow over and within uniform vegetation canopies. Vegetation is accounted for via a drag term in the momentum conservation equation which is a function of the canopy leaf-area density parameter. Predictions from the new proposed subgrid-scale model, classic Smagorinsky type models and one equation closure model are inter-compared against turbulent statistics from experimental measurements

## Numerical study on Shale Mechanical Properties based on Mesoscale Stochastic Digital Models

Xiang Li<sup>\*</sup>, Dongyang Chu<sup>\*\*</sup>, Zhanli Liu<sup>\*\*\*</sup>, Shaoqing Cui<sup>\*\*\*\*</sup>

<sup>\*</sup>Tsinghua University, <sup>\*\*</sup>Tsinghua University, <sup>\*\*\*</sup>Tsinghua University, <sup>\*\*\*\*</sup>Swansea University

### ABSTRACT

With the advancement of hydraulic fracturing techniques, shale gas exploitation has been significantly developed over the past decades. In order to provide essential information for hydraulic fracturing engineering design, it is vital to understand the mechanical properties of shale. However, it has been observed that shale is a complex heterogeneous material that contains multiple types of mineral components. The mineral components percentage and distribution manner differ among different shale samples. For this reason, it is important to establish the precise mesoscale mechanical model of shale. However, to date, most mesoscale digital shale models are developed in order to study permeability characteristics of the fluid, and not much attention has been given to the relation between mineral components of shale and its overall mechanical properties. In this research, mesoscale mechanical models of shale are established based on scanning electron microscopy images. A statistical reconstruction algorithm is introduced to generate stochastic models. As is known, it is difficult to adopt traditional fracture mechanics to investigate crack evolution in complex materials such as shale. The phase field method, on the other hand, employs a diffusive phase field variable to represent the crack surface, avoiding the complexity of modeling and tracing discontinuous crack surfaces. Since no additional criteria are required in dealing with crack deflecting and branching, the method exhibits significant advantages in simulating complex crack evolution. Therefore, a phase field method is implemented to study the damage characteristics and complex crack evolution in the mesoscale shale models. The mechanical properties of shale obtained from simulation results are compared with lab experiments. A three-field-coupling phase field model is further developed based on Biot poroelasticity theory. Solid deformation, fluid seepage, and damage evolution are fully coupled in this numerical model. The model is utilized to study the damage characteristics of shale as fluid is present. [1] Bennett K C, Berla L A, Nix W D, Borja R I. Instrumented nanoindentation and 3D mechanistic modeling of a shale at multiple scales. *Acta Geotechnica* 2015; 10(1):1-14. [2] Walls J D, Diaz E, Cavanaugh T In Shale reservoir properties from digital rock physics, SPE/EAGE European Unconventional Resources Conference & Exhibition-From Potential to Production, 2012. [3] Miehe C, Mauthe S. Phase field modeling of fracture in multi-physics problems. Part III. Crack driving forces in hydro-poro-elasticity and hydraulic fracturing of fluid-saturated porous media. *Computer Methods in Applied Mechanics and Engineering* 2016; 304,619-655.

## Absorbing Boundary Conditions for Atomistic and Electron Structure Calculations

Xiantao Li<sup>\*</sup>, Xiaojie Wu<sup>\*\*</sup>

<sup>\*</sup>Pennsylvania State University, <sup>\*\*</sup>Pennsylvania State University

### ABSTRACT

This talk will present a systematic approach to derive and approximate absorbing boundary conditions (ABC) for dynamics models involving atoms and electrons. The emphasis will be placed on the following issues: 1. Appropriate linearizations. ABCs can only be expressed explicitly for linear models. Ideally, one needs to retain the nonlinear interactions around lattice defects, and linearizes the interactions with the surrounding bath. This is a nontrivial task for multi-body interatomic interactions which extend beyond nearest neighbors. We present a partially-harmonic approximation that achieves this goal. Overall, this approximation is still consistent up to second order. 2. General expressions for the ABCs. We present a Dirichlet-to-Neumann map approach that yields an explicit representation of the boundary conditions, for domains of general geometry, including multiply connected domains. This is motivated by the observation that typical simulations involve multiple material defects. 3. Local approximations of the ABCs. We present a hierarchy of approximations that eliminate the nonlocality of the exact ABCs, which makes the implementation very efficient. 4. Stability. In practice, it is quite easy to end up with unstable boundary conditions. We will show how to determine the coefficients in the approximate ABCs to ensure nonlinear stability, using Lyapunov functionals.

## **Structural and Electromechanical Properties of III-nitride Nanoribbons Using First-principles Calculations**

Xiaobao Li<sup>\*</sup>, Huanlin Zhou<sup>\*\*</sup>, Changwen Mi<sup>\*\*\*</sup>

<sup>\*</sup>Dr., <sup>\*\*</sup>Dr., <sup>\*\*\*</sup>Dr.

### **ABSTRACT**

It has been found that III-nitride monolayers possess promising applications in high power electronic devices and optoelectronics. In this work, we have performed first-principles calculations on the mechanical and electro-mechanical properties of the pristine and chemically-passivated III-nitride nanoribbons. In particular, we investigate the edge stability in terms of the edge stress as well as the deformation for two typical types of edges, i. e. armchair and zigzag edges. It is found that the edges of all three pristine nitride nanoribbons are in compression and the deformation behavior due to the edge stresses along the edges are further confirmed by the molecular dynamics simulations. Moreover, since for such kind of compound nanoribbons, there are two distinct terminated zigzag edges which are also studied in detail in this work. The electromechanical properties are also presented for both pristine and chemically passivated nanoribbons. Our results highlight the importance of the edge properties in the application of 2D III-V monolayer crystalline.

## **Multiscale Modeling and Characterization of Coupled Damage-Healing-Plasticity for Granular Materials by Concurrent Computational Homogenization Method**

Xikui Li<sup>\*</sup>, Zenghui Wang<sup>\*\*</sup>, Qinglin Duan<sup>\*\*\*</sup>

<sup>\*</sup>Dalian University of Technology, <sup>\*\*</sup>Dalian University of Technology, <sup>\*\*\*</sup>Dalian University of Technology

### **ABSTRACT**

A multiscale modeling and characterization method for coupled damage-healing-plasticity occurring in granular material is proposed. The characterization is performed on the basis of multiscale modeling of granular material in the frame of concurrent second-order computational homogenization method, in which granular material is modelled as gradient-enhanced Cosserat continuum at the macroscale. The damage-healing-plasticity is characterized in terms of meso-structural evolution of discrete particle assembly within representative volume elements (RVEs) assigned to selected local material points in macroscopic continuum, with no need to specify macroscopic phenomenological constitutive models, failure criteria along with evolution laws, and associated macroscopic material parameters. The proposed modeling and characterization method for coupled damage-healing-plasticity in granular material is comprised of the following three constituents. The incremental non-linear constitutive relation for the discrete particle assembly of RVE is first established. Then the meso-mechanically informed incremental non-linear constitutive relation of macroscopic gradient-enhanced Cosserat continuum is derived. Finally meso-mechanically informed anisotropic damage and healing factors, anisotropic net damage factors combining both damage and healing effects, plastic strains are defined in the thermodynamic framework. Densities of thermodynamic net damage, plastic and total dissipative energies as scalar internal state variables are provided to compare the effects of damage, healing and plasticity on material failure and structural collapse. The numerical example of strain localization and softening problem is performed to demonstrate the performance and applicability of the proposed multiscale modeling and characterization method of coupled damage-healing-plasticity for granular materials.

## Consistent Coupling of Nonlocal Diffusion

Xingjie Li<sup>\*</sup>, Qiang Du<sup>\*\*</sup>, Xiaochuan Tian<sup>\*\*\*</sup>, Jianfeng Lu<sup>\*\*\*\*</sup>

<sup>\*</sup>University of North Carolina at Charlotte, <sup>\*\*</sup>Columbia University, <sup>\*\*\*</sup>University of Texas at Austin, <sup>\*\*\*\*</sup>Duke University

### ABSTRACT

Nonlocal models have been developed and received lot of attention in recent years to model systems with important scientific and engineering applications. While it is established that the nonlocal formulations can often provide more accurate descriptions of the systems, the nonlocality also increases the computational cost compared to conventional models based on PDEs. The goal is to combine the accuracy of nonlocal models with the computational and modeling efficiency of local PDEs. In this talk, I will introduce a new self-adjoint, consistent, and stable coupling strategy for nonlocal diffusion models, inspired by the quasi-nonlocal atomistic-to-continuum method for crystalline solids. The proposed coupling model is coercive with respect to the energy norms induced by the nonlocal diffusion kernels as well as the  $L_2$  norm, and it satisfies the maximum principle. A finite difference approximation is used to discretize the coupled system, which inherits the property from the continuous formulation. Furthermore, we design a numerical example which shows the discrepancy between the fully nonlocal and fully local diffusion, whereas the result of the coupled diffusion agrees with that of the fully nonlocal diffusion.

## **A Multiscale Framework to Quantify the Competing Failure Mechanisms in Metal Matrix Composites**

Yan Li\*

\*California State University, Long Beach

### **ABSTRACT**

The development of high performance MMCs requires careful microstructure design which can improve fracture toughness while maintaining high strength. Although a great deal of research has focused on the effect of microstructural properties on fracture toughness and strength of MMCs, the relations being established are mostly qualitative. In metal matrix composite materials, reinforcement cracking and interface debonding are two competing failure mechanisms observed during the crack-reinforcements interactions. For ductile MMCs, the fracture resistance depends on the sum of energy spent on both surface generation and the plastic deformation of the matrix material. Interface debonding usually leads to more tortuous crack paths and in turn enhances surface energy dissipation. However, it is not clear if this form of fracture can also lead to more pronounced plastic deformation in the metal matrix. While more significant plastic energy dissipation is beneficial to the toughening of a MMC, it has negative effect on its material strength. The objective of this study is to elucidate the two levels of competitions by considering the effect of microstructure and loading conditions: one being the competition between interface debonding and reinforcement cracking, and the other being the competition between crack formation and the deformation of matrix material. The systematic studies focus on Al/SiC metal matrix composites. The cohesive parameters employed in the computational models are calibrated through Digital Image Correlation analysis.

## 3D Frequency-Domain Elastic Wave Modeling Using the Spectral Element Method

Yang Li<sup>\*</sup>, Ludovic Métivier<sup>\*\*</sup>, Romain Brossier<sup>\*\*\*</sup>

<sup>\*</sup>ISTerre, Univ. Grenoble Alpes, <sup>\*\*</sup>ISTerre, LJK, CNRS, Univ. Grenoble Alpes, <sup>\*\*\*</sup>ISTerre, Univ. Grenoble Alpes

### ABSTRACT

High resolution geophysical seismic imaging by full waveform inversion can be tackled either in time or frequency domains. While it has been proven that frequency-domain can be an approach of choice under the acoustic approximation of the wave equation, taking benefit of recent developments of the computational facilities and optimized finite differences schemes, most of the successful and large scales applications still rely on the time domain formulation. Application of 3D large scale frequency-domain wave modeling is currently limited by the high computational burden resulting from the resolution of huge sparse linear system, i.e., the discretized wave equation. Recent attempts are made either using the multifrontal direct solvers with hierarchically semi-separable (HSS) or block low-rank compression, or using massively parallel iterative solvers with preconditioners like shifted Laplacian or specifically designed method like CARP-CG. These attempts have all been conducted with the finite difference discretization of the wave equation, mainly for visco-acoustic media. However, application in complex area involving complex topographies and free surface boundary conditions lead to severe limitation for the finite difference method. Therefore, in this study, we rely on the finite spectral element method, which has proven to be successful and efficient for considering complex topographies and free surface boundary conditions in the time domain. As the free surface boundary condition is naturally satisfied when considering the weak form of the wave equation, no extra effort need to be made. Wave modeling could also benefit from the high-order accuracy of spectral element method. For instance, only 5 degree of freedom per minimum wavelength is known to be sufficient for P4 spectral element method. Moreover, higher order could also be used in the frequency-domain, as the restriction coming from the CFL condition of the time step does not exist anymore. The mesh could therefore be significantly coarsened at higher order, resulting in a decrease of the linear system size. We start from the most general case where all of the 21 elastic parameter are considered. An anisotropic perfectly matched layer technique and sponge absorbing boundary condition will be investigated to simulate the wave propagation in limited computational area. Several direct solvers and iterative solvers will be studied in solving the derived linear system.

## Dimensionless Damage Factor Method: A New Computational Methodology for Evaluating the Residual Strength of Aluminum Plates

Yanping Li<sup>\*</sup>, Weiguo Guo<sup>\*\*</sup>, Kangbo Yuan<sup>\*\*\*</sup>, Jin Guo<sup>\*\*\*\*</sup>, Xueyao Hu<sup>\*\*\*\*\*</sup>

<sup>\*</sup>School of Aeronautics, Northwestern Polytechnical University, <sup>\*\*</sup>School of Aeronautics, Northwestern Polytechnical University, <sup>\*\*\*</sup>School of Aeronautics, Northwestern Polytechnical University, <sup>\*\*\*\*</sup>School of Aeronautics, Northwestern Polytechnical University, <sup>\*\*\*\*\*</sup>School of Aeronautics, Northwestern Polytechnical University

### ABSTRACT

Abstract: By consulting the relevant literature on calculating the residual strength of cracked aluminium plates, it's found that there is a difference between the experimental results and the calculated values of the existing models. Thus, a more accurate method is expected to predict the residual strength for the aluminium plates. In this paper, we introduce the dimensionless damage factor which is used to quantify the initial damage degree of a plate, and then propose a new computational methodology for evaluating the residual strength of aluminium plates. The dimensionless damage factor can be used as a parameter to describe the material tolerance for damage; it is determined by the ratio between crack length and ultimate plastic zone diameter. (As the ultimate plastic zone diameter is related to apparent fracture toughness and the ultimate tensile strength, their accuracy will have great influence on the predictive value by this method.) For further calculating, establish the function of residual strength reduction coefficient through regression analysis of the data from reference and boundary conditions. The empirical curve of residual strength reduction coefficient decreases with the damage degree increasing. The plates ranged from intact to completely damaged would have the corresponding residual strength reduction coefficients according to their dimensionless damage factors. Illuminated by Jean Lemaitre's damage variable, combining the mechanical parameters and the damage degree, a new methodology presented in the framework of linear elastic fracture mechanics. Then, the comparisons with the other typical two models are carried out, respectively on middle crack tension specimens and multiple site damage specimens. The results show that the dimensionless damage factor method gives the most accurate predictive residual strength, and it is valid on the plates with no crack, a through-thickness crack and multiple site damage. Keywords: Residual strength, Dimensionless damage factor method, Fracture toughness, Residual strength reduction coefficient, Multiple site damage Reference [1] Uwe Zerbst, Markus Heinemann, Claudio Dalle Donne, Dirk Steglich. Fracture and damage mechanics modeling of thin-walled structures-An overview. Engineering Fracture Mechanics 2009; 76:5-43 [2] CHERRY C, MALL S Residual strength of unstiffened aluminum panels with multiple site damage [J] Engineering Fracture Mechanics 1997, 57(6):701-713 [3] Jean Lemaitre. A continuous damage mechanics model for ductile fracture. Journal of Engineering Materials & Technology, 1985, 107 (107) :83-89

## Fluid-Rigid Body Interaction Simulation Based on ISPH Incorporated with Impulse-based Method

Yi Li\*, Mitsuteru Asai\*\*

\*Kyushu University, \*\*Kyushu University

### ABSTRACT

Particle-based fluid-rigid body interaction simulation techniques have been proposed. In our research, ISPH method has been used for fluid simulation and rigid body representation, and the penalty method was utilized for the contact force calculation between rigid bodies. However, precision of the contact force calculated by penalty method is strongly affected by the time increment and the penalty parameter. Then, the impulse-based contact method, which is widely used for the multiple rigid body simulation in computer graphics area, is introduced to ISPH in the fluid-rigid body interaction simulation. The magnitude of contact force in the penalty method is calculated according to the overlap between rigid bodies which can reproduce the procedure of compression and restitution in contact problems. However, it needs a very small time increment. In the meantime, an appropriate time increment in the penalty method is always much smaller than the one in ISPH method. Choosing a smaller time increment will slower the efficiency of the entire simulation because the number of water particles is always hundred times larger than the number of rigid body particles. An impulse-based method is applied, where instead of contact force, impulse is calculated without any calibrations. The velocity change caused by the impulsive force during a very short instant can be easily decided by the coefficient of restitution. By comparing the penalty method with the impulse-based method, it is clear that the impulse-based method can reproduce reasonable and robust rigid body motion with a large time increment. In order to discuss the accuracy of ISPH incorporated with impulse-based method, a comparison between an experiment with several rigid bodies and a simulation result will be demonstrated.

## Mechanical and Thermal Properties of 2D Polycrystalline Graphene Structures

Yinfeng Li\*

\*Shanghai Jiao Tong University

### ABSTRACT

Research on two-dimensional (2D) atomic materials has been a leading topic in condensed matter physics and materials science for many years. A large number of 2D crystals are currently available and isolated atomic crystals can be further reassembled into planar and multilayer heterostructures for desirable electronic and optical properties. In this talk, we present our recent progresses on the mechanical and thermal properties of polycrystalline graphene structures using classical Molecular Dynamics method, density functional theory calculation and disclination theory. Grain boundaries (GBs) as typical defective graphene structure have significant influence on the overall properties of 2D graphene structures. The fracture strength of hydrogenated graphene with tilt GBs composed of pentagon–heptagon defects is systematically investigated and anomalous tunable mechanical and thermal characteristics are revealed for graphene with hydrogenation either on or near the GBs because of the interaction between polar stress fields of hydrogenated pentagon–heptagon defects. GB is also found a vulnerable spot for planar polycrystalline heterostructure of graphene and hexagonal boron nitride under uniaxial tension. The disclination theory is successfully adopted to predict the stress field caused by the lattice mismatch at GB. What's more, the thermal transfer efficiency of hybrid GB is also revealed to depend not only on the mismatch angle of grains but also the direction of thermal flux. Thermal transfer efficiency from graphene to h-BN is higher than that from h-BN to graphene. Detailed analyses for the phonon density of states of GB atoms are carried out for the mismatch angle-dependence of interfacial conductance. Extraordinary dependence of thermal conductivity of polycrystalline graphene on surface hydrogenation and inplane strains are revealed, and PG with different average grain sizes shows different sensitivities to tensile strain. Our results provide useful insights into the application of two dimensional polycrystalline heterostructures for next-generation electronic and flexible devices.

## Understanding Receptor-Mediated Endocytosis of Elastic Nanoparticles Through Coarse Grained Molecular Dynamic Simulation

Ying Li<sup>\*</sup>, Zhiqiang Shen<sup>\*\*</sup>, Huilin Ye<sup>\*\*\*</sup>

<sup>\*</sup>University of Connecticut, <sup>\*\*</sup>University of Connecticut, <sup>\*\*\*</sup>University of Connecticut

### ABSTRACT

For nanoparticle (NP)-based drug delivery platforms, the elasticity of NPs has significant influence on their blood circulation time and cellular uptake efficiency. However, due to the complexity of endocytosis process and inconsistency in the definition of elasticity for NPs in experiments, the understanding about the receptor-mediated endocytosis process of elastic NPs is still limited. In this work, we developed a coarse-grained molecular dynamics (CGMD) model for elastic NPs. The energy change of elastic NPs can be precisely controlled by the bond, area, volume and bending potentials of this CGMD model. To represent liposomes with different elasticities, we systematically varied the bending rigidity of elastic NPs in CGMD simulations. Additionally, we changed the radius of elastic NPs to explore the potential size effect. Through virtual nano-indentation tests, we found that the effective stiffness of elastic NPs was determined by their bending rigidity and size. Afterwards, we investigated the receptor-mediated endocytosis process of elastic NPs with different sizes and bending rigidities. We found that the membrane wrapping of soft NPs was faster than stiff ones at early stage, due to the NP deformation induced large contact area between the NP and membrane. However, because of the large energy penalties induced by the NP deformation, the membrane wrapping speed of soft NPs slows down during the late stage. Eventually, the soft NPs are less efficient than stiff ones during the membrane wrapping process. Through systematic CGMD simulations, we found a scaling law between the cellular uptake efficiency and phenomenal bending rigidity of elastic NPs, which agrees reasonably well with experimental observations. Furthermore, we observed that membrane wrapping efficiencies of soft and stiff NPs with large size were close to each other, due to the stronger ligand-receptor binding force and smaller difference in stiffness of elastic NPs. Our computational model provides an effective tool to investigate the receptor-mediated endocytosis of elastic NPs with well controlled mechanical properties. This study can also be applied to guide the design of NP-based drug carriers with high efficacy, by utilizing their elastic properties.

## Dissipative Particle Dynamics Methods for Mesoscopic Problems

Zhen Li\*, George Karniadakis\*\*

\*Division of Applied Mathematics, Brown University, \*\*Division of Applied Mathematics, Brown University

### ABSTRACT

The traditional dissipative particle dynamics (DPD) model was initially proposed as a minimal working version for mesoscopic simulation of fluids. Regardless of many successful applications of DPD to material science, rheology of complex fluids and computational biology, it only considers the momentum equation governing the evolution of flow field, which precludes the traditional DPD method from modeling many interesting problems involving coupling of flow field with other physical fields, e.g., thermal field, concentration field and electrostatic field. To this end, we have developed several extensions of the DPD method in recent years for tackling the challenges in diverse multiphysics applications involving multiple physical fields, which are beyond the capability of the traditional DPD model. In this talk, we will present three DPD extensions including energy-conserving DPD (eDPD)[1], transport DPD (tDPD)[2] and charged DPD (cDPD)[3]. In particular, the eDPD method solves the energy equations in the DPD framework and is able to consider the coupling of fluctuating hydrodynamics and heat flow, which has been applied to investigation of temperature-induced self-assemblies of thermoresponsive polymers; the tDPD method solves the advection-diffusion-reaction equations and momentum equations in the DPD framework and is able to model mesoscopic diffusive and reactive transport in many biological systems, such as the dynamic process of blood coagulation; the cDPD method solves the equation to consider the solvent explicitly in a coarse-graining sense as DPD particles, while the ion species are described semi-implicitly using a Lagrangian description of ionic concentration fields associated with each moving cDPD particle, which provides a natural coupling between fluctuating electrostatics and hydrodynamics. These DPD extensions consistently incorporate thermal fluctuations and are capable of describing certain mesoscopic features that deterministic macroscopic methods cannot model. References: [1] Z. Li, Y.-H. Tang, H. Lei, B. Caswell and G.E. Karniadakis. Energy-conserving dissipative particle dynamics with temperature-dependent properties. *Journal of Computational Physics*, 2014, 265: 113-127. [2] Z. Li, A. Yazdani, A. Tartakovsky and G. E. Karniadakis. Transport dissipative particle dynamics model for mesoscopic advection-diffusion-reaction problems. *The Journal of Chemical Physics*, 2015, 143: 014101. [3] M. Deng, Z. Li, O. Borodin and G.E. Karniadakis. cDPD: A new dissipative particle dynamics method for modeling electrokinetic phenomena at the mesoscale. *The Journal of Chemical Physics*, 2016, 145: 144109.

## Failure Analysis of Composite Laminates with Big Cutouts

Zheng Li<sup>\*</sup>, Pengcheng Chu<sup>\*\*</sup>, Jianlin Chen<sup>\*\*\*</sup>

<sup>\*</sup>Peking University, <sup>\*\*</sup>Peking University, <sup>\*\*\*</sup>Peking University

### ABSTRACT

According to the extensive application of composite laminates in practical engineering, there are many composite laminates with big cutouts to be designed and applied. However, the stress concentration and the complicated failure modes around the cutout are very difficult to be studied. The progressive failure process induced by the stress concentration needs to be thoroughly investigated because it is essential for predicting the performance of composite structures and designing reliable and safety structures. In the case of more complex structures and complicated stress states, most of the failure criteria are not suitable to predict the propagation of failure and the ultimate strength directly. Therefore, a simulation approach is developed in this paper by combining the finite element method and the progressive damage model to analyze the progressive failure process of composite structures. In this study, the composite laminates with different lay-up and different sizes of big cutouts are considered to figure out the failure behaviors of composite laminates. In the numerical analysis, the onset of failure is predicted by Hashin criteria and the evolution of failure is simulated using a continuum damage model, in which the failure evolution is based on the fracture energy dissipation and the stiffness reduction of matrix is controlled by a set of scalar damage variables. And two kinds of damage degradation model are used to simulation linear and exponential soften relation between stress and strain. The shear nonlinearity was also considered for composite laminates, and shear nonlinearity constitutive relations for the laminates were defined with the Ramberg-Osgood equation. The model has been implemented in the finite element software Abaqus using a UMAT subroutine. All simulation results are compared with experimental tests. The failure evolution in simulation results shows that the proposed model performs well for predicting the failure behavior of composite laminates with big cutouts. We found that the exponential degeneration law performs better than linear degradation law for predicting the ultimate strength for the selected composite laminates. And the simulation using shear nonlinearity gives better results for predicting the nonlinear relation between displacement and force. Furthermore, the finite element based failure model of composite laminates can be used in composite structures with arbitrary configurations under complex stress states to make up for the shortage of analytical failure analysis.

## Extension of Shape-free Low-order Unsymmetric Finite Elements for Geometric Nonlinear Analysis

Zhi Li<sup>\*</sup>, Song Cen<sup>\*\*</sup>, Cheng-Jin Wu<sup>\*\*\*</sup>, Yan Shang<sup>\*\*\*\*</sup>, Chen-Feng Li<sup>\*\*\*\*\*</sup>

<sup>\*</sup>Tsinghua University, <sup>\*\*</sup>Tsinghua University, <sup>\*\*\*</sup>Tsinghua University, <sup>\*\*\*\*</sup>Nanjing University of Aeronautics and Astronautics, <sup>\*\*\*\*\*</sup>Swansea University

### ABSTRACT

**ABSTRACT** Two recent low-order element models, the unsymmetric 4-node, 8-DOF quadrilateral element US-ATFQ4 [1] and the unsymmetric 8-node, 24-DOF hexahedral element US-ATFH8 [2], which exhibit excellent precision and distortion-resistance for linear elastic problems, are successfully extended to geometric nonlinear analysis. Since the original linear elements contain the analytical solutions for pure bending and twisting, how to modify such formulae into incremental forms for nonlinear applications and design an appropriate updated algorithm become the key of the whole job. First, the analytical trial functions should be updated at each iterative step in the framework of updated Lagrangian (UL) formulation that takes the configuration at the beginning of an incremental step as the reference configuration during that step. Second, an appropriate stress update algorithm that the Cauchy stresses are updated by the Hughes-Winget method [3] is adopted to estimate current stress fields. The present geometric nonlinear formulations of element US-ATFQ4 and US-ATFH8 are compiled and implemented in commercial software SIMULA Abaqus via the user element subroutine (UEL). Numerical examples using traditional regular and new distorted mesh divisions are employed to assess the performance of the new formulations, including the slender elastic cantilever beam subjected to end shear force or end moment, the post-buckling nonlinear behavior of the Lee's frame buckling problem and so on. These numerical examples show that the new nonlinear formulations also possess amazing performance for geometric nonlinear analysis, no matter regular or distorted meshes are used. It again demonstrates the advantages of the unsymmetric finite element method with analytical trial functions, although these functions only come from linear elasticity.

**ACKNOWLEDGEMENTS** The authors would like to thank for the financial supports from the National Natural Science Foundation of China (11272181, 11702133), the Tsinghua University Initiative Scientific Research Program (2014z09099) and the Natural Science Foundation of Jiangsu Province (BK20170772).

**REFERENCES** [1] Cen S, Zhou PL, Li CF, Wu CJ. An unsymmetric 4-node, 8-DOF plane membrane element perfectly breaking through MacNeal's theorem. *International Journal for Numerical Methods in Engineering* 2015;103(7):469-500. [2] Zhou PL, Cen S, Huang JB, Li CF, Zhang Q. An unsymmetric 8-node hexahedral element with high distortion tolerance. *International Journal for Numerical Methods in Engineering* 2017;109(8):1130-1158. [3] Hughes TJR, Winget J. Finite rotation effects in numerical integration of rate constitutive equations arising in large-deformation analysis. *International Journal for Numerical Methods in Engineering* 1980;15(12):1862-1867.

## Numerical Simulation of Head Dynamic Process and Potential Mechanism of Brain Injury during Blast Loading

Zhijie Li<sup>\*</sup>, Xiaochuan You<sup>\*\*</sup>, Zhuo Zhuang<sup>\*\*\*</sup>, Zhanli Liu<sup>\*\*\*\*</sup>

<sup>\*</sup>Tsinghua University, <sup>\*\*</sup>Tsinghua University, <sup>\*\*\*</sup>Tsinghua University, <sup>\*\*\*\*</sup>Tsinghua University

### ABSTRACT

Blast-induced traumatic brain injury (b-TBI) is a signature injury of the current military conflicts. And the corresponding mechanism of brain injury and head protection strategy have been the hot research. In this paper, numerical simulation study is conducted to investigate the dynamic response of head and the brain injury mechanics during the blast loading. Based on the software of Hypermesh, a three-dimensional (3-D) finite element model of the human head with high fidelity is constructed, which is to be verified by simulating the impact experiment of cadaver head with ABAQUS software. The simulation and experiment results are in satisfactory agreement, showing the accuracy and validity of the numerical head model. At the same time, based on the coupled Eulerian-Lagrangian (CEL) theory the fluid-structure coupled model of explosive blast and head is developed, and then adopted to conduct the simulation of the head dynamic process under the blast loading with the peak pressure of 500 KPa. The potential mechanism for the brain injury is analyzed from four aspects, namely flow distribution, brain pressure, impulse and acceleration. These corresponding conclusions provide the theoretical basis for the treatment of brain injury and the development of protection equipments.

## Multi-Scale Modeling of Damage and Failure in Heterogeneous Composite Subject to High Strain Rate Impact and Blast

Zhiye Li\*, Zhang Xiaofan\*\*, Somnath Ghosh\*\*\*

\*Department of Civil Engineering, Johns Hopkins University, \*\*Department of Civil Engineering, Johns Hopkins University, \*\*\*Department of Civil Engineering, Johns Hopkins University

### ABSTRACT

This work aims to develop an efficient explicitly multiscale model incorporating material heterogeneities to study multi-physics damage and failure of fiber reinforced composites under extreme dynamic environments. First, micromechanical analysis of S-glass fiber reinforced epoxy composites is performed in conjunction with the phenomenon of stress wave propagation in the representative volume elements (RVEs) subjected to high strain rate deformation. The stress wave propagation process is correctly performed by novel space-time boundary conditions (STBCs) for extreme high strain rate impact or blast. Deformation and failure response of RVE model exhibiting fiber and matrix damage as well as interfacial cohesive crack. The rate-dependent nonlocal damage model is validated by DER 353 Epoxy donut impact experiment. In this calibration-validation study of high-speed impact experiment, adiabatic heating is observed in the specimens and implemented in the thermos-mechanical damage model. The dynamic rate-dependent cohesive models are validated by cruciform experiment and micro-droplet experiment. With model parameters calibrated from experiments, characterization of failure properties and microstructure criteria is studied in realistic microstructure models by using a Voronoi cell characteristic method, e.g. cracking nucleation, growth and spacing decrease. Then macroscopic constitutive damage law is obtained through the homogenized response of the micromechanical model. To connect the damage mechanism in micro-scale with macroscopic damage evolution, a fourth order tensor governing the initiation and evolution of the damage is introduced, and it is calibrated as a function of the macroscopic damage state in heterogeneous materials. After this fourth order tensor is calibrated for a specific composite system, the constitutive damage law can be obtained by this Parametrically Homogenized Continuum Damage model (PHCDM) model without performing a micro-mechanical analysis. Meanwhile, the microscopic damage and failure history at any specific location of a macroscopic model can be recovered from a top-down process of this hierarchical model. Finally, this PHCDM model is incorporated in ABAQUS user-subroutine to describe the material behavior for the composite system, making the analysis of macro-scale structures computationally feasible. This presentation shows theoretical math model and experimentally validated application examples of this multi-scale damage model. Results show that the bilateral combination of micromechanics model and PHCDM model for heterogeneous composite systems can be used for the material-by-design loop and meanwhile able to predict the damage behavior at both micro- and macro- scales.

## **A 9-Node Co-rotational Curved Quadrilateral Shell Element for Smooth, Folded and Multi-Shell Structures**

Zhongxue Li<sup>\*</sup>, Tianzong Li<sup>\*\*</sup>, Loc Vu-Quoc<sup>\*\*\*</sup>, Bassam A. Izzuddin<sup>\*\*\*\*</sup>

<sup>\*</sup>Zhejiang University, <sup>\*\*</sup>Zhejiang University, <sup>\*\*\*</sup>University of Illinois at Urbana-Champaign, <sup>\*\*\*\*</sup>Imperial College London

### **ABSTRACT**

A 9-node co-rotational curved quadrilateral shell element for smooth, folded and multi-shell structures is presented. Its co-rotational framework is defined by the two bisectors of the diagonal vectors generated from the four corner nodes and their cross product. In this framework, the element rigid-body rotations are excluded in calculating the local nodal variables from the global nodal variables. The two smallest components of each nodal normal vector of mid-surface are defined as rotational variables for smooth shell, and three smaller components of two nodal orientation vectors at intersections of folded and multi-shell structures are employed as rotational variables, leading to the desired additive property for all nodal variables in a nonlinear incremental solution procedure. Different from other existing co-rotational finite-element formulations, the resulting element tangent stiffness matrix is symmetric owing to the commutativity of the local nodal variables in calculating the second derivative of strains energy with respect to these nodal variables. To alleviate membrane and shear locking phenomena, the membrane strains and the out-of-plane shear strains are replaced with assumed strains for obtaining the element tangent stiffness matrices and the internal force vector using the Mixed Interpolation of Tensorial Components (MITC) approach. Finally, a series of typical and challenging smooth, folded and multi-shell structures undergoing large displacements and large rotations are solved to demonstrate the reliability, computational accuracy of the proposed formulation.

## **A Cellular Automaton Finite Element Method to Predict Grain Evolution for Directed Laser Fabricated IN718 Alloy**

Yanping Lian<sup>\*</sup>, Zhengtao Gan<sup>\*\*</sup>, Gregory Wagner<sup>\*\*\*</sup>, Wing Kam Liu<sup>\*\*\*\*</sup>

<sup>\*</sup>Northwestern University, <sup>\*\*</sup>Northwestern University, <sup>\*\*\*</sup>Northwestern University, <sup>\*\*\*\*</sup>Northwestern University

### **ABSTRACT**

The grain structure of build part by the additive manufacturing (AM) technology, e.g., Directed Laser Fabrication (DLF), has attracted widespread interest because it plays an essential role in deciding the mechanical property of the build part and can be tailored through the use of reasonable processing parameters in AM. Most of the existing simulation works have been focused on the 2D problem. However, for the accurate quantitative prediction of solidification and grain structure 3D modeling is necessary. In this work, a 3D cellular automaton finite element method is proposed to predict the microstructure of IN718 alloy in DLF, where the thermal field along with the molten pool flow is solved by the finite element method. An enriched grain heterogeneous nucleation scheme is implemented in the cellular automaton model to take into account of both epitaxial grain growth and grain growth from the re-nucleation, following the experimental observation. The simulated microstructure results are shown to be in good agreement with experimental complements, which demonstrates the ability of the proposed method. Moreover, additional simulations are conducted to disclose the influence of the laser scan speed and the laser power on the grain structure and texture, which sheds light on the relationship between the AM process parameters and the as-built grain structure.

## An Improved Koiter-Newton Method for Tracing the Geometrically Nonlinear Response of Structures

Ke Liang\*, Qin Sun\*\*

\*School of Aeronautics, Northwestern Polytechnical University, \*\*School of Aeronautics, Northwestern Polytechnical University

### ABSTRACT

The original Koiter-Newton(KN) method has been approved to be a numerically accurate and computationally efficient algorithm to trace the nonlinear equilibrium path in a stepwise manner, especially in the presence of buckling. In each step, this method works by combining a nonlinear predictor and a few Newton iteration-based corrections. Although the predictor is obtained from the ROM, corrections to the exact equilibrium path relies exclusively on the full model. In this paper, we extend the method such that the reduced order model can be used also in the correction phase. In the proposed predictor-corrector strategy, the exact nonlinear model is used only to calculate force residuals. This significantly reduces the computational cost of the method. As a side product, the method has better error control and more robust step size adaptation strategies, benefiting from the corrections applied in each solution step of the ROM. We demonstrate the potential of the proposed method and the high quality of the analysis results with a set of benchmark and real engineering problems. Both reliability and accuracy of the approach are remarkable. The proposed method show great advantages in computational efficiency, compared to both the original method and the conventional Newton path-following method. Acknowledgement This work was supported by the National Natural Science Foundation of China (Grant No. 11602286, 51375386).  
References [1] Liang, M. Abdalla, Z. Gurdal, A Koiter-Newton approach for nonlinear structural analysis, International Journal for Numerical Methods in Engineering 96(12) (2013) 763–786. [2] Liang, M. Ruess, M. Abdalla, The Koiter-Newton approach using von Kármán kinematics for buckling analyses of imperfection sensitive structures, Computer Methods in Applied Mechanics and Engineering 279(1) (2014) 440–468.

## Predicting Effective Properties of Peridynamic Composites Based on Boundary Element Method

Xue Liang<sup>\*</sup>, Linjuan Wang<sup>\*\*</sup>, Jianxiang Wang<sup>\*\*\*</sup>

<sup>\*</sup>Peking University, <sup>\*\*</sup>Peking University, <sup>\*\*\*</sup>Peking University

### ABSTRACT

The effective properties of composite materials have been intensively and extensively studied within the framework of classical local theory. Today, some composite materials may have hierarchical microstructures such that non-locality may emerge and need to be considered in predicting their properties. Here, we predict the effective elastic properties of composites that are composed of a continuous matrix and discrete inhomogeneities, where both the matrix and inhomogeneities are peridynamic media. To this end, we calculate the displacement field in the composites with the peridynamic boundary element method (PD-BEM). Then, the effective properties are made to correspond to the elastic constants of classical orthotropic composites, and also to the micromodulus functions of the bond-based peridynamic theory. We also examine the effects of various parameters and the correlations with the classical theory.

## Canonical Dual Theory of Discrete Variable Topology Optimization and its Numerical Algorithm

Yuan Liang\*, Gengdong Cheng\*\*

\*Dalian University of Technology, \*\*Dalian University of Technology

### ABSTRACT

The mathematical essence of topology optimization is nonlinear integer programming. To overcome the huge computational burden for solution of large scale integer programming, the popular way is to relax the 0-1 variable constraint and transform the integer programming to continuous variable programming by introduction of the interpolation schemes for the material properties vs design variables as it allows to use gradient based mathematical programming methods. With this strategy, the well-know SIMP (Solid Isotropic Material with Penalty) method achieves great success and popularity. However, there is no doubt that tackling the discrete problems directly is very important. In order to overcome the combination complexity in integer programming, this paper resort to a kind of penalty-dual theory named by Canonical Dual Theory(CDT). This theory is developed by Dvoid Gao[1] in nonconvex mechanics and global optimization. In contrast to the classic Lagrange dual in integer programming, CDT can get any order smooth and differentiable dual function. The present paper develops a CDT formulation of structural topology optimization and applies an effective fixed point iterative algorithm to solve discrete variable topology optimization subproblems which is constructed by sensitivity information. Numerical experiments show that the fixed point iterative algorithm can get approximate solutions with good properties in excellent short time. And this paper shows that the dual gap of this method is negligible. Move limit strategies are supposed to be key role in discrete variables topology optimization. Therefore, this paper also combines some different move limits within the new method. The new method successfully solve the classic minimization of structural compliance, design dependent load problem, multiple constraints problem and heat conduction problems. The results of these problems exhibit that the new method can deal with much more design variables compared to the general branch and bound method. The new method can get black and white solutions and slightly lower compliance than SIMP. On the other hand, in comparison with the BESO method which is also widely used in structural topology optimization, the new method don't need any thresholds for sensitivities or heuristics. Finally, the new method also can solve multi-constraints optimization problems in a unified way and have more hopeful prospects in large-scale discrete topology optimization with local constraints. Reference [1]. Gao D., Gao, D.Y. and Ruan, N. (2010). Solutions to quadratic minimization problems with box and integer constraints. J. Glob. Optim. 47 463484

## Time-extrapolation of Dynamic, Particulate Flows with Recurring Patterns

Thomas Lichtenegger\*

\*Department of Particulate Flow Modelling, Johannes Kepler University, Linz, Austria; Linz Institute of Technology,  
Johannes Kepler University, Linz, Austria

### ABSTRACT

Granular systems exhibit clearly separated, characteristic time-scales. Microscopically, particle collisions last only a few microseconds while the macroscopic motion takes place on the order of (fractions of) seconds. Slow processes like heat transfer or chemical conversion which might happen over minutes or hours eventually render conventional particle-based simulation approaches unfeasible. Inspired by the observation that many systems which evolve over very long durations either run into a steady state or repeat their motion in an approximate, completely irregular fashion, we have recently proposed a novel technique employing recurrence statistics [1] to describe the latter class [2]. This presentation deals with its application to heat transfer in a lab-scale, bubbling fluidized bed. Time-series analysis of the flow fields obtained from CFD-DEM shows that their dynamics starts to reproduce itself after a relatively short duration of a few seconds. After this period, hardly any new states appear, which allows us to extrapolate the bed's behavior using only the information contained within the initial phase. We demonstrate that these fields suffice to study a slow, almost passive process like heat transfer between gas and particles in (semi-)quantitative agreement with experiments over long durations at small fractions of the computational costs of CFD-DEM [3]. Finally, we discuss limitations and envisioned future developments of the method for extremely fast, accurate simulations of large-scale, industrial processes. [1] J.-P. Eckmann, S. O. Kamphorst and D. Ruelle. "Recurrence plots of dynamical systems." *Europhys. Lett.* 4.9 (1987): 973. [2] T. Lichtenegger and S. Pirker. "Recurrence CFD – A novel approach to simulate multiphase flows with strongly separated time scales." *Chem. Eng. Sci.* 153 (2016): 394-410. [3] T. Lichtenegger et al. "A recurrence CFD study of heat transfer in a fluidized bed." *Chem. Eng. Sci.* 172 (2017): 310-322.

## **Multi-scale Mechanics in Bioengineering**

Kim Meow Liew\*

\*City University of Hong Kong

### **ABSTRACT**

Due to the extremely small size of micro- and nano-structures, experimental studies are generally quite difficult. Although experimental studies can capture certain phenomena, it is impossible to understand their delicate properties well through experimental investigations alone. In addition to a large amount of experimental work, theoretical analysis and numerical modeling play an important role in capturing the delicate behavior of complex materials systems. Theoretical and numerical approaches can be generally classified into two categories: microscale method and macroscale method. Microscale method can capture the microscale mechanism of micro- and nano-structures and yield results that are in many cases explicit in nature. However, microscale methods consume a large amount of computational resources, and thus computation is limited to a very small size. This huge computational cost largely restricts their application. Macroscale continuum simulation can largely reduce the degrees of freedom in problems, and the theoretical and numerical analysis of large-size structures thus become possible. However, continuum simulations cannot reflect the microscale physical laws, and are not adequate. The limitations of microscale method as well as macroscale method have stimulated extensive research into multi-scale method that couples microscale method and continuum description. Multi-scale method can overcome the length and time scale limits in an efficient manner, and is emerging as a feasible and efficient approach for complex materials systems. This talk will present recent research work on multi-scale mechanics problems, focussing in bioengineering application.

## **Interface-conformal Hex Meshing Techniques and Mesh Sensitivities in Crystal Plasticity Finite Element Simulations**

Hojun Lim<sup>\*</sup>, Steve Owen<sup>\*\*</sup>, Corbett Battaile<sup>\*\*\*</sup>, James Foulk<sup>\*\*\*\*</sup>

<sup>\*</sup>Sandia National Laboratories, <sup>\*\*</sup>Sandia National Laboratories, <sup>\*\*\*</sup>Sandia National Laboratories, <sup>\*\*\*\*</sup>Sandia National Laboratories

### **ABSTRACT**

Crystal plasticity-finite element (CP-FE) models explicitly capture individual grains within a polycrystalline domain and it is important to accurately reproduce their features using finite elements. In order to better incorporate microstructures in continuum scale models, we use a novel finite element (FE) meshing technique to generate three-dimensional polycrystalline aggregates from a phase field model of grain microstructures. The proposed meshing technique creates hexahedral FE meshes with conformal smooth interfaces between adjacent grains. Three-dimensional realizations of grain microstructures from the phase field model were used in crystal plasticity simulations of polycrystals. It is shown that the conformal meshes significantly reduce artificial stress localizations in voxelated meshes that exhibit the so-called wedding cake interfaces. In addition, mesh sensitivities in CP-FE simulations using polycrystalline and single crystal microstructures are investigated with various constitutive factors.

## **An Alternative Approach of Parallel Preconditioning for 2D Finite Element Problems**

Leonardo Lima<sup>\*</sup>, Sérgio Bento<sup>\*\*</sup>, Riedson Baptista<sup>\*\*\*</sup>, Paulo Barbosa<sup>\*\*\*\*</sup>, Lucia Catabriga<sup>\*\*\*\*\*</sup>,  
Isaac Santos<sup>\*\*\*\*\*</sup>

<sup>\*</sup>UFES, <sup>\*\*</sup>UFES, <sup>\*\*\*</sup>UFES, <sup>\*\*\*\*</sup>UFES, <sup>\*\*\*\*\*</sup>UFES, <sup>\*\*\*\*\*</sup>UFES

### **ABSTRACT**

We propose an alternative approach of parallel preconditioning for finite element analysis. This technique consists in a proper domain decomposition with reordering that produces narrow-band linear systems from finite element discretization, allowing to consider traditional preconditioners as Incomplete LU Factorization (ILU) or even sophisticated parallel preconditioners as SPIKE [1] without significant efforts. We also employ preconditioners based in element-by-element [2] storage with minimal adjustments. Another feature of that approach is the facility to recalculate finite element matrices whether for nonlinear corrections or for time integration schemes. That means parallel finite element application is performed indeed in parallel, including matrices calculations, residue updating, and linear systems calculation. Moreover, our approach provides load balancing and improvement to MPI communications that can be evidenced through consistent studies using an analyzer tools as TAU (Tuning Analysis Utilities). We demonstrate the robustness and scalability of these parallel preconditioning strategies for a set of benchmark experiments, considering two-dimensional fluid flow problems modeled by transport, Euler, and Navier-Stokes equations to evaluate the ILU, SPIKE, and element-by-element preconditioners. We also provide a comparison between our implementation and standard implementations using the Portable, Extensible Toolkit for Scientific Computation (PETSc). [1] L. M. de Lima, B. A. Lugon, and L. Catabriga. An Alternative Approach of the SPIKE Preconditioner for Finite Element Analysis. High Performance Computing (HiPC), 2016 IEEE 23rd International Conference on. IEEE, 2016. [2] L. K. Muller, L. M. de Lima, and L. Catabriga. A Comparative Study of Local and Global Preconditioners for Finite Element Analysis. In: Ibero-Latin American Congress on Computational Methods in Engineering - CILAMCE, 2017, Florianópolis, Brazil. Proceeding of the XXXVIII Ibero-Latin American Congress on Computational Methods in Engineering. Florianópolis, Brazil: ABMEC, 2017. p. 1-19.

# Evaluating High Order Discontinuous Galerkin Discretizations of the Boltzmann Collision Integral in $O(N^2)$ Operations Using the Discrete Fourier Transform

Jeffrey Limbacher\*, Alexander Alekseenko\*\*

\*California State University Northridge, \*\*California State University Northridge

## ABSTRACT

Continuing progress in a number of important applications of slow flows and/or time dependent flows of non-continuum gases requires design of new efficient scalable deterministic methods for solution of the Boltzmann equation. The key difficulty in numerical solution of the Boltzmann equation is evaluation of the multifold collision integral that accounts for interactions of gas molecules. Development of numerical algorithms for efficient and accurate evaluation of the collision integral is at the forefront of recent advances in kinetic theory. We present a novel approach for evaluating the Boltzmann collision operator in  $O(N^2)$  operations where  $N$  is the number of discrete velocity points. The method is formulated for high order nodal discontinuous Galerkin (DG) discretizations of the Boltzmann equation in the velocity variable. At the foundation of the new approach is the convolution form of the Galerkin projection of the collision integral. To achieve efficiency, the solution and the collision kernel are periodically extended and the direct convolution in  $R^3$  is replaced by a circular convolution. The discrete Fourier transform is used to rewrite the collision operator as a weighted convolution in the frequency space. The approach is formulated, implemented, and tested for uniform meshes, however, generalizations to octree meshes are possible. Accuracy of the method was investigated by comparing it to the direct evaluation of convolution and an established DSMC solver. Different forms of the collision operator were investigated. It was found that the non-split form, in which the gain and loss terms are kept together, is the most suitable for fulfillment of the conservation laws. Also, the macro-micro decomposition, in which the solution is represented as a sum of the local Maxwellian and a correction term (not small) was found to help maintain the conservation laws. Evaluation of the collision operator using the discrete Fourier transform results in a two orders of magnitude increase in speed as compared to the direct evaluation.

## **A Versatile Hyperbolic Constitutive Framework for Soft Tissue Elasticity-Application to Skin Mechanics**

Georges Limbert\*

\*University of Southampton

### **ABSTRACT**

Over the last two decades, soft tissue mechanics has been a very active area of research resulting in a wide range of constitutive theories. Nowadays, scientists, engineers and clinicians jointly capitalise on these advances to make practical and quantitative predictions about biological systems and their interactions with engineered devices. This is typically done through the use of computational models developed in concert with dedicated physical experiments. Although constitutive models of soft tissues have reached a high level of sophistication in terms of their ability to capture anelastic and mechanobiological phenomena, as well as their integration of microstructural information, there is still the need for simple versatile phenomenological models featuring a minimum number of physically meaningful constitutive parameters. The objective of this research was to develop such a generic constitutive framework, capable of reproducing a wide range of responses (e.g. low stiffness at moderate strains, strain hardening and locking), whilst also capturing different types of material symmetry for various soft tissues. The constitutive model is based on hyperbolic functions and traditional isotropic and anisotropic tensor invariants but can also accommodate invariants arising from fully decoupled modes of deformation [1] which can capture matrix-to-fibre and fibre-to-fibre interactions. Properties of polyconvexity and stress-free configuration in the reference placement are enforced a priori. A parametric smooth version of the Heaviside step function was also devised to enable a no- or little-compression option when fibres are subjected to compression along their main axis. Constitutive parameters were identified from experimental data obtained from physical tests on skin and arteries samples. The constitutive model was shown to reproduce very well the experimental macroscopic multi-axial properties of these tissues. The constitutive formulation was implemented into a non-linear finite element code using a three-dimensional enhanced strain formulation [2]. Direct sensitivity routines were also developed to assess the influence of constitutive parameters, geometry and loads on the mechanical response of a multi-layer finite element model of the skin subjected to various loading scenarios. The conceptually simple formulation should prove useful for a wide range of biological soft tissues. References [1] Limbert, G. 2011. *J Mech Behav Biomed Mater*, 4 1637-1657. [2] Korelc, J. et al. 2010. *Comput. Mech.*, 46 641-659.

## **Simulations of Turbulent Flow over Periodic Hills with Multiple-relaxation-time Lattice Boltzmann Method on Multi-GPU Cluster**

Chao-An Lin<sup>\*</sup>, Chi-Wei Su<sup>\*\*</sup>, Xiao-Ying Huang<sup>\*\*\*</sup>

<sup>\*</sup>National Tsing Hua University, <sup>\*\*</sup>National Tsing Hua University, <sup>\*\*\*</sup>National Tsing Hua University

### **ABSTRACT**

Laminar and turbulent channel flows over periodic hills were simulated with single-relaxation-time and multiple-relaxation-time lattice Boltzmann method. To speed up the simulation, the computation was conducted on multi-GPU cluster with two-dimensional decomposition by message passing interface(MPI). The laminar flow was simulated at Reynolds number  $Re = 25, 50, 75, 100$  and compared with benchmark solutions for validation. For turbulent flow simulations, the Reynolds number was set to be  $Re = 700$  and the results were in comparison with DNS results. Both results are compared and are in good agreement. In addition, the parallel performance was tested by the strong scaling test on the GPU cluster.

## Consistent Strong Enforcement of Essential Boundary Conditions in Meshfree Methods

Kuan-Chung Lin\*, Michael Hillman\*\*

\*The Pennsylvania State University, \*\*The Pennsylvania State University

### ABSTRACT

Essential boundary condition enforcement in meshfree methods requires special techniques since nodal coefficients of shape functions are not the actual field values. Strong enforcement of boundary conditions at nodes can be accomplished in several ways, such as the transformation method [1], use of a singular kernel [2], and so on. With these approaches, the standard weak form with kinematically admissible approximations is employed, yet between nodes, test functions are generally non-zero, while trial functions also may not satisfy the essential boundary conditions either. In this work, it is first shown that the consequence of employing the standard weak form with these methods is not negligible, as much lower rates of convergence are obtained than expected for meshfree basis functions higher than linear, and in some cases, for linear. Two weighted residual formulations are proposed that allow for test and trial functions which are not kinematically admissible, including a version which yields a symmetric stiffness matrix. When employed with the transformation method, optimal convergence rates are restored, and in general much lower error is obtained in the solution. [1] Chen, J. S., Pan, C., Wu, C. T., and Liu, W. K., 1996. Reproducing kernel particle methods for large deformation analysis of non-linear structures. *Computer Methods in Applied Mechanics and Engineering*, 139(1–4), pp.195–227. [2] Chen, J. S., and Wang, H. P., 2000. New boundary condition treatments in meshfree computation of contact problems. *Computer Methods in Applied Mechanics and Engineering*, 187(3–4), pp.441–468.

## Computational Investigation of Hot-spots Generation by Micocracks in Carbon Nanotube Reinforced Composite under Dynamic Loading

Liqiang Lin<sup>\*</sup>, Justin Wilkerson<sup>\*\*</sup>, Xiaowei Zeng<sup>\*\*\*</sup>

<sup>\*</sup>University of Texas at San Antonio, <sup>\*\*</sup>Texas A&M; University, <sup>\*\*\*</sup>University of Texas at San Antonio

### ABSTRACT

The sensitivity of polymer-bonded explosives (PBXs) can be tuned through adjusting binder material and volume fraction, crystal composition and morphology. To obtain a better understanding on correlation between grain-level failure and hot-spots generation in energetic composites as they undergo mechanical and thermal processes subsequent to impact, a recently developed interfacial zone finite element model (IZFEM) was used to study the dynamic response of polymer-bonded explosives. The IZFEM can capture the contributions of deformation and fracture of the binder phase as well as interfacial debonding and subsequent friction on hot-spots generation. In this study, a 2D computational model of carbon nanotube reinforced polycrystalline composite was developed. The proposed computational model has been applied to simulate hot-spots formation in polymer-bonded explosives with different carbon nanotube volume fraction under dynamic loading. Our simulation showed that the carbon nanotubes will provide additional dissipation pathways for impact energy as well as conduct heat away from energy localizations.

## Performance of AMG-based Preconditioners for Fully-coupled Newton-Krylov Methods for Implicit Continuum Plasma Simulations

Paul Lin<sup>\*</sup>, Roger Pawlowski<sup>\*\*</sup>, John Shadid<sup>\*\*\*</sup>, Edward Phillips<sup>\*\*\*\*</sup>, Eric Cyr<sup>\*\*\*\*\*</sup>

<sup>\*</sup>Sandia National Laboratories, <sup>\*\*</sup>Sandia National Laboratories, <sup>\*\*\*</sup>Sandia National Laboratories, <sup>\*\*\*\*</sup>Sandia National Laboratories, <sup>\*\*\*\*\*</sup>Sandia National Laboratories

### ABSTRACT

Abstract The computational simulation of continuum models of plasma physics systems can be extremely challenging. These difficulties arise from both the strong nonlinear coupling of fluid and electromagnetic phenomena, as well as the significant range of time-scales that the interactions of these physical mechanisms produce. From this point of view, fully-implicit formulations, coupled with effective robust nonlinear iterative solution methods, become attractive, as they have the potential to provide stable, higher-order time-integration of these complex multiphysics systems when long dynamical time-scales are of interest. For the solution of the discrete nonlinear system, the use of fully-coupled Newton-Krylov solution approaches can be advantageous because of their robustness. To enable scalable and efficient solution of the large-scale sparse linear systems generated by the fully-coupled Newton linearization, multilevel/multigrid preconditioners are developed. The multigrid preconditioners are based on two differing approaches. The first technique employs a graph-based aggregation method applied to the nonzero block structure of the Jacobian matrix [1-2]. The second approach utilizes approximate block decomposition methods and physics-based preconditioning approaches that reduce the coupled systems into a set of simplified systems to which multigrid methods are applied [3]. This talk considers the scaling and performance of these algebraic multigrid (AMG) based solution approaches for both MHD and multifluid plasma models with finite element type methods on unstructured meshes. The focus is on large-scale, transient plasma simulations. Studies are presented for scaling and performance on both CPU (IBM Blue Gene/Q and Intel Xeon) and Intel Xeon Phi Knights Landing platforms. References [1] J. Shadid, R. Pawlowski, E. Cyr, R. Tuminaro, P. Weber and L. Chacon, &quot;Scalable Implicit Incompressible Resistive MHD with Stabilized FE and Fully-coupled Newton-Krylov-AMG,&quot; Computer Methods in Applied Mechanics and Engineering, 2016, Vol. 304, pp. 1-25 [2] P.T. Lin, J.N. Shadid, J.J. Hu, R.P. Pawlowski, E.C. Cyr, &quot;Performance of Fully-coupled Algebraic Multigrid Preconditioners for Large-scale VMS Resistive MHD,&quot; Journal of Computational and Applied Mathematics, 2017, in press (<https://doi.org/10.1016/j.cam.2017.09.028>) [3] E. Phillips, J. N. Shadid, E. C. Cyr, and R. Pawlowski. Fast linear solvers for multifluid continuum plasma simulations. Extended abstract and presentation NECDC 2016.

## The Research on Settlement and Damage Characteristics of Pavement Structure under Impulse Load by CDEM (Continuous-discontinuous Element Method)

Qindong Lin<sup>\*</sup>, Chun Feng<sup>\*\*</sup>, Shihai Li<sup>\*\*\*</sup>

<sup>\*</sup>Institute of Mechanics, Chinese Academy of Science, <sup>\*\*</sup>Institute of Mechanics, Chinese Academy of Science, <sup>\*\*\*</sup>Institute of Mechanics, Chinese Academy of Science

### ABSTRACT

The load of Falling Hammer Crusher and Falling Weight Deflectometer can be reduced to instantaneous impulse load. Finite Element Method is usually used to study the impact of impulse load on pavement structure, but it can't accurately describe the damage characteristics. An explicit numerical calculation method CDEM that based on the coupling of FEM and DEM is used to simulate the gradual destruction of the material. With the method of CDEM, the influence of impulse load on the deformation and damage characteristics of pavement structure was discussed. Taking the linear elastic model coupled with Mohr-Coulomb criterion and the maximum tensile stress criterion as constitutive model of element of pavement structure and subgrade material in CDEM. The virtual interface and the real interface in CDEM are described by the brittle fracture Mohr-Coulomb model and the maximum tensile stress criterion. Impulse load is reduced to a trapezoidal load with a certain amplitude and pulse width. Through the comparison with the test results of falling weight deflectometer, the computational accuracy of the CDEM method for calculating the small impact load elasticity problem is proved. By comparing with commercial software Abaqus, the computational accuracy of CDEM simulating plastic rupture problem is proved. The calculation results show that: 1. CDEM can explicitly expresses the initiation and expansion process of cracks. 2. The crack shape of the pavement structure is related to the area, amplitude of the impulse load and pavement structure. Vertical cracks occur in the layers and horizontal cracks occur between the layers. 3. When the cracks occur in the layers, the settlement will increase, this is due to cracks that reduce the structural integrity of the pavement and its ability to dissipate the load. What's more, the increasing proportion of cement concrete pavement is greater than that of asphalt concrete pavement. 4. The settlement of the pavement is positively correlated with the amplitude, time and area of the impulse load. 5. When the layer can be broken, the curve of settlement in one direction will have obvious inflection point. These conclusions have important guiding significance for the research on the crushing of concrete pavement and the settlement of pavement structure under impulse load.

## **A Numerical Method for Simulation of Flow Past a Square Cylinder with Porous Wall**

San Yih Lin<sup>\*</sup>, Ya Hsien Chin<sup>\*\*</sup>, Jeu Jiun Hu<sup>\*\*\*</sup>

<sup>\*</sup>National Cheng Kung University, <sup>\*\*</sup>Overseas Chinese University, <sup>\*\*\*</sup>Shu-Te University

### **ABSTRACT**

The IB-Penalization pressure correction method is developed to simulate a flow past a square cylinder with porous wall. The numerical method can deal with fluid-porous-solid system by using a direct-forcing immersed boundary (IB) method to handle flow past a solid body and a penalization method to handle flow in porous wall. About the fluid field, the method uses a pressure correction method to solve the solutions of incompressible Navier-Stokes equations. The physical model creates intermediate porous media between the solid body and the fluid to modify the boundary layer behavior. First, we use two numerical methods, direct-forcing IB and penalization, to simulate the flow past a solid square cylinder. Two numerical results will be compared each other. Then the IB-Penalization pressure correction method is developed to simulate the flow past a square cylinder with porous wall. A parametric study is performed to investigate the effect of the porosity and thickness on the porous layer.

## **A Nonlinear Gradient-based Reliability Assessment Method (GRAM) for Reliability-Based Design Optimization (RBDO)**

Shu-Ping Lin\*, Po Ting Lin\*\*

\*National Taiwan University of Science and Technology, \*\*National Taiwan University of Science and Technology,  
Taiwan

### **ABSTRACT**

This paper presents a nonlinear Reliability-Based Design Optimization (RBDO) method, which estimates a new reliability assessment based on gradient evaluated at the Most Probable Failure Point (MPFP) and formulates a nonlinear probabilistic constraint at the Allowable Reliability Point (ARP). At first, the MPFP for each performance constraint is determined in terms of minimizing the distance between the design point and the constraint in the original design space (not in the standard normal space). The advantage of finding the MPFP in the original design space is that the new method does not require transformation to the standard normal space, which sometimes is difficult to determine. Next, an approximated constraint function is formulated based on expansion at the MPFP. The approximated constraint function is then shifted along the negative gradient direction, that is evaluated at the MPFP, toward the feasible space by the distance of a Gradient-based Reliability Assessment (GRA), which equals the distance between the design point and the Most Probable Target Point (MPTP). MPTP is located at the position where the failure probability of the shifted constraint function equals to the allowable probability. The second advantage of the proposed method is that it provides a better approximation of the nonlinear probabilistic constraint than traditional first-order reliability methods. Several numerical examples will be examined to show the numerical performances of the proposed Gradient-based Reliability Assessment Method (GRAM).

## **A Balanced-forced Level Set Method on Unstructured Meshes for Thermal Multiphase Flows**

Stephen Lin<sup>\*</sup>, Jinhui Yan<sup>\*\*</sup>, Gregory Wagner<sup>\*\*\*</sup>

<sup>\*</sup>Northwestern University, <sup>\*\*</sup>Northwestern University, <sup>\*\*\*</sup>Northwestern University

### **ABSTRACT**

The interaction between multiple phases (such as solid, liquid and gas) drive many industrial processes, such as additive manufacturing. Physical driving mechanisms driving the free-surface evolution involve surface tension and Marangoni forces at the gas and fluid interface; therefore an accurate computation of these forces is necessary to sufficiently resolve the free-surface evolution. In this work, we present a balanced-force level set formulation on unstructured meshes using a control volume finite element method (CVFEM) for large-scale parallel simulations of thermal multiphase flows that capture the evolution of the liquid, gas and solid phases. We demonstrate that our balanced-force algorithm is able to exactly balance the resulting pressure gradient and surface tension forces for a specified curvature; validation examples show that this balanced-force is necessary to achieve convergence for flows driven by surface force applications. These interfacial forces become significant in engineering applications that exhibit highly localized phenomena including melting and subsequent flow of molten metals in additive manufacturing processes.

## Variational Inequalities for Saddle Point Functionals in Continuum Mechanics and Their Relevance to Error Estimates

Christian Linder<sup>\*</sup>, Andreas Krischok<sup>\*\*</sup>

<sup>\*</sup>Stanford University, <sup>\*\*</sup>Stanford University

### ABSTRACT

We present a variational approach towards identifying conditions for stability and uniqueness of Galerkin methods based on saddle point problems in continuum mechanics and continuum thermodynamics. The framework aims to generalize the inf-sup theory in the context of general problems in an arbitrary number of fields for both linear and nonlinear settings. In utilizing a linearized second derivative test for admissible variations, the proposed framework is purely based on uniqueness properties of a mixed Lagrangian around the solution, thus combining requirements that descend from variational calculus with error estimates for finite-dimensional Galerkin methods. In particular, due to its universal form and its straightforward connection to generalized numerical tests, the proposed framework is trusted to provide a helpful tool for the development of mixed methods that arise in many novel engineering problems due to the coupling of multiple physical phenomena.

## **Defect Estimation within the Limitations of Computational Welding Mechanics**

Lars-Erik Lindgren Lindgren<sup>\*</sup>, Joar Draxler<sup>\*\*</sup>, Andreas Lundbäck<sup>\*\*\*</sup>, Jonas Edberg<sup>\*\*\*\*</sup>

<sup>\*</sup>Luleå University of Technology, Sweden, <sup>\*\*</sup>Luleå University of Technology, Sweden, <sup>\*\*\*</sup>Luleå University of Technology, Sweden, <sup>\*\*\*\*</sup>Luleå University of Technology, Sweden

### **ABSTRACT**

The approaches developed from the 1970ies and onward regarding modelling of welding are also applicable to additive manufacturing when limiting the focus on the macroscopic scale excluding details of the process zone as well as addition of filler material or the existence of powders. The aim of Computational Welding Mechanics (CWM) is to model the overall mechanical performance of the welded component or structure. CWM models can be combined with models for microstructure evolution coupled with thermo-mechanical. The centrepiece in welding simulations is the heat generation process. Its description belongs to the domain of thermo-mechanics in the case of explosive welding, friction welding and friction stir welding. Resistance welding need the inclusion of the electrical field also. However, the process becomes much more complex for fusion welding processes. Weld process modelling (WPM) focuses on modelling the physics of the heat generation. The limiting region between these models is the liquid-solid boundary. They have different time and spatial scales and are not easily solved simultaneously. Therefore most CWM models start with a calibrated heat source model and exclude fluid flow. There are various approaches that have been used over the last decades to estimate the risk for cracking. The talk reviews these approaches and also describes developments for enable better descriptions in the near weld region for crack initiation estimates.

## Modelling of Bulk Metallic Glass Formation in Powder Bed Fusion

Johan Lindwall\*, Victor Pacheco\*\*

\*Luleå University of Technology, \*\*Uppsala University

### ABSTRACT

Additive manufacturing by the powder bed fusion process can provide cooling rates high enough to avoid crystallization, i.e. create bulk metallic glasses. The small melting pool connected to a relatively large volume of cooling material gives cooling rates many orders of magnitude larger than the critical cooling rate for the studied glass forming alloy AMZ4. However, subsequent reheating of built material may cause devitrification, i.e. crystallization of the amorphous phase. The present work aims to simulate the thermal cycles of the powder bed fusion process in order to evaluate and mitigate the risk of devitrification. This is done by combining finite elements simulations with a phase transformation model for the amorphous and crystal phases. The response of AMZ4, in the present case limited to heating of amorphous material from room temperature, was evaluated using DSC measurements with varying low heating rates. This limited set of information is used to construction the lower part of the crystallization diagram based on a JMAK-model. Previous work has developed simulation techniques for efficient simulations of glass formation in powder bed fusion. Temperatures can be computed with sufficient accuracy and considerable reduced computational time compared to a fully detailed model. The simplifications were based on temporal reduction by consolidating the heat source to strings or entire layers by assuming infinite scanning speed in one or two directions. The JMAK- model will now be used combined with these techniques. Further understanding of when and where crystals may be formed can be acquired by the presented work.

## **IMPROVEMENT AND APPLICATION OF THE LARGE SCALE 2D 3D HYBRID TSUNAMI NUMERICAL MODEL**

**GUOMING LING\* JUNICHI MATSUMOTO† ETHAN J. KUBATKO‡  
AND KAZUO KASHIYAMA§**

\*Research and Development Initiative, Chuo University

Kasuga 1-13-27, Bunkyo-ku

Tokyo, Japan

Email address: [lingguoming@civil.chuo-u.ac.jp](mailto:lingguoming@civil.chuo-u.ac.jp)

†National Institute of Advanced Industrial Science and Technology (AIST)

Namiki 1-2-1, Tsukuba

Ibaraki, Japan

Email address: [matsumoto-junichi@aist.go.jp](mailto:matsumoto-junichi@aist.go.jp)

‡Department of Civil, Environment and Geodetic Engineering, Ohio State University

417D Hitchcock Hall, 2070 Neil Avenue

Columbus, OH 43210, U.S.A

Email address: [kubatko.3@osu.edu](mailto:kubatko.3@osu.edu)

§Department of Civil and Environmental Engineering, Chuo University

Kasuga 1-13-27, Bunkyo-ku

Tokyo, Japan

Email address: [kaz@civil.chuo-u.ac.jp](mailto:kaz@civil.chuo-u.ac.jp)

**Key words:** 2D-3D Hybrid Model, Tsunami Simulation, Overlapping Method, Arbitrary Grid.

**Abstract.** This paper presents some improvements and applications of a large-scale 2D-3D hybrid tsunami numerical model which we have developed. The overlapping method based on arbitrary grid is applied as a two-way coupling method to connect a 2D model and a 3D model. For the 2D model, the shallow water equations are applied as the governing equations. For the 3D model, the phase-field model (PFM) governed by the Allen-Cahn equation is applied for the free surface flow. The numerical accuracy of the present method is verified on several numerical

examples.

## 1 INTRODUCTION

Since the tsunami disaster occurred by the 2011 Great East Japan Earthquake, awareness has been improved that not only the prediction of the inundation area of the tsunami but also the damage prediction of structure is extremely important. In practice, the two dimensional (2D) shallow water equations have been widely used for simulating the inundation damage of tsunami. However, in order to compute the fluid force acting on the structure precisely, the three dimensional (3D) free surface flow simulation is needed. But it is still not realistic for simulating tsunami waves from the source area to urban area all by 3D considering the huge computation cost. Therefore, a hybrid model can be an efficient and a reasonable tool by simulating the wave propagation in ocean by a 2D model and in the target area with structures by a 3D model.

In recent years, several 2D-3D hybrid models have been proposed. Some of the 2D-3D hybrid models are based on structured Cartesian grids, e.g. Masamura *et al.* <sup>[1]</sup>, Tomita *et al.* <sup>[2]</sup>, Fukui *et al.* <sup>[3]</sup>, Pringle *et al.* <sup>[4]</sup>, Arikawa *et al.* <sup>[5]</sup>. These models have shown the 2D-3D hybrid models can significantly reduce the calculation load comparing to the fully 3D model, and they also can reproduce the characteristics of 3D flows which cannot be reproduced by the 2D model. However, since these methods use structured grids, meshing the structure or the terrain with a complex geometry exactly is difficult in numerical simulation. To this reason, Takase *et al.* <sup>[6]</sup> proposed a 2D-3D hybrid model based on the stabilized finite element method which can use arbitrary grid. In this model, the multiple point constraint (MPC) method is employed to connect the 2D and 3D models, for which a shared border boundary has to be set between the 2D and 3D domains. The applications were limited to some simple numerical examples. Recently, Mitsume *et al.* <sup>[7]</sup>, Asai *et al.* <sup>[8]</sup> proposed the 2D-3D hybrid models using particle method, but they are one-way coupling models.

The objective of our study is to develop a 2D-3D hybrid model for large-scale tsunami simulation, which can treat with complicate geometry in a two-way coupling. In this paper, we aim to improve the accuracy and the robustness of the 2D and 3D models we used in the proposed 2D-3D hybrid model <sup>[9]</sup>. The shallow water equations are applied as the governing equations for the 2D model, the Navier-Stokes equations and the Allen-Cahn equation are applied as the governing equations for the 3D model. The stabilized finite element method <sup>[6, 10]</sup> is applied for the spatial discretization. The Crank-Nicolson method is applied for the temporal discretization. The Message Passing Interface (MPI) is employed as the parallel computing method. Several numerical examples are simulated to show the validity and efficiency of the present method.

## 2 GOVERNING EQUATIONS

The governing equations for the 2D and 3D models are described in this section.

### 2.1 Shallow water equations for the 2D model

The wave propagation from source area to offshore area is governed by the non-linear shallow water equations,

$$\frac{\partial(U_i H)}{\partial t} + \frac{\partial(U_j U_i H)}{\partial x_j} + \nu_e \frac{\partial^2(U_i H)}{\partial x_j^2} + \frac{g n^2 U_i \sqrt{U_j U_j}}{H^{\frac{1}{3}}} + g H \frac{\partial(H + z)}{\partial x_i} = 0 \quad (1)$$

$$\frac{\partial H}{\partial t} + \frac{\partial(U_i H)}{\partial x_i} = 0 \quad (2)$$

where  $U_i$  is the average velocity in  $x_i$  direction,  $H$  is the total water depth,  $g$  is the gravitational acceleration,  $\nu_e$  is the eddy viscosity coefficient,  $n$  is the Manning's roughness coefficient and  $z$  is the height of bottom.

### 2.2 Navier Stokes equations and Allen Cahn equation for the 3D model

The 3D free surface flow model is governed by the Navier-Stokes equations, continuity equations and the Allen-Cahn equation<sup>[11]</sup>,

$$\rho \left( \frac{\partial u_i}{\partial t} + u_j \frac{\partial u_i}{\partial x_j} - f_i \right) + \frac{\partial p}{\partial x_i} - \mu \frac{\partial}{\partial x_j} \left( \frac{\partial u_i}{\partial x_j} + \frac{\partial u_j}{\partial x_i} \right) = 0 \quad (3)$$

$$\frac{\partial u_i}{\partial x_i} = 0 \quad (4)$$

$$\frac{\partial \phi}{\partial t} + u_j \frac{\partial \phi}{\partial x_j} = -M_a \left[ \xi(\phi) - \kappa_\phi \left( \frac{\partial^2 \phi}{\partial x_j^2} + \kappa \left| \frac{\partial \phi}{\partial x_k} \right| \right) \right] \quad (5)$$

where  $\rho, u_i, f, p, \mu$  are the density, velocity, body force, pressure, viscosity coefficient, respectively.  $\phi$  is the phase function,  $\phi = 1$  denotes fluid,  $\phi = 0$  denotes gas,  $\phi = 0.5$  denotes free surface.  $M_a, \xi(\phi), \kappa_\phi, \kappa$  are defined as,

$$M_a = \frac{2b^2}{\delta^2} M\gamma, \quad b = 2 \tanh^{-1}(1 - 2\lambda), \quad \delta = a_\delta h_\delta$$

$$\xi(\phi) = \frac{\partial f(\phi)}{\partial \phi}, \quad f(\phi) = \phi^2(1 - \phi)^2,$$

$$\kappa_\phi = \frac{\delta^2}{2b^2},$$

$$\kappa = \nabla \cdot \mathbf{n}, \quad \mathbf{n} = \frac{\nabla \phi}{|\nabla \phi|}$$

where  $M, \gamma, \delta, h_\delta, \kappa, \mathbf{n}$  are the interface mobility, interface energy, continuously changing gas-liquid interface width, representative length of element, interface curvature, interface normal vector.

### 2.3 Discretization methods

For the spatial discretization, the stabilized finite element method based on the SUPG method<sup>[10]</sup> is applied to Eqs. (1), (2), (5), the stabilized finite element method based on the SUPG/PSPG method<sup>[6]</sup> is applied to Eqs. (3), (4). For the temporal discretization, the Crank-Nicolson method with second order accuracy is applied. And to solve the simulation linear equations, the element-by-element Bi-CGSTAB (Bi-Conjugate Gradient STABILized) method is applied.

## 4 2D 3D OVERLAPPING METHOD

In this study, the 2D-3D overlapping method shown in the **Figure 1** based on arbitrary grid is developed. In this method, the computational domain is separated into a 2D domain and a 3D domain. An overlap domain for the 2D and 3D domains is set. The domains and the grids of 2D and 3D can be arbitrary. Then the inner boundary of the 2D domain is defined as a 2D connection boundary, while the outer boundary of the 3D domain is defined as a 3D connection boundary. At the 2D connection boundary and the 3D connection boundary, the nodes of 2D and 3D can be located at different places. For the computation, the flow velocities and the water depth computed from the 3D domain are used as the boundary conditions of the 2D connection boundary. As the same, the flow velocities and the water depth computed from 2D domain are used as the boundary conditions of the 3D connection boundary. For the computation of real terrain tsunami simulation, the 3D domain can be chosen anywhere we want to compute precisely. Because of the place for the nodes of 2D and 3D is different, the boundary condition of 2D/3D connection boundary should be computed by making interpolation. The flowchart of

the 2D-3D overlapping method is shown in the **Figure 2**.

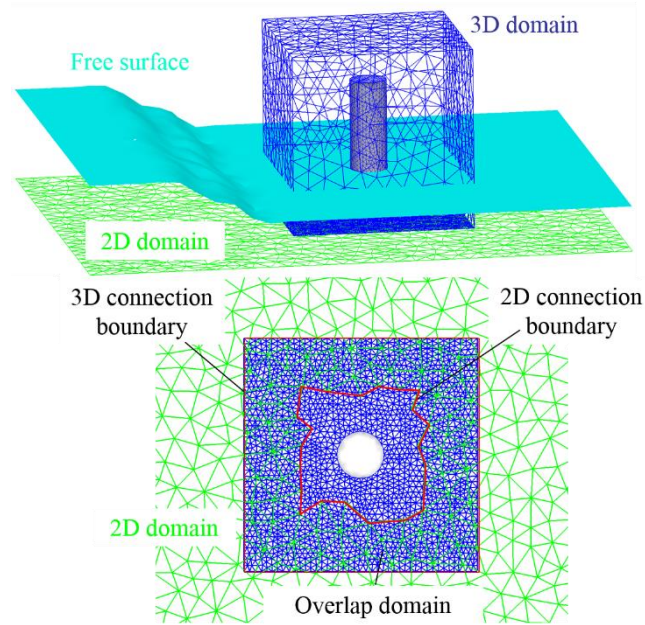


**Figure 1** Overlapping method

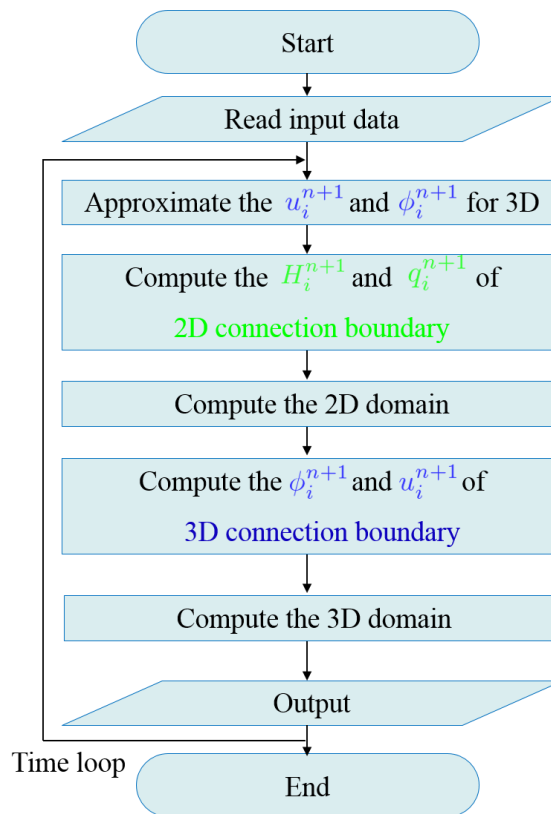


**Figure 2** Flowchart for 2D 3D overlapping method

## NUMERICAL EXPERIMENTS

### 3.1 Runup of solitary wave problem

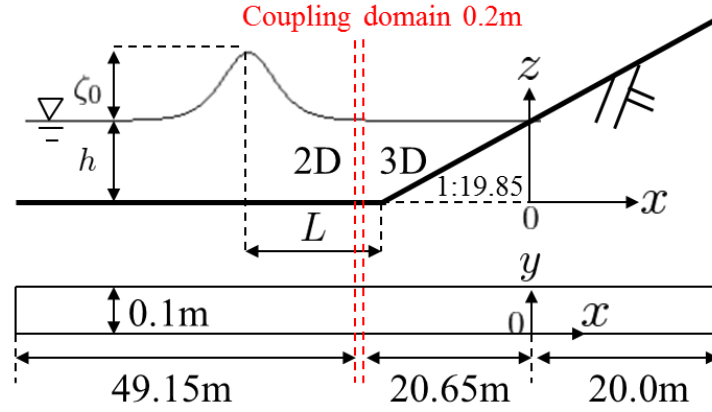


Figure 3 Computational model

The runup of a solitary wave problem shown in **Figure 3** is simulated to investigate the applicability of the 2D-3D hybrid model. The computational results are compared to the experimental results <sup>[12]</sup>, the results of 2D model and 3D model. For the initial conditions, the initial wave height is set by the following equation,

$$\zeta(x, t = 0) = \frac{\zeta_0}{h} \operatorname{sech}^2 \left( \sqrt{\frac{3\zeta_0}{4h}} (x - x_0) \right) \quad (4)$$

the ratio of the wave height  $\zeta_0$  and the static depth  $h$  is set to be 0.3.  $x_0$  is the location of wave crest. The initial flow velocity is set by the following equation,

$$u(x, t = 0) = \zeta(x, t = 0) \sqrt{\frac{g}{h}} \quad (5)$$

The wave crest is located at the half solitary wave length from the front end of the slope.

$$L = \sqrt{\frac{4h}{3\zeta_0}} \operatorname{arccosh} \left( \sqrt{\frac{1}{0.05}} \right) \quad (6)$$

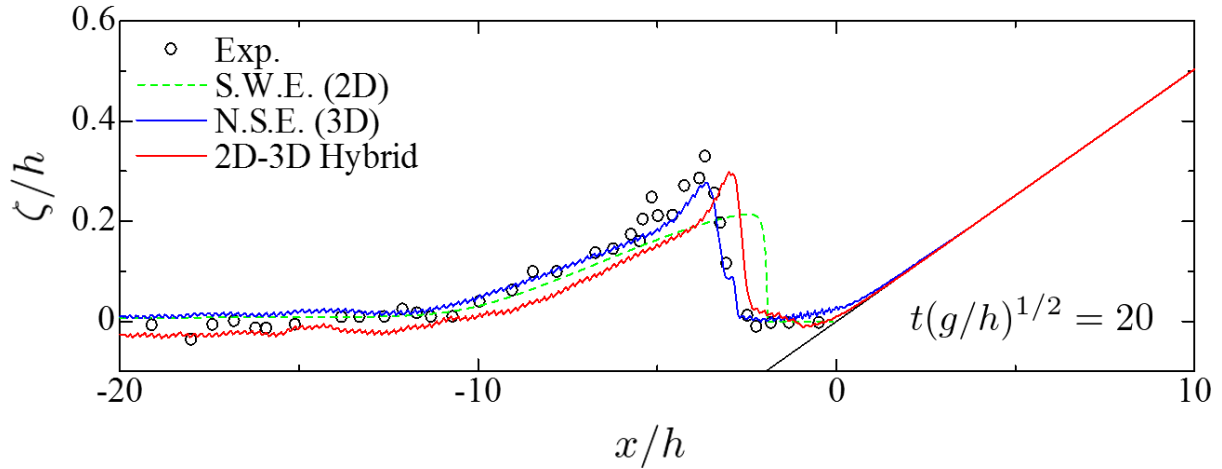


Figure 4 Surface elevation at  $t'=20$

For the computational condition, the mesh size is 0.05m and the time increment is 0.001s.

The comparison of the surface profiles at  $t' = t\sqrt{g/h} = 20$  is shown in the **Figure 4**. From this figure, we can see the result of the 3D model is in the best agreement with the experimental result. The result of the 2D-3D hybrid model show better agreement with the experimental results than the results of the 2D model.

## .2 Tsunami simulation on real terrain

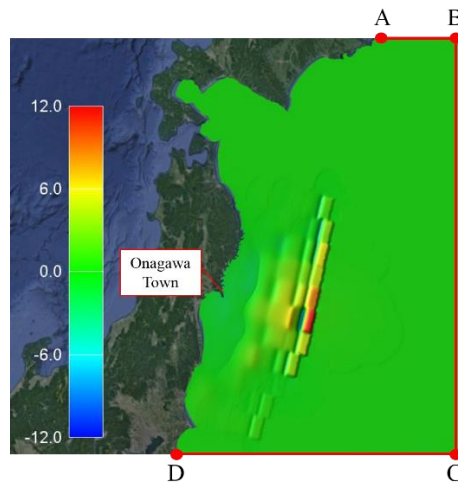


Figure Computational model initial condition

In order to test the applicability of the 2D-3D hybrid tsunami numerical model to the real terrain, the computational model shown in **Figure** is simulated. For this example, the area around the Onagawa town is simulated by 3D while the other area by 2D. For the initial

condition, the fault model of Ver. 8.0 by Satake *et al.* <sup>[13]</sup> is applied. For the boundary conditions, the shoreline is non-slip condition and the ABCD boundary is set open boundary condition. The mesh information of the 2D and 3D domains is shown in **Table 1**. The time increment is 0.1s.

**Figure** shows the computational result at 2000.0s, in the figure, the green denotes the results of 2D domain and the blue denotes the 3D domain. We can see the buildings are flooded by the tsunami waves. The applicability of the present method to the real terrain has been confirmed by this numerical example.

**Table 1 Mesh information**

	2D	3D
Number of nodes	557,252	23,232,416
Number of elements	1,103,938	134,768,640

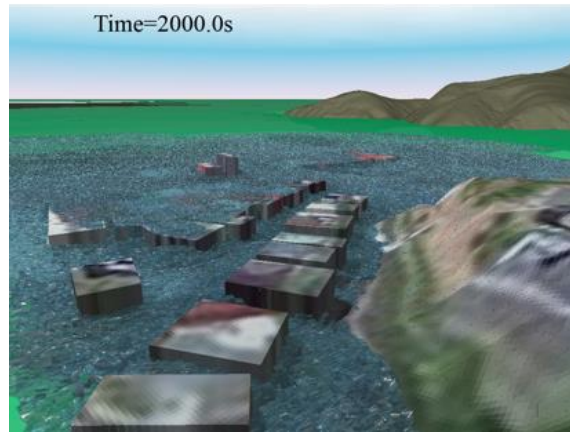


**Figure Computational result at 2 . s**

## CONCLUSIONS

In this paper, a 2D-3D hybrid tsunami numerical model using the overlapping method based on arbitrary grid was developed. By the numerical examples, the following conclusions can be drawn.

- From the runup of solitary wave problem, the numerical result of the present method is in good agreement with the experimental results.
- From the application to the tsunami caused by the Great East Japan Earthquake, the applicability of the present method has been confirmed.

For the future work, we are planning to apply the present 2D-3D hybrid model to solve the

fluid structural interaction (FSI) problems.

## REFERENCES

- [1] Masamura, K., Fujima, K., Goto, C., Iida, K. and Shigemura, T. Numerical analysis of tsunami by using 2d/3d hybrid model. *Journal of JSCE*, (2001), pp. 49-61. (in Japanese)
- [2] Tomita, T. and Kakinuma, T. Storm surge and tsunami simulation in oceans and coastal areas (STOC). Report of the Port and Airport Research Institute, (2005), pp. 83-98.
- [3] Fukui, T., Koshimura, S. and Matsuyama, M. 2D-3D Hybrid Simulation of Tsunami Inundation Flow by Lattice Boltzmann Method. *Journal of Japan Society of Civil Engineers, Ser. B2 (Coastal Engineering)*, Vol. 66(1), (2010), pp. 61-65. (in Japanese)
- [4] Pringle, W., Yoneyama, N. and Mori, N. Two-way coupled long wave - RANS model: Solitary wave transformation and breaking on a plane beach. *Coastal Engineering*, Vol. 114, (2016), pp. 99-118.
- [5] Arikawa, T. and Tomita, T. Development of High Resolution Tsunami Runup Calculation Method Based on a Multi Scale Simulation. Report of the Port and Airport Research Institute, Vol. 53(2), (2014), pp. 3-18. (in Japanese)
- [6] Takase, S., Moriguchi, S., Terada, K., Kato, J., Kyoya, T., Kashiya, K. and Kotani, T. 2D-3D hybrid stabilized finite element method for tsunami runup simulations. *Comput. Mech.*, Vol. 58, (2016), pp. 411-422.
- [7] Mitsume, N., Donahue, A.S., Westerink, J.J. and Yoshimura, S. One-way coupling model based on Boussinesq-type and Navier-Stokes equations for multi-scale tsunami analysis. *Proceedings of the conference on computational engineering and science, CD-ROM, C-5-3*, (2016). (in Japanese)
- [8] Asai, M., Miyagawa, Y., Idris, N., Muhari, A. and Imamura, F. Coupled tsunami simulations based on a 2D shallow-water equation-based finite difference method and 3D incompressible smoothed particle hydrodynamics. *Journal of Earthquake and Tsunami*, Vol. 10(5), (2016). 1640019.
- [9] Ling, G., Matsumoto, J. and Kashiya, K. Large scale tsunami simulation by 2D-3D hybrid method based on arbitrary domain. *COMPSAFE, Chengdu, China*, (2017).
- [10] Takase, S., kashiya, K., Tanaka, S. and Tezduyar, T.E. Space-time SUPG formulation of the shallow-water equation, *International Journal for Numerical Methods in Fluids*, Vol. 64, (2010), pp. 1379-1394.
- [11] Beaucourt, J., Biben, T., Leyrat, A. and Verdier, C. Modeling breakup and relaxation of Newtonian droplets using the advected phase field approach. *Physical Review E*, Vol. 75, (2007), pp. 021405(1-8).
- [12] Synolakis, C.E. The runup of solitary wave. *Journal of Fluid Mechanics*, Vol. 185, (1987).

Guoming Ling, Junichi Matsumoto, Ethan J. Kubatko and Kazuo Kashiya

pp. 523-545.

[13] Satake, K., Fujii, Y., Harada, T. and Namegaya, Y. Time and Space Distribution of Coseismic Slip of the 2011 Tohoku Earthquake as Inferred from Tsunami Waveform Data. *Bulletin of the Seismological Society of America*, Vol. 103, (2013). pp. 1473-1492.

## On the Role of Patient-specific Predictions by Functional MRI Informed Constitutive Modeling

Kevin Linka<sup>\*</sup>, Amelie Schäfer<sup>\*\*</sup>, Mikhail Itskov<sup>\*\*\*</sup>

<sup>\*</sup>Department of Continuum Mechanics, RWTH Aachen University, <sup>\*\*</sup>Department of Continuum Mechanics, RWTH Aachen University, <sup>\*\*\*</sup>Department of Continuum Mechanics, RWTH Aachen University

### ABSTRACT

Osteoarthritis is strongly associated with a degeneration of cartilaginous tissue, which, in turn, is accompanied by tissue softening. One promising non-invasive approach towards its detection appears to be an assessment of multiparametric magnetic resonance (MR) imaging [1,2]. However, so far, there is no reliable correlation between the exact tissue properties and the multiparametric MR image mapping. In this contribution, we developed a constitutive framework in order to inform a cartilage model by sample-specific multiparametric MR maps (T1, T1rho, T2 and T2\*) generated by a clinical 3.0-T MR imaging system. The model predictions of individual patients were fitted against their sample-specific stress responses by enforcing a global set of material parameters. Accordingly, we obtained suitable relations between the specific MR maps and the biomechanical properties. These relations serve as an input for the proposed constitutive law in order to predict the individual stress response of the tested cohort. References [1] Nebelung, S., Sondern, B., Oehrl, S., Tingart, M., Rath, B., Pufe, T., ... & Truhn, D. (2016). Functional MR imaging mapping of human articular cartilage response to loading. *Radiology*, 282(2), 464-474.. [2] K. Linka, M. Itskov, D. Truhn, S. Nebelung, J. Thüning, T2 MR imaging vs. computational modeling of human articular cartilage tissue functionality, *JMBBM*, 74(2017), 477-487.

## Design through Fabrication Systems for Carpentry

Jeffrey Lipton\*, Daniela Rus\*\*

\*MIT CSAIL, \*\*MIT CSAIL

### ABSTRACT

Carpentered items are a critical part of modern lives. They make up the houses people live in along with the furniture and cabinetry inside them. With the Industry 4.0 movement and efforts towards mass customization, laymen are able to design and create a greater number of custom items. This explosion of ability is powered by 3D printing, CNC manufacturing and other robotic fabrication tools. Carpentry however, has few digital design tools that include fabrication. Wood cannot be 3D printed in a meaningful way, and CNC and robotic fabrication methods are expensive and time consuming to setup. Most carpentered items are made by hand with lathes, drill presses and saws. As a result, customization of these items currently requires expert skill, restricting customization to professional and hobbyist carpenters and those who can afford their labor. Recent developments in mobile robotics and digital design tools move us towards mass customization of carpentered items. These advances are predicated on understanding the constraints on the movement of standard carpentry tools and how humans use them. Fabrication and design systems can be made around a tool once its constraints are modeled. Fabrication systems use the model as the basis of path planning and manipulation. Design systems need to know the constraints to ensure parts are in a fabricate-able form. Currently two of the key tools have been modeled, the Jigsaw and the chop saw [1]. These are non-holonomic tools that are model as modified Reeds-Shepp cars. I used this model to make a generic path planning algorithm and combining that with a robotic movement system to turn a jigsaw into a scalable computer controlled cutting machine [1]. For the chop saw I developed fabrication algorithms that control the tolerance stack and allow mobile robots to cut pre-specified lengths of wood with a similar cut quality to a human, despite the robots' movements being imprecise. Through integration of professional CAD systems with user-friendly customization, verification, and robotic fabrication tools, these two tools became the basis of a template design system for co-design of carpentered items. I will discuss motivations and methods for developing constraint models on carpentry tools and discuss how such tools can become the basis of design through fabrication systems for more intricate carpentered items. References [1] J. I. Lipton, Z. Manchester and D. Rus, "Planning cuts for mobile robots with bladed tools," Internation Confrence on Robotics and Automation, pp. 572-579, 2017.

## Optimized Local Bases and Efficient Implementation of Multiscale GFEM

Robert Lipton<sup>\*</sup>, Ivo Babuska<sup>\*\*</sup>, Paul Sinz<sup>\*\*\*</sup>, Michael Stuebner<sup>\*\*\*\*</sup>

<sup>\*</sup>Center for Computation and Technology and Mathematics Louisiana State University, <sup>\*\*</sup>Institute for Computational and Engineering Sciences University of Texas, <sup>\*\*\*</sup>Department of Computational Mathematics and Science and Engineering Mich. State Univ., <sup>\*\*\*\*</sup>University of Dayton Research Institute

### ABSTRACT

We present a computationally efficient method for implementing domain decomposition for multiscale problems. Our approach is to use nearly optimal local bases functions within the Generalized Finite Element Method. Here optimality is measured in terms of the Kolomoragov  $n$ -width. In this talk we describe the new approach and provide several computational examples. We demonstrate the how this method scales favorably with problem size.

## Multiscale Solid Mechanics on Next-Generation Computing Hardware

David Littlewood<sup>\*</sup>, Michael Tupek<sup>\*\*</sup>, J. Antonio Perez<sup>\*\*\*</sup>, Brian Lester<sup>\*\*\*\*</sup>

<sup>\*</sup>Sandia National Laboratories, <sup>\*\*</sup>Sandia National Laboratories, <sup>\*\*\*</sup>University of New Mexico and Sandia National Laboratories, <sup>\*\*\*\*</sup>Sandia National Laboratories

### ABSTRACT

Concurrent multiscale approaches for solid mechanics can resolve small-scale mechanisms within engineering-scale simulations. Their widespread use remains limited, however, due in large part to computational expense. This motivates the adaptation of simulation codes for optimal performance on next-generation computing platforms, which have the potential to enable multiscale and multiphysics models that have been considered intractable to date. In this presentation, we review an ongoing effort to adapt constitutive models within the Library of Advanced Materials for Engineering (LAME) [1] for improved performance on emerging computer architectures characterized by on-node hierarchical parallelism [2]. Increased parallelism is achieved primarily through the Kokkos software package [3], which provides an advanced parallel-for mechanism suitable for the evaluation of constitutive models. Here, memory management is a key issue due to differences in optimal access patterns across disparate architectures. An additional concern is the evolving nature of next-generation hardware, which is addressed by encapsulating hardware-specific source code so that it can be altered at a later date without the need for invasive changes to the material models themselves. The implementation strategy will be discussed, followed by performance analysis of constitutive models in the context of both single-scale and multiscale simulations. Simulations across multiple length scales utilize the well-known FE-squared approach, which associates sub-models that resolve the fine scale with material points in the macroscale model. It is shown that concurrent multiscale modeling is made increasingly viable for engineering-scale simulations by emerging, next-generation computing architectures. [1] W.M. Scherzinger and D.C. Hammerand. Constitutive models in LAME. Report SAND2007-5873, Sandia National Laboratories, Albuquerque, NM and Livermore, CA, 2007. [2] D.J. Littlewood and M.R. Tupek. Adapting material models for improved performance on next-generation hardware. Memorandum SAND2007-5873, Sandia National Laboratories, Albuquerque, NM and Livermore, CA, 2017. [3] H.C. Edwards, C.R. Trott, and D. Sunderland. Kokkos: Enabling manycore performance portability through polymorphic memory access patterns. *Journal of Parallel and Distributed Computing*, 74(12), 2014.

## The Cracks Competition Propagation Simulations for the Composite Adhesively Bonded Joint or Repair Based on Cohesive Zone Model and Hashin Criteria

Bin Liu\*, Rui Yan\*\*

\*Northwestern Polytechnical University, \*\*Xi'an Aeronautical University

### ABSTRACT

Abstract Composites bonded technique are being used widely in the composite joints and repairs of the advanced air vehicle, such as Boeing 747 using bonding junction of 62% among the surface structures, Lockheed C-5A has 3250 m<sup>2</sup> bonding structures. A.B. Harman studied the impact, the compression after impact of composite scarf repair and found that mechanical performance of both the compressional and the tension after impact were affected obviously by the low velocity impact [1]. Generally, the fibers are discontinuous and the adhesive are the new come material for the original matrix and fibers. The damage mechanics FEM model contains the intralaminar solid elements, the interlaminar cohesive zone elements[2,3], and the adhesive cohesive zone elements. In the intralaminar solid elements, fiber fracture, matrix crack and matrix plastic were considered based on the three dimensional Hashin Criteria[4]. The cohesive zone elements considered the composites delamination[5] and adhesive cracks. All the damage elements stiffness would be degraded once the material goes in failure state. The cracks competition propagation was simulated for different loadings. Under the in plane load, the ultimate failure mode is the adhesive shear fracture. The matrix cracks occur at the earliest. Under the out plane impact load, the earliest damage is the delamination and the matrix crack. The delamination dominants the earlier impact stage. When the impact energy increasing to a critical level, the higher-strength adhesive starts cracking. The adhesive cracking also leads to matrix damage. Keywords composite; adhesive; joints; repair; CZM; impact; fracture; delamination Reference [1] A.B. Harman, A.N. Rider. Impact damage tolerance of composite repairs to highly-loaded, high temperature composite structures. Composites Part A: 2011 (42): 1321-1334. [2] B. Liu, F. Xu, W. Feng, R. Yan, W. Xie. Experiment and design methods of composite scarf repair for primary-load bearing structures. Composites Part A: Applied Science and Manufacturing, 2016 (88): 27-38. [3] Panos Papanastasiou, Ernestos Sarris, Cohesive zone models. Woodhead Publishing, 2017:119-144 [4] Z. Hashin. Failure Criteria for Unidirectional Fiber Composites. Journal of Applied Mechanics, 1980 (47): 329-334. [5] Xueling Fan, M.N. Yuan, Q. Qin. Failure mechanisms of Ti-Al<sub>3</sub>Ti metal-intermetallic laminate composites under high-speed impact. Rare Metal Materials and Engineering. 2017,46(3):403-408

## An Efficient and Robust Numerical Integration Scheme for Embedded Interfaces: Application to Fluid-structure Interaction

Bin Liu<sup>\*</sup>, Rajeev Kumar Jaiman<sup>\*\*</sup>

<sup>\*</sup>Department of Mechanical Engineering, National University of Singapore, <sup>\*\*</sup>Department of Mechanical Engineering, National University of Singapore

### ABSTRACT

An efficient, accurate and robust numerical scheme is developed for immersed interface problems with application to fluid-structure interaction (FSI). The incompressible Navier-Stokes equations are solved by the Petrov-Galerkin Finite Element formulation on Cartesian Eulerian grids with finite cell method. In contrast to body-fitted methods, unfitted FEM techniques offer attractive properties for FSI modeling with large displacement and rotation with possible solid-to-solid contact. In a finite-cell unfitted FEM, geometric interfaces of immersed bodies are embedded within each element, termed as a cut cell and the Dirichlet boundary condition is imposed weakly along these interfaces via Nitsche's type method. These interfaces represent a discontinuity embedded in the cut cell, which imposes a difficulty to the conventional numerical integration algorithm. Existing techniques require a sub-division of cut cell into the integration cells and interpolation of scalar values and their gradients from the nodes of the cut cell. Of particular the approximation of the gradients depends on the shape of the cut cell, which leads the degradation of accuracy to resolve complex interface geometry. We introduce a robust and accurate numerical integration technique to deal with the cut cells with embedded discontinuity. Each cut cell is refined into the integration cells. We recognize that elemental matrices of cut cell can be reconstructed at matrix level from the summation of similar matrices from its integration cells. The numerical integration is undertaken in each integration cell with respect to the nodes of its own. Each integration cell takes as minimal supporting area/volume as possible along the discontinuity, thus the accurate and robust interpolation of the scalar values and their gradients are preserved in each integration cell. The proposed numerical integration has been tested on the stationary and rotating circular cylinder and cavity flow problems. Good convergence and stability have been achieved with unfitted grids. Finally, we extend the proposed formulation to fluid-structure interaction application with solid-wall contact effects. References [1] Zou, Zilong, Wilkins Aquino, and Isaac Harari. "Nitsche's method for Helmholtz problems with embedded interfaces." *International Journal for Numerical Methods in Engineering* 110.7 (2017): 618-636. [2] de Prenter, F., et al. "Condition number analysis and preconditioning of the finite cell method." *Computer Methods in Applied Mechanics and Engineering* 316 (2017): 297-327. [3] Natarajan, Sundararajan, D. Roy Mahapatra, and Stephane Bordas. "Integrating strong and weak discontinuities without integration subcells and example applications in an XFEM/GFEM framework." *International Journal for Numerical Methods in Engineering* 83.3 (2010): 269-294.

## Generalized Isogeometric Analysis by a Differential Quadrature Hierarchical Finite Element Method

Bo Liu<sup>\*</sup>, Cuiyun Liu<sup>\*\*</sup>, Yufeng Xing<sup>\*\*\*</sup>

<sup>\*</sup>The Solid Mechanics Research Center, School of Aeronautic Science and Engineering, Beihang University, Beijing 100191, PR China, <sup>\*\*</sup>The Solid Mechanics Research Center, School of Aeronautic Science and Engineering, Beihang University, Beijing 100191, PR China, <sup>\*\*\*</sup>The Solid Mechanics Research Center, School of Aeronautic Science and Engineering, Beihang University, Beijing 100191, PR China

### ABSTRACT

Generalized isogeometric analysis (IGA) by a differential quadrature hierarchical finite element method (DQHFEM) [1] is carried out through representing the geometry by the differential quadrature hierarchical (DQH) basis in the solution space of DQHFEM for dependent variables. The exact CAD geometry, similar to IGA, is matched by a coarse mesh of “DQH elements” using the hierarchical basis. Not only tensor product domains like quadrilateral and hexahedral DQH elements, triangular, tetrahedral and triangular prism DQH elements using Fekete points on the simplexes were also discussed. The DQH method in weak form is called DQHFEM. In DQHFEM, the number of nodes on different edges of an element can be different, and the number of nodes inside an element does not rely on the number of nodes on the edge of the element. So the geometry represented by DQH elements can be easily constructed to be water-tight and to be matched with the nodes of neighboring elements. The DQH method is of high accuracy, so the transformation of exact CAD geometry to be DQH elements will not lose accuracy in general. The DQH method uses high order or very high order basis. A whole NURBS element can be modeled by one DQH element, and any further mesh refinement or further communication with the CAD system is usually not necessary. The accuracy of DQH method can be improved by increasing the order of basis. As is well known that IGA [2] needs mesh refinement in order to keep isoparametric although it does not need to communicate with CAD system. In this work, the DQH elements in physical field is allowed to be sub-parametric or super-parametric, so it is a generalization of the IGA. Water-tight, mesh adaptive and high accuracy properties of the generalized IGA using DQH bases were demonstrated through application of the method to vibration of plate and shell structures. A discussion of obtaining a coarse mesh of “DQH elements” through trimmed NURBS surfaces is also presented. References [1] C.Y. Liu, B. Liu, L. Zhao, Y.F. Xing, C.L. Ma, H.X. Li. A differential quadrature hierarchical finite element method and its applications to vibration and bending of Mindlin plates with curvilinear domains. *Int. J. Numer. Meth. Engng* 109 (2016) 174–197. [2] T.J.R. Hughes, J.A. Cottrell, Y. Bazilevs. Isogeometric analysis: CAD, finite elements, NURBS, exact geometry and mesh refinement. *Comput. Methods Appl. Mech. Engrg.* 194 (2005) 4135–4195.

## Concurrent Design of Additive Manufacturing-Oriented Shell-Infill Graded Lattice Structures Through Explicit Topology Optimization

Chang Liu<sup>\*</sup>, Weishang Zhang<sup>\*\*</sup>, Zongliang Du<sup>\*\*\*</sup>, Xu Guo<sup>\*\*\*\*</sup>

<sup>\*</sup>Dalian University of Technology, <sup>\*\*</sup>Dalian University of Technology, <sup>\*\*\*</sup>Dalian University of Technology, <sup>\*\*\*\*</sup>Dalian University of Technology

### ABSTRACT

Lattice structures with well-designed periodic microstructures have excellent mechanical, thermal, optical and acoustical properties. Structural topology optimization has successfully been used in optimum design of such periodic lattice/porous structures. Nowadays, with the rapid development of modern fabrication technology, it is no longer difficult to fabricate structures with more complicated microstructures. Actually, a structure constituted by graded microstructures can inherit many merits from the ones constitute by uniform periodic microstructures and usually has better performances. In addition, from an aesthetic point of view, using grade structures is also an effective means to make structures having a sense of beauty. Therefore, recent years witnessed a growing interest on developing methods to design graded structures. In the present work, a new approach for designing graded lattice structures is developed based on the Moving Morphable Components/Voids (MMC/MMV) topology optimization framework. For the convenience of additive manufacturing, the structures are designed to have two sub-structures, i.e., a solid shell forming the exterior and graded lattice structures filled in it, which can be optimized simultaneously. The essential idea is introducing a coordinate perturbation in the topology description functions (TDF) for describing the geometries of the components/voids in the design domain, in order to achieve graded structure design by optimizing the coefficients in the perturbation basis functions. Within the current design approach, both the complex solid shell and graded infills with explicitly geometrical parameters can be optimized simultaneously with a very small number of design variables under various loading conditions and coordinate systems. Numerical examples demonstrate the effectiveness and efficiency of the proposed approach.

## Vorticity Tensor and Vorticity Vector Decomposition for Turbulence Study

Chaoqun Liu\*, Yisheng Gao\*\*

\*University of Texas at Arlington, \*\*University of Texas at Arlington

### ABSTRACT

Abstract For long time, there is a lack of mathematical definition for vortex, which is one of major obstacles causing many confusions in turbulence study. Classical theories usually decompose the velocity gradient tensor to a symmetric part which is corresponding to deformation and an anti-symmetric part which is corresponding to vorticity. Many people think vorticity represents fluid rotation, but it is not correct. In this paper the vorticity tensor is further decomposed to an anti-symmetric tensor which is corresponding to rigid rotation and another anti-symmetric tensor which is corresponding to non-rotational shear. The existence and uniqueness of the decomposition are proved. Based on the tensor decomposition, the vorticity vector is decomposed to a vortex vector which is called "Rortex" and a shear vector. This decomposition clearly shows that vorticity is a vector and vortex vector is another vector, but they are different vectors.  $Vorticity=R+S$  is a very important formula to study turbulence and it clearly shows vorticity cannot be used to describe the vortex structure in turbulence since vorticity is not vortex vector and S plays an important role in 3-D viscous flow. Vortex is also not necessary to be a region where vorticity is concentrated since vortex is a region with large R but not large vorticity. Since Rortex only represents fluid rotation, unlike vorticity, it can be generated and ended inside flow field. As a new important physical quantity to represent vortex, through dynamics analysis Rortex can clearly show the vortical structure in turbulence and how turbulence is generated, developed, and sustained. The DNS for boundary layer transition is taken as an example to demonstrate the capability of Rortex to clearly and correctly show the vortex structure in flow transition.

## Buckling Optimization of Variable-Stiffness Composite Panels Based on Flow Field Function

Chen Liu<sup>\*</sup>, Peng Hao<sup>\*\*</sup>, Xuanxiu Liu<sup>\*\*\*</sup>

<sup>\*</sup>Dalian University of Technology, <sup>\*\*</sup>Dalian University of Technology, <sup>\*\*\*</sup>Dalian University of Technology

### ABSTRACT

Buckling is the main failure mode for composite thin-walled panels under axial load or combined load. Cutouts are widely existed in various branches of thin-walled structures to accommodate the need of easy access, inspection, electric lines, especially for launch vehicles, aircrafts, etc. When axial compression load is applied, buckling is usually the governing failure mechanism for these types of structures, and the buckling resistance would be reduced due to the presence of cutouts. Due to the non-uniform in-plane stress distribution, variable-stiffness panel with curvilinear fiber paths is a promising structural concept for cutout reinforcement of composite structures under axial compression, due to the more diverse tailorability opportunities than simply choosing the best straight stacking sequence. Traditional curvilinear fiber path functions lack the local variation capacity of fiber orientation angles to compensate the stiffness loss caused by cutouts. However, traditional representation methods of curvilinear fiber path are usually not flexible for cutout reinforcement. In this study, variable-stiffness panels based on flow field is employed to meet the requirement of cutout reinforcement, since the stress distribution is highly non-uniform for the panel with cutout, and stiffness tailoring is significant for improving the stress distribution and load-carrying efficiency. The cocurrent and equipotential lines are used to parameterize each pair of adjacent plies. The flow field function containing a uniform field and several vortex fields is utilized to represent the fiber path due to its inherent non-intersect and orthotropic features, and a bi-level optimization framework of variable-stiffness panels considering manufacturing constraints is then proposed. The flow field function is utilized to represent the global orientation and local variation of fiber path, which can enhance the design flexibility with only few variables. A typical rectangular panel with multiple cutouts is established to demonstrate the advantage of flow field function and proposed framework. The buckling modes and fiber paths of obtained optimum designs are examined in detail. Also, the effects of boundary condition and manufacturing constraint are investigated. By comparison with other fiber path functions, including linear variation function, cubic polynomial function, contour lines of cubic function. Flow fiber path only needs few variables to finely describe the fiber path, which can provide satisfying and manufacturable fiber paths by combination use of curvature constraint. Results indicate that variable-stiffness panel based on flow field function is a promising structural concept compared to common variable stiffness designs, especially for cutout reinforcement of composite structures under axial compression.

## **Modeling Strong and Weak Discontinuities without Element-partitioning in Reservoir Models**

Chuanqi Liu<sup>\*</sup>, N. Sukumar<sup>\*\*</sup>, Jean H. Prevost<sup>\*\*\*</sup>

<sup>\*</sup>Princeton University, <sup>\*\*</sup>University of California at Davis, <sup>\*\*\*</sup>Princeton University

### **ABSTRACT**

For reservoir, faults are either barriers to flow or fluid flow conduits. By using the extended finite element method, faults can be introduced into a three-dimensional reservoir mesh without meshing them explicitly and a structured mesh suffices since the faults can arbitrarily cut the elements. To capture the various properties of the faults, the enrichment functions in the model can be strongly (faults working as barriers) or weakly (faults working as fluid flow conduits) discontinuous. We implement a new integration scheme without element-partitioning to obtain the residual of the pressure equation. In the integration scheme, the integration of homogeneous monomials over each polyhedron is converted into the integration of the same monomials over the one-dimensional edges of the polyhedron by using Stokes's theorem and Euler's homogeneous function theorem. Several numerical examples are given to assess the performance of this new integration scheme in terms of computational time. It is found that the new integration scheme is over 50% more efficient than the integration scheme using element-partitioning procedure.

## **A Multi-scale Modeling Approach for Computational Design of Knitted Textiles**

Dani Liu<sup>\*</sup>, Seid Koric<sup>\*\*</sup>, David Breen<sup>\*\*\*</sup>, Antonios Kotsos<sup>\*\*\*\*</sup>

<sup>\*</sup>Theoretical & Applied Mechanics Group, Department of Mechanical Engineering & Mechanics, Drexel University, Philadelphia, PA, <sup>\*\*</sup>National Center for Supercomputer Applications-NCSA, University of Illinois Urbana-Champaign, <sup>\*\*\*</sup>Department of Computer Science, Drexel University, Philadelphia, PA, <sup>\*\*\*\*</sup>Theoretical & Applied Mechanics Group, Department of Mechanical Engineering & Mechanics, Drexel University, Philadelphia, PA

### **ABSTRACT**

Knitted textiles are viewed in this talk as hierarchically structured materials. Compared to the manufacturing methods for materials such as fiber-reinforced composites, modern knitting machines provide much finer control which is comparable to CAD-based advanced manufacturing methods and capable of creating a variety of structures using a range of input materials. The mechanical behavior of knitted textiles, however, is difficult to be predicted by traditional computational methods due to their complex architectures. This talk presents results from a developing computational framework for modeling and design of knitted textiles. Specifically, predictions of mechanical behavior of knitted textiles are first obtained by employing direct numeric simulation (DNS) using 3D Finite Element Analysis (FEA). Given the geometrical details of the entangled yarns included in the 3D models used, the DNS approach is capable of investigating the influence of various design parameters at the yarn level, including loop architecture, material properties, as well as interfacial interactions. However, since knitted textiles are treated as free standing structures both kinetic and kinematic effects become important resulting in significant increase of the computational degrees of freedom as a function of domain size analyzed. To address this issue DNS of the mechanical behavior of knitted textiles are for the first time conducted on High Performance Computing (HPC) using the explicit FEA method which was compared to implicit analysis. The results presented demonstrate satisfying accuracy and higher order efficiency with reduced memory requirements of the explicit method which allows for improved efficiency in simulations of larger computational domains, while also demonstrate that HPC could be a valuable resource for computational material design applied to advanced manufacturing. Furthermore, efforts to develop Reduced Order Models (ROM) for knitted textiles based on the available DNS results are also presented which are shown to provide an alternative approach to predict multiscale behavior in addition to consist a tool that could be leveraged in future microstructure optimization investigations. Moreover, to address the issue of size effects a first order, two-scale homogenization scheme was modified and applied by considering the yarn-level knitted textile models as a material point in the far field. The equivalent macro stress and consistent material stiffness were derived from the micro-level where specific 3D textile models were used. The macro field with unknown material properties was linked to the micro-level by a user subroutine which can convey the equivalent macro stress and stiffness in a looped form of the FE code.

## Modeling Competing Hydraulic Fracture Propagation with the Extended Finite Element Method

Fushen Liu<sup>\*</sup>, Peter Gordon<sup>\*\*</sup>, Dakshina Valiveti<sup>\*\*\*</sup>

<sup>\*</sup>ExxonMobil Research and Engineering Company, <sup>\*\*</sup>ExxonMobil Research and Engineering Company,  
<sup>\*\*\*</sup>ExxonMobil Upstream Research Company

### ABSTRACT

Hydraulic fracturing process is essential in enhancing productivity in low permeability reservoirs. In practice, it is common to create several perforation clusters to facilitate simultaneous growth of multiple hydraulic fractures per stage. However, the reported production log data suggests that only a small portion of perforation clusters in a stage may be effectively contributing to the overall production. The uneven fracture propagation results from the nonlinear coupling of wellbore friction, perforation friction, fracture propagation and stress interaction. We present a stabilized extended finite element framework to numerically study competing hydraulic fracture propagation in one stage. The framework is capable of modeling fully-coupled hydraulic fracturing processes including fracture propagation, elasto-plastic bulk deformation and fluid flow inside both fractures and the wellbore. Dynamic fluid allocation among fractures during propagation is solved, by considering both wellbore pressure loss and perforation pressure loss. With the numerical examples, we identify and verify the dimensionless parameters determining the transition from uniform fracture propagation to preferential fracture propagation.

## Thermo-viscoplastic Analysis with Robust Solution Strategy for Extrusion

Guomai Liu<sup>\*</sup>, Xiaoliang Qin<sup>\*\*</sup>, Hongyan Yuan<sup>\*\*\*</sup>

<sup>\*</sup>Fujian University of Technology, <sup>\*\*</sup>Fujian University of Technology, <sup>\*\*\*</sup>University of Rhode Island

### ABSTRACT

Extrusion is a plastic deformation process in which a billet is heated and pressed to flow through a die opening of a much smaller cross-sectional area than the original billet. In recent years, numerical simulation using finite element method has been increasingly used in extrusion die design. The challenges of extrusion simulation come from the large distortion of rate sensitive materials and the coupling of the material flow and heat transfer. It is hard to model extrusion process in a Lagrangian reference frame because the excessive element distortion will fail the analysis as the material pass through the die. Element remising and results mapping are usually required in a Lagrangian reference frame. However, the re-meshing method is computationally costive. The extrusion process can be effectively modeled by treating the problem as a steady flow of viscoplastic material in an Eulerian frame. In this work, a stabilized Eulerian formulation for fully coupled thermal-mechanical steady state viscoplastic flow is presented. Plastic heat generation and frictional heat are considered in this work. Streamline Upwind Petrov-Galerkin (SUPG) method is used to stabilize the incompressible equation and the convection term in heat transfer equation. A mixed P2-P1 tetrahedral element is developed to enhance the stability further. Anand&apos;s viscoplastic constitutive material model is used in this study. A two-step cut off strain rate reduction solution method is introduced to provide a robust and efficient convergence by solving the Anand&apos;s model in the Eulerian formulation using the Newton-Raphson method. The Eulerian formulation is implemented in an OpenMP finite element program called OnExtrude. Two numerical examples are studied to validate the accuracy and efficiency of the Eulerian formulation.

# OPTIMIZATION OF RESIN PELLET SHAPE FOR IMPROVING FLOWABILITY

JIHONG LIU

DAIKIN INDUSTRIES, LTD.  
1-1, Nishi-Hitotsuya  
Settsu, Osaka 566-8585, Japan  
jihong.liu@daikin.co.jp; <http://www.daikin.com/>

**Key words:** Optimal Pellet Shape, Hopper, Flowability, Dynamic Explicit FEM.

**Summary:** *In this paper, we proposed a simulation approach based on the dynamic explicit FEM (Finite Element Method) to evaluate the flowability of resin pellets in a hopper of an extruder. Using the simulation approach, we clarified that the shape of the resin pellets had a large influence on its flowability, and found the optimal pellet shapes that can improve the flowability of the resin pellets in the hopper.*

## 1 INTRODUCTION

The demand for LAN (Local Area Network) cables is greatly increasing with the rapid progress of information technology. LAN cables are made up of electrical wires which are coated with resins. The resins are usually manufactured into pellets of about several millimeters for easy processing.

It is sometimes seen that the coating layer on the electrical wires is not uniform. One of the reasons for this is presumed to be that the outflow rate of the resin pellets from a hopper of an extruder is not constant and the resin pellets are not stably supplied to the electrical wires during coating processes.

Although it is empirically known that the shape of resin pellets affects the outflow behavior of the resin pellets from a hopper, only a few theoretical researches and simulation studies on it have been conducted <sup>[1, 2]</sup>. There are two reasons for this. One is that the governing equations of resin pellets motion are not yet established theoretically due to the fact that resin pellets are discrete and the interactions between resin pellets are complicated. Another is that it is difficult to simulate actual flow phenomenon of resin pellets in a hopper because of the limitations on the scale of resin pellets simulation model and calculation time.

At present, the shape of resin pellet is mainly determined based on the experience and intuition of engineers. In order to improve the stability of the coating layer of electrical wires, it is desired to elucidate the influence of the shape of resin pellets on its flowability in a hopper of an extruder.

In this paper, we proposed a simulation approach based on the dynamic explicit FEM (Finite Element Method) to evaluate the flowability of resin pellets in a hopper of an extruder, which fill into the hopper by free-fall and then flow out from the hopper by gravity.

In particular, first, we verified simulation results in a small scale model by statistical method to ensure the randomness of the filled state of resin pellets in the hopper and established a simulation approach of resin pellet flow. Next, we confirmed that we can deduce simulation results in a large scale model from those in a small scale model. Then, using the simulation approach, we clarified that the shape of resin pellets has a large influence on its flowability and found an optimal pellet shape of oblate and prolate spheroid respectively that can improve the flowability of resin pellets in a hopper. Finally, we confirmed that the optimal resin pellet shape is in dependent of the amount of pellets, kind of material and angle of hopper. It is an interesting phenomenon that the optimal oblate and prolate spheroid have a reciprocal relationship between ratios of equatorial diameter to polar diameter respectively.

## 2 FLOW SIMULATIONS OF RESIN PELLETS IN A HOPPER

The above-mentioned simulation approach is described in detail below. In this paper, we model a resin pellet by using finite elements. A resin pellet cluster includes a plurality of the resin pellets, and we create its simulation model that can be calculated using a workstation.

### 2.1 Analysis model

In this paper, we assume that the shape of a resin pellet can be expressed approximately by a spheroid. Here, as shown in Figure 1, a resin pellet is modeled with solid elements, and a hopper is modeled with shell elements.

In the simulations, first, a resin pellet cluster placed in a higher position than the hopper free-falls to the hopper whose outlet is closed with a lid, and thereby creates a random filled state of resin pellets in the hopper. Next, the randomly filled resin pellets flow out from the hopper under the action of gravity by removing the hopper outlet lid, and the outflow time of the resin pellets from the hopper is calculated.

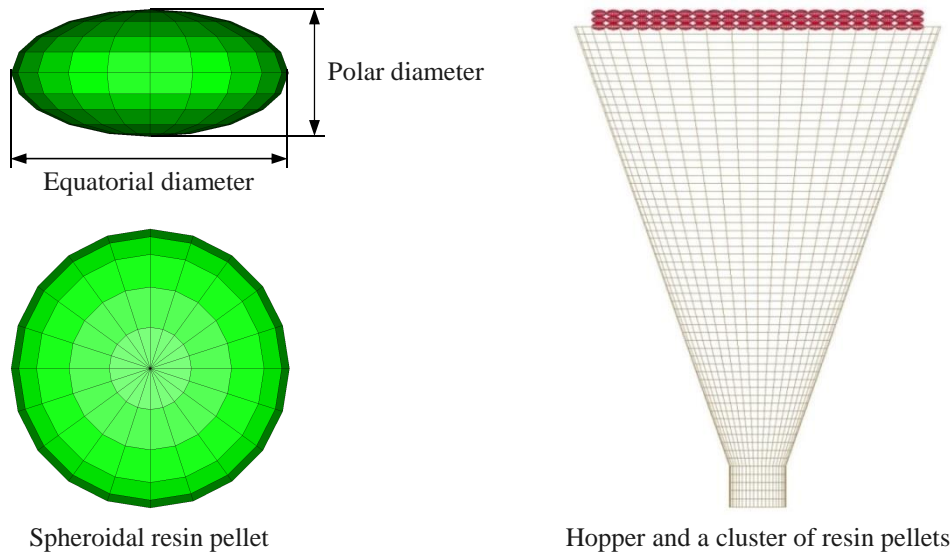


Figure 1. Finite element model of a spheroidal resin pellet, a hopper and a cluster of spheroidal resin pellets in a higher placement position than the hopper

## 2.2 Verification of simulation results

Simulations are performed on the filling of FEP (tetrafluoroethylene-hexafluoropropylene copolymer) pellet clusters with different initial placement state into a hopper and the outflow of filled FEP pellets from the hopper. Nonlinear dynamic explicit software LS-DYNA<sup>[3,4]</sup> is used in the simulations.

### 2.2.1 Creation of filled state of pellets and verification of its randomness

Figure 2 shows the FEP pellet clusters with mass of 10g and different initial placement state No.1 to No.7, and the filled state of pellets in the hopper owing to free fall. According to the results, it seems that there is no difference in randomness in the filled state of the pellets corresponding to the initial placement state No.1 to No.7. Figure 3 shows the distributions of the pellet center distances in each filled state of the pellets. It is seen that the each filled state of the pellets shows almost the same distribution, and it can be judged that they have equivalent randomness and that there is no difference between them.

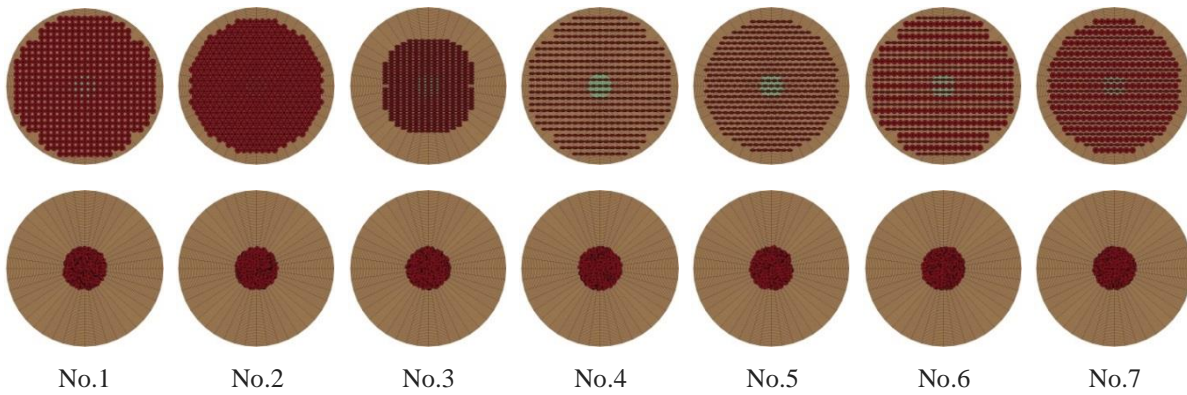


Figure 2. The FEP pellet clusters of 10g with different initial placement state (upper row) and the filled state of the pellets in the hopper due to the free-fall (lower row).

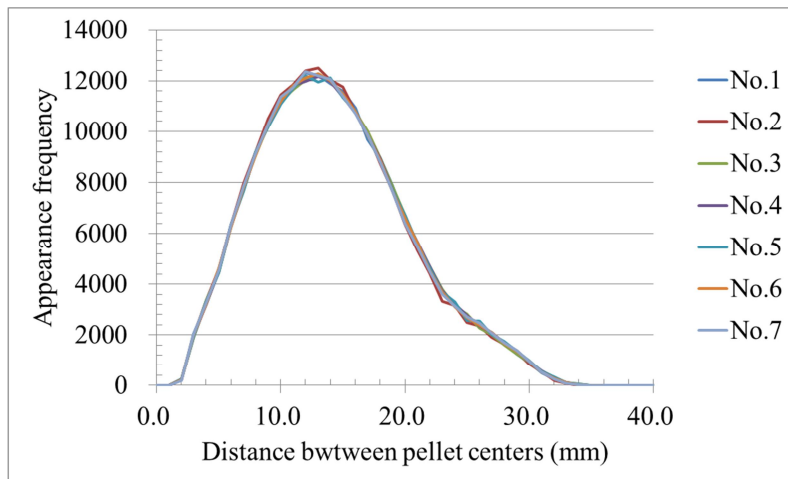


Figure 3. Appearance frequency distributions of the distance between pellet centers of 10g FEP pellet clusters

Figure 4 shows the filling process of the FEP pellets of 10g into a hopper and the outflow process of the filled FEP pellets from the hopper as an example.

### 2.2.2 Outflow time of pellets from a hopper

Figure 5 shows the simulation results of the outflow time of the FEP pellet clusters No.1 to No.7 with mass of 10g, 20g and 30g from the hoop, respectively. According to the results, it is found that there is a slight difference in the outflow time of the pellets due to the differences in initial placement state. The outflow time of the pellets is statistically processed and the relationship between the number of simulations and the variation coefficient of the outflow time is shown in Figure 6. It is found that the coefficient of variation of the outflow time of the pellets is as low as 2% or less in either case. It can be also seen from Figure 6 that the coefficient of variation of the outflow time decreases with an increase in the amount of the pellets. For example, when the pellet cluster is 10g, the variation coefficient of the outflow time is about 2%, but in the case of the pellet cluster of 30g, it is obvious that the variation coefficient of the outflow time decreases to 1% or less. It can be also seen from Figure 6 that when the amount of the pellets reaches 30g or more, the variation coefficient of the outflow time due to the differences in the number of simulations does not change.

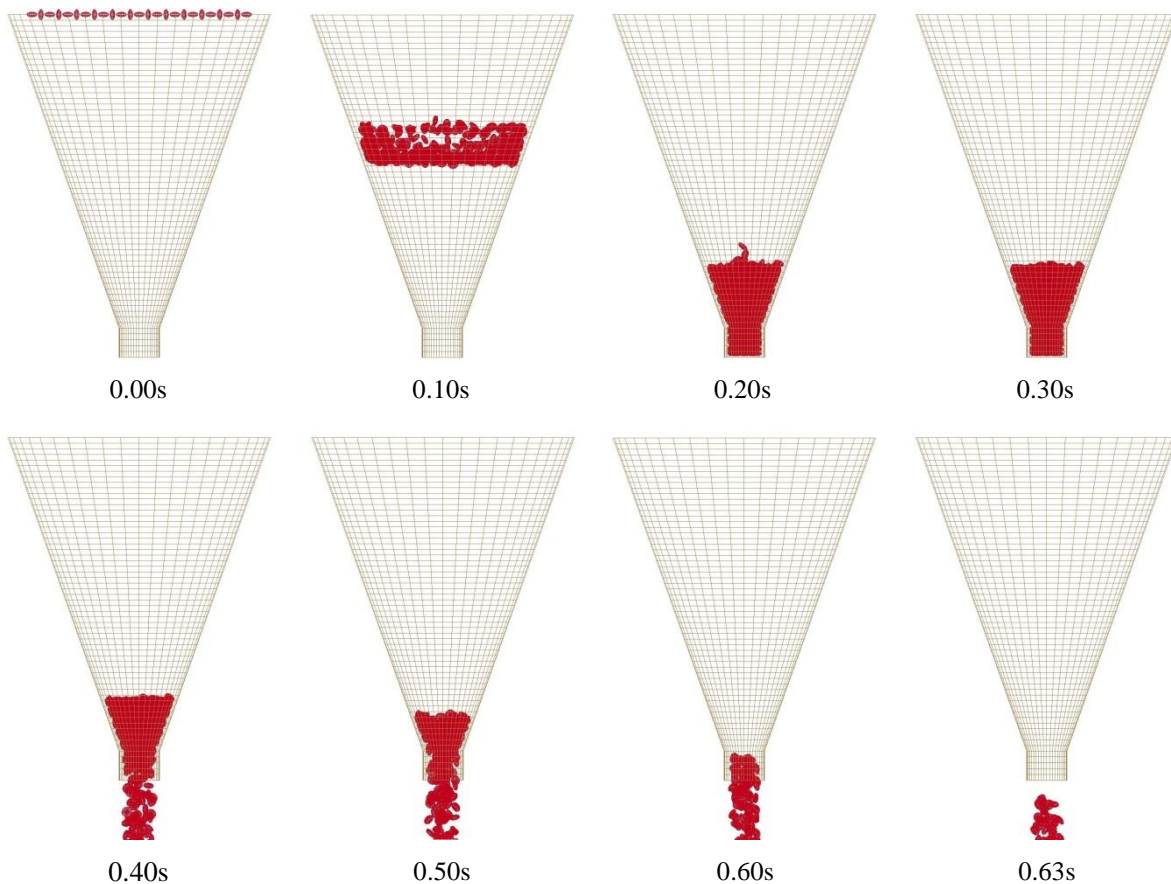


Figure 4. Filling of the FEP pellets of 10g into a hopper and the outflow of the FEP pellets from the hopper

To summarize the simulation results of the outflow time of the FEP pellets described above, it is expected that the statistical influences will not be given to the simulation results of the filled state of the pellets in the hopper and the outflow time of the pellets from the hopper if any pellet cluster of any initial placement state is used. This means that the simulation results of the filled state of pellets in a hopper and the outflow time of the pellets from the hopper obtained by using any pellet cluster of any initial placement state have statistically the same randomness.

### 2.2.3 Relationship between amount of resin pellets and outflow time

It is revealed that there is no statistical differences in the filled state of pellets in a hopper and the outflow time of the pellets from the hopper even if the initial placement state of the pellets is different. In this section, we simulate the filling of the FEP pellets into the hopper

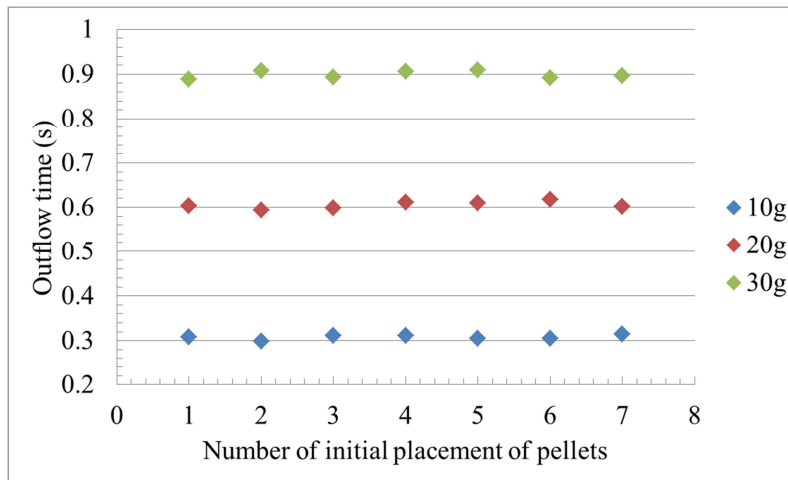


Figure 5. Changes in outflow time due to the differences in initial placement state of FEP pellets and in mass

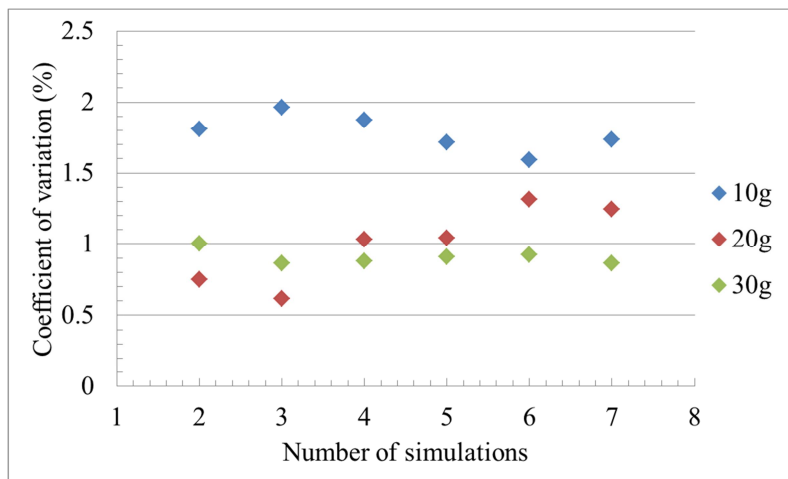


Figure 6. Number of simulations and coefficient of variation of outflow time of FEP pellets with different mass

and the outflow of the pellets from the hopper when the initial placement state No.7 is used to increase the mass of the pellets up to 80g at intervals of 10g.

The relationship between the mass of the FEP pellets and the outflow time of the pellets from the hopper is shown in Figure 7. At the same time, an approximate curve showing the relationship between the mass and the outflow time of the FEP pellets is also shown in the Figure 7. It can be seen that the relation between the mass and the outflow time of the FEP pellets from the hopper can be approximated by a linear function equation  $y=0.0299x$ . Here,  $x$  is the mass (g) of the FEP pellets, and  $y$  is the outflow time of the FEP pellets from the hopper. Using this formula, it is possible to easily predict the outflow time of the FEP pellets of arbitrary mass.

In this paper, the accuracy of the predicted outflow time of the FEP pellets by the formula is verified with the case of the FEP pellets of 300g as an example. Since the simulation model of the pellets of the same mass is large in scale and the calculation time is enormous and not realistic, we predict the outflow time of the pellets on a real scale using simulation results in a small scale model and indirectly verify the accuracy of the simulation.

Table 1 shows the comparisons between the test results and the predicted results of the outflow time of the FEP pellets with mass of 300g. Here, it is assumed that the variation coefficient of the simulation results due to the randomness of the filled state of the pellets is 1%. According to the results, it is revealed that the average error between the predicted results and the test results is 5.97%, which is sufficiently good from the viewpoint of engineering. We think that the simulation approach used in this paper is valid because the predicted results and the test results almost agree with each other. As one of the causes of the differences between the predicted results and the test results, uncertainty of the friction coefficient between the pellets, between the pellets and the hopper can be mentioned. In addition to this, the pellets of uniform shape and size are used in the simulations, but the pellets in the test are not completely uniform shape and size. This is also considered to be the cause of the differences between the predicted results and the test results.

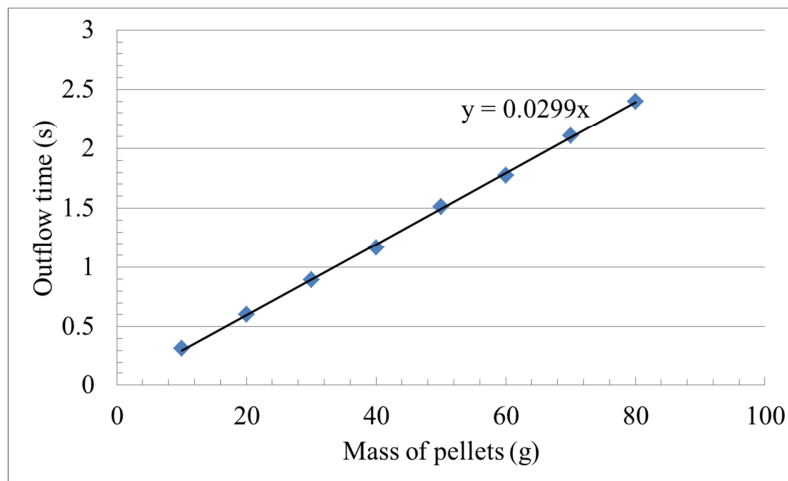


Figure 7. Relationship between the mass of the FEP pellets and the outflow time of the FEP pellets from the hopper, and an approximate formula to predict the outflow time of the FEP pellets of arbitrary mass

Table 1. Predicted and test outflow time of FEP pellets of 300g

Results		Error (%)		
Test	Prediction	Avg.	Max.	Min.
9.54±0.054	8.97±0.090	5.97	7.44	4.49

To summarize the above analysis results, it is found that filling of the pellets into the hopper and outflow of the pellets from the hopper can be predicted by the simulations using the dynamic explicit FEM. This makes it possible to grasp the flow behavior of the pellets having different shapes by the simulations.

### 3 SEARCHES FOR PELLET SHAPE FOR IMPROVING FLOWABILITY

Conventionally, the pellet shape is determined by trial and error based on the experience and intuition of engineers and therefore the theoretical and simulation studies on the pellet shape are insufficient. In this section, we elucidate the influence of the pellet shape on the flowability of the pellets using the above proposed simulation approach and reveal the optimal pellet shapes that can improve flowability of the pellets in a hopper.

#### 3.1 Case of similar pellet shape

Figure 8 shows some examples of similar spheroidal pellet shape having the same ratio of equatorial diameter to polar diameter. Here, the unit of the diameter is millimeter and the ratio is denoted as  $\lambda$ . Figure 9 shows the changes in the outflow time of the FEP pellets from the hopper due to the differences in mass and equatorial diameters of the pellets having the same  $\lambda$  of 2.1875. It is revealed that when the mass is the same, the outflow time becomes linearly shorter as the equatorial diameter of the pellet becomes smaller. This means that, in the case of the pellets having a similar shape, smaller pellets can flow out more smoothly from the hopper and the flowability is better. It is to be noted that since the pellets tend to become more electrostatic as the pellets become smaller, it is necessary to determine the actual pellet size considering the balance between flowability and chargeability.

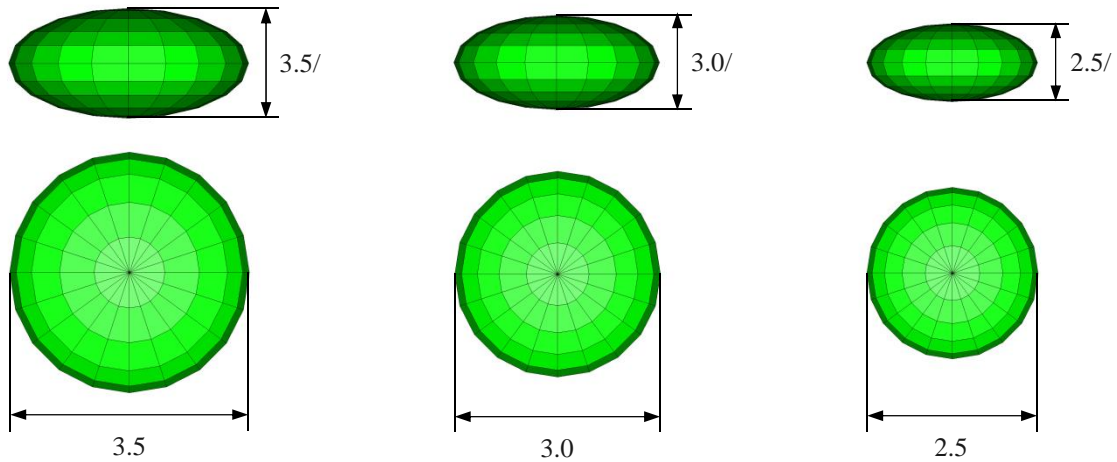


Figure 8. Some similar spheroidal pellets with the same ratio of equatorial diameter to polar diameter,

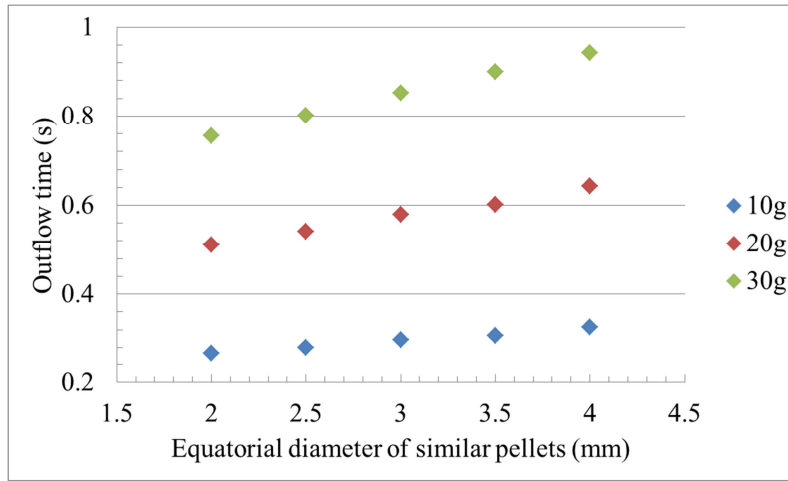


Figure 9. Equatorial diameter, mass and outflow time of FEP pellets with the same of 2.1875

### 3.2 Case of isovolumetric pellets with a different shape

Figure 10 shows some examples of isovolumetric spheroidal pellets in which the ratio of equatorial diameter to polar diameter is varied. Figure 11 shows the changes in the outflow time of the isovolumetric spheroidal FEP pellets of 10g with the varying ratio of equatorial diameter to polar diameter. According to the results, it is revealed that an optimal oblate spheroid and a prolate spheroid with good flowability exist compared to the sphere which is perceived to have the best flowability. Specifically, for example, when the ratio of equatorial diameter to polar diameter is 2.19, it is found that the flowability of the pellets is the most excellent. On the other hand, in the optimal prolate spheroid, the ratio of equatorial diameter to polar diameter is 0.47. It is strangely found that the optimal oblate and prolate spheroid have a reciprocal relationship ( $0.47 \times 2.19 = 1.00$ ) between ratios of equatorial diameter to polar diameter respectively.

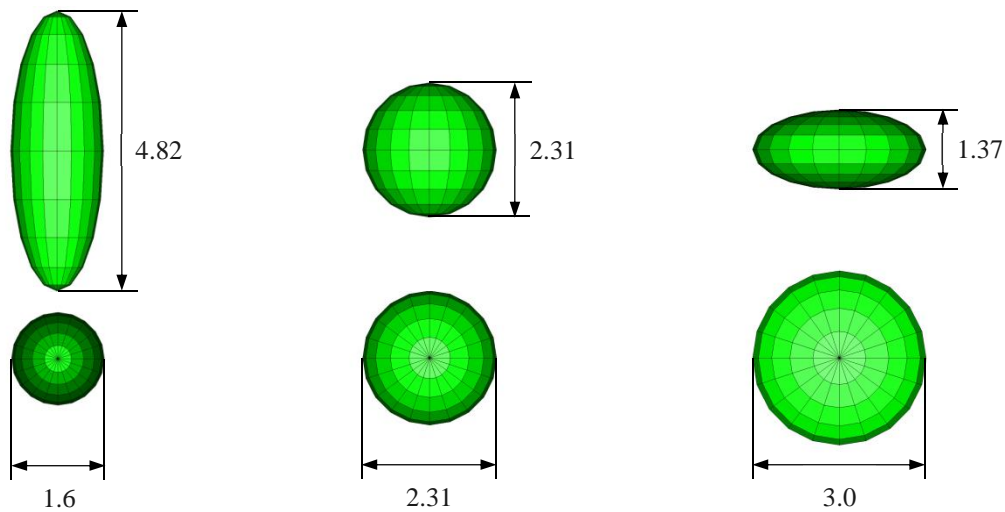


Figure 10. Some isovolumetric spheroidal pellets with varying ratio of equatorial diameter to polar diameter

Concerning the generality of the optimal pellet shapes, it is confirmed below by the simulations based on the above approach whether the optimal pellet shapes for improving flowability of the pellets are in dependent of the amount of pellets, kind of material and angle of hopper.

### 3.2.1 Influence of amount of pellets

Figure 12 shows the change in the outflow time due to the difference in the ratio of equatorial diameter to polar diameter and in the FEP pellets with mass of 10g and 20g. It is found that even when the amount of the pellets is changed, the optimal pellet shapes for improving flowability does not change. That is, the optimal pellet shapes do not depend on the amount of pellets.

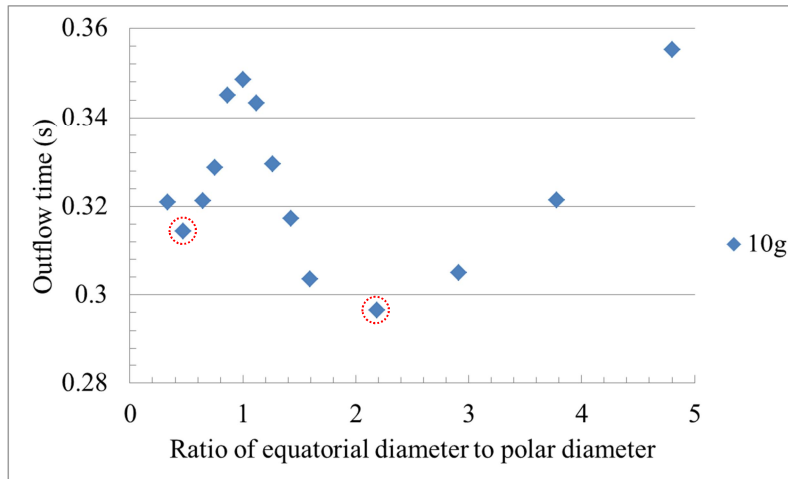


Figure 11. Relationship between the ratio of equatorial diameter to polar diameter and the outflow time of the FEP pellets of 10g

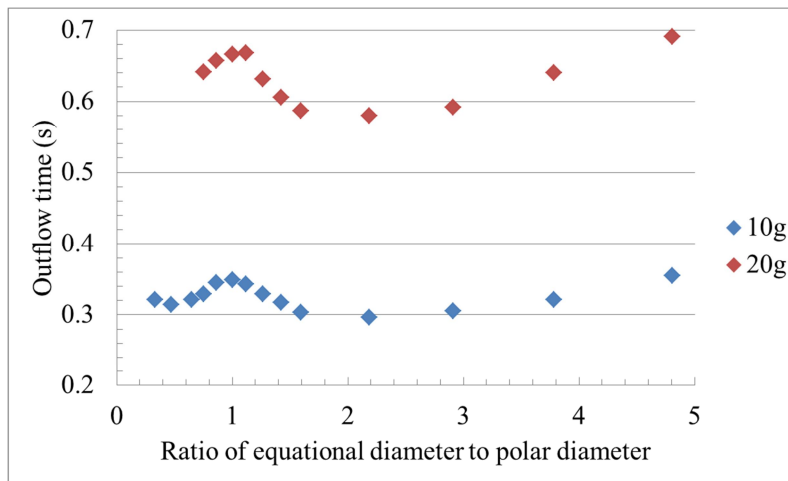


Figure 12. Change in the outflow time due to differences in the ratio of equatorial diameter to polar diameter and in the FEP pellet mass of 10g and 20g

### 3.2.2 Influence of material type of pellets

Figure 13 shows the change in outflow time due to the differences in the ratio of equatorial diameter to polar diameter and in the material type of the FEP and PE (polyethylene) pellets. It turned out that even if the material type of the pellets are changed from FEP to PE, the optimal pellet shapes for improving flowability does not change. That is, the optimal pellet shapes do not depend on the material type.

### 3.2.3 Influence of hopper angle

Figure 14 shows the outflow time of the FEP pellets of 10g due to the difference in the ratio of equatorial diameter to polar diameter when the hopper angle is changed. It is seen that the optimal shapes for improving flowability do not change even if the hopper angle is different. This means that the optimal pellet shapes are independent of the hopper angle.

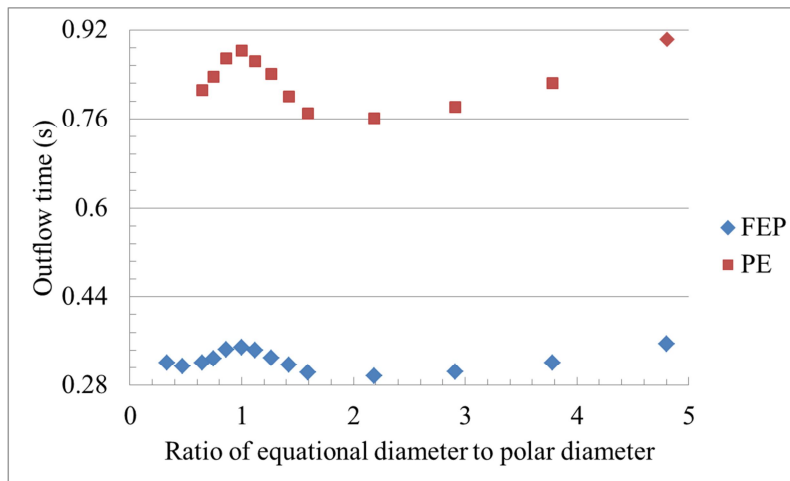


Figure 13. Outflow time of the FEP and PE pellets of 10g

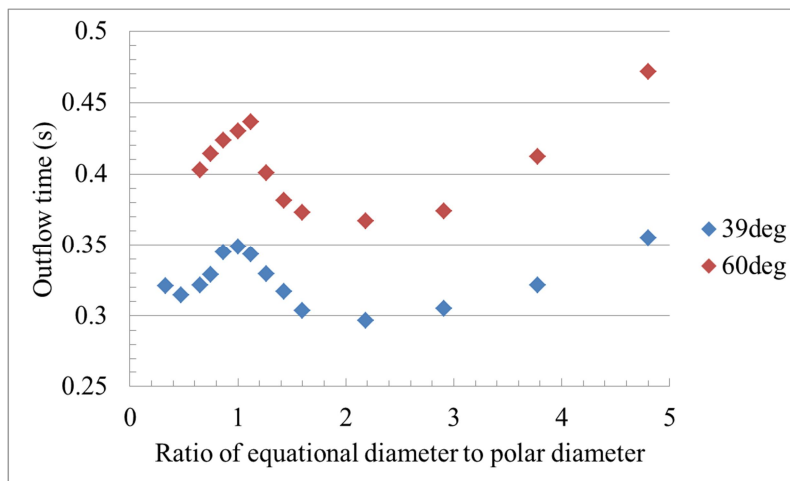


Figure 14. Outflow time of the FEP pellets of 10g with different hopper angles

## 4 CONCLUSIONS

In this paper, using the simulations based on the dynamic explicit FEM, we found the optimal pellet shapes with an oblate and a prolate spheroid respectively, which can improve the flowability of the pellets in a hopper. The ratios of equatorial diameter to polar diameter in the optimal oblate and prolate spheroid are 2.19 and 0.47, respectively.

It is confirmed by the simulations that the optimal spheroid shapes of the pellets are independent of the amount of pellets, the kind of material and the angle of a hopper.

It is also an interesting phenomenon that the optimal oblate and prolate spheroid have a reciprocal relationship between ratio of equatorial diameter and polar diameter respectively.

The optimal oblate spheroid shape is applied to our Neoflon FEP pellets and contributed to the improvement of the pellet flowability and its commercial value.

## REFERENCES

- [1] Potente, H. and Pohl, T. C. Polymer pellet flow out of the hopper into the first section of a single screw, *International Polymer Processing* (2002) 17:11-21.
- [2] Rowe, R. C, York, P., Colbourn, E. A. and Roskilly, S. J. The influence of pellet shape, size and distribution on capsule filling. A preliminary evaluation of three-dimensional computer simulation using a Monte-Carlo technique, *International Journal of Pharmaceutics* (2005) 300:32-37.
- [3] LSTC, LS-DYNA KEYWORD USER'S MANUAL VOLUME I, II, Version 971 R6.1.0 (2012).
- [4] JSOL Corporation, LS-DYNA Usage Guide, Second Edition (2012).

## **ALTO: A Super-Lightweight Topology Optimization Method and Its Application to Support Structure Design for Additive Manufacturing**

Jikai Liu\*, Albert To\*\*

\*University of Pittsburgh, \*\*University of Pittsburgh

### **ABSTRACT**

This research introduces a new topology optimization method, named ALTO (Accelerated Lightweight Topology Optimization). The basic idea of ALTO is to arbitrarily place a number of plates inside the design domain and then perform simultaneous optimization of the shape and material distribution of each plate, as well as the layout of the plates. Unlike conventional topology optimization methods where a 3D background mesh is needed, only the 2D shell element mesh is used to discretize each plate in ALTO, while the shape of each plate is represented by a negative-signed distance function. To ensure smooth convergence and accuracy, finite element nodes will be placed on the joint connections between plates in each optimization iteration. These geometric representation and discretization strategies allow for a rigorous and robust topology optimization method to be formulated. As indicated by its name, this new method has two key advantages: (i) high computational efficiency since no 3D background mesh is required; and (ii) extremely small material volume fraction (such as below 0.02), since material volume is calculated by counting the plate elements, and thickness of the plates can approach a very small value. Effectiveness of the proposed method is proved by studying a few numerical examples. Other than the basic method description, the method will be used to address a tough problem: support structure design in additive manufacturing. Support structure is often encountered in additive manufacturing, which functions in supporting the printing of large overhangs. However, utilizing support structure consumes extra metallic powders, lengthens the printing process, and requires post-machining to remove it after printing. Therefore, overhang free topology optimization has attracted the attention but the overhang free design often severely deviates from the unconstrained optimal. In such a situation, lightweight support structure design through topology optimization is appealing but has been less focused, i.e. residual distortion/stress constrained topology optimization. This problem is challenging due to the involved transient thermo-mechanical analysis is computationally expensive, and to address this problem, we have proposed the inherent strain theory based fast method for residual distortion prediction which have demonstrated pretty good prediction result. Therefore, the inherent strain based ALTO algorithm for super lightweight support structure design will be explored in this research.

## A Unified Continuum and Variational Multiscale Formulation for Fluids, Solids, and Fluid-structure Interaction

Ju Liu<sup>\*</sup>, Alison Marsden<sup>\*\*</sup>

<sup>\*</sup>Stanford University, <sup>\*\*</sup>Stanford University

### ABSTRACT

Traditionally, there has been a dichotomy in computational mechanics: the governing equations for fluids are typically written in terms of the velocity and pressure, while the governing equations for solids are often written in terms of the displacement. This difference is fundamentally due to different stress responses in the constitutive laws, and it leads to developments of different numerical strategies for fluids and solids. It is desirable to formulate a unified framework for fluids and solids to facilitate construction of a consistent and unified numerical framework. Furthermore, a unified framework will benefit the algorithm design for fluid-structure interaction problems. In this work, we first present a unified continuum modeling framework for viscous fluids and hyperelastic solids using the Gibbs free energy as the thermodynamic potential [2]. This framework naturally leads to a pressure primitive variable formulation for the continuum body, which is well-behaved in both compressible and incompressible regimes. Then we perform variational multiscale (VMS) analysis for this general continuum body. The resulting VMS formulation recovers the residual-based variational multiscale formulation for the Navier-Stokes equations. For hyperelastic materials, the VMS formulation provides a mechanism to circumvent the inf-sup condition for low-order tetrahedral elements [1, 3]. After that, we present a novel unified formulation for fluid-solid coupled problems. We show that the proposed numerical scheme enjoys several appealing numerical properties. Numerical examples will be presented to provide corroboration. Lastly, we will discuss possible extensions in biomedical and engineering applications. References [1] A.J. Gil, C.H. Lee, J. Bonet, M. Aguirre. A stabilised Petrov-Galerkin formulation for linear tetrahedral elements in compressible, nearly incompressible and truly incompressible fast dynamics. *Computer Methods in Applied Mechanics and Engineering*, 276:659–690, 2014. [2] J. Liu and A.L. Marsden. A unified continuum and variational multiscale formulation for fluids, solids, and fluid-structure interaction. [arXiv:1711.01322](https://arxiv.org/abs/1711.01322) [physics.comp-ph]. [3] G. Scovazzi, B. Carnes, X. Zeng, and S. Rossi. A simple, stable, and accurate linear tetrahedral finite element for transient, nearly, and fully incompressible solid dynamics: a dynamic variational multiscale approach. *International Journal for Numerical Methods in Engineering*, 106:799–839, 2016.

## Mixed Precision Iterative Methods for Complex Symmetric Systems

Lijun Liu<sup>\*</sup>, Masao Ogino<sup>\*\*</sup>, Kazuaki Sekiya<sup>\*\*\*</sup>

<sup>\*</sup>JST ACT-I, <sup>\*\*</sup>Information Technology Center, Nagoya University, <sup>\*\*\*</sup>Graduate School of Information Science,  
Nagoya University

### ABSTRACT

Electricity devices play an important role in our daily life and in the development of human society. In the processes of designing electricity devices and controlling the quality, electromagnetic field simulations are required. In the electromagnetic field simulations, complex systems of linear equations are generated. In some cases, e.g. the finite element formulation of the E method for Maxwell equations including displacement current, the complex systems are symmetric. To solve complex symmetric systems, many numerical methods are proposed and widely used. When the coefficient matrix is dense and has no special properties to enable fast matrix-vector multiplication, full GMRES is usually the method of choice. If the coefficient matrix is sparse or if storage becomes a problem for full GMRES, COCG, COCR, QMR, MINRES-like\_CS[1], CSYM[2], CS-MINRES-QLP[3] are used. Except for GMRES, the bases of the other methods are computed by recursion and not fully stored. Since all the computations are implemented in finite precision arithmetic, the algorithms are unstable, and the performance of the methods are not only affected by the methods themselves but also depending on the machine precision. To overcome the algorithm's instability and provide adequate accuracy, high precision arithmetic is useful. For the current machines, GCC Version 4.6 or later provides `__float128` type as a system software support, and the IBM POWER9 has hardware support of 128-bit quad-precision floating-point operations. And also, many arbitrary precision algorithms and libraries have been developed using the fixed precision arithmetic. However, computations with high precision are usually time-consuming. In this work, we develop mixed precision iterative methods for complex symmetric systems to achieve high accuracy and at the same time decrease runtime. Keywords: mixed precision arithmetic, complex symmetric, iterative methods

References [1] M. Ogino, A. Takei, S. Sugimoto, and S. Yoshimura, "A numerical study of iterative substructuring method for finite element analysis of high frequency electromagnetic fields", *Comput. Math. Appl.*, (2016). [2] A. Bunse-Gerstner, R. Stöver, "On a conjugate gradient-type method for solving complex symmetric linear systems", *Linear Algebra Appl.* 287 (1999) 105–123. [3] S., Choi, "Minimal Residual Methods for Complex Symmetric, Skew Symmetric, and Skew Hermitian Systems", Report ANL/MCS-P3028-0812, Computation Institute, University of Chicago, (2013).

## DEM-SPH Coupling Simulation with Dilated Polyhedral Elements

Lu Liu\*, Shunying Ji\*\*

\*Dalian University of Technology, \*\*Dalian University of Technology

### ABSTRACT

The Minkowski sum theory is adopted to generate the dilated polyhedral element which is used for the discrete element method (DEM). The constrained minimization problem in the contact detection between dilated polyhedra employs an envelope function which replaces the true dilated polyhedron shape. The parameters of the envelope function are studied about the influence to the efficiency and accuracy of the contact detection. Meanwhile, a bond model is adopted in DEM to simulate the breaking process of continuum. The weakly compressible smooth particles hydrodynamics (SPH) is adopted to simulate the liquid in the coupling with DEM. The force between DEM particles and SPH particles uses the repulsive force model. The GPU-based parallel technology, CUDA is used to accelerate the simulation. Typical simulation examples are simulated by the DEM-SPH model to calibrate the parameters and validate the results. The ice-water coupling including the fracture of ice is simulated by the DEM-SPH coupling model. Real scaled physical model of ice-water coupling is implemented for engineering in cold regions. The results is analyzed and validated with standards to evaluate the accuracy of the simulation ultimately.

## **Meshfree Particle Simulation of Explosive/impact Welding**

Moubin Liu\*

\*Peking University

### **ABSTRACT**

Explosive welding (EXW) involves processes like the detonation of explosive, impact of metal structures and strong fluid-structure interaction, while the whole process of explosive welding has not been well modeled before. In this paper, a novel smoothed particle hydrodynamics (SPH) model is developed to simulate explosive welding. In the SPH model, a kernel gradient correction algorithm is used to achieve better computational accuracy. A density adapting technique which can effectively treat large density ratio is also proposed. Typical phenomena in EXW such as the wavy interface, jetting formation, temperature and pressure distribution at the interfaces and melting voids are investigated by the present SPH simulations, which are usually difficult for grid based methods. The mechanisms of wave formation are investigated, specially, two well-known mechanisms namely, the jet indentation mechanism and the vortex shedding mechanism are studied with the present simulations. Based on the well captured interfacial morphologies, the weldability windows for the impact welding (IMW) are given and are compared with the experimental and theoretical results. Furthermore, the weldability windows for EXW with respect to explosive quantity and initial welding angle are obtained. Meanwhile, welding limits and effective explosive quantity for EXW are discussed in detail.

# RATIONAL BEZIER TRIANGLES FOR THE ANALYSIS OF ISOGOMETRIC HIGHER ORDER GRADIENT DAMAGE MODELS

Ning Liu Ann E. Jeffers<sup>†</sup>

\*Department of Civil and Environmental Engineering, University of Michigan  
2350 Hayward Street  
Ann Arbor, Michigan, 48109, USA  
Email address: ningliu@umich.edu

<sup>†</sup> Department of Civil and Environmental Engineering, University of Michigan  
2350 Hayward Street  
Ann Arbor, Michigan, 48109, USA  
Email address: jffrs@umich.edu; website: <https://sites.google.com/umich.edu/jeffers>

**Key words:** Isogeometric Analysis, Higher-Order Gradient Damage Model, Feature Preserving, Rational Bézier Triangles, Lagrange multipliers.

**Abstract.** The computational approach of modeling smeared damage with quadrilateral elements in isogeometric analysis (e.g., using NURBS or T-splines) has limitations in scenarios where complicated geometries are involved. In particular, the higher-order smoothness that emerges due to the inclusion of higher-order terms in the nonlocal formulation is not always easy to preserve with multiple NURBS patches or unstructured T-splines where reduced continuity is observed at extraordinary points. This drawback can be bypassed with the use of Bézier triangles for domain triangulation. The use of a triangular meshing scheme significantly increases the flexibility in the discretization of arbitrary spaces and facilitates the handling of singular points that result from sharp changes in curvature. Moreover, the process of mesh generation can be completely automated and does not require any user intervention. We also adopt in this research an implicit higher-order gradient damage model in order to fix the non-physical mesh dependency exhibited in continuum damage analysis. For the solution of the fourth- and sixth-order gradient damage models, Lagrange multipliers are adopted to elevate the global smoothness to a desired order in an explicit fashion. The solution algorithm initializes with the cylindrical arc-length method and switches to a dissipation-based arc-length control for better numerical stability as the damage evolves. A number of numerical examples with singularities demonstrated improvements in terms of efficiency and accuracy, as compared to the damage models represented by Powell-Sabin triangles.

## 1 INTRODUCTION

Continuum damage analysis has limitations in approximating diffusive fracture due to the lack of an internal length scale that propagates damage. We address this problem by the use of nonlocal higher-order gradient damage models [1], where nonlocality is introduced by a damage variable that is a function of the nonlocal quantity, which is evaluated as the Taylor expansion of the volume average of the local quantity. Higher-order terms in the Taylor approximation of the nonlocal integral are included due to the lack of accuracy of the second-order gradient damage model.

The formulations of fourth- and sixth-order gradient damage models require a global smoothness of  $C^1$  and  $C^2$ , respectively. The high-order continuity of basis functions can be automatically satisfied with the use of Non-Uniform Rational B-splines (NURBS) [2,3] and T-splines [4] in isogeometric analysis (IGA). However, it is not always easy to preserve the high-order smoothness when modeling complicated geometries, where reduced continuity is observed at multi-patch interfaces or extraordinary points in unstructured T-splines. In such cases, domain triangulation appears to be a powerful tool for parameterization as it is not topologically constrained to the four-sided meshgrid. The use of Powell-Sabin (PS) triangles in fourth-order gradient damage models was studied in [5] and showed promising results. However, due to the definition of PS triangles, which are required to contain all the associated PS points in order to obtain positive basis functions, the control points of PS triangles are positioned randomly. This may be inconvenient in cases where Dirichlet/Neumann boundary conditions have to be specified at a given point. Moreover, the definition of quintic PS triangles for  $C^2$ -continuity is complicated, compared to enforcing higher-order continuities on Bézier triangles. Additionally, it is not clear how the PS triangle formulation could be extended to three dimensions for tetrahedral meshing.

As an alternative, we adopt rational Bézier triangles [6,7] for domain triangulations. The process of mesh generation starts from  $C^0$  Bézier triangles, meaning that one can resort to a wide number of existing meshing tools and automate the meshing process. To raise the global continuity to a desired order, Lagrange multipliers are used to impose continuity constraints in an explicit fashion. Due to the use of the rational form of the Bézier triangles, exact boundary can be fully recovered. Moreover, in order to capture small geometric features and increase the flexibility in discretization, a Delaunay-based feature-preserving triangulation is adopted. This turns out to be beneficial in capturing the initiation and early-stage propagation of damage. Additionally, instead of uniformly refining the mesh, we adopt a local refinement approach called Rivara's method [8] that bisects marked triangles while keeping the final mesh conformal and well-conditioned. The method is used to locally refine the regions where damage initiates and propagates.

In this contribution, the implicit fourth- and sixth-order gradient damage models are considered, since the inclusion of higher-order terms has the potential to accurately approximate the nonlocal solution, with minimal computational effort. The solution initializes with the cylindrical arc-length control [9] and switches to a dissipation-based arc-length control [10] for better numerical stability with the evolution of damage. Numerical examples demonstrate the benefits of higher-order gradient damage models, as well as the accuracy and ease of generalization into arbitrary high-order global smoothness in the use of the feature-preserving rational Bézier triangles.

## 2 DELAUNAY BASED FEATURE PRESERVING TRIANGULATION

Our solution procedure initiates with a closed NURBS curve as input and makes use of a number of existing meshing technologies (e.g., TriGA [6,7]). The main idea is a Delaunay-based triangulation with a series of Laplacian smoothing operation. The algorithm attempts to construct a high-quality polygon approximation of the original NURBS curves (Fig. 1b and 1c), which is then followed by a quadtree decomposition (Fig. 1d) that matches the local geometry features to evaluate the element size distribution needed to resolve the geometry. The algorithm optimizes the control point placement and mesh topology through an iterative process (Fig. 1e and 1f). In particular, a constrained Delaunay triangulation is performed in each iteration with a series of Laplacian smoothing operation. After a high-quality triangulation is obtained, the polynomial degree is raised to cubic and the control points at the domain boundary are replaced by the control points of the original NURBS to exactly recover the boundary. The solution process is briefly discussed in the following and illustrated in Fig. 1.

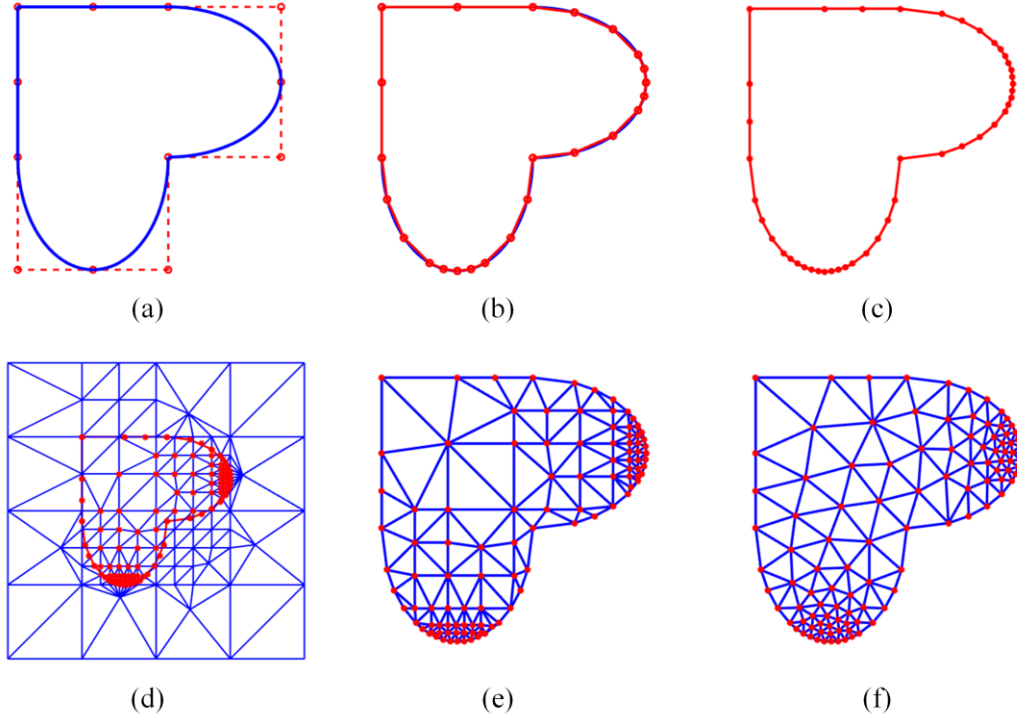


Fig. 1. Delaunay-based feature-preserving triangulation: (a) input NURBS curve; (b) initial polygon approximation after step 1; (c) final polygon approximation after step 2; (d) quadtree decomposition and control points considered for triangulation; (e) constrained Delaunay triangulation (CDT) at the first iteration; and (f) final CDT.

**A . Initial polygon approximation.** The step is controlled by the relative difference between the length of the curve for each knot span and the length of the corresponding polygon that approximates it. The algorithm iteratively subdivides the input NURBS curve until the relative differences for all the knot spans are below a given threshold.

**B . quadtree decomposition.** In this step, a quadtree background mesh is constructed and used to further refine the polygon. Specifically, the algorithm generates a bounding box, which is then recursively subdivided until the dimension of each box matches the local geometry feature size. A size function is also evaluated at the quadtree vertices based on the minimum neighboring box dimension. Next, the quadtree mesh is triangulated (Fig. 1d) so that the size function can be linearly interpolated at the polygon control points. Knot insertion is performed if the ratio of the edge length to the size function is above a given threshold.

**C . Delaunay based triangulation with inner smoothing.** The polygon approximation from Step ( ) is triangulated using the quadtree decomposition. The initial control points of the mesh are taken as a combination of the fixed polygon nodes and the internal nodes from the quadtree mesh (Fig. 1e). The algorithm optimizes the node placement and mesh topology via an iterative process. In particular, a constrained Delaunay triangulation is constructed at every iteration. Nodes are then added or removed from the mesh to meet the required element size distribution. A Laplacian smoothing operation such as a spring-based smoothing is then performed. The process iterates until all the triangles meet the element size constraints.

**D . Polynomial degree elevation and boundary recovery.** In this step, we raise the polynomial degree to cubic via linear interpolation. Additionally, knot insertion is performed on the input NURBS curves until the knots corresponding to the polygon vertices have multiplicity 3. As a result, there exist four control points at each knot span corresponding to the edge control points of the boundary triangles. The control points at the boundary are then substituted by the control points of the input NURBS curves for exact boundary recovery.

### 3 LOCAL REFINEMENT

As is commonly acknowledged, it is unnecessary and computationally costly to uniformly refine the mesh. Therefore, we adopt a local refinement scheme (i.e., Rivara’s method [8]) that is capable of generating high-quality mesh while keeping the final mesh conforming and well-conditioned. The algorithm firstly bisects marked triangles and then iteratively bisects non-conforming triangles until the mesh becomes conforming. A pseudo-code is provided in Fig. 2.

---

**Algorithm 1** Rivara’s method of bisecting triangles for local refinement

---

```

1: for all marked triangles  $\tau \in \Gamma$  do
2:   Bisect  $\tau$  by the midpoint  $P$  of the longest edge.
3: end do
4: Find the set of non-conforming triangles  $\tau_n \in \Gamma_n$ 
5: while cardinality of  $\Gamma_n \neq 0$  do
6:   Bisect  $\tau_n$  by the midpoint  $Q$  of its longest side
7:   if  $P \neq Q$  then
8:     Join  $P$  and  $Q$ 
9:   end if
10: Find the set of non-conforming triangles  $\Gamma_n$ 
11: end do

```

---

Fig. 2. A pseudo-code for Rivara’s method of bisecting triangles for local refinement

## 4 HIGHER ORDER GRADIENT DAMAGE MODELS

### 4.1. Continuum formulation

The nonlocal damage analysis is a coupled analysis where a diffusion equation representing the damage propagation needs to be solved in addition to the equilibrium equation representing the structural deformation. On the one hand, the structural deformation can be expressed as

$$\frac{\partial \sigma_i}{\partial x_i} = 0 \quad (1)$$

and may be subjected to Dirichlet boundary conditions  $u_i = \bar{u}_i$  on  $\partial\Omega_u$  and Neumann boundary conditions  $\sigma_i n_i = h_i$  on  $\partial\Omega_h$ .

On the other hand, the representation of damage propagation requires an additional scalar variable  $\omega \in [0,1]$ , with  $\omega = 0$  the undamaged state and  $\omega = 1$  the fully damaged state. As a result, the stress-strain relationship can be written as

$$\sigma_i = (1 - \omega) \epsilon_i \quad (2)$$

where  $\epsilon_i$  is the elasticity tensor and  $\epsilon$  is the infinitesimal strain tensor

$$\epsilon_i = \frac{1}{2} \left( \frac{\partial u_i}{\partial x} + \frac{\partial u}{\partial x_i} \right) \quad (3)$$

The damage variable  $\omega$  is a function of a monotonically increasing history parameter  $\kappa$ ,  $\omega = \omega(\kappa)$ . The evolution of  $\kappa$  is controlled by the Kuhn-Tucker conditions:

$$f \leq 0, \dot{\kappa} \geq 0, \dot{\kappa} f = 0 \quad (4)$$

with  $f$  the loading function,  $f = \bar{\eta} - \kappa$ , and  $\bar{\eta}$  the nonlocal equivalent strain. The nonlocal equivalent strain  $\bar{\eta}$  can be calculated using the average of the local equivalent strain  $\eta$  over a finite volume  $\Omega$

$$\bar{\eta}(x) = \frac{\int_{\hat{x} \in \Omega} g(x, \hat{x}) \eta(\hat{x}) d\hat{x}}{\int_{\hat{x} \in \Omega} g(x, \hat{x}) d\hat{x}} \quad (5)$$

with  $g(x, \hat{x})$  the weighting function,

$$g(x, \hat{x}) = \exp\left(-\frac{\|x - \hat{x}\|}{2l_c^2}\right) \quad (6)$$

and  $l_c$  the internal length parameter.

In order to avoid a computationally expensive evaluation of the above volume integral, the Taylor expansion of the local equivalent strain  $\eta$  is often employed. In particular,

$$\eta(\hat{x}) = \eta|_{\hat{x}=x} + \frac{\partial \eta}{\partial \hat{x}_i} \Big|_{\hat{x}=x} (\hat{x}_i - x_i) + \frac{1}{2} \frac{\partial^2 \eta}{\partial \hat{x}_i \partial \hat{x}_j} \Big|_{\hat{x}=x} (\hat{x}_i - x_i)(\hat{x}_j - x_j) + O((\hat{x}_i - x_i)^3) \quad (7)$$

Substituting Eq. (7) into Eq. (5) and assuming that the integral ranges from negative infinity to infinity result in the explicit gradient formulation of the nonlocal equivalent strain

$$\bar{\eta}(x) = \eta(x) + \frac{1}{2} l_c^2 \frac{\partial^2 \eta(x)}{\partial x_i^2} + \frac{1}{8} l_c^4 \frac{\partial^4 \eta(x)}{\partial x_i^2 \partial x_j^2} + \frac{1}{48} l_c^6 \frac{\partial^6 \eta(x)}{\partial x_i^2 \partial x_j^2 \partial x_k^2} + \dots \quad (8)$$

In order to include the second- and fourth-order terms from Eq. (8),  $C^1$ - and  $C^2$ -continuous basis functions are required, respectively. As an alternative, the implicit gradient formulation can be obtained through differentiation and multiplication of Eq. (8)

$$\eta(x) = \bar{\eta}(x) - \frac{1}{2} l_c^2 \frac{\partial^2 \bar{\eta}(x)}{\partial x_i^2} + \frac{1}{8} l_c^4 \frac{\partial^4 \bar{\eta}(x)}{\partial x_i^2 \partial x_j^2} - \frac{1}{48} l_c^6 \frac{\partial^6 \bar{\eta}(x)}{\partial x_i^2 \partial x_j^2 \partial x_k^2} + \dots \quad (9)$$

The above implicit formulation only requires  $C^0$ -continuity for the second-order gradient model and is therefore suitable for standard FEA. However, the accuracy of the solution is often not satisfactory. In our approach, the fourth- and sixth-order gradient damage terms are also considered through the use of Lagrange multipliers [7] to raise global continuity.

Combining Eq. (1) and Eq. (9) leads to the govern equations for the higher-order gradient damage model. Through multiplication of a perturbation term  $\delta u$  and  $\delta \bar{\eta}$  to Eq. (1) and Eq. (9), respectively, and integration by parts over the domain  $\Omega$ , the weak form can be obtained

$$\int_{\Omega} \frac{\partial \delta u_i}{\partial x} \sigma_i d = \int_{\partial \Omega_n} \delta u_i h_i d \quad (10)$$

$$\int_{\Omega} \delta \bar{\eta} \bar{\eta} + \frac{1}{2} l_c^2 \frac{\partial \delta \bar{\eta}}{\partial x_i} \frac{\partial \bar{\eta}}{\partial x_i} + \frac{1}{8} l_c^4 \frac{\partial^2 \delta \bar{\eta}}{\partial x_i \partial x_j} \frac{\partial^2 \bar{\eta}}{\partial x_i \partial x_j} + \frac{1}{48} l_c^6 \frac{\partial^3 \delta \bar{\eta}}{\partial x_i \partial x_j \partial x_k} \frac{\partial^3 \bar{\eta}}{\partial x_i \partial x_j \partial x_k} d = \int_{\partial \Omega_n} \delta \bar{\eta} \eta d$$

## 4.2. Discretization

The domain of interest is discretized into  $n$  elements by the feature-preserving triangulation in Section 2. We can rewrite the displacement  $u$ , the nonlocal equivalent strain  $\bar{\eta}$  and their derivatives in terms of the Bézier basis functions and the deformation of the associated control points

$$u = \mathbf{R}_u \mathbf{u}, \varepsilon = \mathbf{B}_u \mathbf{u}, \bar{\eta} = \mathbf{R}_{\bar{\eta}} \bar{\eta}, \frac{\partial \bar{\eta}}{\partial x_i} = \mathbf{B}_{\bar{\eta}} \bar{\eta}, \frac{\partial^2 \bar{\eta}}{\partial x_i \partial x} = \mathbf{B}_{\bar{\eta}\bar{\eta}} \bar{\eta}, \frac{\partial^3 \bar{\eta}}{\partial x_i \partial x \partial x} = \mathbf{B}_{\bar{\eta}\bar{\eta}\bar{\eta}} \bar{\eta} \quad (11)$$

where

$$\begin{aligned} u &= [u_x \quad u_y], \varepsilon = [\varepsilon_{xx} \quad \varepsilon_{yy} \quad 2\varepsilon_{xy}], \frac{\partial \bar{\eta}}{\partial x_i} = \begin{bmatrix} \frac{\partial \bar{\eta}}{\partial x} & \frac{\partial \bar{\eta}}{\partial y} \end{bmatrix}, \\ \frac{\partial^2 \bar{\eta}}{\partial x_i \partial x} &= \begin{bmatrix} \frac{\partial^2 \bar{\eta}}{\partial x^2} & \frac{\partial^2 \bar{\eta}}{\partial y^2} & \sqrt{2} \frac{\partial^2 \bar{\eta}}{\partial x \partial y} \end{bmatrix}, \\ \frac{\partial^3 \bar{\eta}}{\partial x_i \partial x \partial x} &= \begin{bmatrix} \frac{\partial^3 \bar{\eta}}{\partial x^3} & \frac{\partial^3 \bar{\eta}}{\partial y^3} & \sqrt{3} \frac{\partial^3 \bar{\eta}}{\partial x^2 \partial y} & \sqrt{3} \frac{\partial^3 \bar{\eta}}{\partial x \partial y^2} \end{bmatrix}, \end{aligned} \quad (12)$$

$$\mathbf{R}_u = \begin{bmatrix} \mathbf{R} & \\ & \mathbf{R} \end{bmatrix}, \mathbf{B}_u = \begin{bmatrix} \frac{\partial \mathbf{R}}{\partial x} & \frac{\partial \mathbf{R}}{\partial y} \\ \frac{\partial \mathbf{R}}{\partial y} & \frac{\partial \mathbf{R}}{\partial x} \end{bmatrix}, \mathbf{R}_{\bar{\eta}} = \mathbf{R}, \mathbf{B}_{\bar{\eta}} = \begin{bmatrix} \frac{\partial \mathbf{R}}{\partial x} & \frac{\partial \mathbf{R}}{\partial y} \end{bmatrix},$$

$$\mathbf{B}_{\bar{\eta}\bar{\eta}} = \begin{bmatrix} \frac{\partial^2 \mathbf{R}}{\partial x^2} & \frac{\partial^2 \mathbf{R}}{\partial y^2} & \sqrt{2} \frac{\partial^2 \mathbf{R}}{\partial x \partial y} \end{bmatrix}, \mathbf{B}_{\bar{\eta}\bar{\eta}\bar{\eta}} = \begin{bmatrix} \frac{\partial^3 \mathbf{R}}{\partial x^3} & \frac{\partial^3 \mathbf{R}}{\partial y^3} & \sqrt{3} \frac{\partial^3 \mathbf{R}}{\partial x^2 \partial y} & \sqrt{3} \frac{\partial^3 \mathbf{R}}{\partial x \partial y^2} \end{bmatrix}$$

Substituting the discretized form into Eq. (10) leads to

$$\begin{aligned} \delta \mathbf{u} \left( \int_{\Omega} \mathbf{B}_u (1-\omega) \mathbf{C} \mathbf{B}_u d \mathbf{u} - \int_{\partial \Omega_n} \mathbf{R}_u \mathbf{h} d \right) &= 0 \\ \delta \bar{\eta} \left( \int_{\Omega} \mathbf{R}_{\bar{\eta}} \mathbf{R}_{\bar{\eta}} + \frac{l_c^2}{2} \mathbf{B}_{\bar{\eta}} \mathbf{B}_{\bar{\eta}} + \frac{l_c^4}{8} \mathbf{B}_{\bar{\eta}\bar{\eta}} \mathbf{B}_{\bar{\eta}\bar{\eta}} + \frac{l_c^6}{48} \mathbf{B}_{\bar{\eta}\bar{\eta}\bar{\eta}} \mathbf{B}_{\bar{\eta}\bar{\eta}\bar{\eta}} d \bar{\eta} - \int_{\Omega} \mathbf{R}_{\bar{\eta}} \eta d \right) &= 0 \end{aligned} \quad (13)$$

## NUMERICAL EXAMPLES

In this section, we consider the classical L-shaped domain and its variant, which is an L-shaped domain with curved inside corner. For both problems, we employ a 28-point quadrature rule for integration over the triangle. We also use quintic elements in order to impose higher-order continuity.

### 1 L shaped domain

As the first numerical example, we consider the classical L-shaped domain problem. The setup of the problem is shown in Fig. 3(a). The thickness of the plate is  $t=200$  mm. The material

is linear elastic, with the Young's modulus  $E=10\text{GPa}$  and Poisson's ratio is  $\nu=0.2$ . A state of plane stress is assumed.

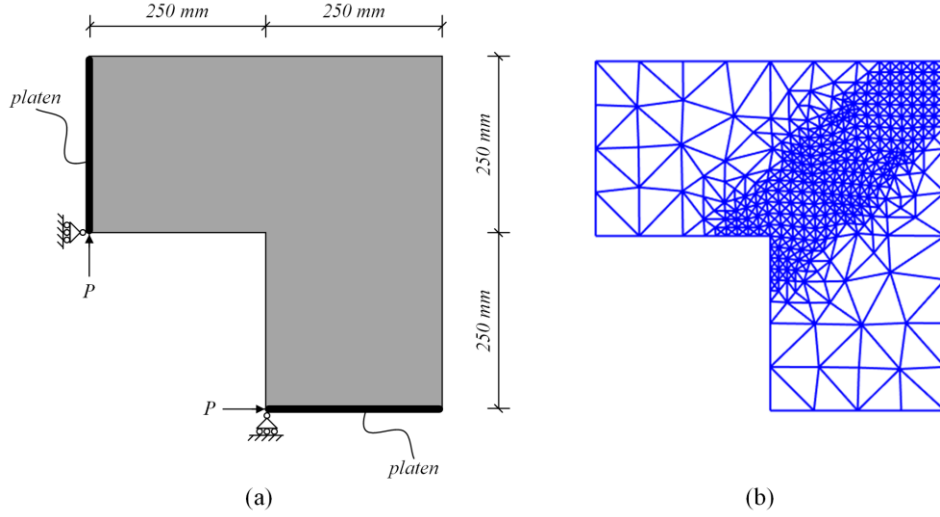


Fig. 3. The classical L-shaped domain: (a) the problem setup, and (b) the resulting mesh after applying Rivara's method five times (number of control points (NCP): 12631).

The two platens at the ends of the plate are realized by imposing linear constraints in the form of Lagrange multipliers. The modified von Mises local equivalent strain is used

$$\eta(\varepsilon) = \frac{-1}{2(1-2\nu)} I_1(\varepsilon) + \frac{1}{2} \sqrt{\left(\frac{-1}{1-2\nu} I_1(\varepsilon)\right)^2 + \frac{12}{(1+\nu)^2} J_2(\varepsilon)} \quad (14)$$

with  $I_1(\varepsilon)$  the first invariant of the strain tensor,  $J_2(\varepsilon)$  the second invariant of the deviatoric strain tensor, and  $\beta$  representing a parameter that accounts for the variation in strength between compression and tension,  $\beta = 10$ .

The damage law employed in this example is

$$\omega(\kappa) = \begin{cases} 0 & \kappa \leq \kappa_0 \\ 1 - \frac{\kappa_0}{\kappa} (1 - \alpha + \alpha \exp(\beta(\kappa_0 - \kappa))) & \kappa > \kappa_0 \end{cases} \quad (15)$$

with  $\kappa_0 = 4 \times 10^{-4}$ ,  $\alpha = 0.98$  and  $\beta = 80$ . The internal length parameter is  $l_c = 5\sqrt{2}\text{mm}$ .

Instead of uniformly refining the entire domain, we directly apply Rivara's method to locally refine the diagonal region, which is the region that damage will propagate. Fig. 3(b) shows the final mesh after applying Rivara's method five times to the region bounded by two lines  $y \geq x - 75$  and  $y \leq x + 75$ , with the inside corner taken as the origin.

The force-displacement relationships are plotted in Fig. 4, where they are also compared to the solutions from literature using T-splines [1] and PS triangles [5]. The displacement is

measured at the location the point load is applied to. For this problem, we use the nonlocal solution using T-splines as our reference solution. By comparing the solutions of different order gradient formulations on the locally refined mesh (LRM), we observe an obvious improvement in accuracy with the inclusion of the fourth- and sixth-order terms. In comparison to the result of the fourth-order gradient damage formulation using PS-triangles, our solution appears to be more accurate. In terms of NCP, the solution using PS-triangles uses 26463 control points, whereas our LRM only employs 12631 control points, which demonstrates significant computational saving.

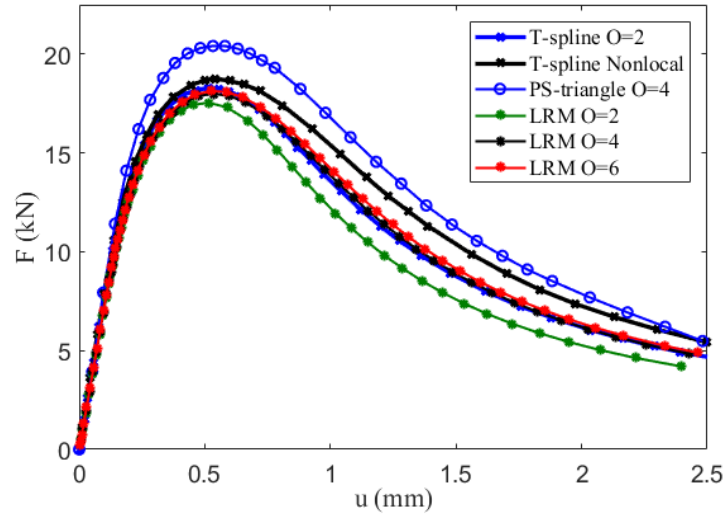


Fig. 4. The force-displacement relationships of the L-shaped domain

To better illustrate the accuracy of the proposed approach, the contour plots for the damage propagation and maximum principal stress distribution at  $u = 1.95\text{mm}$  are also plotted in Fig. 5.

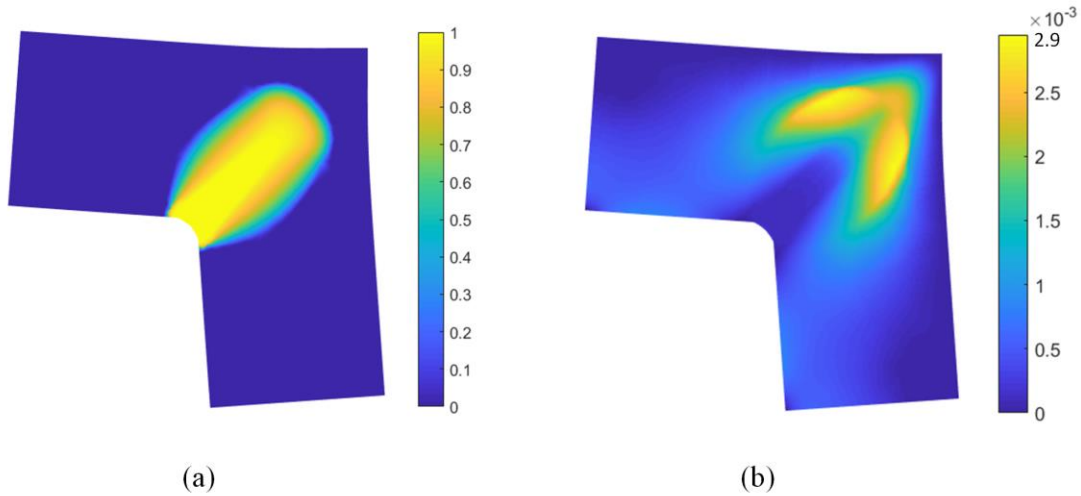


Fig. 5. Control plot for the L-shaped domain at  $u = 1.95mm$  (the deformation is amplified by a factor of 20): (a) damage propagation and (b) maximum principal stress distribution.

## .2 L shaped domain with curved inside corner

For the second example, only a slight change is made to the L-shaped domain, with the inside corner being curved instead of at a right angle (see Fig. 6(a)). Our aim is to investigate the performance of the feature-preserving algorithm on capturing the damage initiation and the early-stage damage diffusion. The sixth-order gradient damage formulation is adopted.

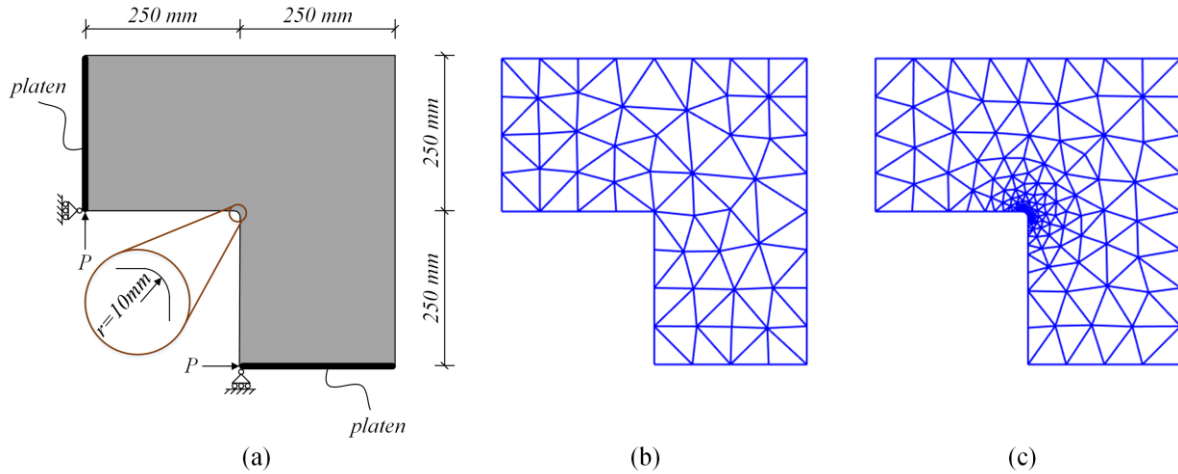


Fig. 6. The L-shaped domain with curved inside corner: (a) the problem setup, (b) the initial mesh, and (c) the feature-preserving triangulation

The final mesh from the feature-preserving meshing algorithm is plotted against the initial mesh of the classical L-shaped domain without before the local refinement technique is applied (see Fig. 6(b)). As we can see, the inside corner is resolved with high resolution (Fig. 6(c)).

The force-displacement relationships obtained using the above two meshes are plotted in Fig. 7. In comparison to the result obtained using the mesh in Fig. 6(b), we see a more accurate prediction of the entire deformation path using the mesh in Fig. 6(c), especially in the damage initiation phase that corresponds to the onset of yielding. The feature-preserving mesh is able to provide a fairly accurate solution up to  $u \approx 0.4mm$ , after which the damage propagates into the region of relatively large elements and locally refinement as demonstrated in the first numerical example is needed. In general, the feature-preserving triangulation can be employed to predict the early-stage damage propagation, and then a coupled adaptive meshing should be used to refine meshes in the direction of damage growth.

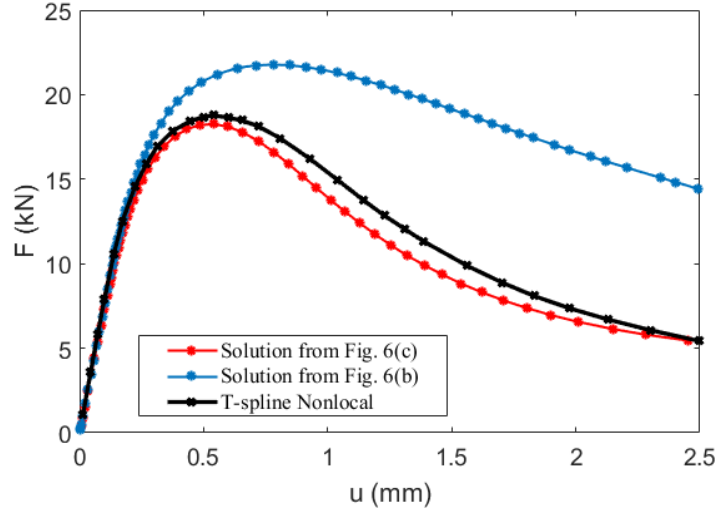


Fig. 7. The force-displacement curves obtained using the two mesh cases in Fig. 6

To better demonstrate the capability of the feature-preserving triangulation in capturing the early-stage damage propagation, the contour plots of damage growth at  $u = 0.43mm$ ,  $u = 0.90mm$  and  $u = 1.25mm$  are provided in Fig. 8.

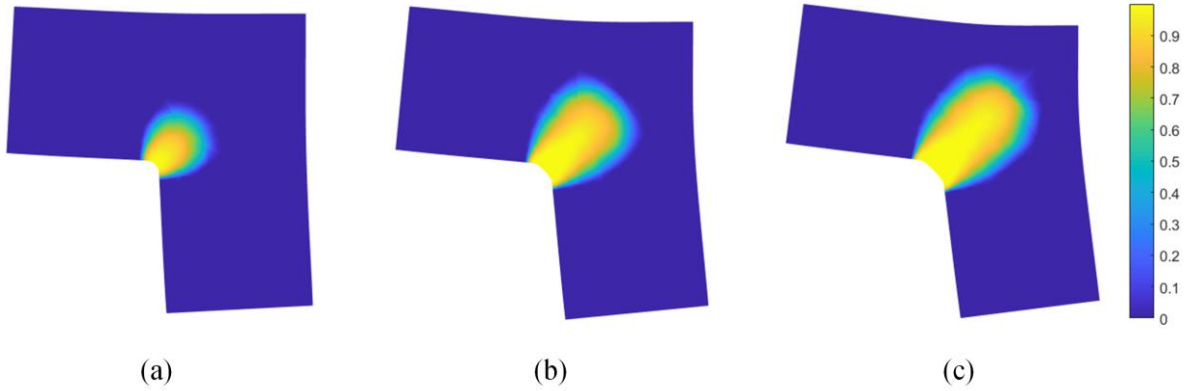


Fig. 8. The contour plots of damage growth in the L-shaped domain with curved inside corner (deformation is amplified by a factor of 50) at (a)  $u = 0.43mm$ , (b)  $u = 0.90mm$  and (c)  $u = 1.25mm$

## . CONCLUSION

The Delaunay-based feature-preserving rational Bézier triangles are a powerful tool in modeling smeared damage, especially in cases where complicated geometries are involved. They not only bypass the reduced continuity issue in NURBS and T-splines, but they also increase the flexibility in discretization. As is indicated in the second example, a general modeling framework can be constructed where the feature-preserving meshing can be employed to predict the damage growth at an early stage. As the damage propagates, a suitable

local refinement technique such as the Rivara's method can be adopted to further refine the mesh in the direction of damage growth. Furthermore, the use of Lagrange multipliers makes it possible to impose higher-order continuity constraints to the resulting mesh. In terms of the formulation of the implicit gradient damage models, the inclusion of higher-order terms results in a more accurate prediction of the deformation path, while the additional computational effort is trivial. The accuracy and efficiency of the proposed modeling approach are verified by a number of numerical examples, where superiority is observed over other domain triangulation methods such as PS triangles.

Nevertheless, it must be mentioned that domain triangulation is not an undisputedly better approach over quadrilateral meshing techniques (e.g., T-splines). An obvious defect of domain triangulation methods is that typically high-order polynomials (e.g., quartic and quintic) have to be used in order to enforce higher-order global continuity. In contrast,  $C^2$  continuity can be easily achieved with cubic NURBS/T-splines.

## REFERENCES

- [1] C. V. Verhoosel, M.A. Scott, T.J.R. Hughes, R. de Borst, An isogeometric analysis approach to gradient damage models, *Int. J. Numer. Methods Eng.* 86 (2011) 115–134.
- [2] N. Liu, A.E. Jeffers, Adaptive isogeometric analysis in structural frames using a layer-based discretization to model spread of plasticity, *Comput. Struct.* 196 (2018) 1–11.
- [3] N. Liu, A.E. Jeffers, Isogeometric analysis of laminated composite and functionally graded sandwich plates based on a layerwise displacement theory, *Compos. Struct.* 176 (2017) 143–153.
- [4] Y. Bazilevs, V.M. Calo, J.A. Cottrell, J.A. Evans, T.J.R. Hughes, S. Lipton, M.A. Scott, T.W. Sederberg, Isogeometric analysis using T-splines, *Comput. Methods Appl. Mech. Eng.* 199 (2010) 229–263.
- [5] S. May, R. de Borst, J. Vignollet, Powell-Sabin B-splines for smeared and discrete approaches to fracture in quasi-brittle materials, *Comput. Methods Appl. Mech. Eng.* 307 (2016) 193–214.
- [6] L. Engvall, J.A. Evans, Isogeometric triangular Bernstein-Bézier discretizations: Automatic mesh generation and geometrically exact finite element analysis, *Comput. Methods Appl. Mech. Eng.* 304 (2016) 378–407.
- [7] N. Liu, A.E. Jeffers, A geometrically exact isogeometric Kirchhoff plate: Feature-preserving automatic meshing and  $C^1$  rational triangular Bézier spline discretizations, *Int. J. Numer. Methods Eng.* (2018) 1–15.
- [8] M.C. Rivara, Algorithms for refining triangular grids suitable for adaptive and multigrid techniques, *Int. J. Numer. Methods Eng.* 20 (1984) 745–756.
- [9] N. Liu, P. Plucinsky, A.E. Jeffers, Combining Load-Controlled and Displacement-Controlled Algorithms to Model Thermal-Mechanical Snap-Through Instabilities in Structures, *J. Eng. Mech.* 143 (2017) 1–11.
- [10] C. V. Verhoose, J.J.C. Remmers, M.A. Gutiérrez, A dissipation-based arc-length method for robust simulation of brittle and ductile failure, *Int. J. Numer. Methods Eng.* 77 (2009) 1290–1321.

## Understanding Evolution Mechanisms of Site-specific Grain Structures during Metal Additive Manufacturing

Pengwei Liu<sup>\*</sup>, Yanzhou Ji<sup>\*\*</sup>, Zhuo Wang<sup>\*\*\*</sup>, Chunlei Qiu<sup>\*\*\*\*</sup>, Alphons A. Antonysamy<sup>\*\*\*\*\*</sup>,  
Long-Qing Chen<sup>\*\*\*\*\*</sup>, Xiangyang Cui<sup>\*\*\*\*\*</sup>, Lei Chen<sup>\*\*\*\*\*</sup>

<sup>\*</sup>Hunan University, <sup>\*\*</sup>Pennsylvania State University, <sup>\*\*\*</sup>Mississippi State University, <sup>\*\*\*\*</sup>Cardiff University, <sup>\*\*\*\*\*</sup>GKN Aerospace Filton, <sup>\*\*\*\*\*</sup>Pennsylvania State University, <sup>\*\*\*\*\*</sup>Hunan University, <sup>\*\*\*\*\*</sup>Mississippi State University

### ABSTRACT

A multiscale model is developed to investigate the evolution mechanisms of site-specific grain structures during additive manufacturing (AM) of metallic alloys, using Ti-6Al-4V fabricated by selective electron beam melting (SEBM) as an example. These rapid processes are difficult to observe in experiments. Specifically, finite-element method is utilized to predict the thermal response at macroscale during SEBM, and the extracted thermal information is then input into a temperature-dependent phase-field model to simulate the grain growth at mesoscale. The thermal-gradient-dictating grain nucleation and anisotropic grain boundary energy are incorporated to account for the strongly anisotropic grain structures and textures. The development of large vertical columnar grains in the thick wall and inward growing slanted columnar grains in the thin wall can be attributed to the competition and collaboration between the thermal gradient and the crystallographically preferred grain orientations, as shown from the different growth stages in the simulations. The simulation results reveal that the thermal gradients control the grain nucleation angles during a layer-wise printing, and play a dominant role in grain structure development at the initial and intermediate stages. As the printing proceeds, the developed large columnar grains, either vertical or slanted, prohibit and swallow the nucleated grains in the newly deposited layer. The crystallographically preferred grain orientations gradually take over and contribute more to the grain texture development. The present study potentially offers valuable insights and guidance toward designing AM conditions to tailor the grain structures and textures. Keywords: Grain structures; Evolution mechanisms; Additive manufacturing; Titanium alloys; Phase-field method; Finite-element.

## **Concurrent Topology Optimization of Macrostructures and Microstructures of Viscoelastic Materials under Periodic Dynamic Loads**

Qiming Liu\*, Xiaodong Huang\*\*

\*Swinburne University of Technology, Australia, \*\*Swinburne University of Technology, Australia

### **ABSTRACT**

The damping characteristics of the viscoelastic materials are often utilized in the applications of dynamic structures, whereas there is no report on concurrent topology optimization of dynamic structures and their viscoelastic materials. Based on the bi-direction evolutionary structural optimization (BESO) method, this paper proposes a two-scale topology optimization algorithm which minimizes the dynamic compliance of structures by employing viscoelastic materials with optimal damping characteristics. The macrostructure is constructed by viscoelastic composite, whose microstructure is represented by periodic unit cells (PUCs). The effective properties of the viscoelastic composite are extracted by the homogenization theory and further integrated into the analysis of macrostructures. The sensitivity analysis with regard to design variables at macro- and micro- scale levels is conducted for iteratively updating the topologies at both scale levels synchronously. Numerical results show the developed topology algorithm can obtain the optimal topologies of the structure at the macro-scale level and microstructure of its viscoelastic material at the micro-scale level simultaneously, so that the resulting structure possesses the minimum dynamic compliance and the maximum damping under the prescribed weight.

## Liquid Evaporation-Driven Self-Assembly of 3-D Architected Structures: Atomistic Modeling and Simulations

Qingchang Liu\*, Baoxing Xu\*\*

\*University of Virginia Charlottesville, \*\*University of Virginia Charlottesville

### ABSTRACT

Low-dimensional deformable 2-D graphene have attracted tremendous attention for its many unique properties. However, a single piece of graphene is too delicate to be useful in most applications, for example, high-performance electrodes in energy storage, filters for waste water/gas treatments in environmental systems, and lightweight structures. Assembling these nanomaterials into three-dimensional (3-D) scaffolds to achieve superior overall performance with multiple functionalities has attracted growing interests, yet this is challenging in manufacturing. In particular, graphene tends to aggregate/restack due to strong van der Waals attraction such as restacking of 2-D flat graphene sheets, which not only results in a tremendous reduction of their accessible surface area and poor mass/ion transport, but also degrades with processing and/or application environments such as mechanical loadings, hence adversely affecting their properties and subsequent applications. A liquid evaporation-assisted manufacturing technique is considered to provide a facile route, where 2-D graphene will experience large deformation and severe instability under evaporation-induced compression to create spacings when assembled, which is highly desirable to minimize restacking and retain the large surface areas of graphene in the assembled 3-D architectural structures. In the present study, we develop an atomistic modeling and simulation technique to first probe the deformation and self-folding mechanism of individual 2-D graphene suspended in a liquid environment, and then extend it for understanding crumpling and assembling multiple 2-D graphene sheets by liquid evaporation. The proposed modeling and simulations results will help finding key controlling parameters including concentration, evaporation rate in experiments and provide a direct guidance for evaporation-assisted manufacturing technique.

## **A Coupled Finite Element Method/Peridynamic for 2D Dynamic Fracture Analysis**

Shuo Liu<sup>\*</sup>, Bing Wang<sup>\*\*</sup>, Guodong Fang<sup>\*\*\*</sup>, Jun Liang<sup>\*\*\*\*</sup>

<sup>\*</sup>Harbin Institute of Technology, <sup>\*\*</sup>Harbin Institute of Technology, <sup>\*\*\*</sup>Harbin Institute of Technology, <sup>\*\*\*\*</sup>Beijing Institute of Technology

### **ABSTRACT**

Abstract: A new coupling scheme of peridynamic (PD) and finite element method (FEM) is proposed in this paper to analyze the 2D brittle material transient crack propagation problem. The coupling scheme makes full use of the advantages of PD to deal with discontinuous problems and the high efficiency of FEM. It is easy to perform, without setting the overlap region between PD and FEM. By using the adaptive partitioning of the solution domain, the PD model is used only in the vicinity of the crack to reduce the computational effort. In the coupling region, the stiffness of FEM and the interaction between PD particles are assembled into a global stiffness matrix. Ghosts test analysis verifies the reliability of the coupling method. The numerical example shows that the proposed coupling scheme has high accuracy and efficiency in the simulation of dynamic crack bifurcation problems. Key words: coupling, damage; crack propagation and bifurcation; FEM; peridynamic

## Harmonic Balance Method for Unsteady One-Dimensional Periodic Flows

Wei Liu<sup>\*</sup>, Zhenxia Chai<sup>\*\*</sup>, Ming Zeng<sup>\*\*\*</sup>, Xiaoliang Yang<sup>\*\*\*\*</sup>

<sup>\*</sup>National University of Defense Technology, <sup>\*\*</sup>National University of Defense Technology, <sup>\*\*\*</sup>National University of Defense Technology, <sup>\*\*\*\*</sup>National University of Defense Technology

### ABSTRACT

In recent years, the harmonic balance method (HBM) has been developed as a novel nonlinear frequency domain method for modeling periodic unsteady flows. In this paper, two one-dimensional computational fluid dynamics (CFD) codes were developed to investigate the behavior of the harmonic balance method. The first work investigated harmonic balance solutions of one-dimensional inviscid wave equation subject to a variety of periodic boundary conditions. Next, harmonic balance solutions of the inviscid Burgers's equation were investigated. Accuracy will be determined through comparison with accurate results and conventional time domain method's results. The impact of number of harmonics, amplitude and frequency of the boundary conditions, and grid density on the harmonic balance solution were investigated. Computational results demonstrate that a flow that is smoothly unsteady without moving discontinuities will require fewer harmonics for HBM computation than a flow containing a moving shock to achieve the same accuracy with the time domain method. As amplitude increased, solutions for boundary conditions containing moving waves ranging from smooth disturbances to strong discontinuities. The larger of amplitude, the stronger of the discontinuities, and the more harmonics are required for HBM computation. In contrast, as the disturbance frequency increased, the number of harmonics required for HBM computation usually decreased. The results also show that the coarse grid can eliminate the non-physical oscillations resulted in beneficial smoothing, but the coarse grid damping effect caused considerable degradation in higher-frequency solution. The harmonic balance method was more sensitive to grid density than the time domain method.

## **A Simulation Toolkit for the Microstructure Modelling Guided Design of the Damage Tolerant High-strength Steel**

Wenqi Liu<sup>\*</sup>, Sebastian Münstermann<sup>\*\*</sup>, Junhe Lian<sup>\*\*\*</sup>

<sup>\*</sup>RWTH Aachen University, <sup>\*\*</sup>RWTH Aachen University, <sup>\*\*\*</sup>RWTH Aachen University

### **ABSTRACT**

A simulation toolkit is developed in this study for the damage tolerant microstructure design of the advanced high strength steel. Toolkit is an improved integrated computational materials engineering approach fostering sustainable component design option. It provides a method of tailoring steels for a specific industry application and improving material performance by new mechanism. In this study, crash box manufactured by a dual-phase steel sheet (DP1000) in the automotive industry is focused on. With the help of macro- and micro-mechanical models, the component performance, i.e. the crashworthiness of crash box, can be transferred to the required mechanical property profiles and the optimized microstructure features. Toolkit starts at the targeted component performance, crash box tests are performed on the drop tower to characterize the crashworthiness. An Extended Modified Bai Wierzbicki (eMBW) damage considering the effects of stress state, strain rate and temperature on the plasticity and damage/fracture behavior is developed for transfer the component performance to the required macromechanical property profiles. An extensive experimental program at lab scale is designed to calibrate the material parameters and validate the model, involving dog-bone specimens, notched tension specimens, central-hole specimens, and punch specimens to cover a wide range of stress states. These tests are performed at quasi-static and high speeds conditions to obtain the plasticity and fracture description of material response at various strain rates and temperatures. For the linking between the microstructure features and the mechanical properties, the representative microstructure model is employed allowing consideration of the microstructure parameters and at the same time bridging the equivalent quantities from microstructure to macroscopic level by incorporating a crystal plasticity material model. To balance the representativeness and computational capability of the 3D representative volume elements (RVEs), A criterion considering the effects of RVE size and mesh discretization is proposed to characterize the RVE representativeness. Nanoindentation tests are carried out on both ferrite and martensite to calibrate the crystal plasticity parameters. The micromechanical models are validated by uniaxial tensile test, with which the flow curve of the reference material is naturally captured. For microstructure optimization, the integrated microstructural features, such as phase fraction, grain size, grain shape, texture, and second phase morphology et.al., are taking into account for their effects on the macroscopic mechanics. Finally, the tailored damage tolerant microstructure is designed for the targeted component performance.

## **Data-Driven Process-Structure-Property Simulation Models for Additive Manufacturing**

Wing Kam Liu\*

\*Northwestern University

### **ABSTRACT**

This talk presents our latest work on the comprehensive materials modeling of process-structure-property relationships for additive manufacturing (AM) materials. The numerous influencing factors that emerge from the AM process motivate the need for novel rapid design and optimization approaches. For this, we propose data-mining as an effective solution. Such methods - used in the process-structure, structure-properties and the design phase that connects them - would allow for a design loop for AM processing and materials. As a specific application, the developed data-driven simulation models are employed to study, understand, and manipulate thermo-capillary flow in additive manufacturing. Thermo-capillary flow, driven by Marangoni stress and buoyant force, dramatically affect the heat and mass transfer, solidification behavior, and microstructure formation in the melt pool. It is still challenging to understand the thermo-capillary flow and to manipulate it so as to tailor microstructure and properties in AM of Superalloys. Surfactants, which are the elements or compounds remarkably affecting surface tension of liquid metal, are introduced. The effects of surfactants on thermo-capillary flow is demonstrated as well as the possibility of manipulating thermo-capillary flow by adding specific surfactant. The surfactant-affected thermo-capillary flow in AM will be discussed.

## **Welcome Remarks**

Wing Kam Liu\*, Jacob Fish\*\*

\*Northwestern, \*\*Columbia University

### **ABSTRACT**

Opening words of welcome.

## **An Efficient Strategy for Large Scale 3D Simulation of Heterogeneous Materials**

Xiaodong Liu<sup>\*</sup>, Julien Réthoré<sup>\*\*</sup>, Antonius A. Lubrecht<sup>\*\*\*</sup>, Marie-Christine Baietto<sup>\*\*\*\*</sup>, Philippe Sainsot<sup>\*\*\*\*\*</sup>

<sup>\*</sup>Ecole Centrale de Nantes, <sup>\*\*</sup>Ecole Centrale de Nantes, <sup>\*\*\*</sup>INSA-Lyon, <sup>\*\*\*\*</sup>INSA-Lyon, <sup>\*\*\*\*\*</sup>INSA-Lyon

### **ABSTRACT**

The development of imaging techniques based on X-ray tomography permits one to obtain the inner structure and the details of materials at a microscopic scale. To take into account such detailed information as an input for numerical simulations is becoming more and more common. The difficulties are the computational cost, mesh generation in the context of finite element simulation and the high discontinuities of material properties (Gu et al., 2016) which can lead to convergence problems. The subject of this presentation is the application of MultiGrid methods coupled with homogenization methods for coarse grid operators (Sviercoskiet al., 2015). The method allows us to solve large scale 3D thermal conduction problems in a material with highly heterogeneous properties. Hybrid MPI-OpenMP parallel computing has been used to save computational time. The material structure is obtained from a real X-ray tomography image. The influence of material heterogeneity is analyzed as well as the ratio of material properties for the thermal conduction. The efficiency of the strategy of using MultiGrid coupled with homogenization based coarse grid operators shows the possibility to carry out numerical simulations at microscopic scale with a low computational cost. References Gu, H., Réthoré, J., Baietto, M.-C., Sainsot, P., Lecomte-Grosbras, P., Venner, C. H., Lubrecht, A. A., 2016. An efficient multigrid solver for the 3d simulation of composite materials. *Computational materials science* 112, 230–237. Sviercoski, R. F., Popov, P., Margenov, S., 2015. An analytical coarse grid operator applied to a multiscale multigrid method. *Journal of Computational and Applied Mathematics* 287, 207–219.

# NONLINEAR DYNAMIC LATERAL RESPONSES OF CURVED RAILWAY TRACK ASSOCIATED WITH HIGH-FREQUENCY SQUEAL NOISES

CHAYUT NGAMKHANONG<sup>1,2</sup>, XIN LIU<sup>3</sup>, AND SAKDIRAT KAEWUNRUEN<sup>1,2</sup>

<sup>1</sup>Department of Civil Engineering, School of Engineering,  
University of Birmingham, Birmingham B152TT, United Kingdom  
Email address; cxn649@student.bham.ac.uk, s.kaewunruen@bham.ac.uk

<sup>2</sup>Birmingham Centre for Railway Research and Education, School of Engineering,  
University of Birmingham, Birmingham B152TT, United Kingdom

<sup>3</sup>Department of Civil Engineering, Beijing Jiaotong University,  
Haidian district, Beijing 100044, China  
Email address; 15125863@bjtu.edu.cn

**Key words:** Dynamic Response, Railway Track, Lateral Responses, Curved Railway Track, Squeal Noise.

**Abstract.** In urban environment, curve squeal is a strongly tonal noise emitted from wheel/rail contact caused by the passage of the train in tight curve rail. Wheel/rail contact can cause a traveling source of sound and vibration, which constitutes high-pitch noise pollution inducing a considerable concern of rail asset owners, commuters and people living or working along the rail corridor. The sound and vibration can be expressed in various forms and spectra. The undesirable sound and vibration on curves are often called squeal noises. This type of noise is commonly emitted in tight curve rails and can be annoying to nearby residents due to its tonal nature and uncertain excitation mechanism. This paper studies the effect of curve radii on the possible occurrence of curve squeal, which is devoted to systems thinking the approach and dynamic assessment in resolving railway curve noise problems. Curve track models in three-dimensional space have been built using finite element package, STRAND7. The moving train loads are applied in order to simulate nonlinear dynamic responses of curve track associated with squeal noise. The simulations of railway tracks with different curve radii have been carried out to develop state-of-the-art understanding into lateral track dynamics. Parametric studies have been conducted to evaluate static and dynamic responses. The dynamic responses of the track are found to be sensitive to the change of curve radii. The resonance peak in the lateral direction is related to the agreement of corresponding natural frequency of rail and the vibration excitation frequency under an individual rolling velocity. The outcome of this study will help provide some key parametric insights into fundamental dynamics of track in the lateral direction and establish the development of the dynamic design of curve track.

## 1 INTRODUCTION

Railway vibration and noise are a serious concern as it makes an annoyance to people nearby and affects property in the surrounding area [<sup>1-3</sup>]. Wheel/rail interaction is a traveling source of

excitation, sound radiation and vibration along the railway corridors. The sound and vibration can be in various forms and spectra. There are many types of noise occurred on railway track during train passage; ground-borne, impact, rolling, squeal and flange. However, one of the loudest and most annoying noise sources from railways is squeal noise [4] which is often occurred on curved track. The occurrence of squeal induces significant environmental impacts immensely annoying people living nearby due to its high frequencies characteristics [5]. Curve squealing occasionally arises when railway vehicles run through tight curves at low speed [4, 6]. Table 1 shows different types of railway noise associated with different frequencies. It can be seen that the frequency range concerned with squeal noise is between 1000 and 5000Hz.

Table 1 Frequency range for different types of railway noise [7-9].

Noise type	Frequency range (Hz)
Ground-borne vibration	4-80
Impact noise	50-250 (speed dependant)
Rolling noise	30-5000
Squeal noise	1000-5000
Flange noise	5000-10000

It should be noted that [10-13] unsteady lateral creepage at the wheel/rail contact is thought to be the prime reason of squeal noise, while other mechanisms such as longitudinal creepage and flange contact, do not necessarily eliminate squeal noise thereby are determined to be of secondary importance [14-16]. Previous work indicated that squeal only occur when the curve radius is smaller than  $100b$ , where  $b$  is the bogie wheelbase [17]. The results of on-site measurements also presented that there is no significant reduction in wheel squeal associated with limiting operation speed. According to the data collected from fields, it is suggested that diverse range of curving behaviour are largely relevant to curve radii. Although there are many possible treatments [18-20] that can be taken for mitigating the effects of squeal such as improving curving behaviour, modifying rail profiles, adding lubrications or friction modifiers, increasing the damping of wheel or rail, it is still uncertain to what extent the track lateral response is affected by rail radii, cants etc. It is noted that lateral track dynamic characteristic has not been fully investigated. The various curve radii, cants and lateral loads are taken into account in this study.

This paper illustrates the dynamic influences of curve radii, cants, lateral loads on the lateral dynamic vibrations, which are the possible mechanism for development of curve squeal under mode-coupling theory. The study is devoted to systems thinking the approach and dynamic assessment in resolving railway curve noise problems. Finite element package, STRAND7 has been used to build the curve track models in three-dimensional space. The dynamic responses of curve track have been simulated by applying a moving train load. The simulations of railway tracks with different curve radii have been implemented to develop a comprehensive understanding of lateral track dynamics, containing dynamic behaviors of rail, cant, gauge and overall track responses.

## 2. TRACK MODEL

The track model comprises two-dimensional Timoshenko beam, which takes into account shear deformation and rotational bending effects. This beam has been proven to be the best options for modelling rail and concrete sleeper due to its bending characteristics in both vertical and lateral directions to reflect the behaviour of thick beam [21-22]. It is noted that Timoshenko beam is suitable for solving the problem of beam subjected to high-frequency excitation when the wavelength approaches the thickness of the beam. The 60kg rail cross section (Area: 17659.8mm<sup>2</sup>; Second moment of Area: 43.2x10<sup>6</sup>) are considered in this track model [23]. While, the trapezoidal cross-section is allocated to the sleeper elements with medium section (204mm top-wide, 250mm bottom-wide and 180mm deep). The non-linear tensionless beam support can be used to demonstrate ballast under the sleeper. It is noted that the tensionless support allow beam to lift over the support while the tensile support is omitted [24]. Thus, this option can correctly reflect the real ballast characteristics [25]. It is noted that the partial support condition is believed to vastly conform with real condition of standard gauge tracks. The rail pads at the rail seat are simulated by using series of spring dash-pot elements. The high-density polyethylene pads are assigned to these spring-dashpot elements both in vertical and lateral direction. It should be noted that the model has been developed and validated previously using experimental parameters, field data and previous laboratory results [26-28]. The finite element models in three-dimensional space for an in situ railway track with both curve and tangent are presented in Figure 1.

Table 2 Material properties.

Parameters	Characteristic value	Unit
<b>Rail</b>		
Length, $l_r$	10.8	m
Gauge, $g$	1.5	m
Modulus, $E_r$	2e5	MPa
Poisson's ratio, $\nu_r$	0.25	-
Density, $d_r$	7850	Kg/m <sup>3</sup>
<b>Railpad</b>		
Vertical stiffness, $k_{pv}$	17	MN/m
Lateral stiffness, $k_{pl}$	70	MN/m
<b>Sleeper</b>		
Length, $l_s$	2.5	m
Spacing, $s$	0.6	m
Modulus, $E_s$	3.75e4	MPa
Shear modulus, $G_s$	1.09e4	MPa
Density, $d_r$	2740	Kg/m <sup>3</sup>
<b>Ballast</b>		
Stiffness, $k_b$	13	MN/m

The curve radius of railway track considered varies from 100m to 600m. Cant is also considered with the range from 100cm to 300cm. It is simplified to 2points loads (1 axle) with a speed of 10m/s and 100kN in magnitude, 2m apart (common passenger bogie centre), on each

side of the rail track. The impulse excitations of a period of 0.0001s starting at 0.005s are assigned. In order to cover high frequency squeal noise, the calculation time step is set to be 0.00005. While, the lateral loads are set to be the proportion of vertical loads (Lateral to Vertical, L/V). The schematic lateral load case used is shown in Figure 2.

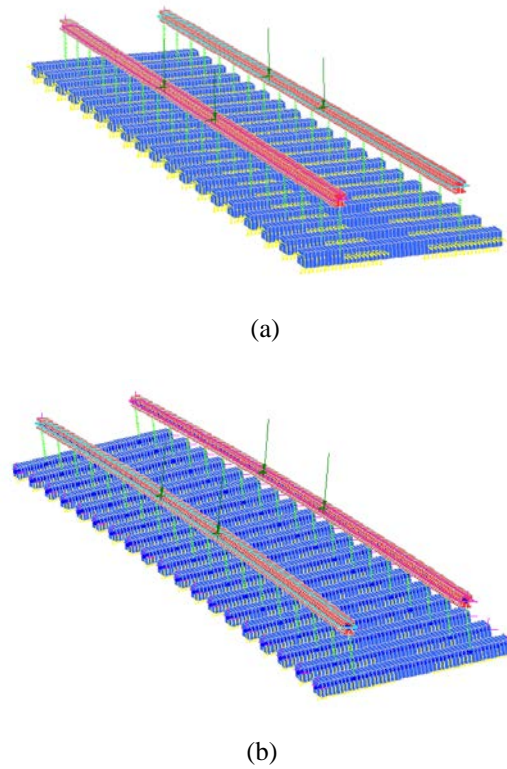


Figure 1 Dynamic track models: (a) The model of curve track (b) The model of tangent track.

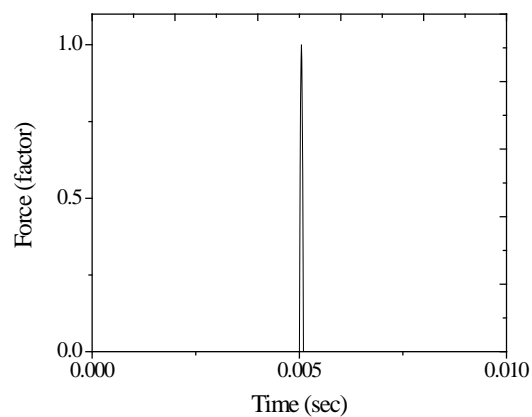


Figure 2 Schematic load case.

### 3 RESULTS AND DISCUSSIONS

The Nonlinear Transient Solver in STRAND7 is used to solve the dynamic responses of curved track. The eigenfrequencies and corresponding eigenmodes are calculated up to 10kHz in order to cover modes of squeal noises vastly. For curve track, the parameters concerned are curve radius, cants and lateral loads. The moving loads are applied with the velocity of 10m/s and thus the calculation time of 5s is considered for the whole process. In this study, lateral track displacement, lateral track velocity and lateral track mobility are presented.

#### 3.1 Displacement responses

Dynamic lateral displacements of rail under different lateral load intensity are shown in Figure 3. The vertical loads are fixed to be 100kN as a benchmark for passenger train bogie, while the lateral loads varies from 5kN to 40kN. It can be seen that railway track with higher curve radius or tangent track have severe lateral displacement than that with tight curve. This is because the tight curve has higher lateral resistance and stiffness. It is interesting to note that the trends of rail lateral displacement with respect to curve radius are nonlinear as can be seen in Figure 3. In addition, as for track with 300cm cant, the lateral responses tend to be nonlinear as well as railway track without cant. However, it is noted that the increase of cant can significantly reduce lateral displacement by about 20-30%. As for from 100m to 200m curve radius, about 78% increase of lateral displacement of track without cant is observed. While, only 3.2% increasing rate is expected to occur from 500m to 600m radius. It can be concluded that, for large curve, lateral displacement has a slight change with the increase of radius and thus the radius plays a little role on dynamic response of large curved track but play a significant role on dynamic responses of tight curve. Therefore, the possibility of occurrence of curve squeal noise might be decreased on large curved track.

The obtained results demonstrate that the increase of track radius has a significant positive effect on the reduction of lateral responses which might decrease the possibility of curve squeal. This implies that lateral displacement responses are more sensitive corresponding to low radii, which gave evidence on the appearance of squeal during train negotiating tight curves. It can also be observed from the graph that the lateral track displacement of tangent track is similar to the value of track with a radius of 600m. For large curve radius, the lateral displacement of the track no longer change significantly with increasing radius therefore the increase of radius plays a little role on the dynamic amplitude of track. In reality, this phenomenon is evident from the less flange contact between wheel and rail while train traveling in large curve. The results above indicate that the increased track radius has positive effect on reducing curve squeal and squeal noise would disappear when the curve radius comes to a certain value.

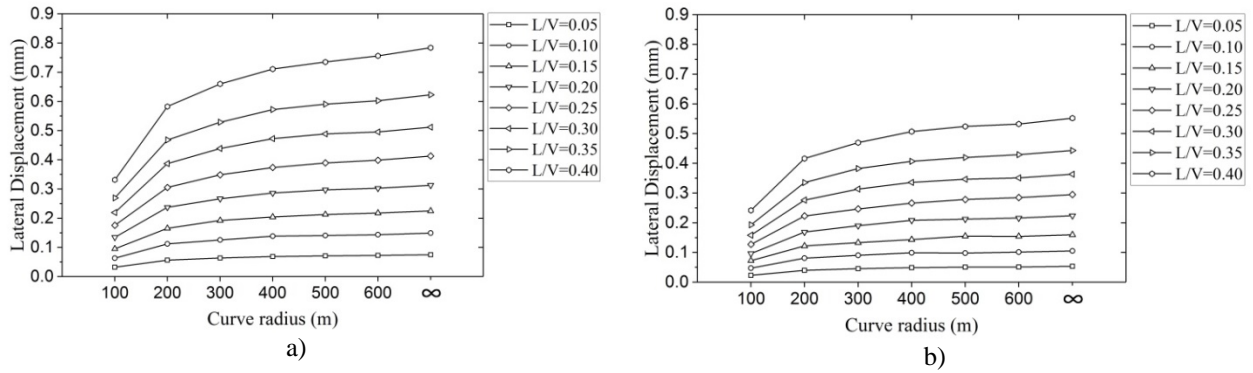


Figure 3 Dynamic lateral displacements of track at rail seat with different curve radius a) without cant (b) with 300mm cant.

### 3.2 Lateral velocity

The time histories of lateral rail velocity are presented in Figure 4. It is noted that the velocity of 10m/s and lateral loads of 20kN are taken into account in this part. Overall, it is shown that the velocity at mid-span is slightly higher than that at rail seat. It is also interesting to note that the peak of the lateral velocity at rail does not occur at the position where train load is applied. This is because there is a delay for the happening of maximum responses. The responses induced by the first sets of loads are smaller than that induced by following train load as a result of the superposition effects of moving loads.

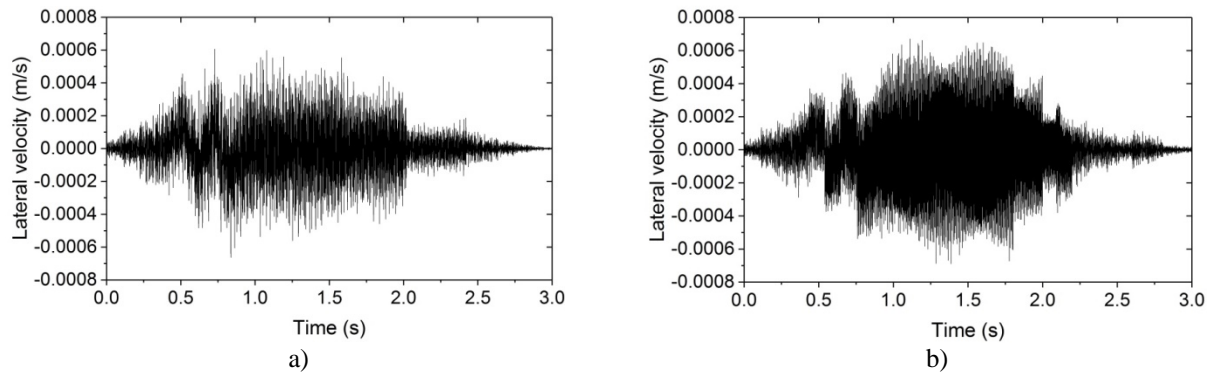


Figure 4 Rail lateral velocity of track with 100m radius under L/V=0.2 at a) rail seat b) mid-span.

The dynamic excitations are comprehensively displayed in terms of the lateral mobilities of the track. The lateral mobility spectrums obtained by a fast Fourier transform are shown in Figure 5 as a comparison of three types of track by virtue of logarithmic distribution in dB re.10<sup>-9</sup> m/s. Overall, it is clearly seen that the curve track with smaller radius has the higher lateral mobilities, in both positions as expected especially between 1000Hz and 5000Hz which is the range of squeal noise. Interestingly, the increasing of curve radius in both cases moves pinned-pinned resonance to higher frequencies and the depth of resonances are effectively reduced. For

example, the sharp peaks at 730Hz, which corresponding to pin-pin resonant frequencies, significantly drop by 20dB with the transition of track radius from 200m to 500m.

This is due to the fact that curve radius considerably affects track dynamics. However, in the low frequency range, the lateral mobilites are generally unaffected by the curve radius. As for the frequency range of 1000-5000Hz, the responses from the various cases incur apparently differences due to the influence of wheel/rail interaction during train passage on curve. By comparison with curve track, tangent track globally exhibits much lower noise levels in high frequency, which implies curve squeal is not likely to occur on tangent track.

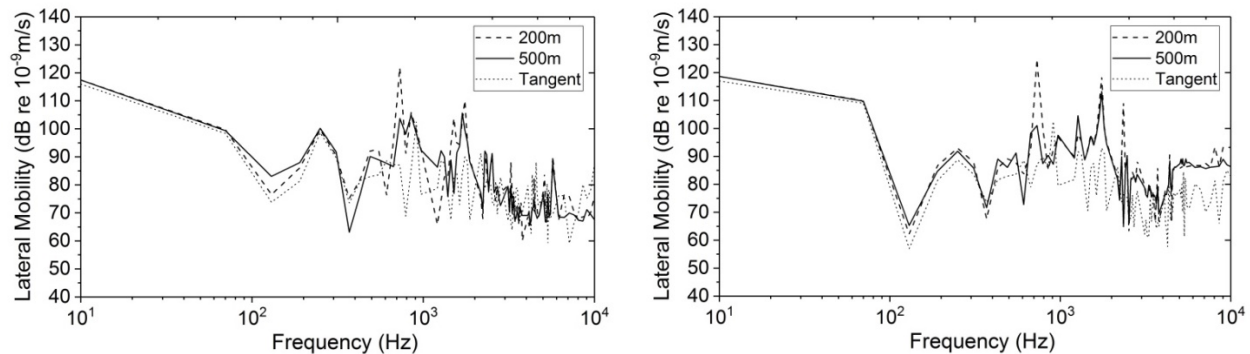


Figure 5 Spectra of the rail lateral mobility at (a) rail seat and (b) mid-span.

## 4 CONCLUSIONS

In this study, numerical simulation has been conducted to identify the lateral dynamic characteristics of both tangent and curved tracks with the consideration of track radii, cants and lateral loads. Track models have been established in three-dimensional space using a finite element package STRAND7. The results obtained are clearly shown that the increase of curve radius and cants have a positive effect on reducing lateral dynamic responses. The lateral displacement responses are more sensitive corresponding to low curve radii as clearly seen in the results between 100m and 200m radii. It has been noted from the literature that the frequency ranges of between 1000 and 5000Hz are corresponding to the squeal noise. In this region, it is observed that the vibration velocity of 200m radius curved track is lower than that of 500m radius and tangent tracks. Hence, increasing of track radius tends to vastly control the squeal noise at higher frequencies. This study put insight into the dominant influences of different track parameters to track lateral dynamic behaviors. Further studies and more experimental results are needed to investigate associated with these influencing parameters.

## ACKNOWLEDGEMENTS

The authors are sincerely grateful to the European Commission for the financial sponsorship of the H2020-RISE Project No. 691135 “RISEN: Rail Infrastructure Systems Engineering Network”, which enables a global research network that tackles the grand challenge of railway infrastructure resilience and advanced sensing in extreme environments ([www.risen2rail.eu](http://www.risen2rail.eu)) [29].

## REFERENCES

- [1] Connolly, D.P., Marecki, G.P., Kouroussis, G., Thalassinakis, I. and Woodward, P.K., 2016. The growth of railway ground vibration problems — a review. *Sci. Total Environ.* (2016) 568: 1276–1282.
- [2] Kouroussis, G., Van Parys, L., Conti, C. and Verlinden, O. Prediction of ground vibrations induced by urban railway traffic: an analysis of the coupling assumptions between vehicle, track, soil, and buildings. *Int. J. Acoust. Vib.* (2013) 18(4): 163–172.
- [3] Ngamkhanong, C., Kaewunruen, S. and Costa, B.J.A. State-of-the-Art Review of Railway Track Resilience Monitoring. *Infrastructures.* (2018) 3.
- [4] Thompson, D. Chapter 9 – Curve Squeal Noise. in: *Railw. Noise Vib.* (2009) :315–342. doi:10.1016/B978-0-08-045147-3.00009-8.
- [5] Wickens, A. *Fundamentals of Rail Vehicle Dynamics: Guidance and Stability.* (2003).
- [6] Liu, X., Ngamkhanong, C. and Kaewunruen, S. Nonlinear Dynamic of Curved Railway Tracks in Three-Dimensional Space. *IOP Conference Series: Materials Science and Engineering.* (2017) 280(1).
- [7] Ngamkhanong, C. and Kaewunruen, S. The effect of ground borne vibrations from high speed train on overhead line equipment (OHLE) structure considering soil-structure interaction. *Science of the Total Environment.* (2018) 627: 934-941.
- [8] Eadiea, D.T., Santoroa, M. and Kalousek, J. Railway noise and the effect of top of rail liquid friction modifiers: changes in sound and vibration spectral distributions in curves. *Wear.* (2005) 258: 1148–1155.
- [9] Liu, X. and Meehan, P.A. Investigation of the effect of relative humidity on lateral force in rolling contact and curve squeal. *Wear.* (2014) 310(1-2): 12-19. doi.org/10.1016/j.wear.2013.11.045.
- [10] Remington, P.J. Wheel/rail squeal and impact noise: What do we know? What don't we know? Where do we go from here? *J. Sound Vib.* (1987) 116: 339-353.
- [11] Fingberg, U. A model for wheel-rail squealing noise. *J. Sound Vib.* (1990) 143: 365-377.
- [12] Thompson, D.J. and Jones, C.J.C. A review of the modelling of wheel–rail noise generation. *J. Sound Vib.* (2000) 231: 519-536.
- [13] De Beer, F.G., Janssens, M.H.A. and Kooijman, P.P. Squeal noise of rail-bound vehicles influenced by lateral contact position. *J. Sound Vib.* (2003) 267: 497-507.
- [14] Koch, J.R., Vincent, N., Chollet, H. and Chiello, O. Curve squeal of urban rolling stock- Part 2: Parametric study on a 1/4 scale test rig. *J. Sound Vib.* (2006) 293: 701–709. doi:10.1016/j.jsv.2005.12.009.
- [15] Pieringer, A. A numerical investigation of curve squeal in the case of constant wheel/rail friction. *J. Sound Vib.* (2014) 333: 4295–4313. doi:10.1016/j.jsv.2014.04.024.
- [16] Vincent, N., Koch, J., Chollet, H. and Guerder, J. Curve squeal of urban rolling stock - Part 1: State of the art and field measurements. *J. Sound Vib.* (2006) 293: 691- 700.
- [17] Rudd, M.J. Wheel/rail noise – Part II: Wheel squeal. *Journal of Sound and Vibration.* (1976) 46: 381–394.
- [18] Nelson, J.T. *Wheel/rail noise control manual.* TCRP Report 23, 1997.
- [19] Kruger, F. *Schall- und Erschütterungsschutz im Schienenverkehr.* Expert Verlag, Renningen, (2001).
- [20] Muller, B., Jansen, E. and De Beer, F.G. Curve squeal WP3 tool box of existing measures. Union Internationale des Chemins de Fer, report prepared by SBB and TNO, (2003).
- [21] Grassie, S.L. Dynamic Modelling of Concrete Railway Sleepers. *J. Sound Vib.* (1995) 187:

- 799–813. doi:10.1006/jsvi.1995.0564.
- [22] Kaewunruen, S. and Remennikov, A.M. Experimental simulation of the railway ballast by resilient materials and its verification by modal testing. *Exp. Tech.* (2008) 32: 29–35. doi:10.1111/j.1747-1567.2007.00298.x.
- [23] Standards Australia. AS1085.1 Rail. Australia: Sydney, (2001).
- [24] Kaewunruen, S. and Remennikov, A.M. Effect of a large asymmetrical wheel burden on flexural response and failure of railway concrete sleepers in track systems. *Engineering Failure Analysis.* (2008) 15(8): 1065-1075.
- [25] Ngamkhanong, C., Kaewunruen, S. and Baniotopoulos, C. A review on modelling and monitoring of railway ballast, *Structural Monitoring and Maintenance.* (2017) 4(3):195-220. doi: 10.12989/smm.2017.4.3.195.
- [26] Kaewunruen, S., Lewandrowski, T. and Chamniprasart, K. Nonlinear modelling and analysis of moving train loads on interspersed railway tracks. 6th ECCOMAS Thematic Conference on Computational Methods in Structural Dynamics and Earthquake Engineering, Rhodes Island, Greece, 15–17 June 2017.
- [27] Kaewunruen, S., Lewandrowski, T. and Chamniprasart, K. Dynamic responses of interspersed railway tracks to moving train loads. *International Journal of Structural Stability and Dynamics*, (2018) 18(1),1850011. doi: 10.1142/S0219455418500116
- [28] Kaewunruen S, Freimanis A and Goto, K. Impact responses of railway concrete sleepers with surface abrasions. 25th International Congress on Sound and Vibration, 8-12 July 2018, Hiroshima, Japan.
- [29] Kaewunruen, S., Sussman, J.M. and Matsumoto, A. Grand challenges in transportation and transit systems. *Frontiers in Built Environment.* (2016) 2(4). doi:10.3389/fbuil.2016.00004.

## The Time Stepping Analysis by XFEM with a New Enrichment Scheme

Xuecong Liu<sup>\*</sup>, Qing Zhang<sup>\*\*</sup>, Xiaozhou Xia<sup>\*\*\*</sup>

<sup>\*</sup>Hohai University, <sup>\*\*</sup>Hohai University, <sup>\*\*\*</sup>Hohai University

### ABSTRACT

Due to there is no need to re-mesh to adapt to the crack geometry in the simulation of failure, the extended finite element method (XFEM) has been widely used. In this talk, we want to present a new enrichment scheme of crack which is based on the framework of XFEM, and the stability of explicit time integration algorithm for dynamic problem is concerned. Based on the classical crack tip enrichment function, many new forms has been developed, such as using singular basis form [1] and Improved XFEM [2]. The new proposal enrichment scheme here is in the matrix form, the characteristics of the classical enriched functions are preserved completely by combining the classical function basis, and only two additional degrees of freedom related to tip are added at each node of the crack tip element. The governing equations are derived and evolved into the discretized form. The lumped mass and the explicit time algorithm are applied for dynamic problem. With different grid densities and different forms of Newmark scheme, the Dynamic Stress Intensity Factor (DSIF) is computed to reflect the dynamic response. DSIF is also as a parameter of judging the stability of numerical method. The applicability and availability of the proposed scheme has been sufficiently verified through the numerical examples, and the critical time stepping in different situations are listed and analyzed to illustrate the factors that affect the numerical stability. It is concluded that the grid density and the form of iterative method have obvious effects on stability. The critical time stepping varies with the grid density and the parameters of iterative method. In addition, a similar conclusions can be obtained by the standard FEM with the lumped mass, and the ratios of the two methods' critical time are relatively stable. Furthermore, the simulation results are found in good agreement with each other when they are stable and the computational efficiency will be involved during the presentation. Keywords: XFEM, DSIF, dynamic loading, time stepping References: [1] T.Menouillard, J.H. Song, Q. Duan, T. Belytschko: Time dependent crack tip enrichment for dynamic crack propagation. *Int. J. Fract.*, 2010, 62 (1-2): 33-69. [2] R. Tian, L. Wen: Improved XFEM: An extra-dof free, well-conditioning, and interpolating XFEM. *Comput. Methods Appl. Mech. Engrg.*, 2015, 285 (3): 639-658.

## Numerical Investigation on the High-velocity Impact of Micron Particles in the Cold Spray

Yan Liu<sup>\*</sup>, Chenyang Xu<sup>\*\*</sup>, Xiong Zhang<sup>\*\*\*</sup>

<sup>\*</sup>Tsinghua University, <sup>\*\*</sup>Tsinghua University, <sup>\*\*\*</sup>Tsinghua University

### ABSTRACT

The cold spray (CS) technique has been considered as a competitive additive manufacturing technique owing to its outstanding properties[1]. The key process of the CS technique is that the micron particles are accelerated to a high speed, and then the particles impact on and are bonded to the substrate. The working temperature is much lower than the melting point, so that the deposit layer has a low level of porosity, nice bonding strength and only compressive residual stress. The bonding mechanism of the CS technique, however, is still under investigation due to the strong nonlinearities aroused by the high-velocity impact. The traditional finite element method (FEM) may encounter mesh distortion and difficulties in modeling material failure when it is used to simulate the high-velocity impact process. In this presentation, the material point method (MPM) is successfully applied to investigate the high-velocity impact of micron particles in the cold spray process. The MPM[2], as one kind of meshfree particle methods, have many advantages over the traditional FEM when investigating the high-velocity impact process. No mesh distortion exists, and the fracture and fragmentation can be naturally simulated in the MPM framework. The high-velocity impacts of single micron copper particle or micron particle cluster onto the copper substrate are successfully simulated with the MPM. The configurations obtained by simulation agree well with the experimental results. The deformation of the sprayed particles and the substrate, the jetting at the rim of the particle, and the stress distribution are discussed in detail. Possible bonding mechanism between the sprayed particle and the substrate is also discussed based on the simulation results. [1] Sova A, Grigoriev S, Okunkova A, Smurov I. Potential of cold gas dynamic spray as additive manufacturing technology. *Int. J. Adv. Manuf. Technol.*, 69: 2269-2278, 2013. [2] Zhang X, Chen Z, Liu Y. *The material point method: A continuum-based particle method for extreme loading cases*. London: Academic Press, 2017

## Structured Grid Based Method with Modified Boundary Basis Functions for Solid and Structure

Yanan Liu<sup>\*</sup>, Keqin Ding<sup>\*\*</sup>, Zhirong Yang<sup>\*\*\*</sup>

<sup>\*</sup>China Special Equipment Inspection and Research Institute, <sup>\*\*</sup>China Special Equipment Inspection and Research Institute, <sup>\*\*\*</sup>China Special Equipment Inspection and Research Institute

### ABSTRACT

Structured Grid Based method with Modified Boundary Basis Functions for Solid and Structure Yanan Liu, Keqin Ding and Zhirong Yang China Special Equipment Inspection and Research Institute In this paper, the basis functions based on a structured grid are used for global approximation in solution domain. A boundary region is considered and the B-Spline basis functions are used to approximate the boundary curves (surfaces in 3D) and describe this boundary region. In this boundary region, boundary basis functions are constructed based on the same B-Spline basis functions used for representing the boundary region and corresponding weight functions are created for modification of the global basis functions and the boundary basis functions. The modified basis functions maintain high order continuity and can at least reconstruct linear polynomial. Based on the modified basis functions, the solution is created to satisfy the essential boundary conditions automatically. Meanwhile, the high accuracy of the solution near the essential boundaries can be guaranteed. Furthermore, the solutions also can be constructed to perform local refinement in the local region in which complex deformation exists. The present method has been used to solve some 2D and 3D elasticity problems. The numerical results are compared with analytical results and finite element analysis solutions to show that the new method is accurate, stable and effective. Keywords: Structured grid; Boundary region; Boundary basis functions; Local refinement

## Numerical Study on Seismic Behavior of a Resilient Steel Bridge Pier

Yang Liu<sup>\*</sup>, Ying-ting Lv<sup>\*\*</sup>, Zi-xiong Guo<sup>\*\*\*</sup>, Qun-xian Huang<sup>\*\*\*\*</sup>

<sup>\*</sup>College of Civil Engineering, Huaqiao University, <sup>\*\*</sup>College of Civil Engineering, Huaqiao University, <sup>\*\*\*</sup>College of Civil Engineering, Huaqiao University, <sup>\*\*\*\*</sup>College of Civil Engineering, Huaqiao University

### ABSTRACT

An resilient steel bridge pier with replaceable steel slit dampers has been developed to meet the needs of rapid restoration of performance and functionality of bridge structures after earthquakes. This design concept is based on concentrating the damage in specially detailed components, which can be controlled and easily replaced once the damage occurs during the earthquake. Refined finite element model of the resilient steel bridge pier was established with ABAQUS and verified using existing experimental data. Numerical simulation on the seismic performance of the resilient steel bridge pier under constant axial load and cyclic horizontal load was then carried out. The main studied parameters are the axial compression ratio( $n$ ), effective slenderness ratio(?) and shear strength of the steel slit damper. It is indicated that with reasonable design principle, which is "strong column – weak damper", satisfactory seismic behavior, including high strength and stiffness, ample ductility, stable hysteretic behaviors, can be achieved for the resilient steel bridge pier. The plastic damage is concentrated on the steel slit dampers under large displacement reversals, while the main structure components remain nearly elastic.

## Fast BEM for Modeling Cracks in 3D Using the Dual BIE Formulation

Yijun Liu\*, Yuxiang Li\*\*, Shuo Huang\*\*\*

\*University of Cincinnati, \*\*University of Cincinnati, \*\*\*University of Cincinnati

### ABSTRACT

In this talk, we present some results in modeling crack problems in 3-D using the fast boundary element method (FastBEM). The BEM is based on the dual boundary integral equation (BIE) formulation, using a linear combination of the displacement and traction BIE. Fast multipole method is applied to solve the BEM equations and constant boundary elements are used in the discretization. The use of the constant elements is more efficient for solving large-scale BEM models of crack propagation problems. Numerical examples are presented to show the efficiency and accuracy of the developed approach. It is found that with enough numbers of boundary elements, the constant elements can be applied effectively to solve crack problems in 3-D solids, and it is more efficient compared with the FEM (ANSYS) in both the meshing and solution times. References: [1] Y. J. Liu, "On the displacement discontinuity method and the boundary element method for solving 3-D crack problems," *Engineering Fracture Mechanics*, 164, 35-45 (2016). [2] Y. J. Liu, Y. X. Li, and W. Xie, "Modeling of multiple crack propagation in 2-D elastic solids by the fast multipole boundary element method," *Engineering Fracture Mechanics*, 172, 1-16 (2017).

## Locomotion Mechanism and Energy Efficiency of Soft Robots

Yilun Liu<sup>\*</sup>, Yingbo Yan<sup>\*\*</sup>, Langquan Shui<sup>\*\*\*</sup>

<sup>\*</sup>State Key Laboratory for Strength and Vibration of Mechanical Structures, School of Aerospace, Xi'an Jiaotong University, Xi'an 710049, China, <sup>\*\*</sup>State Key Laboratory for Strength and Vibration of Mechanical Structures, School of Aerospace, Xi'an Jiaotong University, Xi'an 710049, China, <sup>\*\*\*</sup>State Key Laboratory for Strength and Vibration of Mechanical Structures, School of Aerospace, Xi'an Jiaotong University, Xi'an 710049, China

### ABSTRACT

In nature, a variety of limbless locomotion patterns flourish, from the small or basic life forms (Escherichia coli, amoebae, etc.) to the large or intelligent creatures (e.g., slugs, starfishes, earthworms, octopuses, jellyfishes, and snakes). Many bioinspired locomotion of soft robots have been developed in the past few decades. The locomotion/velocity efficiency and energy efficiency are two important characteristics to evaluate the performance of soft robot system. In this work, we first propose a broad set of innovative designs for soft mobile robots, based on the kinematics and dynamics of two representative locomotion modes (i.e., worm-like crawling and snake-like slithering). Inspired by and going beyond the existing biological systems, these designs include 1-D (dimensional), 2-D, and 3-D robotic locomotion patterns enabled by the simple actuation of continuous beams to achieve various locomotion functions, including crawling, rising, running, creeping, squirming, slithering, swimming, jumping, turning, turning over, helix rolling, wheeling, etc. The locomotion efficiency, functionality and adaptability for different locomotion modes are further analyzed. Then, a general framework is established to evaluate the energy efficiency of mobile soft robots by considering the efficiency of the energy source, actuator and locomotion, and some insights for improving the efficiency of soft robotic systems are presented. Four key factors related to the locomotion energy efficiency are identified, that is, the locomotion modes, material properties, geometric sizes, and actuation states. The results presented herein indicate a large space for improving the locomotion and energy efficiency of soft robots, which is of practical significance for the future development and application of soft robots.

## A Phase Field Formulation for Cohesive Fracture with Application to Shock Wave Lithotripsy

Yingjie Liu<sup>\*</sup>, Rudy Geelen<sup>\*\*</sup>, John Dolbow<sup>\*\*\*</sup>, Pei Zhong<sup>\*\*\*\*</sup>

<sup>\*</sup>Duke University, <sup>\*\*</sup>Duke University, <sup>\*\*\*</sup>Duke University, <sup>\*\*\*\*</sup>Duke University

### ABSTRACT

This study concerns a novel phase field formulation for modeling cohesive-type fracture. Phase field formulations have become increasingly popular for simulating fracture due to their inherent strengths in representing complex fracture patterns, e.g., branching, kinking, merging, and etc. [1]. However, the applicability of many phase field formulations is limited by their basis on a Griffith model of fracture. An advanced phase field formulation is developed in this work that is distinguished by the fact that it converges to a cohesive model of fracture as the regularization length vanishes. In this work, we demonstrate how such an approach builds a foundation for the simulation of fracture in advanced materials with complex microstructure, bulk constitutive laws, and non-conventional fracture behavior. In the present study, in particular, it is applied to simulations of shock wave lithotripsy (SWL). SWL has proven to be a highly effective treatment for the removal of kidney stones [2]. The shock waves break up kidney stones through a dynamic fatigue process involving the contribution of various stress waves propagating inside the stones and cavitation produced in the surrounding liquid medium. In this work, we present a fully coupled acoustic-structural-fracture model for the simulation of SWL. Numerical experiments show ring-shaped cracks on the top surfaces of idealized stones, as well as radial cracks on the bottom surfaces. The details of the fracture patterns are shown to be sensitive to both the position and strength of the acoustic source driving the process. These findings are validated against experimental observations. Keywords: Phase Field; Cohesive Fracture; Anisotropic Solids; Shock Wave Lithotripsy References: [1] Miehe, C., Hofacker, M. and Welschinger, F., 2010. A phase field model for rate-independent crack propagation: Robust algorithmic implementation based on operator splits. *Computer Methods in Applied Mechanics and Engineering* 199, 45-48. [2] Weizer, A.Z., Zhong, P., and Preminger, G.M., 2007. New Concepts in Shock Wave Lithotripsy. *Urologic Clinics of North America* 34, 375-382.

## Multiscale Microstructural Database for Concurrent Modeling of Nonlinear Softening Material with Damage and Failure

Zeliang Liu\*, Wing Kam Liu\*\*

\*Livermore Software Technology Corp., \*\*Northwestern University

### ABSTRACT

Accurate and efficient computational methods for predicting fracture and damage of engineering materials are essential to design and failure analysis of materials with non-uniform or heterogeneous microstructural properties. Successful material models need to capture the non-trivial inter-dependence between material constituents at small scales that lead to dramatic performance effects in the macroscale response. Mechanistic understanding of this structure-property relation will also enable a collection of material microstructural database, which will accelerate material design and manufacturing. Traditional fracture mechanics and continuum damage mechanics are phenomenological macroscopic methods which are not sensitive to the material microstructures and require extensive testing and model calibration for new materials. In this work, we aim to solve the damage problem using a multiscale data-driven modeling framework, so that the macroscale material law is directly extracted from the homogenization of the microscale model. A new three-step homogenization scheme is presented, where the strain localization is distributed in the representative volume element (RVE) and the microscale equilibrium condition becomes well-posed even with the strain softening effect. The homogenization will continuously provide the effective behavior in the localization region, which is independent of the RVE size. The only material length parameter in the concurrent simulation is in the macroscale, and it can be measured or calibrated from numerical or physical experiment. The microscale RVE homogenization can capture the complex damage mechanism due to material heterogeneities, and explicitly provide a microstructure-sensitive material damage model for the macroscale without predefining the form. To increase the efficiency of the multiscale concurrent calculations, the self-consistent clustering analysis (SCA) with a new generalized formulation is proposed. By grouping material points with similar mechanical behavior into clusters, the number of degrees of freedom can be greatly reduced. With the microstructural database built in the offline stage, a reduced Lippmann-Schwinger equation is formulated and solved using a self-consistent scheme in the online stage. By comparing with direct numerical simulations (DNS) for plastic materials, the proposed method is shown to be accurate, with good convergence under refinement and computationally efficient. In the concurrent simulation, the predicted macroscale fracture patterns are observed to be sensitive to the combinations of microscale constituents, showing the capability of the SCA microstructural database.

## Recent Development in Computational Mechanics of Soft Materials and Machines – an Overview

Zishun Liu\*

\*International Center for Applied Mechanics; State Key Laboratory for Strength and Vibration of Mechanical Structures, Xi'an Jiaotong University, China

### ABSTRACT

Abstract: The elegance of nature's designs has inspired scientists to create soft machines. With development of soft machines, the mechanics of soft materials which are used by soft machines becomes an emerging field of applied mechanics. Therefore, the mechanical behaviors of soft materials are new and very current research topics, i.e. the large deformation studies of hydrogels, liquid crystal elastomers, dielectric elastomers and shape memory polymers (SMPs). In last decades, computational methods have become main approaches for studying mechanics of soft materials. Thus different numerical simulation methods are proposed to predict deformation behavior of soft materials, for example, FEM method, meshless method, molecular dynamics simulation etc. It is very imperative to review and discuss the advances of different computational methods. In this presentation, we will review some of the recent works aligned with the direction of providing a better understanding of computational soft materials (gels, SMPs etc.). Then the transient deformation process of polymeric gels and numerical implementation for large deformation kinetics of polymeric gels are studied using the finite element method (FEM). The neutral and environmentally sensitive (such as temperature, pH-value, magnetics and light) hydrogels are investigated. For the SMPs study, we developed different constitutive models which can be used for different SMP materials and can be used for large strain large deformation analyses. To validate the model, simulated and predicted results are compared with experimental results. Finally, as many issues related to the mechanics of hydrogel and SMPs deformation behaviors remain open, we will list some outlines for plausible future directions in the research of computational mechanics of soft materials/machines. Furthermore, we will overview the recent development of computational mechanics in the study of soft materials and machines over the worldwide, especially; the advances of computational mechanics for soft materials in different research groups will be discussed and reviewed.

## **A Nonlocal Damage-Plasticity Model Based on a Smooth Elastic-Plastic Transition**

Michal Livnoni\*, Mahmood Jabareen\*\*

\*Technion – Israel Institute of Technology, \*\*Technion – Israel Institute of Technology

### **ABSTRACT**

Standard rate-independent elastic-plastic formulations use a yield function to separate elastic response and plastic response. Specifically, the consistency condition, which requires the yield function to vanish during loading, causes a sharp transition between elastic and plastic response with a break in the slope of the stress-strain curve. To eliminate this undesired response, a large deformation model, characterized by a smooth elastic-inelastic transition has been proposed (Hollenstein et al. 2013, Jabareen 2016). Also, their model unifies rate independent as well as rate dependent responses. Further, it is well-known that classical continuum damage models may not be able to capture the real mechanical behavior of materials due to localization associated with strain softening. In addition, if no adjustments are made, the region of localization will depend on the mesh size of the spatial discretization. The necessity to model damage, which is controlled by the microstructure, has driven the development of the nonlocal and gradient damage formulations. Nonlocal plasticity models incorporate a nonlocal variable defined as the spatial weighted average of a corresponding local field over the entire body. Often, the nonlocal quantity formulation includes an intrinsic length parameter that affects the weight amplitude in the vicinity of a material point. In the present study, an extension of a smooth inelasticity model to include softening and localization based on a strongly non local gradient-enhanced formulation is presented. A strongly objective integration scheme is developed based on the introduction of the relative deformation gradient – the deformation mapping between the last converged and current configuration. Also, a finite element formulation has been developed, which incorporates three variational fields for the equilibrium equations and an additional field for the Helmholtz type equation for the gradient-enhanced formulation. The numerical implementation of the proposed model will be presented, and the capabilities of the developed finite element will be demonstrated by few examples.

## Rate-Dependent Phase-Field Fracture Model for Rubbers and its Experimental Validation

Pascal Loew<sup>\*</sup>, Bernhard Peters<sup>\*\*</sup>, Lars A. A. Beex<sup>\*\*\*</sup>

<sup>\*</sup>University of Luxembourg, SISTO Armaturen S.A., <sup>\*\*</sup>University of Luxembourg, <sup>\*\*\*</sup>University of Luxembourg

### ABSTRACT

The failure of rubber-like materials depends amongst others on the strain-rate. In this presentation we discuss an isothermal phase-field fracture model for rate-dependent failure of rubber components. Miehe et al.[2] were the first to formulate a rate-independent phase-field damage model for rubbery polymers. Stumpf et al.[3] laid out the framework for thermodynamic consistent linear thermo-viscoelastic damage models. Extending these ideas, we formulate our new model. Introducing a crack phase field overcomes difficulties associating with the computational study of sharp discontinuities. This is particularly convenient when cracks branch and coalesce. The size of the crack phase field is determined by the length scale parameter  $l_0$ . As a material parameter, depending on the microstructure, the length scale  $l_0$  has a high influence on the local solution near the crack tip [1]. We demonstrate the performance of our model by conducting a series of tension tests for various geometries and clamp velocities. First, we compare the measured and numerical calculated global force-displacement curve and see a good agreement. Further, we measure the local strains near the crack tip by application of the Digital Image Correlation technology. Again, we can observe a good matching between experimental data and the numerical solution indicating a correct calibration of the length scale  $l_0$ . Finally, we are showing a numerical example of several cracks coalescing to one. The resulting crack path agrees well with the experimentally determined. References [1] Geers, M. G. D., Borst, R., Brekelmans, W. A.M. and Peerlings, R. H. J. Validation and internal length scale determination for a gradient damage model: application to short glass-fibre-reinforced polypropylene International Journal of Solids and Structures (1999) 36, pp. 2557-2583. [2] Miehe, C. and Schaezel, L.-M Phase field modeling of fracture in rubbery polymers. Part I: Finite elasticity coupled with brittle failure Journal of the Mechanics and Physics of Solids (2014) 65, pp. 93-113. [3] Stumpf, H. and Hackl, K. Micromechanical concept for the analysis of damage evolution in thermo-viscoelastic and quasi-brittle materials. International Journal of Solids and Structures (2003) 40, pp. 1567-1584.

## **Textile Geometry Processors for Virtual Textiles and Textile Composites**

Stepan Lomov\*

\*KU Leuven

### **ABSTRACT**

Textiles, including textile reinforcements for composites, are fibrous materials, hence they are multi-scale and hierarchical. Modelling of textile fibrous structures is a necessary element of a simulation chain which streams the material description from fibre data and description of a textile manufacturing parameters via the fibrous assembly geometry model to the manufacturing and then performance of a final material or product, be it a textile reinforced composite, a textile element of an architectural structure or a nano-fibre based knited antenna. The paper presents a general philosophy of a virtual textile. It has as its key a Textile Geometry Processor, which accepts textile data (such as weave structure, yarns spacing, yarn dimensions etc.), parameters of the fibrous assembly (such as fibre volume fraction, layered geometry) and local (in relation to a scale of model) overall deformation of the textile (shear, compression etc.), and creates a geometrical model of the textile ready for use in the manufacturing and performance simulations of mechanical and physical phenomena (deformation response, damage initiation and development, flow through the material, electromagnetic properties, thermal conductivity etc). The paper describes general principles and a concrete realisation of a textile geometry processor, implemented in WiseTex and VoxTex software of the author. Two types of the textile data inputs are considered: models of the fibres geometry based on the interlacing topology description and micro-computed tomography data. The geometrical model of a unit cell (representative volume) of the textile is transformed into a "general purpose" meso-level finite element (FE) model of the unit cell, allowing further in-depth simulation of the textile or a textile composite properties and behaviour. The modelled textile structures can be seen as stochastic realisations with certain characteristics of their variability. The concept of the textile geometry processor allows implementation of the stochasticity and its advancement to Monte-Carlo variability modelling. The open data structure of the input allows multi-parametrical optimisation of the fibrous assembly.

## Using the Material Point Method to Model Fracture and Multi-body Interactions Within a Single Velocity Field

Christopher Long<sup>\*</sup>, Duan Zhang<sup>\*\*</sup>, Yuri Bazilevs<sup>\*\*\*</sup>, Georgios Moutsanidis<sup>\*\*\*\*</sup>

<sup>\*</sup>Los Alamos National Laboratory, <sup>\*\*</sup>Los Alamos National Laboratory, <sup>\*\*\*</sup>University of California San Diego,  
<sup>\*\*\*\*</sup>University of California San Diego

### ABSTRACT

A chief drawback of using the Material Point Method (MPM) for brittle failure is that a material cannot separate unless a crack has grown to at least one grid cell in thickness. This problem is exacerbated by the use of the Dual Domain Material Point Method (DDMP), which extends the numerical stencil of the particle-grid interactions. Thus, the resolution issues are inherent for brittle failure, as crack width is typically very small, creating artificially thick failure zones. We propose and will discuss a numerical methodology to construct a damage field on the particles which can be used to detect cracks that are sub-gridscale in thickness, and can then be used to separate materials which are otherwise still connected through the Eulerian mesh. This has been previously achieved by detecting a crack and partitioning the particles into multiple interacting velocity fields. [1] We achieve the same effect using a single velocity field through selective force and momentum transfers from particle to grid and vice-versa when a crack is present. The same methodology can be applied to model multi-body interactions and self-contact, by marking the surface particles of an object as a “crack”. Smooth Particle Hydrodynamics (SPH) and Reproducing Kernel Particle Method (RKPM) are introduced to MPM and are used to integrate the crack/damage field in lieu of traditional transfer methodologies. This allows us to model the gradient of the damage field more accurately, which allows us to compute the normal direction to the crack. We will present several numerical demonstrations of this capability, and compare to benchmarks in fracture mechanics. Additionally, we will compare to experimental results of quasi-statically loaded glass spheres (not a Brazil test). These experiments provide several benchmarks for comparison, including the average load at failure, average fractured particle size, and deflection to failure. The implementation of the single-velocity field fracture model will enable us to predict the correct average number of large fragments and ratio of large to small fragments using a much coarser resolution than has previously been required. [1] Homel, M. A., and Herbold, E. B. (2017) Field-gradient partitioning for fracture and frictional contact in the material point method. *Int. J. Numer. Meth. Engng*, 109: 1013–1044. doi: 10.1002/nme.5317.

## **DEM Modelling of Ice Load on Conical Structures under Influence of Cone Angle**

Xue Long<sup>\*</sup>, Shunying Ji<sup>\*\*</sup>

<sup>\*</sup>Dalian University of Technology, <sup>\*\*</sup>Dalian University of Technology

### **ABSTRACT**

The conical structures are applied to effectively reduce the ice load and avoid serious damage to the structures caused by the sea ice. The reasonable parameters for the design of the anti-ice cone are important to show the anti-ice performance of cones. According to the failure characteristics of sea ice, the discrete element method (DEM) with a parallel-bond model is adopted to simulate the interaction between sea ice and conical structure. The accuracy of the DEM model is verified by comparing the calculated ice load and the failure process of sea ice with the test data of the Hamburg Ship Model Basin (HSVA). The simulation results show that the cone ice load increases with the increase of the cone angle, while the average broken length of sea ice decreases with the cone angle. It is found that the failure modes of sea ice are transformed from bending failure to crushing failure as the cone angle increases. Therefore, the anti-ice cone with 60° to 70° cone angle has a better performance to prevent the damage caused by the interaction with ice. The DEM simulations can provide a meaningful basis for the design of anti-ice structures.

## A Plastic-damage Model of Concrete Subjected to Reversed Loading

Yuchuan Long<sup>\*</sup>, Yuming He<sup>\*\*</sup>, Chentao Yu<sup>\*\*\*</sup>

<sup>\*</sup>Chongqing University, China, <sup>\*\*</sup>Sichuan College of Architectural Technology, China, <sup>\*\*\*</sup>Chongqing University, China

### ABSTRACT

A plastic-damage model was developed by using essential concepts of continuum damage mechanics and plastic flow theory, within the framework proposed by Lee and Fenves[1]. First, the mathematic expression of the model was given in this paper. It employed a non-associated plastic flow rule to model the evolution of irrecoverable deformation. The concept of energy-loss mechanism was utilized to develop the evolutionary rule of damage by defining the damage factor in terms of the fracture energy and accumulated dissipating energy. Then, the influence of mesh size on tensile damage factor was investigated using the crack band theory to alleviate the mesh sensitivity. The crack band theory, which modifying the stress-strain relation according to mesh size, was not sufficient to obtain objective responses under cyclic loading. To eliminate the effect of mesh size under unloading and reloading states, the equivalent relation of damage factor for different meshes was derived based on the assumption that the inelastic and plastic components of strain were concentrated in the damaged elements. According to the relation, the damage factor defined by the energy-loss mechanism was mesh-objective and equal to the equivalent damage factor corresponding to crack band width. Last, this model was implemented into ABAQUS and used to model concrete tests conducted by Kupfer[2] and Hordijk[3]. Numerical results such as stress-strain curves and load-deflection ones agreed well with those obtained from tests. The load-deflection responses obtained with different mesh were in close agreement when using the crack band theory and equivalent relation of damage factor, which indicates the equivalent relation of damage could eliminate the effect of mesh size. Moreover, the equivalent damage factors corresponding to crack band width in the cases of different mesh size were consistent to each other and therefore it could be used as a damage index to evaluate the damage degree of concrete structure. These numerical examples drew a conclusion that the plastic-damage model could model the nonlinear responses of concrete structures subjected to reversed loading. [1] Lee J, Fenves GL. Plastic-damage model for cyclic loading of concrete structures[J]. Journal of Engineering Mechanics, ASCE, 1998, 124(8): 892-900. [2] Kupfer H, Hilsdorf H K, Rusch H. Behavior of concrete under biaxial stresses[J]. Journal of ACI, 1969, 66(8): 656-666. [3] Hordijk D A. Local approach to fatigue of concrete[D]. Dissertation, Delft University of Technology, 1991.

## Large Scale Approach of Dynamic Shear Localization-induced Failure of Viscoplastic Structures

Patrice Longère<sup>\*</sup>, André Dragon<sup>\*\*</sup>, Hannah Lois-Dorothy<sup>\*\*\*</sup>

<sup>\*</sup>Institut Clément Ader, <sup>\*\*</sup>Pprime, <sup>\*\*\*</sup>Institut Clément Ader

### ABSTRACT

Lightweight materials such as titanium alloys are widely employed in aircraft and other structures. The latter, while possessing high strength, are susceptible to a dynamic instability phenomenon called adiabatic shear banding which leads to a premature structural failure. Adiabatic shear bands (ASBs) are narrow shear localized regions resulting from thermomechanical instability and occur under high strain rate loading (involving quasi adiabatic conditions) as a consequence of the competition between hardening and softening mechanisms. The linear perturbation method is applied in the context of dynamic plasticity to determine the shear localization onset. Different softening mechanisms (e.g. thermal softening vs. dynamic recrystallization) triggering the adiabatic shear banding are studied (see [1]). A constitutive model is developed within a large scale postulate wherein the shear localization band is embedded within the representative volume element (RVE) and further finite element – and not the opposite as usually done. This facilitates numerical implementation of the model on large structures without the need for mesh refinement in the critical zones. The model describes the progressive anisotropic material deterioration induced by the ASB and further micro-voiding in the band wake as well as the kinematic consequences of the deterioration mechanisms at stake (ASB, micro-voiding) until the ultimate fracture (see [2], [3]). The model is implemented as user material subroutine in the engineering finite element computation code LS-DYNA and its performances are evaluated considering some initial boundary value problems such as dynamic shearing of hat shaped structure and ASB assisted chip serration in high speed machining. References [1] Longère, P., “Respective/combined roles of thermal softening and dynamic recrystallization in adiabatic shear banding initiation,” *Mech. Mater.*, vol. 117, pp. 81–90 (2018). [2] Longère, P. and Dragon, A., “Enlarged finite strain modelling incorporating adiabatic shear banding and post-localization microvoiding as shear failure mechanisms,” *Int. J. Damage Mech.*, vol. 25-8, pp. 1142-1169 (2016). [3] Dorothy, H.L., Longère, P. and Dragon, A., “Coupled ASB-and-microvoiding-assisted dynamic ductile failure,” *Procedia Eng.*, vol. 197, pp. 60–68 (2017).

## **A Numerical Framework to Analyze Fracture in Composite Materials: From Simulated Crack Resistance Curves to Homogenized Softening Laws**

Cláudio S. Lopes<sup>\*</sup>, Miguel Herráez<sup>\*\*</sup>, Carlos González<sup>\*\*\*</sup>

<sup>\*</sup>IMDEA Materials Institute, Madrid, Spain, <sup>\*\*</sup>IMDEA Materials Institute, Madrid, Spain, <sup>\*\*\*</sup>IMDEA Materials Institute, Madrid, Spain

### **ABSTRACT**

A numerical framework to obtain the crack resistance curve (R-curve) and its corresponding softening law for fracture analysis in composite materials under small scale bridging is presented [1]. The use case addresses the intralaminar transverse tensile fracture of a unidirectional ply of carbon fiber-reinforced polymer AS4/8552. The R-curve is computed for this material using a micromechanical embedded model corresponding to the intralaminar transverse tensile fracture toughness characteristic. The model combines an embedded cell approach with the Linear Elastic Fracture Mechanics (LEFM) displacement field to analyze the local crack growth problem including fiber/matrix interface debonding and bridging of matrix ligaments as the main energy dissipation mechanisms. Due to the complexity of the problem, the methodology is illustrated to study the bidimensional propagation of a crack in a fiber reinforced unidirectional ply, including the fiber/matrix interface debonding and the ductile tearing of the matrix ligaments between fibers as energy dissipation mechanisms. This crack propagation problem is also known as the intralaminar crack propagation under transverse tension, characterized by the fracture toughness  $G_{2+}$ . The bidimensional formulation of the problem impedes the inclusion of higher length scale toughening mechanisms, as for instance, fiber bridging due to the lack of parallelism between fibers, so the material toughness and R-curve behavior obtained should be understood as lower bounds or initiation values rather than propagation over a finite crack length of some millimeters. Parametric analyses were carried out to assess the influence of the properties of the material constituents on the R-curve behavior and on the corresponding homogenized cohesive laws. Homogenized softening laws for the crack propagation problem in a unidirectional ply are presented for a wide range of micromechanical parameters including constituent properties as the fiber/matrix interface and matrix plastic/damage behavior. [1] M. Herráez, C. González, C.S. Lopes, A numerical framework to analyze fracture in composite materials: From R-curves to homogenized softening laws, *International Journal of Solids and Structures* (2017) 1–13, In Press.

## Thermal Characterization of a Concrete Sample during Hydration Process by Solution of the Inverse Problem

Ruben Lopez<sup>\*</sup>, Antonio Aquino<sup>\*\*</sup>, Sebastian Farina<sup>\*\*\*</sup>, Fernando Diaz<sup>\*\*\*\*</sup>, Carlos Sauer<sup>\*\*\*\*\*</sup>,  
Belen Martinez<sup>\*\*\*\*\*</sup>

<sup>\*</sup>National University of Asuncion. Faculty of Engineering, <sup>\*\*</sup>National University of Asuncion. Faculty of Engineering,  
<sup>\*\*\*</sup>National University of Asuncion. Faculty of Engineering, <sup>\*\*\*\*</sup>National University of Asuncion. Faculty of  
Engineering, <sup>\*\*\*\*\*</sup>National University of Asuncion. Faculty of Engineering, <sup>\*\*\*\*\*</sup>National University of Asuncion.  
Faculty of Engineering

### ABSTRACT

During the curing process of concrete, chemical exothermic reactions with temperature increase and heat release take place. Studying the development of early thermal and mechanical properties of concrete becomes of primary importance, since the heat release throughout hydration process and the associated effects, such as temperature gradients, may lead to crack generation. To simulate this thermal behavior, it is necessary to obtain the thermal parameters. In this work, computational implicit algorithms using the Conjugate Gradient (CG) method were developed and applied aiming to obtain thermal conductivity  $k$  and specific heat  $c$  of concrete samples during the hydration process, solving the inverse problem. The algorithms were based on temperatures obtained by sensors placed on samples, having in count that the heat generation is minimum since the fourth day of the hydrating process, in order to reduce the ill-posed characteristic of the inverse problem. In addition, to reduce the computational cost of a pure implicit algorithm, the Douglas-Gunn alternate direction implicit (ADI) method was chosen, maintaining at the same time the unconditional stability of the implemented algorithm. Validation of the numerical method was done comparing the parameters obtained by the numerical model with experimental results. Samples manufactured with different cement kinds, and therefore having different strength, were studied. Comparison of temperature evolution curves and thermal parameters of interest was done. Results were, in general, coherent and satisfactory. The proposed model allows the solution of the heat transfer equation avoiding the chemical kinetics modelling, which is well-known for its complexity. Despite this, all the chemical phenomena related to heat generation are indirectly represented. For the studied samples, concretes with similar strength values produced similar Temperature-time plots, except for some pozzolanic samples. These pozzolanic samples produced a delayed temperature increase profile, and therefore delayed heat generation, and their peak temperatures were also noticeably lower than those corresponding to compound cement of similar strength. It could also be observed that the bigger the strength the bigger the temperature peak and thermal constants, except for some pozzolanic samples. In general, the results were satisfactory, which leads to conclude that the thermal characterization of concrete is achieved by means of these implicit numerical methods

## Simulation of a Quadcopter Rotor in Hover at High Altitude

Omar D. Lopez Mejia<sup>\*</sup>, Luisa F. Prado Arellano<sup>\*\*</sup>, Santiago Mendoza Silva<sup>\*\*\*</sup>, Jaime A. Escobar<sup>\*\*\*\*</sup>

<sup>\*</sup>Universidad de los Andes, <sup>\*\*</sup>Universidad de los Andes, <sup>\*\*\*</sup>Universidad de los Andes, <sup>\*\*\*\*</sup>ADVECTOR

### ABSTRACT

Unmanned Aerial Vehicles (UAVs) have become an important technology for civil applications in last years. Among the different platforms available in UAVs, quadcopters are preferable due to its easier control in flight for drone operators and because of their rapid take-off capabilities. Typically, the research community has focused on the control system of these vehicles and simplifying the aerodynamic problem [1]. It is well known that the description and understanding of the wake of the rotor of a rotorcraft is a very complex fluid dynamic problem. The global efficiency of a quadcopter is highly dependant on the aerodynamic performance of the rotor and the interaction of the induced flow between the rotors and the fuselage [2]. In-flight testing of quadcopters is difficult due to space limitations and control of atmospheric conditions. Bench-testing of quadcopter rotors is commonly done, but limited in the information that can be obtained. In this context, Computational Fluid Dynamics (CFD) can play an important role in a clear understanding of the dynamics of such a complex flow. In the present work, CFD is used in order to quantify the influence of atmospheric conditions such as those found in Colombia (high altitude) in the aerodynamic performance of the rotor of the quadcopter ARAKNOS v2 developed by the Colombian company ADVECTOR. Numerical simulations are performed using the commercial software ANSYS-Fluent v17. The rotation is implemented with the Multiple Reference Frame (MRF) model and using the Spalart-Allmaras turbulence model with curvature correction. The influence of the four rotors is included by means of a double symmetry used in the implemented computational domain. Numerical results of torque and power were compared with experimental data measured in hover flight. It was also found that the temperature, atmospheric pressure and humidity have a great influence in the aerodynamic performance (Torque and power coefficients) of the rotor. A difference of approximately 20% was found between the experimental and computational results which can be attributed to the influence of the fuselage which is not included in the computational model. REFERENCES [1] Hoffmann, G. M., Huang, H., Waslander. S. L., and Tomlin C. J., &quot;Quadrotor Helicopter Flight Dynamics and Control: Theory and Experiment&quot; AIAA Guidance, Navigation and Control Conference and Exhibit: AIAA-2007-6461. American Institute of Aeronautics and Astronautics, 2007. [2] Potsdam, M., and Pulliam, T., &quot;Turbulence Modelling Treatment for Rotorcraft Wakes,&quot; San Francisco CA : Specialist&apos;s Conference on Aeromechanics, 2008.

## **Nucleation and Propagation of Fracture and Healing in Elastomers: A Phase-Transition Theory & Numerical Implementation**

Oscar Lopez-Pamies<sup>\*</sup>, Aditya Kumar<sup>\*\*</sup>, Gilles Francfort<sup>\*\*\*</sup>

<sup>\*</sup>University of Illinois at Urbana-Champaign, <sup>\*\*</sup>University of Illinois at Urbana-Champaign, <sup>\*\*\*</sup>NYU

### **ABSTRACT**

A macroscopic theory is proposed to describe, explain, and predict the nucleation and propagation of fracture and healing in elastomers undergoing arbitrarily large quasistatic deformations [1]. The theory, which can be viewed as a natural generalization of the phase-field approximation of the variational theory of brittle fracture of Francfort and Margio (1998) to account for physical attributes innate to elastomers that have been recently unveiled by experiments at high spatio-temporal resolution, rests on two central ideas. The first one is to view elastomers as solids capable to undergo finite elastic deformations and capable also to phase transition to another solid of vanishingly small stiffness: the forward phase transition serves to model the nucleation and propagation of fracture while the reverse phase transition models the possible healing. The second central idea is to take the phase transition to be driven by the competition between a combination of strain energy and hydrostatic stress concentration in the bulk and surface energy on the created/healed new surfaces in the elastomer. From an applications point of view, the proposed theory amounts to solving a system of two coupled and nonlinear PDEs for the deformation field and an order parameter, or phase field. A numerical scheme is presented to generate solutions for these PDEs in  $N = 2$  and  $3$  space dimensions. This is based on an efficient non-conforming finite-element discretization, which remains stable for arbitrarily large deformations and elastomers of any compressibility, together with an implicit gradient flow solver, which is able to deal with the large changes in the deformation field that can ensue locally in space and time from the nucleation of fracture. We conclude by presenting sample simulations of the so-called poker-chip and Gent-Park experiments and confronting those with experimental results for various types of elastomers.

## A Discontinuous Galerkin Immersed Boundary Method Using Unstructured Anisotropic Mesh Adaptation and Penalization Techniques

Marco Lorini<sup>\*</sup>, Cécile Dobrzynski<sup>\*\*</sup>, Vincent Perrier<sup>\*\*\*</sup>, Mario Ricchiuto<sup>\*\*\*\*</sup>

<sup>\*</sup>Inria Bordeaux Sud-Ouest, Team Cardamom, <sup>\*\*</sup>Inria Bordeaux Sud-Ouest, Team Cardamom, <sup>\*\*\*</sup>Inria Bordeaux Sud-Ouest, Team Cagire, <sup>\*\*\*\*</sup>Inria Bordeaux Sud-Ouest, Team Cardamom

### ABSTRACT

When dealing with meshing for Computational Fluid Dynamics (CFD) simulations, two possible methods can be employed. An attractive alternative to the well-known body-fitted approach is the use of embedded boundary methods, which are arousing interest mainly because they simplify the mesh generation process, particularly in the case of moving bodies. This kind of methods are characterized by the fact that the mesh covers the entire domain, so that a special treatment for the elements close to the body surface is needed. We propose an Immersed Boundary Method (IBM) in which the wall boundary conditions are taken into account through a penalization technique, i.e. through the addition of a penalty term to the Navier-Stokes equations. The localization of the solid bodies is done via a level set method, employing the signed distance function (SDF). With the combination of anisotropic mesh adaptation and unstructured simplicial meshes, the accuracy of the definition of the solid boundaries, not explicitly discretized, can be improved without increasing too much the computational cost of the simulation. The method was already proposed by some of the authors for a Finite Element (FE)/Finite Volume (FV) scheme [1] and Residual Distribution Schemes (RDS) [2] while it is now extended to the Discontinuous Galerkin (DG) context. DG methods are FE methods in which the solution of the variational form of the problem is approximated by piecewise polynomial functions with no global continuity requirement. Nowadays they are finding use in very diverse applications because of their robustness, accuracy and flexibility. These aspects combined with the compactness of the scheme have been advantageous for the parallel implementation of the proposed method. The presentation will first briefly cover the motivations and scope of the work. Details on the penalized Navier-Stokes equations and on the evaluation of the penalization operator will be also given before discussing the DG discretization of the equations employed in our solver as well as the mesh adaptation procedure. Results on two- and three-dimensional test cases will conclude the presentation. (1) Abgrall R., Beaugendre H. and Dobrzynski C., "An immersed boundary method using unstructured anisotropic mesh adaptation combined with level-sets and penalization techniques", *Journal of Computational Physics* 257 (2014) 83 - 101. (2) Nouveau, L., Beaugendre H., Dobrzynski C., Abgrall R. and Ricchiuto M., "An adaptive, residual based, splitting approach for the penalized Navier Stokes equations", *Comput. Methods Appl. Mech. Engrg.* 303 (2016) 208 – 230.

## Fast Isogeometric Solvers for Implicit Dynamics Simulations of Heat Transfer and Elastic Wave Propagation Problems

Marcin Los<sup>\*</sup>, Maciej Paszynski<sup>\*\*</sup>, Victor Calo<sup>\*\*\*</sup>

<sup>\*</sup>AGH University, Krakow, Poland, <sup>\*\*</sup>AGH University, Krakow, Poland, <sup>\*\*\*</sup>Curtin University, Perth, Western Australia

### ABSTRACT

The alternating directions method (ADS) was first introduced in 1960 [1] to deal with finite difference simulations for time-dependent problems. Nowadays, the method has been rediscovered as a tool to deal with simulations of difficult computational problems, such as time-dependent Maxwell equations, or incompressible flows [2]. The method introduces intermediate time steps to separate the differential operator and obtain a multi-diagonal structure of the matrices enabling for linear computational cost factorization. The alternating direction method has been recently rediscovered by [3] for fast solution of the isogeometric L2 projection problem in the context of isogeometric finite element method. In there, we do not have a time steps, but rather the projection problem discretized with tensor products B-spline basis functions. It has also been used for explicit dynamics isogeometric simulations [4]. In this talk, we show how to successfully apply the alternating direction method for isogeometric finite element method simulations of implicit dynamics. Namely, we focus on a parabolic problem and discretize it with B-spline basis functions in the spatial dimension, and we use implicit scheme for time discretization. We introduce intermediate time steps and separate our differential operator into a summation of the blocks, acting along particular axes in the intermediate time steps. We show that resulting stiffness matrix can be represented as multiplication of the two (in 2D) or three (in 3D) multiple diagonal matrices, each one with B-spline basis functions along with a particular axis of the spatial system of coordinates. As a result of our algebraic transformations, we get a system of linear equations that can be factorized in linear  $O(N)$  computational cost in every time step of the implicit method. We verify our method by simulating heat transfer and linear elasticity problems. We also demonstrate that our implicit method is unconditionally stable for heat transfer problems (i.e., parabolic). We conclude our presentation with a discussion on the limitations of the method. The work has been supported by National Science Centre, Poland grant no. 2017/26/M/ST1/00281 [1] G. Birkhoff, R.S. Varga, D. Young, Alternating direction implicit methods, *Advanced Computing* 3 (1962) 189–273. [2] J. L. Guermond, P. Mineev, A new class of fractional step techniques for the incompressible Navier-Stokes equations using direction splitting, *Comptes Rendus Mathematique* 348(9-10) (2010) 581–585. [3] L. Gao, V.M. Calo, Fast Isogeometric Solvers for Explicit Dynamics, *Computer Methods in Applied Mechanics and Engineering*, 274 (1) (2014) 19-41

## On Almost Pixel-exact Real-time Rendering of High-order Solution on Unstructured Meshes

Adrien Loseille\*, Rémi Feuillet\*\*

\*INRIA, \*\*INRIA

### ABSTRACT

OpenGL 4 with GLSL shading language have become a standard on many common architectures (Mac, Linux, Windows, , ...) from a couple of years. In the mean time, high-order methods (for flow solution and for meshing algorithm) are emerging. Many of them have proven their abilities to provide accurate results on complex (3D) geometries. However, the assessment of a particular meshing algorithm or of a high-order numerical scheme strongly relies on the capacity to validate and inspect visually the current mesh/solution at hand. However, having at the same time, an accurate and interactive visualization process for high-order mesh/solution is still a challenge as complex process are usually involved in the graphic pipeline: non linear root finding, ray tracing, GPU programming, ... In this presentation, we discuss the current status and issues of using the (raw) OpenGL 4 pipeline to render curved high-order entities, and almost pixel-exact solutions. We illustrate this process on meshes and solutions issued from high-order curved from CAD and with high-order interpolated solutions.

## Numerical Flow Analysis and Optimal Management of a Fishway Model

Mohammed Louaked\*

\*Caen University, France

### ABSTRACT

The need to preserve and enhance natural stocks of diadromous and resident fish have been recognized for, at least, the past century. Dams cut off the migratory route of fish. A fishway or fish-pass is an hydraulic structure that enable fish to overcome obstructions to their spawning and other river migration, and is built whenever it is required, based on ecological, economical, or legal considerations. The purpose of this work is to find the optimal form of fishway so that most many fish can go through rivers in the best conditions. The work involves modeling, mathematical analysis and numerical approximation of a coupled problem between a primal hyperbolic system and adjoint problem for the cost function of the optimal structure. We also obtain an expression for the gradient of the objective function via the adjoint system. Finally, we give numerical results obtained for the pools channel under study. References [1] A. Harten, (1983), High resolution schemes for hyperbolic conservation laws; J. Comp. Physics, 49, 357-393. [2] M. Louaked, (2008), TVD adaptive mesh redistribution scheme for the shallow-water equations; Int. J. Num. Meth. Fluids, 56, 1391-1397. [3] M. Louaked, A. Saidi, (2009), Pointwise control and hybrid scheme for water quality equation; Nonlinear Analysis, 71, 2337-2349. [4] M. Louaked, N. Seloula, S. Shuyu and S. Trabelsi, (2015), A pseudocompressibility method for the incompressible Brinkman-Forchheimer equations; Differential Integral Equations, 28, 3-4, 361-382. [5] Pk. Sweby, (1984), High-resolution schemes using flux limiters for hyperbolic conservation-laws ; Siam J. Numer. Analysis, 21, 995-1011, 361-382.

## Asymmetric Breathing Motions of Nucleosomal DNA and the Role of Histone Tails

Sharon Loverde\*, Kaushik Chakraborty\*\*

\*CUNY College of Staten Island, \*\*CUNY College of Staten Island

### ABSTRACT

The most important packing unit of DNA in the eukaryotic cell is the nucleosome [1]. It undergoes large-scale structural re-arrangements during different cell cycles [1,2]. For example, the disassembly of the nucleosome is one of the key steps for DNA replication, whereas reassembly occurs after replication. Thus, conformational dynamics of the nucleosome is crucial for different DNA metabolic processes. We perform three different sets of atomistic molecular dynamics (MD) simulations of the nucleosome core particle at varying degrees of salt conditions for a total of 0.7 microseconds simulation time. We find that the conformational dynamics of the nucleosomal DNA tails are oppositely correlated from each other during the initial breathing motions [3]. Furthermore, the strength of the interaction of the nucleosomal DNA tail with the neighboring H2A histone tail modulates the conformational state of the nucleosomal DNA tail. With increasing salt concentration, the degree of asymmetry in the conformation of the nucleosomal DNA tails decreases as both tails tend to unwrap. This direct correlation between the asymmetric breathing motions of the DNA tails and the H2A histone tails, and its decrease at higher salt concentrations, may play a significant role in the molecular pathway of unwrapping. Following, we perform even longer simulations (~ 5 microseconds) of the nucleosome core particle at high salt concentration (2 M NaCl). We find the formation of a bulge/loop of nucleosomal DNA that is initiated by the collapse of the H2B N-terminal tail. Using Umbrella Sampling, we next explore the initial stages of unwrapping at these high salt concentrations using the radius of gyration of the nucleosomal DNA tail as a reaction coordinate. [1] McGinty, R. K, Tan, S. Chemical Reviews 115, 2255 (2015). [2] Muller, M. M, Muir, T. W. Chemical Reviews 115, 2296 (2015). [3] Chakraborty, K., Loverde, S.M. Journal of Chemical Physics 147, 165101 (2017).

# THE ENERGY FLUX INTEGRAL BASED FRACTURE CRITERION FOR ELASTIC PLASTIC CRACK GROWTH

Longkun Lu, Shengnan Wang

School of Aeronautics, Northwestern Polytechnical University  
No. 127, Youyi Road (West), Beilin  
Xi'an City, Shaanxi Province, China  
1768614416@qq.com (L.K. Lu), wangshna@nwpu.edu.cn (S.N. Wang)

**Key words:** energy flux integral, elastic plastic crack growth, crack tip configurational force.

**Summary:** *The crack tip energy flux integral is derived from energy or power balance formula containing crack tip. This integral is found to be path independent and represents the power available for separating the crack surfaces during the crack propagation. On the foundation of this integral, a parameter is defined and this parameter is proved to be equal to the minus project of crack tip configurational force along crack growth direction. That is, this parameter is identical to the near tip J integral proposed by Simha et al (J. Mech. Phys. Solids. 2008;56: 2876-95), which is the thermodynamic crack driving force. Thus, a fracture criterion based on this parameter is proposed and its critical value is proved to be equal to the cohesive strength of cohesive model.*

## 1 INTRODUCTION

Plastic unloading is inevitable during crack propagation in elastic plastic materials. Thus, for elastic plastic growing cracks, deformation theory of plasticity ceases to be valid and increment theory of plasticity is required. Furthermore, increment theory of plasticity is not mature enough and intricate to apply. In other words, it is quite difficult to find

a parameter that can characterize the elastic plastic growing crack tip fields. However, the general crack tip integrals proposed by Moran and Shih <sup>[1]</sup> have captured our attention. Moran and Shih have derived the general crack tip integrals based on momentum balance containing the crack tip. This work reminds us that energy balance is always satisfied and energy method may provide a novel view of elastic plastic growing cracks. And this paper attempts to shed some lights on this area.

Unlike the conventional way, the fracture process region (FPZ) <sup>[2]</sup> is our focus. FPZ is a region near the crack tip where the microstructural fracture processes take place. From the standpoint of physical meaning, a parameter representing the states of FPZ can really reflect the fracture properties of materials. Usually, FPZ is small and it may be idealized as the crack tip in some cases <sup>[2]</sup>.

In this paper, the energy flux dissipated in FPZ is studied. And we found that this flux can be expressed as a path independent integral. In fact, this integral is also a kind of crack tip integral proposed by Moran and Shih <sup>[1]</sup>. In Section 2, we have derived this energy flux integral through two methods, energy and power balance <sup>[3]</sup>. And no restriction is imposed on the material response. Since this integral can be regarded as power available for separating the crack surfaces during crack growth, a force-like parameter  $F_T$  can be defined through power is equal to force multiplied by velocity. That is,  $F_T$  is the force conjugated to the crack tip velocity and it is the thermodynamic crack driving force. In Section 3, the relation between  $F_T$  and crack tip configurational force is established. And  $F_T$  is found to be equal to the minus project of crack tip configurational force along crack growth direction, which is identical to the near tip  $J$  integral proposed by Simha et al <sup>[4]</sup>. In Section 4, a fracture criterion based on  $F_T$  is proposed. And the critical value of  $F_T$  is proved to be the cohesive energy of cohesive zone model. In Section 5, a puzzle arising in our minds is presented and some conjectures are also given. Conclusions are summarized in Section 6.

## 2 THE ENERGY FLUX AND CRACK DRIVING FORCE

The energy flux is first derived by energy balance containing crack tip. For a 2D elastic plastic continuum,  $A$  denotes its occupation and  $\Gamma$  denotes its boundary. And then according to equilibrium equation, we can obtain

$$\int_{\Gamma} \sigma_{ij} n_j u_i d\Gamma = \int_A \sigma_{ij} u_{i,j} dA \quad (1)$$

Body force is ignored and Cartesian coordinates are used in Eq. (1).  $n_j$  is the outer normal of the boundary  $\Gamma$ . The left side represents the external load work and the right side is the internal stress work.

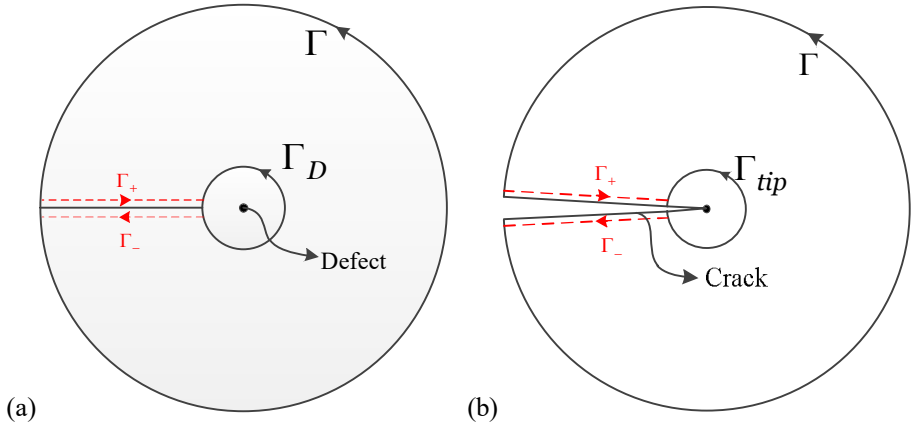


Fig. 1 The contour path when a defect is contained

As shown in Fig. 1 (a), if a defect exists in this body, the defect must be excluded to guarantee the validity of Green theorem. Consider  $\Gamma_D$  is an arbitrary curve surrounding the defect but included by  $\Gamma$ .  $A_D$  is the area surrounded by  $\Gamma_D$ . Because of the overlap between  $\Gamma_+$  and  $\Gamma_-$ , Eq. (1) turns into

$$\int_{\Gamma-\Gamma_D} \sigma_{ij} n_j u_i d\Gamma = \int_{A-A_D} \sigma_{ij} u_{i,j} dA \quad (2)$$

Eq. (2) is also applicable to the crack case. As shown in Fig. 1 (b), the defect will become a crack when  $\Gamma_+$  and  $\Gamma_-$  are separated. And Eq. (2) will keep invariable if the crack surface is traction free. Replace  $\Gamma_D$  with  $\Gamma_{tip}$  ( $A_{tip}$  is the area enclosed by  $\Gamma_{tip}$ ), further result can be obtained,

$$\int_{\Gamma} \sigma_{ij} n_j u_i d\Gamma - \int_A \sigma_{ij} u_{i,j} dA = \int_{\Gamma_{tip}} \sigma_{ij} n_j u_i d\Gamma - \int_{A_{tip}} \sigma_{ij} u_{i,j} dA \quad (3)$$

If  $\Gamma_{tip}$  is chosen as the boundary of FPZ,  $\Gamma_{tip}$  is fixed and  $\Gamma$  can be chosen arbitrarily. Therefore, the left side of Eq. (3) is path independent. The line integral is the work applied to the region enclosed by  $\Gamma$  and the area integral is the strain energy stored in (or dissipated by) the materials. The physical meaning of the left side of Eq. (3) is the energy flowing into the crack tip. In addition, as shown by Broberg<sup>[2]</sup>, material separations take place in FPZ and continuum mechanics does not work. We assume that all of the external work is dissipated by micro damage and then the second term of the right hand will vanish. Thus,

$$\int_{\Gamma_{tip}} \sigma_{ij} n_j u_i d\Gamma = \int_{\Gamma} \sigma_{ij} n_j u_i d\Gamma - \int_A \sigma_{ij} u_{i,j} dA \quad (4)$$

Eq. (4) can also be explained by idealizing FPZ as the crack tip. In this case,  $\Gamma_{tip} \rightarrow 0$ . Since  $\sigma_{ij} u_{i,j}$  has a singularity less than  $r^{-2}$ , the term  $\int_{A_{tip}} \sigma_{ij} u_{i,j} dA$  vanishes. When crack grows in this body,

$$\frac{d}{da} \int_{\Gamma_{tip}} \sigma_{ij} n_j u_i d\Gamma = \frac{d}{da} \left[ \int_{\Gamma} \sigma_{ij} n_j u_i d\Gamma - \int_A \sigma_{ij} u_{i,j} dA \right] \quad (5)$$

Where  $a$  is the crack length. FPZ will also move with respect to this crack tip and it is reasonable to assume FPZ is invariable in size<sup>[5]</sup>. By fixing  $\Gamma$  in space, Eq. (5) will turn into

$$\Theta = \int_{\Gamma_{tip}} \sigma_{ij} n_j \dot{u}_i d\Gamma = \int_{\Gamma} \sigma_{ij} n_j \dot{u}_i d\Gamma - \int_A \sigma_{ij} \dot{u}_{i,j} dA \quad (6)$$

The superposed dot denotes the time derivative. Eq. (6) can also be obtained by power balance during crack propagation. Xiao S et al <sup>[3]</sup> have provided power available for separating the crack surfaces,

$$\text{Power} = \int_{\Gamma} \sigma_{ij} n_j \dot{u}_i d\Gamma - \int_A \sigma_{ij} \dot{u}_{i,j} dA \quad (7)$$

The first term of the right hand side is the power of the external force and the second term is the power of the internal force. From the angle of power balance, the total power of external load can be divided into two parts: One part is the power dissipated by the internal load, and the other is dissipated by FPZ. When the contour is the boundary of FPZ, the external power is totally dissipated by FPZ. And then Eq. (6) can be obtained.

$\Theta$  is the energy flux integral, which represents the energy flowing into FPZ. This integral has already been proved to be path independent during the derivation process. In addition, the energy flux integral can be considered as the power dissipated in FPZ (or the power available for separating the crack surfaces).

Since power is the product of load multiplied by velocity, a force like parameter can be defined as follows,

$$\Theta = F_T \cdot \dot{a} \quad (8)$$

Where  $\dot{a}$  is the crack growth velocity and  $F_T$  is the force conjugated to  $\dot{a}$ .  $F_T$  can thus be regarded as the thermodynamic crack driving force.

### 3 ENERGY FLUX AND CONFIGURATIONAL FORCE

Now we will recall Eq. (6) in initial undeformed configuration. Thus Cauchy stress tensor  $\sigma$  will become Piola-Kirchhoff stress tensor  $\mathcal{S}$ . The contour  $\Gamma_{tip}$  will turn into  $\Gamma_{tip}^{un}$  and the normal vector  $\mathbf{n}$  will become  $\mathbf{m}$ . Fig. 2 has shown this conversion. And then

$$\Theta = \int_{\Gamma_{tip}} (\boldsymbol{\sigma} \cdot \mathbf{n}) \dot{\mathbf{u}} d\Gamma = \int_{\Gamma_{tip}^{un}} (\mathbf{S} \cdot \mathbf{m}) \dot{\mathbf{u}} d\Gamma \quad (9)$$

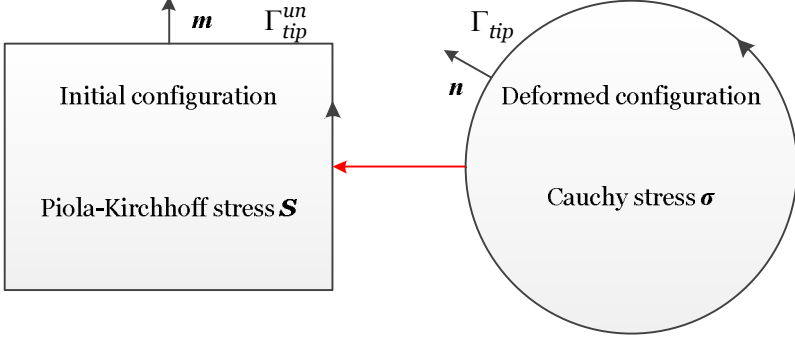


Fig. 2 Initial and deformed configuration

As provided by Moran and Shih<sup>[1]</sup>, the displacement fields satisfy

$$\dot{\mathbf{u}} \sim -\dot{a}_{un} \hat{\mathbf{e}} \cdot \frac{\partial \mathbf{u}}{\partial \mathbf{X}} \text{ as } \Gamma_{tip}^{un} \rightarrow 0 \quad (10)$$

In Eq. (10),  $\dot{a}_{un}$  is the crack growth velocity in initial configuration and  $\hat{\mathbf{e}}$  is the direction of crack growth.  $\mathbf{X}$  is the Lagrange coordinate and  $\mathbf{x}$  is the corresponding spatial coordinate. Thus, Eq. (9) becomes

$$\Theta = \int_{\Gamma_{tip}^{un}} (\mathbf{S} \cdot \mathbf{m}) \dot{\mathbf{u}} d\Gamma = -\dot{a}_{un} \hat{\mathbf{e}} \cdot \int_{\Gamma_{tip}^{un}} (\mathbf{S} \cdot \mathbf{m}) \frac{\partial \mathbf{u}}{\partial \mathbf{X}} d\Gamma \quad (11)$$

Since  $\mathbf{u} = \mathbf{x} - \mathbf{X}$  and substitute it into Eq. (11),

$$\Theta = -\dot{a}_{un} \hat{\mathbf{e}} \cdot \int_{\Gamma_{tip}^{un}} (\mathbf{S} \cdot \mathbf{m}) (\mathbf{F} - \mathbf{I}) d\Gamma = -\dot{a}_{un} \hat{\mathbf{e}} \cdot \int_{\Gamma_{tip}^{un}} (\mathbf{F}^T \cdot \mathbf{S}) \mathbf{m} d\Gamma \quad (12)$$

In Eq. (12),  $\mathbf{F}$  is the deformation gradient and the second equality has used  $\int_{\Gamma_{tip}^{un}} (\mathbf{S} \cdot \mathbf{m}) d\Gamma = 0$ , which is provided by Simha et al<sup>[4]</sup>.

Consider that  $\Gamma_{tip}^{un}$  is the boundary of FPZ in initial configuration and

the materials in FPZ always undertake microscope fracture. And then all of the external work is dissipated by microscope separations. That is no stored energy exists in FPZ (namely  $\Gamma_{tip}^{un}$ ). If  $\varphi$  is the stored energy density, we can obtain

$$\int_{\Gamma_{tip}^{un}} (\varphi \mathbf{I}) \mathbf{m} d\Gamma = 0 \quad (13)$$

Eq. (13) can also be explained as follows: When FPZ is idealized as the crack tip, usual continuum mechanics is applicable near the crack tip and  $\varphi$  can be considered as stress work density. The elastic plastic growing crack tip field has a weaker singularity than static crack tip field<sup>[6]</sup>. Thus the singularity of  $\varphi$  is less than  $r^{-1}$  and Eq. (13) satisfies.

By adding Eq. (13) into Eq. (12),

$$\Theta = \dot{a}_{un} \hat{e} \cdot \int_{\Gamma_{tip}^{un}} (\varphi \mathbf{I} - \mathbf{F}^T \cdot \mathbf{S}) \mathbf{m} d\Gamma \quad (14)$$

The crack tip driving force proposed by Simha et al<sup>[4]</sup> is

$$J_{tip} = \hat{e} \cdot \int_{\Gamma_{tip}^{un}} (\varphi \mathbf{I} - \mathbf{F}^T \cdot \mathbf{S}) \mathbf{m} d\Gamma \quad (15)$$

And thus

$$\Theta = J_{tip} \cdot \dot{a}_{un} \quad (16)$$

It is noting that Eq. (16) is derived in initial configuration. Pull Eq. (16) forth to current configuration, Eq. (8) will be obtained. That is, the energy flux integral is indeed consistent with the thermodynamics crack driving force. And the parameter  $F_T$  proposed in Section 2 is equal to the minus project of crack tip configurational force along crack growth direction. In other words,  $F_T$  is identical to the Simha near tip  $J$  integral.

#### 4 ENERGY FLUX BASED CRACK GROWTH CRITERION

Crack growth will happen only when micro-separations ahead of the

crack tip coalesce with the main crack. That is, the energy flowing into the crack tip must be large enough to support the above process in order to make crack propagate. Therefore, due to its physical meaning, the energy flux integral is a suitable fracture parameter. To keep the same dimension as  $J$  integral, we choose  $F_T$  here. And thus the crack growth criterion can be expressed as

$$F_T = F_T^c \quad (17)$$

$F_T^c$  is the critical value of  $F_T$ , which is dependent on the fracture micro-mechanisms taking place in FPZ. According to Anderson<sup>[7]</sup>, the mechanisms depend on material properties and stress state (constraint level). And thus, for the same material and stress state, it is reasonable to assume that  $F_T^c$  is invariant during crack growth.

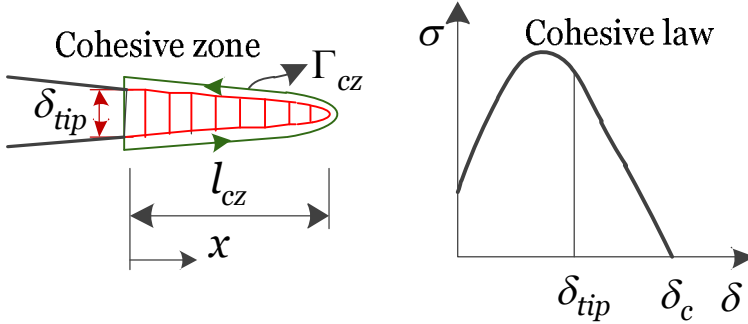


Fig. 3 Cohesive zone model

To determine  $F_T^c$ , FPZ can be idealized as the cohesive zone ahead of crack tip<sup>[8-9]</sup>. The model is shown in Fig. 3, where  $l_{cz}$  is the length of the cohesive zone,  $\delta_{tip}$  is the separation distance at the crack tip,  $\delta_c$  is the critical separation when crack will grow and  $\Gamma_{cz}$  is the contour around the cohesive zone. The contour  $\Gamma_{cz}$  can be divided into two parts: the

upper and lower part. We have  $n_1 = 1, n_2 = 0$  on the upper part; and for the lower part, we have  $n_1 = -1, n_2 = 0$ . Besides, all stress components except  $\sigma_{22}$  are zero. Thus, the power dissipated in cohesive zone is

$$F_T \cdot \dot{a} = 2 \int_0^{l_{cz}} \sigma_{22} \dot{u}_2 dx = \int_0^{l_{cz}} \sigma(\delta) \dot{\delta} dx \quad (18)$$

Where  $\sigma_{22} = \sigma(\delta)$  and  $\delta = 2u_2$ . Since  $\delta(0) = 0, \delta(l_{cz}) = \delta_c$  and  $da = -dx$ ,

$$F_T = \int_0^{l_{cz}} \sigma(\delta) \frac{d\delta}{da} dx = \int_0^{\delta_c} \sigma(\delta) d\delta \quad (19)$$

Therefore, we can conclude that  $F_T^c$  is equal to the cohesive energy  $\Gamma_0$  for cohesive zone model.

M (T) and C (T) specimens tested in reference <sup>[10]</sup> are used to verify Eq. (19). These specimens are 3 mm thick and made of AL 5083 H321 (L-T). The Young's modulus  $E$  is 68000 MPa and Poisson's ratio  $\nu$  is 0.33. Scheider et al <sup>[10]</sup> have utilized cohesive zone model to predict crack extension of these specimens. The predicted results coincide with these tested results quite well when  $\Gamma_0 = 10 \text{ N/mm}$ . Table 1 has shows the specimen geometry and initial load.  $W$  is the total width,  $a_0$  is the initial crack length and  $F_i$  is the applied load when crack initiates.

Table 1. Specimen geometry and initial load

Specimen type	$W$ (mm)	$a_0$ (mm)	$F_i$ (KN)
M (T)	100	15	39
M (T)	300	30	81
C (T)	50	25	2
C (T)	150	75	3.6

Since  $F_T^c$  is invariant during crack growth, the  $F_T$  value under  $F_i$  is equal to  $F_T^c$ . We assume that the crack tip fields are controlled by  $K$  factor when crack initiates. Combined Eq. (6) with (8),

$$F_T = - \int_{\Gamma} \sigma_{ij} n_j \frac{\partial u_i}{\partial x} d\Gamma + \int_A \sigma_{ij} \frac{\partial u_{i,j}}{\partial x} dA \quad (20)$$

By substituting linear elastic crack tip fields into Eq. (20),

$$F_T = \frac{3+\nu}{4} \frac{K^2}{E} \quad (21)$$

From  $F_i$  we can get the stress intensity factor when crack initiates, and then  $F_T^c$  can be obtained. Table 2 has summarized the validity results. All of these errors except 150 mm wide C (T) are less than 2%. The discrepancies of 150 mm wide C (T) may be due to the inappropriate application of linear elastic crack tip fields. Nonetheless, we can get from Table 2 that  $F_T^c$  is indeed consistent with the cohesive energy.

Table 2. Comparison between  $F_T^c$  and  $\Gamma_0$

Specimen	M (T)-100	M (T)-300	C (T)-50	C (T)-150
$F_T^c$ (N/mm)	9.87	9.83	10.15	10.97
Error	-1.3%	-1.7%	1.5%	9.7%

## 5 DISCUSSIONS

A puzzle exists here: For growing cracks,  $F_T$  is the thermodynamic crack driving force and thus  $F_T^c$  is indeed the fracture toughness. And we have shown that  $F_T^c$  is equal to  $\Gamma_0$  of cohesive zone model. But  $\Gamma_0$  alone is not enough to capture crack propagation in cohesive zone model. Any two parameters of  $\Gamma_0$ ,  $\sigma_{\max}$  and  $\delta_c$  are required ( $\sigma_{\max}$  is the cohesive strength of cohesive law) in cohesive zone model.

There exist two conjectures about this puzzle:

The first conjecture is that  $F_T = F_T^c$  must be satisfied to keep crack growing but this equality is not enough to represent the whole features of crack propagation. And another condition is required. Maybe there exists an energy ratio  $R_E$  for these structures. And  $R_E$  is defined as  $F_T^c$

divided by the total dissipated work ( $F_T^c$  plus plastic dissipation). This ratio may be a truly geometry parameter, which is just dependent upon the geometry. Once the formula of  $R_E$  is obtained, the crack growth behavior can be totally decided by  $F_T^c$ .

The second conjecture is that  $F_T=F_T^c$  is enough to represent the whole features of crack propagation. And there exist some conditions which are ignored by cohesive zone model. Usually, we choose cohesive law just on the basis of predicted results. That is, the cohesive parameters are first obtained from simple specimens and then are used to predict the crack growth behaviors of complex structures. And we guess that there may some standard procedure to get these parameters or some extra conditions that control these parameters. That is, once  $F_T^c$  is given, the corresponding cohesive law may be directly obtained. In this case,  $F_T=F_T^c$  is enough to control the crack growth.

## 6 CONCLUSIONS

The crack tip energy flux integral is obtained from energy or power balance containing crack tip. This integral is also path independent. Besides, this integral can be considered as the power available for separating the crack surfaces or power dissipated in FPZ. Based on this physical meaning, a force-like parameter  $F_T$  conjugated to the crack tip velocity is defined. And  $F_T$  is found to equal to the minus project of crack tip configurational force along crack growth direction, which is identical to near tip  $J$  integral proposed by Simha et al <sup>[4]</sup>. Thus, a crack growth criterion based on  $F_T$  is proposed by us. Besides, we also prove that the critical value of  $F_T$  is equal to cohesive energy of cohesive zone model.

## REFERENCE

[1] Moran B, Shih CF. Crack tip and associated domain integrals from

- momentum and energy balance. *Eng. Fract. Mech.* 1987;27: 615-42.
- [2] Broberg KB. *Cracks and fracture*. USA: Academic Press; 1999.
- [3] Xiao S, Wang HL, Liu B, Hwang KC. The surface-forming energy release rate based fracture criterion for elastic-plastic crack propagation. *J. Mech. Phys. Solids*. 2015;84:336-57.
- [4] Simha NK, Fischer FD, Shan GX, Chen CR, Kolednik O. J-integral and crack driving force in elastic-plastic materials. *J. Mech. Phys. Solids*. 2008;56:2876-95.
- [5] Tvergaard V, Hutchinson JW. The relation between crack growth resistance and fracture process parameters in elastic-plastic solids. *J. Mech. Phys. Solids*. 1992;40:1377-97.
- [6] Rice JR, Drugan WJ, Sham TL. Elastic-plastic analysis of growing cracks. *Fracture Mechanics: Twelfth Conference, ASTM STP 700*, American Society for Testing and Materials. 1980:189-21.
- [7] Anderson TL. *Fracture mechanics: fundamental and applications*. USA: CRC Press; 2017.
- [8] Barenblatt GI: The mathematical theory of equilibrium cracks in brittle fracture. *Adv Appl Mech*. 1962;7:55-129.
- [9] Dugdale DS: Yielding of steel sheets containing slits. *J Mech Phys Solids*. 1960;8:100-104.
- [10] Scheider I, Schodel M, Brocks W, Schonfeld W. Crack propagation analyses with CTOA and cohesive model: Comparison and experimental validation. *Eng. Fract. Mech.* 2006;73:252-63.

## Phase Field Modeling of Hydraulic Fracture Propagation in Complex Formation Condition

Qianli Lu<sup>\*</sup>, Jianchun Guo<sup>\*\*</sup>, Lei Chen<sup>\*\*\*</sup>

<sup>\*</sup>Southwest Petroleum University, <sup>\*\*</sup>Southwest Petroleum University, <sup>\*\*\*</sup>Mississippi State University

### ABSTRACT

Unconventional reservoir, especially shale reservoir, is featured with rock heterogeneity, in-situ stress anisotropy and abundant natural fractures. Due to these features, diverting, branching, offsetting and some other phenomena could occur while Hydraulic fracture propagate in the rock of unconventional reservoir. Commonly used sharp fracture topology models, such as the finite –element method (FEM), often suffer in complex fracture geometry due to computationally expensive remeshing and some other special handlings when fracture diverts or branches. In this paper, phase-field method (PFM) which is featured with diffusive fracture interface is proposed to quantitatively study the fracture propagation in complex formation condition with rock heterogeneity, stress anisotropy and natural fracture. The evolution of phase field is established by solving the energy balance between elastic energy, dissipation and external work by variational approach. The displacement field is solved by solid material wave equation with damping term. The advantage of this method is that no special handling or additional constitutive rule is needed to track the fracture interface and the fracture tip, and is free from pre-defining the propagation path, because the fracture diverting and branching is the solution of global optimal of the total energy of the system based on variational principal. The model is validated through fracture width, stress field and propagation against analytical model, ABAQUS and displacement discontinuity method. A hydraulic fracture interacts with an angled single natural fracture and a hydraulic fracture propagates in a shale main formation with a stiff heterogeneous strip across it are investigated. Study reveals that the approaching angle ( $\alpha$ ) of natural fracture (NF) has great impact on hydraulic fracture propagation. For  $\alpha > 72^\circ$ , hydraulic fracture directly penetrates natural fracture, and cannot initiate the natural fracture; for  $\alpha$  around  $63^\circ$ , hydraulic fracture penetrates and also initiates natural fracture, both fracture propagate simultaneously; for small  $\alpha < 45^\circ$ , HF initiates NF, but cannot penetrate NF, fracture propagates along NF. In heterogeneous strip simulation, parametric study shows that fractures will branch as long as Young's modulus ratio ( $ER = E_{strip}/E_{main}$ ) exceeds a critical value. The critical value increases accordingly as the principal in-situ stress difference ( $S_d$ ) goes up. These results indicate that formation with around  $63^\circ$  approaching angle natural fractures, relatively low  $S_d$  and high  $ER$  has higher possibility to generate fracture network to increase production. The findings in this study could provide valuable insights in predicating and creating complex hydraulic fracture patterns.

## Development of Commercial Finite Element Software Using Kratos Multiphysics Framework

Qiukai Lu<sup>\*</sup>, Erwan Beauchesne<sup>\*\*</sup>, Tadeusz Liszka<sup>\*\*\*</sup>, Mahender Reddy<sup>\*\*\*\*</sup>

<sup>\*</sup>Altair Engineering, Inc., <sup>\*\*</sup>Altair Engineering, Inc., <sup>\*\*\*</sup>Altair Engineering, Inc., <sup>\*\*\*\*</sup>Altair Engineering, Inc.

### ABSTRACT

Kratos Multiphysics platform developed as open source at CIMNE, Barcelona, [1], has been used to study thermo-mechanical analysis of material behavior during additive manufacturing (AM, called also 3-D printing) process. Kratos provides Finite Element solver basis, which relies on a set of open source components, including mesh and field variable data structures, matrix assembly, linear system solvers, and even parallelism for both shared and distributed memory systems. These, and other advanced features are under active development by the Kratos community, new ones are constantly being added to the code base, enable developers to quickly implement and test new solution algorithms. This development presents both opportunities to receive cutting edge functionality, and challenges to keep up with constantly changing, fluid environment. In this research, we developed proprietary features specific to AM simulation. These include customized meshing algorithms, moving heat source models, element activation strategies as well as material models. Some of the Altair development related to Kratos has been offered to Kratos community - this includes help in automated builds and testing, as well as interface layer to Altair pre- and post-processing products (Hyper Mesh(R), Hyper View(R), and H3D file format standard). In this talk we will present various aspects of the software development practices utilized by Altair to facilitate practical collaboration between open source and commercial software. We will also present a few results from the Altair AM solver. [1] Kratos Multiplicity (Version 5.2) [Computer software]. Retrieved January 12, 2018, from <https://github.com/KratosMultiphysics/Kratos>

## An Improved FPM Method in the Discontinuous Interface Problems

Wang Lu\*, Xu Fei\*\*

\*Northwestern Polytechnical University, \*\*Northwestern Polytechnical University

### ABSTRACT

An Improved FPM Method in the Discontinuous Interface Problems Wang Lu<sup>1</sup>, Yang Yang<sup>1</sup>, Xu Fei<sup>1</sup> (1.School of Aeronautics, Northwestern Polytechnical University, Xi'an 710072, Shaanxi, P. R. China) Abstract: FPM (Finite Particle Method) is an important improvement of SPH (Smoothed Particle Hydrodynamics) method, which effectively improves the calculation accuracy of boundary particles. However, when the discontinuous physical field is solved by FPM, the accuracy in the vicinity of discontinuous interface is greatly reduced, and non-singularity of the matrix must be satisfied in FPM method, which requires an elaborate handling of the interface. Therefore, based on DSPH (Discontinuous SPH) method which is an improvement of traditional SPH for discontinuous problems, this paper proposed an improved FPM method — DSFPM(Discontinuous Special FPM) method, which considers discontinuous interface, aiming to improve the computational accuracy at interface and further improve the stability of FPM method and reduce the computational method. In this paper, the estimation accuracy of DSFPM method was analyzed firstly, and then the algorithm flow diagram of DSFPM method to deal with the different engineering problems is demonstrated. Next, DSFPM, DSPH and FPM methods are used to simulate the small deformation problem — elastic aluminum blocks impact, by comparing velocity and stress of the aluminum blocks, we verified the accuracy and computational efficiency of DSFPM method. Finally, the simulation of large deformation problem is realized by combination of DSFPM with DFPM (Discontinuous FPM) methods. Key words: FPM; interface; DSFPM; accuracy; computational cost References: [1] Liu MB, Liu G.R. Restoring particle consistency in smoothed particle hydrodynamics[J]. Applied Numerical Mathematics, 2006, 56(1):19-36. [2] Liu M B, Liu G R, Lam K Y. A one-dimensional meshfree particle formulation for simulating shock waves [J]. Shock Wave, 2003, 13: 201-211. [3] F. Xu, Y. Zhao, R. Yan, T. Furukawa. Multi-dimensional Discontinuous SPH method and its application to metal penetration analysis [J]. International Journal for Numerical Methods in Engineering. 2013,93:1125-1146.

## Enhancing the Efficiency of Multiple Image Processing Tasks in Automatic Optical Inspection (AOI)

Wei-Hao Lu\*, Po Ting Lin\*\*

\*National Taiwan University of Science and Technology, Taiwan, \*\*National Taiwan University of Science and Technology, Taiwan

### ABSTRACT

Automatic Optical Inspection (AOI) has been widely used in machinery and manufacturing industries. To complete each specific AOI mission, multiple image processing tasks, such as color balancing, contrast enhancement, filtering, transformation, pattern detection, etc., are used in a systematic arrangement with proper decisions of control parameters. As the complexity of the inspection mission increases, the required time to complete the entire image processing tasks increases dramatically. One way to speed up the image processing tasks is to use multithread computing in Graphics Processing Units (GPUs). However, the improvement by GPUs has a limit because the number of multiple image processing tasks remain the same. To further enhancing the efficiency, we investigated the effectiveness of each process (or each individual operation) and reduced the least effective processes in the entire multi-tasking processes. The balance between the process reduction and the image processing performance is optimized in terms of minimizing the computation time and maximizing the image processing accuracy simultaneously. Several numerical examples are examined to show the performance of the proposed method.

## Computational Welding Vademecum for Parametric Studies: Identification of Nonlinear Material Properties

Ye Lu<sup>\*</sup>, Nawfal Blal<sup>\*\*</sup>, Anthony Gravouil<sup>\*\*\*</sup>

<sup>\*</sup>Univ Lyon, INSA-Lyon, CNRS UMR5259, LaMCoS, F-69621, France, <sup>\*\*</sup>Univ Lyon, INSA-Lyon, CNRS UMR5259, LaMCoS, F-69621, France, <sup>\*\*\*</sup>Univ Lyon, INSA-Lyon, CNRS UMR5259, LaMCoS, F-69621, France

### ABSTRACT

In spite of the impressive progresses in computer science, traditional approaches remain prohibitive when dealing with nonlinear multiparametric problems, like inverse identification or optimization of welding, additive manufacturing or other complex processes. The use of model order reduction [1] can make available, at a cheaper cost, computational vademecum. Fast decisions can be then made by engineers. In this study, a novel non-intrusive reduced order strategy for construction of multiparametric welding computational vademecum is presented. This is based on an optimized database containing a limited number of standard finite element solutions selected in the underlying parameter space. These solutions can be obtained with any appropriate commercial code. An offline learning procedure based on Higher-Order Proper Generalized Decomposition method (HOPGD) [2, 3] is then carried out for searching a separated representation of the parametric solutions (space, time and controlled parameters). Once the separated parameter functions are constructed, new solutions for new parameter values (non-considered in precomputed set) are rapidly obtained by unidirectional interpolation methods at the online stage. The interpolation accuracy is controlled by an adaptive sparse grid sampling strategy in the parameter space. As an example, the multiparametric welding computational vademecum coupled with an online guidance algorithm is applied to inverse identification of non-linear constitutive model parameters. [1] A. Falcó, N. Montés, F. Chinesta, L. Hilario, M. C. Mora, On the Existence of a Progressive Variational Vademecum based on the Proper Generalized Decomposition for a Class of Elliptic Parameterized Problems. *Journal of Computational and Applied Mathematics* (2018). [2] D. Modesto, S. Zlotnik, A. Huerta, Proper generalized decomposition for parameterized helmholtz problems in heterogeneous and unbounded domains: Application to harbor agitation, *Computer Methods in Applied Mechanics and Engineering* (2015). [3] Y. Lu, N. Blal, A. Gravouil. &quot;Multi-parametric space-time computational vademecum for parametric studies: Application to real time welding simulations.&quot; *Finite Elements in Analysis and Design* (2018).

## Getting the Best of Damage Mechanics and Peridynamics: A Unified Approach for Objective Simulation of Material Degradation up to Complete Failure

Gilles Lubineau<sup>\*</sup>, Fei Han<sup>\*\*</sup>, Yan Azdoud<sup>\*\*\*</sup>, Yongwei Wang<sup>\*\*\*\*</sup>

<sup>\*</sup>KAUST, <sup>\*\*</sup>KAUST, <sup>\*\*\*</sup>KAUST, <sup>\*\*\*\*</sup>KAUST

### ABSTRACT

Despite many different approaches have been developed, the objective (mesh-independent) simulation of evolving discontinuities, such as cracks, remains a challenge. Current techniques are highly complex or involve intractable computational costs, making simulations up to complete failure difficult. We propose a framework as a new route toward solving this problem that adaptively couples local-continuum damage mechanics with peridynamics to objectively simulate all the steps that lead to material failure: damage nucleation, crack formation and propagation. Local-continuum damage mechanics successfully describes the degradation related to dispersed microdefects before the formation of a macrocrack. However, when damage localizes, it suffers spurious mesh dependency, making the simulation of macrocracks challenging. On the other hand, the peridynamic theory is promising for the simulation of fractures, as it naturally allows discontinuities in the displacement field. Here, we present a hybrid local-continuum damage/peridynamic model. Local-continuum damage mechanics is used to describe “volume&amp;quot; damage before localization. Once localization is detected at a point, the remaining part of the energy is dissipated through an adaptive peridynamic model capable of the transition to a “surface&amp;quot; degradation, typically a crack. We believe that this framework, which actually mimics the real physical process of crack formation, is the first bridge between continuum damage theories and peridynamics. This approach leverages at best both techniques as 1) damage mechanics helps in locating at low-cost where a peridynamics model should be introduced and 2) the peridynamics models helps in stabilizing the damage mechanics solution once the localization is achieved. Two-dimensional numerical examples are used to illustrate that an objective simulation of material failure can be achieved by this method.

## Simulation of Micro-Scale Shear Bands Using Peridynamics with an Adaptive Dynamic Relaxation Method

Jiangyi Luo\*, Veera Sundararaghavan\*\*

\*University of Michigan, Ann Arbor, \*\*University of Michigan, Ann Arbor

### ABSTRACT

Size effects play an important role in material response. In classical elasticity, stress at a point is locally dependent on the strain at the same point which leads to prediction of singularities at crack tips and dislocation cores. It is therefore difficult for crystal plasticity finite element methods to properly predict strain localizations, in the form of fine shear bands, which have been observed by recent experiments. In contrast, the non-local method, peridynamics, is capable of handling damage and propagation of discontinuities. In peridynamics, strain at a point is calculated by tracking the motion of surrounding particles. An intrinsic length scale is introduced by the particle influence horizon to control the material responses. Recent results based on a crystal plasticity peridynamic model with an implicit Newton-Raphson solver have shown advantages of capturing finer shear bands in planar polycrystals. However, for crystal plasticity, the computation cost of calculating the tangent modulus matrix in implicit methods is high. In this presentation, we will present a peridynamic (PD) implementation of crystal plasticity with an adaptive dynamic relaxation method. Non-ordinary state-based peridynamics and the Newmark's dynamic method with artificial damping are employed to capture strain localizations in polycrystalline microstructures based on a rate-independent crystal plasticity model. The computational efficiency of the explicit PD model is demonstrated to be superior to the implicit PD model for modeling crystals. The stress field distribution, texture formation, and homogenized stress-strain response predicted by the finite element method and the new dynamic PD model are compared in numerical simulations. Finer strain localization bands are observed in the latter model. The effect of influence horizon size on localization bands are studied and instability is observed in PD results with larger horizon radius. Our future work will include: 1. More sophisticated controls of instability in peridynamics, such as introducing stress points; 2. 3D simulations to understand the effect of crystal structure on the activation and propagation of shear bands more accurately. Reference Luo, J., Ramazani, A. and Sundararaghavan, V., 2018. Simulation of micro-scale shear bands using peridynamics with an adaptive dynamic relaxation method. International Journal of Solids and Structures, 130, pp.36-48.

## **Coarse-grained Formulation of Point Defect Absorption at Interfaces and Its Application in Modelling Grain Boundary Migration Under Irradiation**

Jing Luo<sup>\*</sup>, Yichao Zhu<sup>\*\*</sup>, Yang Xiang<sup>\*\*\*</sup>, Xu Guo<sup>\*\*\*\*</sup>

<sup>\*</sup>Dalian University of Technology, <sup>\*\*</sup>Dalian University of Technology, <sup>\*\*\*</sup>The Hong Kong University of Science Technology, <sup>\*\*\*\*</sup>Dalian University of Technology

### **ABSTRACT**

Interfaces are known to be ideal sink sites for point defects. Hence the introduction of high density interfaces provides an effective mean for developing materials with high irradiation tolerance. Nevertheless, limited works have been seen on modelling interface evolution induced by underlying point defect-interface interaction. In this talk, with use of matched asymptotic technique, we manage to upscale the (micro-scale) interaction between point defects and the constituting dislocation of low-angle grain boundaries (GBs), so as to derive a (macro-scale) Robin-type jump boundary condition. In comparison with the existing GB sink efficiency models, the derived condition takes into account (for the first time) the effect due to the point defects that penetrate GBs. Thus the study for GB sink efficiency in polycrystal is enabled. With use of the obtained jump Robin condition, we first derive a formula predicting sink efficiency of point defects for polycrystalline material as a function of its constituting grain sizes. Then in conjunction with the equation for point defect evolution in grain interiors, the GB migration behavior in the presence of irradiation is simulated. It is found that in contrast to the widely-used curvature-derived law, (which predicts symmetric evolution for cylindrical GBs), the GB deforms asymmetrically under irradiation. This work has laid a solid foundation for the investigation of interaction between interfaces and point defects, and useful insights for the dynamical behavior of interface are provided. This is essential for further investigations on nanocrystalline material behavior under irradiation.

## Concrete Fragmentation Driven by Kinetic Energy of Forming Particles: Penetration of Projectiles of Various Impact Inclinations and Velocities

Wen Luo<sup>\*</sup>, Zdeněk Bažant<sup>\*\*</sup>

<sup>\*</sup>Northwestern University, <sup>\*\*</sup>Northwestern University

### ABSTRACT

The apparent increase of strength of concrete at very high strain rates experienced in projectile impact (10 s<sup>-1</sup> to 106 s<sup>-1</sup>), called 'dynamic overstress', has recently been explained by the theory of release of local kinetic energy of shear strain rate in finite size particles about to form. This theory gives the particle size and the additional kinetic energy density that must be dissipated in finite-element codes. In previous research, it was dissipated by additional viscosity, in a model partly analogous to turbulence theory. In the model presented here, it is dissipated by scaling up the material strength. Microplane model M7 is used and its stress–strain boundaries are scaled up by factors proportional to the -4/3rd power of the effective deviatoric strain rate and its time derivative. The scaled M7 model is seen to predict correctly the crater shapes and exit velocities of projectiles penetrating concrete walls of different thicknesses. Apart from orthogonal impacts, oblique impacts of projectiles into thin and thick concrete targets are also simulated. The choice of the finite strain threshold for element deletion criterion, which can have a big effect, is also studied. It is proposed to use the highest threshold above which a further increase has a negligible effect. References Bažant, Z.P., and Caner, F.C. (2013). "Comminution of solids caused by kinetic energy of high shear strain rate, with implications for impact, shock and shale fracturing." Proc., National Academy of Sciences 110 (48), 19291—19294 Bažant, Z.P., and Caner, F.C. (2014). "Impact comminution of solids due to local kinetic energy of high shear strain rate: I. Continuum theory and turbulence analogy." J. of the Mechanics and Physics of Solids 64, 223--235 (with Corrigendum, Vol. 67 (2014), p. 14). Bažant, Z.P., and Su, Yewang (2015). "Impact comminution of solids due to progressive crack growth driven by kinetic energy of high-rate shear." ASME J. of Applied Mechanics 82 (March), pp. 031007-1--031007-5. Su, Yewang, Bažant, Z.P., Zhao, Youxuan, Salviato, M., and Kirane, K. (2015). "Viscous energy dissipation of kinetic energy of particles comminuted by high-rate shearing in projectile penetration, with potential ramification to gas shale." Int. J. of Fracture 193 (1), 77-85.

## **A New Strong Formation Finite Element Method for Fracture Analysis of Functionally Graded Materials**

Jun Lv<sup>\*</sup>, Xiao-Wei Gao<sup>\*\*</sup>

<sup>\*</sup>State Key Laboratory of Structural Analysis for Industrial Equipment, Dalian University of Technology, Dalian 116024, China, <sup>\*\*</sup>State Key Laboratory of Structural Analysis for Industrial Equipment, Dalian University of Technology, Dalian 116024, China

### **ABSTRACT**

In this paper, elastostatic crack analysis in continuously non-homogeneous, isotropic and linear elastic functionally graded materials and structures (FGMs) is presented. A new strong formation finite element method, Elemental Differential Method (EDM), is applied for this purpose, which establishes the system equations directly based on the equilibrium equations. The key aspect of this method is based on the direct differentiation of the shape functions of isoparametric elements used to characterize the geometry and physical variables of the solids. We develop a set of analytical expressions for computing first and second order partial derivative of the shape functions with respect to global coordinates. And then a new collocation approach is proposed to collocate the equilibrium equations collocated at the internal nodes inside elements, and collocate the traction equilibrium equations at the interface and outer surface nodes. Compared with standard FEM, the EDM does not require a variational principle to set up the computational system equation and no integrals are involved to form the coefficients of the system. Moreover, the stress results in EDM are calculated based on the constitutive relationship and can reflect the stress concentration phenomenon better than FEM. Special attention of the analysis is devoted to the computation of the most important crack-tip characterizing parameters of cracked FGMs, namely the stress intensity factors. Numerical examples for 2d and 3d crack problems in FGMs are presented and discussed to show the effects of the material gradation on the crack-opening-displacements and the stress intensity factors.

## **Symbolic-Numeric Methods for Solving Differential Equations in Scientific Computing**

Dmitry Lyakhov\*

\*King Abdullah University of Science and Technology

### **ABSTRACT**

Differential equations are the central objects in physical simulations. However, very rare cases admit exact analytical expressions as solutions. Typically, simulations of complex systems require to solve them numerically. This approach also suffers from drawbacks and limitations, like significant stiffness of the underlying physical systems. This usually requires tiny numerical step sizes to resolve accurately the behavior or to significant improvement of numerical method. Another problem is the lack of physical plausibility in long-term behavior, because it is hardly available to preserve physically important quantities like conservation laws at the discrete level. In this talk we describe modern methods of group analysis of differential equations and differential algebra in order to overcome these difficulties. First of all, we introduce the notion of symmetries and conservation laws, and how to construct symbolically methods to preserve them at the discrete level. Then, we present general algorithms from differential algebra in order to show how to extract all possible information from a differential system without solving it explicitly. Finally, theoretical approaches are illustrated by several relevant examples from scientific computing.

## **ProMesher: A Novel Code for Preprocessing of High-Order Finite Elements Applied to High-Speed Penetrations**

Eric Lynd<sup>\*</sup>, Kent Danielson<sup>\*\*</sup>, Mark Adley<sup>\*\*\*</sup>

<sup>\*</sup>Geotechnical and Structures Laboratory, Engineering Research and Development Center, <sup>\*\*</sup>Geotechnical and Structures Laboratory, Engineering Research and Development Center, <sup>\*\*\*</sup>Geotechnical and Structures Laboratory, Engineering Research and Development Center

### **ABSTRACT**

As part of modeling a deformable penetrator impacting a target, meshing of a pointed-nose projectile finite element model can be a non-trivial task requiring significant user interaction. For applications with nearly incompressible materials, such as typical metal plasticity models, the potential for significant locking issues generally precludes the use of “automatic” unstructured meshers using first-order tetrahedrons. In recent years, however, the authors have developed robust 2nd order finite elements for lumped-mass explicit methods that do not lock and thus can accurately model high-speed penetration events with unstructured meshes. Consequently, it is now possible to employ “automatic” meshers which utilize a variety of 2nd order mapping strategies for efficiently running analyses traditionally limited by select numerical phenomena. This presentation describes a code, developed by the authors, that easily creates high-quality hex-dominant finite element projectile meshes employing combinations of 2nd order element types TET15, WEG21, and HEX27. The code, penned ProMesher (Projectile Mesher), exploits inherent characteristics of the higher-order finite elements that can greatly simplify/automate the meshing and lead to significant reductions in required computation time. ProMesher can greatly improve productivity of analysts as well as provide the automation necessary for shape optimization and large tradespace analyses. Benefits of the computational approach for the case of high projectile penetration are demonstrated.

## **A Multiscale Control Volume Framework Using a Non-orthodox MPFA-D for the Simulation of Two-phase Flows on Truly Unstructured Grids**

Paulo Lyra<sup>\*</sup>, Artur Souza<sup>\*\*</sup>, Lorena Barbosa<sup>\*\*\*</sup>, Darlan Carvalho<sup>\*\*\*\*</sup>

<sup>\*</sup>Federal University of Pernambuco (UFPE), <sup>\*\*</sup>Federal University of Pernambuco (UFPE), <sup>\*\*\*</sup>Federal University of Pernambuco (UFPE), <sup>\*\*\*\*</sup>Federal University of Pernambuco (UFPE)

### **ABSTRACT**

The advances in geostatistical modeling and characterization allow information from different scales to be integrated in order to generate geocellular models whose resolution typically range on the hundreds of millions cells, meanwhile the standard petroleum reservoir simulators handle only a fraction of this amount. In this way, multiple direct simulations on these high-resolution grids become infeasible. To overcome this limitation, scale-transferring methods have been devised. In essence, they allow high-resolution geostatistical data to be integrated onto the flow simulation grid. Among them, two branches of schemes stand out: the upscaling and the multiscale methods. Roughly speaking, the first generally employs a sort of homogenization of the field property, even when there is no formal separation between the scales. In these schemes a solution is found at the coarse-scale space leading to fast and robust results, but on the cost of losing information on the geological scale. To overcome this problem Multiscale Finite Volume Methods (MsFVM) devise conservative operators which are used to project the discrete system of equation onto the coarse-scale, solve the resulting coarse system and by using a set of operators, project back the solution onto the higher-resolution grid. Nonetheless, the MsFVM fail to deal with high-resolution geological properties on general grids as the multiscale operators are often calculated using a TPFA, which is only consistent for k-orthogonal grids. Furthermore, MsFVM lacks the framework capable of generating the geometric entities needed for simulation on unstructured coarse-scale meshes. The Multiscale Restricted Smoothed Basis (MsRSB) method creates this framework and expands the multiscale approach to unstructured coarse meshes. However, it fails to produce consistent solutions on fine-scale unstructured grids and for arbitrary permeability tensors as it also uses TPFA. In this article, we couple a MultiPoint Flux Approximation (MPFAD) with a Diamond stencil with the MsRSB to produce a consistent framework using unstructured grids on all scales. Additionally, we experiment with state of the art correction functions used to improve that quality of the multiscale flux in order to simulate some of the benchmark layers of the SPE. This framework showed prominent results producing accurate solutions for two-phase flow simulation in heterogeneous and mildly anisotropic medium with unstructured grids on coarse and fine scale.

## **Nonlinear Free Vibration Analysis of Defective FG Nanobeams Embedded in Elastic Medium**

Zheng Lyu\*, Zhiping Qiu\*\*

\*Institute of Solid Mechanics, Beihang University (BUAA), Beijing 100191, China, \*\*Institute of Solid Mechanics, Beihang University (BUAA), Beijing 100191, China

### **ABSTRACT**

Defects in atomic structure can deteriorate the mechanical properties of nanomaterials. These defects can be used to tailor the local characteristics of nanostructures and to achieve new functionalities, which is crucial to the potential application in nano electromechanical systems. The existing model cannot fully reflect accurate mechanical behaviors of nanostructures with material defects. Apparently, developing a more realistic model accounting for the nanomaterial defects is an interesting research topic. The presentation focuses on the effect of the material defects on nonlinear vibration behavior of embedded functionally graded (FG) nanobeam. The concept of defect degree is freshly introduced to quantify the material defects. Then a defective FG nanobeam model for nonlinear vibration behavior is developed in the framework of nonlocal strain gradient theory. The proposed defective model is an extension of the perfect model, which not only exhibits good performance in revealing the effect of material defect on vibration behavior, but also could be degenerated into the perfect model by eliminating defect degree. Based on set theory, two methods, i.e., sensitivity based interval analysis method (SIAM) and iterative algorithm based interval analysis method (IAM), are presented to solve the defective model for predicting nonlinear vibration frequency. The comparison between SIAM and IAM is discussed in the presentation. Subsequently, the detailed parametric investigations are carried out to understand the combined effects of the material defects and size-dependent parameter, elastic medium as well as power-law index on the vibration frequency. Some significant conclusions are given, which will offer guidance in the reliability design of new nanodevices. Our preliminary investigations suggest that the defective model and two numerical methods can also be applied to other nanostructures with material defects in various engineering problems. At the end of the presentation, further work on this field is put forward.

## EXPLORING THE LIMITS OF EFFICIENCY FOR BENDING-ACTIVE STRUCTURES

CARLOS LÁZARO\*†, JUAN BESSINI†, AND SALVADOR MONLEÓN†

\*†Departamento de Mecánica de los Medios Continuos y Teoría de Estructuras  
Universitat Politècnica de València, Camino de Vera s/n, 46022 Valencia, Spain  
carlafer@mes.upv.es

**Key words:** active bending, tied arch, scale effect, activation forces, buckling resistance.

**Abstract.** This paper discusses the relationship between structural shape, activation forces and activation stress levels in bending-active tied arches. The study focuses on planar arches composed of a bent rod, lower spanning cables and three equally spaced perpendicular deviators. A general relation between activation forces and structural shape has been established. Numerical experiments have provided activation stress levels with reference to rise-to-span ratios and rod slenderness. Serviceability limits for different proportions and lengths have been also analyzed. Results are given in terms of non-dimensional magnitudes and are applicable to variable scales and cross-section properties.

### 1 INTRODUCTION

Bending-active structures constitute a recent field of interest in research and practice<sup>1</sup>. They consist of initially straight slender members that are elastically bent to reach a post-buckled curved configuration and then stabilized by means of constraints, cables or membranes in tension. Finding the initial equilibrium configuration is one of the main difficulties during the conceptual phase due to the high non-linearity of the structural response of active members<sup>2</sup>. To address this issue, computational form-finding methods are being developed and comprise an active research field.

Nonetheless, the number of investigations focused on the assessment of the structural performance and efficiency of bending-active structures is limited. Lienhard<sup>1</sup> includes the study of several typical cases subject to simple loadings after they reach the initial active state and analyzes the proportion of the different contributions to the stiffness for different configurations by means of FEM software. Lázaro *et al.*<sup>3</sup> analyze the response of circular and elastica-shaped active arches subject to a point load, and quantify the relation between geometric stiffness, tangent stiffness and the angle at arch ends for different values of the slenderness. Douthe<sup>4</sup> considers strength and stiffness criteria to assess the applicability of different materials for active grid-shell members.

The design of a bending-active structure involves a tradeoff between member strength and magnitude of the pre-deformation: significant member curvatures are needed to reach a suitable shape; they require slender members to keep stresses low enough in the target configuration. However, very slender members may lead to insufficient stiffness of the structure. In the design of gridshell-like structures, the structural configuration is typically targeted to obtain certain shape definition and the effect of external loads may not be the most critical. However, in the case of footbridges they must bear heavier loads and it is crucial to achieve a certain stiffness.



Figure 1: Prototype of a lightweight footbridge based on the active bending principle

The broad objective of our research is to find patterns of relationship between form, activation forces, and limits of utilization of bending-active structures that may be used in the field of footbridges. At this stage we stick to simple planar structures composed of a continuous flexible rod that is activated by cables and deviators (Figure 2). We will use the term *bending-active tied arch* to refer to them. The structural concept is a hybrid between a tied arch and a cable beam and is suited to resist self-weight and service live loads. We consider structures with three deviators to limit the number of cases and the complexity of the study. More complex and stiff three-dimensional systems can be built combining a pair of planar bending-active tied arches. (figure 1).

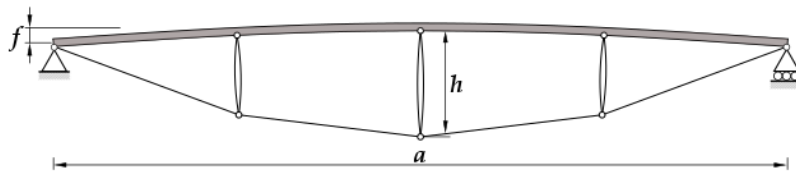


Figure 2: Three-deviator bending-active tied arch

In section 2, we start from fixed lengths and given cross-sections of rod and deviators. Introducing prestressing forces in cables, four different structural configurations that keep deviators perpendicular to the rod are form-found. From these results we establish a relation between the cable force ratio and the rise-to-span ratio of the activated structure, which is applicable for any scale. Through a series of numerical experiments, in section 3 we have obtained stress levels after the activation of the structure as functions of the rise-to-span ratio and the slenderness of the active member. Finally, further numerical analysis has led to establish relations between shape, length and slenderness associated to the serviceability limit state and ultimate limit state of the structure.

## 2 RELATIONSHIP BETWEEN SHAPE AND ACTIVATION FORCE

In a first step, we generate four different configurations for a bending-active tied arch with three equally spaced, perpendicular deviators. Simulations are carried out using Sofistik. The upper rod is a 4 m long continuous member with circular hollow cross-section with  $EI = 23.72 \text{ kN m}^2$ . The lengths of the deviators are  $h = 0.4 \text{ m}$  (central) and  $0.3 \text{ m}$  (lateral). Cables are not continuous; therefore, cable forces will be different in each cable segment.

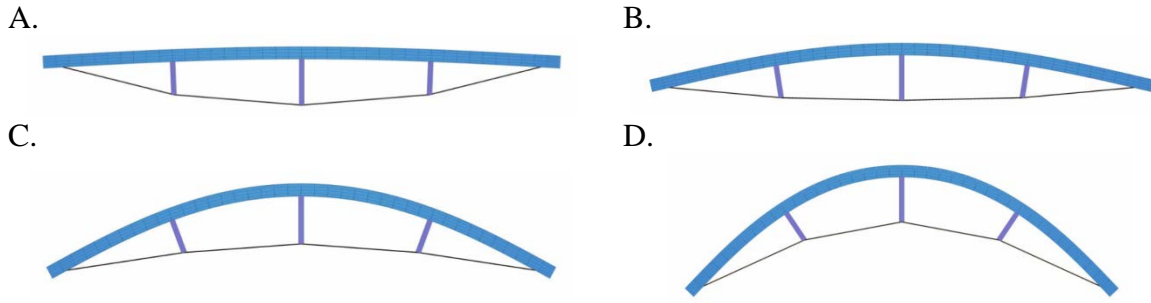


Figure 3: Four configurations for the hybrid structure with equal segment lengths and stiffness

For each self-stressed configuration, a force  $T^0$  has been introduced in the outer cable segments; the force  $T^l$  in the inner cable segments has been chosen to achieve perpendicularity between rod and deviators at nodes. Table 1 lists characteristic data for each structure.

Table 1: Values of activation forces and resulting geometric ratios for each configuration

	A	B	C	D
$T^0$ (kN)	2.71	10.58	21.77	32.9
$T^l$ (kN)	2.62	10.43	22.2	35.41
$T^l / T^0$	0.97	0.99	1.02	1.08
$a$ (m)	3.996	3.947	3.753	3.366
$f/a$	0.0178	0.0727	0.1639	0.284

These results can be generalized for flexible members of any length and stiffness with equally spaced, perpendicular deviators whose proportions be: length of central deviator equal to 10% of the length of the rod; length of lateral deviators equal to 75% of the central deviator. Each segment of the rod behaves as a segment of inflexional elastica whose scale is determined by the critical length (Lázaro *et al.*<sup>5</sup>)  $l_c = \pi\sqrt{EI/T}$ . The ratio  $l_c^0/l_c^l$  between critical lengths of the outer and inner rod segments defines the shape of the whole structure. Consequently, the shapes and forces that have been obtained using specific sizes and dimensions of members can be scaled by increasing the critical lengths of each segment while keeping their ratio. Therefore, the relation between any non-dimensional size ratio and the activation force ratio in cables  $T^l / T^0$  may be stated with generality for this structural type. Figure 4 represents the rise-to-span ratio and the depth-to-span ratio vs. the cable force ratio.

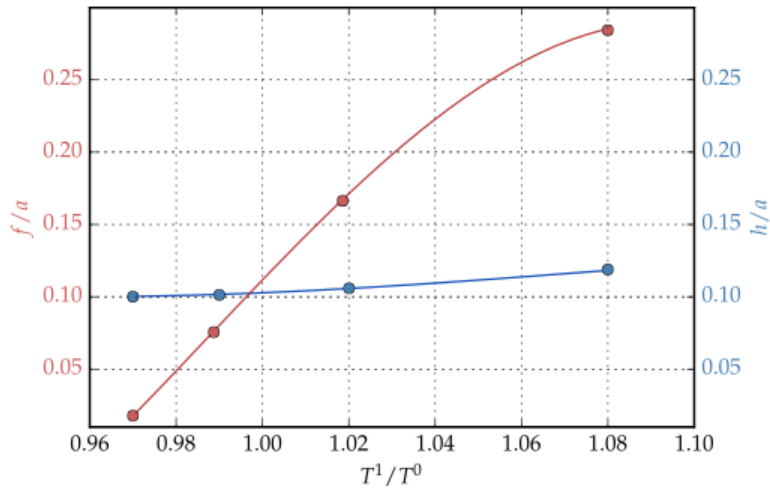


Figure 4: Relation between activation forces and proportions for tied arches with three deviators

Using figure 4 and the results in table 1, the configuration associated to a desired shape and size can be easily determined. For example, a 12 m span and 2.4 m rise arch ( $f/a = 0.2$ ) has a force ratio  $T^1/T^0 = 1.03$  (Figure 2). For this  $f/a$  ratio, in the original structure,  $a = 3.68$  m and  $T^0 = 25$  kN. The scaling factor for the desired structure will be  $12/3.68 = 3.26$ ; therefore  $EI/T^0$  should be  $3.26^2 = 10.627$  times larger than in the original one. This can be done with a  $3.26 \cdot 4$  m = 13.04 m long rod, using a stronger cross section, or decreasing the activation force, or a combination of both.

### 3 STRESS LEVELS AFTER ACTIVATION

The next step has been to establish limits to normal stresses in the bent rod after activation.

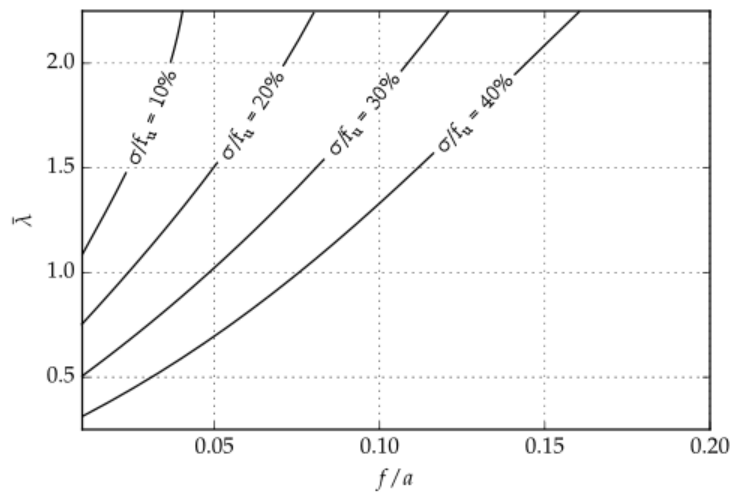


Figure 5: Stress ratio levels after activation in terms of rod slenderness and rise-to-span of the structure

For a single elastica, it can be shown that there is a direct relation between rise-to-span ratio and slenderness of the flexible rod for a given material, shape of cross section and level of normal stress due to bending. The following definition of slenderness has been selected:  $\bar{\lambda} = \frac{s}{\pi} \sqrt{\frac{A}{I}} \sqrt{\frac{f_u}{E}}$ ,

where  $s$  is the length of the rod between deviators. As the bending-active tied arch is composed of a series of elastica sections, a similar relation between rise-to-span and slenderness is to be expected for a given structural topology. We have carried a series of numerical experiments with the same setup as in section 2. We have chosen GFRP for the rod (material properties of GFRP are  $E = 30$  GPa,  $f_u = 400$  MPa) and circular hollow cross-sections with thickness equal to 10% of the radius. Stresses in the rod have been evaluated for 12 values of  $\bar{\lambda}$  and 40 values of the rise-to-span ratio. We have represented curves corresponding to several ratios of stress-to-ultimate-strength (Figure 5). As expected, higher rises lead to higher  $f/a$  ratios for the same slenderness. This diagram complements the results of section 2. Once the shape and size of the structure have been defined, it allows to select the minimum slenderness of the flexural member compatible with a prescribed stress level.

#### 4 PERFORMANCE FOR SERVICE LOADS

To study the performance for service loads, it is necessary to define the cross-section of the activating cables and the magnitude of loading. The cable area has been selected so that its slenderness be 10 times the rod slenderness. The mechanical properties of the selected cables are:  $E = 105$  GPa and  $f_u = 1570$  MPa. Point loads corresponding to 40% of  $5$  kN/m<sup>2</sup> distributed on a variable wide which corresponds to the 10% of the rod length have been applied as frequent service load. Mid-span deflections have been evaluated for different lengths.

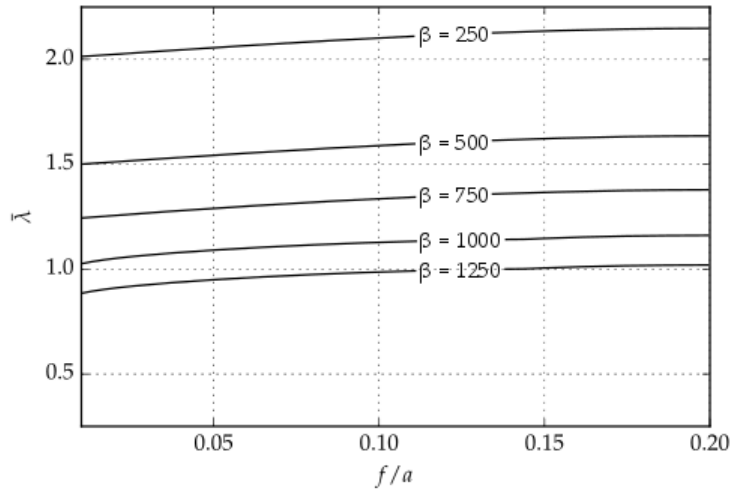


Figure 6: Deflections from  $L/250$  to  $L/1250$  for different lengths and a given load in terms of slenderness and shape

## 5 PERFORMANCE FOR ULTIMATE LOADS

A similar study has been carried out to assess the behavior at ultimate limit states. Structural proportions and cross-section dimensions are the same as the previous analysis. The design value for the point loads is obtained by the application of the partial factor for actions  $\gamma_f = 1.35$ . For several structures, we have checked normal forces and bending moments in the rod performing second order analysis of the structural model. Figure 7 shows the region of the slenderness-shape diagram where according to EN 1993-1-1 (Eurocode 3) the utilization ratio is less than 1, for different lengths and a given design load.

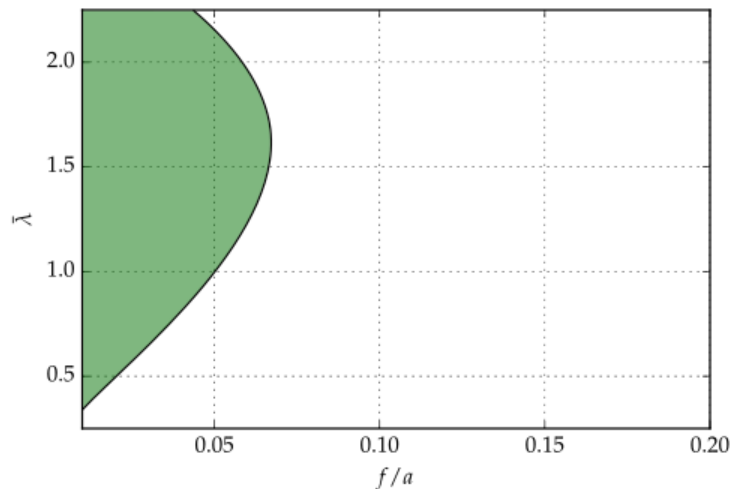


Figure 7: Safe region (green) against buckling for the model examples.

## 6 CONCLUSIONS

We have studied the activation process and the performance of bending-active tied arches with three perpendicular deviators. General non-dimensional relations between activation forces and structural shape, as well as stress levels in terms of shape and slenderness of the flexural member have been established. We have also studied the serviceability limit state and the ultimate limit state for prescribed loads and cable areas. Further research needs to be done to establish the limits of applicability of this type of active arch.

## 6 ACKNOWLEDGEMENTS

The authors gratefully acknowledge the financial support from the Spanish Ministry of Economy and Competitiveness through grant BIA2015-69330-P (MINECO) and the support from CALTER Ingeniería and SOFISTIK AG for providing a software license.

## REFERENCES

- [1] Lienhard, J. *Bending-Active Structures: form-finding strategies using elastic deformation in static and kinetic systems and the structural potentials therein*. Universität Stuttgart, (2014).
- [2] Bessini, J., Lázaro, C. and Monleón, S. A Form-finding method based on the geometrically exact rod model for bending-active structures. *Engineering Structures*, (2017); 152:549–558. <https://doi.org/10.1016/j.engstruct.2017.09.045>.
- [3] Lázaro, C., Monleón, S. and Bessini, J. Tangent Stiffness in loaded elastica arches. *Proceedings of the IASS Symposium 2017. International Association for Shell and Spatial Structures*, (2017).
- [4] Douthe, C. *Etude de structures élancées précontraintes en matériaux composites, application à la conception des gridshells*. *Engineering Sciences [physics]*. Ecole des Ponts ParisTech, (2007).
- [5] Lázaro, C., Monleón, S. and Casanova, J. Can the force density method be extended for active bending structures? *Proceedings of the IASS Symposium 2015. International Association for Shell and Spatial Structures*, (2015).
- [6] Bessini, J., Piñol, R., Lázaro, C. and Monleón, S. Design of an experimental lightweight footbridge based on the active bending principle. *Proceedings of the IASS Symposium 2018. International Association for Shell and Spatial Structures*, (2018).

## Pseudospin-spin Dynamics in AC-driven Single-layer Silicene

Alexander López<sup>\*</sup>, Antonio Di Teodoro<sup>\*\*</sup>, Francisco Mireles<sup>\*\*\*</sup>, John Schliemann<sup>\*\*\*\*</sup>, Benjamin Santos<sup>\*\*\*\*\*</sup>

<sup>\*</sup>Escuela Politécnica del Litoral, <sup>\*\*</sup>Universidad San Francisco de Quito, <sup>\*\*\*</sup>Universidad Autónoma de México,  
<sup>\*\*\*\*</sup>University of Regensburg, <sup>\*\*\*\*\*</sup>INRS-Energie et Materiaux Varennes

### ABSTRACT

We study the pseudospin-spin fluctuation dynamical effects in single layer silicene due to the interplay of a periodically driven perpendicular electric field and the Rashba spin-orbit interaction. We find that spin non conserving processes of the real spin, induced by the rather weak Rashba coupling, manifest themselves as shifts of the resonances in the quasienergy spectrum in the low coupling regime to the driving field. Moreover, we find an interesting cooperative effect among the, in principle, competing spin-orbit contributions. This is explicitly illustrated by a perturbative analytical solution of the dynamical equations. In addition, we show that a finite Rashba spin-orbit interaction is necessary in order to get a non vanishing out of plane pseudospin polarization. We discuss the possible experimental detection schemes of our theoretical results and their relevance in new practical implementation of periodically driven interactions in silicene physics.

